



UNIVERSIDAD DE CHILE
FACULTAD DE CIENCIAS FÍSICAS Y MATEMÁTICAS
DEPARTAMENTO DE ASTRONOMÍA

**CHARACTERIZATION OF THE VARIABILITY OF BLAZARS IN THE
RADIO BAND**

TESIS PARA OPTAR AL GRADO DE MAGÍSTER EN CIENCIAS,
MENCIÓN ASTRONOMÍA

VÍCTOR ALBERTO NAVARRO ARÁNGUIZ

PROFESOR GUÍA:
WALTER MAX-MOERBECK ASTUDILLO

MIEMBROS DE LA COMISIÓN:
PAULINA LIRA TEILLERY
VALENTINO GONZÁLEZ CORVALÁN
ROBERTO ASSEF TREBILCOCK

Este trabajo ha sido parcialmente financiado por:
FONDECYT INICIACIÓN 1190853

SANTIAGO DE CHILE
2023

CARACTERIZACIÓN DE LA VARIABILIDAD DE BLAZARES EN BANDA DE RADIO

Los blazares son un tipo de galaxia de núcleo activo con jets relativistas orientados muy cercano a la línea de visión entre el objeto y el observador. Estos objetos emiten radiación sobre todo el espectro electromagnético, con una gran variabilidad desde radio a rayos gama. El proceso físico de estas emisiones no está claro del todo, teniendo dos posibles escenarios: uno del tipo leptónico, donde la emisión de sincrotrón y el efecto Compton-inverso predominan; o del tipo hadrónico, donde la emisión es de sincrotrón producto de electrones y protones que son acelerados a energías ultrarelativistas dentro del jet. La variabilidad observada en las curvas de luz de blazares muestran un comportamiento estocástico y típicamente aperiódico. Para estudiar las curvas de luz, los astrónomos utilizan comúnmente la densidad de potencia espectral (PSD), reflejada en el periodograma de la curva de luz.

El método actualmente más utilizado para caracterizar la PSD de una curva de luz es computacionalmente costoso, lento y poco adecuado para modelos de PSD complejos, es por ello que en este trabajo introducimos el uso de una nueva técnica basada en los algoritmos *Population Monte Carlo* (PMC) y *Approximate Bayesian Computation* (ABC). Esta técnica resuelve de forma eficiente el ajuste de una PSD usando desde un modelo de ley de potencia simple a modelos mas complejos como aquellos que incluyen una frecuencia de quiebre. La nueva técnica tarda unos minutos en ajustar un modelo, mientras métodos previos requieren de horas para obtener resultados sobre el modelo simple. Ajustamos un total de 1290 curvas de luz en radio de OVRO con un largo aproximado de 12 años. Encontramos que 1000 de ellas se ajustan bien usando el modelo simple, obteniendo resultados consistentes con estudios anteriores. Determinamos que esta caracterización permite predecir con un 74 % de exactitud si una fuente emite o no en rayos γ . Por otro lado, 38 objetos resultan tener una frecuencia de quiebre en su periodograma, siendo esto más probable (3σ) en fuentes que emiten en rayos γ , así como en objetos con redshift $z < 1$ y factor de Doppler $\delta > 10$.

Físicamente se espera que todos los objetos tengan una frecuencia de quiebre en su periodograma. Al corregir las frecuencias de quiebre encontradas usando el redshift y el factor de Doppler, obtenemos un tiempo característico de 8.64 ± 5.34 años en el sistema de referencia de la fuente. Al hacer la misma corrección en la frecuencia mínima de todos los objetos notamos que varios objetos sin quiebre alcanzan valores en el mismo rango de los objetos que si tienen quiebre. Esto sugiere que: (i) el mecanismo que genera la variabilidad en estos objetos es distinto; o (ii) se trata de objetos con escalas físicas distintas. Sugerimos que un estudio sobre la masa del agujero negro y luminosidad de estos objetos podría entregar respuestas.

CHARACTERIZATION OF THE VARIABILITY OF BLAZARS IN THE RADIO BAND

Blazars are a type of Active Galaxy Nucleus (AGN) with relativistic jets closely oriented to the line of sight between the object and the observer. This type of object emits radiation over the entire electromagnetic spectrum, having large variability from radio to γ -ray. The physical processes responsible of these emissions remain unclear. Astronomers theorize about two possible scenarios: in the leptonic scenario, the synchrotron emission and inverse-Compton scattering predominate; or an hadronic context, where synchrotron emission is produced by electrons and protons being accelerated to ultrarelativistic energies inside the jet. The observed variability of blazars described in their light curves shows an stochastic behavior that is typically aperiodic. In order to study these light curves, astronomers commonly use the power spectral density (PSD), which is reflected in the light curve's periodogram.

The currently most common method used to characterize the PSD of light curves is computationally expensive, slow and not well suited for the fit of complex PSD models, that is why in this work we introduce a new technique based in the Population Monte Carlo (PMC) and Approximate Bayesian Computation (ABC) algorithms. This technique efficiently solves the fit of a PSD from a simple power-law model to a more complex one which incorporates a break frequency, taking only a few minutes to complete. In contrast, the previous method takes hours to achieve the same results for the simple power-law model. We fit a total of 1290 light curves in radio from OVRO dataset, each one with a length of about 12 years. We find that 1000 of them are well-fitted using a simple power-law model, obtaining consistent results with previous studies. We determine that this characterization allow us to predict with an accuracy of about 74 % if a source emits or not γ -rays. On the other hand, we found 38 objects with a well-defined break frequency in their periodogram, from what we conclude it is more likely (3σ) to find a break in sources emitting γ -rays, as well in sources with a redshift $z < 1$ and a Doppler factor $\delta > 10$.

Physically we expect that all objects must have a break in frequency in their periodogram at some point. After correcting for the redshift and the Doppler factor in the found break frequencies, we find a characteristic time of 8.64 ± 5.34 years in the source rest frame. We also apply this correction to the minimum frequency of all objects, noticing that several objects without a break reach minimum values in the same range as object with a break. This suggests that: (i) the mechanism to generate variability is different in these objects; or (ii) we are looking at objects with different physical scales. We suggest that a study about the black hole mass and luminosity of these objects could give answers.

*A mi familia,
por su apoyo constante y creencia en mí,
que me impulsó a llegar a la meta.*

*“Nadie puede entender perfectamente a otra persona,
ya es bastante difícil entenderse a uno mismo
(...) tal vez por eso la vida es tan interesante.”*

Agradecimientos

Quiero expresar mi más sincero agradecimiento a todas las personas que me acompañaron en este proceso, el cual fue algo difícil, tedioso y confuso para mi.

En primer lugar quiero agradecer a mi familia, por darme siempre ese leve empujón que me permitió seguir adelante y motivarme a no renunciar al trabajo que estaba haciendo. A mi padre, por enseñarme a afrontar la vida siempre con firmeza, que si el camino esta difícil lo mejor es ir a paso lento y también por su confianza en mí. A mi madre, por estar siempre atenta a cómo me encontraba emocionalmente y darme a entender que sea cual sea la decisión que tomase, ella siempre estaría a mi lado. A mis hermanas Andrea y Claudia, y mi hermano Ignacio, por darme esos momentos de esparcimiento que eran necesarios y mostrar siempre un apoyo incondicional.

A mi profesor, Walter Max-Moerbeck, que logró llevar a puerto el resultado final de esta investigación. Gracias por haberme confiado este trabajo y por todos sus consejos, tanto académicos como de la vida. Fue un honor trabajar con usted, tiene todos mis respetos.

A los amigos que me han acompañado desde el liceo, con los que he compartido grandes momentos desde mi adolescencia y lo que llevo de adultez. A pesar de los problemas que hemos tenido, agradezco que estén ahí para mi y quieran escucharme cuando más lo he necesitado. Infinitas gracias por querer entenderme y darme su apoyo.

Al grupo de amigos con los que conecté en la universidad, que hicieron que mi estadía en ese lugar fuera mucho más amena y que a pesar del tiempo aún mantenemos contacto. Gracias por todas esas tardes hablando de videojuegos, animé y de papas fritas.

A Jocelyn, con quien he compartido muchos bellos momentos y aventuras este último año. Espero seguir compartiendo muchos más momentos contigo. Muchas gracias por acompañarme, entregarme tu amor y darme apoyo en mis peores momentos.

A las personas que en su momento me acompañaron pero ya no están y que me han enseñado un montón de la vida, a valorar el presente y aprender sobre mis errores.

Por supuesto a mis mascotas, Nacho, Milka y Mei, que entregan esa tranquilidad y sentido de hogar cada vez que voy a visitarlos a la casa de mis padres.

Finalmente, quiero dejar unas palabras para Lucas Saavedra, amigo y compañero, el cual fue víctima de la pandemia y de un sistema que aún deja mucho que desear. Siempre fuiste una gran persona compañero, solo muere quien se olvida.

Table of Content

1. Introduction	1
1.1. Motivation	1
1.2. Active Galactic Nuclei	2
1.3. Observational characteristics of Blazars	5
1.4. Theoretical Models of Blazars	8
1.5. Previous studies on the characterization of blazars variability	9
2. Observations	11
2.1. OVRO dataset	11
2.2. Data cleaning and data selection	12
3. Modeling variability of blazars	17
3.1. Signal Processing	18
3.1.1. Fourier Transform	18
3.1.2. Convolution	18
3.1.3. Window functions	19
3.1.4. Power Spectral Density	19
3.1.5. Periodogram	20
3.1.6. Aliasing	20
3.1.7. Nyquist frequency	21
3.2. Simulation of light curves	21
3.2.1. Fourier Decomposition	22
3.3. Comparing observed and simulated light curves	25
3.4. Summary	26
4. The PMC-ABC algorithm	28
4.1. Credible Intervals	29
4.2. Approximate Bayesian Computation	30
4.3. Population Monte Carlo	30
4.4. PMC-ABC: The CosmoABC package	31
4.5. Fitting PSD models	34
4.5.1. Prior distributions	35
4.5.2. Distance function	38

5. Testing the PSD fitting method	41
5.1. Selecting good CosmoABC parameters	42
5.2. Simple power-law model	46
5.2.1. Power-law index β	48
5.2.2. Noise level P_{noise}	53
5.3. Broken power-law model	56
5.3.1. Low power-law index β_l	57
5.3.2. Break frequency f_{br}	64
5.4. Comparison against least-squares method	68
6. PSD fit results	70
6.1. Well-defined fit and model selection	71
7. Discussion	78
7.1. Comparison with previous results	84
7.2. Power law with and without break	87
7.3. Break-frequency analysis	91
7.4. FSRQ vs BL Lac	96
7.4.1. Broken model	96
7.4.2. Simple model	97
7.5. γ -ray sources	99
7.5.1. Broken model	99
7.5.2. Simple model	100
7.6. Redshift range	102
7.6.1. Broken model	102
7.6.2. Simple model	104
7.7. Doppler factor range	105
7.7.1. Broken model	105
7.7.2. Simple model	107
7.8. Radio characterization as γ -ray source predictor	108
8. Conclusion	114
Bibliography	116
Annex A. Mathematics and Code	120
A.1. Data cleaning by using spline functions	120
A.2. Light Curve simulation and periodogram binning	121
A.3. Bayes' Theorem	122
A.4. Parseval's Theorem over white noise	122
A.5. Generalized Linear Model in H2O	123
A.6. Doppler correction	123

Annex B. Figures	125
Annex C. Tables	137

Table Index

2.1.	Summary of some statistics of the 1290 selected observations from OVRO dataset after applying the data cleaning process.	15
5.1.	Important statistics about the blazar light curves used to make the second part of the tests where simulated light curves use the same time sampling of these observed objects. It also includes information of the uniform case.	50
5.2.	Location of the first 5 and last binned points for each observation used for testing in log scale including the uniform case.	60
6.1.	Results of the non-consistency of parameters β_h and β_l . The percentage is with respect to all the 1290 fitted observations.	73
6.2.	Summary statistics of parameters $\log A$ and β of the 1010 objects having $\sigma(\beta)_{68.3\%} < 1.5$ and no well-defined break frequency.	74
6.3.	Summary statistics of parameters $\log A$, $\log f_{br}$, β_l and β_h of the 39 objects having a well-defined break frequency.	75
7.1.	Summary statistics of parameters $\log A$ and β of the 1000 objects having $\sigma(\beta)_{68.3\%} < 1.5$ and no well-defined break frequency after excluding sources with large values of beta as discussed in the text.	81
7.2.	Summary statistics of parameters $\log A$, $\log f_{br}$, β_l and β_h of the final 38 objects having a well-defined break frequency after a selection process.	82
7.3.	Classification of the final 1000 sources well-defined by the simple power-law model.	83
7.4.	Classification of the final 38 sources well-defined by the broken power-law model.	84
7.5.	Power-law index β for two objects obtained by Max-Moerbeck (2013) using almost 4 years of OVRO data, and Goyal et al. (2022) along with our results using CosmoABC for almost 12 years of OVRO data.	86
7.6.	Different results for each classification about the estimation of \hat{p} assuming that finding a well-defined break frequency can be modeled as a Binomial distribution $B(n, p)$	88
7.7.	Anderson-Darling test for each parameter with respect to the distributions of objects with and without a break frequency.	91
7.8.	Results of the log break frequency in the source rest frame $\log f_{br,corr}$ and the corrected time $t_{br,corr}$ after using equation 7.1 for different classifications. . . .	95
7.9.	Summary statistics of the different parameters tested for the broken power-law model with respect to the optical spectrum classification.	97

7.10.	Similar to Table 7.7, but the Anderson-Darling test is with respect to the observed spectrum classification FSRQ and BL Lac for all sources fitted using the broken power-law model, being 24 of them FSRQ and 7 BL Lac.	97
7.11.	Summary statistics of the different parameters tested for the simple power-law model with respect to the optical spectrum classification.	98
7.12.	Similar to Table 7.7, but the Anderson-Darling test is with respect to the observed spectrum classification FSRQ and BL Lac for all sources fitted using the simple power-law model, being 692 of them FSRQ and 168 BL Lac.	98
7.13.	Summary statistics of the different parameters tested for the broken power-law model with respect to being a γ -ray source.	100
7.14.	Similar to Table 7.7, but the Anderson-Darling test is with respect to the 33 γ -ray sources and the 5 non γ -ray sources fitted using the broken power-law model.	100
7.15.	Summary statistics of the different parameters tested for the simple power-law model with respect to being a γ -ray source.	101
7.16.	Similar to Table 7.7, but the Anderson-Darling test is with respect to the 562 γ -ray sources and the 438 non γ -ray sources fitted using the simple power-law model.	101
7.17.	Summary statistics of the different parameters tested for the broken power-law model with respect to two predefined redshift ranges.	103
7.18.	Similar to Table 7.7, but the Anderson-Darling test is with respect to the 27 sources with a redshift range $0 < z \leq 1$ and the 7 having $z > 1$ fitted using the broken power-law model.	103
7.19.	Summary statistics of the different parameters tested for the simple power-law model with respect to two predefined redshift ranges.	104
7.20.	Similar to Table 7.7, but the Anderson-Darling test is with respect to the 427 sources with a redshift range $0 < z \leq 1$ and the 460 having $z > 1$ fitted using the simple power-law model.	105
7.21.	Summary statistics of the different parameters tested for the broken power-law model with respect to two predefined Doppler factor ranges.	106
7.22.	Similar to Table 7.7, but the Anderson-Darling test is with respect to the 6 sources with a Doppler factor range $0 < \delta \leq 10$ and the 27 having $\delta > 10$ fitted using the broken power-law model.	106
7.23.	Summary statistics of the different parameters tested for the simple power-law model with respect to two predefined redshift ranges.	107
7.24.	Similar to Table 7.7, but the Anderson-Darling test is with respect to the 427 sources with a Doppler factor range $0 < \delta \leq 10$ and the 460 having $\delta > 10$ fitted using the simple power-law model.	107
7.25.	Three different models for the logistic regression with respect of being or not a γ -ray source.	109

7.26.	Coefficients of each predictor and model with their respective errors and p -values according to H2O framework	111
7.27.	Confusion Matrices of the three predictive models of being or not a γ -ray.	112
C.1.	Results of fitting the simple power-law model over the 1290 selected observations from OVRO dataset.	137
C.2.	Results of fitting the broken power-law model over the 1290 selected observations from OVRO dataset.	181

Figure Index

1.1.	Schema of an AGN, based on Figure 1 from Urry & Padovani (1995).	4
1.2.	SED of PKS1510-089 and Mrk 421.	6
1.3.	Light curves of 3C 279 at different frequencies	8
2.1.	Light curve of J1706+0953 before and after the cleaning process.	13
2.2.	Light curves of C1047+7238 and J2358-1020 after the cleaning process.	15
2.3.	Histogram of some statistics of the 1290 selected observations from OVRO dataset after applying the data cleaning process.	16
3.1.	Light curves generated using both power-law models described in the thesis, a simple one and one with a characteristic break frequency. At the right of each light curve its periodogram is displayed.	23
3.2.	Effect of the Hanning window in both power-law models.	25
4.1.	Diagram of the PMC-ABC algorithm used by CosmoABC. A detailed explanation of the algorithm is described in Ishida et al. (2015).	34
4.2.	Histograms of the estimation of the noise level P_{noise} using errors σ_e from the observation of PKS 1510-089.	37
4.3.	Possible values for $\log A$ if we consider that the periodogram of all selected observations fits a simple power-law model $P(f) = Af^{-\beta}$ with possible β values between 0 and 5.	38
4.4.	Distance function χ^2 for a simulated light curve with parameters $\beta = 2$ and $\log A = 5$ without noise using different combinations of parameters.	39
4.5.	Same as Figure 4.4 but showing $\log A$ and β separately.	40
5.1.	MAE and dispersion at HDI of 68.3% of model parameters $\log A$, $\log P_{\text{noise}}$ and β versus running time for different CosmoABC configurations in the simple power-law model context.	44
5.2.	Example of the posterior results for $M = 200$ before and after continuing the CosmoABC iteration increasing the number of draws of the last particle system to $M = 1000$	46
5.3.	Comparison of the accuracy metrics for each parameter and running times when using $M = 200$, $M = 200$ continuing the last particle system to achieve 1000 draws ($M = 200+\text{continue}$) and $M = 1000$	46
5.4.	Periodograms to fit for each test of the simple power-law model.	47
5.5.	Results for the uniform case with $\beta = 2$	48

5.6.	Corner plot using the collection of 100 experiments for the uniform case with $\beta = 2$	49
5.7.	Boxplot and MAE for the mode of the 100 experiment posteriors done for each observation and simulated β including the uniform case.	51
5.8.	Dispersion of each parameter and percentage of experiments deviated from the simulated value using HDI at 68.3 % for each observation and simulated β . . .	53
5.9.	Boxplot and MAE for the mode of the 100 experiment posteriors done for each observation and simulated $\log P_{\text{noise}}$ including the uniform case.	55
5.10.	Dispersion of each parameter and percentage of experiments deviated from the simulated value using HDI at 68.3 % for each observation and simulated $\log P_{\text{noise}}$. . .	56
5.11.	Periodograms to fit for each test of the broken power-law model.	57
5.12.	Results for the uniform case with $\beta_l = 0$	58
5.13.	Corner plot using the collection of 100 experiments for the uniform case with $\beta_l = 0$	59
5.14.	Boxplot and MAE for the mode of the 100 experiment posteriors done for each observation and simulated β_l including the uniform case.	62
5.15.	Dispersion of each parameter and percentage of experiments deviated from the simulated value using HDI at 68.3 % for each observation and simulated β_l . . .	63
5.16.	Boxplot and MAE for the mode of the 100 experiment posteriors done for each observation and simulated $\log f_{\text{br}}$ including the uniform case.	66
5.17.	Dispersion of each parameter and percentage of experiments deviated from the simulated value using HDI at 68.3 % for each observation and simulated $\log f_{\text{br}}$. . .	67
5.18.	Results of fitting the simple power-law model using a non linear least-squares method and CosmoABC.	69
5.19.	Comparison between CosmoABC and least-squares with respect to the MAE of each parameter for the different time sampling used.	69
6.1.	Distribution of parameter β and its dispersion at level of HDI 68.3 %, showing the two proposed threshold for $\sigma(\beta)_{68.3\%}$ at 1.5 and = 3.	72
6.2.	Check of consistency between β_h and β_l for objects 2230+114 and J0721+7120 at HDI levels 68.3 %, 95.5 % and 99.7 %.	73
6.3.	Distribution of the dispersion of $\log f_{\text{bf}}$ at HDI level 68.3 % and its comparison with the difference between β_h and β_l for the different assumptions of having a well-defined break frequency.	74
6.4.	Histogram of $\log A$ and β values and their dispersion at 68.3 % of the 1010 objects having $\sigma(\beta)_{68.3\%} < 1.5$ and no well-defined break frequency.	75
6.5.	Histogram of $\log A$, $\log f_{\text{br}}$, β_l and β_h and their dispersion at 68.3 % of the 39 objects having a well-defined break frequency.	75
6.6.	Results of fitting the simple power-law model over object PKS 1510-089. . . .	76
6.7.	Results of fitting the broken power-law model over object CLJ1333+5057. . . .	77
7.1.	Light curves of 10 sources well-defined by the simple power-law model but with a β out of the expected range from 0 to 4.	79

7.2.	Light curves of J0654+4514 fitted with the power-law break model having $\beta_h > 5$ and J1759+2343 fitted with the simple power-law model having $\beta > 5$	80
7.3.	Fitted periodogram for both objects from Figure 7.2.	80
7.4.	Light curve and periodogram of J1405+0415 with and without anomalous points	82
7.5.	Comparison of the β values obtained by this thesis and previous results from Max-Moerbeck (2013)	85
7.6.	Distribution of the dispersion in the β values obtained by this thesis and previous results from Max-Moerbeck (2013) along with a scatter plot of these dispersions.	86
7.7.	Results from Table 7.6 displayed as error bars plot for each classification.	88
7.8.	Comparison of distributions of redshift and Doppler factor between the 1000 sources best fitted with the simple power-law model and the 38 best fitted with the broken power-law model.	90
7.9.	Same as Figure 7.8 but for parameters in radio-band: log of the mean flux and log of the variance of the flux.	90
7.10.	Same as Figure 7.8 but for γ -ray parameters: log of the mean flux, spectral slope and log variability index.	91
7.11.	Break frequency and characteristic time with their respective error bars versus the redshift in the observer frame and the source rest frame.	93
7.12.	Similar to Figure 7.11 but for each AGN classification separately.	94
7.13.	Similar to Figure 7.11 but for the classification of being or not a γ -ray source.	94
7.14.	Distribution of the corrected minimum frequency of all fitted objects and the corrected break frequencies found	96
7.15.	Density and cumulative histograms for the simple power-law model and radio parameters with respect to the observational classes FSRQ and BL Lac.	99
7.16.	Density and cumulative histograms for the simple power-law model and radio parameters with respect to the being or not a γ -ray source.	102
7.17.	Linear Regression results between $\log f_{br}$ and γ -ray parameters for the redshift range $0 < z \leq 1$	104
7.18.	Density and cumulative histograms for the simple power-law model and radio parameters with respect to redshift ranges $0 < z \leq 1$ and $z > 1$	105
7.19.	Density and cumulative histograms for the simple power-law model and radio parameters with respect to Doppler factor ranges $0 < \delta \leq 10$ and $\delta > 10$	108
7.20.	ROC curves and variables importance of the three predictive models of being or not a γ -ray.	110
7.21.	ROC curves of Model 1 and PSD parameters used individually on the prediction of being or not a γ -ray.	111
7.22.	Plot of the probability of being a γ -ray source with respect to β and $\log A$ following results of Model 1.	113
B.1.	Light curves of microquasars CygX-3, SS433, GRS 1915+105 and LS I +61 303 removed from the analysis.	125
B.2.	Histogram of the kurtosis for all 1859 OVRO objects	126

B.3.	Light curve of three objects and histograms of their flux densities each one representing the range of kurtosis described in Appendix A.1.	126
B.4.	Light curves of the 39 objects well-fitted using the broken power-law model (Part 1).	127
B.5.	Light curves of the 39 objects well-fitted using the broken power-law model (Part 2).	128
B.6.	Light curves of the 74 non-consistent objects from Section 7.1 with $\beta_{\text{old}} > \beta_{\text{new}}$ (Part 1).	129
B.7.	Light curves of the 74 non-consistent objects from Section 7.1 with $\beta_{\text{old}} > \beta_{\text{new}}$ (Part 2).	130
B.8.	Light curves of the 74 non-consistent objects from Section 7.1 with $\beta_{\text{old}} > \beta_{\text{new}}$ (Part 3).	131
B.9.	Light curves of the 74 non-consistent objects from Section 7.1 with $\beta_{\text{old}} > \beta_{\text{new}}$ (Part 4).	132
B.10.	Light curves of the 3 non-consistent objects from Section 7.1 with $\beta_{\text{old}} < \beta_{\text{new}}$	133
B.11.	Scatter plot along with a KDE plot at 10 levels of the model parameters from the broken power-law model versus other parameters for FSRQ and BL Lac.	133
B.12.	Scatter plot along with a KDE plot at 10 levels of the model parameters from the simple power-law model versus other parameters for FSRQ and BL Lac.	133
B.13.	Scatter plot along with a KDE plot at 10 levels of the model parameters from the broken power-law model versus other parameters for γ -ray and non γ -ray sources.	134
B.14.	Scatter plot along with a KDE plot at 10 levels of the model parameters from the simple power-law model versus other parameters for γ -ray and non γ -ray sources.	134
B.15.	Scatter plot along with a KDE plot at 10 levels of the model parameters from the broken power-law model versus other parameters for redshift $0 < z \leq 1$ and $z > 1$	135
B.16.	Scatter plot along with a KDE plot at 10 levels of the model parameters from the simple power-law model versus other parameters for redshift $0 < z \leq 1$ and $z > 1$	135
B.17.	Scatter plot along with a KDE plot at 10 levels of the model parameters from the broken power-law model versus other parameters for Doppler factor $0 < \delta \leq 10$ and $\delta > 10$	136
B.18.	Scatter plot along with a KDE plot at 10 levels of the model parameters from the simple power-law model versus other parameters for Doppler factor $0 < \delta \leq 10$ and $\delta > 10$	136

Chapter 1

Introduction

1.1. Motivation

Astronomy has evolved by leaps and bounds over the last years. The new technologies that come along with new observatories have enabled us to observe objects that were impossible to detect and also improve poor data of previously observed objects, thereby allowing newer studies and thus achieving a better understanding of the objects in the universe. Observed data has been always the fundamental source of information for astronomers. In the past, we were restricted to ground-based telescopes and only to observe in the infrared and visible frequencies of the electromagnetic spectrum. As time passed the technological advances helped us to increase the limited frequency band, allowing us to observe from radio to γ -ray frequencies, which meant new perspectives to study astronomical sources and hence new ways to characterize objects by their behavior at different frequencies. The arrival of radio-telescopes has been a revolutionary leap in astronomy and has evolved from being a field that only study rare sources as radio galaxies to study objects with very faint flux densities as radio-quiet active galactic nuclei (Padovani 2016). To illustrate the capabilities of radio-astronomy, the Event Horizon Telescope Collaboration group has employed very-long baseline interferometry over a network of radio-telescopes around the globe to get impressive results of two different supermassive black holes, the one from the radio galaxy Messier 87 (Event Horizon Telescope Collaboration et al. 2019) and Sagittarius A* located at the center of our galaxy (Event Horizon Telescope Collaboration et al. 2022).

The arrival of new tools also means an increment of the data that can be obtained using telescopes. In some cases the flow of data can even exceed the speed at which astronomers publish their results, so the improvement of the techniques is also necessary in order to work with massive data. Projects as the Legacy Survey of Space and Time (LSST) from Vera C. Rubin Observatory will deliver a huge amount of data with open access, producing an estimated of 20 terabytes of data per night¹.

¹ <https://www.lsst.org/about/dm>

This thesis deals with a large data set and its characterization using a new technique. We characterize the variability of blazars, a type of active galactic nuclei with strong relativistic jets oriented very close to the line of sight of the observer (Urry & Padovani 1995). These objects have been characterized at various frequencies fitting a power-law like power spectrum density (PSD) over the periodogram of the sources (e.g. Kataoka et al. 2001; Uttley et al. 2002; Abdo et al. 2010c; Sobolewska et al. 2014; Max-Moerbeck et al. 2014b; Nilsson et al. 2018; Ryan et al. 2019; Goyal 2020; Żywucka et al. 2020; Goyal 2021). We will use sources observed during more than 12 years using data from the Owens Valley Radio Observatory (OVRO) at 15 GHz in the radio band. We propose the usage of a new method to fit the PSD, which allowed us to fit more than 1000 different sources from the OVRO catalog using more complex PSD models with reliable error estimates on the model parameters. The final method aims to be used not only in radio data but also at all the possible frequencies, specially at γ -ray, since blazars are the principal objects that emit in that band (Abdollahi et al. 2020). Observations from the Large Survey of Space and Time (LSST) on the Vera C. Rubin Observatory, or the Cherenkov Telescope Array (CTA), both of which will work at γ -ray band, will also benefit of the improved capabilities of this method which includes generality and reduced computational time.

1.2. Active Galactic Nuclei

Active galaxies are galaxies with a very bright region at its center that exceeds the luminosity produced by star formation. This region is known as the active galactic nucleus (AGN) and presents emission over a wide range of the electromagnetic spectrum. The accepted explanation about the emission of AGN is that it comes from a luminous accretion disk surrounding a central supermassive black hole, whose interaction produces an outflow of collimated plasma ejected perpendicular to the disk, known as jet (Urry & Padovani 1995). This ejected plasma in some cases reaches relativistic speeds and may extend to million of parsecs (Blandford et al. 2019).

Traditionally AGN have been separated into two main classes depending on the ratio between flux density at radio (5 GHz, F_r) and optical (B -band, F_o). We assign the term radio-loud (RL) to sources with ratio $F_r/F_o \geq 10$, while the radio-quiet (RQ) sources are below this value (Kellermann et al. 1989). There are some features that distinguish RL from RQ AGN: (i) The host galaxy of RL AGN are mostly elliptical (Zheng et al. 2020) while for RQ sources the host cover the full range of morphologies with a few of them hosted by bulge-dominated galaxies; (ii) RL AGN emissions are almost all non-thermal, while RQ AGN are dominated by thermal emission which is a contribution between the accretion disk and the host galaxy; (iii) RL AGN show a strong relativistic jet that may extend out to Mpc, on the other hand RQ AGN present only small, weak and slow outflows extended to kpc (e.g. Middelberg et al. 2004); (iv) RL AGN emit at GeV (γ -ray band) and in some cases up to TeV frequencies, while RQ AGN have a cut-off at a few hundred keV. A larger explana-

tion of these differences may be found in Section 2.3 of the review by Padovani (2016). This classification has been a subject of discussion in recent years, Padovani (2017) argue that the radio-to-optical flux ratio is valid only for broad-lined and unobscured AGN where the optical flux can be attributed directly to the accretion disk, which is not the case for recent studies of source population in deep radio fields. In Padovani (2016), the classification of RL and RQ AGN is replaced by *jetted* and *non-jetted* AGN respectively, emphasizing that the big difference resides in the presence (or lack) of a strong relativistic jet as described in (iii).

From all the discovered AGN, RQ sources are the most common (e.g. Ivezić et al. 2002; Padovani 2011; Kellermann et al. 2016) while RL AGN correspond to the rarest objects due to their relativistic jets. Besides the main classification explained above, there are different observational classes of AGN, each one showing different features. One of the most relevant attempts to unify all classes is the so-called unified model, which describe that the difference between the observational classes is mainly due the orientation of the source as seen from the point of view of the observer. This unified model starts with the argument from Readhead et al. (1978) that the orientation of the observed radio sources could explain the curvature of the jets and then evolved to more sophisticated models as the one from Urry & Padovani (1995), where an schematic model of an AGN is defined. Figure 1.1 illustrates this schema showing all the basic components of an AGN and how the line of sight changes the classification of the source. These AGN components play important roles in the emission of radiation, so a brief explanation of each component is described below. At the center lies a supermassive black hole surrounded by an accretion disk, being the black hole characterized by a mass that is in the range $\sim 10^6 - 10^{10} M_{\odot}$ and by its spin, the latter which may have influence on the accretion disk size and the launch of relativistic jets (e.g. Narayan et al. 2014). The accretion flow provided by the disk is the principal energy source in AGN, producing radiation in a wide range from UV to soft- X -rays. Above the accretion disk, a magnetic corona of hot electrons produces strong X -rays. These components are surrounded by the broad-line region, an extensive region of clouds of gas at high velocity and heated by the radiation of the accretion disk. Beyond these clouds a torus of dust and gas obscures the radiation from the central engine and emits radiation in the IR. Its geometric distribution and physical nature remains unclear, however, it is known that its obscuring material generates different AGN classes that depends on the line of sight of the observer, being Type 1 objects that show their central engine and broad line region while for Type 2 objects where the observer only gets a direct view of a farther slow moving clouds called the narrow-line region due the obscuration produced by the torus. Finally, a jet of plasma perpendicular to the accretion disk moving typically at relativistic speed dominates the emission in the γ -rays and in some cases also the radio band.

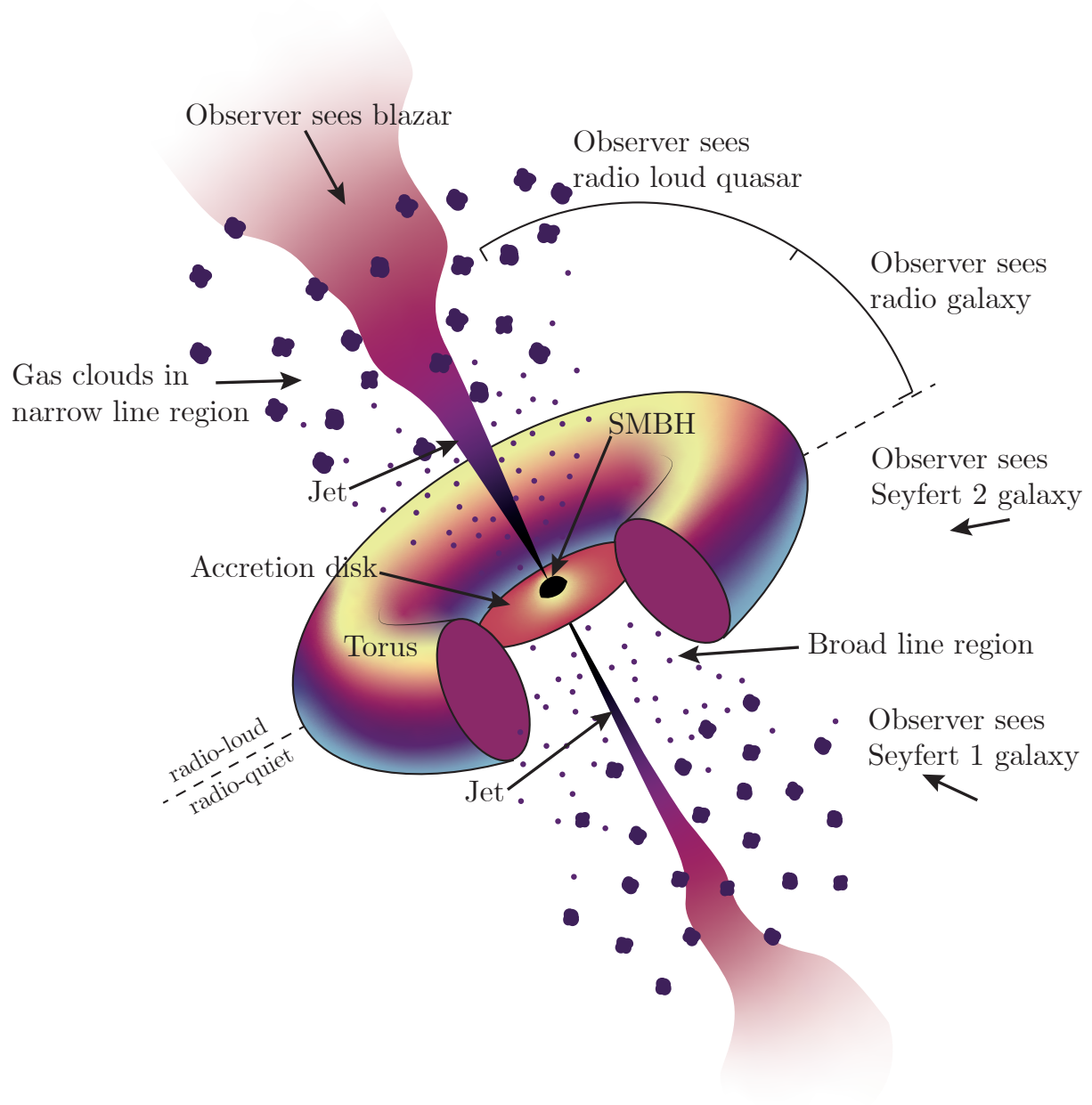


Figure 1.1: Schema of an AGN, based on Figure 1 from Urry & Padovani (1995).

Even though this unified model achieves a successful explanation of the differences over the majority of observed AGN using the orientation as the only parameter, recent studies indicate that others parameters may also have important effects. One important parameter to mention is the Eddington ratio, defined as the ratio between the observed luminosity and the Eddington luminosity $L_{\text{Edd}} = 1.3 \times 10^{46} (M/M_{\odot}) \text{ erg/s}$, which refers to the maximum luminosity that a body can achieve with an equilibrium between radiation pressure and gra-

vitational force. There is evidence that AGN with higher Eddington ratio exhibit a stronger accretion flow, producing a more luminous emission from the accretion disk in optical and UV frequencies. An extended discussion of AGN classification, together with a characterization at different electromagnetic frequencies are reviewed in Padovani et al. (2017), whose main results come from the ESO workshop “*Active Galactic Nuclei: what’s in a name?*” that occurred in 2016².

This work is interested in the class of AGN with strong relativistic jets oriented very close to the line of sight of the observer called blazars. As described before, this class emits radiation in the wide electromagnetic spectrum, from radio to very high energy γ -rays, being the most luminous type of object in the sky at γ -ray band. In the following sections we will discuss the observational characteristics of blazars and in their theoretical models. We will also discuss previous studies and methods employed to characterize the variability of blazars, and how our proposed method works.

1.3. Observational characteristics of Blazars

Blazars emit non-thermal radiation over the entire electromagnetic spectrum with strong variability from radio to γ -rays (von Montigny et al. 1995) due the interaction of energetic particles with the jet outflow. Their Spectral Energy Distribution (SED), a plot of the energy of the source with respect to frequency space, covers the whole electromagnetic spectrum reaching even the TeV range. It has a distinctive shape with two broad peaks, one from IR to X -ray and the second peak at high energy from X -ray to γ -ray. Blazars are sub-divided into different types depending on the low-energy peak also called the synchrotron peak $\nu_{\text{synch peak}}$ since it is generally attributed to synchrotron radiation. Blazar objects with $\nu_{\text{synch peak}} < 10^{14}$ Hz are called low-synchrotron-peaked (LSP), while cases with $\nu_{\text{synch peak}} > 10^{15}$ Hz are denominated high-synchrotron-peaked (HSP). Objects with its $\nu_{\text{synch peak}}$ between these two limits correspond to intermediate-synchrotron-peaked (ISP) (Abdo et al. 2010a). Figure 1.2 shows an example of the blazars PKS 1510-089 and Mrk 421, which correspond to LSP and HSP type respectively.

Another sub-division of blazar types is defined from a spectroscopic perspective, which is based on the width of the emission lines. Flat-spectrum radio quasars (FSRQ) are defined as objects with strong broad emission lines while BL Lacs, whose name is a reference to the source BL Lacertae, have weak and narrow emission lines with an equivalent width of $< 5\text{\AA}$ (Urry & Padovani 1995). Connecting these sub-classes with the $\nu_{\text{synch peak}}$ criteria, FSRQ are predominantly LSPs while BL Lacs encompass from LSP to HSP objects, with a predominance in the latter type of objects (e.g. Boettcher 2012; Padovani et al. 2017, and references therein).

² <https://www.eso.org/sci/meetings/2016/AGN2016.html>

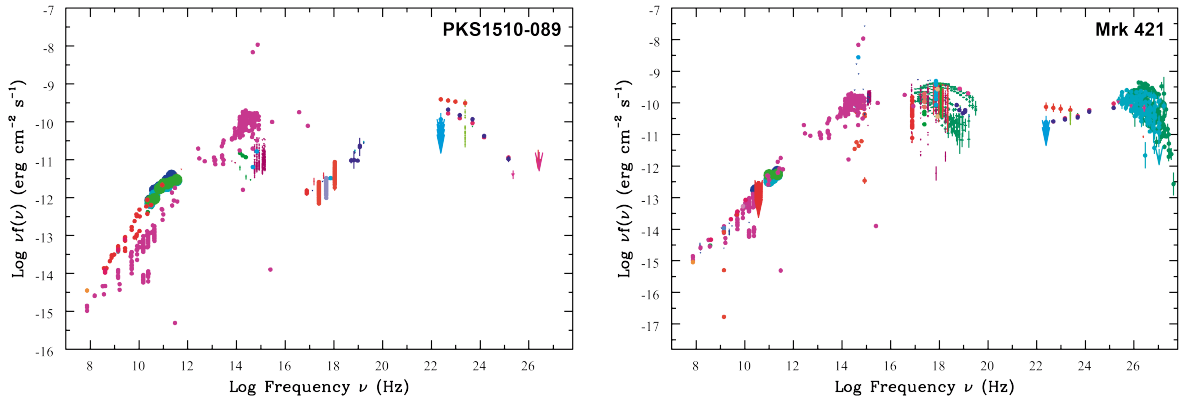


Figure 1.2: SED of PKS1510-089 and Mrk 421. Left: SED of PKS1510-089 as an example of a LSP type. Right: SED of Mrk 421 as an example of a HSP type. Both SEDs were generated using the *SED Builder tool*³ from SSDC on August 25, 2022.

The variability of blazars, as appears in all the different observed light curves for the object 3C 279 plotted in Fig. 1.3, can have timescales from minutes to days or from months to years. The unpredictable behavior of this observed variability, which is typically aperiodic, suggests its origin in a stochastic process intrinsic to the source (Liodakis et al. 2018b). Typically, there is an increment in variability amplitude together with a decrease in timescale as the blazar SED reach higher frequencies. Blazars also present flares, an outburst of higher energy and shorter duration as the usual variability, which is translated into a very-high flux variation with a defined shape. When a flare is detected in radio band, it is very likely that it will also be detected in γ -ray. These detections at different frequencies are lagged in time and finding their correlation can help us to understand the location of the γ -ray emission (e.g. Max-Moerbeck et al. 2014a), which is hard to locate due to the inability to resolve angular sizes in γ -ray of the core of blazars which have subparsec scales.

Another key aspect of blazar observational characteristics is the Doppler factor δ , which arises due to the relativistic motion of the jet outflow towards the observer. The Doppler factor is related to the jet speed and the angle between the jet and the line of sight to the observer. This relativistic beaming results in the observed radiation being amplified, which affects the observed brightness and variability timescales of blazars. A larger Doppler factor indicates a stronger boosting effect, making the source appear brighter and more variable than it would be if the jet were not moving relativistically.

Despite the fact that there is no scientific consensus about the causes of the variability at long-term timescales, the Power Spectral Density (PSD), which describes the amount of power by time in a given frequency, has proven to be useful in characterizing the variability. The PSD typically has a power-law shape $P(f) \propto 1/f^\beta$ where the frequency f has dimensions

³ <https://tools.ssdsc.asi.it/SED/>

of time^{-1} and has been fitted over multiples sources at different wavelengths (e.g. Chatterjee et al. 2008; Abdo et al. 2010c; Max-Moerbeck et al. 2014b). Other studies argue that in some cases exists a different β -value at low and high frequency, with a characteristic break frequency f_{break} (e.g., McHardy et al. 2004; Sobolewska et al. 2014; Żywucka et al. 2020). This break would represent a characteristic variability timescale and may yield information concerning the underlying driving process (e.g., Finke & Becker 2015; Ryan et al. 2019). A first approach in optical band given by Żywucka et al. (2020) suggests an emission dominated by the accretion disk at low frequencies, specially for FSRQ blazars.

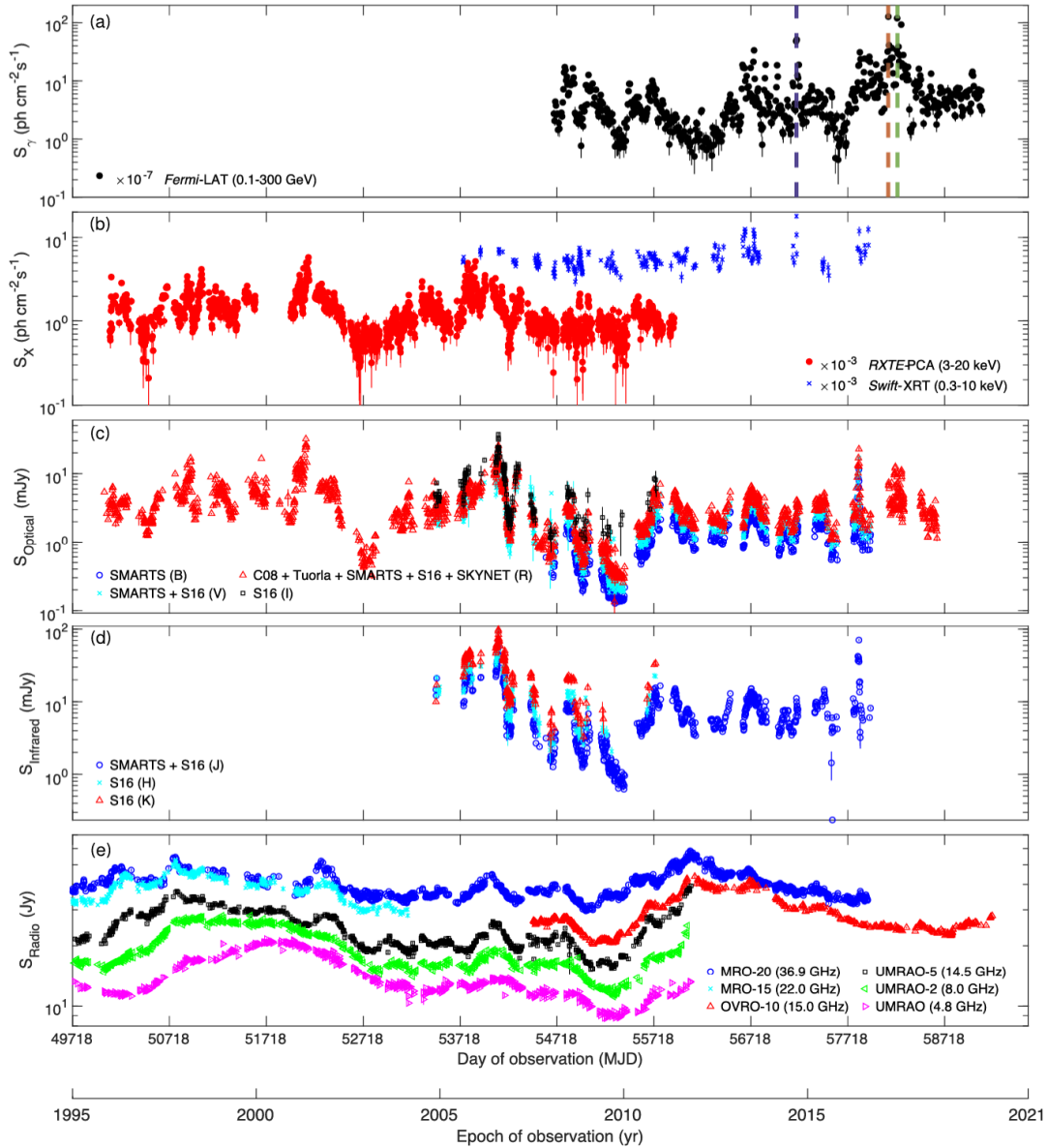


Figure 1.3: Light curves of 3C 279 at different frequencies. Panel (a) shows γ -ray photon fluxes, panel (b) X -ray photon fluxes, panel (c) optical flux densities, panel (d) infrared flux densities and panel (e) radio band flux densities. This figure is reproduced from Goyal et al. (2022), corresponding to Figure 1 from that paper.

1.4. Theoretical Models of Blazars

As described in the previous section, blazars emit over the wide electromagnetic spectrum. However, the physical processes responsible for these emissions remain unclear. The theoretical models of blazars are all based on the SED shape, where the main focus is to explain the peaks at low and high energy. There is a consensus that the low-energy peak from radio to soft X -ray has a leptonic origin produced by synchrotron radiation of relativistic electrons in the jet environment. On the other hand, the origin of the high-energy peak remains unclear.

Some authors claim that it also has a leptonic origin, where the high energy γ -ray emission could be explained by inverse-Compton scattering due to the interaction between photons and electrons (e.g. Maraschi et al. 1992; Padovani et al. 2003; Ackermann et al. 2011). Others authors propose an hadronic scenario where the high energy is produced by the energy lost through synchrotron emission of protons or by secondary particles in electromagnetic cascade initiated by photon-pair production (e.g. Mannheim & Biermann 1992; Böttcher et al. 2013; Cerruti et al. 2015). The hadronic scenario implies that high-energy blazars could also be neutrino emitters from the decay of charged pions. This is supported by IceCube Collaboration et al. (2018), where a detection of a high-energy neutrino coincide (3.5σ significance) with a flare at γ -ray of blazar TXS 0506+056. Recent studies with respect to this source also suggest a lepto-hadronic scenario, arguing that the dominance of one over the other will depend on the nature of the source (e.g. Ansoldi et al. 2018; Cerruti et al. 2019).

1.5. Previous studies on the characterization of blazars variability

Due to technological and physical limitations, scientists currently cannot fully understand and model all the components of a blazar. Thus, astronomers require other methods to study blazars variability. The current method implies comparing observational and simulated data, assuming that the latter characterizes very well the real behavior. As described before, blazars show a typical PSD with power-law like shape. This suggests that their light curves come from a stochastic process intrinsic to the source. One of the first approaches to model this behavior comes from Timmer & Koenig (1995), where light curves for AGN are generated from a random signal following a normal distribution (also called white noise) which is multiplied by a power spectrum $P(f)$ on the frequency domain. The resulting light curve corresponds to the real components of the inverse Fourier transform from the previous multiplication. Since this method is based on reproducing the Fourier Transform of the light curves, it is also called Fourier Decomposition. Another method is described in Kelly et al. (2014), where Continuous-time Auto-Regressive Moving Average (CARMA) models are used to generate light curves, which are approximated as the solution of a stochastic differential equation. CARMA assumes that the PSD is a sum of Lorentzian functions, giving the modeling of PSD some flexibility.

Although the PSD is the most common tool for light curve analysis (as examples using Fourier Decomposition we have Uttley et al. (2002) for X-ray band; Max-Moerbeck et al. (2014b) for radio band; Isobe et al. (2015) and Meyer et al. (2019) for γ -ray band; Żywucka et al. (2020) and Goyal (2021) for optical band, while for the usage of CARMA models we have as examples Kelly et al. (2014) for X-ray and optical band; Ryan et al. (2019) and Tarnopolski et al. (2020) for γ -ray band), it is not the only way to diagnose this kind of time series. Astronomers frequently use the Auto-correlation function (ACF), which gives

a measure of the correlation of the signal fluctuations as a function of time lag. The ACF and the PSD are highly related, being the PSD the frequency counterpart of the ACF into Fourier domain, i.e., the PSD correspond to the Fourier transform of the ACF (Wiener et al. 1930). Another useful tool is the Structure Function (SF), which is claimed to be better for light curves with gaps but has some known problems as discussed in Emmanoulopoulos et al. (2010). The SF is described as a function of the variance of the signal and its ACF, and has been applied multiples times to study AGN variability (e.g. Emmanoulopoulos et al. 2010; Kozłowski 2017; Yuk et al. 2022). It is important to mention that SF is better suited for studying AGN variability at short timescales, whereas the PSD is more useful for long timescales (Moreno et al. 2019). The scope of this thesis is to characterize blazar variability at long timescales, therefore, it employs the PSD as the main tool to accomplish it.

For this thesis we employ the Fourier Decomposition method since one of its objectives is to improve the actual most common PSD fitting method used, which also employs the Fourier Decomposition to simulate light curves. In this method the observed light curve is compared to multiple simulations from a PSD model $P(\boldsymbol{\theta})$ with given $\boldsymbol{\theta}$ parameters using a χ^2 -like test between the periodogram of the real light curve and the mean periodogram of all simulations. This test is then compared to the χ^2 distribution of all the sampled light curves, getting a significance level for which the current PSD model can be rejected known as p -value. This p -value is then calculated for the same PSD model but for a wide range of $\boldsymbol{\theta}$ values, being finally the best fitted model the one with the highest p -value (see Max-Moerbeck et al. 2014b for a better explanation). The search for the best parameters of the PSD model is currently done using brute force, i.e., the method tries all the given combinations before returning the best fit. This made the actual method very inefficient, taking hours to finish a fit, which is restrictive when it is required to fit hundreds and even thousands of observations.

We introduce the usage of the PMC-ABC algorithm as an improvement of the actual method, which stands for Population Monte Carlo (PMC) and Approximate Bayesian Computation (ABC), capable to retrieve the best fit in a more efficient way and providing more reliable uncertainty estimates for each parameter. The ABC approach allows the user to fit a model with no necessity of a likelihood function, which is exactly our case where no likelihood function exists for the PSD of unevenly sampled data. In the PMC-ABC algorithm one of the most important concepts is the definition of a distance function where a χ^2 -like test is applied on a similar way than the previous method. PMC-ABC has the big difference that the search is done starting from a prior for each PSD parameter and the results of each new iteration depends on the results of the previous iteration, finishing the process when a convergence criterion is reached and getting a posterior distribution for each PSD parameter which leads to more reliable uncertainties. An extensive explanation of the PMC-ABC algorithm appears on Chapter 4.

Chapter 2

Observations

2.1. OVRO dataset

The Owens Valley Radio Observatory (OVRO) has been monitoring since 2008 over 1800 sources with two flux density measurements per source per week on average, i.e., a cadence of about 3 days. Its telescope, called “40 m telescope”, is a parabolic reflector with a diameter of 40 meters and a focal ratio of $f/0.4$, it has an aperture efficiency of $\eta_A \sim 0.25$ and a receiver operating in the Ku band at 15 GHz with 3.0GHz bandwidth (Richards et al. 2011). Although the aperture efficiency has a low value, it corresponds to the optimal value in order to accomplish the monitoring program. This is explained by the necessity of an underillumination effect over the antenna when a large sample of objects is monitored, which increases the beamwidth and reduces observational errors and the exposure to thermal noise. The OVRO team has shown empirically that there is no improvement increasing the aperture efficiency since the thermal noise is already at low levels, so the actual value is acceptable to achieve the program.

The OVRO team in principle apply a source selection driven by considerations such as:

1. Given the radio variability properties of blazars and its dependency on other observables, the sample must allow a division in subsamples with enough members per subsample.
2. The main goal is to cross-correlate radio light curves with *Fermi* (Abdo et al. 2010b) γ -ray light curves. Thus, gamma-ray loud blazars should be chosen. On the other hand, some of these blazars have apparently similar properties that non γ -ray blazars. Therefore, and in order to answer this inconsistency, a comparable number of non γ -ray blazars should be also included.

The program started using the 1158 sources of the Candidate Gamma-Ray Blazar Survey (CGRaBS; Healey et al. 2008) with declination -20° which satisfies all the previously described considerations. Other sources were added to the program over time, mainly the one associated to *Fermi* detections and others objects that were studied in F-GAMMA (Fuhrmann et al. 2016) or VERITAS (Weekes et al. 2002) programs and were not in the CGRaBS catalog, some microquasars, cataclysmic variables and also a few bright radio galaxies whose

jets exhibit unusual properties. There are some extra sources that are not classified as blazars but were used to provide calibration for the telescope.

Koay et al. (2019) have studied the variability of the 1158 CGRaBS sources using data of the OVRO program up till 2018. Although the effect of interstellar scintillation (ISS) is usually irrelevant at 15 GHz, they show that actually ISS has an important role in the intra and interday variability of the sources, especially those located at sightlines with high electron column densities. When Richards et al. (2011) was published, approximately 1500 sources were being monitored. At the moment of this study, this number increases to 1859 different objects.

As a way to ensure good results on our characterization of the OVRO data via fitting the PSD, we employ a data cleaning process to all observations in order to remove outlier data points that could cause an anomalous shape in their periodograms. Finally, an object selection mainly based on discarding light curves with very high noise level, with less than 6 years of observation and with less than 20 observed points per year is also applied, in order to dismiss poorly sampled light curves that are not worth to fit.

2.2. Data cleaning and data selection

The acquisition of astronomical data is subject to multiple problems such as observational errors and interruptions due the weather and even from the telescope itself due a malfunction of one of its parts. These kinds of problems appear in the context of light curves as an increase in the uncertainty of the flux for a given observation or as an atypical point in the light curve with an extremely large (or low) flux with respect to the average, which does not resemble a flare, since flares in the radio-band typically have a duration of weeks. In the worst scenario the source cannot be observed on a interval of time, producing gaps in the final light curve. In some cases the observed flux has a very low Signal-to-Noise ratio (SNR), which means that the observation is not significant. All of these problems are present in the OVRO dataset as well as other astronomical datasets, so a cleaning process is required in order to use the light curves for our purpose of characterizing them using the PSD, mainly because these anomalous points would modify enormously the shape of the periodogram. Here are listed the four cleaning processes applied to all observations, the reader can check this process applied to object J1706+0953 in Figure 2.1, noting that in this case the point 2. was not necessary.

1. **High flux error:** The malfunction of a part of the telescope or a poor weather increase the error of observation. Since the uncertainty of these points may be very high, we remove them using a simple filter that removes the 1% of the points with higher flux errors of each observation.
2. **Many points per day:** Some sources have more than one observation in the same day.

As explained in Koay et al. (2019), the variability of blazars in radio-band have an order of days, so it does not make sense to use many data points per day. Thus, we remove the multiple points per day and keep only the value nearest to the median in time for each day.

3. **Low SNR:** The ratio between the flux density and its error SNR for each observed point give us an idea of how significant the point is. We consider that a threshold of $\text{SNR} = 1$ is enough to clean not significant points from the light curves, thus, we remove all the points with a SNR below this threshold.
4. **Outliers:** Some observations show points with flux densities that differ by a large amount with respect to the source average flux density. These points correspond to outliers and are removed using a cubic spline which reproduce the light curve shape. It is important to notice that a fixed cubic spline will work differently depending on the variability of the source, therefore, we apply different cubic splines with a dependence on the kurtosis of the flux distribution in order to adjust it in the best possible way (See Appendix A.1). This process is not perfect, so to avoid removing non problematic points we remove only the 1% of the total points with larger spline distance only if they have a distance that is deviated more than three (or four, depending on kurtosis) standard deviations with respect to the mean distance.

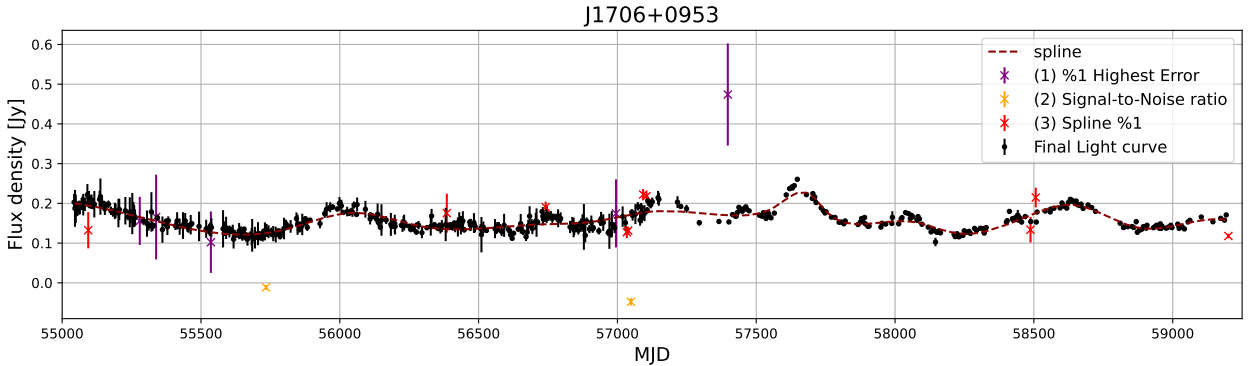


Figure 2.1: Light curve of J1706+0953 before and after the cleaning process. (1) Purple color represents the 1% of points with the highest observational error, which corresponds to a total of 5 points. (2) Orange color represents points with a Signal-to-Noise ratio lower than 1, corresponding to 2 points. (3) Red color represents points deviated more than three standard deviation with respect to the mean distance, which corresponds to a total of 10 points. The segmented line is the spline applied to data, while black points represents the resulting light curve after the cleaning process. Hence, for this object we passed from 493 to 476 points.

After the data cleaning process, an object selection is applied to all 1859 observed objects. This selection correspond to a filtering of the data according to three observational parameters mentioned below.

1. **Ratio between the mean flux density and its mean squared error:** Some objects show more signal than others. Comparing the mean flux level with the mean squared flux error, defined as the average squared difference between each flux error value and the mean flux error level, give us a metric to understand how much of the variance in the light curve is intrinsic to the source and not associated with observational errors. Light curves with a low ratio are dominated by the observational error so the PSD does not contain information about the intrinsic source variability. Therefore, we remove these objects setting a limit to this flux-to-error ratio at 4, meaning that any light curve with a ratio higher than 4 is well defined. From all observations, there are 1319 observations that satisfy this criterion. Figure 2.2 shows an example of light curves with a very low and high ratio, which correspond to objects C1047+7238 and J2358-1020 respectively.
2. **Total years of observations:** Since we are looking for variability at long-term timescales, we are not interested in light curves that have been observed in a short period of time. So a minimum of 6 years of observations is required. From the 1319 resultant observations from the previous point, 19 of them are removed using this criterion, thereby reducing the number of selected observations to 1300. Some of these 19 objects were added to the program more recently, while others were removed for having low flux densities or being problematic to observe (e.g. too close to the galactic plane).
3. **Mean number of observed points per year:** In order to characterize the objects we consider that a minimum number of points per year is required. In the perfect case each observation should have 2 points per week, which correspond to a total of 108 points per year. From the 1300 objects of the previous criterion, most of them have between 20 to 70 points per year on average, while only 6 observations are below this range. Hence, we keep only the objects with more than 20 points per year, reducing the number of observations to 1294.

We determine that this set of 1294 objects shows a well defined variability and thus we were able to characterize them¹. We also remove 4 objects from the final set which correspond to microquasars since their behavior is different to blazars in the sense that they show high variability in a short period of time and their properties are different with respect to quasars. Hence, from the 1294 we remove objects CygX-3 (CygnusX-3), SS433, GRS 1915+105 and LS I +61 303 (Figure B.1 shows their light curves), keeping finally 1290 objects from OVRO dataset. Figure 2.3 shows the histogram of some important statistics of these observations such as the number of points, the total observed time in years and the mean cadence. We display a summary of these statistics in Table 2.1 in order to get a better idea of how these objects are defined.

¹ Note that the cleaning and selection processes are applied uniformly to all sources for this work, anyway, studies of individual sources can relax the constraints of the selection process and/or apply better cleaning methods if desired.

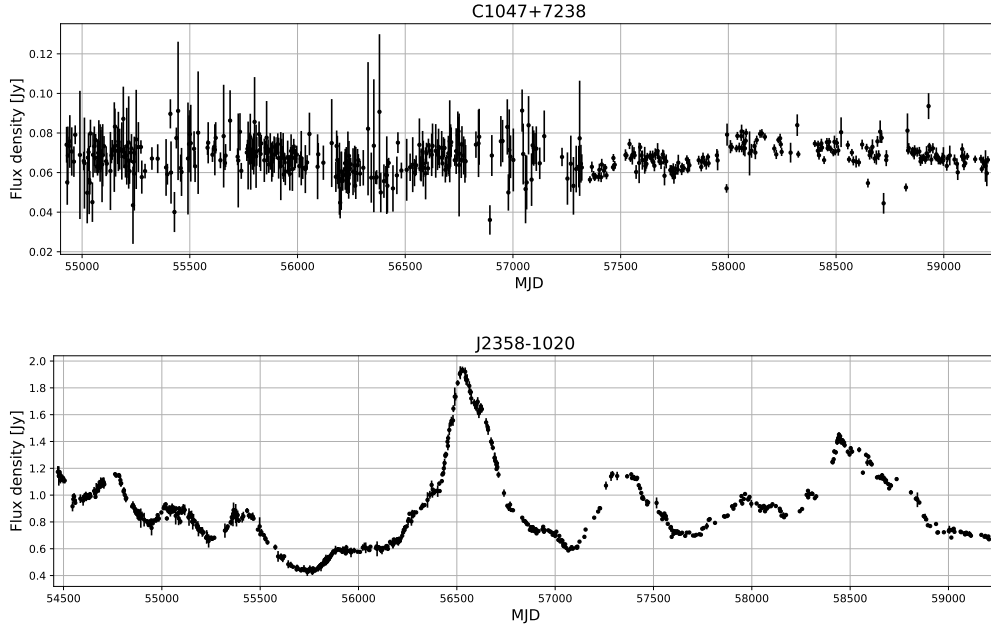


Figure 2.2: Light curves of two objects after the cleaning process. C1047+7238 shows very low variability and flux density (top), having a ratio between the mean flux and its mean squared error of about 1. On the other hand, J2358-1020 shows high variability and flux density (bottom), having a ratio of about 245. By imposing the criteria of a variability ratio greater than 4 all light curves similar to C1047+7238 are not selected.

Table 2.1: Summary of some statistics of the 1290 selected observations from OVRO dataset after applying the data cleaning process.

Variable	Mean	St dev.	Min	Median	Max
N points	535.43	112.71	231.00	532.00	1658.00
Observed time [years]	12.07	1.27	7.37	12.91	13.00
Points per year	44.25	7.75	25.53	43.51	144.77
Median Δt [days]	5.00	0.85	1.01	4.99	7.91
Mean Δt [days]	8.48	1.35	2.52	8.40	14.36
Std. Δt [days]	11.03	2.03	4.42	10.77	20.14
1st largest Gap [days]	108.16	33.57	71.75	99.72	516.48
2nd largest Gap [days]	86.03	13.58	48.87	83.81	170.61
3rd largest Gap [days]	76.08	11.90	38.91	75.49	154.52

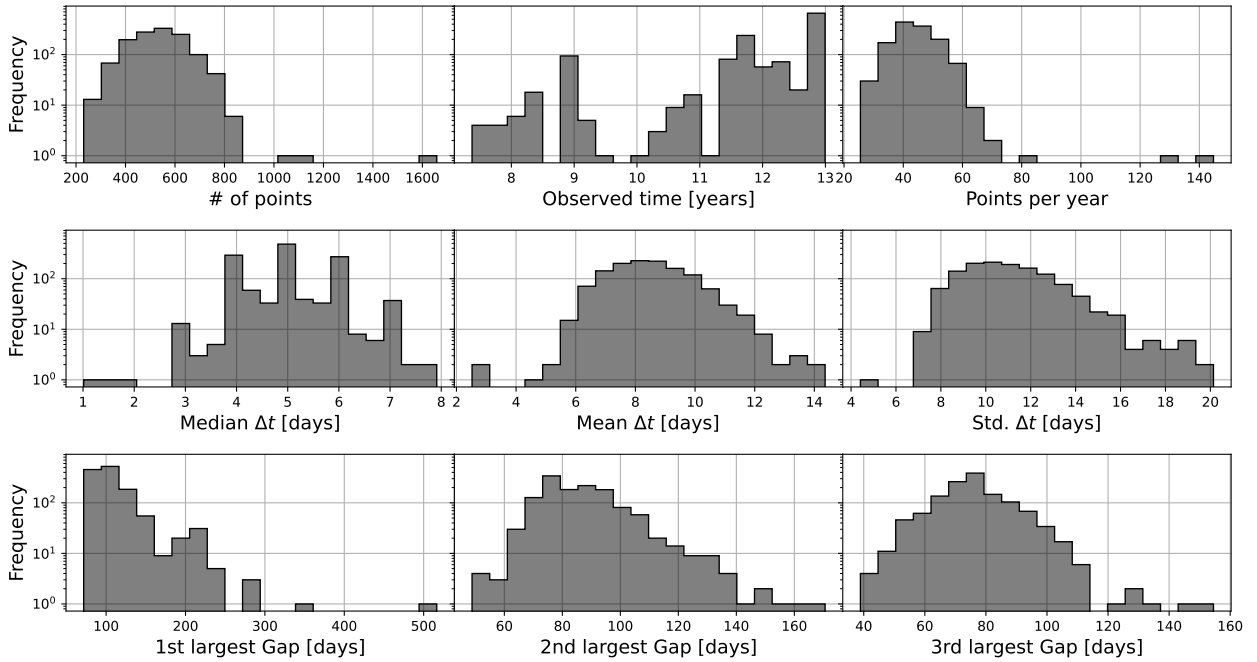


Figure 2.3: Histogram of some statistics of the 1290 selected observations from OVRO dataset after applying the data cleaning process.

As can be seen the mean cadence of all observations differs from the 3 days expected as was described by OVRO team, having on average 8.48 days per observed flux with a standard deviation of 1.35. On the other hand, all observations show gaps having the two largest ones an average of about 108 and 86 days respectively. This means that there are almost three months of no data over all observations and that this happens two times over all the observation time. We take into consideration this discrepancy on the data along with the presence of gaps on our method for fitting the PSD as is discussed in the next chapter.

Chapter 3

Modeling variability of blazars

The observation of an astronomical object at a certain time gives us its brightness. If the object is observed many times in a period of time we obtain its flux per time in that period. These observations, usually called light curves, represent the brightness variability of the observed object. The light curve is one of the principal sources in astronomy, being very useful to study the behavior of the object. As a classical example we have the cepheids, a class of variable stars that shows periodicity in its light curve, which is explained by a radial pulsation in its outer layers. Another example is the detection of exoplanets via transit photometry method, where the light curve of a star that remains mostly constant in brightness shows a drop in a period of time shorter than the length of the light curve. This drop in brightness is originated by an object that passes in front of the telescope and could indicate that an exoplanet is orbiting that star.

In the case of a light curve from an AGN, it does not show any particular behavior at first sight with the exception of flares. Thus, astronomers have to study light curves from AGNs using different tools. One of these tools is the use of signal processing theory: from a mathematical point of view a light curve corresponds to a time series, hence, it can be studied as a signal in the time domain. The study of AGNs using signal processing techniques allow us to identify and characterize the variability, which eventually allow us to generate light curve simulations.

The following chapter explains the mathematics from signal processing theory in Section 3.1, which mainly comes from books “*The Fourier transform and its applications*” (Bracewell 1986) and “*The fast Fourier transform and its applications*” (Brigham 1988). The process of how we use signal processing to model the variability of blazars and simulate light curves is explained in Section 3.2.

3.1. Signal Processing

A signal corresponds to data that carries information about a system or phenomenon (Priemer 1991). The study of signals, or signal processing theory, is one of the richest fields from electrical engineering, with applications on communications, medicine, computation, astronomy and many other areas. This field consists mainly of transforming information from signals into another form of signals as output, allowing to filter, decompose or map to a different space depending on the transformation method used. From a mathematical approach, a signal is a function that depends on variables such as space or time. In time-domain signals we can talk about time-continuous signals if we are in front of a signal that is well defined in all the time domain, or time-discrete signals if it is only defined at discrete instants of time. Given the limitations of the electrical systems to measure signals from sources in a continuous way, and since the light curves are time-domain signals, we always will be referring to them as time-discrete signals.

In order to model and characterize blazars, a series of signal processing concepts are used. Each one of them is explained in the next subsections.

3.1.1. Fourier Transform

The Fourier transform of a time-domain signal X is defined as

$$\text{if } X \in \text{time-continuous domain: } \mathcal{F}[X(t)] = \tilde{X}(f) = \int_{-\infty}^{\infty} X(t)e^{-i(2\pi f)t} dt \quad (3.1)$$

$$\text{if } X \in \text{time-discrete domain: } \mathcal{F}[X[n]] = \tilde{X}[f] = \sum_{n=-\infty}^{\infty} X[n]e^{-i(2\pi f)n} \quad (3.2)$$

where $e^{i\theta} = \cos \theta + i \sin \theta$ is Euler's formula. The Fourier transform corresponds to the decomposition of the signal in a frequency-domain, i.e., returns the spectrum of frequencies that characterize a signal.

Note that the discrete Fourier transform is defined in all the time-domain, which is not realistic as light curve observations have always a finite number of points measured. Hence, the discrete Fourier transform for a finite signal of length $|X| = N$ like a light curve is defined as

$$\mathcal{F}[X[n]] = \hat{X}[f] = \sum_{n=1}^N X[n]e^{-i\frac{2\pi f}{N}n} = \sum_{n=1}^N X[n] \left(\cos \left[\frac{2\pi f}{N}n \right] - i \sin \left[\frac{2\pi f}{N}n \right] \right) \quad (3.3)$$

3.1.2. Convolution

Given two functions f and g , the convolution, expressed as $(f * g)$, corresponds to a function that expresses the superposition between f and the inverted and shifted version

of g . Visually it refers to how the shape of one function is modified by the other one. The convolution between f and g is defined as

$$(f * g)(t) = \int_{-\infty}^{\infty} f(\tau)g(t - \tau)d\tau \quad (3.4)$$

The convolution has properties of commutativity, associativity and distributivity. Another important property from convolution algebra is the convolution theorem, which states that a convolution in the time-domain is equal to a multiplication in the frequency-domain $\mathcal{F}[f * g] = \mathcal{F}[f]\mathcal{F}[g]$, or vice versa, that the multiplication in time-domain is equal to a convolution in the frequency-domain $\mathcal{F}[fg] = \mathcal{F}[f] * \mathcal{F}[g]$.

We can employ the convolution function to represent the time-discrete Fourier transform from the continuous form convolved with a Dirac comb at Δt , i.e., a Dirac function defined each Δt times. In this way we are saying that the time-discrete Fourier transform $\hat{X}[f]$ has a period of Δt .

3.1.3. Window functions

Window functions are used to take a subset of a signal, sometimes also to taper it. This process is called windowing and is one of the most important processes where signals need to be studied. A window function is defined as zero in almost all the domain, except in a certain interval where the function can have values lower or equal than 1. To windowing a time-domain signal $X(t)$ the signal must be multiplied by the window function $W(t)$. These window functions are used to control some properties of the Fourier Transform like its spectral resolution or to control contamination from nearby frequencies.

The choice of a particular window depends on the nature of the situation. There are plenty of window functions, two of them are the Rectangular and Hanning window, being the latter used in this study. For a finite time interval $[0, T]$, they are defined as

$$\text{Rectangular window: } W_R(t) = \begin{cases} 1 & \text{if } 0 \leq t \leq T \\ 0 & \text{otherwise} \end{cases} \quad (3.5)$$

$$\text{Hanning window: } W_H(t) = \begin{cases} \cos\left(\pi\frac{(t-T/2)}{T}\right)^2 & \text{if } 0 \leq t \leq T \\ 0 & \text{otherwise} \end{cases} \quad (3.6)$$

3.1.4. Power Spectral Density

Mathematically, the PSD describes the amount of power present in the signal as a function of frequency. Given the stochastic behavior of blazar light curves, we can assume that we are in front of a stochastic process, which refers to a randomly defined signal. For a stochastic process $X(t)$ with autocorrelation function $R_{XX}(\tau) = E[X(t)\overline{X(t + \tau)}]$, the Wiener-Khinchin

theorem (Wiener et al. 1930) says that the PSD of the process correspond to the Fourier transform of the autocorrelation function, i.e.,

$$P(f) = \mathcal{F}[R_{XX}(\tau)] = \int_{-\infty}^{\infty} R_{XX}(\tau) e^{-i(2\pi f)\tau} d\tau \quad (3.7)$$

Or, if we are in a discrete time space with $X[n]$ and autocorrelation function $R_{XX}[k]$, then the PSD is

$$P(f) = \sum_{k=-\infty}^{\infty} R_{XX}[k] e^{-i(2\pi f)k} \quad (3.8)$$

Retrieving the PSD from blazar light curve observations is the fundamental work of this thesis. It shows us how the power of the observations varies at different frequencies defined as 1/days. There are plenty models of PSD to fit with the observations, all of them based on a power-law like shape $\text{PSD} \sim f^{-\beta}$, that is, it decays exponentially with the frequency.

Note that the PSD is defined in all the time-domain, so, getting the power spectrum of a light curve is certainly impossible. We can have an estimation of the PSD using a discrete and finite signal of length $|X| = N$, this is also called a periodogram, and as N approaches infinity and the Δt sample scale of the light to zero then it converges to the true PSD.

3.1.5. Periodogram

As said before, the periodogram is an estimation of the PSD for a discrete and finite signal of length $|X| = N$. Mathematically, it is defined as the squared modulus of the Fourier transform

$$\text{Per}(f) = C |\mathcal{F}[X]|^2 = C \left(\left[\sum_{n=1}^N X[n] \cos\left(\frac{2\pi f}{N} n\right) \right]^2 + \left[\sum_{n=1}^N X[n] \sin\left(\frac{2\pi f}{N} n\right) \right]^2 \right) \quad (3.9)$$

where the multiplicative factor C is used to normalize in a convenient way depending on the task (generally to match the power of the PSD). If the elements $X[i]$ and $X[i + 1]$ are separated by Δt in time for all $i = 0, \dots, N - 1$, then we have

$$P(f) = \lim_{\substack{N \rightarrow \infty \\ \Delta t \rightarrow 0}} \text{Per}(f) \quad (3.10)$$

3.1.6. Aliasing

We say that a signal has aliasing if two or more frequency components are indistinguishable. This is a problem that all the discrete and finite signals have due to some frequencies that overlap each other when the Fourier transform is obtained. By definition the calculation of the Fourier transform requires an infinite signal, but what the method sees for a discrete signal is the periodic repetition of its spectrum. This creates distortions in the final spectrum we-

re high-frequency components are mistaken as low-frequency components, producing aliasing.

Since we are talking about discrete and also finite signals, the final spectrum described by the periodogram, is the convolution between the Fourier transform, a Dirac comb and a window function in the frequency space.

$$\text{Per}(f) = C|W(f) * \text{III}_{\frac{1}{\Delta t}}(f) * \tilde{X}(f)|^2 \quad (3.11)$$

This convolution, in particular when the window function applied corresponds to a Rectangular one, raises an issue called spectral leakage generated by the Fourier transform of the window function, in which side lobes can increase the power of certain frequencies depending on the signal. Max-Moerbeck et al. (2014b) describes this effect and how the usage of a Hanning window reduces this problem.

3.1.7. Nyquist frequency

The Nyquist frequency corresponds to the highest frequency such that a signal can be represented in a discrete way with no aliasing. For a signal with sampling rate Δt , the Nyquist frequency correspond to half of the sampling frequency $f_{\text{Nyq}} = \frac{1}{2} \frac{1}{\Delta t}$.

3.2. Simulation of light curves

In our case with astronomical sources, we can assume that we are in front of stochastic processes due the random behavior of the light curves. Therefore, the main task is to find and define a method able to generate stochastic processes $X(t)$ with the same observed variability seen by OVRO and with a PSD that follows a given model $P(f)$.

The currently used methods are based on white noise, which refers to a random signal such that its values at different times has no statistic correlation, typically following a normal distribution with mean of zero and variance σ^2 . The most common algorithm to accomplish the simulation of light curves is based on the Fourier Decomposition (Timmer & Koenig 1995), where the phase and amplitude of the Fourier transform of the data are randomized and then multiplied with a power-law shape to obtain the light curve $X(t)$. There are also different methods as the Continuous-time Auto-Regressive Moving Average (CARMA) by Kelly et al. (2014), where the light curve $X(t)$ is approximated as the solution of a stochastic differential equation. In next section we will do a comprehensive study of the Fourier Decomposition method since the results of this thesis are based on that method.

3.2.1. Fourier Decomposition

The Fourier Decomposition method refers to the usage of signal processing tools in order to generate light curves and estimate its PSD. The main tool used in this work is the Fourier transform applied in time-domain signals, which allow us to decompose the signal in a frequency-domain and then estimate its PSD using the Periodogram.

Our method to generate light curve with a power-law like shape as PSD employs the algorithm from Timmer & Koenig (1995), which uses the fact that the Fourier transform of a white noise process normally distributed $X(t) \sim \mathcal{N}(0, \sigma^2)$ corresponds to a complex gaussian random variable as described by the spectral estimation's theory (Priestley 1989) (see Appendix A.2), and the Fast Fourier Transform (FFT) algorithm (Cooley & Tukey 1965) that allow us to rapidly compute the Discrete Fourier Transform. The Fourier Decomposition algorithm has been already used in Uttley et al. (2002) for the study of Seyfert galaxies PSD and has been improved in Max-Moerbeck et al. (2014b). The current method is a variation of this last article. For an even number of samples N , a time sampling period t_{Samp} in days and a power spectrum density $P(f)$, the model does:

1. Generate the real and complex components of the Fourier transform with $\frac{N}{2}$ samples for positive frequencies from a normal distribution $\mathcal{N}(0, 1)$.
2. Following the conventions of the frequency order of FFT and inverse FFT, construct the negative values of the Fourier transform concatenating the conjugated of the positives frequencies at reverse order to the previous samples.
3. Construct the frequencies as $f_i = i/(Nt_{\text{Samp}})$ for $i \in [1, N/2]$. The frequencies of samples from $N/2 + 1$ to N are the same but at reverse order.
4. At this point we obtain white noise from $\mathcal{N}(0, 1)$. Multiply the Fourier components by $\sqrt{\frac{1}{2}P(f)}$.
5. Get the flux as the real part of the inverse Fourier transform of the previous result using the inverse FFT algorithm. Get the time as $t_i = i t_{\text{Samp}}$ for $i \in [0, N - 1]$.

We run the algorithm for N even only given that the FFT algorithm benefits from this due the symmetry of this case, resulting in a faster application than for the uneven case. Since the shape of the PSD is given by $P(f)$, this method allows us to simulate different power-law models. In particular, we use two models:

1. Simple Power-law model with amplitude A and index β , and noise level P_{noise} :

$$P(f) = A f^{-\beta} + P_{\text{noise}} \quad (3.12)$$

2. Broken power-law model with amplitude A , break frequency f_{br} , low index β_l , high index

β_h for frequencies before and after break frequency respectively, and noise level P_{noise} :

$$P(f) = \begin{cases} A f_{\text{br}}^{\beta_l - \beta_h} f^{-\beta_l} + P_{\text{noise}} & \text{if } f < f_{\text{br}} \\ A f^{-\beta_h} + P_{\text{noise}} & \text{if } f \geq f_{\text{br}} \end{cases} \quad (3.13)$$

where for both models the amplitude A is defined as the power at frequency of one day. Note that the noise levels are independent of frequency, thus, in order to add it to the light curve we first simulate an independent white noise scaled on its Fourier components by the constant $\sqrt{\frac{1}{2}P_{\text{noise}}}$ which is added to the Fourier components of the simulated PSD $P(f)$ before getting the fluxes in point 4. Figure 3.1 shows a light curve simulated using each one of the two models previously mentioned with common parameters $A = 1$, $P_{\text{noise}} = 100$, $\beta = \beta_h = 2$, and parameters $\beta_l = 0$, $f_{\text{br}} = 180^{-1}$ [1/days] for the broken power-law case. The similarity on the structure of both light curves is because we generated them using the same random state.

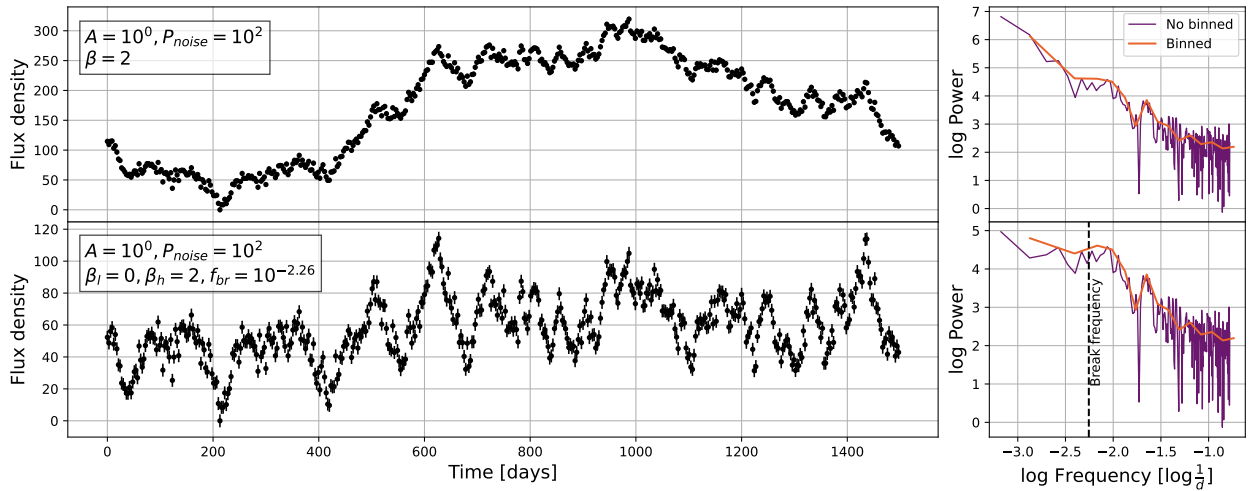


Figure 3.1: Light curves generated using both power-law models described in the thesis, a simple one and one with a characteristic break frequency. At the right of each light curve its periodogram is displayed. Top: Light curve from the simple power-law model with parameters $A = 1$, $P_{\text{noise}} = 100$ and $\beta = 2$. Bottom: Light curve from the broken power-law model with parameters $A = 1$, $P_{\text{noise}} = 100$, $\beta_l = 0$, $\beta_h = 2$ and $f_{\text{br}} = 180^{-1}$ [1/days]. Note that both light curves show a similar structure, this is because both are generated from the same random state.

As previously mentioned, the periodogram is a useful tool to estimate the PSD of a signal and thus its calculation is fundamental to the characterization of the variability of blazars. For a light curve with flux density s_i at time t_i and N even points such that $i = 1, \dots, N$, the periodogram is given by the following expression (Max-Moerbeck et al. 2014b)

$$\text{Per}(f_k) = \frac{2T}{N^2} \left(\left[\sum_{i=1}^N s_i \cos(2\pi f_k t_i) \right]^2 + \left[\sum_{i=1}^N s_i \sin(2\pi f_k t_i) \right]^2 \right) \quad (3.14)$$

where $f_k = k/T$ for $k = 1, \dots, N/2$ and $T = N(t_N - t_1)/(N - 1)$. The maximum frequency corresponds to the Nyquist frequency $f_{\text{Nyq}} = N/2T$. In our case the multiplicative factor $C = 2T/N^2$ is defined such that the integral of the periodogram from f_i to f_j is equal to the variance contributed to the light curve in this frequency range following Parseval's Theorem. Note that this normalization affects the simulated light curves for a PSD model in the sense that its periodogram will differ by a $2T/N^2$ factor in power from the PSD. Therefore, this factor must be considered in the point 4. of the method to simulate light curves.

One important contribution by Max-Moerbeck et al. (2014b) is the usage of a Hanning window instead of a Rectangular window. Their article shows that a Hanning window has lower side lobes and therefore, reduces the spectral leakage, known in this context also as red-noise leakage. The effect of this red-noise leakage increases as parameter β increases when studying the simple power-law model and authors coincide that a Hanning window is good enough for $\beta \leq 4$. Figure 3.2 shows a test of the Hanning window over both power-law models for a series of simulations. To make the plot we take an average of 1000 periodograms for each set of model parameters, all of them coming from a simulated light curve with an evenly space sampling time of 3 days and a total of 1500 points. For the case of the simple power-law model all parameters but β were fixed. It shows how for $\beta = 5$ the periodogram starts to differ from the expected behavior, especially at low frequencies. For $\beta = 6$ and larger values the Hanning windows does not work for the simple model. However, for the broken power-law model where all parameters are also fixed with the exception of β_h , the Hanning windows works for all the tested β_h values. This suggests that when fitting a power-law with a break model the value of β_h is not limited by the bound of the simple model case. Finding a power-law index greater than 5 or 6 would be very rare since there is no literature reporting those values. An extended analysis of the Hanning window for the power-law break model will give an idea of the limits of this window function, but it is out of the scope of this thesis.

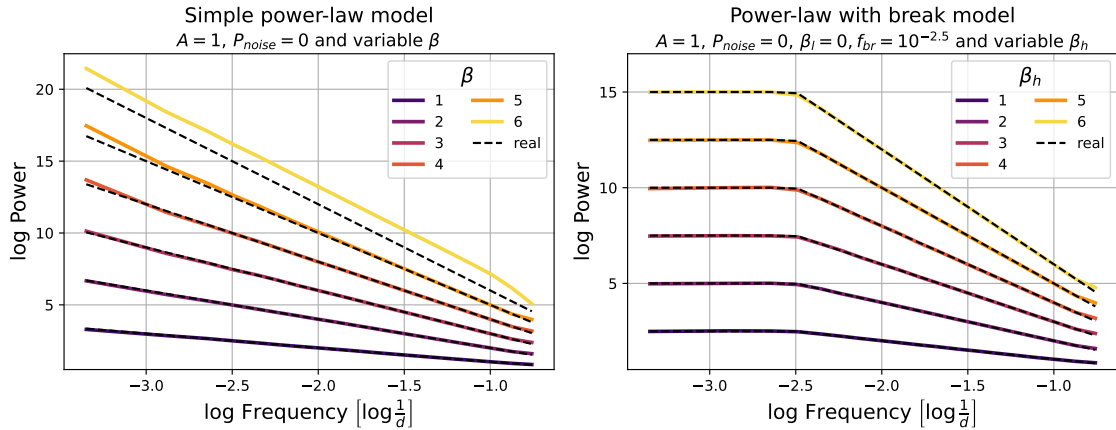


Figure 3.2: Effect of the Hanning window in both power-law models. Left: Simple power-law model without noise, $A = 1$ and a variable β . Right: Broken power-law model without noise, $A = 1$, $\beta_l = 0$, $\log f_{br} = -2.5$ and a variable β_h . The curves correspond to an average of 1000 periodograms for an evenly space sampling time of 3 days and a total of 1500 points. The segmented black line correspond to the expected behavior.

3.3. Comparing observed and simulated light curves

There are three important considerations before comparing observations and simulations when using the Fourier Decomposition method.

- Due to technical capabilities and interruptions in the observation due the weather and the different positions of the different objects observed in a year, observations are typically unevenly sampled. As described in Max-Moerbeck et al. (2014b) this produces a negative effect in the window function were the response of it does not decay when the frequency increases, and thus, the red-noise leakage effect is increased.
- We can obtain a large number of periodograms from a simulation and then average them to obtain a periodogram with low variance. This is not the case for observations, were we have a unique periodogram with high distortion in its components.
- What is the fastest variability of blazars in radio frequency?, i.e., the fastest timescale of the OVRO dataset?. This is necessary to simulate light curves in the best possible way.

The first problem can be solved using interpolation to obtain a constant cadence of observations in the same way described in Max-Moerbeck et al. (2014b). For a total number of points N and a mean time sampling $\langle \Delta t \rangle$, it creates a grid of N evenly spaced points and then assigns values according to the original points that reside between each points of the grid. One question that could remains is what happens with the gaps in the data, Isobe et al. (2015) shows that the interpolation of data gaps induces an over/underestimation of the periodogram's power at the frequency of the average gap size. It is important to note

that our method incorporates this effect also into the simulation, thus, there is no need to intervene gaps.

The second problem is solved by binning the periodogram in logarithmic bins as explained in Papadakis & Lawrence (1993). Data binning refers to aggregate the data in intervals called bins, where typically the central value of each interval is the representative value of each bin. The aggregation function will depend on the purposes of the user, for example, histograms uses the sum of all the values for each bin. Papadakis & Lawrence (1993) compares the binning of the periodogram with average as aggregation function and uses linear and logarithmic bins. It shows that logarithmic bins are better than linear when working with red-noise, since it requires a lower number of data points binned to approximate a normal distribution per observation. This makes the binned periodogram a better estimator of the PSD due that the points have a lower variance and the variance itself will reduce if more data points are collected, in contrast to the full periodogram where the points distribute as χ_2^2 and therefore the variance remains constant even though more data points are collected (See Appendix A.2). Note that the binning of the periodogram reduces its variance with the cost of losing spectral resolution. While this is not very important for the simple power law model, the loss of spectral resolution is negative if we are looking for a break frequency as the broken power-law model requires. Anyway, in these cases where we want to fit PSD models over periodograms, decreasing the variance is more important than the spectral resolution.

Finally, about the third consideration, we must select an appropriate value for the sampling period, t_{Samp} , to accurately simulate blazar light curves. Our approach involves using time data from observations to extract points from a simulated light curve with a fixed t_{Samp} value, which must match the minimum timescale in blazar variability for radio-band. The value chosen for t_{Samp} affects the periodogram due to data point extraction and interpolation applied to the light curve. While selecting a value close to the mean cadence of the light curve can reduce this effect, it does not fully capture the true timescale of blazar variability. Koay et al. (2019) studied the variability of OVRO blazars dataset and found that only $\sim 2\%$ exhibit flux variability on a timescale of 4 days or less. The OVRO monitoring program (Richards et al. 2011) has an expected cadence of 3 days per observation. Based on these factors, we choose a characteristic timescale of $t_{\text{Samp}} = 3$ days for the radio-band. This implies that we expect blazar variability to occur no more rapidly than on a 3-day timescale. Note that this parameter may need to be adjusted for observations at other frequencies, such as γ -rays, which could exhibit a lower variability timescale.

3.4. Summary

The modeling process of a blazar in radio-band along with the required process for the periodogram comparison can be then summarized as follow:

1. For a given PSD, generate a light curve with a time sampling period of 3 days and a total number of samples large enough to cover almost three times the time size of the real light curve as minimum.
2. Get a sub-sampling from the simulated light curve such that it has the exact time sampling of the real light curve. To do this, for each point of the real light curve select the closest simulated sample flux in time.
3. Interpolate the light curve to make it evenly sampled. In our case we use a linear interpolation where each point is separated by the mean time sampling $\langle \Delta t \rangle$. Note that this part could be resolved using a better interpolation. Anyway, this falls outside the scope of this thesis.
4. Remove the mean from the fluxes and move the timescale to its own system such that the first point represents the time $t = 0$. Then apply the Hanning window function to the flux.
5. Get the Fourier Transform using the FFT method. The non-normalized periodogram will correspond to the square of the Fourier Transform. Normalize the periodogram multiplying it by the factor $2T/N^2$.
6. Apply a binning process over the logarithm of the periodogram in order to reduce the variance.

Note that points 3. to 6. are applied to both simulated and real light curve. After this process the resulting binned periodograms can be compared using the preferred method by the user. As described in the Introduction, we employ the PMC-ABC algorithm to generate light curves simulated with different model parameters and compare them with the real one. An extensive explanation of this algorithm and how it is applied to resolve the fitting problem is described in the next Chapter.

Chapter 4

The PMC-ABC algorithm

This chapter introduces the concept behind Bayesian inference and how to summarize the results obtained after fitting a model. It explains how both PMC and ABC algorithms work separately and how to combine them to use them as an efficient algorithm to run Bayesian inference without using a likelihood function. In particular, we refer to the PMC-ABC algorithm's implementation of Ishida et al. (2015) and the considerations required to run the algorithm in the OVRO data such as the prior probability of each model parameter and the distance function to compare real and simulated data.

Getting the parameters which model a process is a common problem in the scientific area, whatever the topic is. From a statistic point of view, the problem can be tackled using a frequentist approach, where each parameter has a fixed value and some statistical tests can be applied to check the goodness of the fit, or using Bayesian inference, where each parameter has a probability distribution and credible intervals can be used to represent the uncertainty about the parameter. The second approach is better than the first one in the sense that it declares that the parameters can have multiples values, some with more important than others. An advantage of using Bayesian inference is the usage of previous information for each parameter, called *priors*, in order to fit the model. For example, if it is necessary to update a model with new observations, the previous result can be used as a *prior* in order to update the results with the new data.

When a object or phenomenon has been well studied it is common to use Bayesian inference in order to fit a model, obtaining with that the best set of parameters which characterize the observed data. This method is based on the Bayes' Theorem (See Appendix A.3), which describes the probability that an event A occurs given that another event B is true. Mathematically:

$$P(A|B) = \frac{P(B|A)P(A)}{P(B)} \quad (4.1)$$

where $P(A|B)$ is called *posterior*, $P(B|A)$ is interpreted as the *likelihood* and $P(A)$, $P(B)$

are known as *priors*. From a modeling point of view, Bayes' Theorem can be understood as the probability that a model, the event A , fits the observed data given the data, event B . The likelihood function, which describes how well the model fits the observed data, is a must to apply the Bayesian inference method, otherwise it is impossible to get a posterior. If the likelihood is unknown it is impossible to make inferences of the parameters. Another problem that comes with the usage of Bayesian inference is the time that it takes to compute the probability distribution of the parameters, which is larger than getting a fixed value using the frequentist approach. These limitations have led scientists to create algorithms capable of reproducing results in a similar way as the Bayesian inference method but with no necessity of a likelihood function and thus improving the computation time and allowing a larger set of problems to be studied with these methods. With this in mind, algorithms as *Approximate Bayesian Computation* (ABC) along with *Population Monte Carlo* (PMC) are used as an effective tool in replacement to Bayesian inference. In the next sections both algorithms will be explained, including how they can be used as the adequate tool to fit the PSD of blazars.

4.1. Credible Intervals

As was mentioned before, the results from Bayesian inference correspond to posterior distributions. The values of these distributions need to be represented in a simple way in order to summarize the results of the fit. In this sense, scientists represent the best fit of each parameter along with a credible interval to represent the uncertainty. There are three different ways to summarize a posterior distribution.

1. Using the mean and standard deviation.
2. Using the median and given quantiles.
3. Using the mode and the highest density interval (HDI) at certain level.

These three ways of reporting results are equal for a posterior with a normal-like shape, but differ for posteriors with a skewed distribution. For cases like this it is not appropriate to use the mean and standard deviation. As the posterior has a greater skewness, the median is not useful anymore since it is not reporting the most representative value of the posterior. Given the above, we prefer to use the mode and the HDI to report our results. Thus, if a parameter θ has an HDI at level $x\%$ we can affirm that θ is contained in the range $[\theta_{x\%}^{\text{low}}, \theta_{x\%}^{\text{up}}]$ and then has a dispersion $\theta_{x\%}^{\text{up}} - \theta_{x\%}^{\text{low}}$ at level $x\%$. We represent this dispersion as $\sigma(\theta)_{x\%}$, although we are abusing notation since σ is typically used to represent the standard deviation. As a comparison of the HDI with the others two ways to measure the uncertainty, an HDI at level 68.3% represent the same values as the 1 standard deviation from a normal distribution or quantiles 0.159 and 0.841.

4.2. Approximate Bayesian Computation

The ABC algorithm has its beginnings in Rubin (1984), where a mechanism to find approximations to the posterior distribution is described. This article illustrates only the basic of ABC rejection scheme, and it was not until Tavaré et al. (1997) when the scheme was proposed as an algorithm for posterior inference and then applied in the area of genetics. Beaumont et al. (2002) establishes the term *Approximate Bayesian Computation*, where the ABC methodology is extended weighting the estimated parameters according to its rejection scheme. Since then, the algorithm has been employed in different areas, such as epidemiology, social science and astronomy. As some examples, Schafer & Freeman (2012) used it in a cosmology context as an potential estimator of luminosity functions, while in Robin et al. (2014) is applied to characterize the thick disk of the Milky Way using simulations in contrast with photometric data from SDSS and 2MASS surveys.

For a given observed data \mathcal{D} and model that uses parameters $\boldsymbol{\theta} = \{\theta_1, \theta_2, \dots, \theta_n\}$ to simulate data \mathcal{D}_S , the ABC algorithm can be summarized as follow:

1. Given a prior distribution p_j for each j-th parameter, draw a large number of parameters $\boldsymbol{\theta}^i$. Then simulate data \mathcal{D}_S^i for each one of the draws.
2. Calculate the distance between the simulated and observed data $\rho^i = \rho(\mathcal{D}_S^i, \mathcal{D})$, where $\rho(\cdot, \cdot)$ must be a function that is zero if the simulated and observed data are exactly equal and increase its value as the discrepancy between both increases.
3. Keep only the parameters with $\rho^i < \epsilon$, where ϵ corresponds to a threshold given by the user. If the user requires a larger set of parameters, then return to point 1 and get new draws until obtaining a final set, which will be an approximation of the posterior distribution. This point correspond to the ABC rejection scheme.

It is important to indicate that the choice of the distance function ρ is the most important step of the ABC algorithm in order to get a good estimator of the posterior distribution. Despite having a good model for the observations, a poor-defined distance function will increase the bias of the final result.

4.3. Population Monte Carlo

The PMC algorithm has no clear origin. The algorithm has been attributed to von Neumann on his development of an algorithm to calculate elements of an inverse Matrix or to Metropolis and Ulam in their publication of the first paper about the Monte Carlo method (Iba 2001, and references therein). The main concept of the PMC algorithm is the *importance sampling*, which consists on correcting each posterior iteration by re-weighting the values.

In Markov Chain Monte Carlo (MCMC) methods, as the iterations evolve in time t , each component $x_i^{(t+1)}$ of a vector $\mathbf{x}^{(t)}$ needs to be accepted or rejected to reach convergence. This method has high computational costs, which increases as the dimension of \mathbf{x} increases. The PMC algorithm is introduced on this part by re-calculating the importance weight of each component and drawing the elements with greater weight as the next vector $\mathbf{x}^{(t+1)}$. The method is unbiased at any iteration, meaning that the iteration can be stopped at any time (Cappé et al. 2004). This property allows the user to define its own convergence criterion being this the central property used in the PMC-ABC algorithm, which will be explained in the next section.

Let π be the target distribution of the problem, i.e., we expect that \mathbf{x} distributes as $\sim \pi$. Suppose we have a generating distribution $\hat{\pi}_t$ such that it allow us to generate all the i -components of \mathbf{x} at time t . Defining $t = 1 \dots T$ and $i = 1 \dots M$, the PMC algorithm may be summarized as follows:

1. Generate the $x_i^{(t)}$ elements using $\hat{\pi}_t$
2. Compute the weights $W_i^{(t)}$ using the target and generating distribution :
 $W_i^{(t)} = \pi(x_i^{(t)}) / \hat{\pi}_t(x_i^{(t)})$. Normalize weights such that $W_i^{(t)}$ sum up to 1.
3. Resample the vector $\mathbf{x}^{(t)}$ using the M values with greater weight between the previous values and those generated from the point 1. Go to time $t = t + 1$, if $t \neq T$ then return to point 1, otherwise finish the iteration.

Here, the iteration is stopped according to the definition of parameter T . In the PMC-ABC approach there is no fixed parameter T but a convergence criterion which increase t by 1 and depends on the M values drawn from the generating distribution $\hat{\pi}_t$. We will clarify this in the next section.

4.4. PMC-ABC: The CosmoABC package

The PMC-ABC algorithm corresponds to the union between the previous mentioned algorithms and it allows the user to fit a model with parameters $\boldsymbol{\theta} = \{\theta_1, \theta_2, \dots, \theta_n\}$ in a Bayesian way without a defined likelihood function. The main idea is to use the importance sampling concept from the PMC algorithm to generate set of particles systems S_i containing interim results which are improved iteratively through the ABC algorithm until a convergence criteria is reached. The implementation of the PMC-ABC algorithm used in this thesis is packed in the `Python` package `CosmoABC` written by Ishida et al. (2015), who use it to infer cosmological parameters without a likelihood function over measurements of galaxy cluster number counts. The package has been published as open source¹ and it can be easily

¹ <https://github.com/COINtoolbox/CosmoABC/>

adapted² for solving other kinds of problems.

The algorithm requires some previous user defined parameters and functions in order to run. The more important are the number of draws for the first iteration M_{ini} , the number of particles M in each system S , the distance function $\rho(\cdot, \cdot)$ which compare the simulated data \mathcal{D}_S with the observed data \mathcal{D} , the prior distribution $p_i(\cdot)$ of each model parameter θ_i , the distance threshold given by a percentile ϵ and the convergence criterion Δ necessary to stop the iterations. Figure 4.1 shows a flow chart of the PMC-ABC algorithm used by CosmoABC, a detailed explanation of the algorithm is described in Ishida et al. (2015). We can separate it in three principal steps:

1. **Initialization:** The algorithm starts generating M_{ini} draws of $\boldsymbol{\theta}$ using the priors $p(\boldsymbol{\theta})$, which are then used to generate simulated data \mathcal{D}_S . Then, it calculates the distance of the simulation with respect to the observed data $\rho(\mathcal{D}_S, \mathcal{D})$ for each draw, keeping the $M < M_{\text{ini}}$ draws with the smallest distances and save it as the particle system S_0 with uniform weights $\frac{1}{M}$.
2. **PMC importance sampling:** The algorithm verifies if the convergence criterion Δ , defined as the fraction between the total number of draws K needed to generate the system S_t and M , is reached. For the first particle system this correspond to M_{ini} , while for the next ones depends on the distance values and tends to increase as the distance between \mathcal{D}_S and \mathcal{D} is reduced. If the converge criterion is not reached then a particle system S_{t+1} is created using the ABC approach. The resulting particle system of that approach is re-weighted using

$$W_t^j = \frac{p(\boldsymbol{\theta}_t^j)}{\sum_{i=1}^M W_{t-1}^i \mathcal{N}(\boldsymbol{\theta}_t^j; \boldsymbol{\theta}_{t-1}^i, C_{t-1})} \quad (4.2)$$

Where j refers to the j -ith particle of the S_t system and $\mathcal{N}(\boldsymbol{\theta}_t^j; \boldsymbol{\theta}_{t-1}^i, C_{t-1})$ to a Gaussian PDF with mean $\boldsymbol{\theta}_{t-1}^i$ and covariance matrix C_{t-1} built from S_{t-1} calculated at $\boldsymbol{\theta}^i$. These weights are normalized such that $\sum W_t = 1$ and then passed to the ABC iteration if the convergence criterion is not reached with the actual K value.

3. **ABC iteration:** A new particle system S_t is generated using the previous results. First of all it set the parameter K equal to 0. The algorithm draws a first set of model parameters $\boldsymbol{\theta}_0$ from S_{t-1} and uses it as the mean of a normal distribution with deviation equal to the covariance matrix of the previous system to draw the actual possible model parameters $\boldsymbol{\theta} \sim \mathcal{N}(\boldsymbol{\theta}, C_{t-1})$ and generate simulated data \mathcal{D}_S . These model parameters are added to the system S_t if and only if the distance $\rho(\mathcal{D}_S, \mathcal{D})$ is lower than the ϵ -percentile of distances from the previous system S_{t-1} . If not, the algorithm try to get a new set of parameters $\boldsymbol{\theta}$ in the same way as before. Each try adds 1 to K and the

² The well-known package PyMC for Bayesian Inference in Python also implemented this algorithm at the moment that this thesis was being written.

ABC iteration finishes when the new system contains M particles, then it returns to the PMC importance sampling, to re-weight the new particles and check the convergence criterion using the K value resulting from filling the particle system S_t .

Thereby, CosmoABC replicates and combines both PMC and ABC algorithms and applies an iterative process to obtain the best fit of the input model. As in the ABC algorithm, the user defined distance function $\rho(\cdot, \cdot)$ plays an important role in order to get a precise fit. Since it is necessary to compare the simulated data with the real one, it must be a very well-defined function with no bias among the data and along model parameter's values. It is highly recommended to test and check the properties of the distance function before running the algorithm. Other important user defined elements are the prior distributions $p_i(\theta)$ of each model parameter θ_i . Here, priors works in the same way as in Bayesian inference, where an inconsistent definition can results in a misleading posterior distribution. As in Bayesian inference, the kind of prior also disturbs the shape of the posterior distributions, which can lead to overfitted results. There are three level of Bayesian priors that refers to how important is the evidence: uninformative, weakly-informative and informative priors. An uninformative prior corresponds to a prior that expresses very general information about the parameter θ , frequently defined by an uniform distribution over a wide range of values. When the user has evidence that θ is typically around a certain value, the prior $p(\theta)$ may be defined as a normal distribution with mean in that value and a standard deviation that depends on how confident the user is. If the user is not very confident about the evidence then a reasonable standard deviation can be defined to constrain the value in an acceptable range, which corresponds to a weakly-informative prior. On the other hand, if the user is very confident about the evidence then a small standard deviation can be defined resulting on a posterior distribution largely determined by this prior, which corresponds to an informative prior.

As explained before, CosmoABC requires the definition of some parameters such as the convergence criterion Δ and the number of particles M in each system S . A good definition of these algorithm parameters is fundamental to obtain accurate results in a short computational time. A poor definition results in an insufficient or inefficient fit. As examples, a very low Δ value with an uninformative prior would not allow the algorithm to achieve a good result, while if we set a very high Δ value we could get a good fit at the expense of a larger computation time, but it can be possible that the evolution of the last S_t particle systems were not substantial and thus a lower value would be better in order to stop the algorithm in a lower t .

The next section describes the distance function and prior distributions used in this thesis in order to fit the two mentioned PSD models over the periodogram of the 1290 selected observations from the OVRO dataset described in Section 2.1. Concerning the algorithm parameters selection, Chapter 5 about testing CosmoABC has a detailed explanation of how they are selected.

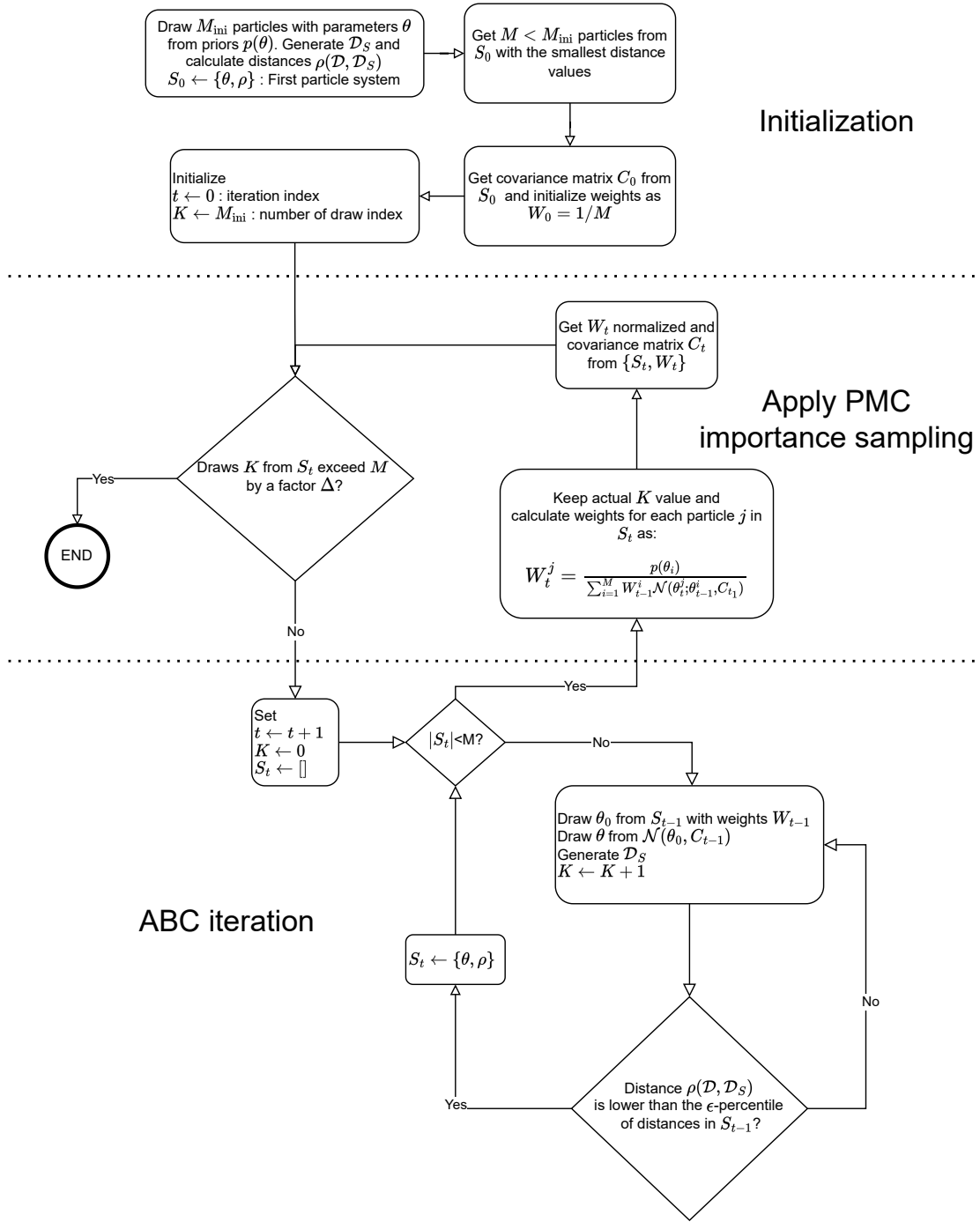


Figure 4.1: Diagram of the PMC-ABC algorithm used by CosmoABC. A detailed explanation of the algorithm is described in Ishida et al. (2015).

4.5. Fitting PSD models

In Subsection 3.2.1 we mentioned the two PSD models that will be fitted to the data: the simple power-law model with parameters $\{A, P_{\text{noise}}, \beta\}$ and the broken power-law model

with parameters $\{A, P_{\text{noise}}, \beta_l, \beta_h, f_{\text{br}}\}$. This means that 3 prior distributions must be defined for the simple model while for the broken power-law model it is necessary to define 5 prior distributions. About the comparison of the simulated data generated by each family of particle systems inside the PMC-ABC algorithm and the observed data, both models require to use the periodogram, so a distance function capable of discriminate each point of it and generate an accounting result is fundamental. Since we are working over power-law like data, it is preferable to work on a logarithmic scale, which also makes sense with the fact that the comparison of light curves is performed using the log-binned periodogram of each one. Hence, we require to define prior distribution for the log-parameters $\log A$, $\log P_{\text{noise}}$, and $\log f_{\text{br}}$. Note also that this transformation allows us to work all the model parameters in the same scale, which is essential for the good behavior of the PMC-ABC algorithm due to the usage of the covariance matrix³.

It is important to note that the model with the break frequency corresponds exactly to an extended version of the simple one. If the observed periodogram does not have a characteristic break frequency then the break model will produce an over-fitted results where β_l will be equal to β_h and thus it could be reduced to the simple model which has only one power-law index β . This means that all periodograms with a shape of a simple power-law can also be fitted using this model, which will typically return a non-defined break frequency, i.e., a posterior distribution with a very high dispersion. Due to this, and since we initially do not know when an object can be characterized using the broken power-law model, we run both models over all the 1290 observations. After fitting the models a model selection method is required and mandatory to check which one is better fitted over the data, we clarify the method applied for the observations in Chapter 6.

4.5.1. Prior distributions

We run the CosmoABC's algorithm using uninformative priors for all parameters included in both models with the exception of the noise level P_{noise} , which uses as evidence a very informative prior instead of an uninformative one. The reason to employ an informative prior for the noise level is because its value is commonly known, being typically subtracted from the periodogram before fitting (e.g. Isobe et al. 2015; Goyal et al. 2022). Since the noise level corresponds to an observational error it does not depend on the object itself, therefore, we can consider it as an independent component of the light curve. An observational error σ_e produces a white noise with power P_{noise} , and, according to Parseval's theorem the integral of the periodogram over all frequencies corresponds to the variance of the time series (See Appendix A.4), i.e.,

³ If the magnitude of model parameters differs by many orders then we are in front of a ill-conditioned covariance matrix, which is as bad as having a singularity. It is always recommended to rescale the parameters of a multivariate normal before using it.

$$\begin{aligned}\sigma_e^2 &= \int_{f_{\text{ini}}}^{f_{\text{fin}}} P(f)df = P_{\text{noise}} \frac{1}{T} \left(\frac{N}{2} - 1 \right) \\ \Rightarrow P_{\text{noise}} &= \sigma_e^2 T \left(\frac{N}{2} - 1 \right)^{-1}\end{aligned}\tag{4.3}$$

This means that $\sigma_e^2 T (N/2 - 1)^{-1}$ should be equal to the noise level. In the context of light curves, σ_e can be interpreted as the average flux density error of all the observed points. It is important to notice that the defined observational error is the result of a probabilistic estimation, thus it can deviate from the real one (see Richards et al. 2011 Section 5.4 for a detailed explanation of the uncertainty estimation in the OVRO dataset). On the other hand, each point has an independent observational error σ_{e_i} , meaning that a possible variation with respect to the average σ_e must be kept in mind. Initially, we consider a quite simple solution to define the noise level prior for a light curve with N points and it is as follows:

1. Obtain 2000 samples of N points where the i -th element is a draw from a normal distribution $\mathcal{N}(0, \sigma_{e_i}^2)$, i.e., with a standard deviation equal to the i -th error
2. Determine the variance of each of the N samples
3. Multiply the result by $T (N/2 - 1)^{-1}$

Figure 4.2 shows the result of this sampling method applied to the object PKS 1510-089. As can be seen in the logarithmic scale, the final distribution of the estimated noise level has a normal shape and it is centered very closely to the mean of $\langle \sigma_e \rangle^2 T (N/2 - 1)^{-1}$. This gives us a very informative prior for P_{noise} . We ran the CosmoABC's algorithm using a normal distribution with the mean and standard deviation of this distribution at a first stage, however, for some objects the fits were not good enough at high frequencies. This effect coincides with the fact that σ_{e_i} values are estimated using a probabilistic method, hence, their values can be deviated from the real one. In order to fix that we relax the standard deviation of the prior using a fixed value at 0.3. In this manner we cover a ± 1 magnitude of deviation with respect to the mean noise level, which is good enough to consider these discrepancies due to the flux density error estimation.

The prior for $\log A$ comes from the possible values depending on β . Since we are trying to fit a power-law model, A will be related to β . In particular, for the simple power-law model $P(f) = Af^{-\beta}$ we can determinate its value as $A = P(f)f^\beta$. If we consider the logarithmic binned periodogram we have $\log A \approx \log P(f_b) + \beta \log f_b$ for all binned frequency f_b . Calculating this value for $\beta \in [0, 5]$ for all observations and over all their binned frequencies give us a range of possible values between -20 and 5 . Figure 4.3 shows the range of possible $\log A$ values for different β values and the full histogram of values for all the 1290 selected observations of the OVRO dataset. Having said that, we consider that a uniform prior $U(-20, 5)$ is perfect for parameter $\log A$. Note that we could have used a different specified range for

each observation based on its own periodogram values, but for the purpose of this thesis we simplify the problem covering all possible values at once.

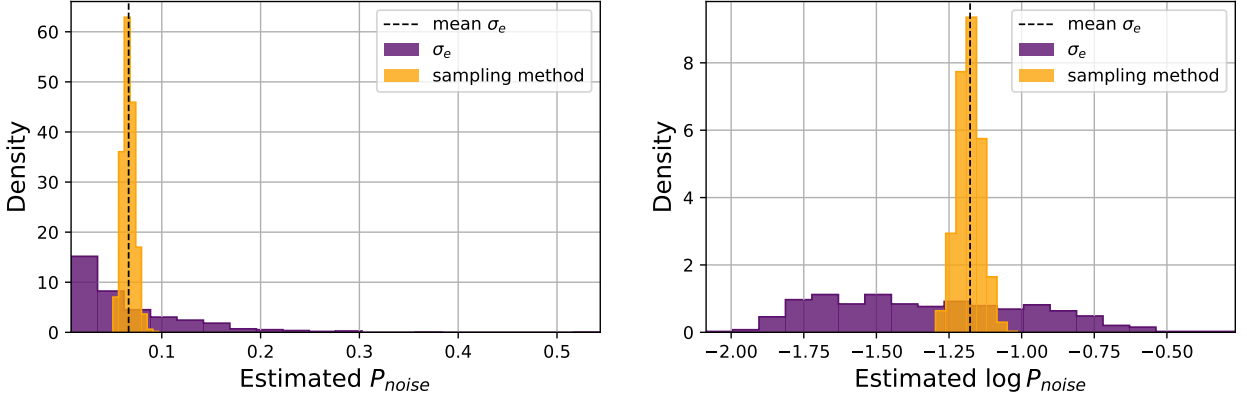


Figure 4.2: Histograms about the estimation of the noise level P_{noise} using errors σ_e from the observation of PKS 1510-089 in linear scale (left) and log scale (right). The direct result from eq. 4.3 for each observational error σ_{e_i} is plotted in purple while in yellow the result from our method described in Section 4.5.1. The result from the sampling method in log scale has a shape of a normal distribution $\mathcal{N}(-1.181, 0.04^2)$, while the log noise level estimated from $\langle \sigma_e \rangle$ gives a noise level at -1.177 .

With respect to priors for the power-law indices β , β_l and β_h , these values have a common uninformative prior that covers all the range of possible values that we expect to obtain defined by a uniform distribution. Initially, the prior should contain all the values where the Hanning window is still good enough, i.e., from 0 to 4. However, we also have to consider that the results can get out of these bounds since they are distributions covering a certain range of values, specially the lower limit for the broken power-law model where β_l will be defined with respect to the most dispersed part of the periodogram. In particular, and as we expect that β_l should have values around 0, we reduce the lower limit to -1.5 . On the other hand, because the Hanning window does not alter the shape of the periodogram for the broken power-law case for $\beta_h = 5$ and only alters the low frequency power of the simple power-law case as was explained in 3.2.1, we decided to include this value in the prior but inspecting the results of the simple case with $\beta > 4$ in detail. Hence, the upper limit is extended to 5.5, having finally an uninformative prior $U(-1.5, 5)$ for all the power-law indices.

Finally, for the broken power-law model the prior for $\log f_{\text{br}}$ corresponds to a uniform distribution defined between all the range of logarithmic binned frequencies. Hence, if $f_{b,i}$ refers to the i -th binned frequency, then the prior is defined as $U(f_{b,\text{min}}, f_{b,\text{max}})$ being $f_{b,\text{min}}$ and $f_{b,\text{max}}$ the minimum and maximum log binned frequency of the light curve respectively.

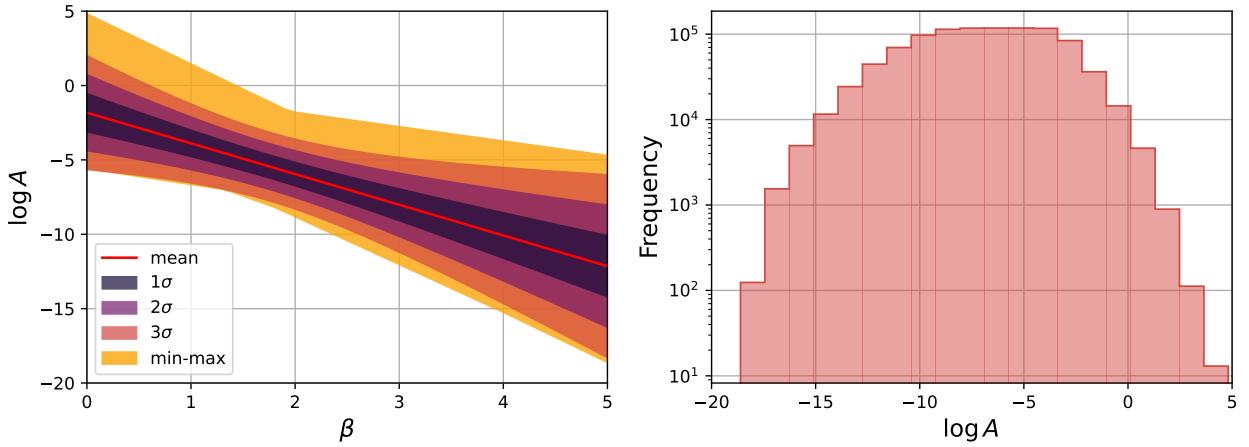


Figure 4.3: Possible values for $\log A$ if we consider that the periodogram of all selected observations fits a simple power-law model $P(f) = Af^{-\beta}$ with possible β values between 0 and 5. Left: Range of $\log A$ values obtained for different β s, the red line correspond to the mean, while the other colors represent the deviations from 1 to 3 standard deviations along with the min-max values. Right: Histogram of all the $\log A$ values.

4.5.2. Distance function

The distance function is the most important part of the ABC algorithm. It is the replacement for the likelihood function and must be able to compare simulated and real data in the best possible way. A good distance function will tell us that two observations have practically zero distance if they are identical or have the same origin, and will have higher values as they differ. As an example, Ishida et al. (2015) explains the usage of a proper distance function for a very simple model of fitting the model parameters of a normal distribution, where the mean and standard deviation of the simulated and real data are compared.

For the case of fitting and comparing periodograms, we employ a similar χ^2 -like test as the one used in previous studies where Fourier Decomposition is applied. The big difference is that we use a weighted version which depends on the number of binned points per bin $N_{\text{bin},i}$. Hence, if P_{sim} and P_{exp} are the binned periodograms of the simulated and real light curve, we define our distance function as

$$\chi^2 = \sum_{i=0}^M W_i^{\text{bin}} (P_{\text{sim},i} - P_{\text{exp},i})^2, \quad \text{with } W_i^{\text{bin}} = \frac{\sqrt{N_{\text{bin},i}}}{\sum_{i=0}^M \sqrt{N_{\text{bin},i}}} \quad (4.4)$$

where W_i^{bin} is the normalized weight of each bin and M the total number of bins of the binned periodogram. The idea is to penalize the bins with less data points averaged, which coincide with the higher values of the periodogram, i.e., with the power at lower frequency. This way the distance function is not biased by the extreme parts of the periodogram which is problematic when comparing power-law like shapes with very different slopes.

Figure 4.4 shows the behavior of our distance function when the expected observations correspond to simulated data generated using the simple power-law model with parameters $\beta = 2$, $\log A = 5$ and no noise levels. Since the periodogram has high variance in all of its points, two different experiments for the same parameters will give different distance values, hence, we average a total of 100 distances for each combination of parameters. Note that the distance between the expected and simulated periodogram does not go to zero as we approach the exact parameters, however, it has a global minimum and thus it is still valid for the ABC algorithm. The figure also shows some correlation between these model parameters, i.e., there is a sort of degeneracy between β and $\log A$. Figure 4.5 shows the behavior of both parameters β and $\log A$ separately. It is clear that when parameters $\log A = 5$ and $\beta = 2$ are chosen then the global minimum is achieved.

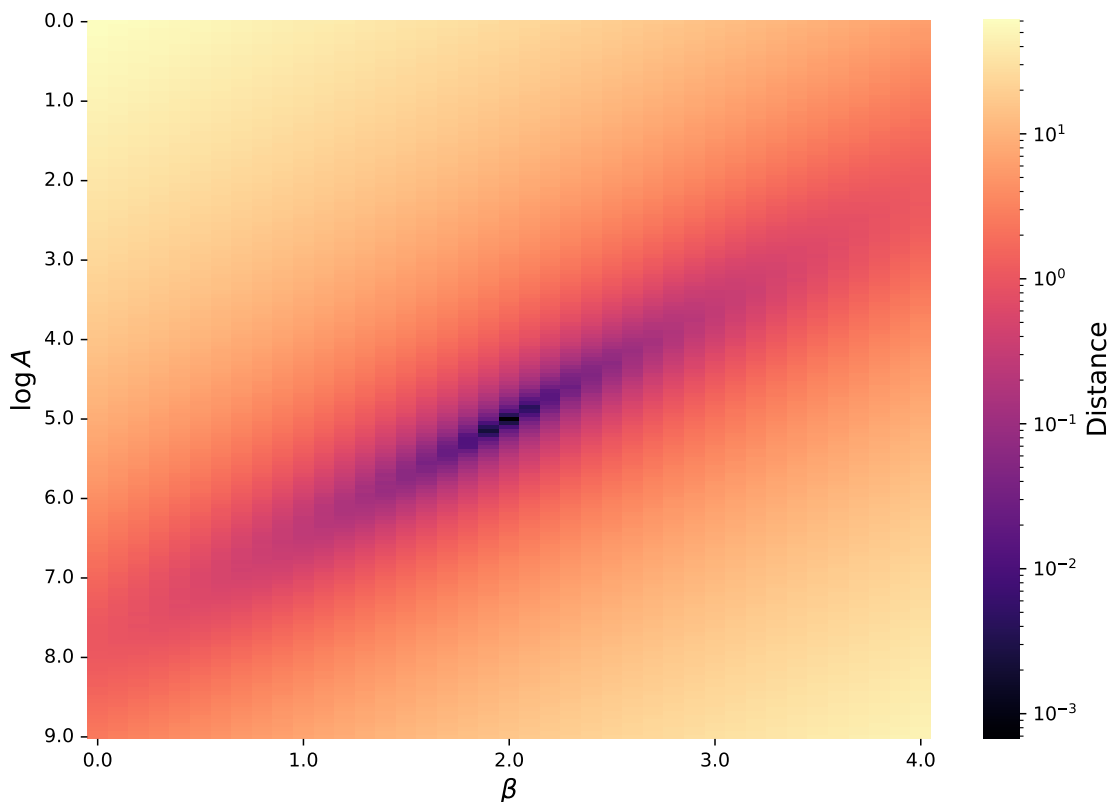


Figure 4.4: Distance function χ^2 for a simulated light curve with parameters $\beta = 2$ and $\log A = 5$ without noise using different combinations of parameters. Note that as β and $\log A$ approach the real value the distance decreases.

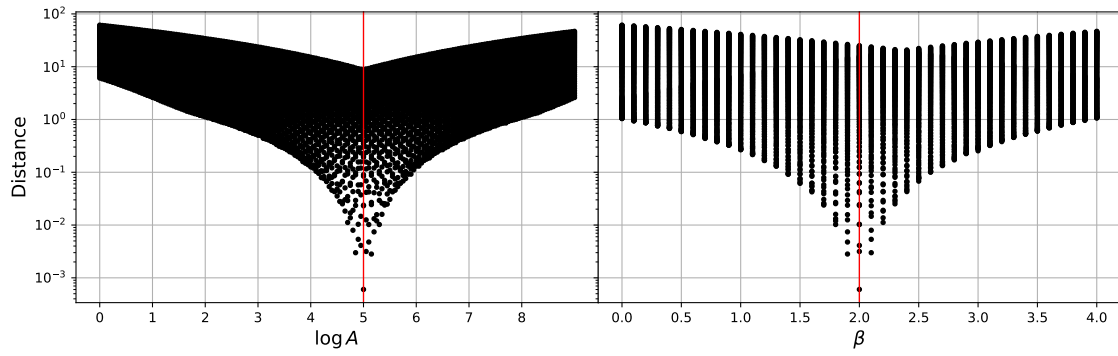


Figure 4.5: Same as Figure 4.4 but showing $\log A$ and β separately. Left: Distance with respect to parameter $\log A$. Right: Distance with respect to parameter β . Both plots shows a red vertical line denoting the expected value.

Chapter 5

Testing the PSD fitting method

The output from a CosmoABC run returns a distribution for each of the model parameters given as input. The closeness of the distribution to the real one will be highly correlated to the quality of the data, which will be defined by the length N of the light curve and the cadence Δt in days. As explained in 3.1.5, the longer the curve and faster the cadence, the periodogram will be a better estimator of the PSD, and therefore, the light curve will be of better quality for a CosmoABC fit. Since the real values of simulated light curves are defined by the user, we can study the accuracy and limitations of the CosmoABC approach to characterize the variability of blazar in a controlled environment. In order to accomplish this task, a battery of tests using particular values in length N , cadence Δt and parameters for the mentioned PSD models are performed.

Before running CosmoABC the user has to setup a set of parameters required for a consistent iteration of the PMC-ABC algorithm. These parameters relate to definitions of the particle systems such as the number of particles and draws for each i -th system, and also convergence definitions as the distance threshold and convergence criterion necessities for the ABC part. The definition of these algorithm parameters, in particular the convergence criterion Δ , have high impact in the running time ¹ and accuracy of CosmoABC. A large number of tests with different PSD models were done in order to study the accuracy and limitations of CosmoABC, specially for the broken power-law model, where retrieving the break frequency depends on how long and good is the light curve. These tests are performed using the time sampling of three typical light curves with a length of approximately 12 years, each of them having gaps and no constant cadence: PKS 1510-089, J0204-1701 and J1121-071. Another set of tests were done for the well-defined case where the time sampling has constant cadence and thus there are no gaps in the data, the idea of these tests is to check how good CosmoABC performs on a perfect scenario.

¹ We executed the CosmoABC algorithm using an Intel Xeon Gold 5220R CPU at 2.2 GHz with a total of 48 threads and 128GB of RAM DDR4 at 2666 MHz. The running times mentioned on this Chapter corresponds to the total time running the algorithm over these 48 threads. We also tested the algorithm on another computer with an Intel Xeon Silver 4110 CPU at 2.1GHz with a total of 16 threads and 128GB of RAM DDR4 at 2400 MHz. The running time on this computer was almost double for the same fits.

5.1. Selecting good CosmoABC parameters

As explained in the Introduction, CosmoABC requires a set of algorithm parameters to work. There are four parameters with high impact in the accuracy and running time to consider:

- M_{ini} : Number of model parameter sets drawn for the first iteration
- M : Number of simulated light curves, particles, in the particle system S
- ϵ : Distance threshold (percentile)
- Δ : Convergence parameter

The CosmoABC algorithm was explained in Chapter 4, we can summarize the usage of these parameters in the following way. Starting from the priors of each model parameter, draw M_{ini} sets of model parameters from them and generate simulated light curves for each one, then keep the $M < M_{\text{ini}}$ light curves with lower distance with respect to the real one. For the next particle systems S_t , the algorithm draws a new set of model parameters using the covariance matrix of the previous particle system S_{t-1} and weights W_{t-1} previously defined. For each set of model parameters, it generates a new simulated light curve which is compared with the ϵ percentile of distance of S_{t-1} . If the simulation has a lower distance, then is added to the particle system S_t . The drawing from S_{t-1} is repeated until S_t has M particles. On this process, the total number of draws that were necessary to achieve the M particles for the new system S_t are saved in the algorithm parameter K . If K is $\frac{1}{\Delta}$ times greater than M then the algorithm has fulfilled the convergence criterion and ends.

Depending on the value of each algorithm parameter the CosmoABC run will be more or less accurate, and also it will take more or less time to finish. A direct relationship between the accuracy and running time of the algorithm is expected. If the time that takes to fit the observed data is not important, then it is preferable to use the parameters with the best accuracy. On the other hand, if the time is important, for example, if the observed data consists of many independent datasets and the time to finish is limited, the optimal parameters will be the ones with low running time and good enough accuracy. Thus, there is no clear definition for the last case and it will depend always on the problem being solved. It is important to note that it is highly recommended to use a value of $M_{\text{ini}} \gg M$. As was previously mentioned the first iteration draws M_{ini} random values from the prior of each model parameter and then keeps only the M with smallest distance with respect to the real data. Thus, the space of parameters of the first system will have a large probability of having the best model parameters if M_{ini} has a high value, which will be finally reflected in a lower running time.

To determine the best CosmoABC configuration, we perform a grid search over the parameters $M_{\text{ini}} = \{20000, 50000\}$, $M = \{200, 500, 1000\}$ and $\Delta = \{0.01, 0.05, 0.1\}$, while keeping

the distance threshold fixed at $\epsilon = 0.75$. Two metrics are considered to define the accuracy: the Mean Absolute Error (MAE) of the mode of the posterior distribution from each model parameter, which corresponds to how far away the estimated result is with respect to the real value on average $\text{MAE} = \sum_i^N |\theta_{\text{exp}_i} - \theta_{\text{obs}_i}|/N$; and the dispersion of the model parameters, which correspond to the HDI at 68.3% ($\sigma_{68.3\%}$) and represents the error bars of each result. In a compromise between obtaining significant results and finishing the tests in a reasonable time we decided to use 20 simulations for each different CosmoABC configuration, where all simulations were done using the simple power-law model with parameters $\log A = -5$, $\log P_{\text{noise}} = -6$ and $\beta = 2$. Figure 5.1 summarizes these results showing these accuracy metrics versus running time. The resultant MAE for each one of the model parameters is weakly dependent of the CosmoABC configuration, being the parameter $\log P_{\text{noise}}$ the only one that shows a clearly direct relationship between accuracy and running time, which are related to the values of Δ and M . As we can see, the MAE decreases as M increases and Δ decreases while the running time gets longer with the same setup. With respect to the dispersion metric, all plots show that the error bar size remains mostly constant independent of M , which has only a negative effect in the running time. The dispersion decreases as Δ also decreases, meaning that Δ has a high impact on the error bar sizes. About the number of draws of the first iteration M_{ini} , there are no big differences for both accuracy metrics between using a value of 20000 or 50000.

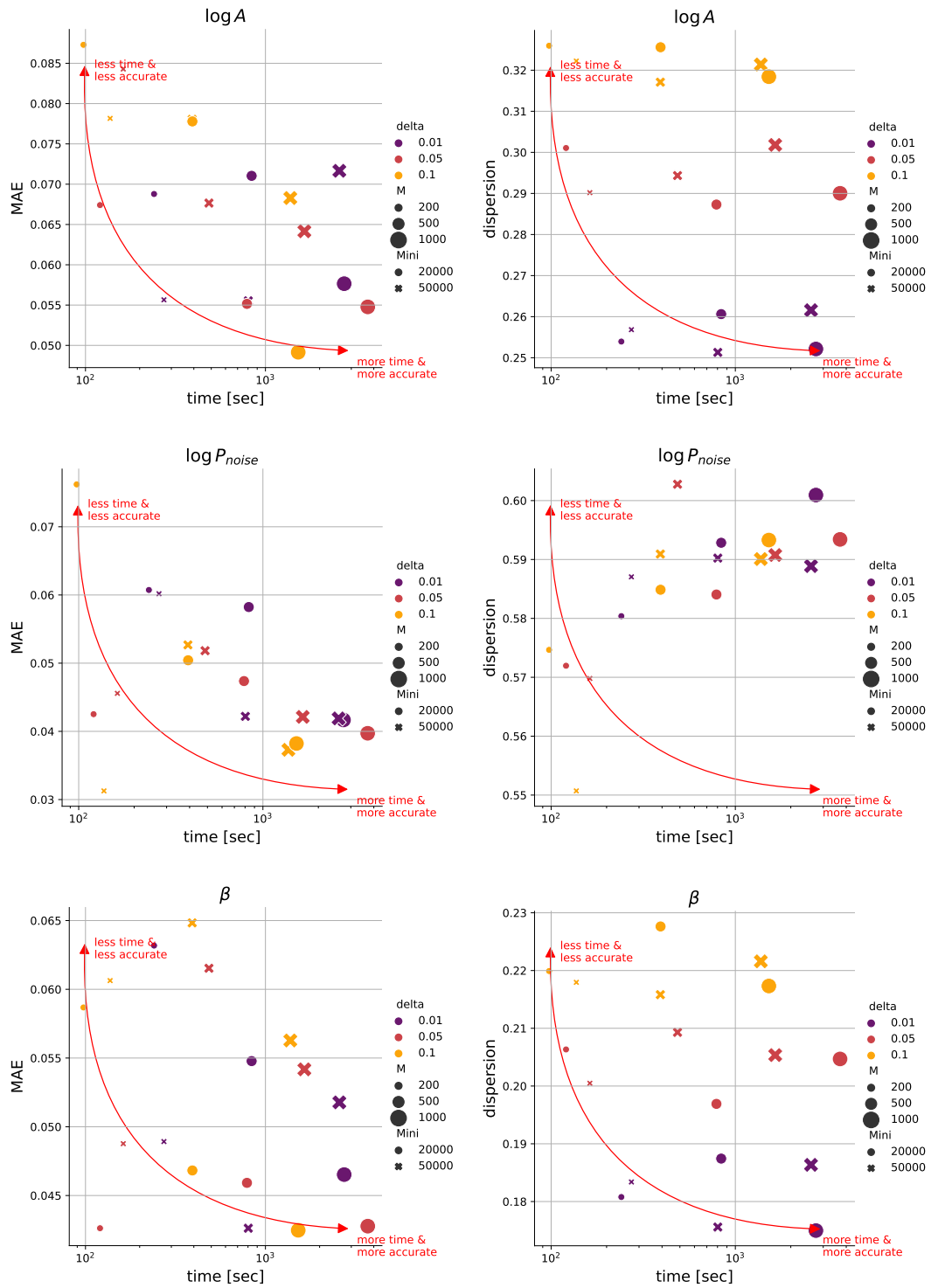


Figure 5.1: MAE and dispersion at HDI of 68.3 % of model parameters $\log A$, $\log P_{\text{noise}}$ and β versus running time for different CosmoABC configurations for a total of 20 simulations using a simple power-law model with parameters $\log A = -5$, $\log P_{\text{noise}} = -6$ and $\beta = 2$. The colors correspond to different Δ values, while size and style correspond to M and M_{ini} respectively. The red line is included just to guide the reader. Hence, we determine that the best CosmoABC parameters for our proposes are $M_{\text{ini}} = 20000$, $M = 1000$ and $\Delta = 0.01$.

We consider that a low dispersion is essential for our fits, therefore, we use $\Delta = 0.01$ as the optimal value², while $M_{\text{ini}} = 20000$ is sufficient. There is an important observation with respect to the CosmoABC parameter M . Since CosmoABC is an approximation of a MCMC method, one expects that the number of draws of the posterior should be enough to get a well defined distribution of each parameter. We consider in a first instance that 1000 draws correspond to a good value to accomplish this criterion when fitting observations, while 200 is appropriate for testing the CosmoABC capabilities. Anyway, we consider to also use 200 draws for real data and extrapolate the final particle system to a new one with 1000 draws. In terms of the CosmoABC algorithm, this is achieved by continuing the iteration for the last particle system of $M = 200$ but using $M = 1000$ instead. The impact of doing this is illustrated in Figure 5.2 for one of the experiments using $M_{\text{ini}} = 20000$ and $\Delta = 0.01$. It shows how the distribution gets a better shape after continuing the last particle system, which only produce a very slight change in the median and standard deviation values. A summary comparison related to accuracy metrics and running time between the case of $M = 200$ with and without continuing together with the full case for $M = 1000$ is shown in Figure 5.3. The error of fitting each parameter is lower when $M = 1000$ is used directly as can be seen in the MAE plot but the differences are negligible. The error bar sizes remain constant and almost equal for all the cases, which can be also seen in Figure 5.1 when using $\Delta = 0.01$. Concerning the running time, continuing the last particle system in order to achieve 1000 draws takes approximately 7 minutes on average, while running the full case with $M = 1000$ takes approximately 45 minutes, which is more than six times longer. This suggests that if we want results in a short period of time and also to have a well defined posterior distribution of each parameter the most efficient way is to continue the last particle system and increase its number of draws as described here. For comparison, the older method takes on the order of hours to complete the fit, demonstrating the improved efficiency of the new approach.

² We also ran some tests with $\Delta < 0.01$ and found that the improvement was not significant compared to the currently chosen value.

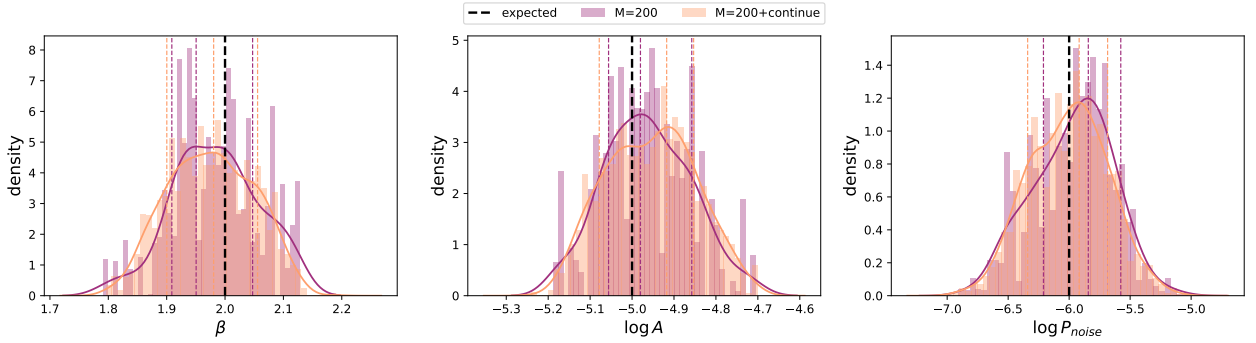


Figure 5.2: Example of the posterior results for $M = 200$ before and after continuing the CosmoABC iteration increasing the number of draws of the last particle system to $M = 1000$. The expected parameters correspond to $\log A = -5$, $\log P_{\text{noise}} = -6$ and $\beta = 2$ and are shown as the black segmented lines. The central segmented line represents the mode of each distribution, while the other lines corresponds to HDI at 68.3%. There are a total of 40 bins per histogram.

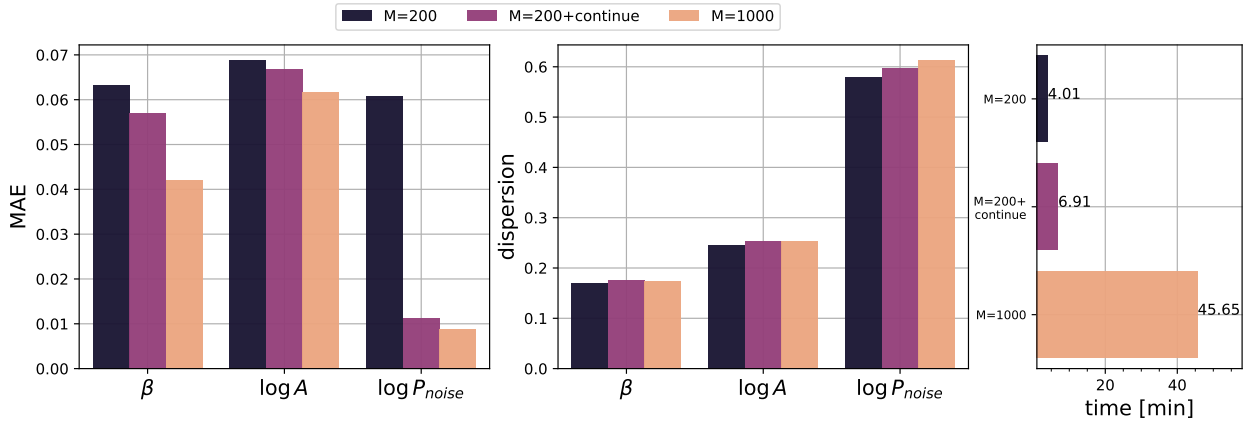


Figure 5.3: Comparison of the accuracy metrics for each parameter and running times when using $M = 200$, $M = 200$ continuing the last particle system to achieve 1000 draws ($M = 200+\text{continue}$) and $M = 1000$. The MAE for all parameters is illustrated in the left, the error bar sizes $\sigma_{68.3\%}$ of them in the middle and the CosmoABC's running time in the right.

Before using the PMC-ABC algorithm over real data, we run a battery of tests to ensure that the fitting process using CosmoABC is well done. The main idea is to characterize the scope and limitations of CosmoABC for different combinations of PSD model parameters, using the simple power-law model and the broken power-law model.

5.2. Simple power-law model

For the PSD as a simple power-law model, we define the following tests:

1. **Power-law index β** : Fixed A and P_{noise} for different β values

We want to know how CosmoABC fits β values when the noise level is lower than the amplitude of the PSD. Therefore, we set $\log A = -5$ and $\log P_{\text{noise}} = -6$, while for β we base the testing values with respect of the space where the Hanning window works well, setting then $\beta \in [0, 3.5]$ with $\Delta\beta = 0.5$.

2. **Noise level P_{noise}** : Fixed β and A for different P_{noise} values

In this case the idea is to check how big can the noise level be with respect to the amplitude before we cannot retrieve the real values of parameters A and β . For an observation with a cadence of 3 days, the maximum frequency correspond to $f_{\text{max}} = \frac{1}{3 \times 2} \approx 0.166 \left[\frac{1}{\text{day}} \right]$. Then, if we set $\log A = -5$ and $\beta = 2$, the minimum log power will be $\log P_{\text{min}} \approx -5 + 2 \times \log(0.0166) \approx -3.44$. This means that the periodogram would be affected³ only for values of $\log P_{\text{noise}} > -3.44$. Therefore, to check the capabilities of CosmoABC with respect to the noise level, we set $\log A = -5$, $\beta = 2$ and $\log P_{\text{noise}} \in [-4, 0]$ using $\Delta \log P_{\text{noise}} = 1$.

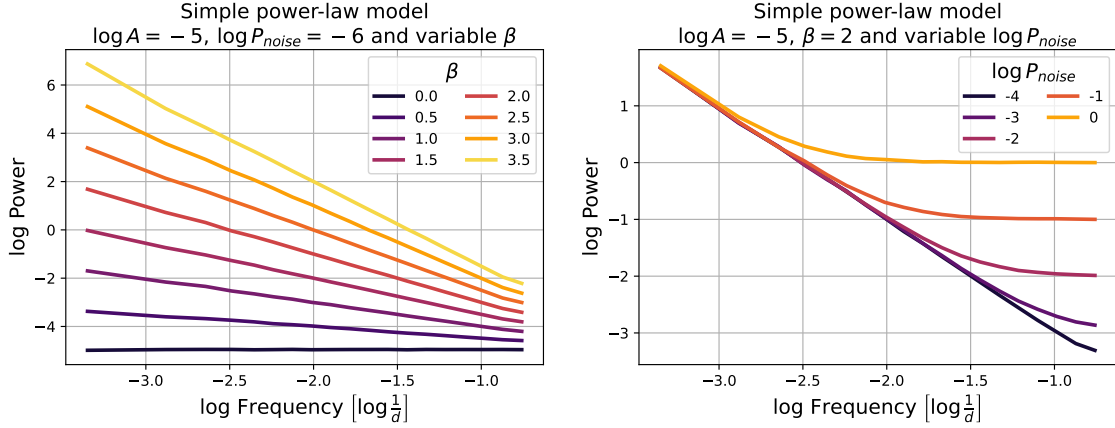


Figure 5.4: Periodograms to fit for each test of the simple power-law model. Left: Visualization of the effect of increasing the power-law index β with $\log A = -5$ and $\log P_{\text{noise}} = -6$. Right: Same as the left but varying the noise level P_{noise} and using $\beta = 2$. The curves correspond to an average of 1000 periodograms for an evenly space sampling time of 3 days and a total of 1500 points.

Figure 5.4 shows a visualization of the effect over the periodogram for this set of model parameters. Due to the high variability of the periodogram, for each test we simulate and fit 100 different light curves in order to get a quantitative result of the method. Since CosmoABC fits the parameters in a bayesian way, the final results will correspond to distributions over the parameters, which is generally described as a normal distribution. Thus, by using a HDI at 68.3% we expect that the posterior of each model parameter contains the simulated

³ Note that this reasoning apply for the ideal case where observation were done each 3 days. If the observations were done only once per week we can approximate the cadence to 7 days, giving us $\log P_{\text{min}} \approx -2.7$

value about 68.3% of times.

Using the proposed CosmoABC configuration $M_{\text{ini}} = 20000$, $M = 200$, $\epsilon = 0.75$ and $\Delta = 0.01$ each light curve takes approximately 4 minutes to be fitted on our machine, which means that for the test of 100 different simulated light curves with 8 different β values, the final running time will be $4 \times 100 \times 8 = 3200$ minutes, approximately 53.3 hours. As a comparison, if we consider that with the older technique a fit takes almost 1 hour, then our approach is 15 times faster.

5.2.1. Power-law index β

A first iteration of these tests is done over simulated light curves with a fixed and evenly spaced sampling time of 3 days, with a total of 1500 points (i.e., 12.3 years). This iteration corresponds to the ideal case of study where an object is observed exactly with a cadence of 3 days, and the reasoning behind this responds to two important things as explained in Chapter 2: the expected number of observations per week of the OVRO program; and following Koay et al. (2019), only about 2% of the observed blazars of the OVRO program exhibit significant flux density variation on timescale of 4 days. Hence, we define 3 days as the lower limit in variation for the radio-band. Figure 5.5 shows the results of this uniform case with $\beta = 2$ over 100 experiments. The result of each test is represented by the mode and the HDI at 68.3% ($\sigma_{68.3\%}$) of the posterior as the best fit and error bar respectively. The error bar is blue if it reaches the expected value, otherwise has a red color. It is important to mention that if all the posteriors look like a normal distribution, we expect a failure of about 32%. Note that the estimated P_{noise} is always close to the expected value since the prior is obtained in the same way the noise level is simulated as described in section 4.5.1.

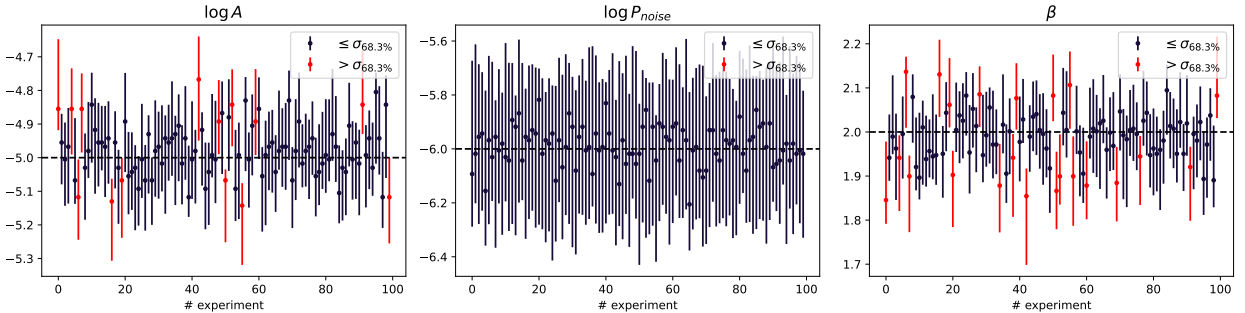


Figure 5.5: Results for the uniform case with $\log A = -5$, $\log P_{\text{noise}} = -6$ and $\beta = 2$. The point represents the mode of the posterior while the error bar size corresponds to the HDI at 68.3%. The red color corresponds to experiments whose dispersion does not coincide with the expected values: for $\log A$, there are 14% of them outside this range, while for β is 22%. If each result looks like a normal distribution, we expect a failure of about 32%.

We can summarize the results for the 100 experiments using a corner plot, a typical plot to

summarize the estimated parameters in a Bayesian approach. Since each experiment is done independently from each other, we can take the average of each parameter for all the 100 experiments and plot the result. Figure 5.6 illustrates the corner plot for $\beta = 2$, showing that on average the 100 experiments are centered in the expected values which are represented by red lines. It is important to notice that this case is far away from the reality where only one fit is done for each observation, but it helps us to understand the range of values that CosmoABC achieves for each posterior.

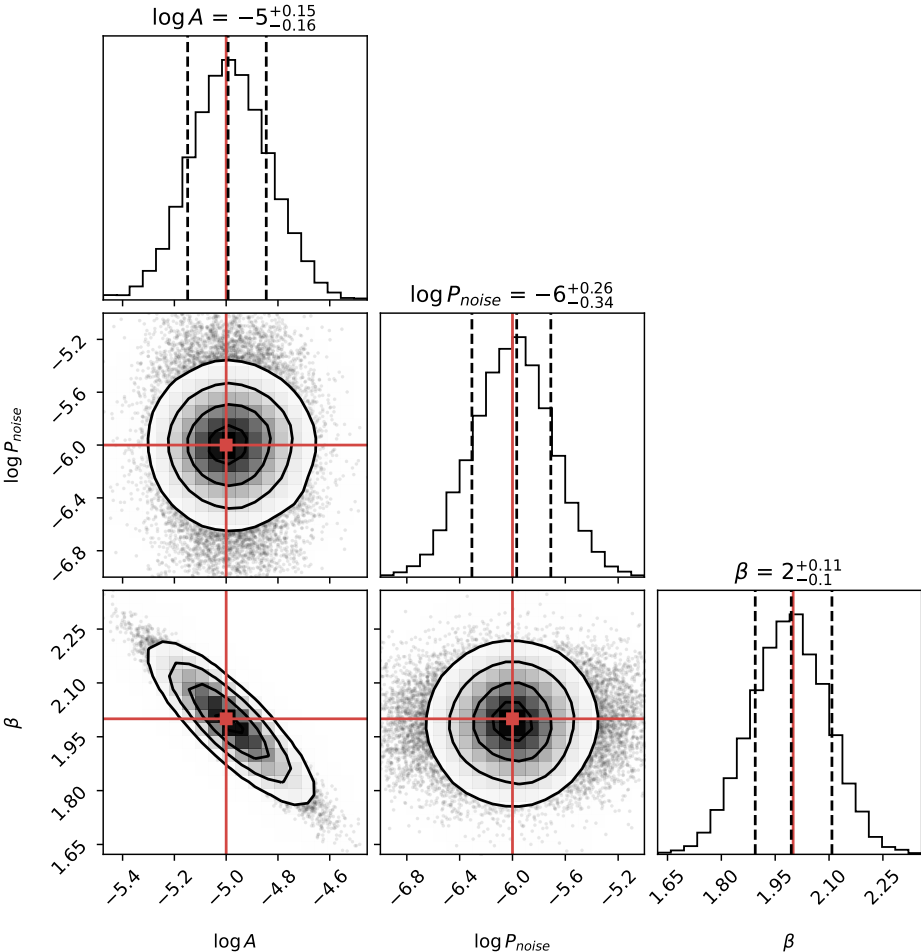


Figure 5.6: Corner plot using the collection of 100 experiments for the uniform case with $\log A = -5$, $\log P_{\text{noise}} = -6$ and $\beta = 2$. It shows histograms of each model parameter together with a 2d-kernel estimation for each combination. The red lines represent the simulated value, while the central segmented lines correspond to the mode of the distribution. The others segmented lines correspond to HDI at 68.3%.

The previous tests are distant to the real case when observations need to be fitted, but it is necessary to define a starting point and ensuring the method is working properly. In reality, no observation has an evenly spaced sampling, which means interpolation is mandatory to

achieve a good periodogram as explained in section 3.3. Therefore, a second part of these tests uses simulated light curves with a time sampling equal to certain observations which define the worst and typical cases of the observed data in a window of 12 years of observation. The selected observations are blazars PKS 1510-089, J0204-1701 and J1121-0711, some important statistics of them are shown in Table 5.1, such as the total number of points, total observed time, mean cadence, and min/max log frequency of its periodogram.

Table 5.1: Important statistics about the blazar light curves used to make the second part of the tests where simulated light curves use the same time sampling of these observed objects. It also includes information of the uniform case.

	<i>uniform</i>	PKS 1510-089	J0204-1701	J1121-0711
N points	1500	450	602	361
observed time [year]	12.33	11.75	12.96	12.93
points per year	121.6	38.31	46.44	27.92
median Δt [day]	3	5.98	4.9	6.98
mean Δt [day]	3	9.55	7.87	13.11
1st largest gap [day]	3	96.83	223.28	155.69
2nd largest gap [day]	3	90.73	72.79	153.6
min $\log f$ [$\log \frac{1}{\text{day}}$]	-3.65	-3.63	-3.68	-3.68
max $\log f$ [$\log \frac{1}{\text{day}}$]	-0.78	-1.28	-1.2	-1.42

Here, we select PKS 1510-089 and J0204-1701 as typical cases, where J0204-1701 has an extended gap of 223 days, which is almost 2/3 of a year. J1121-0711 correspond to the worst case scenario, having the lowest number of points per year. In order to compare the results of fitting light curves using the different time sampling of each selected observation, a boxplot of the mode of the 100 experiment posteriors for all simulated β values is displayed in Figure 5.7, which also include the uniform case and a plot of the MAE of each model parameter. The boxplot allows us to understand the distribution of the mode, while the MAE how far away we are from the expected result. It is clear that the uniform case is the best fitted case, followed by J0204-1701, PKS 1510-089 and J1121-0711.

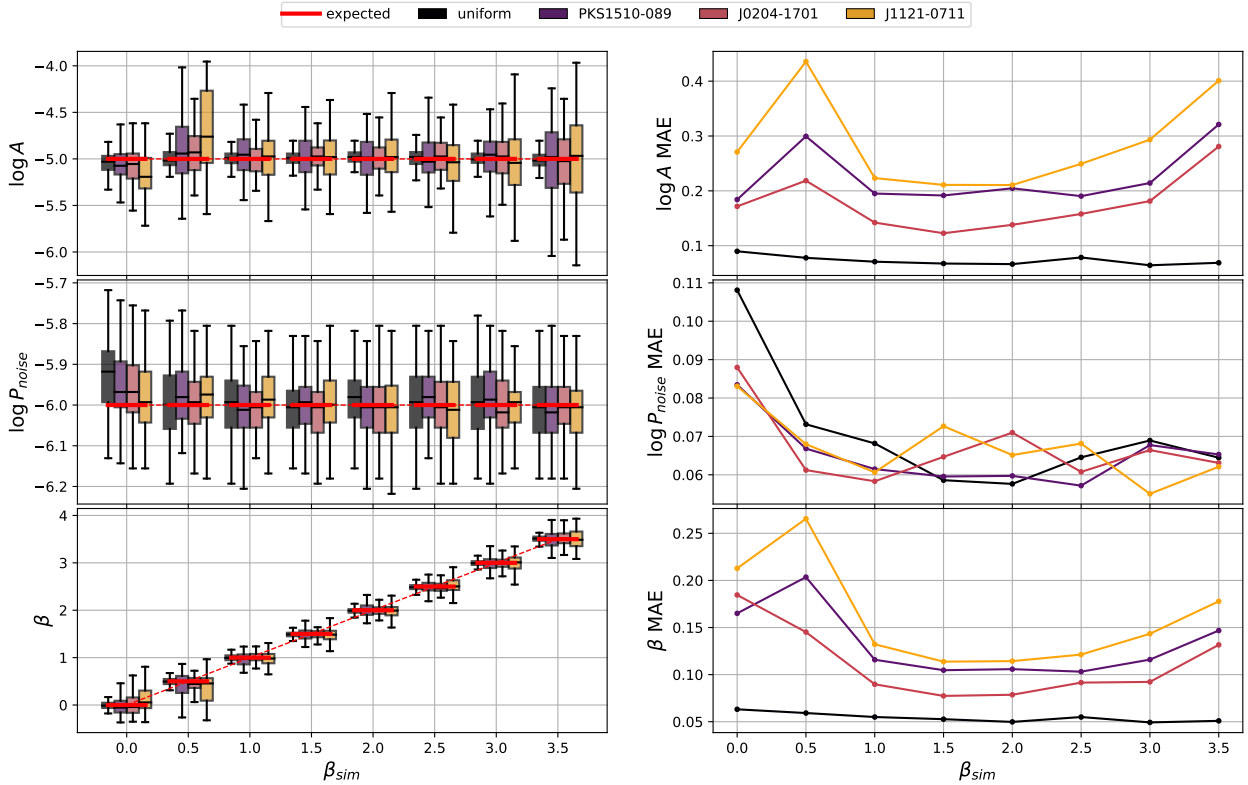


Figure 5.7: Boxplot (left) and MAE (right) for the mode of the 100 experiment posteriors done for each observation and simulated β including the uniform case. The red horizontal bars in the boxplot indicate the expected values for that parameter, while the different time samplings from the observations are described by the different colors.

The MAE is a metric whose value depends on the order of magnitude of each parameter. It is important to note that although the usage of a logarithmic scale for A and P_{noise} allow us to check the results in a simple way, it might lead to a confusion about the magnitude of the error. As an example, a MAE of 0.3 in a logarithmic scale corresponds to an error of two times greater than the expected value. An explanation about the MAE values for each parameter and time sampling is presented below.

- **Amplitude A**

The MAE for the uniform case is the lowest for all β_{sim} as expected. Since for $\beta_{\text{sim}} \leq 0.5$ the spectrum looks like white-noise, we expect difficulties to retrieve the real value in this range⁴. As the spectrum becomes a red-noise the obtained amplitude A decrease its MAE until $\beta_{\text{sim}} < 3$, with J1121-0711 the worst case with a MAE of ~ 0.25 which corresponds to a error of ~ 1.8 in a linear scale. For $\beta_{\text{sim}} \geq 3$ the interpolation and subsequent use of the window function makes the result worse, increasing the MAE in all the cases where the time sampling came from an observation.

⁴ The case $\beta = 0.5$ is curious and unexplained. It shows a high MAE with respect to the others when using the time sampling from observations

- **Noise level P_{noise}**

As explained before, the parameter P_{noise} is easily estimated from the simulated light curve using eq. 4.3. This means that the prior used for this parameter is very constrained around the real value, which finally results in a very low MAE regardless of the time sampling of the light curve. There is only one discrepancy for β_{sim} , where we are in front of a white noise and thus it is not very clear how to compensate the effect of P_{noise} with respect to the others parameters A and β . In this scenario the uniform case has the worst value with a MAE of ~ 0.11 , which corresponds to an error of ~ 1.3 in a linear scale.

- **Power-law index β**

The behavior for β is pretty similar to the parameter A , showing a similar increment at $\beta_{\text{sim}} = 0.5$. For simulated power-law indices greater than 0.5 the MAE is always lower than 0.2, being J1121-0711 the worst case. Note that the uniform case has almost a constant MAE of only 0.05, which means that for the ideal scenario the PMC-ABC algorithm is capable of retrieving all β_{sim} values with very high precision.

Another important metric is the percentage of experiments whose parameter posterior distributions have a deviation greater than expected. Since we are using an HDI at 68.3% and the experiments are randomly generated, we expect that about 32% of the experiments should have error bars not containing the simulated parameter. Figure 5.8 shows these results together with the error bar sizes using HDI at 68.3% ($\sigma_{68.3\%}$) for all the different observations and simulated β values. We found that the experiments for all the observations behave as expected, being $\beta_{\text{sim}} = 0$ the one with the greater dispersion. With respect to the percentage of experiments out of range, the number of deviating tests is very close to the expectation for all time sampling and β_{sim} values, hence, we conclude that the error bars are a good representation for the uncertainty in the model parameters. Of all the tests the observation for J1121-0711 is the worst, particularly for $\beta_{\text{sim}} = 0.5$, having 40% of the experiments outside the range. Note that the negligible percentage of experiments outside this range for $\log P_{\text{noise}}$ along with the constant dispersion make sense with the fact that its prior has very well defined bounds as explained before.

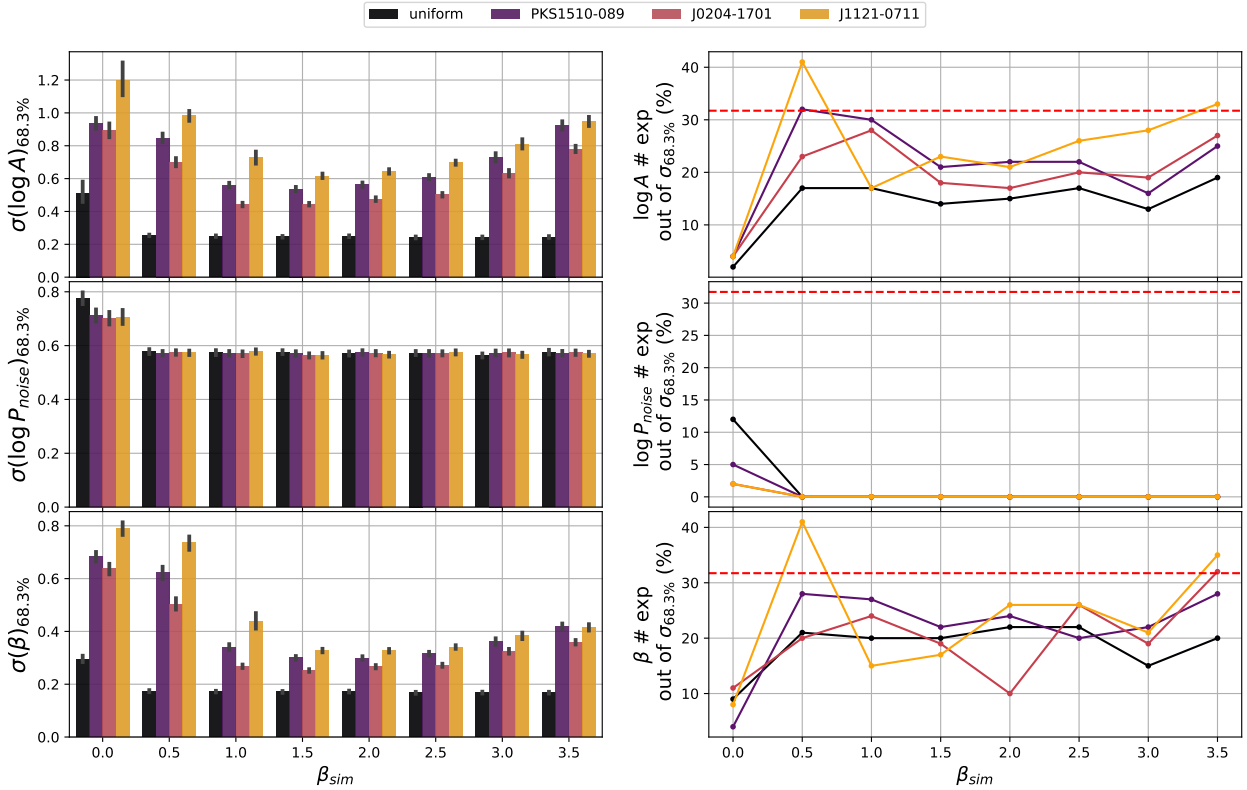


Figure 5.8: Dispersion of each parameter (left) and percentage of experiments deviated from the simulated value using HDI at 68.3% (right) for each observation and simulated β . The segmented red line indicates the expected percentage of experiments out of the range for the defined HDI interval. The number of deviating tests is very close to the expectation demonstrating that the error bars are a good representation for the uncertainty in the parameter.

5.2.2. Noise level P_{noise}

The fitted A and β parameters should show a greater dispersion and deviation from the expected value as the noise level increases. Figure 5.9 shows the boxplot of the mode for each parameter and its respective MAE in the same way as Figure 5.7 for the previous test, but for all simulated $\log P_{\text{noise}}$ values. Results for simulated values -4 and -3 are pretty similar with a low MAE for all parameters, but it increases after -2 and gets larger as the simulated noise level increases. Figure 5.10 is useful to explain the wide range of possible values for both $\log A$ and β when the noise level reaches -1 and 0 . This figure shows the dispersion and the percentage of experiments out of range for the HDI level 68.3% in the same way as Figure 5.8 for the previous test. Here it is illustrated how the CosmoABC results are less accurate as the noise level increases. An extended interpretation of these results is presented below.

- **Amplitude A**

The error of retrieving the amplitude increases as the noise level increases as expected,

being the uniform case the best one. The wide range of values from -4 to -12 shown in the boxplot is explained by the large dispersion for these noise levels, having error bar sizes greater than 4 magnitudes when time sampling from observations are used for a log noise level of -1 and even greater than 5 for a log noise level of 0. Note that these results for log noise levels between 4 and -1 are not as bad as they seem since CosmoABC is indicating that practically for all of them the percentage of experiments deviated is pretty similar to the expected threshold. For the case of $P_{\text{noise}_{\text{sim}}} = 0$ just the uniform case is in the range, while when using a time sampling from an observation about 80% of the experiments are out of the range, meaning that the the parameter $\log A$ practically cannot be retrieved. We expect this behavior since at this point the light curve looks like white-noise and thus parameters $\log A$ and β are degenerate.

- **Noise level P_{noise}**

The explanation is the same described in the previous test. An interesting phenomenon occurs with the dispersion of its posterior, which appears to decrease as the noise level increases and consequently the PSD approaches to a white noise. Note that the MAE for the uniform case also decrease with the increment of the noise level.

- **Power-law index β**

The behavior of β is pretty similar to parameter A , increasing its dispersion and deviation as the noise level increases. When time sampling from observations are used, the dispersion have values greater than 1 and 2 for log noise levels -1 and 0 respectively, indicating that the resultant posteriors decreases its precision as the PSD is being covered by the observational noise. About the percentage of experiments out of the range the β shows a behavior as expected. Note that for a log noise level equal to 0 the parameter takes practically any value as can be seen in the boxplot.

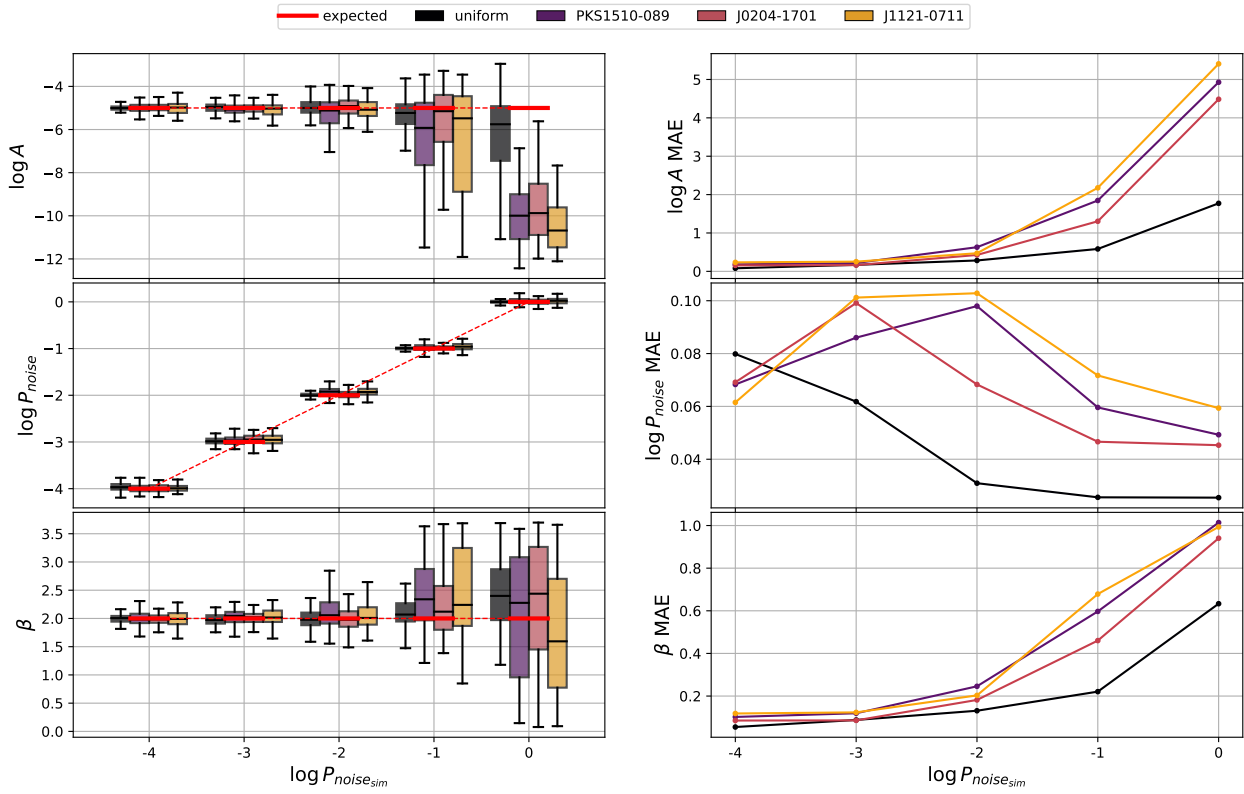


Figure 5.9: Boxplot (left) and MAE (right) for the mode of the 100 experiment posteriors done for each observation and simulated $\log P_{\text{noise}}$ including the uniform case. The red horizontal bars in the boxplot indicate the expected values for that parameter, while the different time samplings from the observations are described by the different colors.

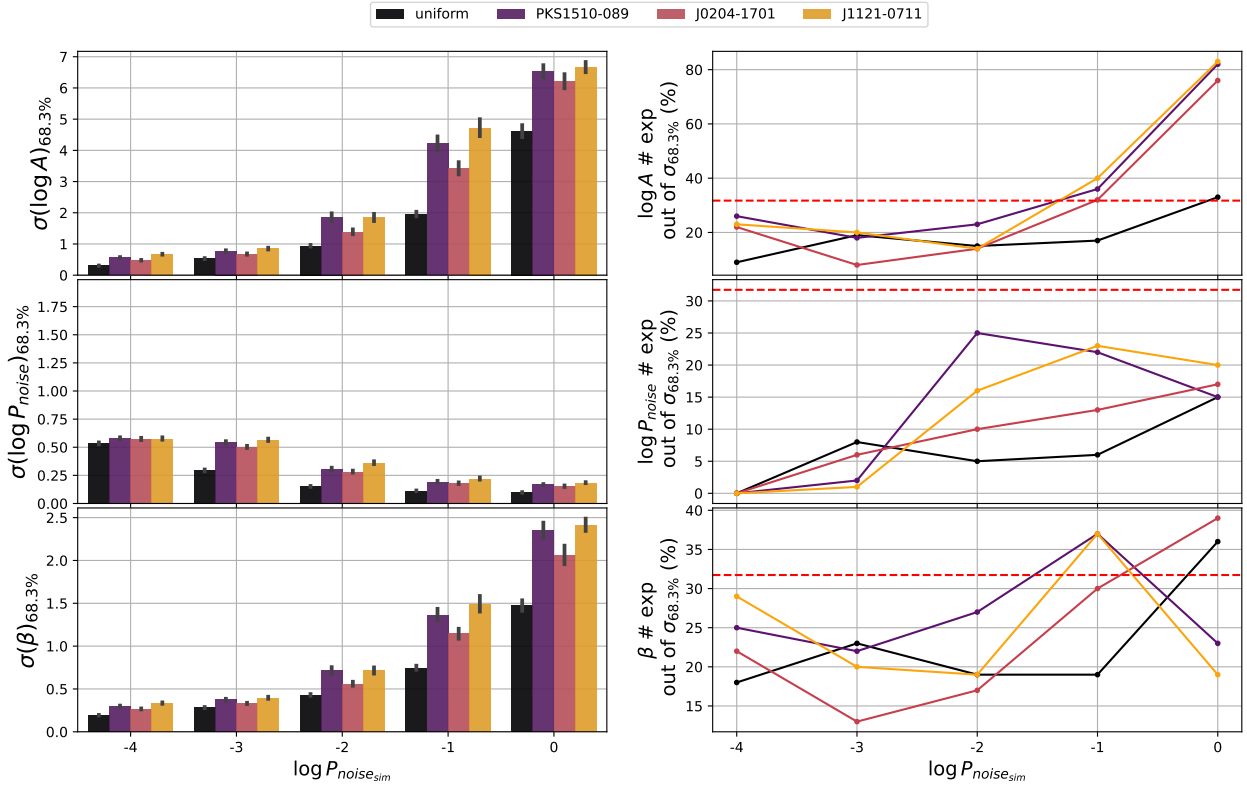


Figure 5.10: Dispersion of each parameter (left) and percentage of experiments deviated from the simulated value using HDI at 68.3% (right) for each observation and simulated $\log P_{\text{noise}}$. The segmented red line indicates the expected percentage of experiments out of the range for the defined HDI interval.

5.3. Broken power-law model

In the case of the broken power-law model, the purpose of these tests are checking the capabilities of CosmoABC to retrieve β_l as its value approaches the value of β_h , and knowing which is the range of action with respect to the break frequency f_{br} . Therefore, we define the following tests:

1. **Low power-law index β_l :** Fixed A , P_{noise} , β_h and f_{br} . Different $\beta_l \leq \beta_h$ values

As described before, we want to know if CosmoABC is capable of retrieve β_l as its value approaches β_h . We expect that when $\beta_l \sim \beta_h$ the algorithm will not be able to retrieve a well defined f_{br} and β_l or β_h will be miscalculated, with only one of them having a value similar to the fixed value β_h . For these tests we set $\log A = -5$, $\log P_{\text{noise}} = -6$, $\beta_h = 2$, $\log f_{\text{br}} = -2.5$ and $\beta_l \in [0, 2]$ using $\Delta\beta_l = 0.5$.

2. **Break frequency f_{br} :** Fixed A , P_{noise} , β_h and β_l . Different f_{br} values

In this case we want to know if the algorithm can retrieve all the parameters changing the location of the break. Although for frequencies lower than f_{interp} the periodogram is highly affected by the interpolation, the method used to simulate light curves shares

the same effect, allowing CosmoABC to also retrieve the cases $f_{\text{br}} \leq f_{\text{interp}}$. We set $\log A = -5$, $\log P_{\text{noise}} = -6$, $\beta_h = 2$ and $\beta_l = 0$, where the latter means that the observed object has a cutoff frequency at f_{br} . With respect to the values for the break frequency, the idea is to cover all the frequency range of the observations. Therefore, we use the logarithm of the break frequency with values $\log f_{\text{br}} \in [-3.5, -0.75]$ using $\Delta \log f_{\text{br}} = 0.25$.

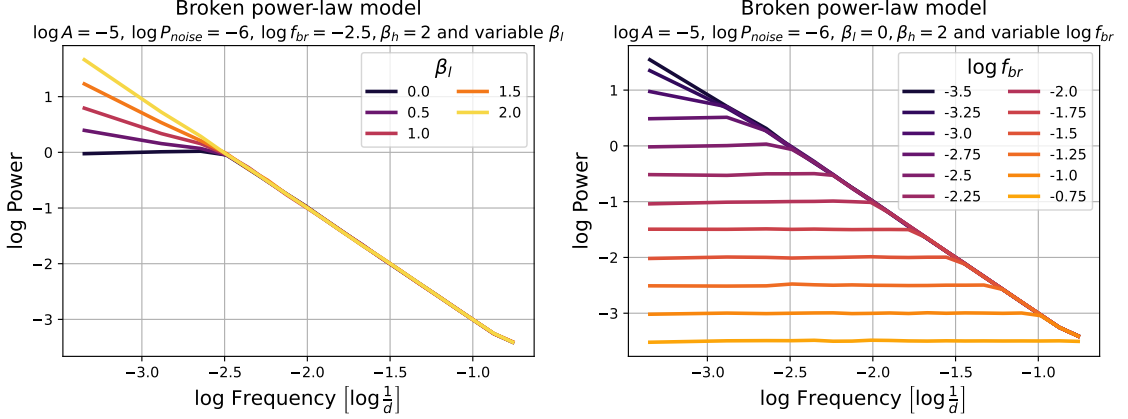


Figure 5.11: Left: Visualization of the effect of increasing the low power-law index β_l with $\log A = -5$, $\log P_{\text{noise}} = -6$, $\log f_{\text{br}} = 2.5$ and $\beta_h = 2$. Right: Same as the left but varying the break frequency f_{br} and using $\beta_h = 0$. The curves correspond to an average of 1000 periodograms for an evenly space sampling time of 3 days and a total of 1500 points.

Figure 5.11 shows a visualization of the effect over the PSD for these set of parameters. All tests for the broken power-law model are done in the same way as the tests for the simple power-law model, i.e, it uses 1000 simulated light curves using different time samplings from observations described in Table 5.1.

5.3.1. Low power-law index β_l

As explained above, we expect a miscalculation of parameters f_{br} , β_l and β_h as β_l reaches the value of β_h . A value of $\beta_l \neq \beta_h$ for a clearly defined break frequency f_{br} indicates a change in the behavior of the object in the timescale $t_{\text{br}} = \frac{1}{f_{\text{br}}}$. As an example, if $t_{\text{br}} = 3$ years and $\beta_l = 0$ then the light curve will show a defined structure only in time windows of 3 years where the flux of each observation is correlated to the previous one according to β_h . For time windows larger than 3 years the object loses all its “memory” and its behavior is the same as white noise. This behavior changes as β_l increases its value until reaches the value β_h where the object has the same behavior in all time windows, which correspond exactly to the simple power-law model case. Figure 5.12 shows the result over 100 experiments using $\beta_l = 0$, $\beta_h = 2$ and $\log f_{\text{br}} = -2.5$ in a similar way to the simple power-law model test for β . In addition to the parameters that define the broken power-law model, the figure also shows

the results for $\log A_{\text{low}}$, which correspond to the logarithmic amplitude for frequencies lower than f_{br} and is defined as $\log A_{\text{low}} = \log A + (\beta_l - \beta_h)f_{\text{br}}$.

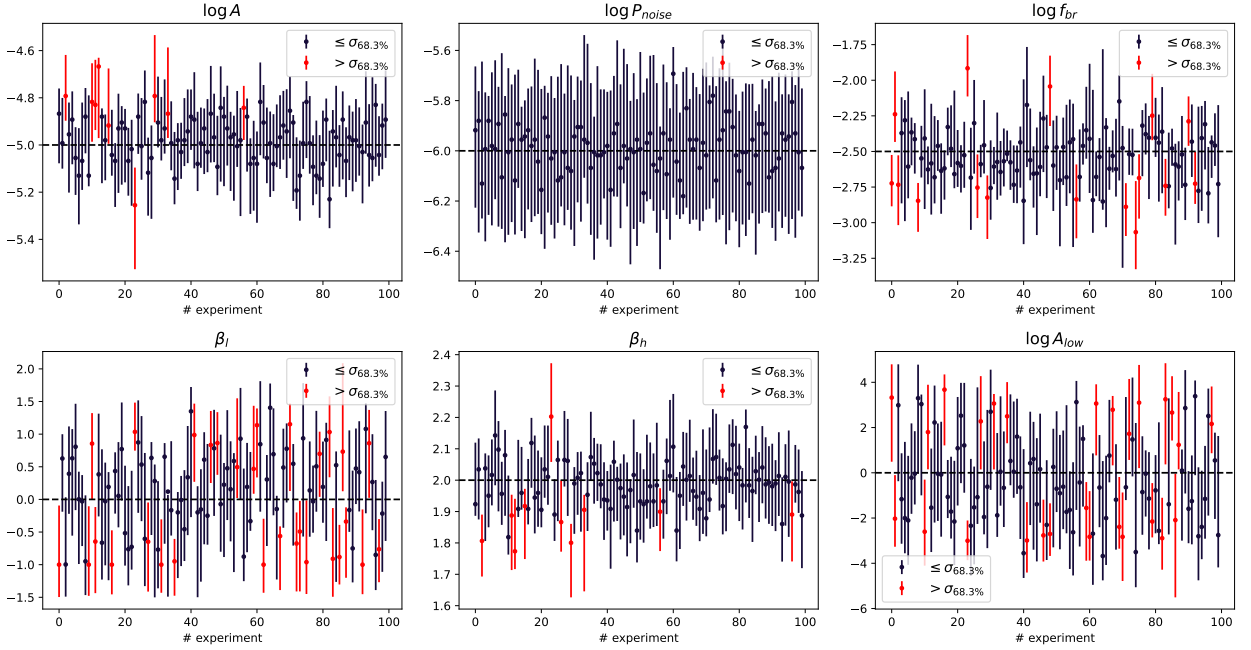


Figure 5.12: Same as Fig. 5.5 but for the broken power-law model using $\log A = -5$, $\log P_{\text{noise}} = -6$, $\beta_l = 0$, $\beta_h = 2$ and $\log f_{\text{br}} = -2.5$. The percentage of experiments whose dispersion does not coincide with the expected values are 9% for $\log A$, 16% for $\log f_{\text{br}}$, 30% for β_l and 10% for β_h . The Figure also shows the results for $\log A_{\text{low}}$, which correspond to the logarithmic amplitude for frequencies lower than f_{br} , having 27% of the experiments out of range.

Following the figures of Section 5.2.1, Figure 5.13 shows a summary of the 100 experiments using $\beta_l = 0$, $\beta_h = 2$ and $\log f_{\text{br}} = -2.5$ in a corner plot. It is interesting to note the wide region that covers β_l from -1 to 1 . The explanation of this behavior lies in the low number of points at log frequencies lower than -2.5 (~ 316 days) and the binning of the periodogram: since by definition each point of the periodogram has an error equal to its magnitude as explained in Section 3.3, a low number of binned points still will have high dispersion⁵ and thus the slope will be highly affected by the dispersion of each binned point between the break and minimum binned frequency, which in this case corresponds to $\log f_{\text{br}} = -2.5$ and $\log f_{b,\text{min}}^{\text{uniform}} = -3.65$ respectively. Using the current setup of a minimum of 4 data points per bin, a binning factor of 1.3 (0.11 in log scale) and a increase factor of 1.1, the uniform case has only 3 binned points of 4 data points each one in this range, which explains the high dispersion that exists in this frequency range.

⁵ According to Papadakis & Lawrence (1993) the ideal number of binned points should be 20 to achieve a normal distribution. However, our method does not require normal distributed points so we consider that binning the periodogram at any level will be always helpful.

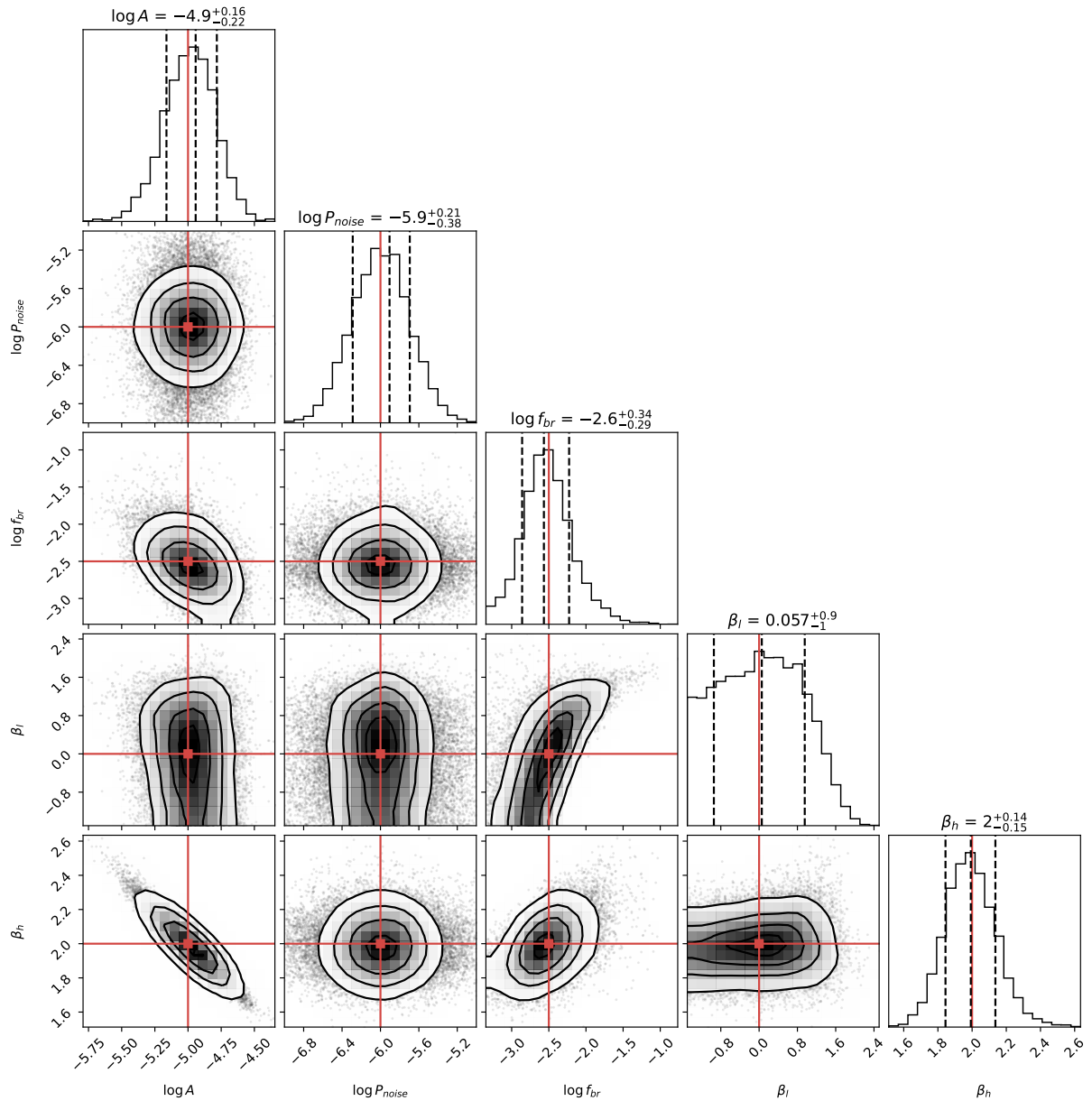


Figure 5.13: Same as Fig. 5.6 but for the broken power-law model using $\log A = -5$, $\log P_{\text{noise}} = -6$, $\beta_l = 0$, $\beta_h = 2$ and $\log f_{\text{br}} = -2.5$. The red lines represent the simulated value, while the central segmented lines correspond to the mode of the distribution. The others segmented lines correspond to HDI at 68.3%.

Figure 5.14 shows the boxplot of the mode for each parameter and its respective MAE for each observation and simulated β_l including the uniform case. As described in the previous paragraph, the value of β_l is biased due the low number of points in the range $[\log f_{b,\text{min}}, \log f_{\text{br}}]$. For all observations including the uniform case, the first 3 binned points contains only 4 points, while the fourth binned point contains 5 points. Only J204-1701 and J1121-0711 has a fourth binned point in the mentioned range of frequency, meaning that the error in retrieving β_l for these observations should be lower than the uniform case and PKS 1510-089.

Another effect to consider is the space between binned frequencies. As explained in Section 3.3, when frequencies are separated by a value larger than the binning factor, the factor is increased by an increase factor until the binned point has at least 4 data points. On the other hand, if the separation between frequencies is lower than the binning factor, then the binned point averages all data points in a range of frequency equal to the binning factor. Table 5.2 shows the location of the first binned points of each observation including the uniform case. As can be seen, the separation of these binned points exceeds the log binning factor due to the reduced number of data points in this range. Thus, the binning algorithm alters the frequency space of the periodogram and consequently also the capabilities to recover the true value of f_{br} .

Table 5.2: Location of the first 5 and last binned points for each observation used for testing in log scale including the uniform case. The separations $\Delta \log f_b$ between the first 5 binned points are 0.47, 0.24, 0.16 and 0.13. From the 6th to the last binned frequency the separation remains constant and equal to the log binning factor 0.11.

$\log f_b$ position	1st	2nd	3rd	4th	5th	...	last
uniform	-3.35	-2.88	-2.64	-2.49	-2.35	...	-0.74
PKS 1510-089	-3.33	-2.86	-2.62	-2.47	-2.33	...	-1.31
J0204-1701	-3.37	-2.9	-2.67	-2.51	-2.38	...	-1.24
J1121-0711	-3.37	-2.9	-2.67	-2.51	-2.38	...	-1.46

Following the structure of the previous tests for the simple power-law model, Figure 5.15 shows the dispersion and the percentage of experiments out of range for a HDI interval of 68.3%, for all the different time samplings. The interpretation of this Figure and the previous one for each parameter is presented below:

- **Amplitude A**

The behavior of the mode of the experiments is pretty similar for all the simulated β_l values, being the uniform case the best one with $MAE < 0.1$ and dispersion of 0.3 on average. The worst case is J1121-0711 having a typical $MAE > 0.3$ and a dispersion of 1.2 on average. When an observation is used as time sampling, the minimal dispersion obtained is almost 3 times greater than the dispersion of the uniform case, which means that there is more uncertainty when an interpolation process is required. Finally, the percentage of experiments out of range is lower than 26% for all the observations including the uniform case.

- **Noise level P_{noise}**

The explanation is the same described in the previous tests.

- **Break frequency f_{br}**

A bias in the break frequency appears as β_l reaches the value of β_h for all time sampling as can be see in the MAE plot. The dispersion also increases under the same scenario,

getting values greater than 1 magnitude which is translated to a uncertainty in the characteristic break timescale from days to years or even decades. The percentage of experiments out of range of the uniform case is larger for almost all simulated β_l values, with a 37 for $\beta_{l_{\text{sim}}} = 1$ which exceeds the expected percentage.

- **Low power-law index β_l**

The high dispersion with values greater than about 1.5 and the MAE around 0.2 to 0.8 across all observations including the uniform case respond the low number of points in the range $[\log f_{b,\text{min}}, \log f_{\text{br}}]$ as mentioned in previous paragraph.

- **High power-law index β_h**

The behavior is quite similar to the power-law index of the simple model, being the uniform and J1121-0711 the best and worst cases respectively. The dispersion remains constant for all simulated β_l values lower than 1.5 and has a minor increment as $\beta_{l_{\text{sim}}}$ reaches $\beta_{h_{\text{sim}}}$.

- **Amplitude at low frequencies A_{low}**

The parameter $\log A_{\text{low}}$ depends directly on all other parameters except the noise level, meaning that its MAE and dispersion correspond to a combination of the MAE and dispersion of the other parameters. In this case the MAE and dispersion has the same shape as the parameter β_l , with only some minor variations. It is important to recall that this auxiliary parameter is just a linear combination of the model parameters and is not directly fitted by CosmoABC.

These results indicate that the degeneracy of the model when β_l approaches β_h affects principally the parameter f_{br} . Given the definition of the broken power-law model, the location of the break frequency loses importance as CosmoABC detects that β_l and β_h have the same values, and therefore its uncertainty increases as can be seen in its dispersion level when $\beta_l = \beta_h = 2$.

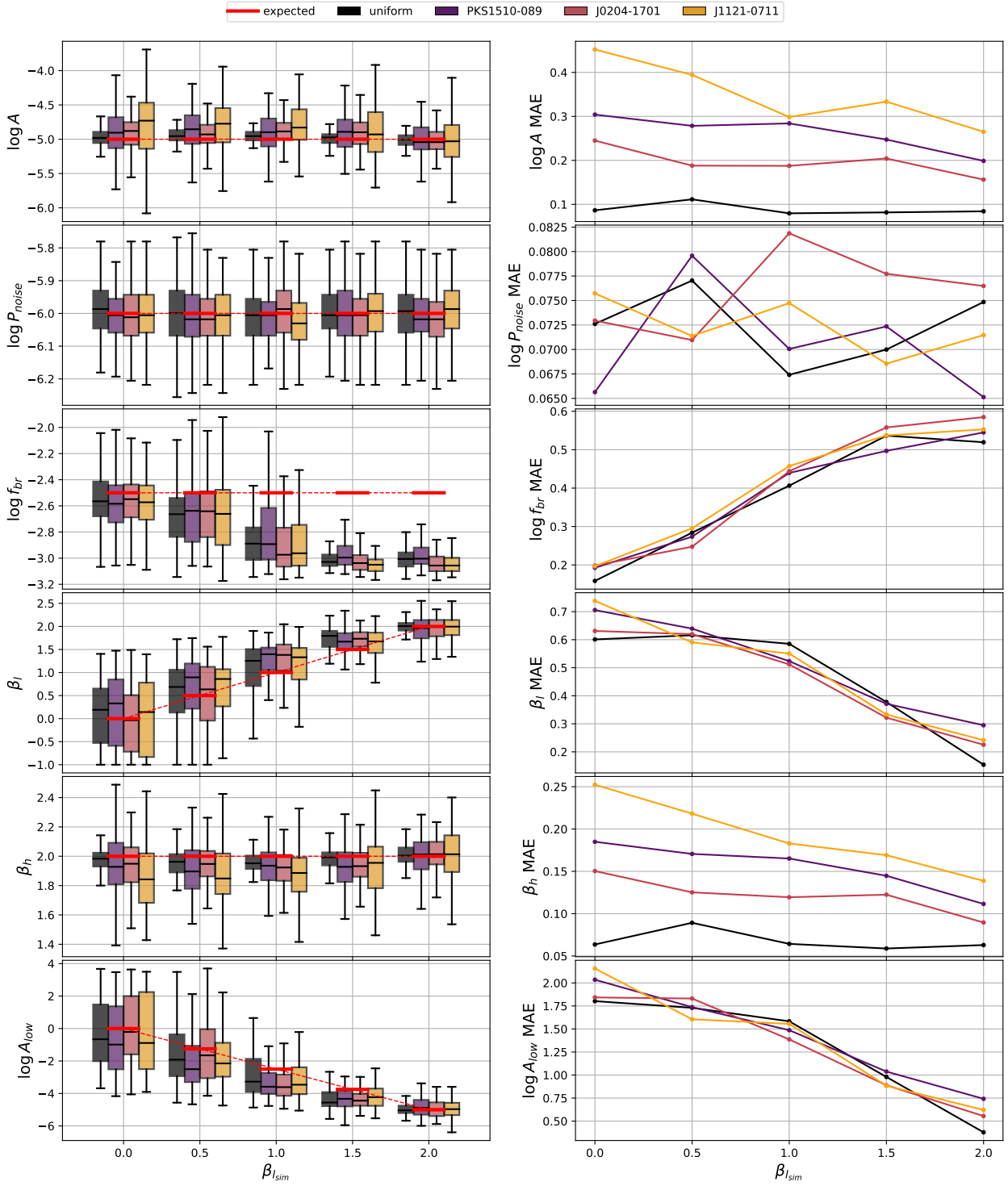


Figure 5.14: Boxplot (left) and MAE (right) for the mode of the 100 experiments done for each observation (including the uniform case) and simulated β_l with fixed parameters $\beta_h = 2$ and $\log f_{br} = -2.5$. The red horizontal bars in the boxplot indicate the expected values for that parameter, while the different time samplings from the observations are described by the different colors.

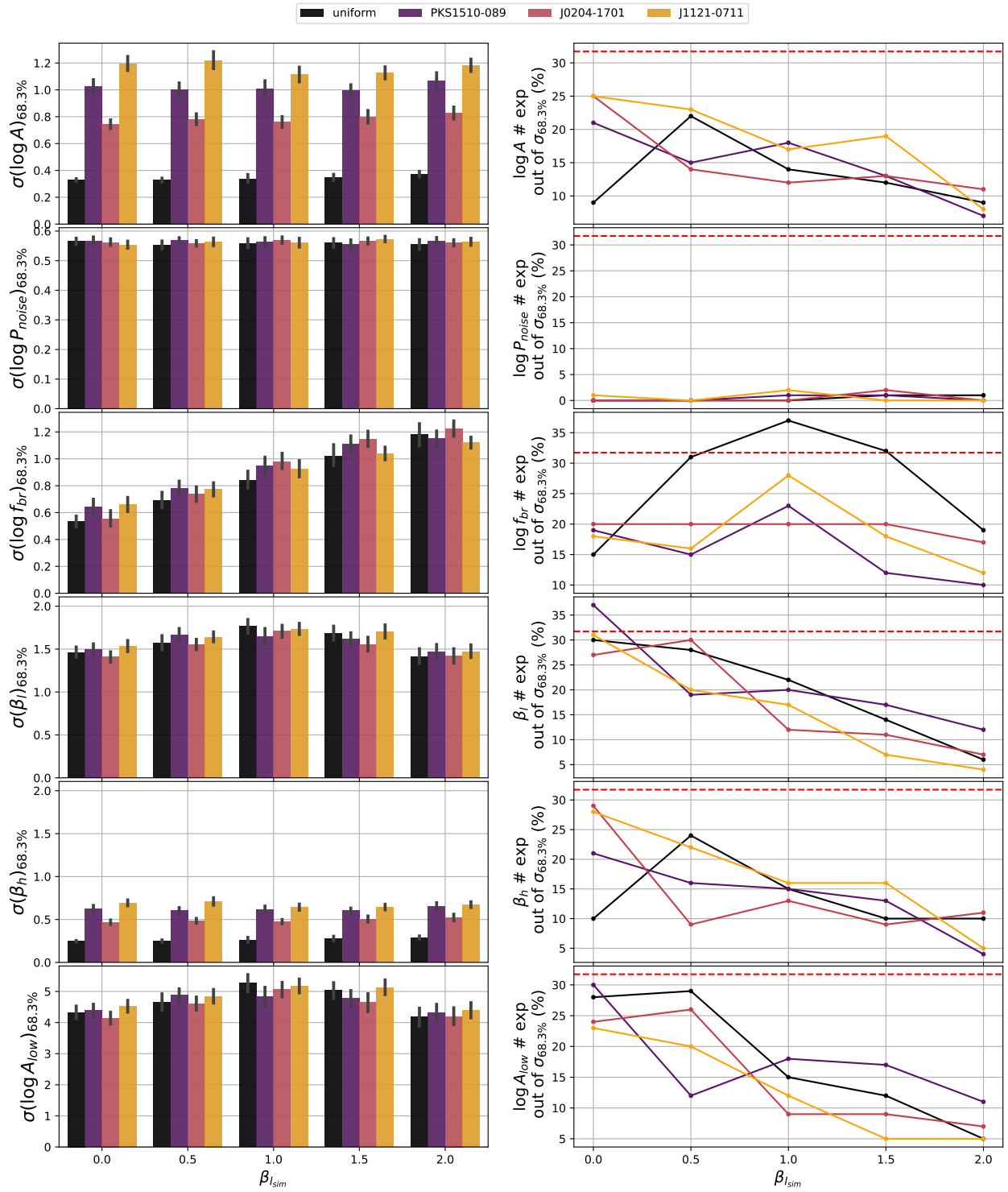


Figure 5.15: Dispersion of each parameter (left) and percentage of experiments deviated from the simulated value using HDI at 68.3% (right) for each observation and simulated β_l with fixed parameters $\beta_h = 2$ and $\log f_{br} = -2.5$. The segmented red line indicates the expected percentage of experiments out of the defined HDI interval.

5.3.2. Break frequency f_{br}

The last set of tests refer to the break frequency position. It is important to mention that the range of simulated $\log f_{\text{br}}$ values exceed the lower and upper binned log frequency limits for some time samplings as can be seen in Table 5.2. When the simulated log break frequency is -3.5 all observations including the uniform case do not have points before the break and thus CosmoABC should miscalculate the parameters β_l and $\log f_{\text{br}}$ near this simulated break. We expect a similar miscalculation at the other end of simulated break frequencies but for parameter β_h instead of β_l . When the simulated log break frequency is -1.25 there are five points for the uniform case and one for J0204-1701, while PKS 1510-089 and J1121-0711 have no points after this value. For greater values only the uniform case has points, having three and one points for log break frequencies -1 and -0.75 respectively. If we consider the broken power-law model as described in equation 3.13, in both cases we are reducing the model to the simple one with a difference on the amplitude and power-law index. For the cases when $\log f_{b,\text{min}} \sim \log f_{\text{br}}$ the model is reduced to $P(f) \approx Af^{-\beta_h} + P_{\text{noise}}$ while when $\log f_{b,\text{max}} \sim \log f_{\text{br}}$ it is reduced to $P(f) \approx A_{\text{low}}f^{-\beta_l} + P_{\text{noise}}$.

Following all other subsections about tests, Figure 5.16 shows the boxplot of the mode for each parameter and its respective MAE for each observation and simulated $\log f_{\text{br}}$ including the uniform case, while Figure 5.17 shows the dispersion and the percentage of experiments out of range for a HDI interval of 68.3%, for all the different time samplings and same simulated values. An interpretation of these results for each parameter is presented below.

- **Amplitude A**

The MAE and dispersion for $\log f_{\text{br, sim}} \leq -2.5$ are very similar to the results of the simple power-law model with different simulated β values. After that value both accuracy metrics increase as the simulated break frequency increase. The number of experiments out of range exceeds the expected percentage as $\log f_{b,\text{max}}$ approaches to $\log f_{\text{br, sim}}$, failing at a log break frequency -1.75 for J1121-0711 and PKS 1510-89 with 44% and 36% of the experiments out of range respectively, -1.5 for J0204-1701 with a percentage of 85% and for -1 for the uniform case with a percentage of 89%. This behavior supports the idea that when $\log f_{b,\text{max}} \approx \log f_{\text{br, sim}}$ the characteristic amplitude of the model is A_{low} .

- **Noise level P_{noise}**

The explanation is the same described in the previous tests.

- **Break frequency f_{br}**

The MAE shows values less than about 0.25 for all cases between the range of log break frequencies $[-3, -1.75]$. This range goes to -1.25 for the case of uniform time sampling since it keeps a sufficient number of points after the break. CosmoABC can not retrieve the break frequency position for frequencies that reach the bounds of the observation timescale as can be seen in the percentage of experiments out of range and in the

dispersion plot where the error bars have sizes ≥ 1 magnitude, which is translated into a uncertainty in the characteristic break timescale from days to years or even decades.

- **Low power-law index β_l**

The MAE for $\log f_{\text{brsim}} \leq -2.75$ has values greater than about 0.5, suggesting that it is quite difficult to retrieve the correct β_l in this range, which is confirmed by the percentage of experiments out of range in this interval. This make sense looking at the low number of points that have the binned periodogram before these breaks as described in Table 5.2: for log break frequencies at -3.5 , -3.25 , -3.0 and -2.75 there are zero, one, one and three points respectively. Note how the percentage of experiments out of range matches the expected percentage for log break positions ≥ -2.75 , which suggests that the parameter β_l is important for the model after this break. About the dispersion, it has mean values between 1 and 2 for all observations excluding the uniform case which has an uncertainly lower than 1 between the range $[-2, -1]$ of simulated log break frequencies.

- **High power-law index β_h**

The behavior of β_h is quite similar to β_l but for the other extreme of simulated log break frequencies. The action range of this parameter goes from log break -3.5 to -2.25 for all cases, even reaching $\log f_{\text{brsim}} = -1.25$ for the uniform time sampling. The dispersion remains mostly constant till these upper limits on break frequency are reached, with values very similar to the previous tests for different simulated β_l values. After these upper limits the dispersion and MAE of β_l increases similar to parameter A , which confirm us that this area is dominated by parameters A_{low} and β_l .

- **Amplitude at low frequencies A_{low}**

The results for A_{low} are the opposite of A in the same sense as results for β_l are the opposite of β_h as explained before, having a high number of values out of range for $\log f_{\text{brsim}} \leq -2.7$. The dispersion and MAE follows the same shape of parameter β_l in the same way that the previous test.

The high percentage of deviated experiments for parameters $\log A$, $\log f_{\text{br}}$, β_l and β_h are telling us that CosmoABC is underestimating their error bar sizes, so we cannot be sure about the results at these simulated log break frequencies. Given this, and that our main focus is on the experiments where the time sampling comes from observations, we determine that under this criteria the $\log f_{\text{br}}$ is well-defined in the range $[-3, -1.75]$ for light curves of length ~ 12 years. With respect to β_l , the parameter is well-defined for log break frequencies greater than -2.75 , while β_h for a log break lower than -2.0 . Therefore, we expect that $[-2.75, -2]$ will be the optimal range for all the observations since we are using light curves with a minimum of 6 years, which correspond to a log frequency of approximately -3.34 .

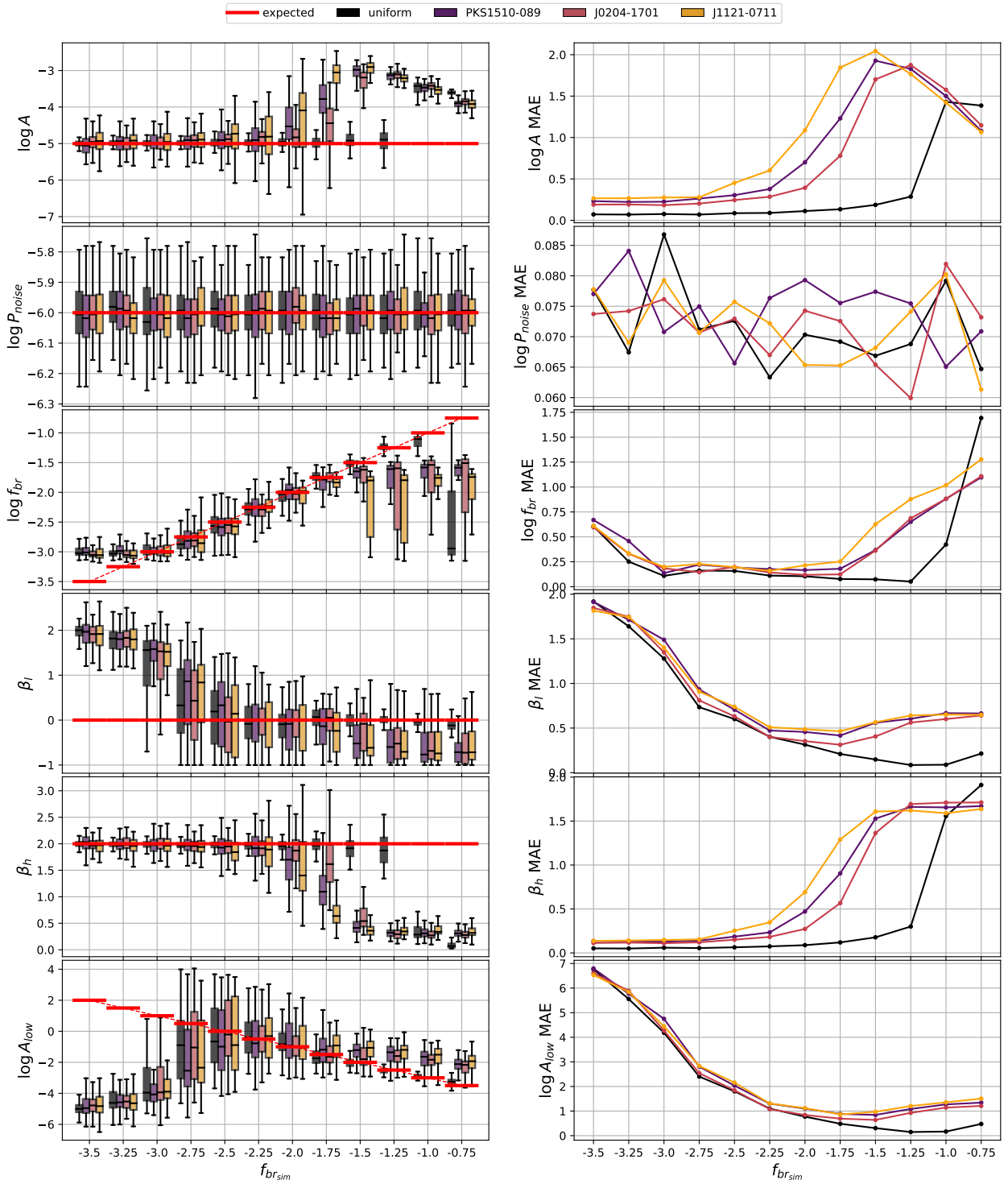


Figure 5.16: Boxplot (left) and MAE (right) for the mode of the 100 experiments done for each observation (including the uniform case) and simulated $\log f_{br}$ with fixed parameters $\beta_l = 0$ and $\beta_h = 2$. The red horizontal bars in the boxplot indicate the expected values for that parameter, while the different time samplings from the observations are described by the different colors.

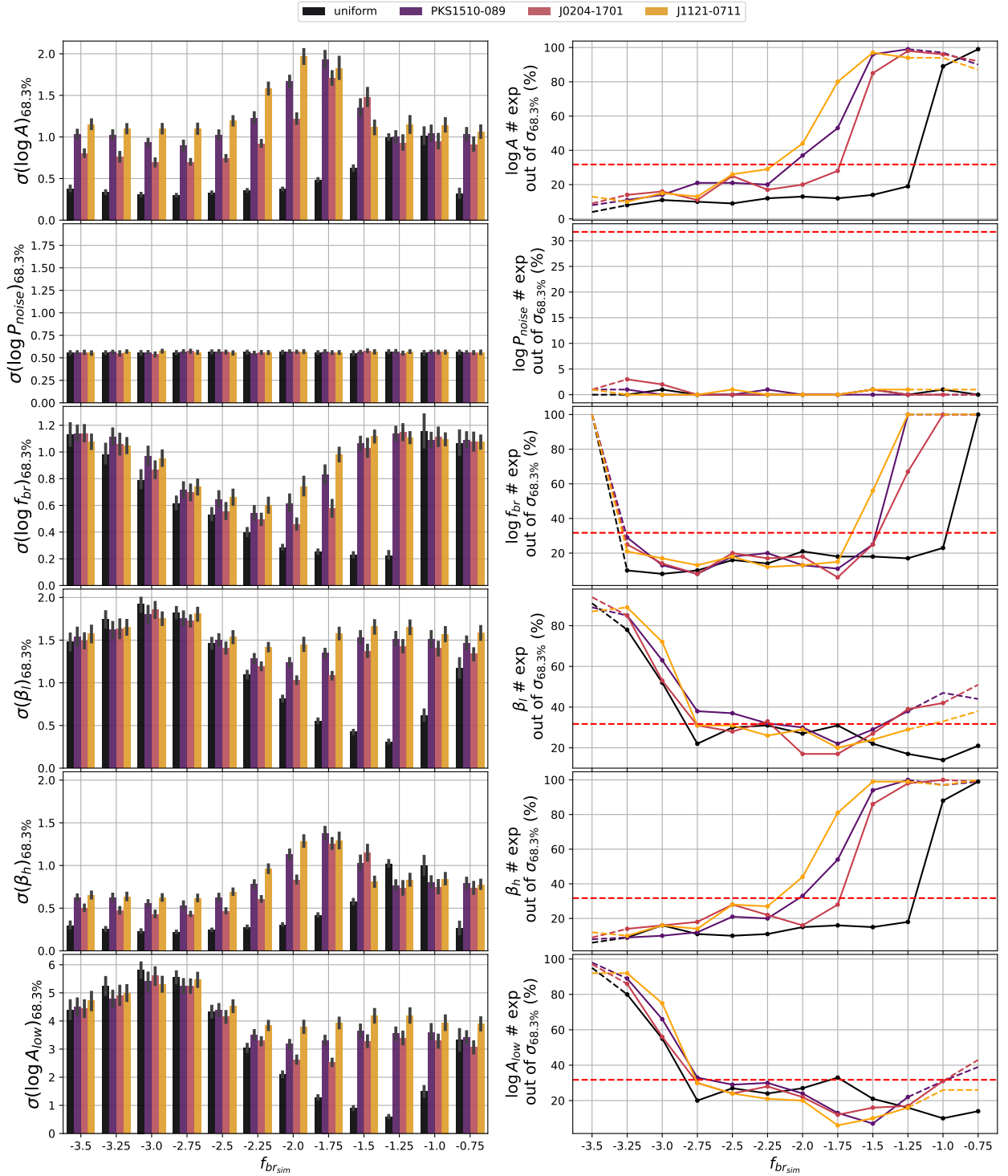


Figure 5.17: Dispersion of each parameter (left) and percentage of experiments deviated from the simulated value using HDI at 68.3% (right) for each observation and simulated f_{br} with fixed parameters $\beta_l = 0$ and $\beta_h = 2$. The segmented horizontal red line indicates the expected percentage of experiments out of the defined HDI interval. The segmented lines that extend the out of range plot indicate that we are outside the timescale bounds from each time sampling.

5.4. Comparison against least-squares method

As a first approach the problem of fitting a model over the periodogram could be solved using a method of least-squares, however, there are some important limitations. First of all, it is recommended to use the method over points having a normal distribution in order to get a consistent result. As explained in Appendix A.2, it is necessary to log bin a total of 20 points to accomplish this task, which turns into a big problem if we want to keep points at lower frequencies. Secondly, the interpolation and window function produce a deformation in the periodogram shape as described in Section 3.3, which will induce a miscalculation of the power-law index and noise level if the fit of the model is applied directly to the data. The reader can see this effect in figures 1, 2, and 4 from Max-Moerbeck et al. (2014b) where the authors applied a linear fit directly to the binned periodogram to illustrate the discrepancy between the β used to simulate the periodogram and the one obtained from the linear fit.

We compare CosmoABC with the method *Curve Fit* from the package *Scipy* for *Python*, which correspond to a non linear least-squares method to fit a function to data in order to compare CosmoABC with a least-squares method. We use the same setup for the log binning applied to the periodogram of the tests: 4 data points per bin, a binning factor of 1.3 and a increase factor of 1.1. We ran Curve Fit over the same simulations generated for the experiments of Section 5.2.1 testing the parameter β of the simple power-law model. Curve Fit received as input eq. 3.12 and the following starting points for each parameter: $\log A_0$ equals to the minimum log power of the periodogram; $\beta_0 = 2$; and $\log P_{\text{noise}_0}$ as the same value used for the mean of the prior distribution employed in CosmoABC. The Figure 5.18 shows the results of both methods over the different time samplings, showing that Curve Fit fits with a higher bias for all parameters in comparison to CosmoABC. The best case of Curve fit correspond to the uniform time sampling that has no interpolation effects, which is far away from the reality of observation as has been mentioned multiple times in this Chapter.

Continuing the comparison of both methods, Figure 5.19 illustrates the MAE of each method and time sampling in the same plot for each parameter. The least-squares method fits $\log A$ well for $\beta_{\text{sim}} = 0.5$, while for all other values the results are really bad compared with CosmoABC, excepting the uniform case. The parameter P_{noise} shows an extremely high MAE for Curve fit for all $\beta_{\text{sim}} > 0$, showing that the method is not capable of recovering the noise level. Finally, the parameter β shows values that double the MAE of CosmoABC for $\beta_{\text{sim}} > 0.5$, while that for β_{sim} equal to 0.5 and 3.5 Curve Fit behave very similar to CosmoABC. Anyway, it is important to recall that since the majority of observations correspond to blazars, we expect to find power-law indices around 2 to 2.5 and thus CosmoABC will give you better results. Furthermore, a least-squares method returns error values coming from an estimator while CosmoABC returns the complete posterior distribution and hence the user can better understand the fitted parameter.

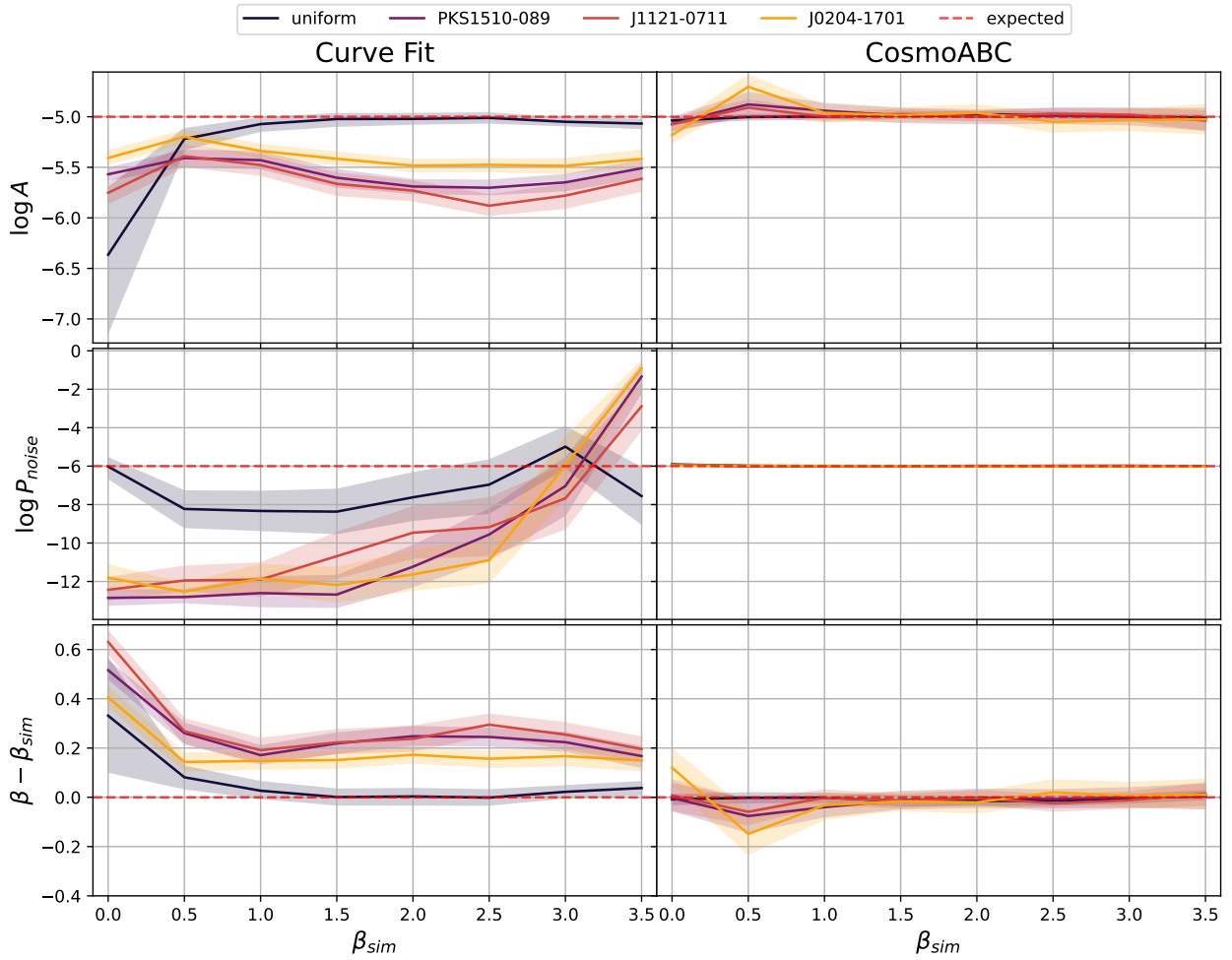


Figure 5.18: Results of fitting the simple power-law model using a non linear least-squares method (left) and CosmoABC (right). Each color refers to a the same time samplings used in the tests, while the segmented red line to the expected value for each parameter. Error bars correspond to the confidence interval at 95 %.

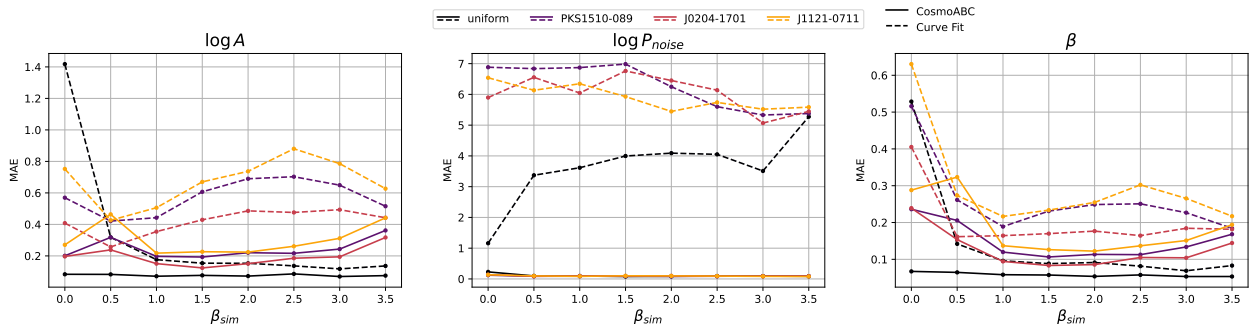


Figure 5.19: Comparison between CosmoABC (solid lines) and least-squares (segmented lines) with respect to the MAE of each parameter for the different time sampling used.

Chapter 6

PSD fit results

After understanding the capabilities of CosmoABC to retrieve the expected values for a different set of models and parameters, we ran the algorithm over the 1290 selected observations from OVRO program. About the CosmoABC parameters used, we employ the same ones described in Section 5.1, i.e., $M_{\text{ini}} = 2000$, $\Delta = 0.01$ and $\varepsilon = 0.75$. In order to obtain well defined posterior distributions in a reasonable computational time, we use the strategy of continuing the last particle system from a previous iteration with $M = 200$ to a new particle system with $M = 1000$ (so called $M = 200+\text{continue}$ in the same section). With this configuration the total running time for all the observations is of approximately 157 hours, which corresponds to 6.5 days.

Since we do not know which observation has a break or not, we run both models over all the observations. This means that almost 2 weeks of computation are required to obtain all the results. After getting the posterior for all the parameters from both power-law models it is necessary to select the model that fits better each periodogram. The principal idea is to check consistency between β_l and β_h for the broken power-law model to consider the existence or not of a break frequency. We explain this model selection method in the next section of this chapter.

For the priors, we employ the strategy explained in 4.5.1 where we use uninformative priors for all parameters except for the logarithm of the noise level $\log P_{\text{noise}}$, where we employ a normal distribution as an informative prior derived from the light curve errors. For the case of parameters β , β_l and β_h we use the distribution $U(-1.5, 5.5)$. In the case of the broken power-law model we use as prior for $\log f_{\text{br}}$ a uniform distribution over the binned logarithm frequency $\log f_b$ defined between its minimum and maximum, i.e., $U(\log f_{b,\text{min}}, \log f_{b,\text{max}})$. Due to the results from testing CosmoABC capabilities we expect to obtain results only in the range of log frequencies $[-2.75, -2]$ for light curves of length ~ 12 years. Finally, we use a uniform distribution $U(-20, 5)$ as prior for the logarithm of the amplitude $\log A$ in order to cover all the possible values of the selected observations.

Considering that CosmoABC returns distributions for each parameter, we report the three typical levels of HDI 68.3%, 95.5% and 99.7% for each parameter and observation as different dispersion levels, while the mode of each parameter defines its best value. We separate the result of each model in two tables displayed in Appendix C being Table C.1 and Table C.2 the summary results for the simple power-law model and the broken power-law model respectively. Note that these tables report the results with an extra flag distinguishing which objects are *well-defined* according to some definitions. We describe our considerations for these definitions in the next section along with the model selection, i.e., checking if the object is better fitted using the simple power-law model or with the broken power-law model.

6.1. Well-defined fit and model selection

The HDI levels give us an idea of how dispersed is each model parameter, this allow us to declare that a periodogram was correctly fitted or not depending on how large is this dispersion. To get an idea, let's assume that we fit the periodogram of an observation with the simple power-law model and found that the power-law index β has a HDI at 68.3% (which would be equal to 1 standard deviation if the posterior distributes as a normal distribution) that cover practically the same range defined for its prior. This is a hint that CosmoABC was not capable of fitting the periodogram, which is the consequence of a light curve with a very low signal or a wrong cleaning process. In practice, we define two thresholds for this HDI level: the first declares sources as *well-defined fits*, while the second one put a flag on observations where we cannot be completely sure about the fit. All observations with a dispersion in β greater than the second threshold are simply considered a bad fit.

Figure 6.1 shows the distribution of the dispersion of β at HDI level 68.3% along with the distribution of β and a comparison with $\log A$. The first threshold is defined at $\sigma(\beta)_{68.3\%} = 1.5$, covering almost a 80% of the distributions for the dispersion of β . Specifically, we keep 1048 observations for this threshold. We define the second threshold arbitrarily at $\sigma(\beta)_{68.3\%} = 3$, which is just twice the value of the first threshold. If we use this second threshold, we keep 1247 observations, which represents 96.7% of the total. Recalling the definition of the simple power-law model, we expect that the parameters $\log A$ and β satisfy a relation of the form $\log A \propto -\beta$. From Figure 6.1(b) we can check that this criteria for the definition of *well-defined fits* allow us to identify observations that break this relationship which correspond mostly to fits with $\sigma(\beta)_{68.3\%} > 3$ (purple squares). On the other hand, Figure 6.1(d) show us how this criterion removes observations with a fitted β near their limits 0 and 5 respectively.

As was mentioned in Chapter 5 about testing, the broken power-law model can be fitted over a periodogram showing a simple power-law shape. The problem is that not all model parameters will be well-defined, having a final posterior with a very high dispersion for the

break frequency or for one of the power-law indices β_h, β_l . In order to find which observation is well-defined by this model we could do a similar approach as the previous one using the dispersion of the $\log f_{br}$. However, we note that the following model selection method gives us not only an idea of which model fits better but it also allows us to check the observations that are well-defined using this model.

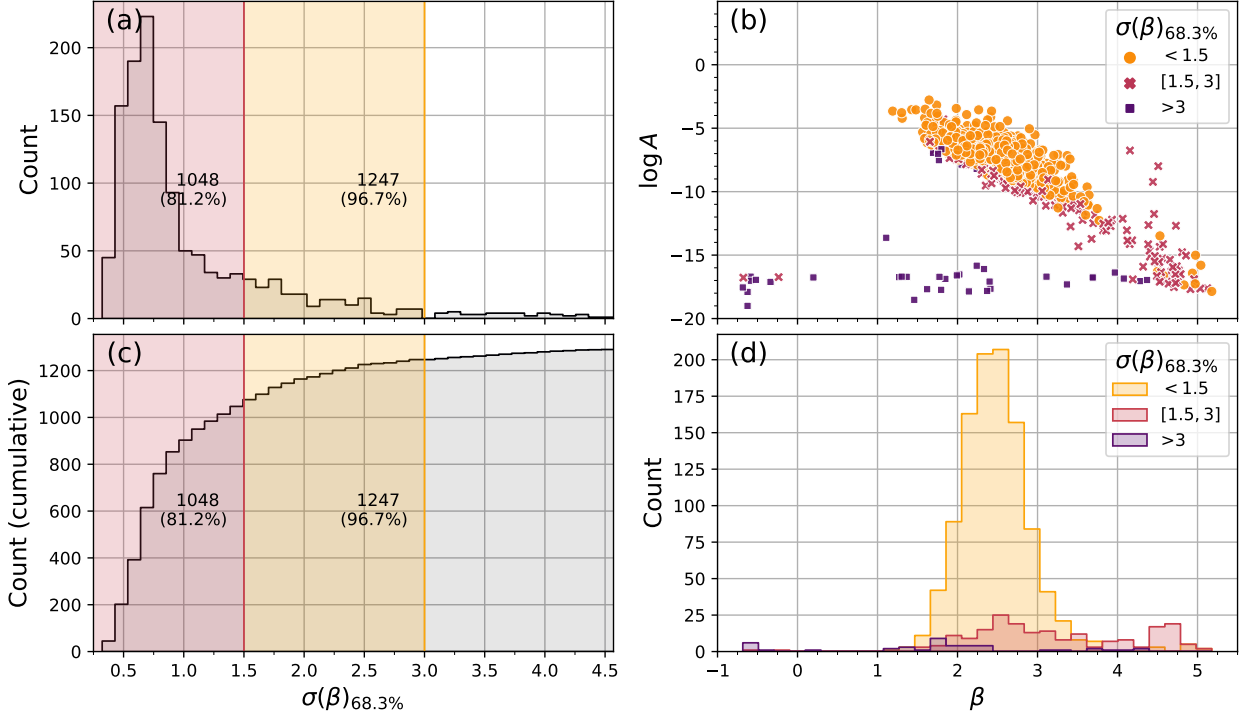


Figure 6.1: Distribution of parameter β and its dispersion at level of HDI 68.3%, showing the two proposed threshold for $\sigma(\beta)_{68.3\%}$ at 1.5 and = 3. (a) Distribution of $\sigma(\beta)_{68.3\%}$. If we consider the threshold at 1.5 (red) then 1048 observations meet this criterion (81.2%), while for threshold 3 (orange) we keep 1247 observations (96.7%). (b) Comparison between β and $\log A$ for each defined dispersion range. Note that a relationship $\log A \propto -\beta$ should be fulfilled due the definition of the simple power-law model. (c) Cumulative distribution of $\sigma(\beta)_{68.3\%}$. Same description as (a). (d) Distribution of β for each defined dispersion range.

We check the *non-consistency* of parameters β_h and β_l at different HDI levels. We say that there is no consistency between both parameters if the HDI values of the parameters do not intersect. In particular, we use 3 HDI levels: 68.3%, 95.5% and 99.7%. Figure 6.2 shows an example of this method over the fits of objects 2230+114 and J0721+7120. For 2230+114 we have no consistency just for 68.3%, while for J0721+7120 β_h and β_l are not consistent for all the levels. In a similar way to the concepts of the model selection of the simple power-law model, we state that sources with no consistency at 99.7% level provide very strong evidence for the existence of a break frequency. For sources with no consistency at 95.5% level, some evidence is provided, while for those with only no consistency at 68.3%, the result cannot

be regarded as confident. Table 6.1 displays the number of non-consistent sources for each HDI level, having for the most confident only 39 sources, which corresponds to 3.02 % of the total.

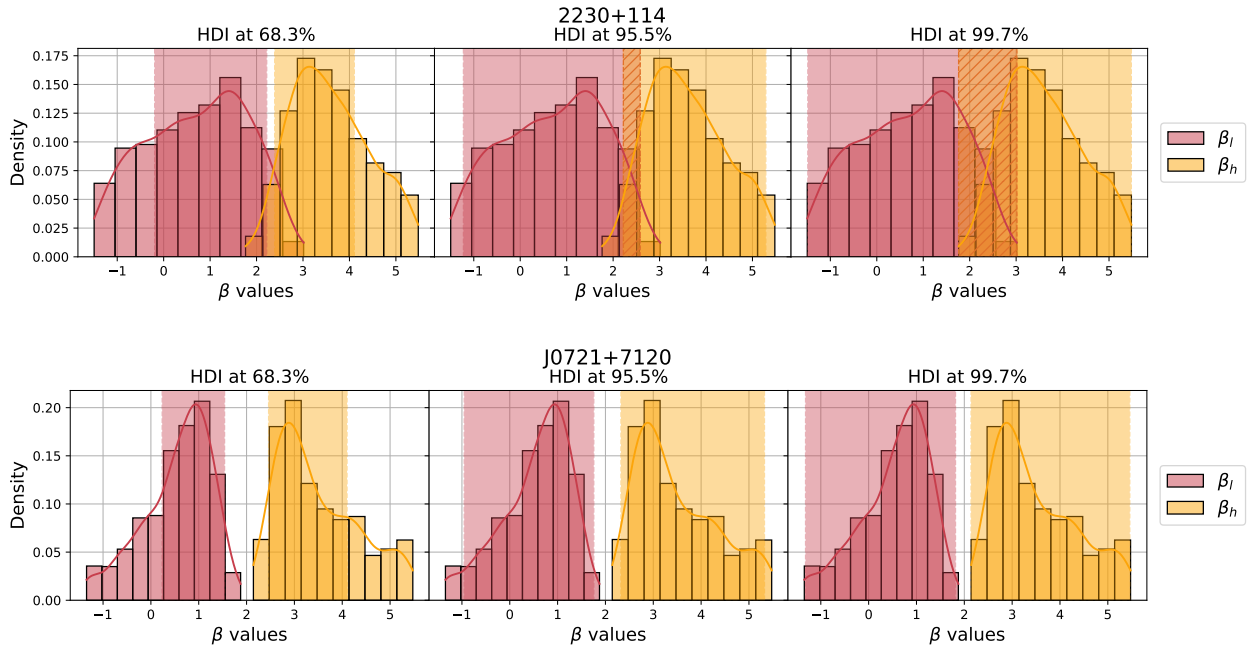


Figure 6.2: Check of consistency between β_h and β_l for objects 2230+114 (top) and J0721+7120 (bottom) at HDI levels 68.3 %, 95.5 % and 99.7 %. We say that there is no consistency between β_h and β_l parameters if their HDI values do not intersect, which is evidence for the need of a break frequency in the PSD model.

Table 6.1: Results of the non-consistency of parameters β_h and β_l . The percentage is with respect to all the 1290 fitted observations. These results indicate that for the HDI at highest level we have 39 observation with a well-defined break frequency.

HDI level	Not Consistent sources	Percentage from total
68.3 %	212	16.43 %
95.5 %	115	8.91 %
99.7 %	39	3.02 %

As we describe before, this model selection method give us also an idea of how good was the fit of the break frequency. Figure 6.3 shows the distribution of $\sigma(\log f_{br})_{68.3\%}$ and which ratio represent each of the different assumptions of having a well-defined break frequency described by the model selection criterion. We can note that the lower dispersion mostly corresponds to a non-consistency at HDI level 99.7 % (dark purple). The figure also shows how this dispersion behaves versus the difference $\beta_h - \beta_l$ where we can notice the difference for the highest level is greater than 2 (purple plus signs).

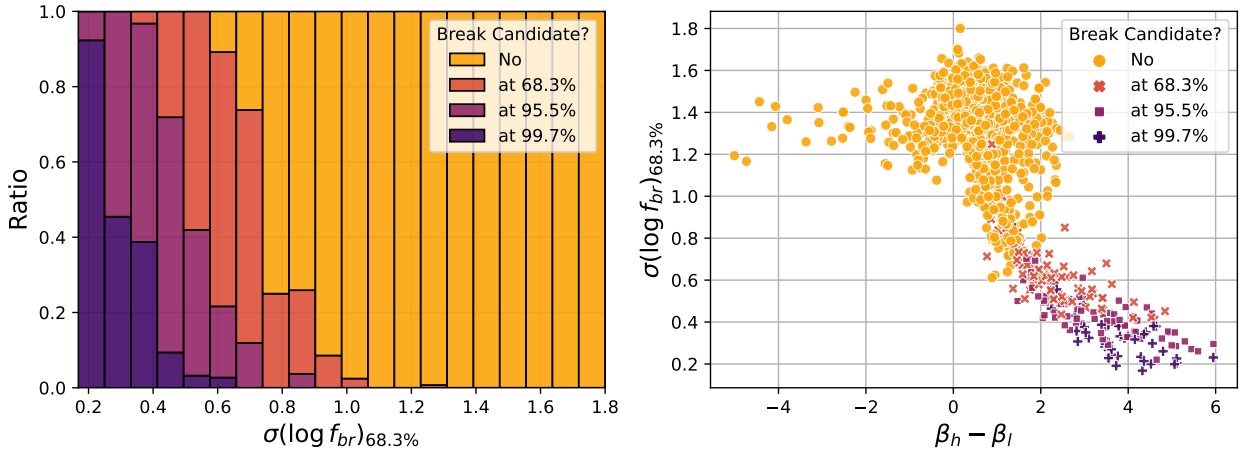


Figure 6.3: Distribution of the dispersion of $\log f_{\text{br}}$ at HDI level 68.3% and its comparison with the difference between β_h and β_l for the different evidences of having a well-defined break frequency. Left: Distribution of $\sigma(\log f_{\text{br}})_{68.3\%}$ and proportion of observations (ratio) that represent each evidence level for each bin. Right: Behavior of $\sigma(\log f_{\text{br}})_{68.3\%}$ as a function of the difference between β_h and β_l .

From the 1048 sources defined as well-defined fits for having $\sigma(\beta)_{68.3\%} < 1.5$, 38 of them have significantly different β_h and β_l using the criteria at 99.7%, meaning that they are better fitted using the broken power-law frequency. There is only one object that does not pass the criteria for $\sigma(\beta)$ but it has a well-defined break frequency. Hence, 1010 objects are defined as sources with a simple power-law periodogram and 39 objects as sources with a broken power-law periodogram.

Figures 6.4 and 6.5 show histograms of the model parameters for the simple power-law and the broken power-law models respectively along with the dispersion of each parameter at HDI level 68.3%. Table 6.2 shows summary statistics of each parameter for the simple power-law model and Table 6.3 shows the same for the broken power-law model. Note that parameter $\log f_{\text{br}}$ is defined very close to the expected range.

Table 6.2: Summary statistics of parameters $\log A$ and β of the 1010 objects having $\sigma(\beta)_{68.3\%} < 1.5$ and no well-defined break frequency.

	Mean	St dev.	Min	Q0.25	Median	Q0.75	Max
$\log A$	-7.265	1.550	-17.861	-7.931	-7.081	-6.406	-2.779
β	2.487	0.451	1.301	2.209	2.452	2.706	5.178

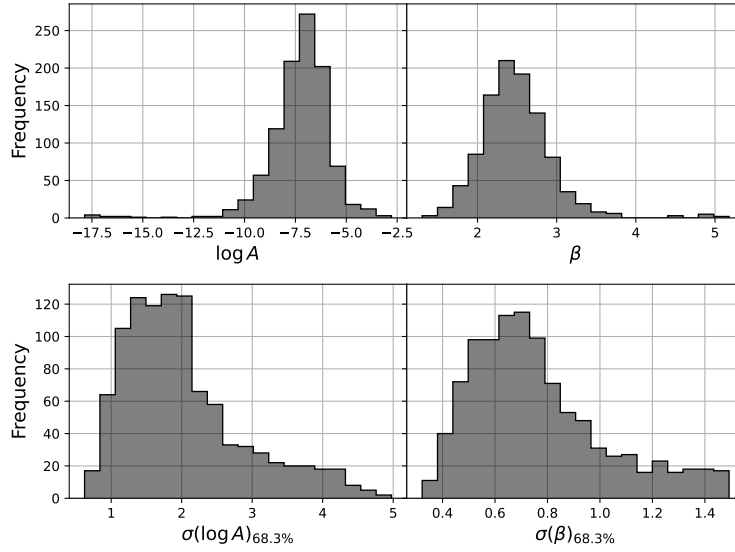


Figure 6.4: Histogram of $\log A$ and β values and their dispersion at 68.3 % of the 1010 objects having $\sigma(\beta)_{68.3\%} < 1.5$ and no well-defined break frequency.

Table 6.3: Summary statistics of parameters $\log A$, $\log f_{br}$, β_l and β_h of the 39 objects having a well-defined break frequency, i.e., having no consistency between β_h and β_l at HDI of 99.7 %.

	Mean	St dev.	Min	Q0.25	Median	Q0.75	Max
$\log A$	-9.467	1.883	-13.222	-11.127	-9.070	-8.132	-4.780
$\log f_{br}$	-2.389	0.288	-2.834	-2.609	-2.421	-2.237	-1.683
β_l	0.275	0.851	-1.206	-0.290	0.352	1.011	1.575
β_h	4.083	0.749	-2.863	3.444	4.054	4.780	5.178

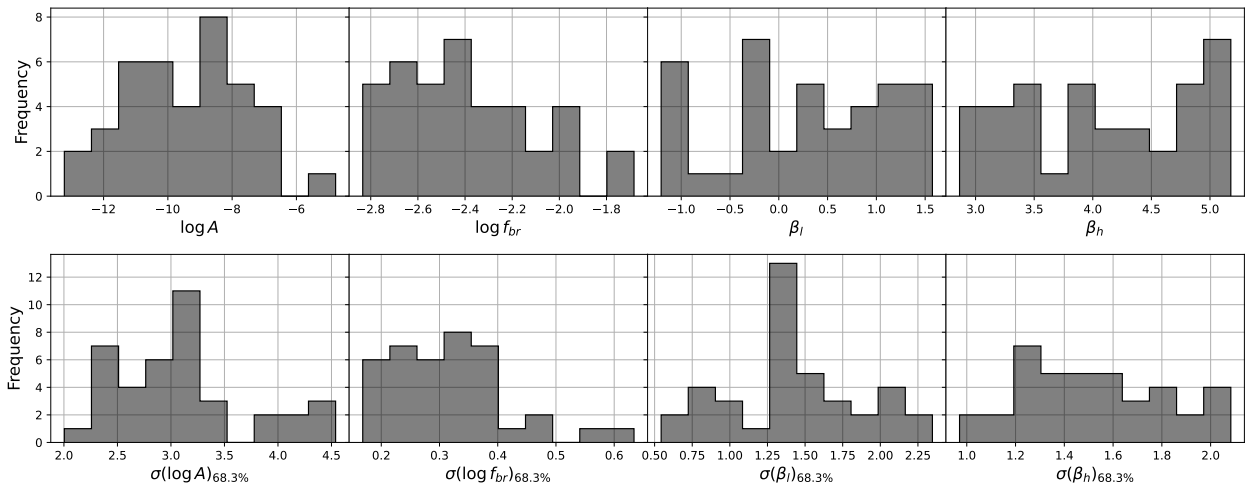


Figure 6.5: Histogram of $\log A$, $\log f_{br}$, β_l and β_h and their dispersion at 68.3 % of the 39 objects having a well-defined break frequency, i.e., having no consistency between β_h and β_l at HDI of 99.7 %.

We can check the results for object PKS 1510-089 in Figure 6.6, one of the 1012 objects well-defined using the simple power-law model. On the other hand, Figure 6.7 shows the results for CLJ1333+5057, one of the 39 objects having well-defined break frequency, and particularly it is the only object that does not pass the $\sigma(\beta)_{68.3\%} < 1.5$ criteria. In the plot of the periodogram, the plot of the best fit is generated obtaining the mean of 10 simulations for each posterior combination and aggregating them to obtain a final point that represent the weighted median of each frequency. Using this aggregated points we also obtain the error bars for each plotted point, corresponding to quantiles [0.156, 0.841] and [0.023, 0.977] .

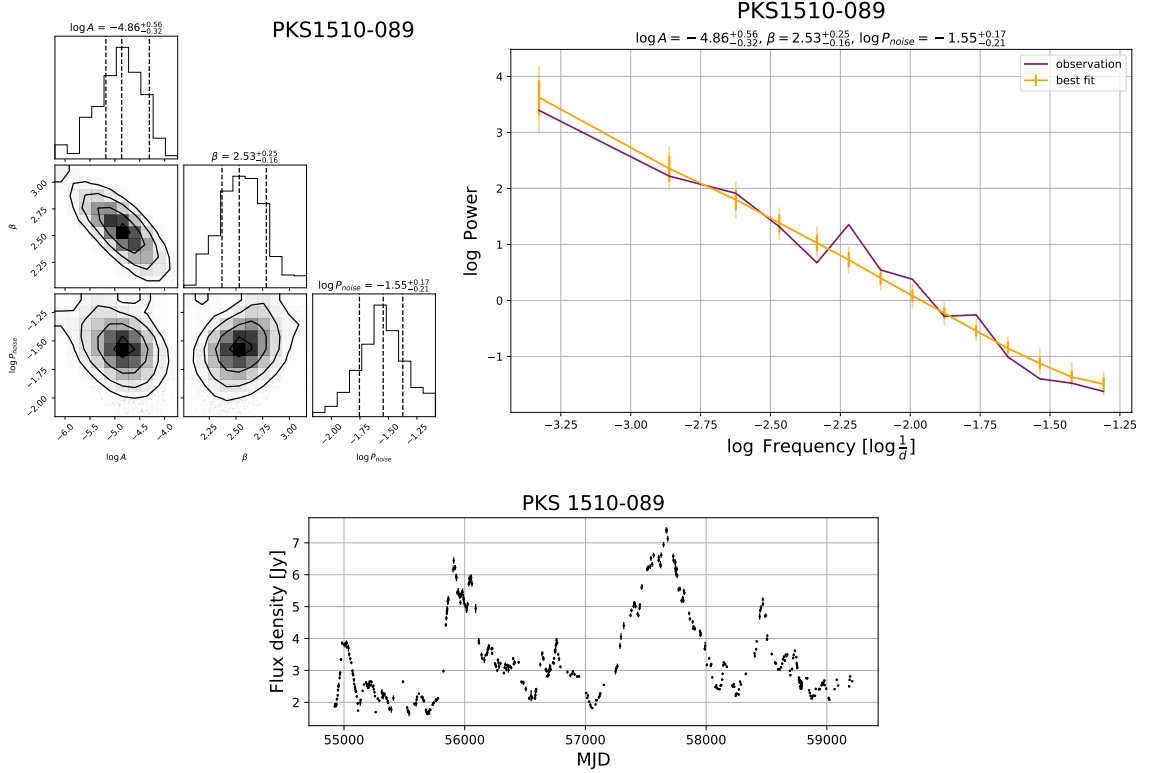


Figure 6.6: Results of fitting the simple power-law model over object PKS 1510-089. Top left: The corner plot between the parameters. Top right: The periodogram with the best fit. The dispersion of each parameter corresponds to the HDI at level 68.3 %. Bottom: The respective light curve.

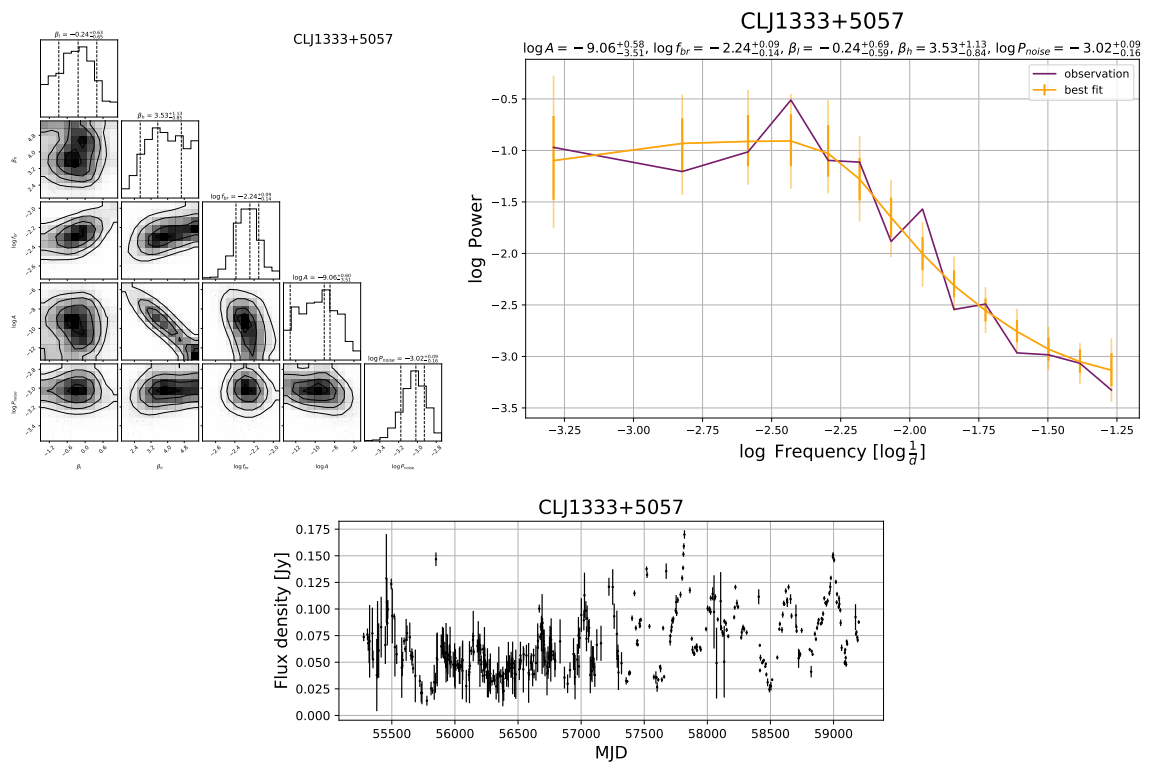


Figure 6.7: Results of fitting the broken power-law model over object CLJ1333+5057. Top left: The corner plot between the parameters. Top right: The periodogram with the best fit. The dispersion of each parameter corresponds to the HDI at level 68.3%. Bottom: The respective light curve.

Chapter 7

Discussion

In order to compare the fitted parameters of each observation with other characteristics of the source, we collected some variables from different source catalogs. Beginning with the flux density in radio-band of each light curve in OVRO catalog, we obtain the mean flux density $\langle F_r \rangle$ and its variance $\text{var}(F_r)$, from the Fermi Gamma-ray Space Telescope (4FGL; Abdollahi et al. 2020) in its second data release DR2 we get which objects are γ -ray sources along with their mean flux density between 1 to 100 GeV $\langle F_\gamma \rangle$, spectral slope β_γ , Variability index Var_γ and the SED class when available. We collected the blazar class classification FSRQ and BL Lac also from the 4FGL-DR2 when available and use other catalogs when is not. These other catalogs are the fifth data release of the BlaZar Catalog (5BZCAT; Massaro et al. 2009), the Candidate Gamma-Ray Blazar Survey (CGRaBS; Healey et al. 2008) and the Combined Radio All-Sky Targeted Eight GHz Survey (CRATES; Healey et al. 2007). The idea is to have a large quantity of sources classified to make a comparison between them. In this sense, we also apply the same strategy to obtain a larger number of redshifts z for our selected observations, adding results from the NASA/IPAC Extragalactic Database (NED; Helou et al. 1991) as a last resort. Finally the Doppler factor δ of various sources, which is related to the relativistic velocity of the emission region (see Appendix A.6), was obtained from Liidakis et al. (2018a).

About the 1010 objects well-defined by the simple power-law model, we look closely at the results for $\beta \geq 4$ since we know that the Hanning window loses effectiveness in this range. A large β value means that the light curve is dominated by timescales longer than the 12 years available in our current observations. Objects with this behavior require more observation time in order to properly fit the periodogram since its current light curve could be hiding the complete behavior of the source. It is important to consider that redshift also plays a fundamental role here, as objects with larger redshifts will show a slower change in variability than objects with lower redshift because of cosmological time dilation, although the effects of relativistic corrections due to fast motion in the jet are probably more important in most blazars. Hence, as a way to verify the radio power-law index (β) of objects that are out of this range, we inspect the light curves of all the 10 sources with $\beta > 4$: J1603+1554 (4.5), J2339-1206 (4.53), J1333+1649 (4.57), J1437+3119 (4.83), J1617-1941 (4.94), CRJ0305-0607

(4.97), J2257+0243 (4.97), 1458+718 (4.97), J1653+3107 (5.04) and J1759+2343 (5.18). Figure 7.1 shows the light curve of all these objects along with their fitted β and redshift z (only if it exists). We consider that all these objects can be removed from the analysis due to two considerations since all of them show a very slow change in their variability, suggesting that β could be even greater. Therefore, we exclude these 10 sources, leaving us with 1039 well-defined objects. 1000 of them being fitted with the simple power-law model, while the remaining 39 with the broken power-law model.

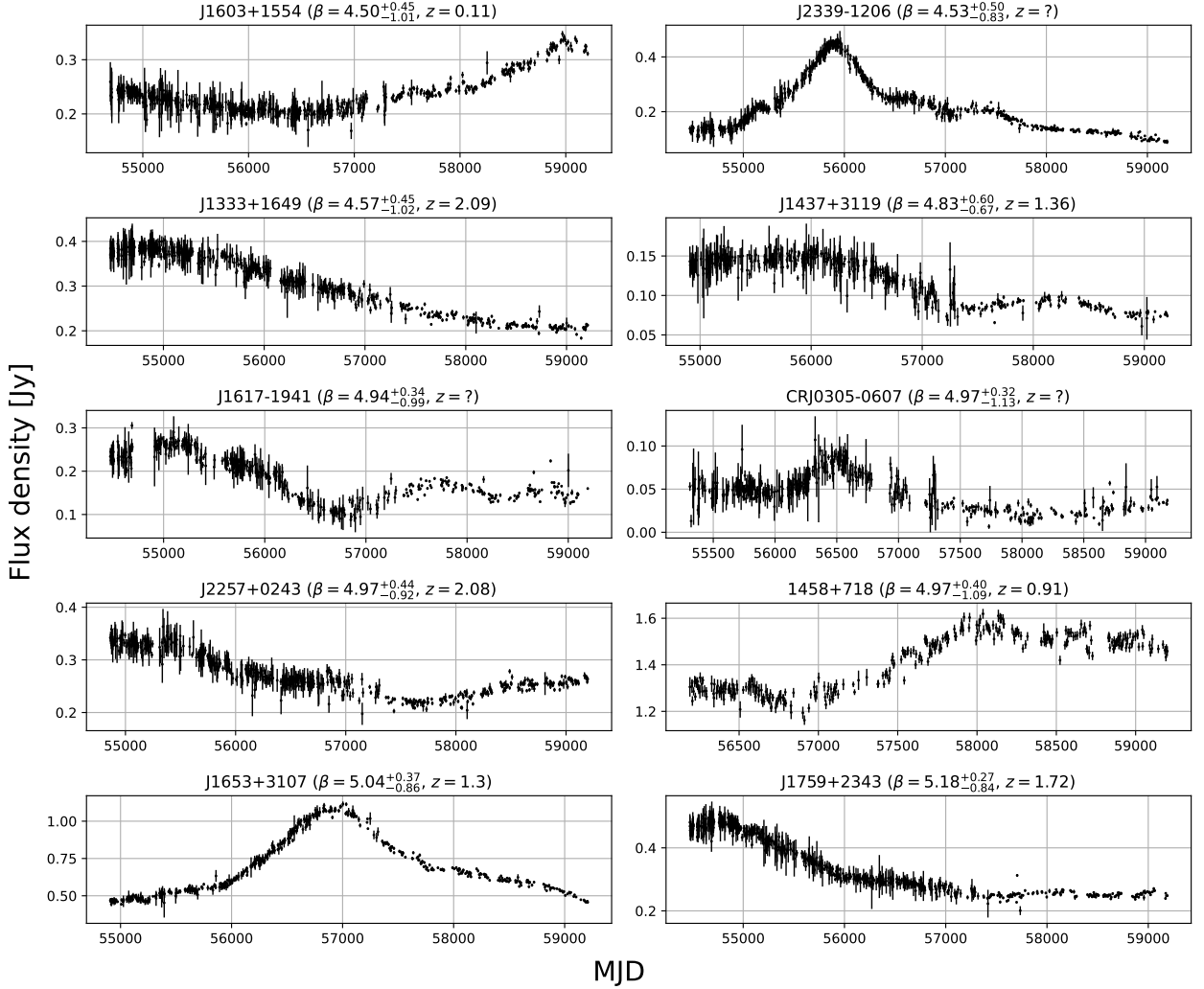


Figure 7.1: Light curves of 10 sources well-defined by the simple power-law model but with a β out of the range $[0, 4]$. All light curves have the common x-axis Modified Julian Day (MJD) and y-axis flux density at Jansky. The name, fitted β and redshift z of each light curve are shown in the titles. Light curves with unknown redshift appear with a ? symbol instead.

A doubt that may remain about these large β values is what occurs in contrast to the broken power-law case where the median of β_h is around 4.05 and the 0.75 quantile is 4.78. The answer is that for all these cases the existence of a break frequency f_{br} means that this high growth in power has a cut-off in a time less than the observational time, so their

light curves show many fluctuations in their flux density with some structure. Figure 7.2 shows the light curves of J0654+4514, the most extreme case of well-defined objects using the broken power-law model having $\beta_h = 5.18^{+0.28}_{-0.93}$ and $\log f_{br} = -2.33^{+0.1}_{-0.09}$, and the source J1759+2343 displayed before, which was well-defined by the simple power-law model and has $\beta = 5.18^{+0.28}_{-0.84}$. As can be seen, J0654+4514 shows fluctuations along all its observation time, while J1759+2343 shows only a gradual change in its variability. Figure 7.3 shows the fitted periodogram of both sources to complement the discussion.

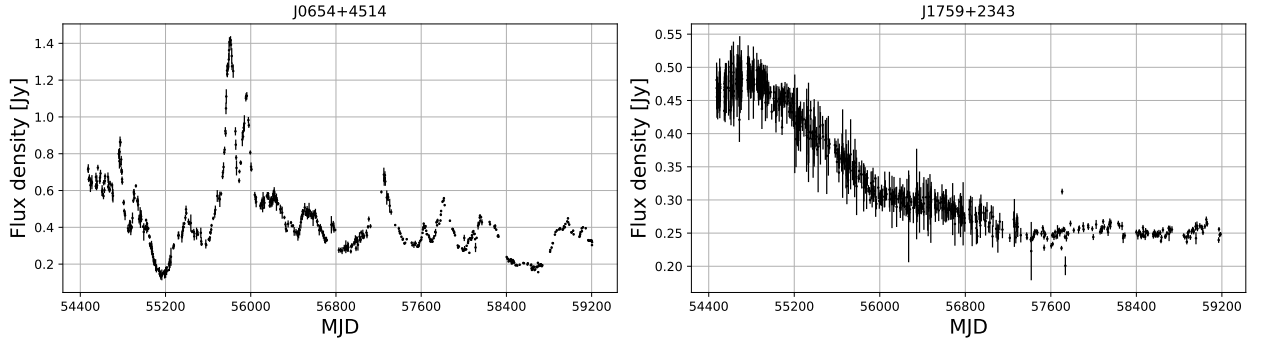


Figure 7.2: Light curves of J0654+4514 (left) fitted with the power-law break model resulting in $\beta_h = 5.18^{+0.28}_{-0.93}$ and $\log f_{br} = -2.33^{+0.1}_{-0.09}$, and J1759+2343 (right) fitted with the simple power-law model having $\beta = 5.18^{+0.28}_{-0.84}$.

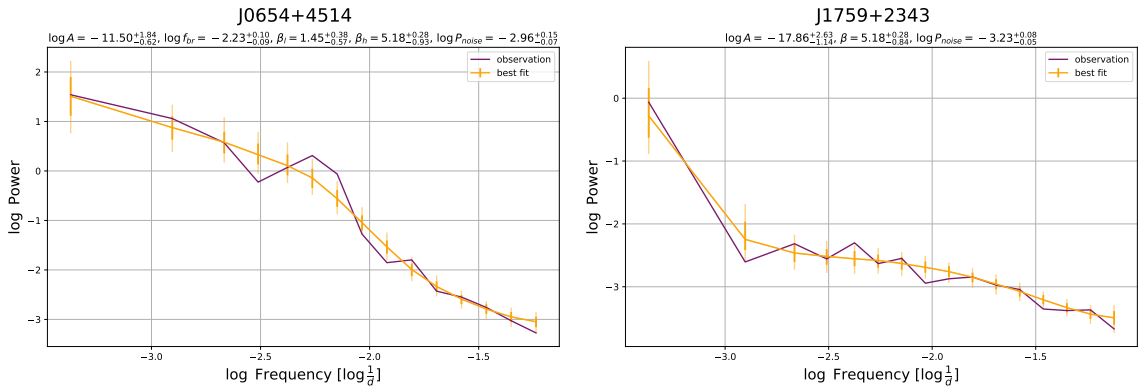


Figure 7.3: Fitted periodogram for both objects from Figure 7.2, J0654+4514 (left) and J1759+2343 (right).

Note that since we remove 10 objects, the summary statistics of $\log A$ and β have been modified. Table 7.1 shows the updated version of Table 6.2. Here we can note that all objects have a power-law index in the range $\beta \in [1.3, 3.8]$.

Table 7.1: Summary statistics of parameters $\log A$ and β of the 1000 objects having $\sigma(\beta)_{68.3\%} < 1.5$ and no well-defined break frequency after excluding sources with large values of beta as discussed in the text.

	Mean	St dev.	Min	Q0.25	Median	Q0.75	Max
$\log A$	-7.174	1.256	-12.271	-7.897	-7.069	-6.393	-2.779
β	2.463	0.386	1.301	2.201	2.446	2.692	3.770

A manual inspection of the light curves from the objects well-defined by the broken power-law model is done as an additional measure. The reason is that if the light curve was not cleaned correctly then an artificial break frequency could appear on the periodogram. Figure B.4 from Appendix shows the light curves of the 39 candidates sorted by $\log f_{\text{br}}$. We note that J1404+0415, which has the lowest $\log f_{\text{br}}$ value and thus it is out of the expected range of log break frequencies, has some atypical points after MJD 56000 with a flux density lower than 0.5 Jy. A more detailed cleaning process, particularly when the spline is applied, would remove these values. Figure 7.4 shows the light curve along with the periodogram with and without this atypical observations. As can be seen, if these anomalous points are removed then the periodogram looks more like having a simple power-law shape than having a break frequency. Hence, we remove J1404+0415 from the objects that are well defined by the broken power-law model. Table 7.2 shows the summary statistics of the model parameters after removing this object from the list of sources with a well-defined break frequency. Note that the log break frequency is defined in the range $\log f_{\text{br}} \in [-2.8, -1.8]$, covering the expected range mentioned in Chapter 5 about testing.

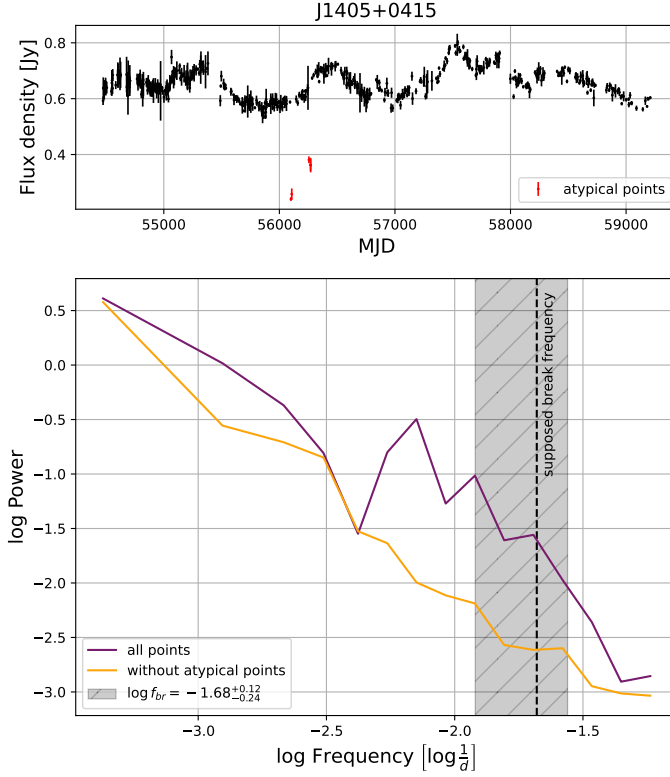


Figure 7.4: Light curve (top) and periodogram (bottom) of J1405+0415 with and without anomalous points. We consider these points atypical since they are out the main behavior of the light curve.

Table 7.2: Summary statistics of parameters $\log A$, $\log f_{\text{br}}$, β_l and β_h of the 38 objects having a well-defined break frequency after a selection process.

	Mean	St dev.	Min	Q0.25	Median	Q0.75	Max
$\log A$	-9.488	1.904	-13.222	-11.255	-9.188	-8.094	-4.780
$\log f_{\text{br}}$	-2.407	0.267	-2.834	-2.611	-2.422	-2.247	-1.798
β_l	0.251	0.849	-1.206	-0.305	0.300	0.976	1.575
β_h	4.085	0.759	2.863	3.443	4.057	4.801	5.178

From the final 1000 objects well-defined by a simple power-law, in the optical spectrum classification context 692 of them are FSRQ and 171 BL Lac. There are other classification as Blazar Candidates of Unknown type (BCU) and Flat-Spectrum Radio Source (FSRS), the complete list of classification with their respective reference and number of objects appears on Table 7.3. About the SED classification from 4FGL-DR2, 493 of them are LSP, 29 ISP and 10 are HSP. In the γ -ray context, 563 of them are γ -ray sources while the others 438 are not. 889 sources have a known redshift and 765 have a known Doppler factor δ . On the other hand, from the final 38 well-defined objects having a break frequency, in the optical spectrum classification context 24 of them are FSRQ and 7 BL Lac, while the the remaining objects are classified as BCU (3), NLSy1 (3) and RDG (1). Table 7.4 contains the references

for each classification. If we check the SED classification, 30 of them are LSP and 2 are ISP. In the γ -ray context, 33 of them are γ -ray sources while the others 5 are not. Only 34 sources have a known redshift, while 33 have a known Doppler factor δ .

Table 7.3: Classification of the final 1000 sources well-defined by the simple power-law model. Objects with OVRO as reference come from various sources and need to be verified. Note that objects classified as BL Lac-galaxy dominated, CSS, FSRQ, NLRG, NLSy1, RDG and SSRQ can be also be classified as AGNs.

Classification	Reference	N° objects
AGN	4FGL	1
	CGRABS	3
	OVRO	1
BCU	4FGL	38
	BZCAT	14
BL Lac	4FGL	157
	BZCAT	11
	CGRABS	1
	OVRO	2
BL Lac-galaxy dominated	BZCAT	7
CSS	4FGL	1
	O'Dea (1998)	2
FSRQ	4FGL	357
	BZCAT	315
	CGRABS	16
	CRATES	1
	OVRO	3
FSRS	CRATES	56
NLRG	CGRABS	4
NLSy1	4FGL	1
	OVRO	1
RDG	4FGL	7
SSRQ	4FGL	1

Table 7.4: Classification of the final 38 sources well-defined by the broken power-law model.

Classification	Reference	N° objects
BCU	4FGL	3
BL Lac	4FGL	6
	BZCAT	1
FSRQ	4FGL	20
	BZCAT	4
NLSy1	4FGL	3
RDG	4FGL	1

7.1. Comparison with previous results

The previous largest study of PSD characterization in radio-band comes from Max-Moerbeck (2013), a PhD thesis that fits a total of 424 objects from OVRO dataset with light curves observed between mid-2007 and the end of 2012 in order to study the relationship between radio and γ -ray emission of blazars. Max-Moerbeck (2013) used the Power Spectral RESPonse (PSRESP) described in Uttley et al. (2002), which is based on the Fourier Decomposition method to simulate light curves, reporting the best β obtained along with the p -value of each test and error bars at percentile 68.3%. When considering only our fits for the same objects as Max-Moerbeck (2013), we obtained results for 388 of them. The exclusion of the other 36 objects is thoroughly explained in Chapter 6 due to the definition of a well-defined fit. Note that our study involves approximately 12 years of data, whereas Max-Moerbeck (2013) utilized light curves with a maximum duration of nearly 4 years. In addition, there are other differences in the minimum timescale of blazar variability and the length of the simulated light curves. While we use a minimum timescale of 3 days, based on Koay et al. (2019), and a length 3 times longer than the one for the source we fit, Max-Moerbeck (2013) used a minimum timescale of 1 day and a length 4 times longer. Moreover, the cleaning processes between the two studies are different. Despite these disparities and the absence of a direct comparison between both methods, we want to check if there are hints of changes in the variability characteristics of these sources, and to discard any major inconsistencies between these two methods.

To compare the reported results, we examine the consistency of the parameter β using the HDI at 68.3% for our findings and the values β_{low} , β_{up} from Max-Moerbeck (2013). Figure 7.5 shows a comparison of the error bars where β_{old} and β_{new} refers to the β values reported by Max-Moerbeck (2013) and our thesis, respectively. The plot is separated according to the consistency of the results, revealing that 77 out of the 388 objects are not consistent, corresponding to roughly 20%. Population differences at this level are expected for 1σ error bars, that statistically are expected to contain the real value of the estimated parameter 68.3% of the time.

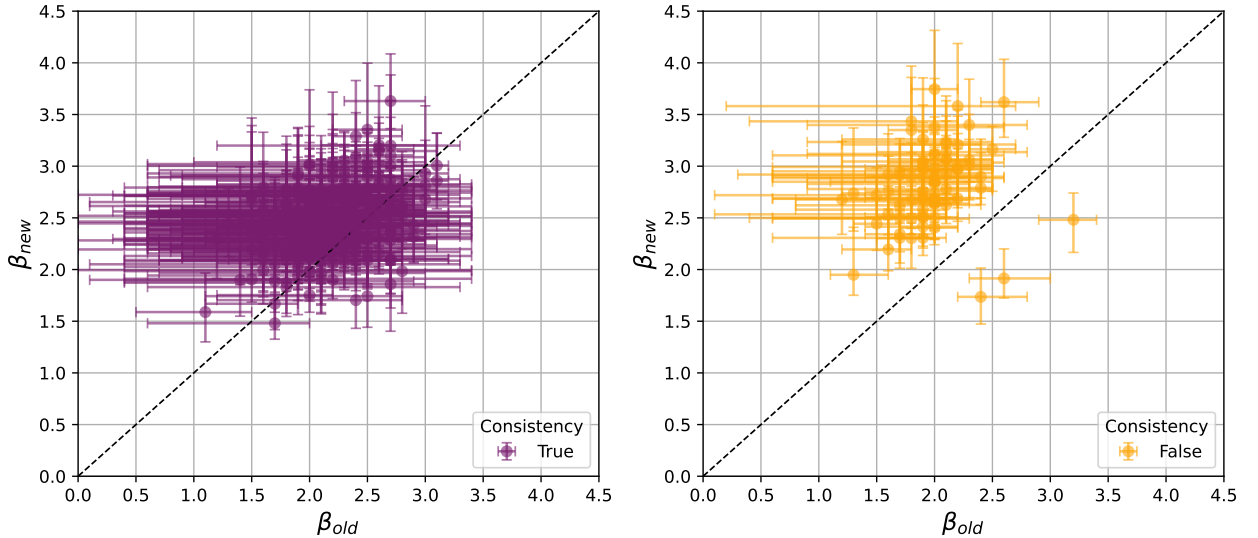


Figure 7.5: Comparison of the β values obtained by this thesis (β_{new}) and previous results β_{old} from Max-Moerbeck (2013). The segmented diagonal black line is to guide the reader. Left: The 311 objects with consistent error bars between bot results. Right: The 77 objects with no consistency.

We note that on average our results are deviated to a larger β value with respect to the older results. Indeed, for our results we have a mean $\langle \beta_{\text{new}} \rangle = 2.54$, while Max-Moerbeck (2013) reported results with a mean $\langle \beta_{\text{old}} \rangle = 2.13$, i.e., an increment of 0.41. From the non-consistent objects, 74 show a β_{new} larger than the previous results, while only 3 objects have a lower new power-law index. We suggest that the differences between both studies mentioned above could explain the non-consistent results and the deviation of β to larger values. Since the light curves used in this thesis were three times longer, they could capture different variability characteristics in the sources. Figures B.6 to B.10 show the light curves of all non-consistent objects with a segmented red line representing the end of 2012, which corresponds to the length of the light curves in Max-Moerbeck (2013). These hypotheses could be tested by fitting these objects using the same period of time, minimum timescale, and cleaning process used by Max-Moerbeck (2013). However, since our method was tested in a self-consistent way as described in Chapter 5, and it is also more flexible and fast, we consider this unnecessary and recommend its adoption for future publications.

If we take a look at the size of the error bars, we find that our results have lower dispersion on average with a mean $\langle \sigma(\beta_{\text{new}})_{68.3\%} \rangle = 0.69$ versus $\langle \sigma(\beta_{\text{old}})_{68.3\%} \rangle = 1.41$ for the previous results. Figure 7.6 shows the distributions for both results, remember that we are using the HDI level at 68.3% while Max-Moerbeck (2013) used the percentile at 68.3%. Despite this discrepancy in the definition of the error bars, we consider that they are still comparable in this context. Obviously, and as was explained in Chapter 6, our results only consider fits with a dispersion lower than 1.5, this is the reason for the cut off into the dispersion for CosmoABC results. If we compare the size of the error bars per fitted object, 300 of them have a dispersion lower than the previous results, having 245 of them consistency on the

β values. On the other hand, 88 are in the opposite scenario having larger error bars with CosmoABC, being 66 of them consistent with the previous β value.

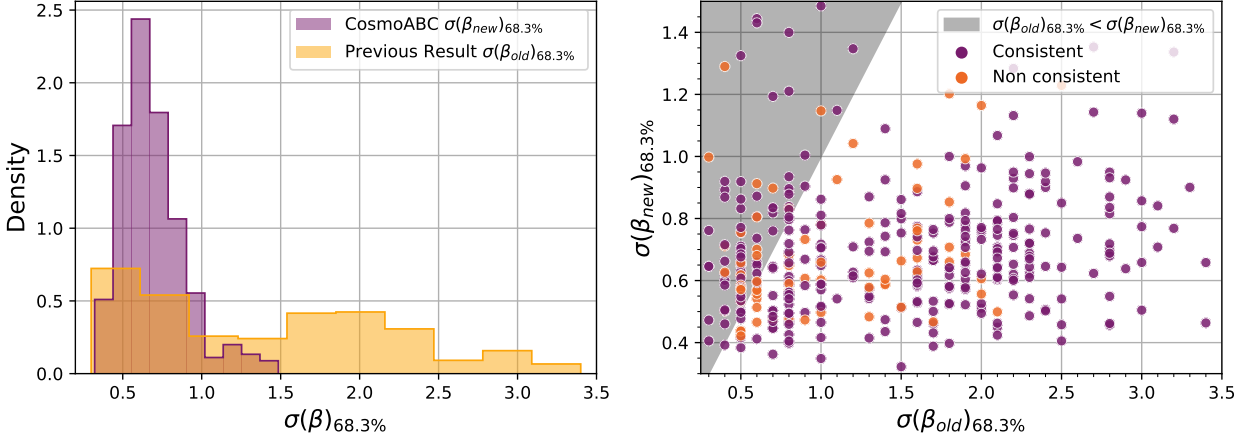


Figure 7.6: Left: Distribution of the dispersion in the β values of the objects that were fitted using CosmoABC (purple) and also were fitted in Max-Moerbeck (2013) (yellow). Our results consider the dispersion at HDI level 68.3%, while the results from Max-Moerbeck (2013) consider percentile at 68.3%. Right: Scatter plot of both dispersions, the gray area corresponds to the area where error bars from Max-Moerbeck (2013) are smaller than the results using CosmoABC.

Additionally, we compare our results with the ones from Goyal et al. (2022), where the periodogram of objects 3C 279 (also known as J1256-0547) and PKS 1510-089 were fitted also with the OVRO data until the end of December 2020. Table 7.5 show the results from this paper along with the fits from Max-Moerbeck (2013) and our fit using CosmoABC. It is clear that we have consistent results for both objects but with a clearly smaller dispersion with respect to Goyal et al. (2022).

Table 7.5: Power-law index β for two objects obtained by Max-Moerbeck (2013) using almost 4 years of OVRO data, and Goyal et al. (2022) along with our results using CosmoABC for almost 12 years of OVRO data.

	β Max-Moerbeck (2013)	β Goyal et al. (2022)	β CosmoABC
3C 279	2.4 ± 0.2	2.5 ± 1.1	$2.43^{+0.34}_{-0.25}$
PKS 1510-089	$2.3^{+0.6}_{-0.7}$	2.1 ± 1	$2.53^{+0.25}_{-0.16}$

Overall, we consider that the proposed fitting method represents an improvement in the sense that it reduces the computation time and allows the user to employ more complex PSD models with good error estimates.

7.2. Power law with and without break

As we described in the chapter before, only 38 of 1038 sources have a well-defined break frequency, which corresponds to approximately to 3.71 % of all objects. All of these 38 sources show a $\beta_l < \beta_h$, which make sense physically speaking since AGNs are not infinite objects with infinite energy and must have a cut-off in its power for a certain low frequency such that for frequencies even lower the power should remains constant. In that sense, it expects that all of them have a break frequency.

We estimate the likelihood of having a well-defined break frequency by defining a Binomial distribution $B(n, p)$ where n is the total number of observations and p the probability of having the break. To estimate the probability we employ the estimator $\hat{p} = \frac{x}{n}$ where x is the number of observations that actually have a break frequency. This estimation is done for different classifications of the data:

1. Blazar Optical Spectrum classification FSRQ and BL Lac
2. SED classification LSP, ISP and HSP
3. γ -ray and non γ -ray sources¹
4. Redshift range $0 < z \leq 1$ and $z > 1$
5. Doppler factor range $0 < \delta \leq 10$ and $\delta > 10$

With the purpose of checking the stability of the estimator \hat{p} and being able to compare the results of each estimator between the different classifications, we obtain a confidence interval using the Jeffreys interval method. The Jeffreys interval method is a Bayesian approach to construct confidence intervals for probability parameters, particularly beneficial for cases with small sample sizes or extreme probabilities². We prefer this method over others as the Normal approximation interval method since it allows to define an upper limit even for the cases where $\hat{p} = 0$. Table 7.6 shows a summary of results for all these classification with its respective \hat{p} and its 95 % confidence interval, while Figure 7.7 displays the \hat{p} of each classification as error bars. Note that the classifications γ -ray sources, redshift range and Doppler factor range show \hat{p} -values that do not intersect each other. We compare the \hat{p} values of each classification using a two proportion z-test, obtaining a significance level of 3σ for all of them. This suggests that it is more likely to find a break frequency on γ -ray sources than in no γ -ray sources, that

¹ To define a source as a γ -ray emitter, we consider that the source must have a γ -ray flux density detectable by the primary instrument of the Fermi Gamma-ray Space Telescope called Large Area Telescope (LAT). Although this definition is not completely exact and newer technologies would give better results, due the current technological limitation we consider that this definition of γ -ray emitters is enough to separate the objects between γ -ray and non γ -ray sources. Hence, we make the assumption that sources that are not in the data catalog release 4FGL-DR2 can be defined as non γ -ray sources.

² Brown et al. (2001) contains an extensive explanation of this method and other methods as well for interval estimation in a Binomial proportion context.

objects with a redshift lower than 1 are more likely to have a break frequency that the ones with a redshift larger than 1, and that objects with a Doppler factor higher than 10 are more likely to have a break frequency that the ones with a Doppler factor smaller than 1.

Table 7.6: Different results for each classification about the estimation of \hat{p} assuming that finding a well-defined break frequency can be modeled as a Binomial distribution $B(n, p)$. x corresponds to the number of observations that actually have a break frequency, n to the total number of observations and $\hat{p} = \frac{x}{n}$ to the estimator of the probability of having a break. $\hat{p}_{low}^{95\%}$ and $\hat{p}_{up}^{95\%}$ indicate the lower and upper bounds of \hat{p} considering a 95 % confidence interval and were calculated using Jeffreys interval method.

	x	n	\hat{p}	$\hat{p}_{low}^{95\%}$	$\hat{p}_{up}^{95\%}$
FSRQ	24	716	0.0335	0.0222	0.0486
BL Lac	7	178	0.0393	0.0178	0.0757
LSP	30	523	0.0574	0.0398	0.0798
ISP	2	31	0.0645	0.0136	0.1912
HSP	0	10	0	0	0.2172
γ -ray source	33	596	0.0554	0.0391	0.0759
no γ -ray source	5	443	0.0113	0.0043	0.0246
$0 < z \leq 1$	27	454	0.0595	0.0405	0.0841
$z > 1$	7	467	0.0150	0.0067	0.0292
$0 < \delta \leq 10$	27	427	0.0632	0.0430	0.0893
$\delta > 10$	6	371	0.0162	0.0068	0.0330



Figure 7.7: Results from Table 7.6 displayed as error bars plots for each classification. (a) Classification using the optical spectrum: FSRQ and BL Lac. (b) SED class from 4FGL-DR2: LSP, ISP and HSP. (c) γ -ray and non γ -ray sources from 4FGL-DR2. (d) Redshift range lower and greater than 1. (e) Doppler factor range lower and greater than 10.

The result for the redshift range and Doppler factor is consistent with the previous discussion about the variability scale, being the objects with low redshift and high Doppler factor the ones observed for a longer timescale in their source frame. Hence, we can say that objects with a redshift $0 < z \leq 1$ are 3.5 times more likely of having a break frequency, and that objects with a Doppler factor $\delta > 10$ are 3.9 times more likely of having a break frequency. In the case of γ -ray sources, they are 4.1 more likely to have a break frequency compared to non γ -ray sources. In this same context, we suggest that the angle of sight θ_{obs} of these sources plays an important role because γ -ray sources typically exhibit very low θ_{obs} values. This is directly connected with the Doppler factor, as objects with a low θ_{obs} also tend to have higher δ values.

To gain an initial understanding that may lead to more interesting findings, we also examine the difference in distributions of parameters redshift z , Doppler factor δ , log of the mean flux in radio $\log\langle F_r \rangle$, log of the variance of the flux in radio $\log \text{var}(F_r)$, log of the mean flux in γ $\log\langle F_\gamma \rangle$, the γ -ray spectral slope β_γ and the log of the variability index $\log \text{Var}_\gamma$ for the 1000 sources well-defined using a simple power-law model and the 38 others with a well-defined break frequency. Figures 7.8, 7.9 and 7.10 show the distributions of these parameters, referring as *Simple* to objects using the simple power-law model and *Broken* to the ones using the broken power-law model. In order to compare these distributions statistically, we employ the Anderson-Darling test (Anderson & Darling 1952) with the null hypothesis that samples from Simple and Broken come from the same distribution, i.e., there is no statistical difference between the distribution of the parameter for the simple power-law model and the broken power-law model. The result of these tests are displayed in Table 7.7, showing that only variables related to the flux density in radio can be rejected at the 1% level. Hence, the redshift and γ -ray variables show distributions significantly different between both models. These results support the previous premise about the different probability of finding a break frequency with respect to a certain redshift range and being or not a γ -ray source.

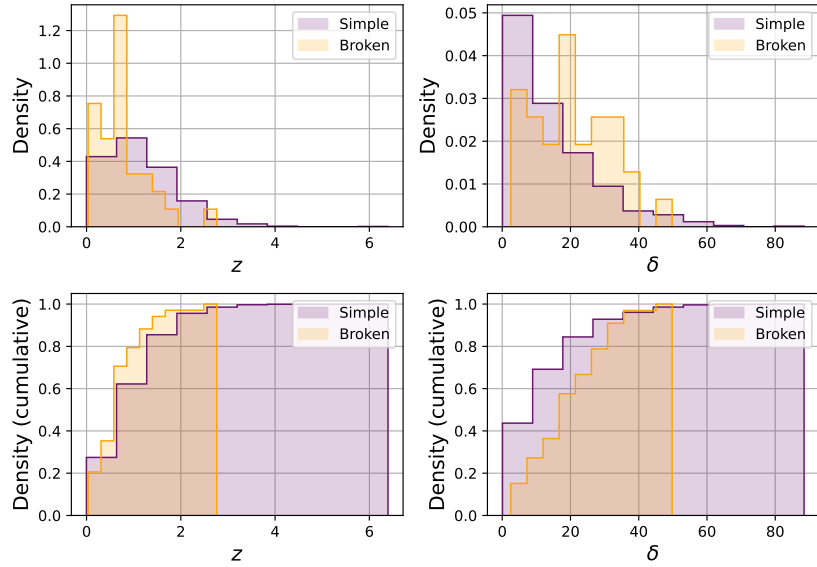


Figure 7.8: Comparison of distributions of parameters redshift z and Doppler factor δ between the results of the 1000 sources best fitted with the simple power-law model (Simple) and the 38 best fitted with the broken power-law model (Broken).

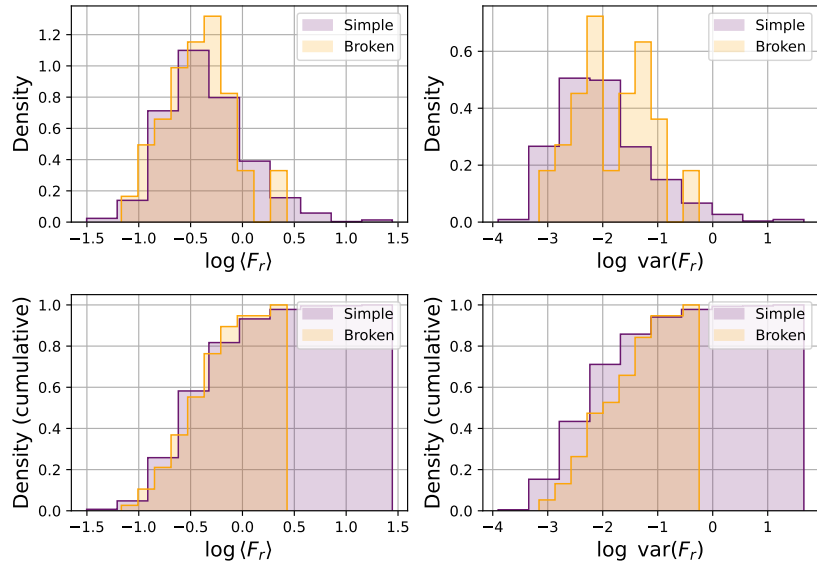


Figure 7.9: Same as Figure 7.8 but for parameters in radio-band: log of the mean flux $\log(F_r)$ and log of the variance of the flux in radio $\log \text{var}(F_r)$.

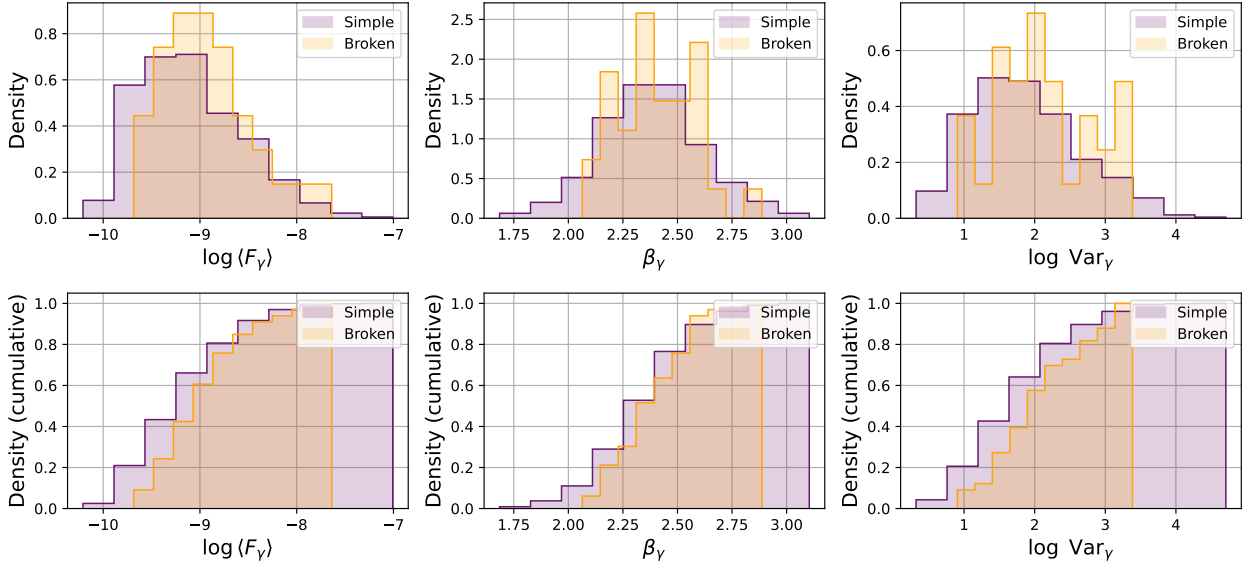


Figure 7.10: Same as Figure 7.8 but for γ -ray parameters: $\log \langle F_\gamma \rangle$, spectral slope β_γ and $\log \text{Var}_\gamma$.

Table 7.7: Anderson-Darling test for each parameter with respect to the distributions of objects with and without a break frequency. The null hypothesis refers to that the samples come from the same distribution, i.e., there is no statistical difference between the distribution of the parameter for the simple power-law model and the broken power-law model, and it is rejected at level 1%.

Parameter	Statistic	p -value	Reject null-hyp at 1%
z	4.702	0.005	Yes
δ	2.598	0.028	No
$\log \langle F_r \rangle$	-0.626	>0.25	No
$\log \text{var} \langle F_r \rangle$	1.583	0.072	No
$\log \langle F_\gamma \rangle$	8.920	<0.001	Yes
β_γ	9.758	<0.001	Yes
$\log \text{Var}_\gamma$	8.301	<0.001	Yes

7.3. Break-frequency analysis

As was previously explained in this thesis, a break on the periodogram means a characteristic time for which the object modifies its behavior changing the slope of the PSD. We can retrieve this characteristic time from parameter $\log f_{\text{br}}$ as $t_{\text{br}} = 10^{-\log f_{\text{br}}}$. Remember that we removed one of the objects fitted with a break frequency, having now a $\log f_{\text{br}}$ distribution with a mean of -2.407 and a standard deviation of 0.267 as can be seen in Table 7.2. For the characteristic time, we obtain a t_{br} distribution with a mean and standard deviation of 0.83 and 0.49 years, respectively. However, we are not considering the difference on timescale due the Doppler effect from the redshift of each source and the relativistic velocity of its

emission region. As we know, for a redshift z , the frequency emitted f_{em} from the source and observed f_{obs} by the observer follows the relationship $f_{\text{em}} = (1 + z)f_{\text{obs}}$. On the other hand, a relativistic emission region with a Doppler factor δ has the relationship $f_{\text{em}} = \delta^{-1}f_{\text{obs}}$ (See Appendix A.6). Connecting both relationships the final correction by the Doppler effect is

$$\begin{aligned} f_{\text{em}} &= \frac{1+z}{\delta} f_{\text{obs}} \\ \Rightarrow f_{\text{obs}} &= \frac{\delta}{1+z} f_{\text{em}} \\ \Rightarrow \log f_{\text{obs}} &= \log \left(\frac{\delta}{1+z} f_{\text{em}} \right) \end{aligned} \quad (7.1)$$

Hence, as long as we know the redshift z and Doppler factor δ of a source we can obtain a corrected break frequency $f_{\text{br,corr}}$, i.e., the break frequency in the rest frame of the source, and with that a corrected characteristic time $t_{\text{br,corr}}$. An important aspect that we must consider is the propagation of errors. Since we are in front of asymmetric uncertainties with respect to δ and $\log f_{\text{br}}$, the error propagation cannot be resolved in the typical way. In this context the easier solution is to do arithmetic with the distributions of each parameter, however, we only have distributions for the break frequency, while for δ we have the error at confidence 68%. A solution for this kind of problem was proposed by Barlow (2004), where the errors are propagated using MCMC with a *linear variable width Gaussian* likelihood³. Using this approach, we can determine the break frequency in the rest frame $f_{\text{br,corr}}$ and characteristic time $t_{\text{br,corr}}$ with their respective error bars. Figure 7.11 shows these corrections for the different AGN classifications, where we assume a redshift error of 0.0001 at confidence 99.75%. We obtain a $\log f_{\text{br,corr}} = -3.42 \pm 0.28 \left[\log \frac{1}{d} \right]$ on average and a characteristic time of $t_{\text{br,corr}} = 8.64 \pm 5.34$ years. The plot of the characteristic time shows three objects with errors out of 3 standard deviations: the FSRQs C1239+0443 and J0457+0645; and the BL Lac J0527+0331. In any case, the scale remains in the order of decades.

³ The `asymmetric_uncertainties` package for Python has an implementation of this method.

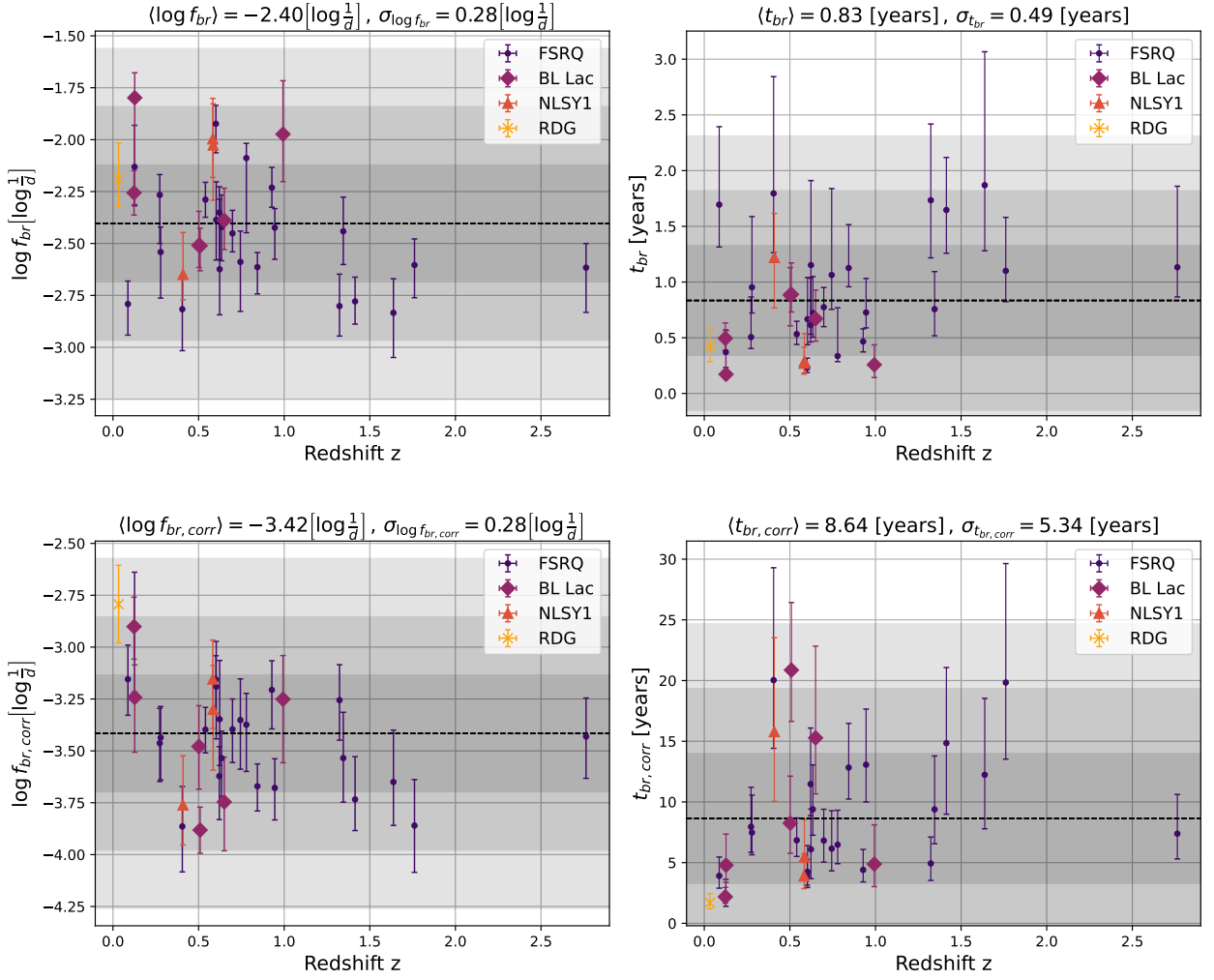


Figure 7.11: Break frequency and characteristic time with their respective error bars versus the redshift in the observer frame (top) and the source rest frame (bottom). Different colors correspond to different AGN classifications, the segmented line correspond to the mean and the gray area to 1 to 3 standard deviations from the mean.

As a way to measure how deviated each AGN classification is from the average result, we obtain the mean and standard deviation of the break frequency in the source rest frame and the characteristic time of each classification. Figure 7.12 show these results, where we have 24 FSRQ, 6 BL Lac and 3 NLSy1. We also calculate the mean for the cases of being or not a γ -ray source, which are illustrated in Figure 7.13 where we have 29 sources emitting in γ -band versus 5 that are not. Note as all of the cases have a $\langle \log f_{br,corr} \rangle$ very close to the average $\langle \log f_{br,corr} \rangle = -3.42$. This result is an indication that all these classifications have a similar break scale, or in other words, that the break frequency has no dependency with respect to the AGN classification or with being or not a γ -ray source. Table 7.8 summarizes the corrections done for each of these classifications.

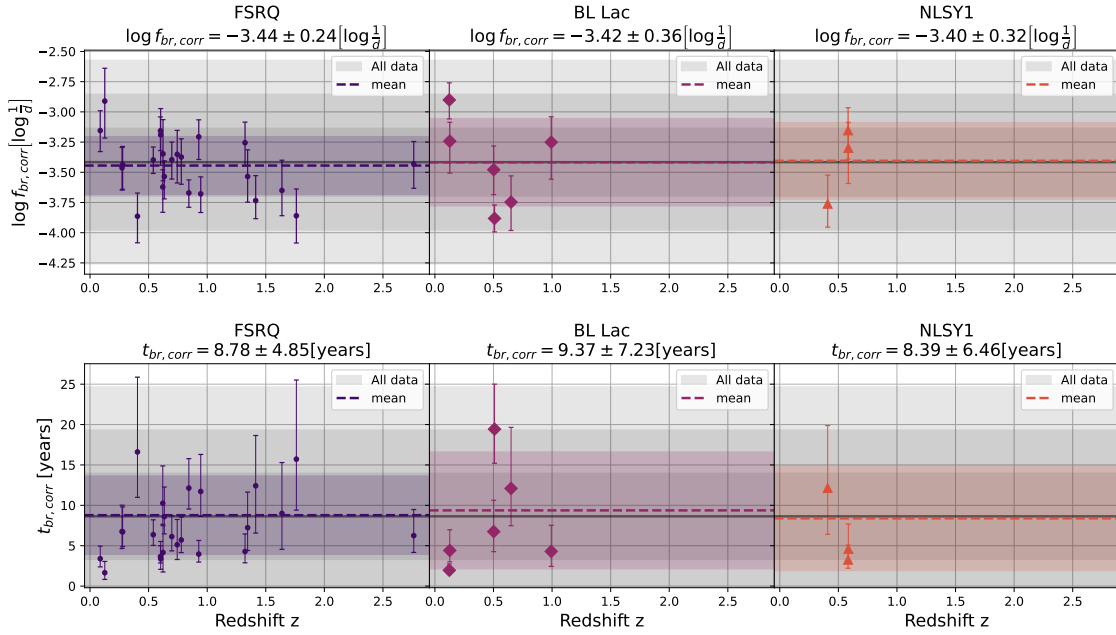


Figure 7.12: Similar to Figure 7.11 but for each AGN classification separately. The gray area represent 1 to 3 standard deviations from the mean (gray line) of all data.

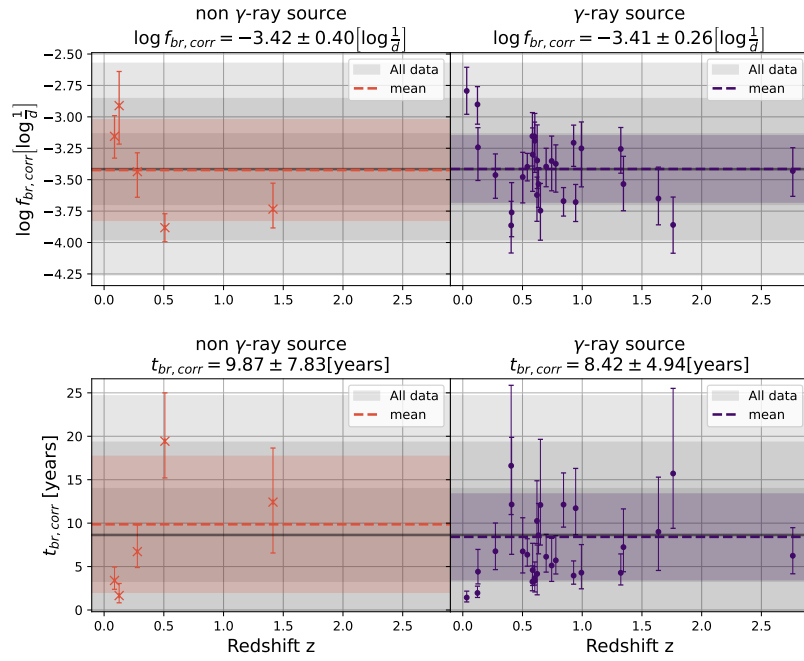


Figure 7.13: Similar to Figure 7.11 but for the classification of being or not a γ -ray source. The gray area represents 1 to 3 standard deviations from the mean (gray line) of all data.

Table 7.8: Results of the log break frequency in the source rest frame $\log f_{\text{br,corr}}$ and the corrected time $t_{\text{br,corr}}$ after using equation 7.1 for different classifications.

Classification	$\log f_{\text{br,corr}} \left[\log \frac{1}{d} \right]$	$t_{\text{br,corr}}$ [years]
All	-3.42 ± 0.28	8.64 ± 5.34
FSRQ	-3.44 ± 0.24	8.78 ± 4.85
BL Lac	-3.42 ± 0.36	9.37 ± 7.23
NLSy1	-3.40 ± 0.32	8.39 ± 6.46
γ -ray	-3.41 ± 0.26	8.42 ± 4.94
non γ -ray	-3.42 ± 0.40	9.87 ± 7.83

An interesting question that arises from these results is, given the correction in the timescale and the reduced number of objects with a well-defined break frequency, is the timescale of the other objects not large enough to find a break? Let's keep in mind that all objects must have a break in their periodogram since the emitted energy is not infinite. This question can be answered looking at the corrected minimum frequency of each object compared to the distribution of break frequencies. Figure 7.14 shows the distribution of corrected minimum frequency for the objects where redshift and the Doppler factor was available, along with the distribution of the corrected break frequencies. As can be seen, there is a large number of objects fitted with the simple power-law model with a minimum frequency similar to the one for the objects fitted with the broken power-law model. Thus, why do we not see a break frequency for these objects? We propose two scenarios:

1. The physical process that produces the variability on the objects with a well-defined break frequency is different to the process of the objects without a break in their periodogram. In this case a further analysis of the objects with a break frequency could give new answers.
2. The difference depends on the mass, luminosity or another physical property of the source. This is consistent with results from McHardy et al. (2006) where they find a plane which relates the break timescale with the mass and bolometric luminosity of the objects, and also with Liidakis et al. (2017) where they find that the mass and luminosity, from microquasars to blazars, are scale invariants.

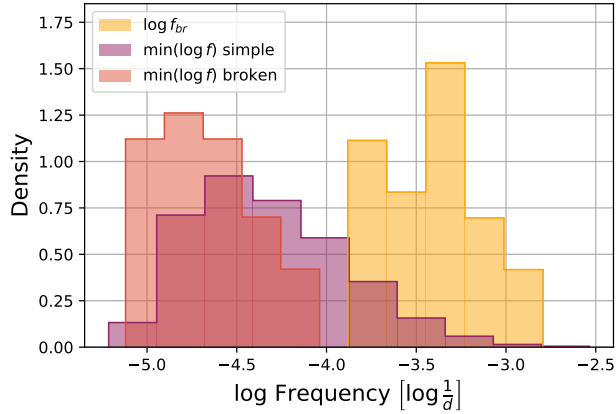


Figure 7.14: Distribution of the corrected minimum frequency of all fitted objects, in purple the best fitted with the simple power-law model and in red the best fitted with the broken power-law model, and the corrected break frequencies found in orange.

7.4. FSRQ vs BL Lac

From the 1038 final objects, 716 of them correspond to FSRQ and 178 to BL Lac. We compare the results between FSRQ and BL Lac on a similar way as how were compared the different observational parameters for objects fitted with both models in Section 7.3 using an Anderson-Darling test, but in this case we run the analysis of the simple power-law model and the broken power-law model separately only for radio parameters and adding the model parameters of each one. The goal is to check for significant statistical differences in the parameter distributions between the two classifications, which may indicate a different origin between the classes.

7.4.1. Broken model

For the broken power-law model 24 objects are classified as FSRQ and 7 as BL Lac. Table 7.9 shows a summary of the statistics for a series of parameter including the ones of the model under this context, while Table 7.10 shows the result of the Anderson-Darling test over these parameters as a way to compare the distributions of FSRQ and BL Lac for each PSD and radio parameter. Although no parameters can be rejected at the 1% level, we consider the sets of FSRQs and BL Lacs are too small to make strong conjectures.

Figure B.11 displays a scatter plot along with a KDE plot of the model parameters versus other parameters as a way to inspect relationships and/or differences between the classification for each parameter. For this case of the broken power-law model fitted between FSRQ and BL Lac we see no substantial difference nor relationships. Perhaps, $\log A$ vs $\log \text{Var}_\gamma$ and $\log f_{\text{br}}$ vs $\log \langle F_\gamma \rangle$ for BL Lac class show some correlation, but again, the set of BL Lac sources is too small to make any strong conjecture.

Table 7.9: Summary statistics of the different parameters tested for the broken power-law model with respect to the optical spectrum classification.

Parameter	Class	Mean	Std.	Q0.25	Median	Q0.75
β_l	BL Lac	0.08	0.82	-0.51	0.13	0.76
	FSRQ	0.28	0.81	-0.27	0.37	0.94
β_h	BL Lac	3.77	0.79	3.04	4.01	4.27
	FSRQ	4.16	0.77	3.45	4.14	4.97
$\log f_{\text{br}}$	BL Lac	-2.25	0.27	-2.45	-2.32	-2.11
	FSRQ	-2.47	0.25	-2.62	-2.45	-2.28
$\log f_{\text{br,corr}}$	BL Lac	-3.42	0.36	-3.68	-3.36	-3.24
	FSRQ	-3.44	0.24	-3.64	-3.43	-3.30
$\log A$	BL Lac	-8.63	2.25	-10.10	-8.89	-7.52
	FSRQ	-9.77	1.83	-11.39	-9.68	-8.33
$\log \langle F_r \rangle$	BL Lac	-0.41	0.35	-0.60	-0.42	-0.35
	FSRQ	-0.42	0.31	-0.62	-0.37	-0.18
$\log \text{var}(F_r)$	BL Lac	-1.80	0.72	-2.15	-2.12	-1.65
	FSRQ	-1.79	0.67	-2.35	-1.61	-1.31

Table 7.10: Similar to Table 7.7, but the Anderson-Darling test is with respect to the observed spectrum classification FSRQ and BL Lac for all sources fitted using the broken power-law model, being 24 of them FSRQ and 7 BL Lac.

Parameter	Statistic	p -value	Reject null-hyp at 1 %
β_l	-0.923	>0.25	No
β_h	0.851	0.146	No
$\log A$	-0.203	>0.25	No
$\log f_{\text{br}}$	1.102	0.115	No
$\log f_{\text{br,corr}}$	-0.158	>0.25	No
$\log \langle F_r \rangle$	-0.510	>0.25	No
$\log \text{var}(F_r)$	-0.328	>0.25	No

7.4.2. Simple model

For the simple power-law model 692 objects are classified as FSRQ and 171 as BL Lac. Table 7.11 shows a summary of the statistics of each parameter under this context, while Table 7.12 shows the result of the Anderson-Darling test on the same way as the previous subsection. In this case the null hypothesis of the model parameters β and $\log A$ can be rejected at level 1 %, note that the summary statistics of these parameters for each class differs considerably, which finally suggests that the PSD characterization is different between FSRQ and BL Lac sources. This give us a clue that the variability on radio-band and the optical spectrum of blazars are linked somehow, so a further study is required to understand

this part. On the other hand, parameters with respect to the flux density at radio-band have a large p -value, therefore, we can not talk about a difference in flux density at radio-band between FSRQ and BL Lac.

Table 7.11: Summary statistics of the different parameters tested for the simple power-law model with respect to the optical spectrum classification.

Parameter	Class	Mean	St dev.	Q0.25	Median	Q0.75
β	BL Lac	2.37	0.35	2.14	2.37	2.57
	FSRQ	2.50	0.39	2.25	2.48	2.73
$\log A$	BL Lac	-6.81	1.23	-7.61	-6.81	-5.99
	FSRQ	-7.26	1.24	-7.94	-7.12	-6.48
$\log\langle F_r \rangle$	BL Lac	-0.40	0.40	-0.66	-0.39	-0.15
	FSRQ	-0.32	0.38	-0.59	-0.37	-0.10
$\log \text{var}(F_r)$	BL Lac	-1.97	0.84	-2.69	-1.97	-1.45
	FSRQ	-1.94	0.82	-2.52	-2.07	-1.48

Table 7.12: Similar to Table 7.7, but the Anderson-Darling test is with respect to the observed spectrum classification FSRQ and BL Lac for all sources fitted using the simple power-law model, being 692 of them FSRQ and 168 BL Lac.

Parameter	Statistic	p -value	Reject null-hyp at 1 %
β	10.050	<0.001	Yes
$\log A$	11.500	<0.001	Yes
$\log\langle F_r \rangle$	2.887	0.022	No
$\log \text{var}(F_r)$	0.404	0.227	No

Since for the simple power-law case we have enough objects, we display the histogram of these parameters in Figure 7.15. The power-law index β for FSRQs are spread over a wider range than BL Lacs. Parameter $\log A$ has a similar behavior since both parameters are connected by the power-law model and all the objects show similar characteristics in their flux density.

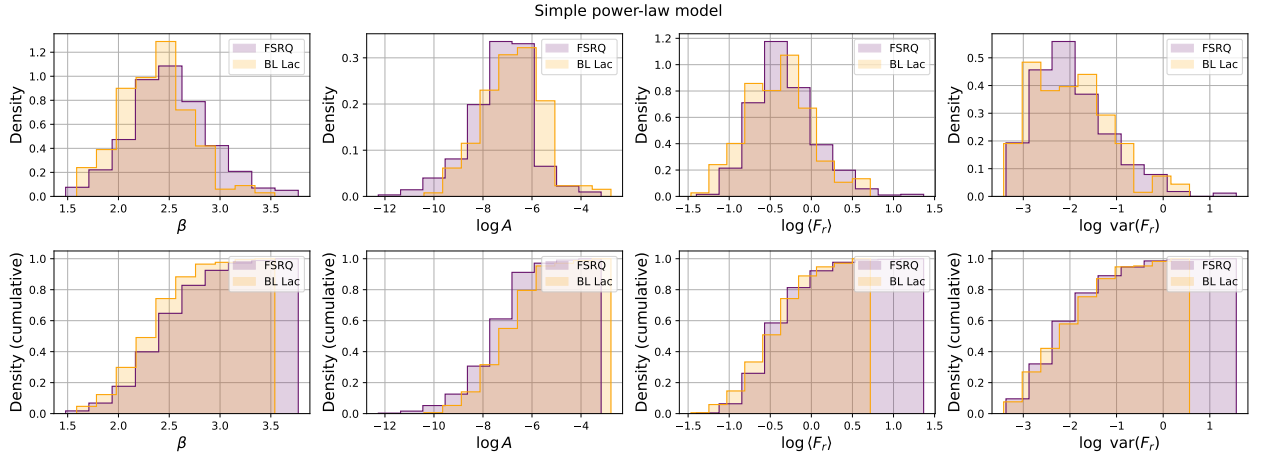


Figure 7.15: Density and cumulative histograms for the simple power-law model and radio parameters with respect to the observational classes FSRQ and BL Lac.

Figure B.12 displays a scatter plot along with a KDE plot on the same way that Figure B.11 but for the simple power-law model case. We do not see any relationship between parameters under this optical spectrum classification.

7.5. γ -ray sources

We run the same Anderson-Darling tests for the simple power-law model and the broken power-law model applied in the previous section, but the classification here is between γ -ray and non γ -ray sources. From the 1038 final objects, 596 are γ -ray sources and 442 are not.

7.5.1. Broken model

For the broken power-law model 33 objects are γ -ray sources and 5 are not. Table 7.13 shows a summary of the statistics of each parameter under this context, while Table 7.14 shows the result of the Anderson-Darling test over these two classifications. None of the parameters can be rejected at level 1%, meaning that for this case there is no difference about the model parameters and flux density at radio-band variables. However, and similar to the previous case about optical spectrum classification, the set of objects for each classification is too small to affirm any conjecture.

Figure B.13 displays a scatter plot along with a KDE plot on the same way that Figure B.11 but for this classification of γ -ray sources. Here, only $\log A$ shows a difference between both classification, we can note also that its p -value in Table 7.14 has a low value and that there is a difference also in its summary values from Table 7.13. It could be possible that the amplitude between γ -ray and non γ -ray sources differs, having the first one larger amplitudes, but again, we require a larger sample to affirm this.

Table 7.13: Summary statistics of the different parameters tested for the broken power-law model with respect to being a γ -ray source.

Parameter	γ -ray	Mean	St dev.	Q0.25	Median	Q0.75
β_l	No	0.05	1.06	-0.58	-0.26	0.64
	Yes	0.28	0.83	-0.26	0.35	0.99
β_h	No	4.60	0.47	4.22	4.85	4.96
	Yes	4.01	0.77	3.35	4.01	4.72
$\log f_{\text{br}}$	No	-2.55	0.27	-2.78	-2.54	-2.51
	Yes	-2.39	0.26	-2.60	-2.41	-2.24
$\log f_{\text{br,corr}}$	No	-3.42	0.40	-3.73	-3.44	-3.15
	Yes	-3.41	0.26	-3.63	-3.40	-3.25
$\log A$	No	-11.20	0.65	-11.51	-11.40	-11.38
	Yes	-9.23	1.90	-10.37	-8.89	-7.92
$\log \langle F_r \rangle$	No	-0.53	0.35	-0.90	-0.35	-0.28
	Yes	-0.39	0.33	-0.60	-0.42	-0.23
$\log \text{var}(F_r)$	No	-1.72	0.85	-2.37	-1.64	-0.91
	Yes	-1.82	0.69	-2.25	-1.82	-1.35

Table 7.14: Similar to Table 7.7, but the Anderson-Darling test is with respect to the 33 γ -ray sources and the 5 non γ -ray sources fitted using the broken power-law model.

Parameter	Statistic	p -value	Reject null-hyp at 1 %
β_l	-0.183	>0.25	No
β_h	0.797	0.154	No
$\log A$	2.582	0.028	No
$\log f_{\text{br}}$	0.021	>0.25	No
$\log f_{\text{br,corr}}$	-0.200	>0.25	No
$\log \langle F_r \rangle$	-0.394	>0.25	No
$\log \text{var}(F_r)$	-0.710	>0.25	No

7.5.2. Simple model

For the simple power-law model 563 objects are γ -ray sources and 437 are not. Table 7.15 shows a summary of the statistics of each parameter under this context, while Table 7.16 shows the result of the Anderson-Darling test on the same way as the previous subsection. Here all the null hypothesis can be rejected except for parameter β . About the flux density at radio-band and $\log A$, γ -ray emitter objects have typically a higher flux density over all the electromagnetic spectrum since they carry more energy than non γ -ray blazars, so these results are compatible with the physics behind blazars. These differences can be also seen in Figure 7.16 where the histogram of each parameter and classification is displayed.

Table 7.15: Summary statistics of the different parameters tested for the simple power-law model with respect to being a γ -ray source.

Parameter	γ -ray	Mean	St dev.	Q0.25	Median	Q0.75
β	No	2.49	0.41	2.21	2.45	2.71
	Yes	2.44	0.36	2.20	2.45	2.68
$\log A$	No	-7.70	1.25	-8.42	-7.58	-6.91
	Yes	-6.76	1.10	-7.43	-6.73	-6.09
$\log\langle F_r \rangle$	No	-0.48	0.31	-0.69	-0.49	-0.31
	Yes	-0.26	0.42	-0.54	-0.29	-0.02
$\log \text{var}(F_r)$	No	-2.33	0.61	-2.76	-2.39	-2.02
	Yes	-1.72	0.86	-2.36	-1.79	-1.20

Table 7.16: Similar to Table 7.7, but the Anderson-Darling test is with respect to the 562 γ -ray sources and the 438 non γ -ray sources fitted using the simple power-law model.

Parameter	Statistic	p -value	Reject null-hyp at 1 %
β	1.227	0.102	No
$\log A$	94.247	<0.001	Yes
$\log\langle F_r \rangle$	55.077	<0.001	Yes
$\log \text{var}(F_r)$	98.998	<0.001	Yes

As in the previous case. Figure B.14 displays a scatter plot along with a KDE plot on the same way that Figure B.13 but for the simple power-law model case. From the KDE levels of $\log\langle F_r \rangle$ and $\log \text{var}(F_r)$, along with the summary statistics of these parameters from Table 7.15, it is clear why the null hypothesis for these radio-band parameters can be rejected. Finally, we do not see any relationship between parameters under this γ -ray source classification.

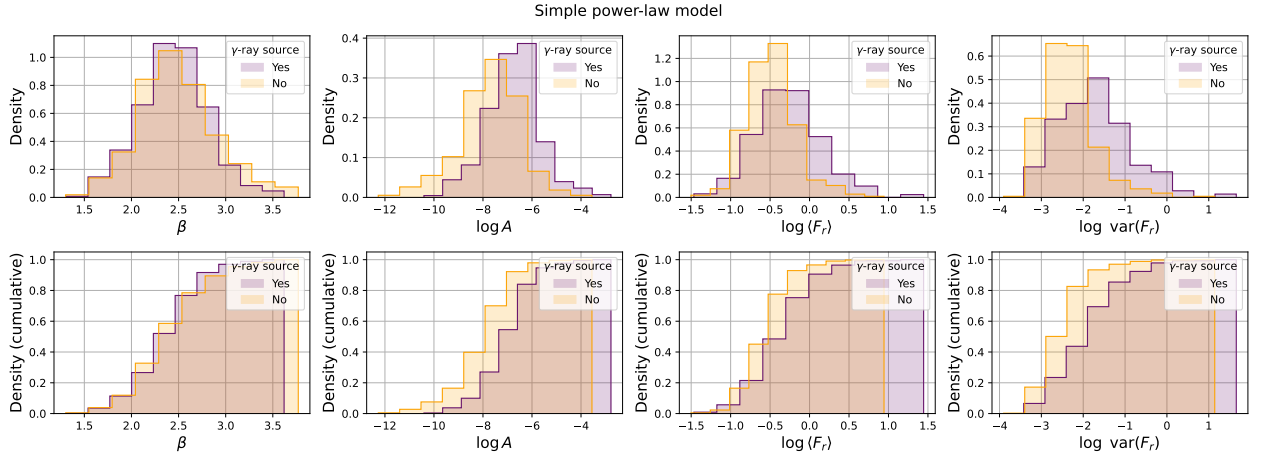


Figure 7.16: Density and cumulative histograms for the simple power-law model and radio parameters with respect to the being or not a γ -ray source.

7.6. Redshift range

Similar to what was done for the optical spectrum classification and the γ -ray sources, we run the same Anderson-Darling tests for the redshift ranges $0 < z \leq 1$ and $z > 1$, having each one 454 and 467 sources of the 1038 final objects respectively.

7.6.1. Broken model

For the broken power-law model 27 objects have a redshift between 0 and 1, while 7 of them have a redshift greater than 1. Table 7.17 shows a summary of the statistics of each parameter under this context, while Table 7.18 shows the results of the Anderson-Darling test. None of the null hypothesis can be rejected at level 1%, meaning that for this case there is no difference about the model and flux density at radio-band variables. However, and as mentioned in the other classifications, for this scenario we have too few samples per classification, so we can not affirm or reject any conjecture.

Table 7.17: Summary statistics of the different parameters tested for the broken power-law model with respect to two predefined redshift ranges.

Parameter	Redshift z	Mean	St dev.	Q0.25	Median	Q0.75
β_l	$0 < z \leq 1$	0.51	0.80	-0.12	0.64	1.05
	$z > 1$	-0.33	0.59	-0.68	-0.26	-0.02
β_h	$0 < z \leq 1$	4.16	0.77	3.45	4.22	4.89
	$z > 1$	3.76	0.73	3.25	3.53	4.15
$\log f_{\text{br}}$	$0 < z \leq 1$	-2.34	0.27	-2.53	-2.39	-2.16
	$z > 1$	-2.62	0.22	-2.79	-2.62	-2.52
$\log f_{\text{br,corr}}$	$0 < z \leq 1$	-3.38	0.28	-3.58	-3.37	-3.20
	$z > 1$	-3.58	0.22	-3.71	-3.59	-3.46
$\log A$	$0 < z \leq 1$	-9.39	1.89	-10.75	-9.31	-8.21
	$z > 1$	-9.59	2.17	-10.85	-9.07	-7.93
$\log \langle F_r \rangle$	$0 < z \leq 1$	-0.33	0.29	-0.55	-0.35	-0.18
	$z > 1$	-0.56	0.39	-0.80	-0.49	-0.32
$\log \text{var}(F_r)$	$0 < z \leq 1$	-1.63	0.64	-2.15	-1.64	-1.32
	$z > 1$	-2.18	0.74	-2.60	-2.34	-1.78

Table 7.18: Similar to Table 7.7, but the Anderson-Darling test is with respect to the 27 sources with a redshift range $0 < z \leq 1$ and the 7 having $z > 1$ fitted using the broken power-law model.

Parameter	Statistic	p -value	Reject null-hyp at 1 %
β_l	3.286	0.015	No
β_h	0.009	>0.25	No
$\log A$	-0.882	>0.25	No
$\log f_{\text{br}}$	2.861	0.022	No
$\log f_{\text{br,corr}}$	-0.322	>0.25	No
$\log \langle F_r \rangle$	0.642	0.179	No
$\log \text{var}(F_r)$	2.673	0.026	No

Figure B.15 displays a scatter plot along with a KDE plot on the same way that Figure B.11 but for this classification of redshift range. The plots $\log f_{\text{br}}$ vs γ -ray parameters show some correlations for the redshift range $0 < z \leq 1$. As we have 27 objects in this range, we went further and fitted a simple linear regression over these parameters which is illustrated in Figure 7.17. We found a low correlation for the log of the break frequency and the log of the flux density in γ -ray ($R^2 = 0.42$), which tell us that there are a certain dependency in the position of the break frequency with respect to the flux density at γ -ray for objects with a redshift $0 < z \leq 1$. Having a larger sample for this range would get us a more consistent result.

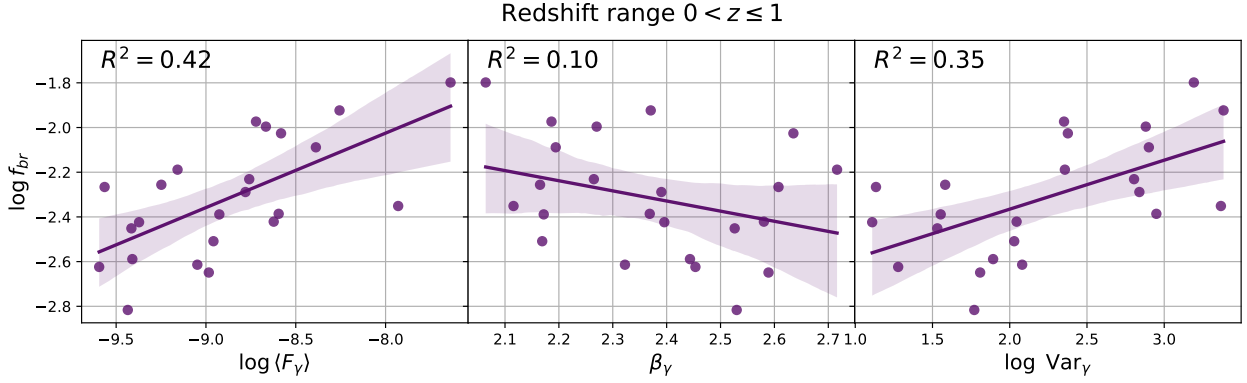


Figure 7.17: Linear Regression results between $\log f_{\text{br}}$ and γ -ray parameters for the redshift range $0 < z \leq 1$.

7.6.2. Simple model

For the simple power-law model 427 objects have a redshift between 0 and 1, while 460 of them have a redshift greater than 1. Table 7.19 shows a summary of the statistics of each parameter under this context, while Table 7.20 shows the results of the Anderson-Darling test on the same way as the previous subsection. Similar to the results between FSRQ and BL Lac for the simple model case, the null hypothesis about flux density at radio-band parameters can not be rejected at level 1%. With respect to the model parameters, there is a difference in $\log A$ where the mean between the two classifications differs almost on ~ 0.5 , while for β the difference is about 0.1. Anyway, we suggest that these results are somehow arbitrary and defining others redshift ranges could give other results. Figure 7.18 shows the histograms of these parameters with respect to this classification.

Table 7.19: Summary statistics of the different parameters tested for the simple power-law model with respect to two predefined redshift ranges.

Parameter	Redshift z	Mean	St dev.	Q0.25	Median	Q0.75
β	$0 < z \leq 1$	2.43	0.38	2.17	2.42	2.67
	$z > 1$	2.51	0.39	2.26	2.48	2.73
$\log A$	$0 < z \leq 1$	-6.91	1.26	-7.66	-6.84	-6.11
	$z > 1$	-7.40	1.23	-8.03	-7.23	-6.60
$\log \langle F_r \rangle$	$0 < z \leq 1$	-0.32	0.44	-0.62	-0.37	-0.07
	$z > 1$	-0.34	0.35	-0.59	-0.38	-0.13
$\log \text{var}(F_r)$	$0 < z \leq 1$	-1.89	0.91	-2.57	-2.02	-1.40
	$z > 1$	-2.01	0.75	-2.56	-2.12	-1.60

Table 7.20: Similar to Table 7.7, but the Anderson-Darling test is with respect to the 427 sources with a redshift range $0 < z \leq 1$ and the 460 having $z > 1$ fitted using the simple power-law model.

Parameter	Statistic	p -value	Reject null-hyp at 1 %
β	6.248	<0.001	Yes
$\log A$	22.802	<0.001	Yes
$\log \langle F_r \rangle$	1.496	0.078	No
$\log \text{var}(F_r)$	1.980	0.050	No

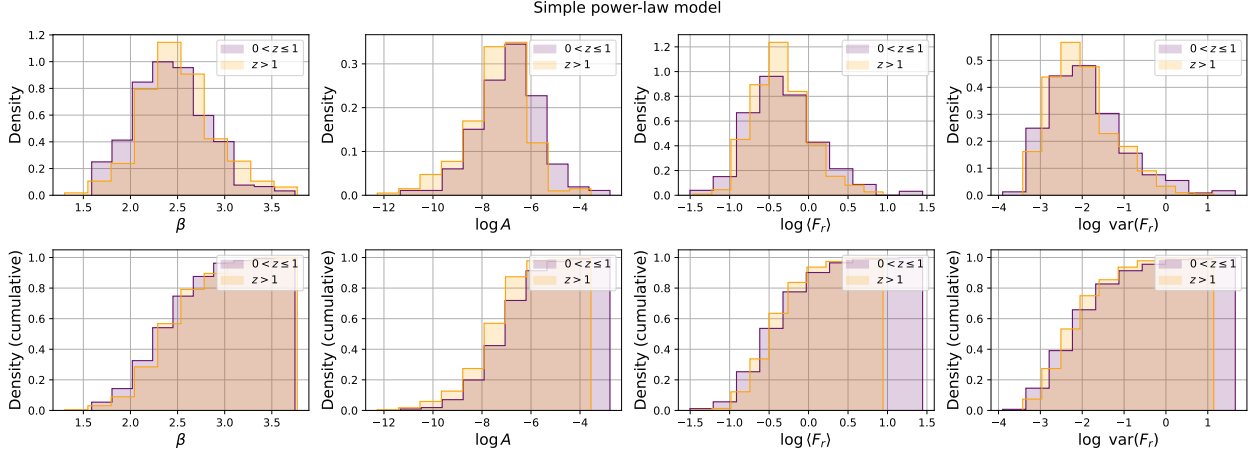


Figure 7.18: Density and cumulative histograms for the simple power-law model and radio parameters with respect to redshift ranges $0 < z \leq 1$ and $z > 1$.

As in the previous case, Figure B.16 displays a scatter plot along with a KDE plot on the same way that Figure B.15 but for the simple power-law model case. Parameter β (and in consequence $\log A$) shows a difference which is confirmed by its p -value from Table 7.20 and the histograms from Figure 7.18. Finally, no relationship between parameters was found for this classification controlling for redshift range.

7.7. Doppler factor range

Similar to what was done for the optical spectrum classification, γ -ray sources and redshift range, we run the same Anderson-Darling tests for the Doppler factor ranges $0 < \delta \leq 10$ and $\delta > 10$, having each one 371 and 427 sources of the 1038 final objects respectively.

7.7.1. Broken model

For the broken power-law model 6 objects have a Doppler factor between 0 and 10, while 27 of them have a value greater than 10. Table 7.21 shows a summary of the statistics of each parameter under this context, while Table 7.22 shows the results of the Anderson-

Darling test. In this context, only the null hypothesis of the break frequency in the source rest frame $\log f_{\text{br,corr}}$ can be rejected at level 1%, which can be also determined observing the mean of both parameters with respect of the Doppler factor range. As was mentioned in the section about the redshift range, this result is somehow arbitrary and defining others Doppler factor ranges could give other results.

Table 7.21: Summary statistics of the different parameters tested for the broken power-law model with respect to two predefined Doppler factor ranges.

Parameter	Doppler factor δ	Mean	St dev.	Q0.25	Median	Q0.75
β_l	$0 < \delta \leq 10$	0.69	0.85	0.22	0.74	1.42
	$\delta > 10$	0.28	0.83	-0.29	0.39	0.98
β_h	$0 < \delta \leq 10$	4.41	0.61	4.27	4.45	4.85
	$\delta > 10$	4.03	0.80	3.37	4.01	4.84
$\log f_{\text{br}}$	$0 < \delta \leq 10$	-2.47	0.31	-2.75	-2.44	-2.21
	$\delta > 10$	-2.39	0.28	-2.60	-2.42	-2.25
$\log f_{\text{br,corr}}$	$0 < \delta \leq 10$	-3.06	0.22	-3.23	-3.03	-2.90
	$\delta > 10$	-3.49	0.23	-3.67	-3.46	-3.33
$\log A$	$0 < \delta \leq 10$	-10.28	1.78	-11.05	-9.94	-8.91
	$\delta > 10$	-9.25	1.97	-10.75	-9.07	-7.61
$\log \langle F_r \rangle$	$0 < \delta \leq 10$	-0.40	0.45	-0.56	-0.48	-0.37
	$\delta > 10$	-0.35	0.26	-0.51	-0.35	-0.18
$\log \text{var}(F_r)$	$0 < \delta \leq 10$	-1.68	0.88	-2.23	-2.15	-1.21
	$\delta > 10$	-1.71	0.61	-2.18	-1.64	-1.33
$\log \langle F_\gamma \rangle$	$0 < \delta \leq 10$	-9.29	0.21	-9.33	-9.21	-9.16
	$\delta > 10$	-8.82	0.50	-9.23	-8.85	-8.59

Table 7.22: Similar to Table 7.7, but the Anderson-Darling test is with respect to the 6 sources with a Doppler factor range $0 < \delta \leq 10$ and the 27 having $\delta > 10$ fitted using the broken power-law model.

Parameter	Statistic	p -value	Reject null-hyp at 1%
β_l	0.261	>0.25	No
β_h	-0.073	>0.25	No
$\log A$	-0.029	>0.25	No
$\log f_{\text{br}}$	-0.233	>0.25	No
$\log f_{\text{br,corr}}$	6.900	<0.001	Yes
$\log \langle F_r \rangle$	-0.055	>0.25	No
$\log \text{var}(F_r)$	-0.418	>0.25	No

Figure B.17 displays a scatter plot along with a KDE plot on the same way that Figure B.11 but for this classification of Doppler factor range. Here is clear the separation by $\log f_{\text{br,corr}}$.

7.7.2. Simple model

For the simple power-law model 365 objects have a Doppler factor between 0 and 1, while 400 of them have a value greater than 1. Table 7.23 shows a summary of the statistics of each parameter under this context, while Table 7.24 shows the results of the Anderson-Darling test on the same way as the previous subsection. Similar to the results between FSRQ and BL Lac for the simple model case, the null hypothesis about the flux density at radio-band parameters can not be rejected at level 1%. About the model parameters, there is a difference in $\log A$ where the mean between the two classifications differs almost on ~ 0.7 , while for β the difference is about 0.1. However, and as was declared before, we suggest that these results are somehow arbitrary and defining others Doppler factor ranges could give other results. Figure 7.19 shows the histograms of these parameters with respect to this classification.

Table 7.23: Summary statistics of the different parameters tested for the simple power-law model with respect to two predefined redshift ranges.

Parameter	Doppler factor δ	Mean	St dev.	Q0.25	Median	Q0.75
β	$0 < \delta \leq 10$	2.57	0.41	2.30	2.53	2.80
	$\delta > 10$	2.44	0.34	2.20	2.43	2.67
$\log A$	$0 < \delta \leq 10$	-7.49	1.27	-8.17	-7.34	-6.62
	$\delta > 10$	-6.81	1.15	-7.54	-6.79	-6.13
$\log \langle F_r \rangle$	$0 < \delta \leq 10$	-0.28	0.38	-0.53	-0.35	-0.07
	$\delta > 10$	-0.30	0.40	-0.60	-0.34	-0.06
$\log \text{var}(F_r)$	$0 < \delta \leq 10$	-1.93	0.80	-2.50	-2.07	-1.53
	$\delta > 10$	-1.80	0.84	-2.43	-1.90	-1.27

Table 7.24: Similar to Table 7.7, but the Anderson-Darling test is with respect to the 427 sources with a Doppler factor range $0 < \delta \leq 10$ and the 460 having $\delta > 10$ fitted using the simple power-law model.

Parameter	Statistic	p -value	Reject null-hyp at 1%
β	11.592	<0.001	Yes
$\log A$	30.673	<0.001	Yes
$\log \langle F_r \rangle$	1.265	0.098	No
$\log \text{var}(F_r)$	2.315	0.036	No

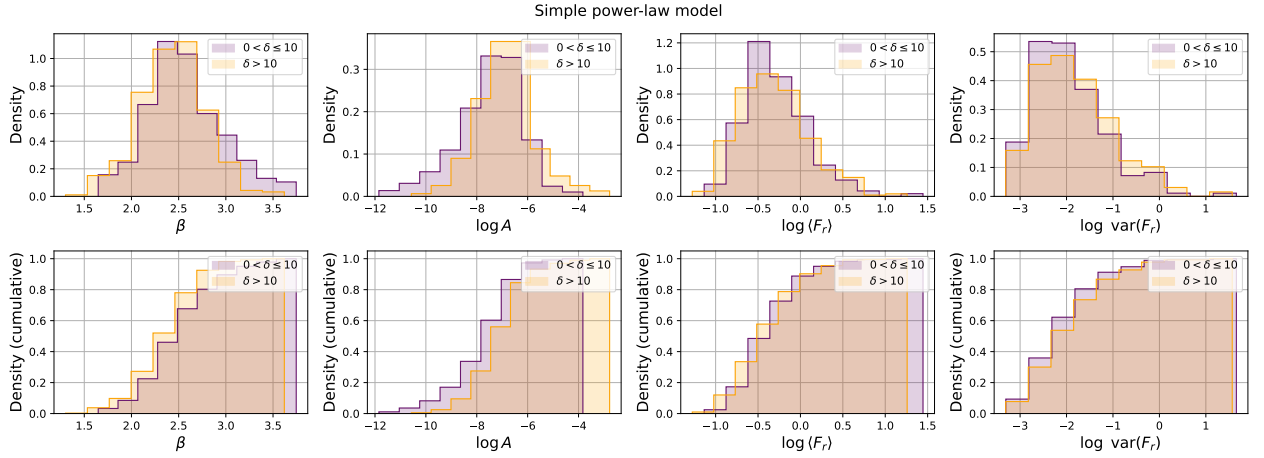


Figure 7.19: Density and cumulative histograms for the simple power-law model and radio parameters with respect to Doppler factor ranges $0 < \delta \leq 10$ and $\delta > 10$.

As in the previous case, Figure B.18 displays a scatter plot along with a KDE plot on the same way that Figure B.17 but for the simple power-law model case. Note that β for the Doppler factor range $0 < \delta \leq 10$ is spread in a wide range than the range $\delta > 10$, while for $\log A$ the Doppler factor range $0 < \delta \leq 10$ reaches lower values than the other range. Both of these differences can be also seen in Figure 7.19.

7.8. Radio characterization as γ -ray source predictor

The Fermi Gamma-ray Space Telescope is able to detect sources emitting in γ -rays doing an all-sky survey. This permits astronomers to detect high-energy γ -ray bursts and to monitor the variability of multiple sources (Atwood et al. 2009). Given that in Section 7.5 we show that γ -ray sources differ with respect to the PSD and radio-band variables, an interesting question that comes up is: can we use the radio characterization of a source to predict if it is a γ -ray emitter? In this way, the radio characterization could be sufficient to define, or not, an object as a γ -ray source, and therefore the observation of new possible γ -ray sources can be based on this hypothesis, pointing preferentially to objects that have a greater probability of emitting in that band.

To answer this question, we train a simple Generalized Linear Model (GLM) using the open source machine learning framework H2O (see Appendix A.5) with a Binomial distribution, also known as logistic regression. Regarding H2O parameters, we set $\alpha = 0$ for ℓ_2 penalties since we use a very reduced number of predictors x . The parameter α controls the balance between ℓ_1 (Lasso) and ℓ_2 (Ridge) penalties in the model, which adds a regularization term to the objective function to prevent overfitting while allowing for the inclusion of all predictors in the model. On the other hand, parameter λ , which controls the trade-off between model complexity and fitting accuracy, is defined by the model itself using an automatic search.

With respect to the predictors used, from the observational data in radio we use the ones derived from the flux density $\langle F_r \rangle$ and $\text{var}(F_r)$, all of them in a log-scale. About the PSD characterization, for simplicity we consider only the 1000 objects well-defined by the simple power-law model, thus we only use the logarithm of the amplitude $\log A$ and the power-law index β . We produce 3 different models in order to compare the importance of the PSD characterization with respect to the observational predictors, which are described in Table 7.25.

Table 7.25: Three different models for the logistic regression with respect of being or not a γ -ray source.

	Predictors	Description
Model 1	$\beta, \log A$	PSD only
Model 2	$\log \langle F_r \rangle, \log \text{var}(F_r)$	Light curve
Model 3	$\beta, \log A, \log \langle F_r \rangle, \log \text{var}(F_r)$	PSD + Light curve

From the 1000 sources used, 563 of them are γ -ray emitters and 437 are not. We employ a 5-folds cross-validation over the data in order to avoid overfitting. For each cross-validation 80% of the data is used for training and the other 20% for validation. Table 7.26 shows the coefficients obtained for each model with their respective errors and p -values. Note that Model 3 shows a very high p value for the log of the flux density variability $\log \text{var}(F_r)$ which means that this parameter can be removed from the model since it has not a significant effect to make predictions. This is consistent with the fact that PSD parameters characterize the variability of the light curve so adding this extra parameter has no impact. Figure 7.20 shows the Receiver Operating Characteristic (ROC) curve, which corresponds to a way to illustrate the ability of a binary classifier for different threshold values. In our context GLM models obtain for each object a probability P of being γ -ray source, then different threshold values will give us different results in the classification. The ROC curve is useful to understand how well a binary classifier model works. A perfect classifier will have a True Positive Rate of 1 and a False Positive Rate of 0, while a random classifier will have a ROC curve on the diagonal, shown on this figure as a segmented black line.

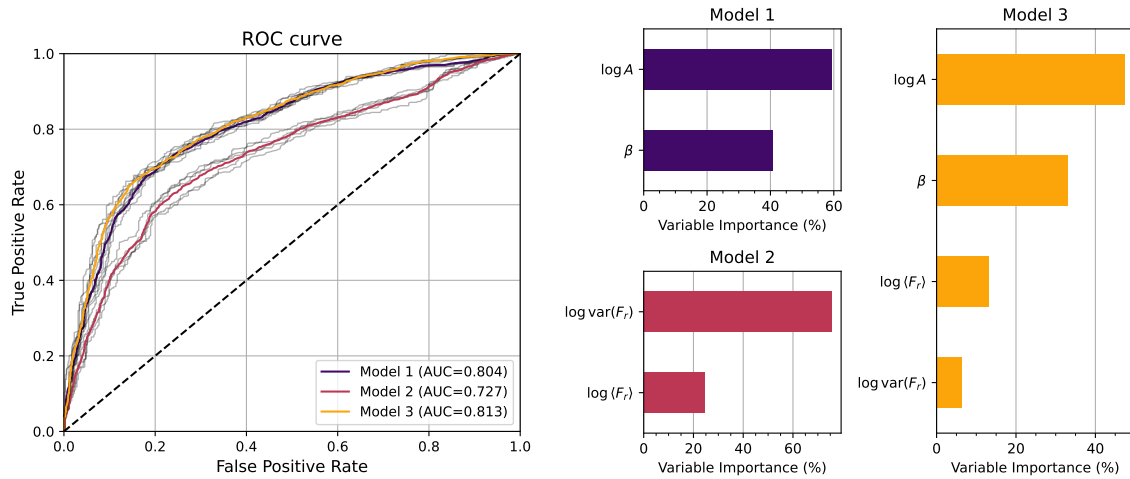


Figure 7.20: ROC curve (left) and variable importance (right) of the three predictive models of being or not a γ -ray. The segmented black line on the ROC plot correspond to the curve that could be obtained using a simple random dummy predictor, while the gray curves corresponds to each one of the 5-folds cross-validation of each model.

The area under the curve (AUC) is used as a way to compare different ROC curves, where here a perfect classifier will have an AUC of 1. If we compare the AUC of the three models, we note that Model 1 is better than Model 2, having an AUC of 0.804 versus 0.727. On the other hand, Model 3 which contains as predictors the variables from Model 1 and Model 2, has an AUC slightly higher than Model 1. This is telling us that the the PSD characterization has a stronger predictive power than the observational derived variables. This is made clear after looking at the same Figure 7.20 where the variable importance of each model is also illustrated. In the case of Model 1, $\log A$ has about 60% in variable importance while β has about 40%, meaning that $\log A$ has more predictive power than β . One question that may arise here is what about using the parameters of the PSD characterization individually on the prediction. Figure 7.21 shows a comparison of the ROC between Model 1 and the usage of $\log A$ and β separately. $\log A$ plays an important role in the prediction, but using it without β is worse than flux density properties of Model 2. Hence, adding the parameter β to the GLM classifier increase the AUC in ~ 0.1 .

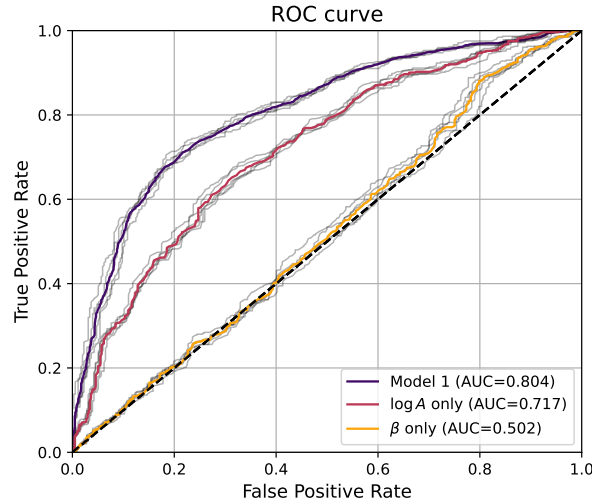


Figure 7.21: ROC curves of Model 1 and PSD parameters used individually on the prediction of being or not a γ -ray. The segmented black line on the ROC plot correspond to the curve that could be obtained using a simple random dummy predictor, while the gray curves corresponds to each one of the 5-folds cross-validation of each model.

Table 7.26: Coefficients of each predictor and model with their respective errors and p -values according to H2O framework

		Coefficients	Std. error	p -value
Model 1	Intercept	3.302	0.523	0.000
	β	3.852	0.353	0.000
	$\log A$	1.726	0.124	0.000
Model 2	Intercept	3.139	0.294	0.000
	$\log \text{var}(F_r)$	1.600	0.184	0.000
	$\log \langle F_r \rangle$	-1.077	0.343	0.002
Model 3	Intercept	3.841	0.825	0.000
	β	4.712	0.634	0.000
	$\log A$	2.068	0.209	0.000
	$\log \text{var}(F_r)$	0.425	0.277	0.126
	$\log \langle F_r \rangle$	-1.843	0.396	0.000

The results of the cross-validation predictions are shown in Table 7.27 as confusion matrices, where the real classification of γ -ray sources is at the left and the predicted ones at the top. The threshold used is the one that maximize the number of true positives and true negatives for each model, being 0.551 for Model 1, 0.532 for Model 2 and 0.54 for Model 3. The accuracy of each model can be obtained as $1 - \text{Total Error}$, resulting in 0.738 for Model 1, 0.688 for Model 2 and 0.746 for Model 3.

Table 7.27: Confusion Matrices of the three predictive models of being or not a γ -ray at the threshold that maximize the true positives and true negatives (called `min_per_class_accuracy` in H2O).

	Real/Pred	No	Yes	Error
Model 1	No	323	114	0.261
	Yes	148	415	0.263
	Total	471	529	0.262
Model 2	No	300	137	0.314
	Yes	175	388	0.311
	Total	475	525	0.312
Model 3	No	326	111	0.254
	Yes	143	420	0.254
	Total	469	533	0.254

Model 1 has similar results to Model 3 but reducing the parameter space to only two variables. The accuracy of Model 1 implies that from four sources approximately three of them are classified correctly, while its AUC of approximately 0.8 is an indicator that we are in the presence of a very good model (Mandrekar 2010). We can illustrate the behavior of Model 1 on a figure following equation A.5 and the coefficients from 7.26 to obtain the probability of being a γ -ray given the PSD parameters as

$$P(X = \text{being a } \gamma\text{-ray source} | \beta, \log A) = \frac{1}{1 + e^{-y(\beta, A)}} \quad (7.2)$$

where $y(\beta, A) \approx 3.3 + 3.9\beta + 1.7\log A$. Figure 7.22 shows the plot of this probability with respect to parameters β and $\log A$, and how this curve separates the plane between both parameters as well. From the figure we can say that $\log A$ has an important effect on the probability, having for values > -7 better probabilities of being a γ -ray source.

We find that logistic regression applied to the condition of being or not a γ -ray source using only the radio characterization gives interesting results, in particular for the case where we only consider the PSD parameters. Although our analysis indicates that including additional radio-band variables did not significantly improve the predictive power, we believe that exploring other properties of the sources may yield better results. Therefore, we suggest that a further analysis using other parameters and experimenting with different classification algorithms could enhance the predictive power. These results should be considered as a starting point for more in-depth investigations in this field.

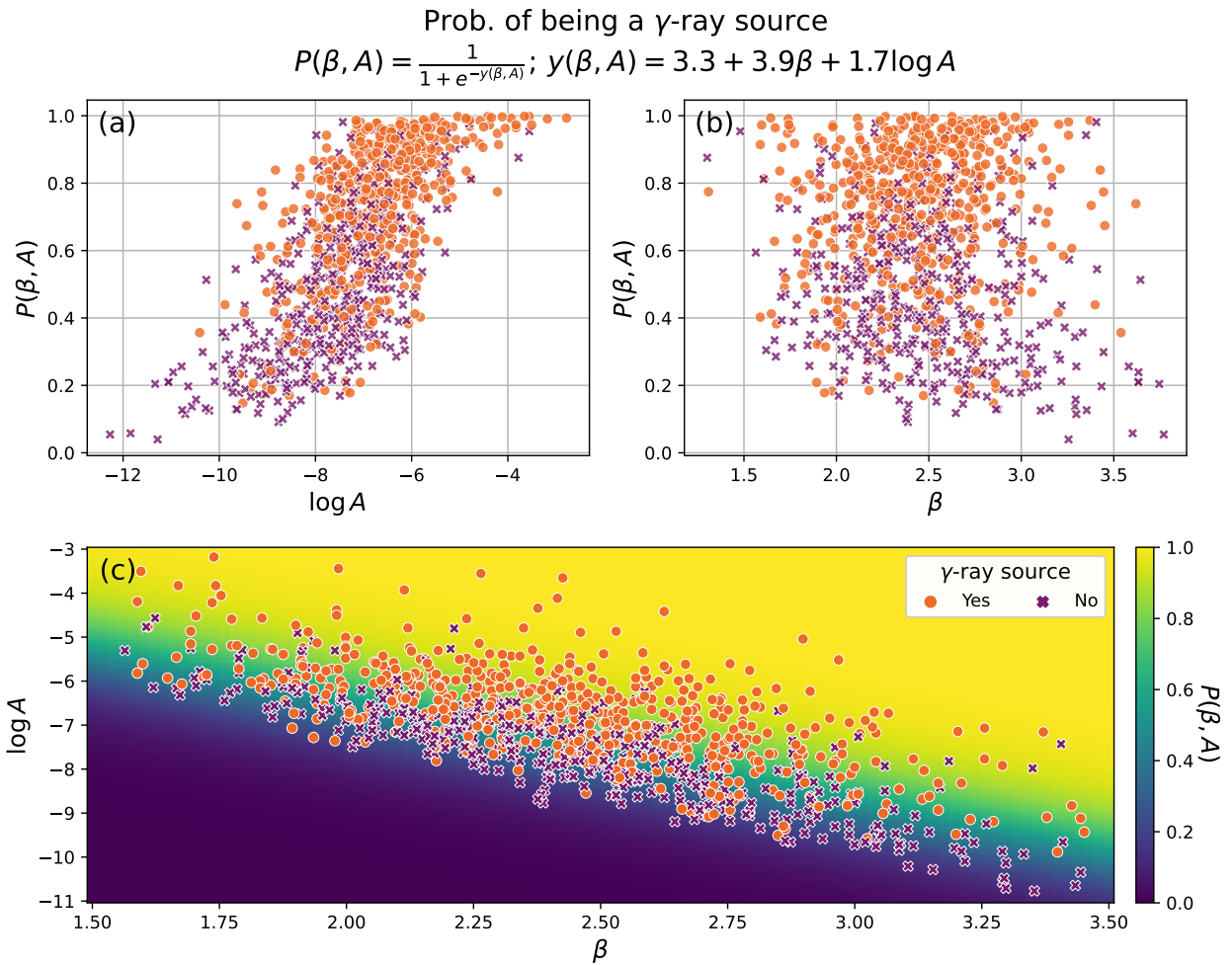


Figure 7.22: Plots of the probability of being a γ -ray source following results of Model 1. (a) with respect to $\log A$. (b) with respect to β . (c) with respect to plane $(\beta, \log A)$.

Chapter 8

Conclusion

The proposed method for fitting light curve periodograms using PMC-ABC provides results more efficiently than previous methods, with shorter computation time, greater flexibility, and consistent error bars, as explained in Chapter 5 on Testing. In particular, the outputs of the method correspond to distributions in the parameter space, giving more information than the frequentist approach in that sense. The PMC-ABC method is also not limited to a grid of search as previous methods, providing more exact results. That said, we propose to extend the usage of the PMC-ABC method to estimate the PSD for unevenly sampled light curves, in particular the time series data that will be generated with CTA and Rubin Observatory. In the near future we plan to extend the use of our current implementation for the radio-band to estimate the PSD of blazar light curves at other frequencies, especially the ones at γ -band from Fermi-LAT and CTA.

About the characterization using the simple power-law model, the power-law index β of FSRQs is spread over a wide range, reaching values larger than 3, whereas BL Lacs predominantly exhibit values below this threshold. In γ -ray sources the power-law index shows no big difference compared to sources not detected in γ -rays. Regarding redshifts, there are some objects with a redshift lower than 1 that have $\beta \sim 1.5$. If we look at the Doppler factor range, objects with a Doppler factor lower than 10 reach values around 3.5 in comparison with objects with a higher Doppler factor, which exhibit values lower than this. Apart from that, the simple power-law model does not show big differences between the different object classifications FSRQ and BL Lac, γ -ray and non γ -ray sources, redshift range lower and higher than 1 and Doppler factor range lower and higher than 10.

We find that 38 out of 1038 sources show a break on the PSD, which corresponds to 3.6% of the well-fitted population. If we look at the characterization using the broken power-law model, no big relationships or differences were found for the different characterization, this is due mainly to the small sample size of objects well-fitted with this model.

We found that the probability of finding an object with a break in its periodogram is

greater for objects at low redshift and with a large Doppler factor, which is consistent with what is expected from cosmological redshift, that displaces a break frequency to a lower value, and relativistic Doppler blueshift that displaces a break frequency to higher values. Because all objects are expected to have a break in their PSD, the effects described above contribute to make the break frequency fall in the currently observable range determined by the length of the observed light curves. This probability is also high in γ -ray sources, which show a preponderance for higher Doppler factors.

About the Doppler effect corrections, all corrected objects show a characteristic break time in the rest frame of the source in the order of decades. When comparing the corrected minimum frequency from objects with no break frequency and the corrected minimum frequency of objects fitted with the power-law break model, we note that many objects with no break frequency have a corrected minimum frequency of the same value than objects with a well-fitted break frequency in the rest frame. Since we did not find a break frequency on these objects, we propose that this discrepancy is due to the nature of the variability of these objects, or that we are in front of objects with different scales in luminosity, mass and/or another physical property. A further analysis aiming to clarify the origin of this difference will give a better understanding of the physical origin of the observed break frequency in radio-bands.

Another interesting result is the possible use of the characterization at radio-band to predict sources emitting γ -rays. The simple power-law characterization with parameters β and $\log A$ shows a high predictive power, with an accuracy of 0.738 and an AUC of 0.804. In particular, we found that the probability of being or not a γ -ray source separates the parameter space in the same shape that describes the β - $\log A$ relationship. We propose that this idea of predicting γ -ray emitters can be extended to include new parameters and/or using a different classification method as a way to guide the observations of γ -band telescopes such as CTA and Fermi-LAT.

Bibliography

- Abdo, A. A., Ackermann, M., Agudo, I., et al. 2010a, [ApJ](#), **716**, 30
- Abdo, A. A., Ackermann, M., Ajello, M., et al. 2010b, [ApJ](#), **715**, 429
- Abdo, A. A., Ackermann, M., Ajello, M., et al. 2010c, [ApJ](#), **722**, 520
- Abdollahi, S., Acero, F., Ackermann, M., et al. 2020, [ApJS](#), **247**, 33
- Ackermann, M., Ajello, M., Allafort, A., et al. 2011, [ApJ](#), **743**, 171
- Anderson, T. W. & Darling, D. A. 1952, *The annals of mathematical statistics*, 193
- Ansoldi, S., Antonelli, L. A., Arcaro, C., et al. 2018, [ApJ](#), **863**, L10
- Atwood, W. B., Abdo, A. A., Ackermann, M., et al. 2009, [ApJ](#), **697**, 1071
- Barlow, R. 2004, [arXiv e-prints](#), [physics/0406120](#)
- Beaumont, M. A., Zhang, W., & Balding, D. J. 2002, *Genetics*, 162, 2025
- Blandford, R., Meier, D., & Readhead, A. 2019, [ARA&A](#), **57**, 467
- Boettcher, M. 2012, [arXiv e-prints](#), [arXiv:1205.0539](#)
- Boettcher, M., Harris, D. E., & Krawczynski, H. 2012, *Relativistic Jets from Active Galactic Nuclei*
- Böttcher, M., Reimer, A., Sweeney, K., & Prakash, A. 2013, [ApJ](#), **768**, 54
- Bracewell, R. N. 1986, *The Fourier transform and its applications*, Vol. 31999 (McGraw-Hill New York)
- Brigham, E. O. 1988, *The fast Fourier transform and its applications* (Prentice-Hall, Inc.)
- Brown, L. D., Cai, T. T., & DasGupta, A. 2001, *Statistical science*, 16, 101
- Cappé, O., Guillin, A., Marin, J.-M., & Robert, C. P. 2004, *Journal of Computational and Graphical Statistics*, 13, 907
- Cerruti, M., Zech, A., Boisson, C., et al. 2019, [MNRAS](#), **483**, L12

- Cerruti, M., Zech, A., Boisson, C., & Inoue, S. 2015, *MNRAS*, **448**, 910
- Chatterjee, R., Jorstad, S. G., Marscher, A. P., et al. 2008, *ApJ*, **689**, 79
- Cooley, J. W. & Tukey, J. W. 1965, *Mathematics of computation*, **19**, 297
- Emmanoulopoulos, D., McHardy, I. M., & Uttley, P. 2010, *MNRAS*, **404**, 931
- Event Horizon Telescope Collaboration, Akiyama, K., Alberdi, A., et al. 2022, *ApJ*, **930**, L12
- Event Horizon Telescope Collaboration, Akiyama, K., Alberdi, A., et al. 2019, *ApJ*, **875**, L1
- Finke, J. D. & Becker, P. A. 2015, *ApJ*, **809**, 85
- Fuhrmann, L., Angelakis, E., Zensus, J., et al. 2016, *A&A*, **596**, A45
- Goyal, A. 2020, *MNRAS*, **494**, 3432
- Goyal, A. 2021, *ApJ*, **909**, 39
- Goyal, A., Soida, M., Stawarz, Ł., et al. 2022, *ApJ*, **927**, 214
- Healey, S. E., Romani, R. W., Cotter, G., et al. 2008, *ApJS*, **175**, 97
- Healey, S. E., Romani, R. W., Taylor, G. B., et al. 2007, *ApJS*, **171**, 61
- Helou, G., Madore, B. F., Schmitz, M., et al. 1991, in *Astrophysics and Space Science Library*, Vol. 171, *Databases and On-line Data in Astronomy*, ed. M. A. Albrecht & D. Egret, **89–106**
- Iba, Y. 2001, *Transactions of the Japanese Society for Artificial Intelligence*, **16**, 279
- IceCube Collaboration, Aartsen, M. G., Ackermann, M., et al. 2018, *Science*, **361**, eaat1378
- Ishida, E. E. O., Vitenti, S. D. P., Penna-Lima, M., et al. 2015, *Astronomy and Computing*, **13**, 1
- Isobe, N., Sato, R., Ueda, Y., et al. 2015, *ApJ*, **798**, 27
- Ivezić, Ž., Menou, K., Knapp, G. R., et al. 2002, *AJ*, **124**, 2364
- Kataoka, J., Takahashi, T., Wagner, S. J., et al. 2001, *ApJ*, **560**, 659
- Kellermann, K. I., Condon, J. J., Kimball, A. E., Perley, R. A., & Ivezić, Ž. 2016, *ApJ*, **831**, 168
- Kellermann, K. I., Sramek, R., Schmidt, M., Shaffer, D. B., & Green, R. 1989, *AJ*, **98**, 1195
- Kelly, B. C., Becker, A. C., Sobolewska, M., Siemiginowska, A., & Uttley, P. 2014, *ApJ*, **788**, 33
- Koay, J., Jauncey, D., Hovatta, T., et al. 2019, *MNRAS*, **489**, 5365

- Kozłowski, S. 2017, *ApJ*, **835**, 250
- Liodakis, I., Hovatta, T., Huppenkothen, D., et al. 2018a, *ApJ*, **866**, 137
- Liodakis, I., Pavlidou, V., Papadakis, I., et al. 2017, *ApJ*, **851**, 144
- Liodakis, I., Romani, R. W., Filippenko, A. V., et al. 2018b, *MNRAS*, **480**, 5517
- Mandrekar, J. N. 2010, *Journal of Thoracic Oncology*, **5**, 1315
- Mannheim, K. & Biermann, P. L. 1992, *A&A*, **253**, L21
- Maraschi, L., Ghisellini, G., & Celotti, A. 1992, *ApJ*, **397**, L5
- Massaro, E., Giommi, P., Leto, C., et al. 2009, *A&A*, **495**, 691
- Max-Moerbeck, W., Hovatta, T., Richards, J. L., et al. 2014a, *MNRAS*, **445**, 428
- Max-Moerbeck, W., Richards, J. L., Hovatta, T., et al. 2014b, *MNRAS*, **445**, 437
- Max-Moerbeck, W. K. 2013, *The relationship between the radio and gamma-ray emission of blazars*, PhD thesis, California Institute of Technology
- McHardy, I. M., Koerding, E., Knigge, C., Uttley, P., & Fender, R. P. 2006, *Nature*, **444**, 730
- McHardy, I. M., Papadakis, I. E., Uttley, P., Page, M. J., & Mason, K. O. 2004, *MNRAS*, **348**, 783
- Meyer, M., Scargle, J. D., & Blandford, R. D. 2019, *ApJ*, **877**, 39
- Middelberg, E., Roy, A. L., Nagar, N. M., et al. 2004, *A&A*, **417**, 925
- Moreno, J., Vogeley, M. S., Richards, G. T., & Yu, W. 2019, *PASP*, **131**, 063001
- Narayan, R., McClintock, J. E., & Tchekhovskoy, A. 2014, in *General Relativity, Cosmology and Astrophysics*, ed. J. Bičák & T. Ledvinka, Vol. 177, 523
- Nilsson, K., Lindfors, E., Takalo, L. O., et al. 2018, *A&A*, **620**, A185
- O’Dea, C. P. 1998, *PASP*, **110**, 493
- Padovani, P. 2011, *MNRAS*, **411**, 1547
- Padovani, P. 2016, *A&A~Rev.*, **24**, 13
- Padovani, P. 2017, *Nature Astronomy*, **1**, 0194
- Padovani, P., Alexander, D. M., Assef, R. J., et al. 2017, *A&A~Rev.*, **25**, 2
- Padovani, P., Perlman, E. S., Landt, H., Giommi, P., & Perri, M. 2003, *ApJ*, **588**, 128
- Papadakis, I. & Lawrence, A. 1993, *MNRAS*, **261**, 612

- Priemer, R. 1991, *Introductory Signal Processing*, Advanced series in electrical and computer engineering (World Scientific)
- Priestley, M. 1989, San Diego: Academic Press, 389
- Readhead, A. C. S., Cohen, M. H., Pearson, T. J., & Wilkinson, P. N. 1978, *Nature*, **276**, 768
- Richards, J. L., Max-Moerbeck, W., Pavlidou, V., et al. 2011, *ApJS*, **194**, 29
- Robin, A., Reylé, C., Fliri, J., et al. 2014, *A&A*, **569**, A13
- Rubin, D. B. 1984, *The Annals of Statistics*, **12**, 1151
- Ryan, J. L., Siemiginowska, A., Sobolewska, M. A., & Grindlay, J. 2019, *ApJ*, **885**, 12
- Schafer, C. M. & Freeman, P. E. 2012, in *Statistical Challenges in Modern Astronomy V* (Springer), 3–19
- Sobolewska, M. A., Siemiginowska, A., Kelly, B. C., & Nalewajko, K. 2014, *ApJ*, **786**, 143
- Tarnopolski, M., Żywucka, N., Marchenko, V., & Pascual-Granado, J. 2020, *ApJS*, **250**, 1
- Tavaré, S., Balding, D. J., Griffiths, R. C., & Donnelly, P. 1997, *Genetics*, **145**, 505
- Timmer, J. & Koenig, M. 1995, *A&A*, **300**, 707
- Urry, C. M. & Padovani, P. 1995, *PASP*, **107**, 803
- Uttley, P., McHardy, I., & Papadakis, I. 2002, *MNRAS*, **332**, 231
- von Montigny, C., Bertsch, D. L., Chiang, J., et al. 1995, *ApJ*, **440**, 525
- Weekes, T., Badran, H., Biller, S., et al. 2002, *Astroparticle Physics*, **17**, 221
- Wiener, N. et al. 1930, *Acta mathematica*, **55**, 117
- Yuk, H., Dai, X., Jayasinghe, T., et al. 2022, *ApJ*, **930**, 110
- Zheng, X. C., Röttgering, H. J. A., Best, P. N., et al. 2020, *A&A*, **644**, A12
- Żywucka, N., Tarnopolski, M., Böttcher, M., Stawarz, Ł., & Marchenko, V. 2020, *ApJ*, **888**, 107

Annex A

Mathematics and Code

A.1. Data cleaning by using spline functions

A spline refers to a curve defined piecewise by polynomials typically of degree 3, which is also called a cubic spline. They are frequently used as a way to interpolate or smooth curves. A spline S is mainly defined by the polynomial degree n and $k - 1$ disjoint intervals, where k is also known as knots. If these intervals are equidistantly distributed then we say that the spline is uniform.

As was described in Chapter 2, we fit a cubic spline over each light curve and remove only the 1% of points with the highest distance between the spline and observed point as long as that distance is deviated more than s standard deviations with respect to the mean distance. The usage of s standard deviations as well as the number of knots k for the cubic spline depends on the kurtosis of the flux density of the light curve.

The kurtosis is a measure of the *tailedness* of a distribution, being equal to zero for a gaussian-like distribution and greater or lower than zero if they tails are defined on a wide or narrow range, respectively. Mathematically, the kurtosis of the random variable X correspond to the fourth standardized moment

$$\text{Kurt}[X] = E \left[\frac{X - \mu^4}{\sigma} \right] \quad (\text{A.1})$$

where μ is the mean and σ is the standard deviation of X . After obtaining the kurtosis of the flux density of all the 1859 light curves of the OVRO dataset and through trial and error, we found three different range of kurtosis that allows us to explicitly state the number of knots of the spline in order to fit on a reasonable way the light curve. These ranges are (i) all values lower than 0; (ii) values between 0 and 10; and (iii) all values greater than 10. Figure B.2 show the histogram of the kurtosis of all OVRO objects, while in Figure B.3 the reader can see light curves and the histogram of their flux densities for each one of defined ranges.

Algorithm 1 shows a pseudo-code of the method to obtain the number of knots k for fitting the spline and the number of standard deviations s for the comparison between the spline and the real data points.

Algorithm 1: Number of knots k and standard deviations s selection for outliers removal using a spline function. F refers to the flux density of the light curve.

```

Data:  $F$ 
 $s \leftarrow 3$                                 /* Initial number of standard deviations */
 $kurt \leftarrow \text{Kurtosis}(F)$              /* Kurtosis of the flux density */
 $N \leftarrow \text{length}(F)$                  /* Length of the light curve */
 $k \leftarrow N$                              /* Initial number of knots */
if  $kurt < 0$  then
  |  $k \leftarrow 2.5N$ 
else if  $kurt \leq 10$  then
  |  $k \leftarrow 4.5N$ 
else
  |  $k \leftarrow 8N$ 
  |  $s \leftarrow 4$ 
end
return  $k, s$ 

```

We employ the method `interpolate.UnivariateSpline`¹ from package `Scipy` for Python in order to fit the spline over a light curve, which also allow us to consider the flux density errors.

A.2. Light Curve simulation and periodogram binning

A white noise process normally distributed $X(t) \sim \mathcal{N}(0, \sigma^2)$ has an autocorrelation function $R_{XX}(\tau) = \sigma^2 \delta(\tau)$. Using the Wiener-Khinchin theorem we obtain a PSD $P(f) = \sigma^2$. On the other hand, from the spectral estimation's theory the Fourier transform of the process $X(t)$ corresponds to a complex gaussian random variable with no correlation at two different frequencies

$$\mathcal{F}[X(t)] = \mathcal{F}(f) = \mathcal{N}\left(0, \frac{1}{2}P(f)\right) + i\mathcal{N}\left(0, \frac{1}{2}P(f)\right) \quad ; \quad \langle \mathcal{F}(f_i)\mathcal{F}(f_j) \rangle = \delta_{ij}$$

Using the periodogram $\text{Per}(f)$ in addition to the fact that the squared normal distribution follows a χ_2^2 , we obtain that the periodogram is

$$\text{Per}(f) \sim \frac{1}{2}P(f)\chi_2^2 \implies \text{Per}(f) = P(f) \pm P(f) \tag{A.2}$$

¹ [scipy.interpolate.univariatespline Documentation](#).

This is the basis of the Fourier Decomposition, meaning that with this method the periodogram as its error follows a χ_2^2 distribution. It is highly recommended to average subsets of periodogram points in order to reduce the error of the periodogram. Indeed, If we average N points that distribute as χ_2^2 , by the central limit theorem we obtain that the new distribution approaches the Normal distribution as $N \rightarrow \infty$. Papadakis & Lawrence (1993) shows how by using an average in logarithmic scale only $N = 20$ are required to achieve a normal-like distribution.

A.3. Bayes' Theorem

The statement of Bayes' theorem comes from the definition of a conditional probability of A given B and viceversa

$$P(A|B) = \frac{P(A \cap B)}{P(B)} \quad ; \quad P(B|A) = \frac{P(A \cap B)}{P(A)}$$

If we solve for $P(A \cap B)$ we obtain that

$$P(A \cap B) = P(A|B)P(B) = P(B|A)P(A)$$

Using the right side of the previous results and solving for $P(A|B)$ we obtain the Bayes' Theorem.

$$\Rightarrow P(A|B) = \frac{P(B|A)P(A)}{P(B)} \tag{A.3}$$

A.4. Parseval's Theorem over white noise

A white noise has a PSD $P(f) = P_{\text{noise}}$. Hence, for a white noise coming from a $\mathcal{N}(0, \sigma_e^2)$, the Parseval's Theorem tell us that

$$\sigma_e^2 = \int_{f_{\text{ini}}}^{f_{\text{fin}}} P(f)df = P_{\text{noise}} \int_{f_{\text{ini}}}^{f_{\text{fin}}} df = P_{\text{noise}}(f_{\text{fin}} - f_{\text{ini}})$$

being f_{ini} and f_{fin} the initial and final frequency respectively. If the white noise is defined over N points, then $f_{\text{ini}} = \frac{1}{T}$ and $f_{\text{fin}} = \frac{N}{2T}$, where $T = N(t_N - t_1)/(N - 1)$ being t_1 and t_N the initial and final time of the time series respectively. Thus, the variance of the time series and the noise level of its periodogram have the following relationship

$$\sigma_e^2 = P_{\text{noise}} \frac{1}{T} \left(\frac{N}{2} - 1 \right) \tag{A.4}$$

A.5. Generalized Linear Model in H2O

Generalized Linear Models² (GLM) are an extension to classical regression models where the outcomes follow normal distributions, allowing also to apply regressions to outcomes with exponential distributions such as poisson, gamma, and binomial distributions. The latter is used for the purpose of making a model of a binary classification, which is also known as logistic regression. In a logistic regression the outcome \hat{y} has the form

$$\log\left(\frac{\hat{y}}{1-\hat{y}}\right) = \beta_0 + x^T \boldsymbol{\beta} = \beta_0 + \beta_1 x_1 + \beta_2 x_2 + \cdots + \beta_N x_N \quad (\text{A.5})$$

where β_0 is the intercept and the others β_i are the coefficients for the N different predictors x . In order to fit the model with the data, H2O maximizes the following penalized likelihood

$$\max_{\boldsymbol{\beta}, \beta_0} \frac{1}{N} \sum_{i=1}^N \left(y_i (x_i^T \boldsymbol{\beta} + \beta_0) - \log(1 + e^{x_i^T \boldsymbol{\beta} + \beta_0}) \right) - \lambda \left(\alpha \|\boldsymbol{\beta}\|_1 + \frac{1}{2} (1 - \alpha) \|\boldsymbol{\beta}\|_2^2 \right) \quad (\text{A.6})$$

where the α parameter controls the distribution between ℓ_1 (LASSO) and ℓ_2 (ridge regression) penalties³, and λ controls the amount of regularization applied to the model.

A.6. Doppler correction

As is well known, the Doppler effect caused by the redshift correspond to

$$1 + z = \frac{f_{\text{em}}}{f_{\text{obs}}}$$

where f_{em} is the frequency of the emitting source in its frame and f_{obs} to the observed emission from that source in the frame of the observer. If we pass to an interval time as $\Delta t = 1/f$, then we obtain that Δt_{em} and Δt_{obs} are related as $\Delta t_{\text{obs}} = (1 + z) \Delta t_{\text{em}}$. However, this Doppler correction is not taking into account the relativistic emission of the source. In relativity, energies E_{em} and E_{obs} are related as $E_{\text{obs}} = \delta E_{\text{em}}$ ⁴, where δ corresponds to the Doppler factor and is defined as

$$\delta \equiv \frac{1}{\Gamma(1 - \beta_{\Gamma} \cos \theta_{\text{obs}})} \quad (\text{A.7})$$

where Γ is known as the Bulk Lorentz factor of the emission region, β_{Γ} the normalized speed of the emission region and θ_{obs} the angle that covers the emitting source in the direction of the emission region viewed from the point of view of the observer, which corresponds to the

² [GLM Documentation in H2O](#)

³ [α parameter in H2O](#)

⁴ see Boettcher et al. (2012) “*Relativistic Jets from Active Galactic Nuclei*”, Chapter 2 for a detailed explanation.

angle of sight of the jet in Blazars. Using the fact that $E = hf$ we obtain that the relativistic Doppler correction is

$$\delta^{-1} = \frac{f_{\text{em}}}{f_{\text{obs}}}$$

Finally, taking into account both redshift and Doppler factor, the final correction corresponds to

$$f_{\text{obs}} = \frac{\delta}{(1+z)} f_{\text{em}} \tag{A.8}$$

$$\Delta t_{\text{obs}} = \frac{(1+z)}{\delta} \Delta t_{\text{em}} \tag{A.9}$$

This implies that the timescale of the source is shortened by a factor $\delta/(1+z)$ with respect to the observed timescale.

Annex B

Figures

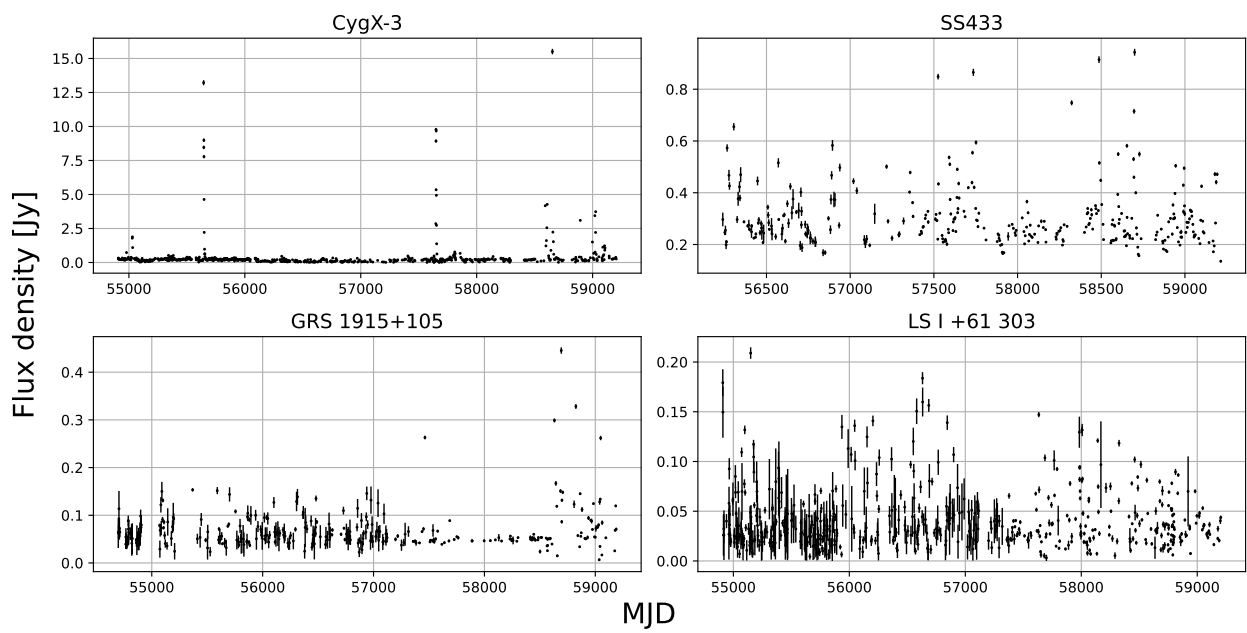


Figure B.1: Light curves of microquasars CygX-3, SS433, GRS 1915+105 and LS I +61 303 removed from the analysis.

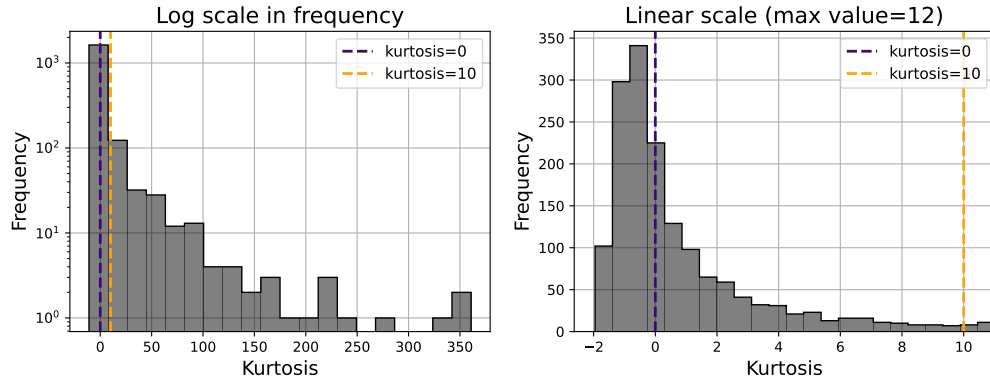


Figure B.2: Histogram of the kurtosis for all 1859 OVRO objects. Left: Logarithmic scale in frequency. Right: Linear scale for values between -2 and 12. Segmented lines at 0 (purple) and 10 (yellow) correspond to the values that change the cubic spline input and thresholds (See Appendix A.1).

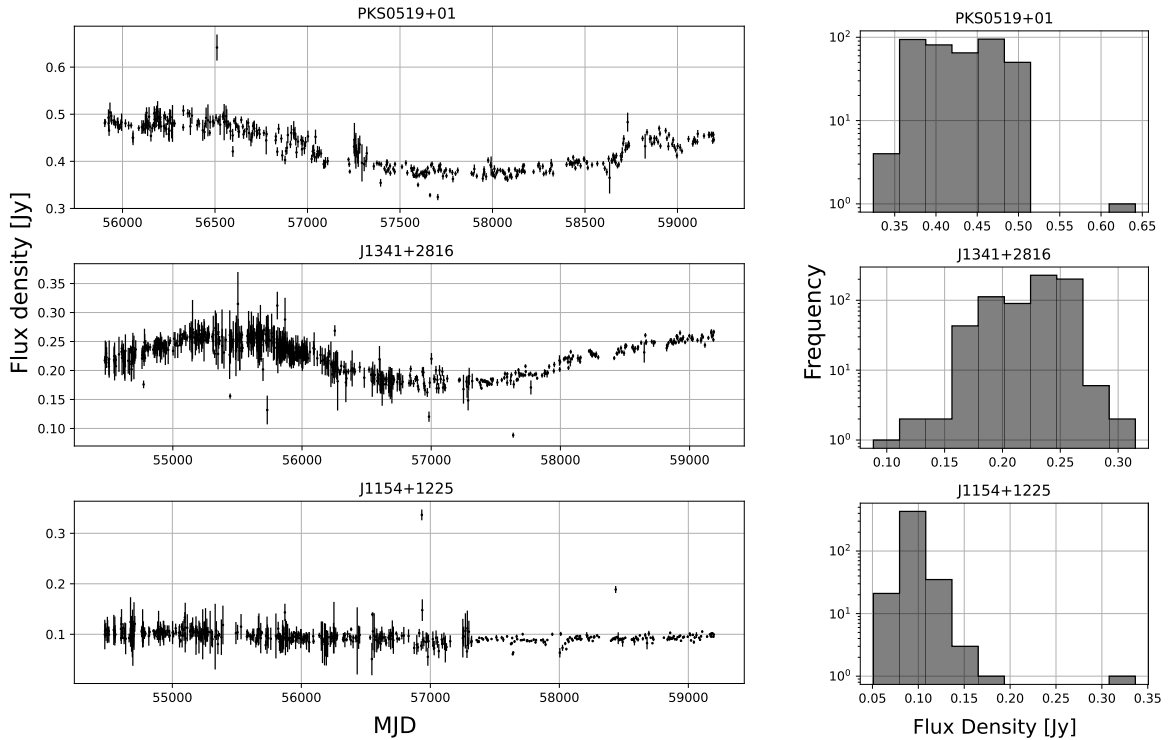


Figure B.3: Light curve of three objects (left) and histograms of their flux densities (right) each one representing the range of kurtosis described in Appendix A.1. PKS 0519+01, J1341+2816 and J1154+1225 have kurtosis of -0.25 , 0.21 and 116.93 respectively.

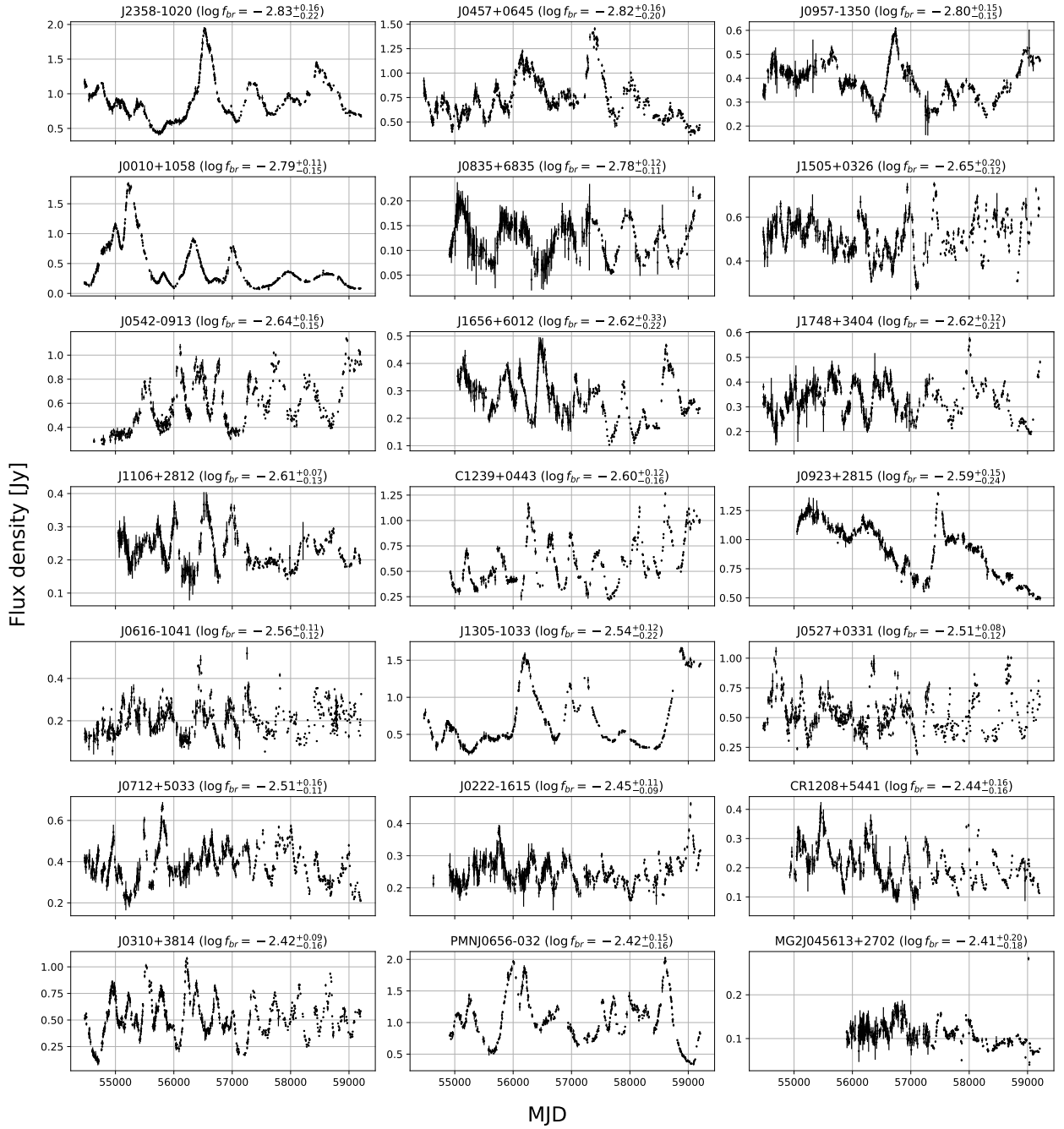


Figure B.4: Light curves of the 39 objects well-fitted using the broken power-law model (Part 1).

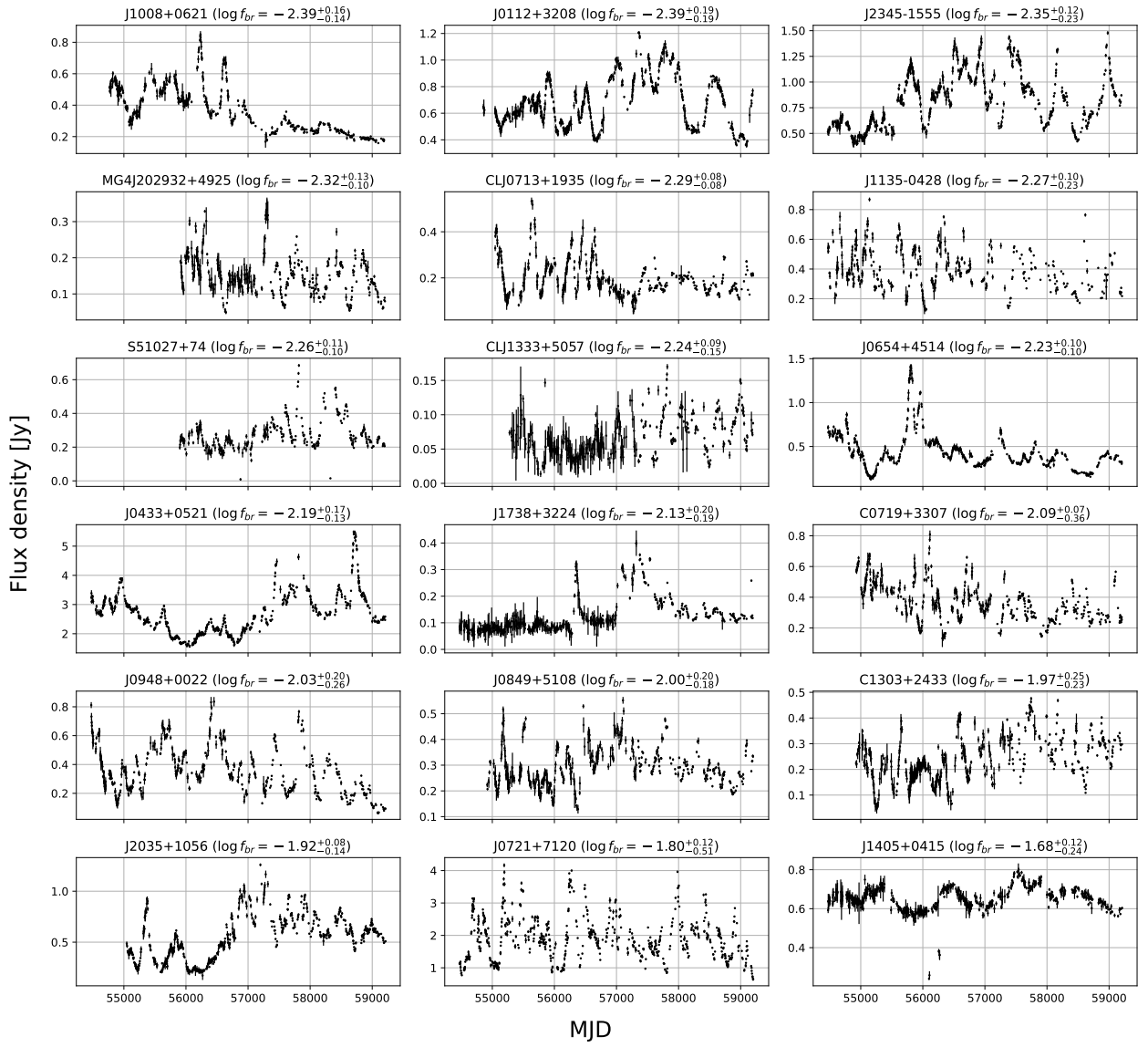


Figure B.5: Light curves of the 39 objects well-fitted using the broken power-law model (Part 2).

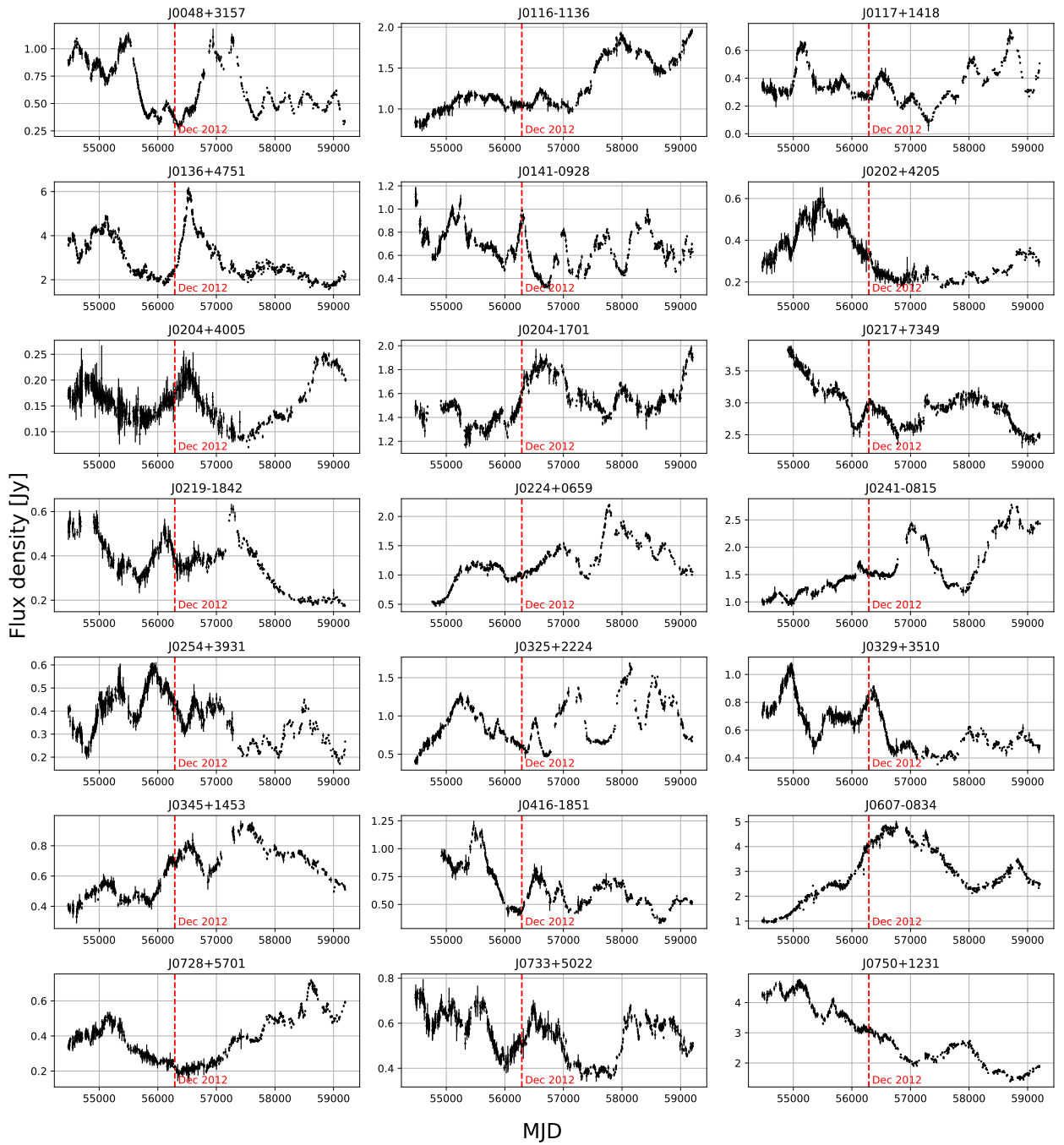


Figure B.6: Light curves of the 74 non-consistent objects from Section 7.1 with $\beta_{\text{old}} > \beta_{\text{new}}$ (Part 1). The red segmented line represents the end of the time period used in Max-Moerbeck (2013).

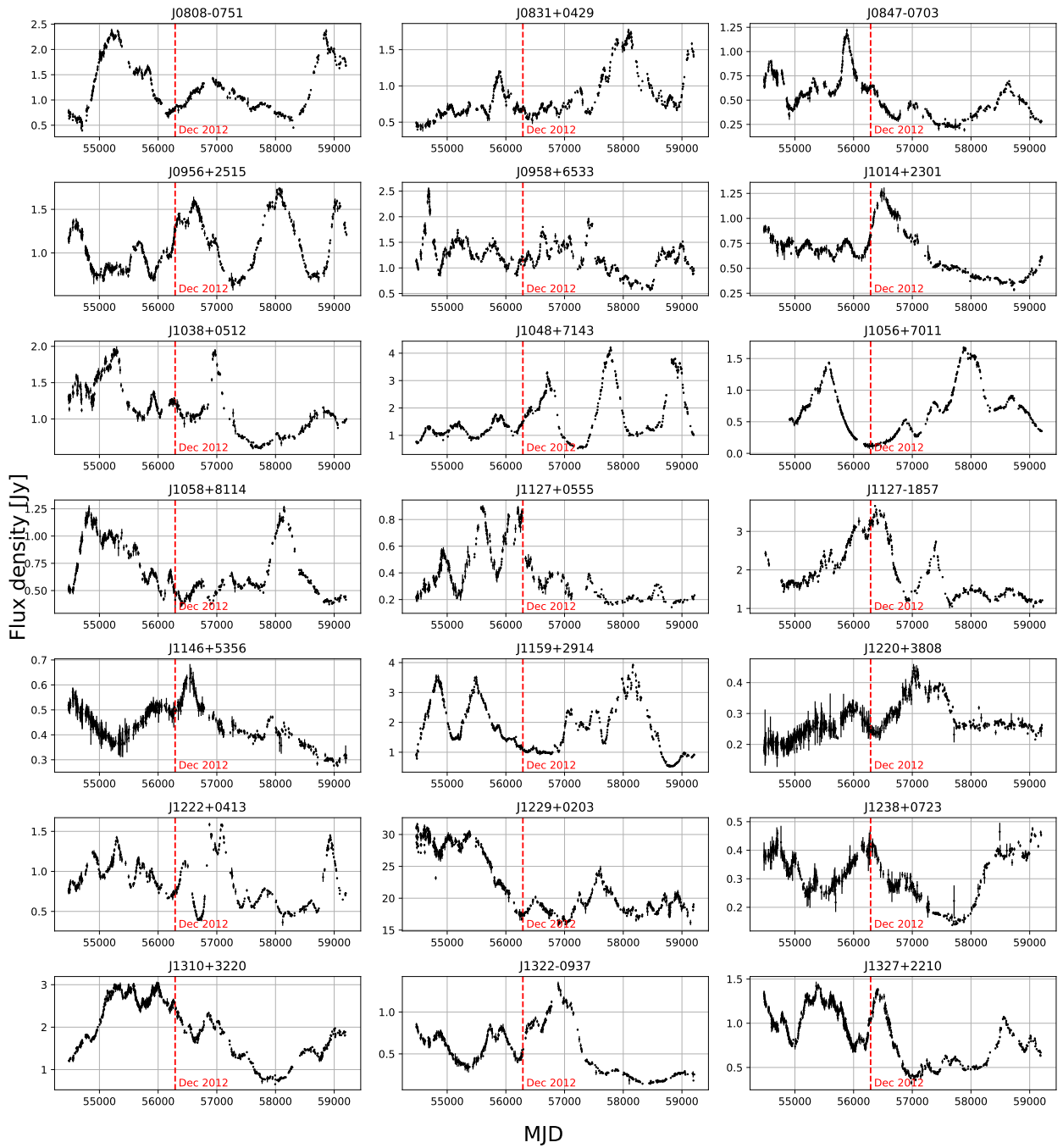


Figure B.7: Light curves of the 74 non-consistent objects from Section 7.1 with $\beta_{\text{old}} > \beta_{\text{new}}$ (Part 2). The red segmented line represents the end of the time period used in Max-Moerbeck (2013).

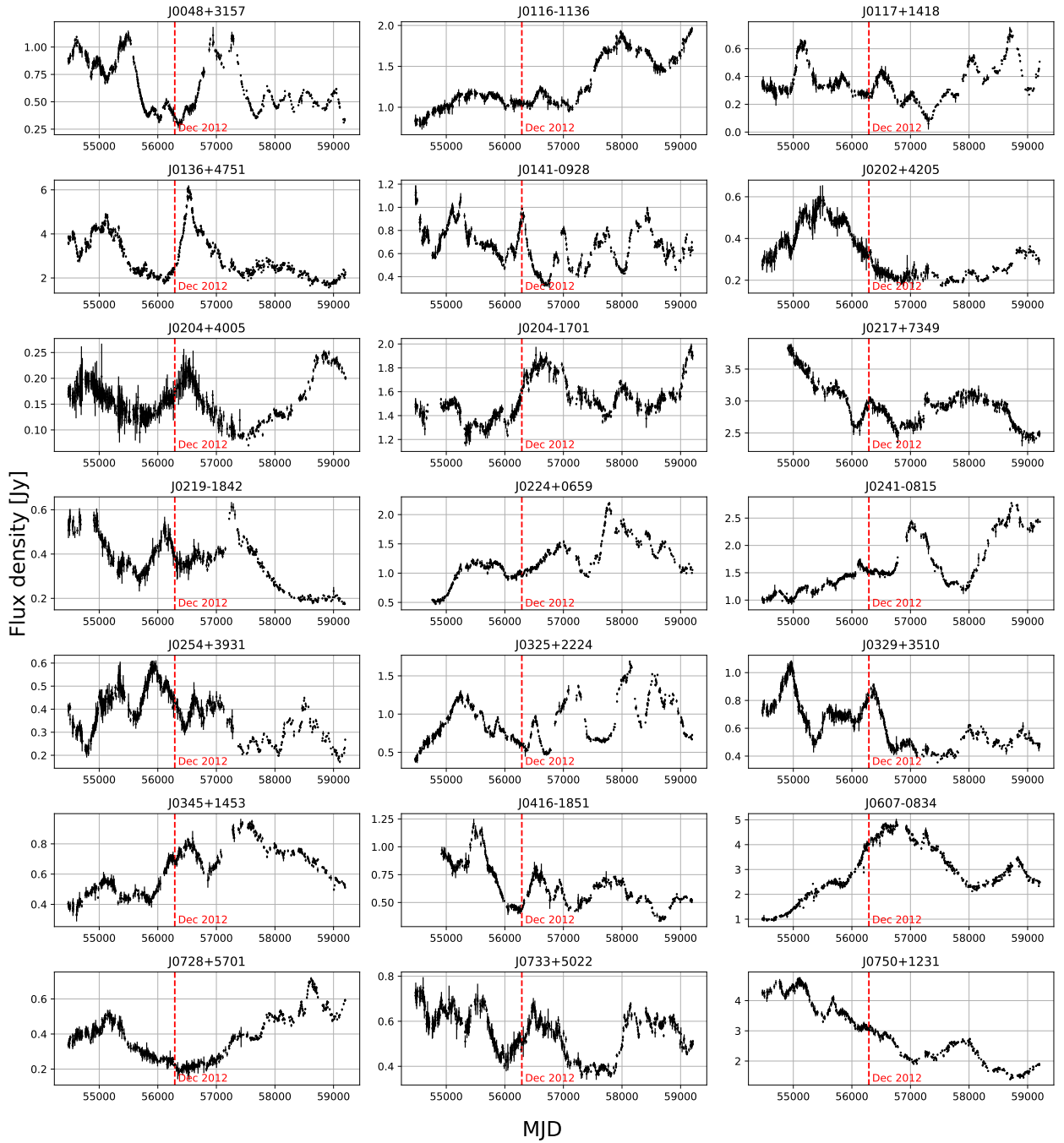


Figure B.8: Light curves of the 74 non-consistent objects from Section 7.1 with $\beta_{\text{old}} > \beta_{\text{new}}$ (Part 3). The red segmented line represents the end of the time period used in Max-Moerbeck (2013).

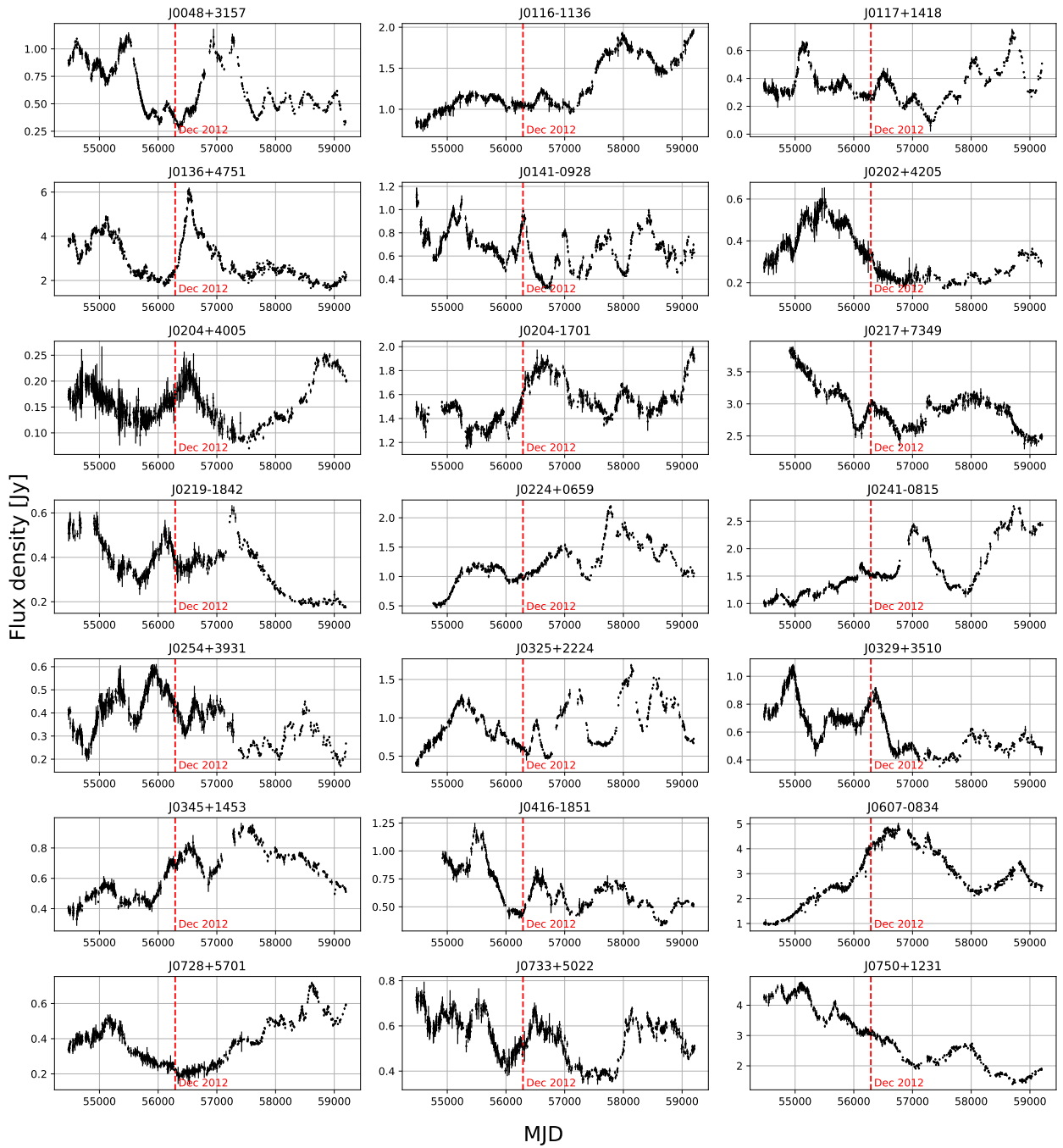


Figure B.9: Light curves of the 74 non-consistent objects from Section 7.1 with $\beta_{\text{old}} > \beta_{\text{new}}$ (Part 4). The red segmented line represents the end of the time period used in Max-Moerbeck (2013).

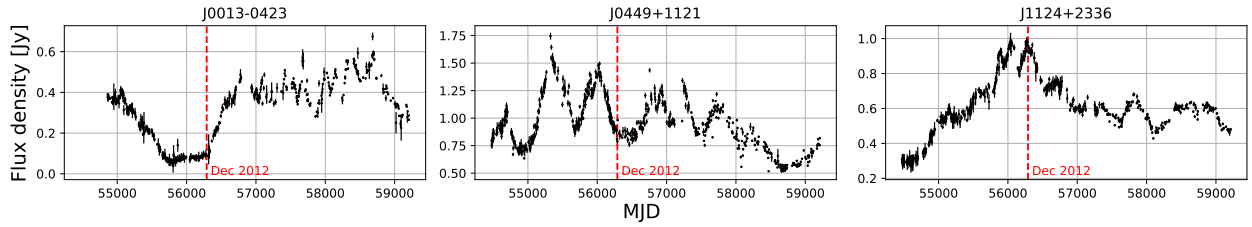


Figure B.10: Light curves of the 3 non-consistent objects from Section 7.1 with $\beta_{\text{old}} < \beta_{\text{new}}$. The red segmented line represents the end of the time period used in Max-Moerbeck (2013).

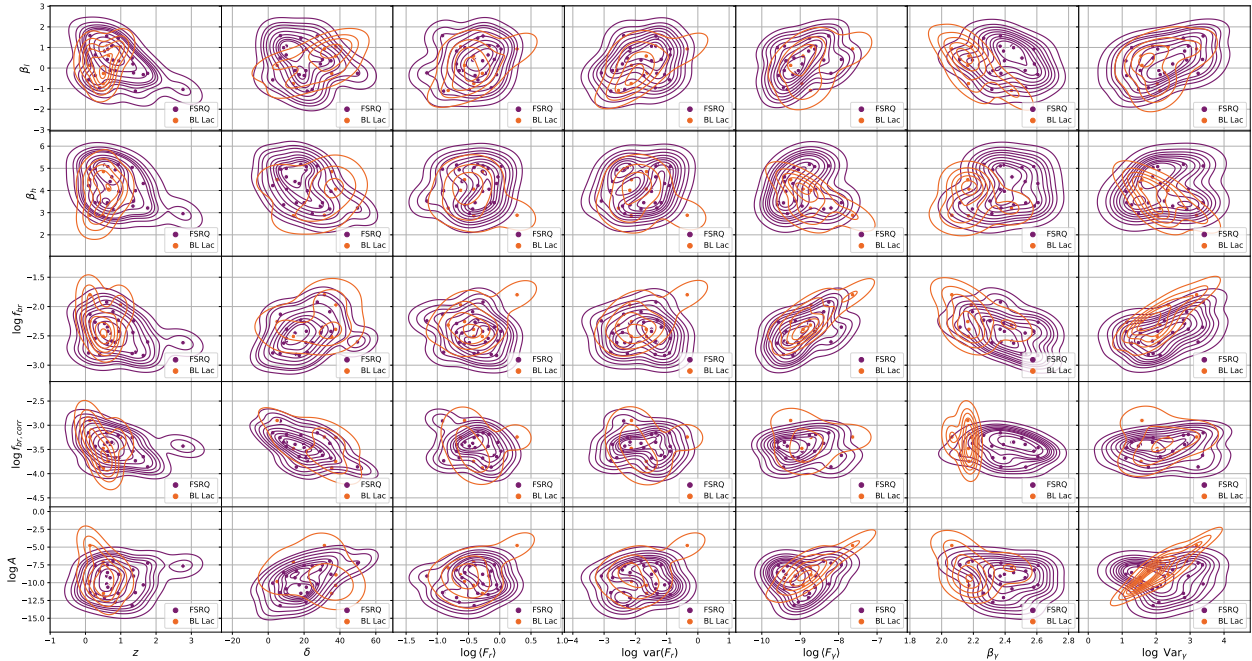


Figure B.11: Scatter plot along with a KDE plot at 10 levels of the model parameters from the broken power-law model versus other parameters for FSRQ (purple) and BL Lac (orange).

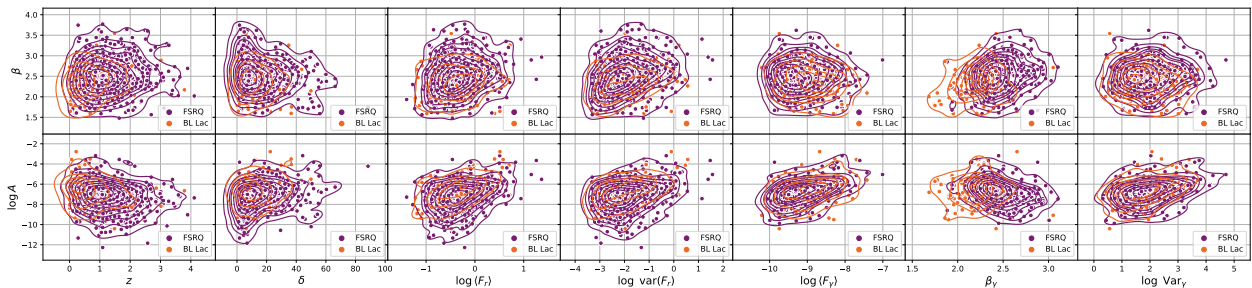


Figure B.12: Scatter plot along with a KDE plot at 10 levels of the model parameters from the simple power-law model versus other parameters for FSRQ (purple) and BL Lac (orange).

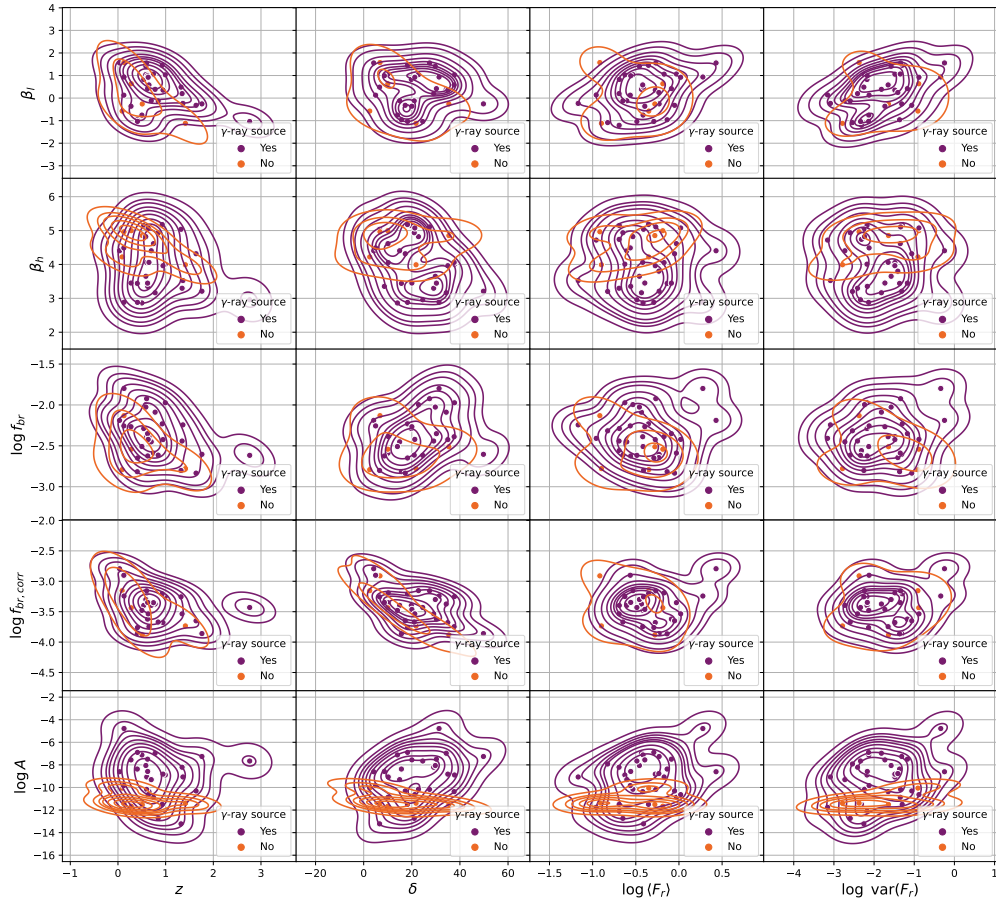


Figure B.13: Scatter plot along with a KDE plot at 10 levels of the model parameters from the broken power-law model versus other parameters for γ -ray (purple) and non γ -ray (orange) sources.

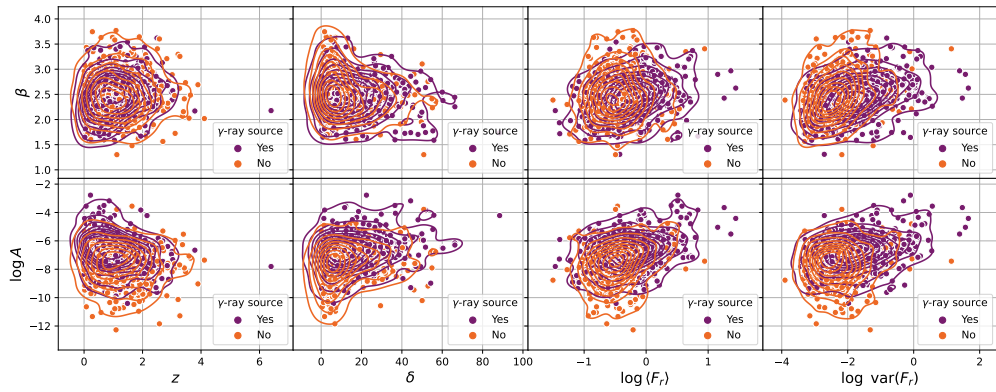


Figure B.14: Scatter plot along with a KDE plot at 10 levels of the model parameters from the simple power-law model versus other parameters for γ -ray (purple) and non γ -ray (orange) sources.

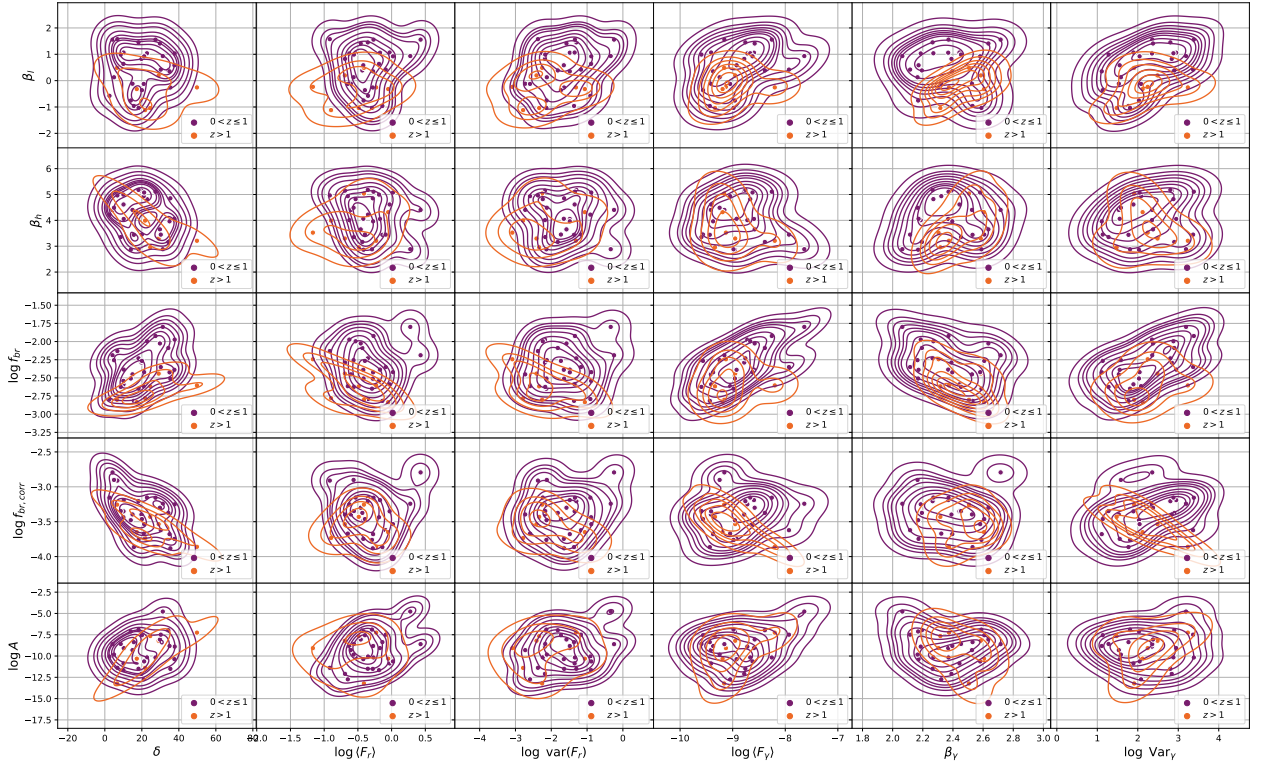


Figure B.15: Scatter plot along with a KDE plot at 10 levels of the model parameters from the broken power-law model versus other parameters for redshift $0 < z \leq 1$ (purple) and $z > 1$ (orange).

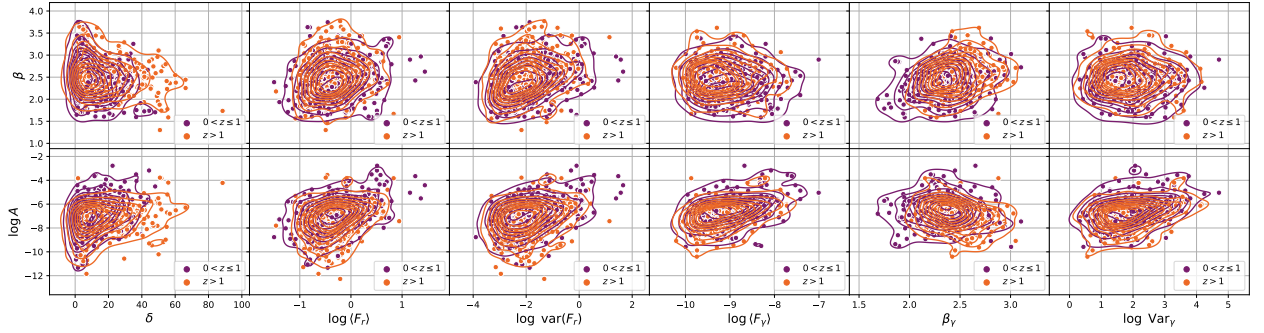


Figure B.16: Scatter plot along with a KDE plot at 10 levels of the model parameters from the simple power-law model versus other parameters for redshift $0 < z \leq 1$ (purple) and $z > 1$ (orange).

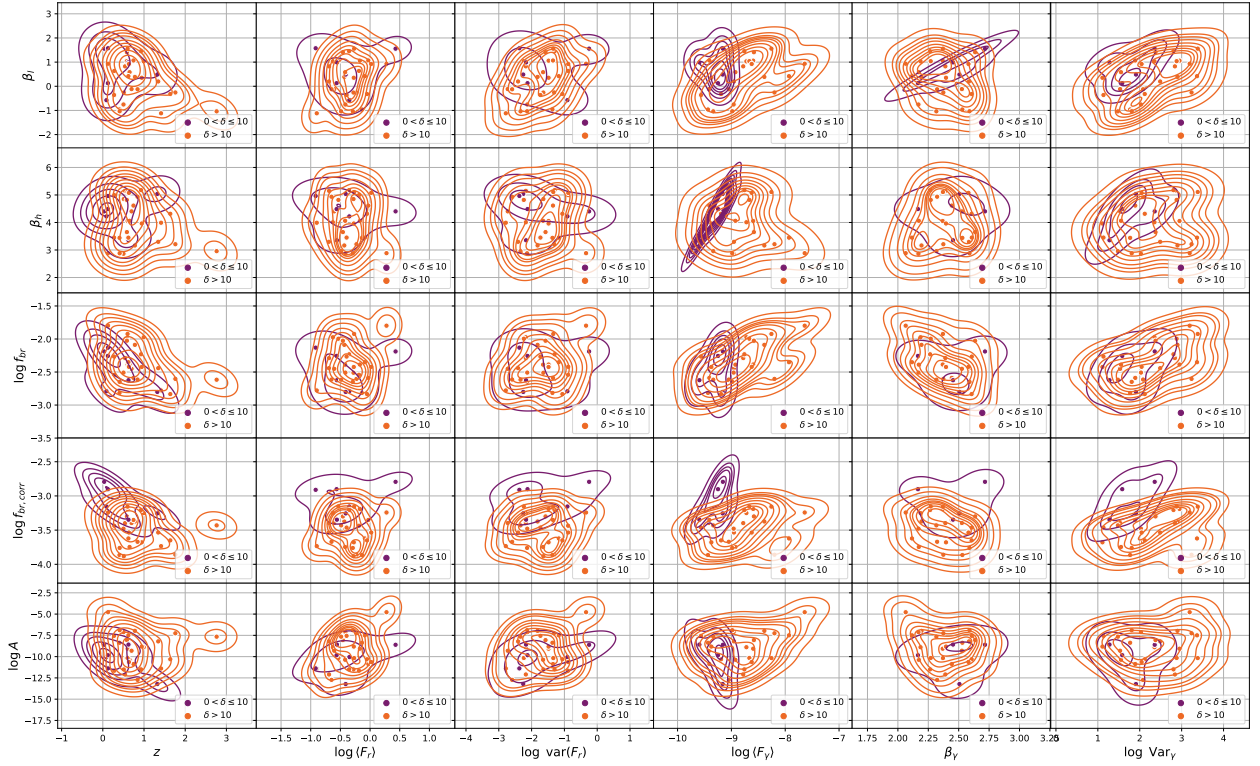


Figure B.17: Scatter plot along with a KDE plot at 10 levels of the model parameters from the broken power-law model versus other parameters for Doppler factor $0 < \delta \leq 10$ (purple) and $\delta > 10$ (orange).

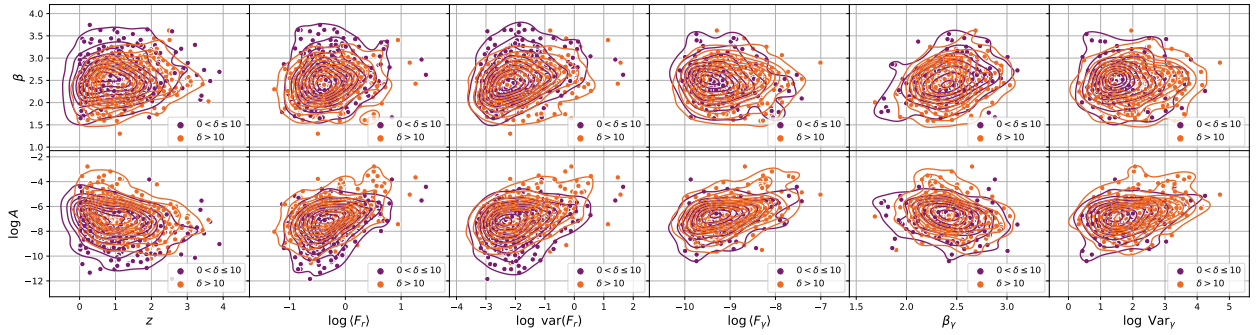


Figure B.18: Scatter plot along with a KDE plot at 10 levels of the model parameters from the simple power-law model versus other parameters for Doppler factor $0 < \delta \leq 10$ (purple) and $\delta > 10$ (orange).

Annex C

Tables

Table C.1: Results of fitting the simple power-law model over the 1290 selected observations from OVRO dataset. Flag refers to sources well-defined by the model, being (*m*) objects with a $\sigma(\beta)_{68.3\%} \in [1.5, 3]$ (medium quality) and (*ℓ*) to $\sigma(\beta)_{68.3\%} > 3$ (low quality). The absence of a flag means having $\sigma(\beta)_{68.3\%} < 1.5$.

Name	Flag	β	$\beta^{95.5\%}$	$\beta^{99.7\%}$	$\log A$	$\log A^{95.5\%}$	$\log A^{99.7\%}$
0010+405		$2.17^{+0.25}_{-0.32}$	$+0.61_{-0.45}$	$+0.73_{-0.69}$	$-5.98^{+0.70}_{-0.54}$	$+1.11_{-1.21}$	$+1.34_{-1.63}$
0059+581		$2.11^{+0.26}_{-0.19}$	$+0.60_{-0.30}$	$+0.69_{-0.52}$	$-3.93^{+0.51}_{-0.47}$	$+0.79_{-1.15}$	$+0.94_{-1.62}$
0136+176	<i>m</i>	$2.53^{+1.53}_{-0.68}$	$+2.89_{-0.75}$	$+2.97_{-1.24}$	$-8.78^{+1.85}_{-4.89}$	$+1.96_{-9.37}$	$+3.12_{-9.83}$
0224+671		$3.12^{+0.32}_{-0.49}$	$+0.84_{-0.74}$	$+1.23_{-0.88}$	$-7.77^{+1.11}_{-0.79}$	$+1.72_{-2.04}$	$+1.98_{-3.04}$
0241+622		$2.48^{+0.30}_{-0.40}$	$+0.68_{-0.57}$	$+0.75_{-0.76}$	$-6.37^{+0.74}_{-0.95}$	$+1.31_{-1.76}$	$+1.58_{-1.94}$
0300+471		$2.32^{+0.35}_{-0.24}$	$+0.71_{-0.47}$	$+0.99_{-0.63}$	$-5.43^{+0.62}_{-0.73}$	$+0.96_{-1.78}$	$+1.44_{-2.38}$
0333+321		$2.46^{+0.40}_{-0.33}$	$+1.02_{-0.64}$	$+1.43_{-0.71}$	$-6.68^{+1.08}_{-0.88}$	$+1.84_{-2.64}$	$+1.89_{-3.73}$
0355+508	<i>m</i>	$2.53^{+0.73}_{-0.79}$	$+1.89_{-1.02}$	$+2.78_{-1.12}$	$-5.47^{+2.17}_{-2.35}$	$+2.65_{-6.30}$	$+2.82_{-9.22}$
0415+379		$2.85^{+0.26}_{-0.33}$	$+0.81_{-0.50}$	$+0.97_{-0.67}$	$-6.17^{+0.78}_{-0.59}$	$+1.50_{-1.62}$	$+1.56_{-2.14}$
0536+145		$2.28^{+0.35}_{-0.41}$	$+1.05_{-0.58}$	$+1.59_{-0.75}$	$-6.01^{+0.53}_{-1.31}$	$+1.18_{-3.05}$	$+1.37_{-4.13}$
0836+710		$2.67^{+0.41}_{-0.42}$	$+0.92_{-0.81}$	$+1.62_{-0.82}$	$-6.69^{+0.80}_{-1.37}$	$+1.53_{-3.11}$	$+2.12_{-4.35}$
0859-140	<i>ℓ</i>	$-0.59^{+2.25}_{-0.91}$	$+4.89_{-0.91}$	$+5.81_{-0.91}$	$-16.70^{+6.61}_{-2.29}$	$+12.80_{-2.30}$	$+14.40_{-2.30}$
1243-072		$2.36^{+0.72}_{-0.46}$	$+1.53_{-1.02}$	$+2.78_{-0.96}$	$-6.63^{+1.20}_{-1.90}$	$+2.36_{-4.58}$	$+2.31_{-8.44}$
1406-076		$2.96^{+0.48}_{-0.40}$	$+1.04_{-0.75}$	$+1.44_{-0.94}$	$-7.82^{+1.20}_{-1.11}$	$+1.84_{-2.82}$	$+2.17_{-4.12}$
1458+718		$4.97^{+0.40}_{-1.09}$	$+0.52_{-2.31}$	$+0.51_{-3.27}$	$-15.01^{+2.69}_{-1.91}$	$+6.94_{-1.96}$	$+9.86_{-1.95}$
1655+077		$3.17^{+0.74}_{-0.49}$	$+1.73_{-0.85}$	$+2.12_{-1.21}$	$-8.42^{+1.66}_{-1.65}$	$+2.88_{-4.60}$	$+2.87_{-6.18}$
1845+797		$2.59^{+0.87}_{-0.55}$	$+2.02_{-0.77}$	$+2.28_{-1.09}$	$-7.49^{+1.58}_{-2.32}$	$+2.71_{-5.55}$	$+2.98_{-6.56}$
1923+210	<i>m</i>	$2.22^{+1.38}_{-0.80}$	$+2.84_{-1.02}$	$+3.16_{-1.14}$	$-6.86^{+2.23}_{-4.12}$	$+2.23_{-9.95}$	$+2.92_{-10.12}$
1924+507	<i>m</i>	$4.78^{+0.67}_{-1.83}$	$+0.72_{-3.24}$	$+0.72_{-3.97}$	$-16.66^{+7.17}_{-1.13}$	$+10.54_{-2.29}$	$+11.82_{-2.32}$
1926+42		$1.79^{+0.32}_{-0.43}$	$+0.87_{-0.68}$	$+1.22_{-0.79}$	$-5.82^{+0.82}_{-1.06}$	$+1.35_{-2.76}$	$+1.69_{-3.55}$

Table C.1: Results of fitting the simple power-law model over the 1290 selected observations from OVRO dataset. Flag refers to sources well-defined by the model, being (*m*) objects with a $\sigma(\beta)_{68.3\%} \in [1.5, 3]$ (medium quality) and (*ℓ*) to $\sigma(\beta)_{68.3\%} > 3$ (low quality). The absence of a flag means having $\sigma(\beta)_{68.3\%} < 1.5$.

Name	Flag	β	$\beta^{95.5\%}$	$\beta^{99.7\%}$	$\log A$	$\log A^{95.5\%}$	$\log A^{99.7\%}$
1RXS002209.2-185333	<i>m</i>	$2.14^{+2.03}_{-0.46}$	$+2.89$ -0.79	$+3.15$ -1.19	$-7.86^{+1.65}_{-6.53}$	$+1.97$ -10.11	$+2.98$ -10.13
1RXSJ154604.6+08191	<i>ℓ</i>	$1.27^{+2.09}_{-1.87}$	$+3.37$ -2.67	$+4.07$ -2.76	$-16.74^{+6.39}_{-2.00}$	$+11.75$ -2.00	$+13.31$ -2.24
2005+403		$1.94^{+0.51}_{-0.28}$	$+1.08$ -0.53	$+1.39$ -0.79	$-5.08^{+0.73}_{-1.27}$	$+1.35$ -2.67	$+1.72$ -3.54
2021+317		$2.32^{+0.87}_{-0.39}$	$+1.70$ -0.73	$+2.54$ -1.03	$-6.56^{+1.29}_{-2.33}$	$+2.10$ -4.71	$+2.47$ -7.42
2037+511		$3.04^{+0.63}_{-0.65}$	$+1.19$ -1.05	$+1.94$ -1.33	$-7.18^{+1.41}_{-1.93}$	$+2.55$ -3.79	$+2.82$ -5.70
2230+114		$2.39^{+0.38}_{-0.26}$	$+0.69$ -0.54	$+0.97$ -0.81	$-6.03^{+0.98}_{-0.56}$	$+1.83$ -1.10	$+2.12$ -1.67
2254+074		$3.04^{+0.34}_{-0.46}$	$+0.85$ -0.72	$+1.21$ -0.96	$-7.83^{+0.73}_{-1.19}$	$+1.49$ -2.35	$+1.96$ -3.46
2351+456	<i>m</i>	$3.19^{+0.91}_{-0.87}$	$+1.94$ -1.33	$+2.27$ -1.53	$-9.48^{+2.29}_{-2.98}$	$+3.30$ -6.36	$+3.80$ -7.36
2353+816		$2.36^{+0.45}_{-0.27}$	$+0.84$ -0.50	$+0.90$ -0.65	$-6.62^{+0.69}_{-1.10}$	$+1.20$ -2.18	$+1.29$ -2.55
3C207		$2.31^{+0.29}_{-0.45}$	$+0.70$ -0.62	$+1.07$ -0.79	$-6.01^{+0.87}_{-1.06}$	$+1.44$ -1.98	$+1.79$ -2.96
3C274	<i>ℓ</i>	$1.11^{+1.11}_{-2.47}$	$+3.39$ -2.54	$+4.02$ -2.61	$-13.63^{+8.54}_{-2.34}$	$+12.59$ -2.03	$+13.73$ -2.35
3C380		$2.12^{+0.30}_{-0.31}$	$+0.70$ -0.50	$+0.87$ -0.94	$-5.24^{+0.91}_{-0.63}$	$+1.47$ -1.57	$+1.65$ -2.18
3C407	<i>m</i>	$2.93^{+1.45}_{-0.66}$	$+2.26$ -1.05	$+2.52$ -1.64	$-9.76^{+1.77}_{-5.23}$	$+2.65$ -8.16	$+4.57$ -8.16
3C48		$1.80^{+0.30}_{-0.24}$	$+0.60$ -0.51	$+0.86$ -0.61	$-5.29^{+0.63}_{-0.64}$	$+1.04$ -1.70	$+1.34$ -2.17
3C66A		$2.53^{+0.27}_{-0.35}$	$+0.64$ -0.59	$+1.00$ -0.82	$-7.43^{+0.97}_{-0.58}$	$+1.57$ -1.56	$+2.11$ -2.65
3EGJ2016+3657		$1.74^{+0.19}_{-0.16}$	$+0.37$ -0.31	$+0.44$ -0.36	$-3.18^{+0.29}_{-0.35}$	$+0.60$ -0.69	$+0.68$ -0.87
3EGJ2027+3429		$1.64^{+0.13}_{-0.22}$	$+0.31$ -0.37	$+0.47$ -0.45	$-2.78^{+0.26}_{-0.40}$	$+0.45$ -0.94	$+0.66$ -1.10
4C+29.48	<i>m</i>	$2.30^{+1.21}_{-0.70}$	$+2.76$ -0.92	$+3.02$ -1.24	$-7.23^{+2.56}_{-3.11}$	$+2.59$ -8.90	$+2.90$ -9.84
4C+45.08		$2.64^{+0.56}_{-0.64}$	$+1.52$ -0.97	$+1.88$ -1.18	$-8.07^{+1.73}_{-1.61}$	$+2.69$ -4.10	$+2.95$ -5.68
5C07.119	<i>m</i>	$2.99^{+1.40}_{-0.87}$	$+2.46$ -1.11	$+2.50$ -1.82	$-10.20^{+2.54}_{-4.59}$	$+3.20$ -8.73	$+4.72$ -8.73
5C12.170		$2.57^{+0.39}_{-0.13}$	$+0.76$ -0.28	$+0.93$ -0.46	$-7.01^{+0.24}_{-0.88}$	$+0.70$ -1.57	$+1.04$ -2.06
6CB194425+834912	<i>ℓ</i>	$1.36^{+1.90}_{-1.88}$	$+3.27$ -2.78	$+3.94$ -2.86	$-16.71^{+8.49}_{-2.16}$	$+12.56$ -2.16	$+14.19$ -2.29
7C1823+6856		$2.75^{+0.48}_{-0.59}$	$+1.15$ -0.88	$+1.93$ -0.92	$-8.62^{+1.53}_{-1.34}$	$+2.49$ -2.89	$+2.56$ -5.07
7C2010+4619		$2.65^{+0.31}_{-0.16}$	$+0.58$ -0.34	$+0.77$ -0.52	$-5.99^{+0.36}_{-0.58}$	$+0.77$ -1.12	$+1.12$ -1.55
87GB114026.7+613850	<i>m</i>	$2.76^{+1.48}_{-0.88}$	$+2.61$ -1.03	$+2.71$ -1.56	$-9.37^{+2.48}_{-5.11}$	$+3.03$ -9.12	$+4.18$ -9.58
87GB182712.0+272717		$2.31^{+0.37}_{-0.47}$	$+0.97$ -0.74	$+1.16$ -1.05	$-7.24^{+0.92}_{-1.19}$	$+1.55$ -2.64	$+1.98$ -3.03
87GB190942.8+160617		$2.68^{+0.77}_{-0.65}$	$+1.55$ -1.10	$+2.37$ -1.32	$-8.14^{+1.64}_{-2.52}$	$+3.18$ -5.39	$+3.17$ -7.21
87GB195252.4+135009		$2.52^{+0.22}_{-0.37}$	$+0.62$ -0.57	$+0.70$ -0.86	$-7.06^{+0.66}_{-0.79}$	$+1.18$ -1.62	$+1.65$ -1.98
A2052	<i>ℓ</i>	$-0.34^{+2.34}_{-1.07}$	$+4.80$ -1.16	$+5.51$ -1.16	$-17.11^{+5.68}_{-1.88}$	$+11.77$ -1.89	$+13.90$ -1.88
A2415	<i>m</i>	$4.70^{+0.74}_{-1.17}$	$+0.74$ -2.59	$+0.76$ -3.22	$-16.09^{+4.59}_{-1.44}$	$+8.64$ -1.90	$+10.16$ -1.86

Table C.1: Results of fitting the simple power-law model over the 1290 selected observations from OVRO dataset. Flag refers to sources well-defined by the model, being (*m*) objects with a $\sigma(\beta)_{68.3\%} \in [1.5, 3]$ (medium quality) and (*ℓ*) to $\sigma(\beta)_{68.3\%} > 3$ (low quality). The absence of a flag means having $\sigma(\beta)_{68.3\%} < 1.5$.

Name	Flag	β	$\beta^{95.5\%}$	$\beta^{99.7\%}$	$\log A$	$\log A^{95.5\%}$	$\log A^{99.7\%}$
ATJ0814-1012	<i>m</i>	$2.13^{+2.09}_{-0.82}$	$+3.09$ -2.80	$+3.30$ -3.51	$-7.74^{+2.23}_{-6.76}$	$+1.89$ -11.26	$+2.85$ -11.26
B20200+30		$1.69^{+0.49}_{-0.18}$	$+0.86$ -0.42	$+1.02$ -0.56	$-5.26^{+0.47}_{-1.04}$	$+0.77$ -2.21	$+1.16$ -2.64
B20242+23		$2.24^{+0.29}_{-0.25}$	$+0.55$ -0.51	$+0.81$ -0.64	$-6.59^{+0.82}_{-0.45}$	$+1.16$ -1.32	$+1.43$ -1.94
B20321+33		$1.77^{+0.17}_{-0.16}$	$+0.31$ -0.32	$+0.43$ -0.43	$-4.59^{+0.31}_{-0.31}$	$+0.57$ -0.71	$+0.75$ -1.04
B20619+33		$1.94^{+0.42}_{-0.32}$	$+0.84$ -0.62	$+1.08$ -0.79	$-5.71^{+0.62}_{-1.27}$	$+1.21$ -2.39	$+1.48$ -2.92
B21846+32B		$2.16^{+0.29}_{-0.25}$	$+0.75$ -0.39	$+0.75$ -0.61	$-5.69^{+0.57}_{-0.61}$	$+0.84$ -1.47	$+1.11$ -1.76
B30509+406		$2.74^{+0.32}_{-0.35}$	$+0.64$ -0.71	$+1.00$ -0.84	$-6.83^{+0.70}_{-0.96}$	$+1.75$ -1.56	$+1.92$ -2.74
B30707+476		$2.10^{+0.45}_{-0.14}$	$+0.74$ -0.31	$+0.75$ -0.71	$-6.27^{+0.44}_{-0.93}$	$+0.95$ -1.70	$+1.32$ -2.15
B30745+453		$2.19^{+0.58}_{-0.35}$	$+1.36$ -0.64	$+1.79$ -0.83	$-7.33^{+1.09}_{-1.38}$	$+1.85$ -3.62	$+1.99$ -5.16
B30757+441		$2.73^{+0.28}_{-0.31}$	$+0.63$ -0.56	$+0.96$ -0.72	$-7.82^{+0.74}_{-0.74}$	$+1.29$ -1.60	$+1.71$ -2.36
B30819+408		$2.67^{+0.34}_{-0.46}$	$+0.72$ -0.71	$+1.05$ -0.83	$-7.67^{+1.23}_{-0.75}$	$+1.63$ -1.94	$+1.99$ -2.58
B30831+442	<i>m</i>	$2.66^{+1.13}_{-0.65}$	$+2.20$ -1.02	$+2.70$ -1.08	$-8.73^{+1.85}_{-3.36}$	$+2.36$ -7.34	$+2.98$ -9.26
B30908+416B	<i>m</i>	$1.97^{+1.39}_{-0.93}$	$+3.21$ -0.86	$+3.47$ -1.08	$-6.66^{+2.08}_{-5.25}$	$+2.11$ -11.22	$+2.36$ -12.34
B31518+423		$2.19^{+0.43}_{-0.52}$	$+0.99$ -0.78	$+1.07$ -1.11	$-6.73^{+1.15}_{-1.72}$	$+1.81$ -3.28	$+2.18$ -3.76
BBJ0723+5841	<i>ℓ</i>	$2.41^{+2.77}_{-0.73}$	$+3.05$ -3.11	$+3.05$ -3.91	$-17.65^{+6.68}_{-2.28}$	$+12.25$ -2.15	$+14.61$ -2.33
BBJ1233-0144		$2.18^{+0.82}_{-0.49}$	$+2.41$ -0.85	$+3.20$ -0.99	$-7.81^{+1.44}_{-2.39}$	$+2.20$ -8.46	$+2.66$ -10.35
BBJ1309+4305		$1.98^{+0.42}_{-0.32}$	$+1.00$ -0.58	$+1.31$ -0.74	$-7.36^{+0.90}_{-1.11}$	$+1.39$ -2.93	$+1.87$ -3.46
BBJ2247+0000		$2.13^{+0.23}_{-0.27}$	$+0.47$ -0.52	$+0.65$ -0.58	$-6.09^{+0.76}_{-0.42}$	$+1.16$ -1.06	$+1.36$ -1.38
BLLacertae		$2.26^{+0.13}_{-0.19}$	$+0.32$ -0.34	$+0.37$ -0.42	$-3.55^{+0.38}_{-0.26}$	$+0.63$ -0.62	$+0.79$ -0.82
BQJ1258-1800		$2.54^{+0.20}_{-0.38}$	$+0.55$ -0.69	$+0.83$ -0.75	$-6.49^{+0.59}_{-0.82}$	$+1.16$ -1.77	$+1.39$ -2.35
BQJ1514+4450		$1.71^{+0.32}_{-0.14}$	$+0.56$ -0.34	$+0.76$ -0.56	$-5.78^{+0.48}_{-0.60}$	$+0.81$ -1.36	$+1.15$ -1.92
BZBJ1131+5809	<i>ℓ</i>	$2.14^{+2.34}_{-0.76}$	$+3.34$ -3.02	$+3.35$ -3.60	$-7.71^{+1.87}_{-7.71}$	$+2.10$ -11.80	$+3.23$ -12.20
C0058+3311		$2.25^{+0.26}_{-0.47}$	$+0.76$ -0.66	$+1.53$ -0.88	$-7.42^{+1.19}_{-0.64}$	$+1.88$ -1.84	$+2.25$ -4.16
C0144+2705		$2.37^{+0.42}_{-0.24}$	$+0.74$ -0.60	$+1.09$ -0.67	$-6.83^{+0.65}_{-0.90}$	$+1.42$ -1.78	$+1.43$ -2.61
C0424+0036		$2.34^{+0.26}_{-0.25}$	$+0.49$ -0.65	$+0.70$ -0.71	$-6.17^{+0.65}_{-0.49}$	$+1.20$ -1.06	$+1.43$ -1.52
C0448+1127		$3.29^{+0.67}_{-0.63}$	$+1.56$ -1.02	$+1.90$ -1.48	$-10.57^{+1.66}_{-2.17}$	$+2.60$ -5.31	$+4.18$ -5.78
C0509+1011		$2.10^{+0.28}_{-0.34}$	$+0.68$ -0.56	$+0.84$ -0.72	$-5.97^{+0.91}_{-0.56}$	$+1.57$ -1.41	$+1.69$ -2.07
C0608-1520		$2.09^{+0.31}_{-0.27}$	$+0.75$ -0.47	$+0.89$ -0.63	$-6.41^{+0.64}_{-0.77}$	$+0.94$ -1.99	$+1.28$ -2.15
C0719+3307		$2.00^{+0.17}_{-0.23}$	$+0.37$ -0.40	$+0.43$ -0.65	$-5.01^{+0.50}_{-0.32}$	$+0.79$ -0.64	$+1.27$ -0.84
C0850+4854		$2.05^{+0.22}_{-0.14}$	$+0.41$ -0.28	$+0.49$ -0.49	$-5.57^{+0.33}_{-0.40}$	$+0.65$ -0.78	$+0.95$ -1.13

Table C.1: Results of fitting the simple power-law model over the 1290 selected observations from OVRO dataset. Flag refers to sources well-defined by the model, being (*m*) objects with a $\sigma(\beta)_{68.3\%} \in [1.5, 3]$ (medium quality) and (*ℓ*) to $\sigma(\beta)_{68.3\%} > 3$ (low quality). The absence of a flag means having $\sigma(\beta)_{68.3\%} < 1.5$.

Name	Flag	β	$\beta^{95.5\%}$	$\beta^{99.7\%}$	$\log A$	$\log A^{95.5\%}$	$\log A^{99.7\%}$
C1012+2439	<i>m</i>	$2.50^{+2.08}_{-0.30}$	$+2.83$ -0.79	$+2.94$ -1.20	$-8.89^{+2.06}_{-6.05}$	$+2.06$ -9.84	$+3.25$ -10.10
C1037+5711		$2.19^{+0.34}_{-0.29}$	$+0.88$ -0.42	$+0.94$ -0.68	$-7.11^{+0.82}_{-0.63}$	$+1.12$ -1.87	$+1.65$ -2.30
C1112+3446		$2.07^{+0.27}_{-0.20}$	$+0.53$ -0.41	$+0.59$ -0.54	$-5.69^{+0.52}_{-0.58}$	$+0.77$ -1.32	$+0.98$ -1.41
C1130-1449		$2.81^{+0.44}_{-0.35}$	$+0.83$ -0.75	$+1.20$ -0.99	$-6.59^{+0.50}_{-1.57}$	$+1.40$ -2.89	$+2.02$ -3.71
C1224+2122		$2.26^{+0.27}_{-0.18}$	$+0.50$ -0.35	$+0.57$ -0.46	$-5.14^{+0.61}_{-0.41}$	$+0.86$ -1.03	$+1.04$ -1.38
C1228+4858		$2.99^{+0.16}_{-0.49}$	$+0.61$ -0.73	$+0.74$ -0.96	$-8.11^{+0.58}_{-1.10}$	$+1.32$ -2.03	$+1.44$ -2.63
C1239+0443		$2.24^{+0.38}_{-0.14}$	$+0.68$ -0.44	$+0.88$ -0.53	$-5.48^{+0.44}_{-0.62}$	$+0.70$ -1.56	$+1.17$ -1.78
C1253+5301		$2.14^{+0.38}_{-0.33}$	$+0.72$ -0.48	$+0.99$ -0.62	$-7.14^{+0.91}_{-1.02}$	$+1.10$ -2.54	$+1.53$ -2.64
C1303+2433		$1.94^{+0.30}_{-0.15}$	$+0.51$ -0.33	$+0.62$ -0.38	$-5.13^{+0.26}_{-0.57}$	$+0.45$ -1.18	$+0.67$ -1.18
C1345+4452		$2.29^{+0.21}_{-0.25}$	$+0.51$ -0.45	$+0.87$ -0.51	$-5.82^{+0.51}_{-0.50}$	$+1.01$ -1.18	$+1.17$ -1.94
C1454+5124		$2.04^{+0.84}_{-0.50}$	$+2.23$ -0.78	$+2.73$ -0.96	$-7.38^{+1.65}_{-2.24}$	$+2.40$ -6.81	$+2.56$ -9.19
C1607+1551		$2.33^{+0.49}_{-0.24}$	$+0.98$ -0.49	$+1.29$ -0.67	$-7.09^{+0.89}_{-1.05}$	$+1.65$ -2.08	$+1.82$ -3.49
C1724+4004		$3.06^{+0.56}_{-0.43}$	$+1.22$ -0.78	$+1.55$ -0.98	$-8.79^{+1.13}_{-1.63}$	$+2.10$ -3.45	$+2.66$ -4.44
C2025-0735		$2.78^{+0.31}_{-0.30}$	$+0.69$ -0.48	$+0.90$ -0.68	$-6.66^{+0.92}_{-0.57}$	$+1.18$ -1.52	$+1.55$ -2.13
C2116+3339	<i>m</i>	$2.34^{+1.76}_{-1.05}$	$+3.07$ -3.13	$+3.10$ -3.71	$-8.33^{+2.57}_{-6.09}$	$+2.54$ -11.08	$+5.12$ -11.50
C2121+1901	<i>m</i>	$4.13^{+1.29}_{-0.98}$	$+1.36$ -2.21	$+1.35$ -3.18	$-13.81^{+3.59}_{-4.23}$	$+7.42$ -5.21	$+9.40$ -5.83
C2212+0646		$2.56^{+0.30}_{-0.18}$	$+0.50$ -0.37	$+0.56$ -0.50	$-7.12^{+0.48}_{-0.54}$	$+0.91$ -1.07	$+1.22$ -1.12
C2225-0457		$2.44^{+0.38}_{-0.25}$	$+0.69$ -0.48	$+0.92$ -0.74	$-5.96^{+0.73}_{-0.85}$	$+1.26$ -1.78	$+1.86$ -2.46
C2311+3425		$2.54^{+0.23}_{-0.29}$	$+0.68$ -0.39	$+0.78$ -0.68	$-6.48^{+0.70}_{-0.41}$	$+1.06$ -1.25	$+1.52$ -1.80
C2325+3957		$1.89^{+0.83}_{-0.47}$	$+2.41$ -0.78	$+3.53$ -0.78	$-7.07^{+1.65}_{-2.03}$	$+2.03$ -8.04	$+2.14$ -11.47
CLJ0024+0349		$1.94^{+0.73}_{-0.51}$	$+1.91$ -0.73	$+2.59$ -0.90	$-7.28^{+1.58}_{-2.08}$	$+1.80$ -6.24	$+2.19$ -8.98
CLJ0043+3426		$1.88^{+0.24}_{-0.30}$	$+0.42$ -0.49	$+0.57$ -0.62	$-6.46^{+0.70}_{-0.60}$	$+1.04$ -1.18	$+1.29$ -1.37
CLJ0048+2235		$2.09^{+0.17}_{-0.28}$	$+0.52$ -0.42	$+0.66$ -0.54	$-6.06^{+0.48}_{-0.53}$	$+0.87$ -1.15	$+1.05$ -1.49
CLJ0105+3928		$1.87^{+0.37}_{-0.30}$	$+0.78$ -0.50	$+0.95$ -0.78	$-5.83^{+0.79}_{-0.81}$	$+1.32$ -2.00	$+1.73$ -2.55
CLJ0115+0356		$1.99^{+0.40}_{-0.14}$	$+0.53$ -0.51	$+0.79$ -0.59	$-6.13^{+0.43}_{-0.74}$	$+0.93$ -1.31	$+1.22$ -1.64
CLJ0212+2244		$2.47^{+0.74}_{-0.46}$	$+1.43$ -1.11	$+2.16$ -1.14	$-8.54^{+1.30}_{-2.16}$	$+2.85$ -4.30	$+3.28$ -6.41
CLJ0342+3859		$1.85^{+0.49}_{-0.20}$	$+0.79$ -0.52	$+1.07$ -0.65	$-6.09^{+0.83}_{-0.79}$	$+1.46$ -1.64	$+1.77$ -2.29
CLJ0713+1935		$1.97^{+0.36}_{-0.28}$	$+0.71$ -0.46	$+1.01$ -0.54	$-5.73^{+0.54}_{-0.88}$	$+1.17$ -1.45	$+1.34$ -2.25
CLJ1333+5057	<i>m</i>	$1.60^{+0.79}_{-2.11}$	$+2.25$ -3.09	$+3.68$ -3.09	$-5.61^{+1.80}_{-7.70}$	$+1.80$ -12.88	$+4.04$ -13.37
CLJ1503+4759		$2.26^{+0.56}_{-0.43}$	$+1.25$ -0.76	$+1.59$ -1.00	$-7.59^{+1.33}_{-1.39}$	$+1.71$ -4.03	$+2.25$ -4.89

Table C.1: Results of fitting the simple power-law model over the 1290 selected observations from OVRO dataset. Flag refers to sources well-defined by the model, being (*m*) objects with a $\sigma(\beta)_{68.3\%} \in [1.5, 3]$ (medium quality) and (*ℓ*) to $\sigma(\beta)_{68.3\%} > 3$ (low quality). The absence of a flag means having $\sigma(\beta)_{68.3\%} < 1.5$.

Name	Flag	β	$\beta^{95.5\%}$	$\beta^{99.7\%}$	$\log A$	$\log A^{95.5\%}$	$\log A^{99.7\%}$
CR0154+0823		$1.69^{+0.22}_{-0.21}$	$+0.53_{-0.42}$	$+0.74_{-0.54}$	$-5.16^{+0.41}_{-0.59}$	$+0.76_{-1.18}$	$+0.98_{-1.77}$
CR1016+0513		$2.46^{+0.46}_{-0.32}$	$+0.81_{-0.60}$	$+0.96_{-1.04}$	$-7.66^{+1.07}_{-0.89}$	$+1.61_{-2.11}$	$+2.65_{-2.57}$
CR1059-1134		$2.43^{+0.13}_{-0.33}$	$+0.40_{-0.50}$	$+0.55_{-0.64}$	$-6.46^{+0.49}_{-0.58}$	$+0.88_{-1.24}$	$+1.19_{-1.65}$
CR1208+5441		$2.26^{+0.12}_{-0.35}$	$+0.44_{-0.52}$	$+0.68_{-0.65}$	$-6.19^{+0.64}_{-0.42}$	$+1.10_{-0.96}$	$+1.15_{-1.59}$
CR1218-0119		$2.10^{+0.39}_{-0.35}$	$+0.68_{-0.72}$	$+0.95_{-0.82}$	$-7.16^{+0.76}_{-1.35}$	$+1.58_{-1.95}$	$+1.96_{-2.62}$
CR1354-1041		$2.45^{+0.18}_{-0.36}$	$+0.49_{-0.57}$	$+0.78_{-0.68}$	$-6.41^{+0.65}_{-0.57}$	$+1.31_{-1.19}$	$+1.40_{-1.98}$
CR1427+2347	<i>m</i>	$3.55^{+1.39}_{-0.42}$	$+1.85_{-1.15}$	$+1.93_{-1.55}$	$-11.37^{+2.19}_{-3.63}$	$+3.96_{-5.57}$	$+4.71_{-6.25}$
CR1542+6129		$2.43^{+0.38}_{-0.41}$	$+1.29_{-0.71}$	$+1.50_{-0.86}$	$-7.83^{+1.26}_{-0.86}$	$+1.47_{-3.67}$	$+2.21_{-3.67}$
CR1553+1256		$2.51^{+0.37}_{-0.33}$	$+0.85_{-0.53}$	$+0.96_{-0.71}$	$-7.06^{+0.93}_{-0.90}$	$+1.22_{-2.33}$	$+1.59_{-2.63}$
CR1903+5540	<i>m</i>	$1.70^{+1.57}_{-0.85}$	$+3.32_{-1.07}$	$+3.71_{-2.95}$	$-6.77^{+1.92}_{-6.06}$	$+2.65_{-11.03}$	$+2.96_{-12.07}$
CR1928-0456	<i>m</i>	$4.40^{+0.63}_{-1.16}$	$+0.88_{-2.27}$	$+1.03_{-2.77}$	$-15.12^{+3.12}_{-2.81}$	$+6.93_{-2.84}$	$+8.70_{-2.86}$
CR2228-0753		$2.45^{+0.39}_{-0.38}$	$+0.78_{-0.65}$	$+1.05_{-0.80}$	$-7.46^{+0.78}_{-1.26}$	$+1.29_{-2.45}$	$+1.84_{-2.78}$
CRJ0305-0607		$4.97^{+0.32}_{-1.12}$	$+0.51_{-2.15}$	$+0.52_{-2.88}$	$-17.34^{+3.46}_{-1.51}$	$+7.21_{-1.59}$	$+9.58_{-1.65}$
CRJ0505-0419		$1.77^{+0.29}_{-0.38}$	$+0.80_{-0.58}$	$+1.25_{-0.83}$	$-5.19^{+0.76}_{-0.84}$	$+1.47_{-1.96}$	$+1.47_{-3.51}$
CRJ1012+0630		$2.42^{+0.52}_{-0.52}$	$+1.42_{-0.67}$	$+1.97_{-0.87}$	$-7.68^{+1.40}_{-1.43}$	$+1.76_{-4.38}$	$+2.07_{-6.39}$
CRJ1142+1547	<i>ℓ</i>	$2.33^{+2.58}_{-0.99}$	$+2.67_{-3.27}$	$+2.96_{-3.82}$	$-16.10^{+6.62}_{-1.90}$	$+11.24_{-1.90}$	$+13.36_{-1.90}$
CRJ1220+7105		$2.14^{+0.30}_{-0.19}$	$+0.55_{-0.25}$	$+0.55_{-0.42}$	$-5.87^{+0.37}_{-0.65}$	$+0.57_{-1.21}$	$+0.94_{-1.21}$
CRJ1305+7854	<i>m</i>	$2.59^{+1.76}_{-0.48}$	$+2.75_{-0.94}$	$+2.86_{-1.27}$	$-9.04^{+1.54}_{-5.59}$	$+3.11_{-8.88}$	$+3.67_{-9.77}$
CRJ1321+8316		$2.17^{+0.54}_{-0.28}$	$+0.83_{-0.63}$	$+1.16_{-0.69}$	$-7.14^{+0.72}_{-1.24}$	$+1.40_{-2.38}$	$+1.71_{-3.67}$
CRJ1803+0341		$2.27^{+0.46}_{-0.27}$	$+0.83_{-0.58}$	$+1.06_{-0.73}$	$-6.78^{+0.52}_{-1.30}$	$+1.27_{-2.32}$	$+1.67_{-2.77}$
CRJ1925-1018	<i>ℓ</i>	$3.11^{+1.64}_{-2.59}$	$+1.67_{-4.59}$	$+2.20_{-4.59}$	$-16.70^{+6.21}_{-2.28}$	$+11.38_{-2.28}$	$+13.51_{-2.29}$
CT_1419-0838		$2.15^{+0.30}_{-0.21}$	$+0.48_{-0.50}$	$+0.69_{-0.54}$	$-5.49^{+0.42}_{-0.77}$	$+0.92_{-1.27}$	$+1.14_{-1.61}$
CT_1625+4118		$2.54^{+0.27}_{-0.38}$	$+0.49_{-0.64}$	$+0.71_{-0.80}$	$-7.73^{+1.07}_{-0.49}$	$+1.50_{-1.35}$	$+1.88_{-1.66}$
CT_2255+2410	<i>m</i>	$2.53^{+1.06}_{-0.48}$	$+2.15_{-0.98}$	$+2.34_{-1.59}$	$-8.98^{+1.48}_{-3.15}$	$+2.80_{-7.04}$	$+3.73_{-7.78}$
GAJ1054+8629	<i>m</i>	$4.71^{+0.47}_{-1.20}$	$+0.68_{-2.27}$	$+0.74_{-3.14}$	$-17.52^{+4.46}_{-1.27}$	$+8.03_{-1.46}$	$+10.77_{-1.47}$
GB10751+485		$1.94^{+0.64}_{-0.55}$	$+2.92_{-0.74}$	$+3.20_{-0.90}$	$-6.51^{+1.13}_{-2.00}$	$+1.53_{-10.37}$	$+2.11_{-10.92}$
GB6J0009+0625		$1.56^{+0.29}_{-0.23}$	$+0.56_{-0.48}$	$+0.83_{-0.62}$	$-5.31^{+0.61}_{-0.55}$	$+0.89_{-1.70}$	$+1.04_{-2.17}$
GB6J0047+5657		$2.00^{+0.49}_{-0.36}$	$+0.96_{-0.67}$	$+1.31_{-0.76}$	$-6.57^{+0.80}_{-1.43}$	$+1.50_{-2.64}$	$+1.85_{-3.80}$
GB6J0515+1527	<i>m</i>	$4.55^{+0.40}_{-1.84}$	$+0.55_{-3.07}$	$+0.94_{-3.39}$	$-16.64^{+5.27}_{-2.22}$	$+9.51_{-2.30}$	$+10.75_{-2.30}$
GB6J0526+6317	<i>ℓ</i>	$3.69^{+1.19}_{-2.82}$	$+1.21_{-5.11}$	$+1.55_{-5.19}$	$-16.79^{+5.39}_{-2.17}$	$+10.90_{-2.21}$	$+14.12_{-2.21}$

Table C.1: Results of fitting the simple power-law model over the 1290 selected observations from OVRO dataset. Flag refers to sources well-defined by the model, being (*m*) objects with a $\sigma(\beta)_{68.3\%} \in [1.5, 3]$ (medium quality) and (*ℓ*) to $\sigma(\beta)_{68.3\%} > 3$ (low quality). The absence of a flag means having $\sigma(\beta)_{68.3\%} < 1.5$.

Name	Flag	β	$\beta^{95.5\%}$	$\beta^{99.7\%}$	$\log A$	$\log A^{95.5\%}$	$\log A^{99.7\%}$
GB6J0636+7138		$2.04^{+0.35}_{-0.30}$	$+0.73_{-0.51}$	$+1.04_{-0.63}$	$-6.59^{+0.56}_{-0.97}$	$+1.07_{-1.84}$	$+1.36_{-2.57}$
GB6J0856+7146		$1.89^{+0.32}_{-0.25}$	$+0.55_{-0.45}$	$+0.68_{-0.67}$	$-5.93^{+0.39}_{-0.76}$	$+0.85_{-1.32}$	$+1.35_{-1.53}$
GB6J0922+0433		$2.05^{+0.37}_{-0.40}$	$+0.82_{-0.75}$	$+1.47_{-0.86}$	$-6.06^{+0.63}_{-1.33}$	$+1.41_{-2.43}$	$+1.61_{-3.94}$
GB6J0941+2721	<i>m</i>	$2.29^{+1.75}_{-0.71}$	$+2.94_{-0.86}$	$+3.06_{-1.36}$	$-7.79^{+2.02}_{-5.84}$	$+2.36_{-9.98}$	$+2.63_{-11.15}$
GB6J1439+3711	<i>ℓ</i>	$4.28^{+1.00}_{-2.97}$	$+1.10_{-5.30}$	$+1.09_{-5.79}$	$-17.05^{+5.54}_{-1.81}$	$+11.63_{-1.93}$	$+12.98_{-1.94}$
GB6J2102+4702	<i>m</i>	$1.84^{+1.31}_{-0.84}$	$+3.16_{-0.84}$	$+3.58_{-0.84}$	$-6.31^{+2.13}_{-4.24}$	$+2.13_{-10.75}$	$+2.13_{-11.68}$
J0001+1914	<i>m</i>	$3.70^{+0.86}_{-0.76}$	$+1.66_{-1.13}$	$+1.77_{-1.81}$	$-12.48^{+2.23}_{-2.69}$	$+3.41_{-5.21}$	$+5.47_{-5.40}$
J0001-1551	<i>m</i>	$4.74^{+0.29}_{-1.47}$	$+0.60_{-2.43}$	$+0.71_{-3.14}$	$-16.31^{+4.76}_{-1.08}$	$+7.81_{-1.65}$	$+9.84_{-1.64}$
J0004+2019		$2.66^{+0.74}_{-0.61}$	$+1.66_{-1.02}$	$+2.79_{-1.30}$	$-8.62^{+1.87}_{-2.16}$	$+2.88_{-5.20}$	$+3.45_{-9.22}$
J0004+4615		$2.36^{+0.38}_{-0.38}$	$+0.79_{-0.76}$	$+1.14_{-0.88}$	$-7.52^{+0.94}_{-1.07}$	$+1.77_{-2.49}$	$+2.03_{-3.20}$
J0004-1148		$2.36^{+0.27}_{-0.20}$	$+0.47_{-0.38}$	$+0.56_{-0.56}$	$-6.64^{+0.45}_{-0.63}$	$+0.96_{-0.99}$	$+1.20_{-1.21}$
J0005+3820		$2.30^{+0.30}_{-0.22}$	$+0.62_{-0.35}$	$+0.73_{-0.59}$	$-6.48^{+0.70}_{-0.48}$	$+0.84_{-1.43}$	$+1.33_{-1.43}$
J0006-0623		$2.63^{+0.18}_{-0.35}$	$+0.45_{-0.57}$	$+0.61_{-0.72}$	$-5.74^{+0.56}_{-0.68}$	$+1.09_{-1.37}$	$+1.61_{-1.53}$
J0009+0628	<i>m</i>	$1.96^{+1.47}_{-0.91}$	$+3.47_{-1.03}$	$+3.47_{-2.85}$	$-7.12^{+2.35}_{-4.89}$	$+1.88_{-11.77}$	$+2.47_{-12.73}$
J0010+1058		$2.88^{+0.45}_{-0.19}$	$+0.70_{-0.46}$	$+0.89_{-0.65}$	$-7.36^{+0.53}_{-0.96}$	$+1.09_{-1.59}$	$+1.66_{-2.03}$
J0010+1724		$2.58^{+0.33}_{-0.43}$	$+0.69_{-0.69}$	$+0.83_{-0.96}$	$-8.12^{+1.31}_{-0.75}$	$+1.84_{-1.94}$	$+2.53_{-2.22}$
J0010+2047		$2.02^{+0.45}_{-0.21}$	$+0.98_{-0.36}$	$+1.02_{-0.59}$	$-6.88^{+0.53}_{-1.15}$	$+0.97_{-2.50}$	$+1.50_{-2.50}$
J0011+0057		$1.96^{+0.43}_{-0.18}$	$+0.81_{-0.42}$	$+1.04_{-0.43}$	$-6.54^{+0.39}_{-1.00}$	$+1.02_{-1.85}$	$+1.08_{-2.47}$
J0012+3353		$2.04^{+0.46}_{-0.36}$	$+0.96_{-0.63}$	$+1.09_{-0.92}$	$-7.29^{+1.30}_{-0.78}$	$+1.80_{-2.46}$	$+2.27_{-2.86}$
J0013+1910		$2.20^{+0.51}_{-0.34}$	$+0.95_{-0.59}$	$+1.04_{-0.87}$	$-7.42^{+1.29}_{-0.95}$	$+1.80_{-2.21}$	$+2.15_{-2.87}$
J0013-0423		$1.91^{+0.29}_{-0.19}$	$+0.56_{-0.31}$	$+0.62_{-0.37}$	$-5.24^{+0.38}_{-0.68}$	$+0.56_{-1.44}$	$+0.75_{-1.63}$
J0013-1513		$2.34^{+0.48}_{-0.33}$	$+0.82_{-0.75}$	$+1.12_{-0.90}$	$-8.31^{+1.36}_{-0.84}$	$+2.15_{-1.95}$	$+2.44_{-2.63}$
J0015-1812		$2.74^{+0.57}_{-0.34}$	$+1.14_{-0.69}$	$+1.80_{-0.98}$	$-8.59^{+1.49}_{-1.13}$	$+2.38_{-2.54}$	$+2.74_{-4.43}$
J0016-0015		$2.26^{+0.26}_{-0.25}$	$+0.51_{-0.49}$	$+0.76_{-0.63}$	$-6.59^{+0.61}_{-0.50}$	$+1.04_{-1.21}$	$+1.20_{-1.86}$
J0017+8135		$2.06^{+0.46}_{-0.37}$	$+1.03_{-0.55}$	$+1.17_{-0.85}$	$-6.27^{+0.78}_{-1.47}$	$+1.39_{-2.74}$	$+1.82_{-3.40}$
J0017-0512		$2.18^{+0.29}_{-0.10}$	$+0.47_{-0.25}$	$+0.54_{-0.40}$	$-6.27^{+0.60}_{-0.26}$	$+0.90_{-0.64}$	$+1.15_{-0.90}$
J0019+2021		$2.30^{+0.37}_{-0.11}$	$+0.48_{-0.36}$	$+0.62_{-0.49}$	$-6.42^{+0.55}_{-0.53}$	$+0.99_{-0.96}$	$+1.36_{-1.15}$
J0019+2602		$2.90^{+0.37}_{-0.34}$	$+0.73_{-0.58}$	$+0.94_{-0.71}$	$-8.17^{+0.83}_{-0.92}$	$+1.53_{-1.79}$	$+1.71_{-2.32}$
J0019+7327		$3.26^{+0.40}_{-0.45}$	$+0.87_{-0.79}$	$+1.12_{-0.87}$	$-7.77^{+1.09}_{-1.07}$	$+1.70_{-2.53}$	$+2.11_{-3.23}$
J0022+0608		$2.25^{+0.25}_{-0.16}$	$+0.46_{-0.35}$	$+0.53_{-0.55}$	$-6.39^{+0.66}_{-0.22}$	$+0.96_{-0.85}$	$+1.25_{-1.06}$

Table C.1: Results of fitting the simple power-law model over the 1290 selected observations from OVRO dataset. Flag refers to sources well-defined by the model, being (*m*) objects with a $\sigma(\beta)_{68.3\%} \in [1.5, 3]$ (medium quality) and (*ℓ*) to $\sigma(\beta)_{68.3\%} > 3$ (low quality). The absence of a flag means having $\sigma(\beta)_{68.3\%} < 1.5$.

Name	Flag	β	$\beta^{95.5\%}$	$\beta^{99.7\%}$	$\log A$	$\log A^{95.5\%}$	$\log A^{99.7\%}$
J0022+4525		$1.84^{+0.58}_{-0.20}$	$+0.94_{-0.55}$	$+1.26_{-0.70}$	$-6.62^{+0.71}_{-1.44}$	$+1.14_{-2.88}$	$+1.76_{-3.61}$
J0023+4456		$2.16^{+0.42}_{-0.27}$	$+0.80_{-0.59}$	$+1.00_{-0.70}$	$-6.83^{+0.58}_{-1.20}$	$+1.35_{-2.30}$	$+1.70_{-2.76}$
J0024+2439		$2.50^{+0.27}_{-0.35}$	$+0.82_{-0.45}$	$+0.82_{-0.64}$	$-7.81^{+0.83}_{-0.74}$	$+1.02_{-2.04}$	$+1.54_{-2.04}$
J0027+2241	<i>m</i>	$3.31^{+1.42}_{-0.41}$	$+1.92_{-1.12}$	$+1.96_{-1.78}$	$-11.66^{+1.23}_{-4.90}$	$+3.54_{-6.28}$	$+5.34_{-6.28}$
J0029+0554		$1.88^{+0.42}_{-0.22}$	$+0.69_{-0.52}$	$+1.02_{-0.62}$	$-6.13^{+0.68}_{-0.92}$	$+1.16_{-1.95}$	$+1.25_{-3.08}$
J0035-1305		$2.41^{+0.68}_{-0.43}$	$+1.47_{-0.60}$	$+1.63_{-0.93}$	$-7.87^{+1.12}_{-2.00}$	$+2.11_{-4.02}$	$+2.15_{-5.06}$
J0037+1109		$2.39^{+0.20}_{-0.33}$	$+0.44_{-0.58}$	$+0.64_{-0.68}$	$-7.08^{+0.75}_{-0.55}$	$+1.17_{-1.33}$	$+1.50_{-1.82}$
J0038+1227		$2.06^{+0.60}_{-0.64}$	$+1.57_{-0.88}$	$+3.05_{-0.88}$	$-7.02^{+1.29}_{-2.03}$	$+2.04_{-4.93}$	$+2.04_{-10.28}$
J0038+1856		$2.51^{+0.45}_{-0.32}$	$+0.68_{-0.77}$	$+0.93_{-0.77}$	$-8.18^{+1.10}_{-0.95}$	$+1.77_{-2.01}$	$+2.14_{-2.73}$
J0038+4137		$1.91^{+0.53}_{-0.24}$	$+0.89_{-0.59}$	$+1.57_{-0.72}$	$-6.74^{+0.76}_{-1.30}$	$+1.49_{-2.57}$	$+1.81_{-4.30}$
J0039+1411		$2.24^{+0.42}_{-0.42}$	$+0.88_{-0.68}$	$+1.11_{-0.86}$	$-7.33^{+1.21}_{-1.10}$	$+1.53_{-3.08}$	$+1.95_{-3.69}$
J0040-0146		$1.78^{+0.42}_{-0.29}$	$+0.93_{-0.53}$	$+1.06_{-0.69}$	$-6.18^{+0.77}_{-1.22}$	$+0.98_{-2.90}$	$+1.51_{-2.90}$
J0042+1009	<i>m</i>	$3.23^{+0.97}_{-0.97}$	$+1.87_{-1.12}$	$+2.22_{-1.52}$	$-10.62^{+2.81}_{-3.18}$	$+3.24_{-6.39}$	$+4.26_{-7.13}$
J0042+2320		$2.25^{+0.27}_{-0.32}$	$+0.57_{-0.60}$	$+0.96_{-0.78}$	$-6.78^{+0.66}_{-0.85}$	$+1.29_{-1.63}$	$+1.68_{-2.57}$
J0046+3900		$2.23^{+0.44}_{-0.36}$	$+0.97_{-0.68}$	$+1.16_{-0.92}$	$-7.63^{+1.05}_{-1.02}$	$+1.89_{-2.49}$	$+2.23_{-3.08}$
J0047+2435		$2.14^{+0.34}_{-0.44}$	$+0.92_{-0.67}$	$+1.26_{-0.75}$	$-7.06^{+0.80}_{-1.06}$	$+1.29_{-2.52}$	$+1.65_{-3.65}$
J0048+3157		$3.06^{+0.38}_{-0.27}$	$+0.77_{-0.51}$	$+0.85_{-0.64}$	$-7.93^{+0.66}_{-0.87}$	$+1.54_{-1.66}$	$+1.59_{-2.29}$
J0049+0237		$2.42^{+0.25}_{-0.29}$	$+0.66_{-0.37}$	$+0.80_{-0.51}$	$-6.86^{+0.52}_{-0.70}$	$+0.90_{-1.46}$	$+1.19_{-1.75}$
J0049+5128		$2.54^{+0.63}_{-0.27}$	$+1.00_{-0.69}$	$+1.47_{-0.84}$	$-7.92^{+0.88}_{-1.51}$	$+1.79_{-2.57}$	$+2.27_{-3.95}$
J0050-0452		$2.19^{+0.32}_{-0.18}$	$+0.52_{-0.50}$	$+0.86_{-0.57}$	$-5.98^{+0.41}_{-0.71}$	$+0.86_{-1.26}$	$+1.09_{-1.92}$
J0050-0929		$2.27^{+0.25}_{-0.14}$	$+0.39_{-0.33}$	$+0.58_{-0.42}$	$-5.61^{+0.38}_{-0.46}$	$+0.66_{-0.98}$	$+0.95_{-1.06}$
J0051-0650		$2.34^{+0.32}_{-0.40}$	$+0.80_{-0.59}$	$+0.88_{-0.84}$	$-6.59^{+0.90}_{-0.92}$	$+1.49_{-2.07}$	$+1.88_{-2.78}$
J0056+1625		$2.29^{+0.23}_{-0.27}$	$+0.53_{-0.39}$	$+0.66_{-0.65}$	$-5.89^{+0.34}_{-0.82}$	$+0.60_{-1.59}$	$+1.02_{-1.94}$
J0057+3021		$1.90^{+0.30}_{-0.35}$	$+0.62_{-0.59}$	$+0.88_{-0.77}$	$-5.94^{+0.77}_{-0.77}$	$+1.18_{-1.86}$	$+1.72_{-2.39}$
J0058+0620		$2.05^{+0.41}_{-0.26}$	$+0.83_{-0.48}$	$+1.08_{-0.59}$	$-6.53^{+0.90}_{-0.82}$	$+1.29_{-2.02}$	$+1.47_{-2.79}$
J0102+4214		$2.04^{+0.17}_{-0.23}$	$+0.41_{-0.32}$	$+0.56_{-0.45}$	$-5.79^{+0.45}_{-0.39}$	$+0.57_{-1.02}$	$+0.83_{-1.06}$
J0105+4819		$2.40^{+0.29}_{-0.35}$	$+0.63_{-0.58}$	$+0.84_{-0.77}$	$-7.21^{+0.97}_{-0.60}$	$+1.37_{-1.65}$	$+1.77_{-2.10}$
J0106+1300		$2.91^{+0.56}_{-0.72}$	$+1.58_{-0.98}$	$+2.06_{-1.39}$	$-9.21^{+1.90}_{-1.94}$	$+2.82_{-4.98}$	$+3.47_{-6.70}$
J0106+2539	<i>m</i>	$2.35^{+2.21}_{-0.33}$	$+2.82_{-0.99}$	$+3.09_{-1.32}$	$-9.52^{+1.26}_{-7.39}$	$+3.20_{-9.48}$	$+4.56_{-9.48}$
J0106+3402		$3.63^{+0.46}_{-0.74}$	$+1.34_{-1.03}$	$+1.77_{-1.31}$	$-11.05^{+1.39}_{-2.07}$	$+2.62_{-4.17}$	$+3.29_{-5.44}$

Table C.1: Results of fitting the simple power-law model over the 1290 selected observations from OVRO dataset. Flag refers to sources well-defined by the model, being (*m*) objects with a $\sigma(\beta)_{68.3\%} \in [1.5, 3]$ (medium quality) and (*ℓ*) to $\sigma(\beta)_{68.3\%} > 3$ (low quality). The absence of a flag means having $\sigma(\beta)_{68.3\%} < 1.5$.

Name	Flag	β	$\beta^{95.5\%}$	$\beta^{99.7\%}$	$\log A$	$\log A^{95.5\%}$	$\log A^{99.7\%}$
J0106-0315	<i>m</i>	$4.56^{+0.57}_{-1.91}$	$+0.85$ -2.89	$+0.89$ -3.47	$-15.26^{+5.80}_{-2.71}$	$+9.34$ -2.71	$+11.07$ -2.70
J0108+0135		$2.41^{+0.32}_{-0.25}$	$+0.69$ -0.44	$+0.93$ -0.61	$-5.83^{+0.78}_{-0.66}$	$+1.14$ -1.58	$+1.75$ -2.04
J0110-0415		$2.39^{+0.28}_{-0.39}$	$+0.81$ -0.59	$+1.02$ -0.72	$-7.61^{+0.74}_{-0.91}$	$+1.39$ -2.12	$+1.54$ -2.91
J0110-0741		$2.65^{+0.35}_{-0.34}$	$+0.63$ -0.61	$+1.01$ -0.83	$-7.87^{+0.74}_{-1.05}$	$+1.41$ -1.93	$+1.93$ -2.50
J0111+3906	<i>ℓ</i>	$1.69^{+2.22}_{-1.01}$	$+3.12$ -3.17	$+3.63$ -3.17	$-6.94^{+2.10}_{-7.68}$	$+2.40$ -11.71	$+4.28$ -12.02
J0111-1317		$2.51^{+0.38}_{-0.22}$	$+0.80$ -0.48	$+1.20$ -0.59	$-7.37^{+0.36}_{-1.16}$	$+1.09$ -2.05	$+1.48$ -3.11
J0112+2244		$2.60^{+0.18}_{-0.26}$	$+0.39$ -0.43	$+0.54$ -0.56	$-6.64^{+0.40}_{-0.59}$	$+0.88$ -0.99	$+1.16$ -1.26
J0112+3208		$2.74^{+0.28}_{-0.22}$	$+0.68$ -0.35	$+0.78$ -0.47	$-6.59^{+0.27}_{-0.78}$	$+0.54$ -1.64	$+0.89$ -1.64
J0112+3522		$2.65^{+0.34}_{-0.21}$	$+0.70$ -0.40	$+0.74$ -0.59	$-7.39^{+0.62}_{-0.78}$	$+1.18$ -1.47	$+1.44$ -2.07
J0113+0222		$1.99^{+0.30}_{-0.33}$	$+0.82$ -0.52	$+0.88$ -0.76	$-5.99^{+0.79}_{-0.87}$	$+1.34$ -2.00	$+1.68$ -2.44
J0113+1324		$2.59^{+0.45}_{-0.46}$	$+0.93$ -0.93	$+1.37$ -0.97	$-8.17^{+1.16}_{-1.18}$	$+2.09$ -2.86	$+2.51$ -3.54
J0113+4948		$2.43^{+0.42}_{-0.28}$	$+0.80$ -0.66	$+1.37$ -0.74	$-6.67^{+0.68}_{-1.14}$	$+1.64$ -2.10	$+1.78$ -3.48
J0115-0127		$2.74^{+0.36}_{-0.34}$	$+0.73$ -0.63	$+0.94$ -0.77	$-7.89^{+1.05}_{-0.76}$	$+1.53$ -1.98	$+2.05$ -2.43
J0116+2422	<i>ℓ</i>	$1.82^{+2.58}_{-1.05}$	$+3.05$ -3.30	$+3.51$ -3.30	$-6.68^{+1.31}_{-9.31}$	$+2.19$ -12.17	$+4.23$ -12.32
J0116-1136		$2.97^{+0.37}_{-0.31}$	$+0.77$ -0.59	$+1.22$ -0.77	$-8.19^{+0.85}_{-0.90}$	$+1.47$ -2.04	$+2.06$ -3.08
J0117+1418		$2.99^{+0.43}_{-0.26}$	$+0.80$ -0.47	$+0.95$ -0.86	$-8.57^{+0.69}_{-1.07}$	$+1.27$ -1.98	$+2.10$ -2.55
J0121+0422		$2.43^{+0.36}_{-0.27}$	$+0.83$ -0.44	$+0.96$ -0.70	$-6.62^{+0.78}_{-0.78}$	$+1.25$ -1.92	$+1.71$ -2.16
J0121+1149		$2.57^{+0.23}_{-0.33}$	$+0.74$ -0.48	$+0.82$ -0.73	$-6.41^{+0.84}_{-0.45}$	$+1.07$ -1.61	$+1.55$ -1.84
J0122+2502		$2.30^{+0.46}_{-0.38}$	$+0.96$ -0.61	$+1.26$ -0.76	$-7.52^{+1.16}_{-1.10}$	$+1.74$ -2.54	$+2.04$ -3.38
J0123+2615	<i>m</i>	$3.27^{+0.63}_{-0.91}$	$+1.54$ -1.33	$+2.10$ -1.51	$-10.95^{+3.07}_{-1.66}$	$+3.72$ -4.87	$+4.10$ -7.51
J0125-0005		$2.39^{+0.31}_{-0.36}$	$+0.75$ -0.48	$+0.75$ -0.75	$-6.78^{+0.86}_{-0.88}$	$+1.50$ -1.80	$+1.73$ -2.24
J0126+2559		$2.18^{+0.25}_{-0.47}$	$+0.59$ -0.74	$+0.84$ -0.92	$-6.52^{+0.72}_{-1.10}$	$+1.36$ -1.86	$+1.77$ -2.53
J0127-0821		$2.54^{+0.53}_{-0.44}$	$+1.14$ -0.66	$+1.72$ -0.85	$-8.29^{+1.23}_{-1.39}$	$+1.76$ -3.12	$+2.19$ -4.36
J0128+4901		$2.12^{+0.17}_{-0.22}$	$+0.35$ -0.41	$+0.48$ -0.41	$-4.79^{+0.43}_{-0.33}$	$+0.70$ -0.86	$+0.75$ -1.05
J0130+0842		$2.31^{+0.53}_{-0.16}$	$+0.87$ -0.47	$+1.24$ -0.60	$-7.44^{+0.88}_{-0.83}$	$+1.63$ -1.63	$+1.67$ -2.64
J0131+3834		$2.65^{+0.80}_{-0.43}$	$+1.65$ -0.86	$+2.65$ -0.91	$-8.43^{+1.32}_{-2.27}$	$+2.51$ -4.72	$+2.51$ -7.76
J0132+4325		$2.26^{+0.29}_{-0.18}$	$+0.56$ -0.32	$+0.60$ -0.60	$-5.89^{+0.38}_{-0.71}$	$+0.67$ -1.39	$+1.13$ -1.49
J0132-1654		$2.66^{+0.27}_{-0.29}$	$+0.61$ -0.49	$+0.76$ -0.62	$-6.46^{+0.51}_{-0.82}$	$+1.07$ -1.45	$+1.33$ -1.92
J0136+4751		$2.75^{+0.34}_{-0.27}$	$+0.83$ -0.51	$+0.95$ -0.83	$-5.61^{+0.70}_{-0.76}$	$+1.12$ -2.08	$+1.87$ -2.23
J0140-1532		$2.15^{+0.41}_{-0.46}$	$+1.08$ -0.63	$+1.37$ -0.81	$-7.32^{+1.07}_{-1.28}$	$+2.03$ -2.89	$+2.11$ -4.07

Table C.1: Results of fitting the simple power-law model over the 1290 selected observations from OVRO dataset. Flag refers to sources well-defined by the model, being (*m*) objects with a $\sigma(\beta)_{68.3\%} \in [1.5, 3]$ (medium quality) and (*ℓ*) to $\sigma(\beta)_{68.3\%} > 3$ (low quality). The absence of a flag means having $\sigma(\beta)_{68.3\%} < 1.5$.

Name	Flag	β	$\beta^{95.5\%}$	$\beta^{99.7\%}$	$\log A$	$\log A^{95.5\%}$	$\log A^{99.7\%}$
J0141-0202		$2.44^{+0.40}_{-0.49}$	$+1.09_{-0.75}$	$+1.63_{-0.90}$	$-7.77^{+1.12}_{-1.20}$	$+1.95_{-3.11}$	$+2.22_{-4.87}$
J0141-0928		$2.49^{+0.32}_{-0.15}$	$+0.55_{-0.37}$	$+0.70_{-0.53}$	$-6.37^{+0.29}_{-0.78}$	$+0.73_{-1.22}$	$+1.01_{-1.53}$
J0143+4129		$2.24^{+0.19}_{-0.33}$	$+0.50_{-0.50}$	$+0.57_{-0.69}$	$-7.01^{+0.90}_{-0.35}$	$+1.09_{-1.32}$	$+1.56_{-1.32}$
J0148+3854		$2.21^{+0.31}_{-0.27}$	$+0.64_{-0.48}$	$+0.71_{-0.61}$	$-7.08^{+0.66}_{-0.78}$	$+1.10_{-1.60}$	$+1.49_{-1.88}$
J0148+4215	<i>m</i>	$2.59^{+1.46}_{-0.84}$	$+2.76_{-0.87}$	$+2.79_{-1.31}$	$-8.97^{+1.81}_{-5.79}$	$+2.28_{-9.94}$	$+3.39_{-9.94}$
J0149+0555		$1.87^{+0.32}_{-0.33}$	$+0.74_{-0.60}$	$+1.06_{-0.70}$	$-6.03^{+0.63}_{-1.03}$	$+1.29_{-2.17}$	$+1.41_{-2.98}$
J0149+1857		$2.89^{+0.38}_{-0.28}$	$+0.95_{-0.48}$	$+1.05_{-0.70}$	$-8.36^{+0.62}_{-1.11}$	$+1.42_{-2.36}$	$+1.80_{-2.76}$
J0151+2744		$2.22^{+0.43}_{-0.24}$	$+0.83_{-0.63}$	$+1.05_{-0.68}$	$-7.11^{+0.78}_{-0.98}$	$+1.56_{-2.37}$	$+1.71_{-2.94}$
J0151-1732		$2.11^{+0.27}_{-0.33}$	$+0.63_{-0.52}$	$+0.87_{-0.67}$	$-6.81^{+0.71}_{-0.77}$	$+1.20_{-1.71}$	$+1.49_{-2.15}$
J0152+2207		$2.53^{+0.28}_{-0.36}$	$+0.81_{-0.57}$	$+0.98_{-0.85}$	$-6.67^{+0.78}_{-0.80}$	$+1.24_{-2.06}$	$+1.96_{-2.52}$
J0154+4743		$2.43^{+0.47}_{-0.37}$	$+1.05_{-0.56}$	$+1.52_{-0.86}$	$-7.73^{+1.26}_{-0.90}$	$+2.04_{-2.09}$	$+2.82_{-3.41}$
J0202+3943		$2.71^{+0.38}_{-0.29}$	$+0.75_{-0.70}$	$+1.13_{-0.70}$	$-8.14^{+0.65}_{-1.07}$	$+1.56_{-1.93}$	$+1.81_{-2.92}$
J0202+4205		$2.92^{+0.39}_{-0.58}$	$+1.15_{-0.78}$	$+1.44_{-1.29}$	$-8.77^{+1.27}_{-1.32}$	$+1.82_{-3.42}$	$+2.99_{-4.61}$
J0202-0559	<i>ℓ</i>	$1.77^{+1.54}_{-1.74}$	$+2.67_{-3.24}$	$+3.50_{-3.24}$	$-6.82^{+2.55}_{-7.18}$	$+2.07_{-12.13}$	$+4.16_{-12.16}$
J0203+1134		$2.48^{+0.37}_{-0.29}$	$+0.82_{-0.43}$	$+0.82_{-0.84}$	$-7.22^{+0.85}_{-0.80}$	$+1.08_{-2.08}$	$+1.97_{-2.07}$
J0203+7232		$2.91^{+0.27}_{-0.52}$	$+0.73_{-0.72}$	$+1.00_{-0.97}$	$-8.62^{+1.12}_{-0.96}$	$+1.94_{-2.07}$	$+2.46_{-2.67}$
J0204+1514		$2.68^{+0.26}_{-0.29}$	$+0.69_{-0.43}$	$+0.80_{-0.67}$	$-7.06^{+0.71}_{-0.64}$	$+1.02_{-1.59}$	$+1.59_{-2.05}$
J0204+4005		$3.43^{+0.53}_{-0.67}$	$+1.30_{-1.07}$	$+1.68_{-1.28}$	$-10.65^{+1.71}_{-1.91}$	$+3.30_{-3.99}$	$+3.30_{-5.68}$
J0204-1701		$2.53^{+0.28}_{-0.33}$	$+0.51_{-0.62}$	$+0.81_{-0.67}$	$-6.74^{+0.91}_{-0.65}$	$+1.51_{-1.45}$	$+1.64_{-2.21}$
J0205+3212		$3.00^{+0.47}_{-0.29}$	$+0.88_{-0.62}$	$+0.99_{-0.88}$	$-7.96^{+0.93}_{-1.05}$	$+1.55_{-2.48}$	$+2.31_{-2.64}$
J0206-1150		$2.63^{+0.27}_{-0.27}$	$+0.55_{-0.51}$	$+0.61_{-0.71}$	$-7.08^{+0.49}_{-0.80}$	$+1.17_{-1.22}$	$+1.40_{-1.64}$
J0209+1352		$2.39^{+0.16}_{-0.33}$	$+0.47_{-0.48}$	$+0.75_{-0.56}$	$-6.96^{+0.68}_{-0.47}$	$+1.11_{-1.14}$	$+1.31_{-1.76}$
J0209+7229		$2.68^{+0.15}_{-0.42}$	$+0.43_{-0.74}$	$+0.71_{-0.80}$	$-6.89^{+0.47}_{-0.87}$	$+1.13_{-1.50}$	$+1.31_{-2.14}$
J0211+1051		$2.45^{+0.20}_{-0.24}$	$+0.46_{-0.44}$	$+0.76_{-0.53}$	$-5.76^{+0.51}_{-0.54}$	$+0.89_{-1.18}$	$+1.04_{-1.70}$
J0211-1558		$2.59^{+0.21}_{-0.54}$	$+0.63_{-0.78}$	$+0.88_{-1.10}$	$-8.23^{+1.20}_{-0.83}$	$+1.82_{-1.98}$	$+2.66_{-2.61}$
J0215-0222		$2.27^{+0.47}_{-0.33}$	$+0.94_{-0.65}$	$+1.04_{-1.08}$	$-7.03^{+0.61}_{-1.53}$	$+1.42_{-2.67}$	$+2.28_{-3.14}$
J0217+0144		$2.68^{+0.19}_{-0.24}$	$+0.44_{-0.41}$	$+0.55_{-0.58}$	$-6.76^{+0.43}_{-0.57}$	$+0.87_{-1.08}$	$+1.18_{-1.42}$
J0217+0837		$2.46^{+0.36}_{-0.20}$	$+0.72_{-0.43}$	$+0.99_{-0.62}$	$-6.41^{+0.47}_{-0.97}$	$+0.98_{-1.82}$	$+1.37_{-2.56}$
J0217+7349		$2.44^{+0.45}_{-0.26}$	$+0.82_{-0.50}$	$+0.94_{-0.81}$	$-6.14^{+0.54}_{-1.23}$	$+1.23_{-2.10}$	$+1.80_{-2.33}$
J0219+0120		$1.92^{+0.21}_{-0.28}$	$+0.48_{-0.47}$	$+0.78_{-0.64}$	$-6.13^{+0.64}_{-0.56}$	$+1.12_{-1.21}$	$+1.50_{-1.84}$

Table C.1: Results of fitting the simple power-law model over the 1290 selected observations from OVRO dataset. Flag refers to sources well-defined by the model, being (*m*) objects with a $\sigma(\beta)_{68.3\%} \in [1.5, 3]$ (medium quality) and (*ℓ*) to $\sigma(\beta)_{68.3\%} > 3$ (low quality). The absence of a flag means having $\sigma(\beta)_{68.3\%} < 1.5$.

Name	Flag	β	$\beta^{95.5\%}$	$\beta^{99.7\%}$	$\log A$	$\log A^{95.5\%}$	$\log A^{99.7\%}$
J0219+4727	<i>m</i>	$3.10^{+1.28}_{-0.47}$	$+1.82$ -1.24	$+2.34$ -1.61	$-11.11^{+2.40}_{-3.07}$	$+3.84$ -5.89	$+4.48$ -7.50
J0219-1842		$2.85^{+0.27}_{-0.39}$	$+0.56$ -0.60	$+0.78$ -0.76	$-8.03^{+0.86}_{-0.70}$	$+1.38$ -1.53	$+1.70$ -1.89
J0220-1305	<i>ℓ</i>	$1.46^{+1.23}_{-2.63}$	$+3.45$ -2.95	$+3.99$ -2.96	$-18.52^{+8.12}_{-2.40}$	$+13.79$ -2.42	$+16.25$ -2.46
J0221+3556		$1.88^{+0.29}_{-0.17}$	$+0.51$ -0.33	$+0.66$ -0.42	$-5.39^{+0.32}_{-0.72}$	$+0.64$ -1.32	$+0.91$ -1.44
J0222-1615		$1.90^{+0.24}_{-0.23}$	$+0.45$ -0.47	$+0.62$ -0.51	$-6.07^{+0.55}_{-0.52}$	$+0.93$ -0.92	$+1.20$ -1.27
J0224+0659		$2.64^{+0.31}_{-0.34}$	$+0.76$ -0.48	$+0.95$ -0.79	$-6.48^{+0.79}_{-0.68}$	$+1.11$ -1.78	$+1.65$ -2.47
J0225+1846		$2.67^{+0.38}_{-0.25}$	$+0.70$ -0.59	$+1.03$ -0.68	$-7.44^{+0.68}_{-0.84}$	$+1.31$ -1.73	$+1.67$ -2.29
J0226-1843		$2.66^{+0.33}_{-0.36}$	$+0.79$ -0.56	$+0.84$ -0.67	$-8.03^{+0.91}_{-0.77}$	$+1.35$ -1.96	$+1.81$ -2.19
J0230+4032		$2.84^{+0.32}_{-0.23}$	$+0.59$ -0.51	$+0.81$ -0.59	$-7.66^{+0.51}_{-0.77}$	$+1.07$ -1.39	$+1.53$ -1.99
J0231+1322		$2.32^{+0.51}_{-0.24}$	$+0.85$ -0.53	$+1.25$ -0.76	$-6.49^{+1.06}_{-0.84}$	$+1.62$ -2.09	$+1.90$ -3.11
J0237+0526	<i>m</i>	$1.98^{+0.97}_{-0.62}$	$+2.35$ -0.95	$+3.28$ -1.14	$-7.44^{+1.85}_{-2.96}$	$+2.65$ -7.42	$+2.61$ -11.35
J0237+2848		$2.59^{+0.20}_{-0.30}$	$+0.46$ -0.49	$+0.80$ -0.60	$-5.91^{+0.64}_{-0.54}$	$+1.15$ -1.01	$+1.38$ -1.74
J0237+3022		$2.71^{+0.65}_{-0.70}$	$+1.43$ -1.08	$+1.86$ -1.28	$-9.07^{+1.92}_{-1.97}$	$+3.16$ -4.19	$+3.16$ -5.37
J0238+1636		$2.67^{+0.21}_{-0.17}$	$+0.48$ -0.36	$+0.58$ -0.44	$-5.62^{+0.46}_{-0.32}$	$+0.78$ -0.86	$+1.01$ -1.24
J0239+0416		$2.74^{+0.22}_{-0.31}$	$+0.55$ -0.66	$+0.90$ -0.66	$-7.44^{+0.57}_{-0.75}$	$+1.25$ -1.56	$+1.36$ -2.37
J0239-0234		$2.42^{+0.24}_{-0.33}$	$+0.71$ -0.46	$+0.74$ -0.59	$-6.56^{+0.96}_{-0.41}$	$+1.03$ -1.78	$+1.43$ -1.78
J0240+1848	<i>m</i>	$3.41^{+1.65}_{-0.37}$	$+1.77$ -1.44	$+1.89$ -1.98	$-12.75^{+2.65}_{-4.24}$	$+5.26$ -5.24	$+7.10$ -5.25
J0241-0815		$2.96^{+0.36}_{-0.26}$	$+0.75$ -0.53	$+1.03$ -0.67	$-7.51^{+0.56}_{-1.00}$	$+1.25$ -2.00	$+1.60$ -2.63
J0242+1101		$3.13^{+0.45}_{-0.39}$	$+1.09$ -0.57	$+1.15$ -0.98	$-8.68^{+0.82}_{-1.39}$	$+1.62$ -2.72	$+2.62$ -3.14
J0242+1742		$2.06^{+0.36}_{-0.25}$	$+0.70$ -0.41	$+0.93$ -0.55	$-6.62^{+0.42}_{-1.05}$	$+1.04$ -1.69	$+1.36$ -2.46
J0242+2653		$1.62^{+0.64}_{-0.16}$	$+1.04$ -0.42	$+1.34$ -0.58	$-6.14^{+0.98}_{-1.08}$	$+1.16$ -2.76	$+1.63$ -3.23
J0243+7120	<i>m</i>	$2.81^{+1.20}_{-0.69}$	$+2.36$ -0.95	$+2.43$ -1.34	$-9.42^{+2.22}_{-3.43}$	$+2.94$ -7.58	$+3.57$ -8.35
J0243-0550		$2.72^{+0.45}_{-0.24}$	$+0.80$ -0.48	$+0.86$ -0.83	$-7.59^{+0.90}_{-0.74}$	$+1.17$ -2.14	$+1.94$ -2.27
J0246-1236		$2.99^{+0.60}_{-0.28}$	$+1.03$ -0.64	$+1.40$ -0.84	$-9.49^{+1.23}_{-1.18}$	$+2.06$ -2.43	$+2.53$ -3.65
J0249+0619		$2.24^{+0.35}_{-0.32}$	$+0.74$ -0.57	$+0.83$ -0.71	$-7.14^{+0.95}_{-0.86}$	$+1.32$ -2.06	$+1.81$ -2.37
J0251+3734		$2.54^{+0.90}_{-0.36}$	$+1.68$ -0.89	$+2.04$ -1.12	$-8.78^{+1.22}_{-2.67}$	$+2.46$ -5.12	$+3.05$ -6.31
J0251+4315		$2.13^{+0.39}_{-0.35}$	$+1.03$ -0.63	$+1.20$ -0.83	$-6.84^{+1.01}_{-0.86}$	$+1.46$ -2.75	$+1.95$ -3.28
J0251+7226		$2.68^{+0.35}_{-0.34}$	$+0.79$ -0.56	$+0.95$ -0.83	$-8.34^{+1.07}_{-0.69}$	$+1.83$ -1.54	$+2.21$ -2.49
J0254+2343		$3.20^{+0.55}_{-0.39}$	$+1.24$ -0.68	$+1.56$ -0.96	$-9.79^{+1.11}_{-1.50}$	$+2.04$ -3.13	$+2.40$ -4.08
J0254+3931		$2.73^{+0.47}_{-0.24}$	$+0.81$ -0.49	$+1.09$ -0.73	$-7.99^{+0.82}_{-0.92}$	$+1.33$ -2.11	$+1.95$ -2.71

Table C.1: Results of fitting the simple power-law model over the 1290 selected observations from OVRO dataset. Flag refers to sources well-defined by the model, being (*m*) objects with a $\sigma(\beta)_{68.3\%} \in [1.5, 3]$ (medium quality) and (*ℓ*) to $\sigma(\beta)_{68.3\%} > 3$ (low quality). The absence of a flag means having $\sigma(\beta)_{68.3\%} < 1.5$.

Name	Flag	β	$\beta^{95.5\%}$	$\beta^{99.7\%}$	$\log A$	$\log A^{95.5\%}$	$\log A^{99.7\%}$
J0256+1542		$2.45^{+0.42}_{-0.27}$	$+0.77$ -0.59	$+1.17$ -0.74	$-7.77^{+0.74}_{-0.99}$	$+1.41$ -2.08	$+1.91$ -2.67
J0257+1847		$2.13^{+0.18}_{-0.32}$	$+0.54$ -0.53	$+0.88$ -0.65	$-6.33^{+0.68}_{-0.45}$	$+1.14$ -1.25	$+1.44$ -2.11
J0257+7843		$2.52^{+0.47}_{-0.67}$	$+1.36$ -0.92	$+1.62$ -1.26	$-8.61^{+1.42}_{-1.85}$	$+2.90$ -3.58	$+3.24$ -5.00
J0257-1212		$2.78^{+0.33}_{-0.44}$	$+0.77$ -0.70	$+0.95$ -0.98	$-8.61^{+0.67}_{-1.34}$	$+1.63$ -2.19	$+2.16$ -2.83
J0258+0541		$2.56^{+0.37}_{-0.34}$	$+0.80$ -0.63	$+1.23$ -0.82	$-7.93^{+1.04}_{-0.82}$	$+1.76$ -1.92	$+2.07$ -3.19
J0259+0747		$2.57^{+0.24}_{-0.37}$	$+0.73$ -0.51	$+1.03$ -0.69	$-6.48^{+0.62}_{-0.77}$	$+1.31$ -1.67	$+1.37$ -2.50
J0259-0018	<i>ℓ</i>	$-0.58^{+3.58}_{-0.78}$	$+5.44$ -0.79	$+5.82$ -0.91	$-17.02^{+6.36}_{-1.93}$	$+12.90$ -1.93	$+15.02$ -1.92
J0309+1029		$2.47^{+0.29}_{-0.23}$	$+0.62$ -0.38	$+0.71$ -0.62	$-6.28^{+0.56}_{-0.66}$	$+0.91$ -1.38	$+1.45$ -1.76
J0309-0559	<i>m</i>	$3.21^{+1.29}_{-0.94}$	$+2.10$ -1.32	$+2.28$ -1.48	$-9.49^{+1.14}_{-6.51}$	$+2.60$ -8.84	$+3.08$ -9.48
J0310+3814		$2.46^{+0.26}_{-0.20}$	$+0.47$ -0.34	$+0.53$ -0.56	$-5.78^{+0.27}_{-0.68}$	$+0.66$ -1.03	$+1.20$ -1.27
J0312+0133		$2.44^{+0.45}_{-0.28}$	$+0.98$ -0.53	$+1.16$ -0.61	$-7.06^{+1.07}_{-0.83}$	$+1.36$ -2.52	$+1.73$ -3.09
J0313+4120		$2.39^{+0.49}_{-0.34}$	$+0.95$ -0.55	$+1.39$ -0.63	$-6.96^{+0.86}_{-1.23}$	$+1.25$ -2.80	$+1.60$ -3.70
J0315-1031		$2.17^{+0.46}_{-0.28}$	$+0.96$ -0.50	$+1.40$ -0.66	$-6.81^{+0.53}_{-1.22}$	$+1.18$ -2.28	$+1.43$ -3.43
J0315-1656		$2.68^{+0.73}_{-0.59}$	$+1.88$ -0.82	$+1.88$ -1.28	$-8.83^{+1.69}_{-2.08}$	$+2.43$ -5.56	$+3.48$ -6.04
J0318-0029	<i>m</i>	$4.66^{+0.42}_{-1.22}$	$+0.73$ -2.29	$+0.83$ -3.01	$-16.55^{+2.91}_{-2.43}$	$+7.07$ -2.40	$+10.20$ -2.43
J0319+4130		$2.63^{+0.42}_{-0.19}$	$+0.70$ -0.48	$+1.05$ -0.60	$-4.42^{+0.66}_{-0.80}$	$+1.29$ -1.56	$+1.58$ -2.53
J0319-1613		$2.99^{+0.51}_{-0.41}$	$+1.11$ -0.84	$+1.36$ -0.94	$-9.24^{+1.39}_{-1.35}$	$+2.00$ -3.53	$+2.45$ -4.23
J0325+2224		$3.01^{+0.25}_{-0.34}$	$+0.63$ -0.55	$+0.74$ -0.62	$-7.19^{+0.55}_{-0.79}$	$+0.85$ -1.73	$+1.28$ -1.84
J0327+0044		$2.30^{+0.45}_{-0.62}$	$+1.07$ -0.85	$+1.75$ -1.02	$-7.67^{+1.17}_{-1.81}$	$+1.85$ -3.43	$+2.42$ -5.32
J0329+3510		$3.01^{+0.48}_{-0.30}$	$+0.96$ -0.59	$+1.32$ -0.73	$-8.53^{+0.86}_{-1.17}$	$+1.59$ -2.47	$+1.98$ -3.09
J0334+0800		$2.16^{+0.41}_{-0.38}$	$+0.87$ -0.57	$+0.97$ -0.81	$-6.99^{+0.58}_{-1.53}$	$+1.28$ -2.52	$+1.74$ -2.66
J0336-1302		$1.95^{+0.43}_{-0.34}$	$+1.02$ -0.55	$+1.06$ -0.77	$-5.93^{+0.85}_{-1.23}$	$+1.31$ -2.68	$+1.67$ -2.97
J0339-0133	<i>m</i>	$3.44^{+1.41}_{-0.71}$	$+2.01$ -1.34	$+2.06$ -1.77	$-11.08^{+1.89}_{-5.21}$	$+3.79$ -7.46	$+4.73$ -7.79
J0339-0146		$2.72^{+0.28}_{-0.31}$	$+0.71$ -0.47	$+0.92$ -0.82	$-5.96^{+0.66}_{-0.76}$	$+1.12$ -1.73	$+1.76$ -2.38
J0343+3622		$2.65^{+0.35}_{-0.38}$	$+0.71$ -0.62	$+0.88$ -0.88	$-7.51^{+0.92}_{-0.92}$	$+1.46$ -2.04	$+1.92$ -2.22
J0345+1453		$2.90^{+0.43}_{-0.42}$	$+0.87$ -0.74	$+0.98$ -0.91	$-8.13^{+1.25}_{-1.07}$	$+1.66$ -2.64	$+2.24$ -2.82
J0348-1610		$2.47^{+0.45}_{-0.36}$	$+1.08$ -0.57	$+1.41$ -0.75	$-7.57^{+0.95}_{-1.30}$	$+1.70$ -2.88	$+2.00$ -3.83
J0351-1153	<i>m</i>	$4.44^{+0.95}_{-1.53}$	$+1.02$ -2.56	$+1.04$ -3.11	$-9.23^{+2.47}_{-5.75}$	$+2.47$ -9.48	$+4.28$ -9.73
J0354+8009		$1.99^{+0.21}_{-0.26}$	$+0.51$ -0.38	$+0.62$ -0.51	$-6.12^{+0.46}_{-0.63}$	$+0.77$ -1.25	$+1.01$ -1.40
J0357+2319		$2.24^{+0.35}_{-0.23}$	$+0.61$ -0.50	$+0.83$ -0.62	$-5.77^{+0.63}_{-0.84}$	$+1.02$ -1.62	$+1.37$ -2.21

Table C.1: Results of fitting the simple power-law model over the 1290 selected observations from OVRO dataset. Flag refers to sources well-defined by the model, being (*m*) objects with a $\sigma(\beta)_{68.3\%} \in [1.5, 3]$ (medium quality) and (*ℓ*) to $\sigma(\beta)_{68.3\%} > 3$ (low quality). The absence of a flag means having $\sigma(\beta)_{68.3\%} < 1.5$.

Name	Flag	β	$\beta^{95.5\%}$	$\beta^{99.7\%}$	$\log A$	$\log A^{95.5\%}$	$\log A^{99.7\%}$
J0359+3220	<i>m</i>	$2.75^{+1.01}_{-0.79}$	$+2.41$ -0.98	$+2.71$ -1.25	$-8.56^{+2.13}_{-3.45}$	$+3.20$ -7.78	$+3.43$ -8.92
J0400+0550		$2.11^{+0.55}_{-0.38}$	$+1.16$ -0.84	$+1.72$ -0.84	$-6.69^{+1.06}_{-1.46}$	$+2.07$ -3.37	$+2.20$ -5.01
J0401+0413		$2.26^{+0.41}_{-0.59}$	$+0.89$ -1.12	$+1.23$ -1.12	$-5.77^{+1.03}_{-1.52}$	$+2.47$ -2.55	$+2.47$ -3.67
J0401+2110		$2.18^{+0.21}_{-0.22}$	$+0.37$ -0.40	$+0.49$ -0.50	$-6.09^{+0.46}_{-0.50}$	$+0.64$ -1.10	$+0.91$ -1.17
J0401-1606	<i>m</i>	$4.67^{+0.49}_{-1.29}$	$+0.51$ -3.12	$+0.66$ -3.46	$-16.31^{+4.18}_{-1.69}$	$+10.46$ -1.52	$+11.60$ -1.69
J0403+2600		$2.54^{+0.42}_{-0.29}$	$+0.82$ -0.58	$+0.93$ -0.77	$-7.04^{+1.03}_{-0.88}$	$+1.64$ -2.11	$+1.86$ -2.60
J0405-1308		$2.80^{+0.33}_{-0.39}$	$+0.76$ -0.69	$+1.39$ -0.73	$-7.03^{+1.01}_{-0.75}$	$+1.89$ -1.72	$+1.93$ -3.21
J0406+0637		$2.55^{+0.36}_{-0.39}$	$+0.62$ -0.79	$+0.91$ -1.02	$-7.44^{+1.34}_{-0.59}$	$+1.93$ -1.62	$+2.53$ -2.31
J0407+0742		$2.15^{+0.22}_{-0.28}$	$+0.60$ -0.41	$+0.66$ -0.58	$-5.51^{+0.60}_{-0.57}$	$+0.91$ -1.36	$+1.23$ -1.64
J0409+1217		$2.78^{+0.57}_{-0.49}$	$+1.15$ -1.02	$+1.88$ -1.09	$-8.54^{+1.48}_{-1.56}$	$+2.73$ -3.36	$+3.01$ -5.73
J0409-1238	<i>m</i>	$3.85^{+0.94}_{-0.78}$	$+1.56$ -1.45	$+1.55$ -1.91	$-12.67^{+2.49}_{-2.90}$	$+5.20$ -4.52	$+5.68$ -5.17
J0412+0010		$2.48^{+0.31}_{-0.43}$	$+0.69$ -0.69	$+0.92$ -0.79	$-8.08^{+1.02}_{-1.01}$	$+1.58$ -2.20	$+1.95$ -2.71
J0412+0438	<i>m</i>	$2.52^{+0.82}_{-0.79}$	$+2.19$ -1.09	$+2.80$ -1.21	$-8.74^{+2.61}_{-2.46}$	$+2.58$ -7.64	$+3.44$ -8.75
J0412+1856	<i>ℓ</i>	$-0.62^{+2.61}_{-0.85}$	$+5.12$ -0.85	$+5.91$ -0.86	$-19.00^{+6.85}_{-2.01}$	$+12.95$ -2.00	$+15.83$ -2.01
J0414+3418	<i>m</i>	$1.61^{+1.65}_{-0.82}$	$+3.72$ -2.27	$+3.72$ -3.03	$-5.76^{+1.91}_{-4.94}$	$+1.62$ -12.24	$+2.52$ -13.09
J0416-1851		$2.83^{+0.19}_{-0.40}$	$+0.41$ -0.69	$+0.59$ -0.83	$-7.18^{+0.51}_{-0.96}$	$+1.10$ -1.53	$+1.55$ -1.87
J0422+0219		$2.66^{+0.17}_{-0.42}$	$+0.47$ -0.61	$+0.64$ -0.78	$-6.94^{+0.93}_{-0.52}$	$+1.54$ -1.18	$+1.85$ -1.61
J0422-0643		$1.61^{+0.18}_{-0.19}$	$+0.37$ -0.34	$+0.54$ -0.48	$-4.77^{+0.32}_{-0.47}$	$+0.66$ -0.80	$+0.86$ -1.18
J0423-0120		$3.04^{+0.28}_{-0.38}$	$+0.74$ -0.46	$+0.79$ -0.68	$-6.71^{+0.83}_{-0.84}$	$+1.46$ -1.72	$+1.72$ -2.11
J0424+0805		$2.40^{+0.43}_{-0.49}$	$+1.05$ -0.77	$+1.49$ -0.97	$-7.96^{+1.50}_{-1.00}$	$+1.81$ -3.41	$+2.60$ -4.31
J0426+0518		$2.44^{+0.44}_{-0.46}$	$+1.14$ -0.81	$+1.30$ -0.95	$-7.51^{+1.09}_{-1.35}$	$+2.30$ -2.75	$+2.30$ -3.93
J0426+2327	<i>m</i>	$2.87^{+1.12}_{-0.64}$	$+2.07$ -1.04	$+2.53$ -1.17	$-9.61^{+2.08}_{-3.42}$	$+2.19$ -7.85	$+3.32$ -7.86
J0426+2350	<i>m</i>	$5.12^{+0.34}_{-1.16}$	$+0.37$ -2.69	$+0.37$ -3.45	$-17.61^{+3.84}_{-1.66}$	$+8.69$ -1.75	$+11.09$ -1.99
J0428+1732	<i>m</i>	$3.72^{+1.45}_{-0.80}$	$+1.73$ -1.63	$+1.78$ -2.20	$-11.82^{+0.88}_{-6.65}$	$+4.35$ -6.71	$+5.63$ -7.16
J0430+1655		$1.72^{+0.37}_{-0.36}$	$+0.89$ -0.43	$+1.10$ -0.62	$-5.91^{+0.61}_{-1.38}$	$+1.06$ -2.63	$+1.31$ -3.00
J0431+1731		$2.03^{+0.56}_{-0.32}$	$+0.99$ -0.61	$+1.51$ -0.65	$-6.83^{+0.74}_{-1.65}$	$+1.61$ -2.90	$+1.89$ -3.77
J0433+0521		$2.58^{+0.30}_{-0.09}$	$+0.45$ -0.26	$+0.48$ -0.43	$-5.36^{+0.24}_{-0.54}$	$+0.55$ -0.90	$+0.85$ -0.99
J0433+2905		$2.17^{+0.20}_{-0.29}$	$+0.44$ -0.45	$+0.56$ -0.57	$-5.89^{+0.56}_{-0.50}$	$+1.00$ -1.02	$+1.22$ -1.39
J0434-1442	<i>m</i>	$2.91^{+0.84}_{-0.70}$	$+1.77$ -0.98	$+2.43$ -1.14	$-8.78^{+2.06}_{-2.48}$	$+2.56$ -5.65	$+2.94$ -7.91
J0437-1844	<i>m</i>	$4.77^{+0.50}_{-1.33}$	$+0.73$ -2.26	$+0.73$ -3.01	$-16.21^{+4.69}_{-1.37}$	$+8.28$ -1.66	$+10.46$ -1.66

Table C.1: Results of fitting the simple power-law model over the 1290 selected observations from OVRO dataset. Flag refers to sources well-defined by the model, being (*m*) objects with a $\sigma(\beta)_{68.3\%} \in [1.5, 3]$ (medium quality) and (*ℓ*) to $\sigma(\beta)_{68.3\%} > 3$ (low quality). The absence of a flag means having $\sigma(\beta)_{68.3\%} < 1.5$.

Name	Flag	β	$\beta^{95.5\%}$	$\beta^{99.7\%}$	$\log A$	$\log A^{95.5\%}$	$\log A^{99.7\%}$
J0438+3004		$2.38^{+0.26}_{-0.46}$	$+0.62_{-0.72}$	$+0.83_{-0.82}$	$-7.23^{+1.16}_{-0.69}$	$+1.70_{-1.80}$	$+1.98_{-2.67}$
J0438-1251		$2.74^{+0.64}_{-0.39}$	$+1.21_{-0.68}$	$+1.89_{-0.90}$	$-7.81^{+1.04}_{-1.74}$	$+1.90_{-3.33}$	$+2.25_{-5.39}$
J0439+0520	<i>ℓ</i>	$1.62^{+1.17}_{-2.65}$	$+3.41_{-2.86}$	$+3.74_{-3.11}$	$-17.69^{+8.77}_{-2.31}$	$+12.48_{-2.30}$	$+14.57_{-2.30}$
J0439+3045		$2.24^{+0.61}_{-0.66}$	$+1.85_{-1.12}$	$+2.31_{-1.08}$	$-7.36^{+1.61}_{-2.09}$	$+2.23_{-6.46}$	$+2.57_{-7.44}$
J0440+1437		$2.99^{+0.51}_{-0.36}$	$+0.99_{-0.81}$	$+1.61_{-0.82}$	$-8.79^{+1.18}_{-1.12}$	$+2.23_{-2.56}$	$+2.53_{-4.30}$
J0442-0017		$2.42^{+0.21}_{-0.38}$	$+0.82_{-0.44}$	$+0.82_{-0.66}$	$-6.13^{+0.74}_{-0.63}$	$+1.02_{-2.06}$	$+1.63_{-2.06}$
J0449+1121		$1.74^{+0.28}_{-0.26}$	$+0.74_{-0.41}$	$+1.05_{-0.50}$	$-4.22^{+0.58}_{-0.71}$	$+1.06_{-1.65}$	$+1.06_{-2.45}$
J0449+6332		$2.75^{+0.48}_{-0.41}$	$+0.99_{-0.70}$	$+1.35_{-0.86}$	$-7.32^{+0.96}_{-1.33}$	$+1.67_{-2.49}$	$+2.03_{-3.33}$
J0452+1236		$2.13^{+0.49}_{-0.54}$	$+1.25_{-0.72}$	$+1.71_{-0.87}$	$-7.12^{+0.95}_{-1.93}$	$+1.79_{-3.85}$	$+1.94_{-5.25}$
J0456+0400		$1.67^{+0.66}_{-0.45}$	$+2.72_{-0.81}$	$+3.78_{-0.80}$	$-6.17^{+1.38}_{-1.61}$	$+1.98_{-9.37}$	$+1.89_{-12.79}$
J0457+0645		$2.40^{+0.48}_{-0.22}$	$+0.94_{-0.48}$	$+1.34_{-0.68}$	$-6.02^{+0.53}_{-1.21}$	$+1.21_{-2.21}$	$+1.45_{-3.59}$
J0501+1356		$2.38^{+0.63}_{-0.35}$	$+1.21_{-0.64}$	$+1.48_{-0.88}$	$-7.87^{+0.93}_{-1.95}$	$+1.48_{-3.90}$	$+2.34_{-4.44}$
J0501-0159		$2.68^{+0.27}_{-0.34}$	$+0.61_{-0.57}$	$+0.69_{-0.72}$	$-6.66^{+0.97}_{-0.55}$	$+1.42_{-1.38}$	$+1.86_{-1.50}$
J0502+1338	<i>m</i>	$2.57^{+1.76}_{-0.46}$	$+2.69_{-0.82}$	$+2.80_{-1.14}$	$-7.67^{+1.43}_{-5.65}$	$+2.63_{-8.78}$	$+2.97_{-9.28}$
J0503+6600		$1.77^{+0.53}_{-0.17}$	$+1.04_{-0.39}$	$+1.06_{-0.71}$	$-6.27^{+0.98}_{-0.82}$	$+1.10_{-2.58}$	$+1.72_{-2.74}$
J0505+0459		$2.51^{+0.34}_{-0.24}$	$+0.72_{-0.54}$	$+0.84_{-0.65}$	$-6.47^{+0.57}_{-0.76}$	$+1.06_{-1.72}$	$+1.34_{-1.94}$
J0508+8432		$2.71^{+0.39}_{-0.53}$	$+0.93_{-0.90}$	$+1.24_{-1.02}$	$-9.08^{+1.40}_{-1.08}$	$+2.13_{-3.14}$	$+2.74_{-3.37}$
J0509+0541		$2.48^{+0.56}_{-0.28}$	$+0.97_{-0.57}$	$+1.27_{-0.68}$	$-7.21^{+1.01}_{-1.30}$	$+1.67_{-2.50}$	$+1.87_{-3.87}$
J0510+1800		$2.68^{+0.26}_{-0.34}$	$+0.71_{-0.46}$	$+0.77_{-0.71}$	$-6.33^{+0.63}_{-0.79}$	$+1.15_{-1.61}$	$+1.73_{-2.01}$
J0511+1357	<i>m</i>	$2.66^{+1.22}_{-0.63}$	$+2.50_{-0.95}$	$+2.72_{-1.13}$	$-8.98^{+1.89}_{-3.77}$	$+2.34_{-8.73}$	$+3.18_{-8.88}$
J0522-0725		$2.30^{+0.65}_{-0.41}$	$+1.77_{-0.60}$	$+1.94_{-0.76}$	$-8.03^{+1.05}_{-1.93}$	$+2.01_{-5.11}$	$+2.03_{-5.90}$
J0527+0331		$1.43^{+0.28}_{-0.28}$	$+0.81_{-0.43}$	$+1.35_{-0.51}$	$-3.54^{+0.48}_{-0.72}$	$+0.86_{-1.92}$	$+0.93_{-3.23}$
J0529-0519		$2.31^{+0.99}_{-0.40}$	$+1.98_{-1.04}$	$+2.87_{-1.20}$	$-7.53^{+1.80}_{-2.22}$	$+3.12_{-5.65}$	$+3.55_{-8.70}$
J0530+1331		$3.44^{+0.58}_{-0.34}$	$+1.04_{-0.83}$	$+1.40_{-1.00}$	$-9.12^{+0.98}_{-1.46}$	$+2.14_{-2.96}$	$+2.65_{-3.99}$
J0532+0732		$2.58^{+0.36}_{-0.17}$	$+0.60_{-0.43}$	$+0.80_{-0.52}$	$-6.12^{+0.47}_{-0.74}$	$+0.93_{-1.48}$	$+1.26_{-1.92}$
J0541+5312	<i>m</i>	$2.30^{+0.99}_{-0.57}$	$+2.46_{-0.76}$	$+3.00_{-1.04}$	$-7.91^{+1.64}_{-2.88}$	$+2.33_{-7.43}$	$+2.67_{-9.68}$
J0541-0541		$1.70^{+0.34}_{-0.27}$	$+0.72_{-0.46}$	$+0.93_{-0.53}$	$-4.52^{+0.47}_{-1.07}$	$+1.02_{-1.90}$	$+1.16_{-2.44}$
J0542+498		$1.91^{+0.31}_{-0.46}$	$+0.86_{-0.70}$	$+0.97_{-0.93}$	$-5.32^{+0.97}_{-0.79}$	$+1.64_{-1.91}$	$+2.11_{-2.75}$
J0542-0913		$2.18^{+0.44}_{-0.27}$	$+0.85_{-0.51}$	$+1.12_{-0.65}$	$-5.31^{+0.73}_{-0.89}$	$+1.17_{-2.12}$	$+1.42_{-2.82}$
J0552+0313		$2.45^{+0.56}_{-0.66}$	$+1.23_{-1.08}$	$+2.03_{-1.08}$	$-6.82^{+1.46}_{-2.08}$	$+2.66_{-3.60}$	$+2.66_{-5.76}$

Table C.1: Results of fitting the simple power-law model over the 1290 selected observations from OVRO dataset. Flag refers to sources well-defined by the model, being (*m*) objects with a $\sigma(\beta)_{68.3\%} \in [1.5, 3]$ (medium quality) and (*ℓ*) to $\sigma(\beta)_{68.3\%} > 3$ (low quality). The absence of a flag means having $\sigma(\beta)_{68.3\%} < 1.5$.

Name	Flag	β	$\beta^{95.5\%}$	$\beta^{99.7\%}$	$\log A$	$\log A^{95.5\%}$	$\log A^{99.7\%}$
J0554+6857	<i>m</i>	$3.00^{+1.42}_{-0.48}$	$+2.06$ -1.08	$+2.39$ -1.46	$-10.28^{+2.71}_{-3.49}$	$+3.06$ -7.39	$+4.07$ -7.63
J0558-1317		$2.23^{+0.42}_{-0.43}$	$+1.15$ -0.62	$+1.21$ -0.96	$-6.71^{+1.39}_{-0.93}$	$+1.58$ -3.26	$+2.46$ -3.44
J0559+5804		$2.49^{+0.48}_{-0.62}$	$+1.65$ -0.69	$+1.76$ -0.99	$-7.96^{+1.47}_{-1.66}$	$+2.38$ -4.26	$+2.63$ -5.43
J0559-1817	<i>m</i>	$4.81^{+0.63}_{-1.12}$	$+0.67$ -2.34	$+0.69$ -2.87	$-14.77^{+3.94}_{-1.95}$	$+7.24$ -2.98	$+8.86$ -2.98
J0606-0724		$2.34^{+0.49}_{-0.29}$	$+0.87$ -0.62	$+1.07$ -0.71	$-7.07^{+0.71}_{-1.35}$	$+1.49$ -2.36	$+1.81$ -2.99
J0607+4739		$2.47^{+0.45}_{-0.37}$	$+0.92$ -0.61	$+0.97$ -0.88	$-7.63^{+1.21}_{-0.92}$	$+1.59$ -2.48	$+2.20$ -2.69
J0607+6720		$2.37^{+0.30}_{-0.40}$	$+0.63$ -0.70	$+0.93$ -0.76	$-6.94^{+0.95}_{-0.93}$	$+1.40$ -2.07	$+1.78$ -2.82
J0607-0834		$2.74^{+0.63}_{-0.36}$	$+1.25$ -0.64	$+1.65$ -0.97	$-6.39^{+1.02}_{-1.72}$	$+1.55$ -3.63	$+2.44$ -5.08
J0609-1542		$2.21^{+0.44}_{-0.23}$	$+0.74$ -0.55	$+1.31$ -0.62	$-4.80^{+0.73}_{-0.86}$	$+1.24$ -1.84	$+1.35$ -3.34
J0610-1847		$2.00^{+0.52}_{-0.51}$	$+1.16$ -0.76	$+1.69$ -0.76	$-5.48^{+1.25}_{-1.52}$	$+1.81$ -3.36	$+1.81$ -5.13
J0612+4122		$2.46^{+0.22}_{-0.35}$	$+0.58$ -0.51	$+0.80$ -0.68	$-7.07^{+0.87}_{-0.52}$	$+1.20$ -1.37	$+1.61$ -1.92
J0616-1041		$1.19^{+0.40}_{-0.43}$	$+1.77$ -0.82	$+2.28$ -2.15	$-3.65^{+0.95}_{-0.84}$	$+1.53$ -4.97	$+1.53$ -16.55
J0617+5701		$2.84^{+0.43}_{-0.36}$	$+1.06$ -0.59	$+1.23$ -0.85	$-8.48^{+0.99}_{-1.03}$	$+1.55$ -2.69	$+2.28$ -3.03
J0617+7816		$2.38^{+0.70}_{-0.46}$	$+1.65$ -0.91	$+2.61$ -0.91	$-7.86^{+1.41}_{-1.86}$	$+2.16$ -5.32	$+2.47$ -8.51
J0618+4620		$2.54^{+0.35}_{-0.37}$	$+0.93$ -0.59	$+1.07$ -0.76	$-7.97^{+0.86}_{-1.08}$	$+1.20$ -2.76	$+1.98$ -2.76
J0619-1140		$1.91^{+0.27}_{-0.23}$	$+0.61$ -0.41	$+0.82$ -0.52	$-5.39^{+0.54}_{-0.68}$	$+1.08$ -1.40	$+1.14$ -2.14
J0624+3856		$2.73^{+0.20}_{-0.46}$	$+0.67$ -0.67	$+0.93$ -0.92	$-8.17^{+1.10}_{-0.63}$	$+1.67$ -2.00	$+2.41$ -2.59
J0625+4440		$2.74^{+0.35}_{-0.31}$	$+0.98$ -0.47	$+1.20$ -0.70	$-7.73^{+0.53}_{-1.11}$	$+1.38$ -2.21	$+1.66$ -2.85
J0626+8202		$2.82^{+0.39}_{-0.54}$	$+0.95$ -0.89	$+1.51$ -0.96	$-8.44^{+1.47}_{-1.07}$	$+2.43$ -2.76	$+2.49$ -4.36
J0629-1959		$2.22^{+0.18}_{-0.35}$	$+0.64$ -0.51	$+0.76$ -0.66	$-5.51^{+0.49}_{-0.74}$	$+0.90$ -1.79	$+1.14$ -2.28
J0630-1323		$2.44^{+0.55}_{-0.29}$	$+0.95$ -0.58	$+1.17$ -0.71	$-7.38^{+0.61}_{-1.71}$	$+1.47$ -2.59	$+1.78$ -3.56
J0631-1410		$2.22^{+0.43}_{-0.16}$	$+0.72$ -0.41	$+0.93$ -0.51	$-6.56^{+0.52}_{-0.98}$	$+1.10$ -1.68	$+1.44$ -2.48
J0637+3322		$2.89^{+0.48}_{-0.60}$	$+0.94$ -1.03	$+1.48$ -1.41	$-9.03^{+1.95}_{-1.03}$	$+2.89$ -2.75	$+3.89$ -4.26
J0638+5933		$1.79^{+0.33}_{-0.17}$	$+0.66$ -0.40	$+0.72$ -0.55	$-5.48^{+0.43}_{-0.76}$	$+0.80$ -1.67	$+1.14$ -1.80
J0639+7324		$2.83^{+0.31}_{-0.32}$	$+0.69$ -0.62	$+1.14$ -0.88	$-7.66^{+0.64}_{-0.99}$	$+1.44$ -1.95	$+1.89$ -3.05
J0642+3509		$2.24^{+0.29}_{-0.47}$	$+0.68$ -0.82	$+0.95$ -0.97	$-7.32^{+1.01}_{-1.01}$	$+1.89$ -2.17	$+2.35$ -3.05
J0642+8811		$3.00^{+0.29}_{-0.46}$	$+0.78$ -0.85	$+1.13$ -0.96	$-8.68^{+1.20}_{-0.80}$	$+2.37$ -1.87	$+2.35$ -2.89
J0644+3914		$2.24^{+0.36}_{-0.31}$	$+0.69$ -0.62	$+1.01$ -0.71	$-7.19^{+0.71}_{-1.01}$	$+1.69$ -1.61	$+1.83$ -3.04
J0646+4451		$2.16^{+0.52}_{-0.13}$	$+0.85$ -0.49	$+1.04$ -0.86	$-5.53^{+0.42}_{-1.14}$	$+1.12$ -2.29	$+1.88$ -2.88
J0650+5616		$2.53^{+0.54}_{-0.34}$	$+0.90$ -0.78	$+1.22$ -0.99	$-8.29^{+0.86}_{-1.59}$	$+2.02$ -2.65	$+2.68$ -3.39

Table C.1: Results of fitting the simple power-law model over the 1290 selected observations from OVRO dataset. Flag refers to sources well-defined by the model, being (*m*) objects with a $\sigma(\beta)_{68.3\%} \in [1.5, 3]$ (medium quality) and (*ℓ*) to $\sigma(\beta)_{68.3\%} > 3$ (low quality). The absence of a flag means having $\sigma(\beta)_{68.3\%} < 1.5$.

Name	Flag	β	$\beta^{95.5\%}$	$\beta^{99.7\%}$	$\log A$	$\log A^{95.5\%}$	$\log A^{99.7\%}$
J0650+6001		$2.26^{+0.28}_{-0.42}$	$+0.78$ -0.67	$+1.01$ -0.73	$-6.63^{+0.63}_{-1.12}$	$+1.35$ -2.18	$+1.53$ -3.30
J0653+3705		$3.05^{+0.58}_{-0.78}$	$+1.47$ -1.26	$+1.99$ -1.38	$-9.54^{+2.28}_{-1.84}$	$+3.72$ -4.71	$+3.72$ -6.82
J0654+4514		$2.72^{+0.25}_{-0.19}$	$+0.43$ -0.45	$+0.58$ -0.46	$-6.74^{+0.50}_{-0.48}$	$+0.84$ -1.00	$+1.04$ -1.17
J0654+5042		$1.84^{+0.27}_{-0.14}$	$+0.50$ -0.28	$+0.51$ -0.41	$-5.94^{+0.21}_{-0.72}$	$+0.54$ -1.10	$+0.79$ -1.25
J0655+4100		$3.08^{+0.80}_{-0.65}$	$+1.53$ -1.31	$+2.25$ -1.39	$-9.47^{+1.77}_{-2.48}$	$+3.44$ -5.17	$+3.51$ -7.49
J0657+2423		$2.49^{+0.42}_{-0.49}$	$+0.98$ -0.69	$+1.34$ -0.88	$-7.59^{+0.90}_{-1.40}$	$+1.48$ -2.96	$+2.00$ -3.68
J0702+2644	<i>m</i>	$2.43^{+0.94}_{-0.63}$	$+2.54$ -0.85	$+2.65$ -1.10	$-8.02^{+1.59}_{-3.16}$	$+2.41$ -9.05	$+2.87$ -9.59
J0702+8549	<i>m</i>	$4.61^{+0.72}_{-2.11}$	$+0.84$ -4.64	$+0.86$ -5.75	$-16.61^{+7.91}_{-0.96}$	$+9.63$ -3.32	$+11.18$ -3.32
J0712+5033		$1.85^{+0.31}_{-0.13}$	$+0.53$ -0.37	$+0.69$ -0.40	$-5.27^{+0.47}_{-0.46}$	$+0.72$ -1.17	$+0.88$ -1.66
J0717+4538		$3.06^{+0.27}_{-0.64}$	$+0.84$ -0.84	$+1.31$ -0.94	$-9.01^{+1.68}_{-0.72}$	$+2.27$ -2.41	$+2.59$ -3.56
J0720+4737		$2.30^{+0.62}_{-0.59}$	$+2.03$ -0.98	$+2.80$ -0.97	$-7.68^{+1.72}_{-1.84}$	$+2.25$ -6.60	$+2.60$ -9.05
J0721+7120		$1.98^{+0.19}_{-0.18}$	$+0.37$ -0.35	$+0.53$ -0.36	$-3.44^{+0.34}_{-0.32}$	$+0.66$ -0.67	$+0.79$ -0.99
J0725+1425		$1.59^{+0.38}_{-0.29}$	$+0.75$ -0.45	$+1.13$ -0.49	$-4.19^{+0.64}_{-0.94}$	$+0.95$ -2.07	$+1.09$ -3.22
J0726+0636		$2.48^{+0.54}_{-0.55}$	$+1.37$ -0.76	$+1.57$ -1.01	$-8.09^{+1.51}_{-1.55}$	$+2.24$ -4.06	$+2.43$ -5.40
J0726+2153		$3.00^{+0.58}_{-0.47}$	$+1.49$ -0.93	$+2.04$ -1.15	$-8.77^{+1.26}_{-1.81}$	$+2.59$ -3.91	$+3.11$ -6.61
J0728+2153		$2.31^{+0.45}_{-0.23}$	$+0.83$ -0.46	$+1.18$ -0.67	$-7.19^{+0.65}_{-1.07}$	$+1.33$ -2.01	$+1.68$ -3.19
J0728+5701		$2.66^{+0.23}_{-0.37}$	$+0.54$ -0.67	$+0.75$ -0.88	$-7.99^{+0.83}_{-0.73}$	$+1.48$ -1.48	$+2.02$ -2.14
J0730+4049	<i>m</i>	$2.48^{+1.70}_{-0.69}$	$+2.50$ -1.16	$+2.63$ -1.56	$-8.61^{+2.54}_{-5.50}$	$+2.76$ -9.12	$+3.59$ -9.35
J0731+2451		$2.57^{+0.67}_{-0.68}$	$+1.76$ -0.90	$+2.18$ -1.02	$-8.63^{+2.12}_{-1.85}$	$+2.14$ -5.90	$+2.71$ -7.13
J0732+2548		$2.10^{+0.32}_{-0.15}$	$+0.48$ -0.32	$+0.64$ -0.53	$-6.11^{+0.31}_{-0.70}$	$+0.65$ -1.14	$+1.13$ -1.60
J0733+0456		$2.39^{+0.44}_{-0.24}$	$+0.77$ -0.51	$+1.12$ -0.75	$-6.74^{+0.51}_{-1.22}$	$+1.01$ -2.26	$+1.56$ -2.98
J0733+5022		$2.62^{+0.33}_{-0.30}$	$+0.73$ -0.67	$+1.07$ -0.78	$-7.46^{+0.80}_{-0.85}$	$+1.44$ -1.95	$+1.81$ -2.66
J0735+4750		$3.05^{+0.63}_{-0.83}$	$+2.06$ -1.06	$+2.35$ -1.58	$-9.49^{+2.59}_{-1.79}$	$+2.93$ -6.96	$+3.97$ -7.96
J0736+2604	<i>m</i>	$3.56^{+0.96}_{-0.71}$	$+1.69$ -1.16	$+1.93$ -1.71	$-12.23^{+2.54}_{-2.79}$	$+3.95$ -5.25	$+5.23$ -5.75
J0738+1742		$2.13^{+0.40}_{-0.34}$	$+0.90$ -0.55	$+1.22$ -0.69	$-5.82^{+0.72}_{-1.26}$	$+1.44$ -2.42	$+1.50$ -3.78
J0739+0137		$2.44^{+0.24}_{-0.23}$	$+0.48$ -0.41	$+0.71$ -0.46	$-5.46^{+0.36}_{-0.61}$	$+0.76$ -1.07	$+0.90$ -1.63
J0740+2852		$2.56^{+0.53}_{-0.25}$	$+0.91$ -0.61	$+1.57$ -0.84	$-8.29^{+0.82}_{-1.29}$	$+1.53$ -2.57	$+2.20$ -4.16
J0741+3112		$2.77^{+0.37}_{-0.41}$	$+0.79$ -0.60	$+1.16$ -0.77	$-7.41^{+1.12}_{-0.83}$	$+2.04$ -1.89	$+2.14$ -2.95
J0742+4900		$2.42^{+0.27}_{-0.18}$	$+0.45$ -0.36	$+0.53$ -0.50	$-6.73^{+0.33}_{-0.73}$	$+0.69$ -1.19	$+1.02$ -1.31
J0742+5444		$2.36^{+0.14}_{-0.25}$	$+0.43$ -0.32	$+0.53$ -0.53	$-6.18^{+0.36}_{-0.46}$	$+0.56$ -0.96	$+0.89$ -1.25

Table C.1: Results of fitting the simple power-law model over the 1290 selected observations from OVRO dataset. Flag refers to sources well-defined by the model, being (*m*) objects with a $\sigma(\beta)_{68.3\%} \in [1.5, 3]$ (medium quality) and (*ℓ*) to $\sigma(\beta)_{68.3\%} > 3$ (low quality). The absence of a flag means having $\sigma(\beta)_{68.3\%} < 1.5$.

Name	Flag	β	$\beta^{95.5\%}$	$\beta^{99.7\%}$	$\log A$	$\log A^{95.5\%}$	$\log A^{99.7\%}$
J0743+1714		$2.72^{+0.36}_{-0.48}$	$+0.81$ -0.89	$+1.17$ -1.01	$-8.37^{+1.53}_{-0.76}$	$+2.60$ -2.18	$+2.53$ -3.11
J0745+1011		$2.25^{+0.36}_{-0.28}$	$+0.74$ -0.44	$+0.80$ -0.79	$-6.13^{+0.52}_{-1.03}$	$+0.79$ -2.22	$+1.47$ -2.28
J0745-0044		$2.34^{+0.46}_{-0.36}$	$+0.83$ -0.61	$+1.06$ -0.75	$-6.92^{+1.18}_{-0.96}$	$+1.79$ -2.08	$+2.26$ -2.71
J0746+2549		$2.55^{+0.20}_{-0.26}$	$+0.43$ -0.40	$+0.58$ -0.49	$-6.94^{+0.60}_{-0.39}$	$+0.88$ -0.91	$+1.13$ -1.12
J0746+2734		$2.57^{+0.39}_{-0.38}$	$+0.77$ -0.81	$+1.19$ -0.88	$-7.38^{+0.73}_{-1.34}$	$+1.86$ -2.29	$+1.88$ -3.55
J0748+2400		$2.67^{+0.22}_{-0.48}$	$+0.65$ -0.68	$+0.91$ -0.81	$-7.29^{+0.98}_{-0.84}$	$+1.71$ -1.62	$+1.97$ -2.26
J0749+7420		$2.46^{+0.42}_{-0.23}$	$+0.83$ -0.43	$+0.95$ -0.69	$-6.94^{+0.45}_{-1.19}$	$+1.06$ -2.15	$+1.49$ -2.53
J0750+1021		$2.27^{+0.41}_{-0.21}$	$+0.71$ -0.50	$+0.95$ -0.72	$-6.99^{+0.40}_{-1.17}$	$+1.31$ -1.85	$+1.61$ -2.80
J0750+1231		$2.78^{+0.40}_{-0.27}$	$+0.69$ -0.58	$+0.94$ -0.75	$-6.91^{+0.86}_{-0.83}$	$+1.48$ -1.85	$+1.94$ -2.51
J0750+1823		$2.39^{+0.27}_{-0.37}$	$+0.52$ -0.66	$+0.62$ -0.95	$-6.71^{+0.57}_{-1.07}$	$+1.20$ -1.71	$+1.80$ -1.95
J0750+4814		$2.46^{+0.24}_{-0.41}$	$+0.66$ -0.62	$+0.88$ -0.81	$-7.18^{+1.23}_{-0.46}$	$+1.55$ -1.67	$+1.98$ -2.01
J0751+3313		$2.66^{+0.36}_{-0.36}$	$+0.70$ -0.63	$+0.98$ -0.79	$-7.82^{+0.62}_{-1.24}$	$+1.60$ -1.85	$+1.85$ -2.64
J0752+3730		$2.16^{+0.38}_{-0.37}$	$+0.70$ -0.56	$+0.80$ -0.75	$-7.12^{+0.72}_{-1.26}$	$+1.31$ -2.07	$+1.62$ -2.30
J0753+5352		$2.29^{+0.30}_{-0.24}$	$+0.67$ -0.50	$+0.85$ -0.65	$-6.22^{+0.61}_{-0.63}$	$+1.02$ -1.60	$+1.44$ -2.18
J0756+6347	<i>m</i>	$2.09^{+1.18}_{-0.52}$	$+2.21$ -0.93	$+2.97$ -1.01	$-7.69^{+1.99}_{-3.10}$	$+2.71$ -7.44	$+2.71$ -9.67
J0757+0956		$2.59^{+0.28}_{-0.37}$	$+0.75$ -0.51	$+1.02$ -0.81	$-6.34^{+0.74}_{-0.79}$	$+1.24$ -1.75	$+1.78$ -2.54
J0802+1809		$1.99^{+0.29}_{-0.39}$	$+0.82$ -0.53	$+0.97$ -0.82	$-6.44^{+0.69}_{-1.05}$	$+1.29$ -2.18	$+1.60$ -2.89
J0805+6144		$2.57^{+0.28}_{-0.36}$	$+0.72$ -0.60	$+0.92$ -0.67	$-7.32^{+0.86}_{-0.71}$	$+1.27$ -2.01	$+1.57$ -2.52
J0805-0111		$2.51^{+0.19}_{-0.25}$	$+0.38$ -0.46	$+0.69$ -0.51	$-6.74^{+0.38}_{-0.60}$	$+0.75$ -1.25	$+0.97$ -1.69
J0806+4504		$2.24^{+0.44}_{-0.38}$	$+0.96$ -0.68	$+1.32$ -0.85	$-7.59^{+1.13}_{-1.03}$	$+2.28$ -2.09	$+2.50$ -3.47
J0807+5117		$2.87^{+0.83}_{-0.53}$	$+1.65$ -1.10	$+2.33$ -1.15	$-9.66^{+1.82}_{-2.27}$	$+4.08$ -4.65	$+3.39$ -7.52
J0807-0541	<i>ℓ</i>	$1.85^{+2.63}_{-1.15}$	$+3.31$ -3.00	$+3.65$ -3.31	$-16.87^{+8.42}_{-2.04}$	$+11.89$ -2.03	$+13.08$ -2.13
J0808+4052		$2.40^{+0.31}_{-0.37}$	$+0.60$ -0.63	$+0.83$ -0.77	$-6.92^{+1.08}_{-0.68}$	$+1.45$ -1.68	$+2.09$ -2.12
J0808+4950		$2.57^{+0.29}_{-0.29}$	$+0.59$ -0.49	$+0.84$ -0.63	$-6.99^{+0.57}_{-0.84}$	$+1.03$ -1.39	$+1.40$ -1.73
J0808+7315	<i>m</i>	$3.57^{+1.31}_{-0.42}$	$+1.88$ -0.95	$+1.88$ -1.62	$-11.57^{+0.90}_{-4.94}$	$+2.92$ -6.37	$+4.83$ -6.37
J0808-0751		$2.64^{+0.31}_{-0.25}$	$+0.69$ -0.39	$+0.82$ -0.60	$-6.86^{+0.68}_{-0.70}$	$+1.21$ -1.51	$+1.62$ -2.18
J0809+5341		$2.37^{+0.19}_{-0.32}$	$+0.50$ -0.44	$+0.63$ -0.63	$-6.83^{+0.71}_{-0.51}$	$+1.05$ -1.17	$+1.54$ -1.47
J0810+4134		$2.73^{+0.48}_{-0.26}$	$+0.82$ -0.56	$+1.17$ -0.81	$-8.76^{+1.14}_{-0.75}$	$+1.88$ -1.83	$+2.48$ -2.55
J0811+0146		$2.34^{+0.23}_{-0.17}$	$+0.44$ -0.33	$+0.59$ -0.41	$-5.43^{+0.37}_{-0.51}$	$+0.68$ -0.99	$+0.89$ -1.31
J0811+4533		$2.27^{+0.65}_{-0.22}$	$+0.91$ -0.67	$+1.25$ -0.78	$-7.78^{+0.79}_{-1.64}$	$+1.40$ -2.97	$+1.95$ -3.67

Table C.1: Results of fitting the simple power-law model over the 1290 selected observations from OVRO dataset. Flag refers to sources well-defined by the model, being (*m*) objects with a $\sigma(\beta)_{68.3\%} \in [1.5, 3]$ (medium quality) and (*ℓ*) to $\sigma(\beta)_{68.3\%} > 3$ (low quality). The absence of a flag means having $\sigma(\beta)_{68.3\%} < 1.5$.

Name	Flag	β	$\beta^{95.5\%}$	$\beta^{99.7\%}$	$\log A$	$\log A^{95.5\%}$	$\log A^{99.7\%}$
J0813+2542		$2.03^{+0.37}_{-0.34}$	$+0.68$ -0.55	$+0.75$ -0.73	$-6.19^{+0.41}_{-1.25}$	$+0.82$ -2.02	$+1.48$ -2.13
J0814+5609		$2.39^{+0.95}_{-0.46}$	$+2.13$ -0.84	$+2.68$ -1.15	$-8.77^{+1.42}_{-2.58}$	$+1.90$ -7.00	$+2.80$ -8.69
J0814+6431		$2.43^{+0.31}_{-0.43}$	$+0.83$ -0.57	$+0.97$ -0.69	$-7.33^{+0.95}_{-0.95}$	$+1.44$ -2.01	$+1.72$ -2.63
J0815+3635		$2.25^{+0.41}_{-0.39}$	$+0.82$ -0.64	$+1.00$ -0.85	$-7.08^{+1.02}_{-1.10}$	$+1.70$ -2.21	$+2.27$ -3.31
J0818+4222		$2.52^{+0.35}_{-0.28}$	$+0.77$ -0.33	$+0.77$ -0.54	$-6.74^{+0.72}_{-0.88}$	$+1.32$ -1.48	$+1.32$ -1.98
J0819+3226		$2.34^{+0.31}_{-0.22}$	$+0.60$ -0.44	$+0.79$ -0.55	$-6.96^{+0.53}_{-0.84}$	$+0.88$ -1.61	$+1.25$ -2.23
J0823+2928		$1.90^{+0.38}_{-0.36}$	$+0.80$ -0.56	$+1.02$ -0.71	$-6.18^{+0.83}_{-1.12}$	$+1.47$ -2.31	$+1.51$ -3.15
J0824+3916		$2.78^{+0.30}_{-0.49}$	$+0.80$ -0.77	$+1.11$ -0.89	$-7.52^{+0.98}_{-1.00}$	$+1.88$ -2.19	$+2.01$ -3.08
J0824+5552		$3.15^{+0.41}_{-0.36}$	$+0.78$ -0.70	$+0.94$ -0.96	$-8.62^{+0.96}_{-0.98}$	$+1.69$ -2.14	$+2.34$ -2.50
J0824-1527	<i>m</i>	$2.93^{+1.03}_{-0.65}$	$+2.21$ -0.97	$+2.48$ -1.33	$-8.96^{+1.78}_{-3.26}$	$+2.90$ -7.00	$+3.85$ -7.60
J0825+0309		$2.95^{+0.17}_{-0.30}$	$+0.37$ -0.52	$+0.58$ -0.62	$-6.84^{+0.60}_{-0.49}$	$+1.08$ -0.99	$+1.26$ -1.47
J0825+1332		$2.08^{+0.28}_{-0.39}$	$+0.71$ -0.55	$+1.04$ -0.67	$-6.72^{+1.04}_{-0.73}$	$+1.25$ -2.28	$+1.58$ -3.08
J0825+6157		$2.80^{+0.66}_{-0.33}$	$+1.36$ -0.63	$+1.90$ -1.07	$-8.77^{+0.96}_{-1.80}$	$+2.06$ -3.44	$+2.75$ -5.23
J0827+3525		$2.21^{+0.46}_{-0.33}$	$+1.14$ -0.53	$+1.44$ -0.85	$-7.39^{+0.71}_{-1.48}$	$+1.40$ -3.07	$+1.64$ -4.37
J0830+2410		$2.90^{+0.26}_{-0.22}$	$+0.51$ -0.45	$+0.82$ -0.53	$-7.21^{+0.48}_{-0.57}$	$+1.01$ -1.12	$+1.20$ -1.74
J0831+0429		$2.58^{+0.21}_{-0.28}$	$+0.51$ -0.42	$+0.71$ -0.60	$-6.43^{+0.55}_{-0.61}$	$+0.96$ -1.25	$+1.30$ -1.61
J0833+0350		$2.14^{+0.52}_{-0.29}$	$+1.23$ -0.48	$+1.49$ -0.65	$-6.77^{+0.64}_{-1.48}$	$+1.38$ -3.31	$+1.59$ -4.19
J0833+4224		$2.38^{+0.31}_{-0.27}$	$+0.72$ -0.47	$+0.83$ -0.58	$-6.83^{+0.56}_{-0.80}$	$+0.95$ -2.00	$+1.27$ -2.31
J0834+6019		$2.92^{+0.42}_{-0.30}$	$+0.68$ -0.81	$+1.12$ -0.81	$-8.29^{+0.69}_{-1.21}$	$+2.01$ -1.94	$+2.01$ -3.11
J0835+6835		$2.18^{+0.39}_{-0.35}$	$+0.99$ -0.44	$+0.99$ -0.75	$-6.78^{+0.60}_{-1.17}$	$+1.19$ -2.30	$+1.57$ -2.71
J0836+2728		$3.22^{+0.37}_{-0.42}$	$+0.74$ -0.74	$+1.17$ -0.89	$-9.47^{+0.98}_{-0.99}$	$+1.98$ -1.89	$+2.39$ -3.24
J0837+2454		$2.37^{+0.41}_{-0.31}$	$+0.86$ -0.58	$+1.40$ -0.67	$-6.92^{+0.71}_{-1.19}$	$+1.45$ -2.52	$+1.51$ -4.02
J0837+5825		$3.29^{+0.54}_{-0.91}$	$+1.36$ -1.36	$+1.71$ -1.57	$-9.87^{+2.58}_{-1.67}$	$+3.30$ -4.51	$+4.22$ -5.34
J0839+0104		$2.28^{+0.31}_{-0.24}$	$+0.56$ -0.50	$+0.81$ -0.55	$-6.53^{+0.45}_{-0.87}$	$+0.89$ -1.59	$+1.20$ -2.09
J0842+1835		$1.94^{+0.45}_{-0.28}$	$+0.80$ -0.65	$+1.35$ -0.72	$-6.42^{+0.96}_{-0.91}$	$+1.30$ -2.36	$+1.59$ -3.34
J0847-0703		$2.79^{+0.34}_{-0.16}$	$+0.62$ -0.42	$+0.77$ -0.47	$-7.32^{+0.47}_{-0.76}$	$+0.77$ -1.37	$+1.20$ -1.74
J0849+5108		$2.02^{+0.26}_{-0.16}$	$+0.37$ -0.39	$+0.51$ -0.62	$-5.39^{+0.35}_{-0.53}$	$+0.81$ -0.78	$+1.22$ -1.07
J0850-1213		$2.42^{+0.33}_{-0.18}$	$+0.51$ -0.43	$+0.64$ -0.48	$-5.72^{+0.64}_{-0.46}$	$+1.01$ -1.01	$+1.00$ -1.48
J0854+2006		$2.41^{+0.29}_{-0.12}$	$+0.46$ -0.32	$+0.63$ -0.43	$-4.12^{+0.44}_{-0.41}$	$+0.66$ -0.94	$+0.96$ -1.13
J0854+5757	<i>m</i>	$4.32^{+0.74}_{-1.04}$	$+0.96$ -2.17	$+1.18$ -2.74	$-15.91^{+3.58}_{-2.09}$	$+7.57$ -2.09	$+9.53$ -2.08

Table C.1: Results of fitting the simple power-law model over the 1290 selected observations from OVRO dataset. Flag refers to sources well-defined by the model, being (*m*) objects with a $\sigma(\beta)_{68.3\%} \in [1.5, 3]$ (medium quality) and (*ℓ*) to $\sigma(\beta)_{68.3\%} > 3$ (low quality). The absence of a flag means having $\sigma(\beta)_{68.3\%} < 1.5$.

Name	Flag	β	$\beta^{95.5\%}$	$\beta^{99.7\%}$	$\log A$	$\log A^{95.5\%}$	$\log A^{99.7\%}$
J0856+2111		$1.67^{+0.49}_{-0.29}$	$+1.08$ -0.60	$+3.05$ -0.80	$-6.32^{+1.04}_{-1.09}$	$+1.63$ -3.02	$+1.93$ -11.10
J0856-1105		$2.53^{+0.29}_{-0.32}$	$+0.56$ -0.51	$+0.81$ -0.62	$-7.02^{+0.88}_{-0.64}$	$+1.05$ -1.68	$+1.52$ -1.97
J0900+4108	<i>m</i>	$2.54^{+1.03}_{-0.51}$	$+2.80$ -0.69	$+2.80$ -1.10	$-8.71^{+1.94}_{-2.75}$	$+2.21$ -8.47	$+2.89$ -9.89
J0901+0448		$3.09^{+0.56}_{-0.55}$	$+1.15$ -0.88	$+1.45$ -1.09	$-9.84^{+1.26}_{-1.92}$	$+2.46$ -3.55	$+3.02$ -4.68
J0902+0443	<i>m</i>	$2.08^{+1.46}_{-0.60}$	$+3.04$ -0.85	$+3.42$ -1.10	$-7.77^{+1.45}_{-4.79}$	$+2.15$ -9.88	$+2.58$ -10.94
J0902+4310		$2.56^{+0.52}_{-0.37}$	$+1.18$ -0.53	$+1.57$ -0.71	$-8.08^{+0.94}_{-1.49}$	$+1.69$ -2.95	$+1.93$ -5.08
J0902+5402	<i>m</i>	$2.48^{+2.01}_{-0.57}$	$+2.98$ -0.73	$+3.01$ -1.25	$-8.77^{+1.77}_{-6.76}$	$+2.34$ -10.33	$+3.15$ -10.90
J0903+6757		$2.46^{+0.40}_{-0.34}$	$+0.80$ -0.59	$+1.22$ -0.81	$-7.48^{+0.66}_{-1.30}$	$+1.46$ -2.36	$+1.94$ -3.05
J0903-1721		$1.90^{+0.24}_{-0.41}$	$+0.69$ -0.54	$+0.87$ -0.66	$-6.26^{+0.86}_{-0.68}$	$+1.47$ -1.66	$+1.42$ -2.66
J0905+2849	<i>m</i>	$3.17^{+0.99}_{-0.85}$	$+2.13$ -1.16	$+2.31$ -1.38	$-10.32^{+2.61}_{-3.20}$	$+2.84$ -7.78	$+3.83$ -8.68
J0906+6930	<i>m</i>	$4.53^{+0.33}_{-1.60}$	$+0.71$ -2.39	$+0.71$ -3.36	$-14.35^{+3.41}_{-3.19}$	$+6.60$ -3.65	$+8.96$ -3.64
J0908+1609	<i>m</i>	$2.97^{+1.19}_{-0.54}$	$+2.45$ -0.79	$+2.46$ -1.24	$-9.71^{+2.09}_{-3.27}$	$+2.55$ -7.53	$+3.41$ -8.26
J0909+0121		$2.78^{+0.30}_{-0.30}$	$+0.85$ -0.56	$+1.16$ -0.70	$-6.99^{+0.77}_{-0.66}$	$+1.46$ -1.92	$+1.73$ -2.47
J0909+0200		$2.16^{+0.30}_{-0.29}$	$+0.69$ -0.49	$+1.00$ -0.64	$-6.73^{+0.63}_{-0.87}$	$+1.26$ -1.73	$+1.53$ -2.29
J0910+2248		$2.73^{+0.46}_{-0.51}$	$+1.60$ -0.57	$+1.60$ -0.98	$-8.66^{+1.29}_{-1.49}$	$+2.11$ -4.20	$+2.48$ -5.25
J0910+3329		$2.34^{+0.64}_{-0.69}$	$+2.03$ -1.07	$+3.06$ -1.07	$-8.03^{+1.78}_{-2.09}$	$+2.79$ -7.71	$+2.49$ -10.36
J0914+0245		$2.75^{+0.38}_{-0.32}$	$+0.84$ -0.61	$+1.03$ -0.73	$-7.92^{+0.74}_{-1.13}$	$+1.62$ -2.20	$+1.90$ -2.83
J0917-1345	<i>m</i>	$2.12^{+2.12}_{-0.52}$	$+3.16$ -0.76	$+3.37$ -1.01	$-7.71^{+1.53}_{-7.79}$	$+1.76$ -11.92	$+2.65$ -12.26
J0919+3324		$2.51^{+0.54}_{-0.42}$	$+1.15$ -0.68	$+1.41$ -0.84	$-8.04^{+1.08}_{-1.72}$	$+1.82$ -3.46	$+2.19$ -4.36
J0920+4441		$2.90^{+0.34}_{-0.41}$	$+0.79$ -0.68	$+1.02$ -0.87	$-7.67^{+1.35}_{-0.58}$	$+2.23$ -1.71	$+2.33$ -2.58
J0921+6215		$2.20^{+0.30}_{-0.38}$	$+0.72$ -0.52	$+1.02$ -0.64	$-6.59^{+0.91}_{-0.79}$	$+1.61$ -1.43	$+1.70$ -2.67
J0922-0529		$2.25^{+0.25}_{-0.36}$	$+0.59$ -0.52	$+0.66$ -0.72	$-6.47^{+0.62}_{-0.92}$	$+0.86$ -2.00	$+1.32$ -2.01
J0923+2815		$2.98^{+0.30}_{-0.32}$	$+0.60$ -0.63	$+0.93$ -0.68	$-7.43^{+0.81}_{-0.61}$	$+1.44$ -1.50	$+1.53$ -2.14
J0923+3849		$2.57^{+0.37}_{-0.15}$	$+0.54$ -0.50	$+0.72$ -0.66	$-7.26^{+0.43}_{-0.84}$	$+1.12$ -1.36	$+1.41$ -1.74
J0923+4125		$2.37^{+0.32}_{-0.25}$	$+0.55$ -0.51	$+0.63$ -0.69	$-6.88^{+0.89}_{-0.46}$	$+1.19$ -1.26	$+1.60$ -1.42
J0925+1658	<i>m</i>	$3.82^{+1.00}_{-1.02}$	$+1.56$ -1.81	$+1.67$ -2.26	$-13.05^{+3.81}_{-3.05}$	$+5.33$ -5.81	$+6.96$ -5.81
J0926+4029	<i>m</i>	$3.86^{+0.87}_{-1.15}$	$+1.45$ -1.76	$+1.52$ -2.43	$-13.07^{+2.49}_{-3.97}$	$+5.33$ -4.90	$+7.13$ -4.90
J0927+3902	<i>m</i>	$1.82^{+2.43}_{-0.47}$	$+3.37$ -0.51	$+3.50$ -0.83	$-4.30^{+1.15}_{-8.47}$	$+1.28$ -11.50	$+1.99$ -11.70
J0928+4446		$2.84^{+0.54}_{-0.28}$	$+1.11$ -0.60	$+1.37$ -0.81	$-9.06^{+0.83}_{-1.40}$	$+1.45$ -3.13	$+2.25$ -3.20
J0929+5013		$2.77^{+0.39}_{-0.28}$	$+0.72$ -0.57	$+1.01$ -0.71	$-7.67^{+0.72}_{-0.92}$	$+1.51$ -1.71	$+1.80$ -2.64

Table C.1: Results of fitting the simple power-law model over the 1290 selected observations from OVRO dataset. Flag refers to sources well-defined by the model, being (*m*) objects with a $\sigma(\beta)_{68.3\%} \in [1.5, 3]$ (medium quality) and (*ℓ*) to $\sigma(\beta)_{68.3\%} > 3$ (low quality). The absence of a flag means having $\sigma(\beta)_{68.3\%} < 1.5$.

Name	Flag	β	$\beta^{95.5\%}$	$\beta^{99.7\%}$	$\log A$	$\log A^{95.5\%}$	$\log A^{99.7\%}$
J0929+8612		$3.20^{+0.44}_{-0.36}$	$+0.96_{-0.74}$	$+1.38_{-0.91}$	$-9.48^{+0.86}_{-1.25}$	$+1.97_{-2.40}$	$+2.46_{-4.08}$
J0930+7420		$2.10^{+0.52}_{-0.50}$	$+1.59_{-0.77}$	$+2.90_{-1.14}$	$-7.16^{+1.27}_{-1.59}$	$+1.79_{-5.64}$	$+2.44_{-9.72}$
J0932+5306		$1.83^{+0.47}_{-0.45}$	$+1.57_{-0.69}$	$+1.57_{-1.27}$	$-5.99^{+0.98}_{-1.19}$	$+1.81_{-4.56}$	$+1.74_{-6.27}$
J0933-0819		$2.21^{+0.31}_{-0.23}$	$+0.56_{-0.53}$	$+0.71_{-0.70}$	$-6.71^{+0.61}_{-0.81}$	$+1.01_{-1.53}$	$+1.54_{-1.56}$
J0933-1139		$1.89^{+0.60}_{-0.42}$	$+1.34_{-0.54}$	$+1.59_{-0.71}$	$-6.16^{+1.24}_{-1.75}$	$+1.39_{-3.89}$	$+1.80_{-4.56}$
J0934+3926		$2.09^{+0.46}_{-0.20}$	$+0.76_{-0.47}$	$+1.00_{-0.75}$	$-6.54^{+0.69}_{-0.98}$	$+1.13_{-2.01}$	$+1.77_{-2.42}$
J0935-1939	<i>ℓ</i>	$2.14^{+1.15}_{-2.95}$	$+2.81_{-3.62}$	$+3.35_{-3.62}$	$-17.86^{+7.77}_{-2.76}$	$+12.14_{-3.06}$	$+15.24_{-3.13}$
J0936-0535		$2.05^{+0.45}_{-0.46}$	$+1.06_{-0.71}$	$+1.42_{-0.94}$	$-6.93^{+1.33}_{-1.23}$	$+2.04_{-3.23}$	$+2.28_{-4.08}$
J0937+5008		$2.02^{+0.22}_{-0.20}$	$+0.52_{-0.36}$	$+0.61_{-0.50}$	$-5.07^{+0.44}_{-0.45}$	$+0.92_{-0.95}$	$+1.02_{-1.28}$
J0938-0708		$2.43^{+0.42}_{-0.50}$	$+0.94_{-0.88}$	$+1.52_{-1.06}$	$-7.91^{+1.94}_{-0.64}$	$+2.24_{-2.89}$	$+2.67_{-4.59}$
J0939+4141	<i>m</i>	$3.02^{+0.71}_{-0.93}$	$+1.96_{-1.34}$	$+2.39_{-1.52}$	$-9.93^{+2.69}_{-2.29}$	$+3.78_{-6.36}$	$+4.08_{-8.49}$
J0940+2603		$1.99^{+0.29}_{-0.34}$	$+0.74_{-0.48}$	$+0.78_{-0.63}$	$-6.37^{+0.51}_{-1.07}$	$+0.94_{-2.08}$	$+1.34_{-2.38}$
J0941+2728		$2.06^{+0.31}_{-0.20}$	$+0.54_{-0.40}$	$+0.69_{-0.49}$	$-6.69^{+0.52}_{-0.78}$	$+1.00_{-1.25}$	$+1.16_{-1.71}$
J0941-1335		$2.13^{+0.37}_{-0.41}$	$+0.83_{-0.67}$	$+1.11_{-0.84}$	$-6.33^{+1.03}_{-1.07}$	$+1.65_{-2.37}$	$+1.92_{-3.35}$
J0942-0759		$1.91^{+0.32}_{-0.14}$	$+0.49_{-0.34}$	$+0.74_{-0.36}$	$-5.53^{+0.24}_{-0.71}$	$+0.70_{-1.03}$	$+0.73_{-1.45}$
J0943+3614	<i>m</i>	$4.15^{+0.48}_{-1.53}$	$+0.98_{-2.22}$	$+1.06_{-2.82}$	$-14.13^{+4.76}_{-2.10}$	$+6.78_{-3.82}$	$+8.57_{-3.87}$
J0945+4636	<i>ℓ</i>	$3.97^{+0.86}_{-2.91}$	$+0.86_{-5.42}$	$+1.47_{-5.43}$	$-16.37^{+5.47}_{-2.62}$	$+10.87_{-2.51}$	$+13.18_{-2.61}$
J0946+1017		$1.92^{+0.32}_{-0.26}$	$+0.57_{-0.48}$	$+0.80_{-0.60}$	$-5.88^{+0.81}_{-0.61}$	$+0.93_{-1.70}$	$+1.44_{-1.70}$
J0948+0022		$2.38^{+0.19}_{-0.23}$	$+0.37_{-0.36}$	$+0.70_{-0.46}$	$-5.78^{+0.39}_{-0.45}$	$+0.66_{-0.79}$	$+0.91_{-1.35}$
J0948+4039		$2.52^{+0.36}_{-0.32}$	$+0.79_{-0.50}$	$+0.84_{-0.84}$	$-6.92^{+0.80}_{-0.92}$	$+1.08_{-2.41}$	$+1.67_{-2.47}$
J0952+3512	<i>m</i>	$3.08^{+0.78}_{-0.89}$	$+2.01_{-1.01}$	$+2.19_{-1.23}$	$-9.52^{+2.67}_{-2.32}$	$+3.23_{-6.02}$	$+3.41_{-7.42}$
J0954+2639		$2.43^{+0.41}_{-0.44}$	$+0.89_{-0.68}$	$+1.21_{-0.85}$	$-8.19^{+1.03}_{-1.23}$	$+1.97_{-2.40}$	$+2.27_{-3.49}$
J0956+2515		$2.69^{+0.26}_{-0.31}$	$+0.60_{-0.40}$	$+0.69_{-0.56}$	$-6.89^{+0.48}_{-0.83}$	$+0.95_{-1.46}$	$+1.24_{-1.73}$
J0957-1350		$2.80^{+0.57}_{-0.18}$	$+0.96_{-0.56}$	$+1.13_{-0.93}$	$-8.08^{+0.56}_{-1.33}$	$+1.40_{-2.24}$	$+2.05_{-2.68}$
J0958+4725		$3.09^{+0.43}_{-0.37}$	$+0.86_{-0.66}$	$+1.11_{-0.84}$	$-8.46^{+1.00}_{-1.04}$	$+1.77_{-2.22}$	$+2.21_{-2.81}$
J0958+5039		$2.72^{+0.59}_{-0.31}$	$+1.16_{-0.67}$	$+1.90_{-0.78}$	$-9.02^{+1.04}_{-1.46}$	$+2.02_{-2.94}$	$+2.49_{-4.78}$
J0958+6533		$2.31^{+0.27}_{-0.17}$	$+0.46_{-0.38}$	$+0.68_{-0.49}$	$-5.39^{+0.53}_{-0.35}$	$+1.04_{-0.72}$	$+1.04_{-1.23}$
J1001+2911		$2.13^{+0.31}_{-0.13}$	$+0.45_{-0.36}$	$+0.61_{-0.44}$	$-5.32^{+0.27}_{-0.59}$	$+0.61_{-1.11}$	$+0.83_{-1.29}$
J1001+3424		$2.44^{+0.54}_{-0.29}$	$+0.92_{-0.68}$	$+1.86_{-0.99}$	$-8.17^{+1.14}_{-1.07}$	$+1.78_{-2.63}$	$+2.77_{-5.26}$
J1002+1216	<i>m</i>	$2.98^{+1.52}_{-0.40}$	$+2.04_{-0.94}$	$+2.28_{-1.26}$	$-10.38^{+1.72}_{-4.50}$	$+2.87_{-7.09}$	$+3.76_{-7.55}$

Table C.1: Results of fitting the simple power-law model over the 1290 selected observations from OVRO dataset. Flag refers to sources well-defined by the model, being (*m*) objects with a $\sigma(\beta)_{68.3\%} \in [1.5, 3]$ (medium quality) and (*ℓ*) to $\sigma(\beta)_{68.3\%} > 3$ (low quality). The absence of a flag means having $\sigma(\beta)_{68.3\%} < 1.5$.

Name	Flag	β	$\beta^{95.5\%}$	$\beta^{99.7\%}$	$\log A$	$\log A^{95.5\%}$	$\log A^{99.7\%}$
J1007+1356		$2.17^{+0.40}_{-0.36}$	$+0.81_{-0.64}$	$+1.10_{-0.78}$	$-6.69^{+1.18}_{-0.91}$	$+1.63_{-2.34}$	$+1.93_{-3.33}$
J1007-0207	<i>m</i>	$2.39^{+0.93}_{-0.83}$	$+2.77_{-0.77}$	$+3.05_{-1.05}$	$-8.17^{+1.69}_{-3.63}$	$+2.89_{-8.34}$	$+2.81_{-10.64}$
J1008+0621		$2.44^{+0.29}_{-0.19}$	$+0.66_{-0.37}$	$+0.88_{-0.49}$	$-6.34^{+0.45}_{-0.65}$	$+0.70_{-1.44}$	$+1.02_{-2.10}$
J1010+3330		$2.20^{+0.37}_{-0.37}$	$+0.81_{-0.61}$	$+0.98_{-0.66}$	$-7.11^{+1.03}_{-0.85}$	$+1.28_{-2.29}$	$+1.58_{-2.61}$
J1010+8250		$2.88^{+0.44}_{-0.33}$	$+0.84_{-0.64}$	$+1.04_{-0.87}$	$-7.64^{+0.67}_{-1.30}$	$+1.33_{-2.51}$	$+1.82_{-2.70}$
J1010-0200		$2.56^{+0.53}_{-0.24}$	$+0.93_{-0.57}$	$+1.05_{-0.89}$	$-7.63^{+0.61}_{-1.45}$	$+1.30_{-2.78}$	$+2.00_{-3.28}$
J1012+2312		$2.21^{+0.34}_{-0.28}$	$+0.60_{-0.58}$	$+0.83_{-0.70}$	$-6.91^{+0.93}_{-0.57}$	$+1.71_{-1.30}$	$+1.74_{-1.92}$
J1013+2449		$2.11^{+0.69}_{-0.61}$	$+3.23_{-0.60}$	$+3.32_{-0.88}$	$-6.62^{+1.71}_{-1.99}$	$+2.04_{-10.35}$	$+2.09_{-11.26}$
J1013+3445	<i>m</i>	$2.77^{+1.21}_{-0.67}$	$+2.32_{-0.98}$	$+2.65_{-1.29}$	$-9.21^{+2.23}_{-3.67}$	$+2.68_{-8.04}$	$+3.66_{-8.46}$
J1014+2301		$3.38^{+0.47}_{-0.36}$	$+0.93_{-0.51}$	$+1.01_{-0.85}$	$-9.09^{+0.89}_{-1.29}$	$+1.52_{-2.41}$	$+2.05_{-2.93}$
J1015+1227		$2.89^{+0.33}_{-0.37}$	$+0.82_{-0.48}$	$+0.93_{-0.74}$	$-8.18^{+0.79}_{-0.91}$	$+1.42_{-1.84}$	$+1.52_{-2.44}$
J1015+6728	<i>ℓ</i>	$3.37^{+1.60}_{-2.27}$	$+1.59_{-4.56}$	$+1.83_{-4.84}$	$-17.31^{+4.98}_{-1.64}$	$+10.79_{-1.67}$	$+13.90_{-1.64}$
J1016+2037		$1.73^{+0.42}_{-0.32}$	$+0.92_{-0.52}$	$+1.19_{-0.70}$	$-5.97^{+0.85}_{-1.14}$	$+1.26_{-2.93}$	$+1.70_{-3.55}$
J1017+6116	<i>m</i>	$3.26^{+1.40}_{-0.85}$	$+1.90_{-1.59}$	$+2.07_{-2.10}$	$-10.85^{+1.45}_{-6.08}$	$+4.39_{-6.96}$	$+5.97_{-7.05}$
J1018+0530		$2.80^{+0.25}_{-0.47}$	$+0.72_{-0.66}$	$+0.87_{-0.85}$	$-7.69^{+0.85}_{-0.99}$	$+1.27_{-2.41}$	$+1.86_{-2.72}$
J1018+3542		$2.99^{+0.29}_{-0.68}$	$+0.97_{-0.95}$	$+1.25_{-1.37}$	$-8.83^{+1.65}_{-0.89}$	$+2.45_{-2.89}$	$+3.12_{-3.99}$
J1019+6320		$2.67^{+0.21}_{-0.30}$	$+0.48_{-0.49}$	$+0.72_{-0.52}$	$-7.08^{+0.57}_{-0.60}$	$+1.07_{-1.22}$	$+1.15_{-1.73}$
J1021+3437		$2.27^{+1.07}_{-0.36}$	$+2.08_{-0.64}$	$+2.49_{-0.92}$	$-8.01^{+1.23}_{-2.91}$	$+2.37_{-5.69}$	$+2.65_{-7.58}$
J1022+4239	<i>m</i>	$3.37^{+0.62}_{-0.88}$	$+1.88_{-1.06}$	$+1.88_{-1.66}$	$-10.56^{+2.09}_{-2.52}$	$+2.48_{-6.80}$	$+4.11_{-6.99}$
J1023+3948		$2.50^{+0.39}_{-0.22}$	$+0.67_{-0.46}$	$+0.90_{-0.66}$	$-6.72^{+0.48}_{-1.07}$	$+1.36_{-1.56}$	$+1.46_{-2.25}$
J1024+1912		$2.54^{+0.56}_{-0.59}$	$+1.19_{-1.14}$	$+2.07_{-1.17}$	$-7.83^{+1.42}_{-2.07}$	$+2.73_{-4.20}$	$+3.02_{-6.50}$
J1025+1253		$2.51^{+0.38}_{-0.42}$	$+0.83_{-0.69}$	$+1.01_{-0.92}$	$-7.24^{+0.86}_{-1.26}$	$+1.63_{-2.20}$	$+2.09_{-3.00}$
J1025-0509	<i>m</i>	$3.93^{+0.53}_{-1.29}$	$+1.47_{-1.66}$	$+1.56_{-2.03}$	$-12.21^{+3.47}_{-2.14}$	$+5.04_{-4.85}$	$+5.68_{-5.74}$
J1028+0255		$3.02^{+1.04}_{-0.39}$	$+1.70_{-1.06}$	$+2.12_{-1.07}$	$-9.58^{+1.23}_{-2.91}$	$+2.63_{-5.73}$	$+2.92_{-7.16}$
J1029-1852	<i>m</i>	$3.21^{+0.75}_{-0.85}$	$+1.75_{-1.24}$	$+2.26_{-1.37}$	$-9.32^{+2.20}_{-2.67}$	$+3.48_{-5.99}$	$+3.48_{-8.31}$
J1033+0711		$2.25^{+0.44}_{-0.50}$	$+1.08_{-0.69}$	$+1.36_{-0.80}$	$-7.29^{+0.95}_{-1.67}$	$+1.87_{-3.23}$	$+2.16_{-4.24}$
J1033+4116		$2.53^{+0.45}_{-0.38}$	$+0.99_{-0.62}$	$+1.03_{-0.96}$	$-6.67^{+0.87}_{-1.31}$	$+1.44_{-2.98}$	$+2.06_{-3.25}$
J1033+6051		$2.60^{+0.38}_{-0.15}$	$+0.69_{-0.37}$	$+0.91_{-0.42}$	$-6.12^{+0.56}_{-0.65}$	$+0.89_{-1.67}$	$+1.09_{-1.89}$
J1036+1440	<i>ℓ</i>	$1.99^{+2.36}_{-0.79}$	$+3.44_{-2.84}$	$+3.44_{-3.32}$	$-7.12^{+1.63}_{-7.51}$	$+1.63_{-11.74}$	$+3.76_{-11.85}$
J1036+2203		$1.83^{+0.37}_{-0.25}$	$+0.78_{-0.42}$	$+1.09_{-0.60}$	$-6.16^{+0.53}_{-0.99}$	$+1.22_{-1.83}$	$+1.24_{-2.79}$

Table C.1: Results of fitting the simple power-law model over the 1290 selected observations from OVRO dataset. Flag refers to sources well-defined by the model, being (*m*) objects with a $\sigma(\beta)_{68.3\%} \in [1.5, 3]$ (medium quality) and (*ℓ*) to $\sigma(\beta)_{68.3\%} > 3$ (low quality). The absence of a flag means having $\sigma(\beta)_{68.3\%} < 1.5$.

Name	Flag	β	$\beta^{95.5\%}$	$\beta^{99.7\%}$	$\log A$	$\log A^{95.5\%}$	$\log A^{99.7\%}$
J1038+0512		$2.85^{+0.31}_{-0.28}$	$+0.53_{-0.59}$	$+0.78_{-0.66}$	$-6.68^{+0.74}_{-0.67}$	$+1.20_{-1.36}$	$+1.37_{-2.05}$
J1039-1541		$2.00^{+0.22}_{-0.25}$	$+0.45_{-0.45}$	$+0.60_{-0.63}$	$-5.21^{+0.41}_{-0.69}$	$+0.68_{-1.40}$	$+0.85_{-1.89}$
J1041+0610		$2.64^{+0.38}_{-0.54}$	$+0.79_{-0.85}$	$+1.24_{-1.04}$	$-7.61^{+1.59}_{-0.76}$	$+2.44_{-2.03}$	$+2.88_{-3.13}$
J1041+5233		$2.57^{+0.43}_{-0.27}$	$+0.77_{-0.56}$	$+1.16_{-0.64}$	$-7.39^{+0.61}_{-1.29}$	$+1.49_{-1.87}$	$+1.57_{-3.05}$
J1043+2408		$2.57^{+0.21}_{-0.26}$	$+0.45_{-0.43}$	$+0.64_{-0.54}$	$-6.13^{+0.54}_{-0.53}$	$+0.87_{-1.07}$	$+1.08_{-1.48}$
J1044+5322		$2.07^{+0.18}_{-0.46}$	$+0.53_{-0.64}$	$+1.00_{-0.75}$	$-6.41^{+0.49}_{-1.19}$	$+1.30_{-1.81}$	$+1.49_{-2.98}$
J1044+8054		$2.75^{+0.31}_{-0.30}$	$+0.75_{-0.42}$	$+0.87_{-0.67}$	$-7.28^{+0.59}_{-0.90}$	$+1.19_{-1.78}$	$+1.61_{-2.20}$
J1045+0624	<i>m</i>	$2.73^{+1.90}_{-0.45}$	$+2.46_{-1.00}$	$+2.76_{-1.49}$	$-9.56^{+2.47}_{-5.40}$	$+2.73_{-8.43}$	$+4.34_{-8.43}$
J1046+5354		$2.47^{+0.36}_{-0.33}$	$+0.94_{-0.62}$	$+1.34_{-0.73}$	$-7.83^{+0.93}_{-0.94}$	$+1.56_{-2.68}$	$+1.93_{-3.68}$
J1047-1308	<i>m</i>	$4.66^{+0.50}_{-1.33}$	$+0.65_{-2.54}$	$+0.75_{-3.73}$	$-15.36^{+3.57}_{-2.59}$	$+7.84_{-2.59}$	$+11.14_{-2.59}$
J1048+7143		$2.51^{+0.38}_{-0.21}$	$+0.67_{-0.46}$	$+0.87_{-0.53}$	$-5.38^{+0.37}_{-0.99}$	$+0.97_{-1.53}$	$+1.07_{-2.14}$
J1048-1909		$2.42^{+0.43}_{-0.35}$	$+0.91_{-0.58}$	$+1.32_{-0.76}$	$-6.14^{+0.65}_{-1.46}$	$+1.37_{-2.61}$	$+1.68_{-3.79}$
J1051+2027		$2.52^{+0.36}_{-0.25}$	$+0.73_{-0.49}$	$+0.81_{-0.69}$	$-7.47^{+0.77}_{-0.73}$	$+1.20_{-1.70}$	$+1.57_{-2.14}$
J1051+2119	<i>m</i>	$3.05^{+0.77}_{-0.95}$	$+1.87_{-1.21}$	$+2.17_{-1.51}$	$-9.07^{+2.31}_{-2.99}$	$+3.20_{-6.66}$	$+3.49_{-7.82}$
J1054-0713	<i>m</i>	$2.78^{+0.91}_{-0.65}$	$+2.14_{-0.81}$	$+2.41_{-1.23}$	$-9.53^{+2.40}_{-2.45}$	$+2.63_{-6.82}$	$+3.61_{-7.67}$
J1056+7011		$3.62^{+0.41}_{-0.34}$	$+0.77_{-0.73}$	$+1.05_{-1.05}$	$-9.63^{+1.25}_{-0.70}$	$+1.80_{-1.94}$	$+2.65_{-2.27}$
J1058+0133		$3.26^{+0.51}_{-0.33}$	$+1.00_{-0.75}$	$+1.65_{-0.90}$	$-7.07^{+0.83}_{-1.38}$	$+1.69_{-3.01}$	$+2.18_{-4.55}$
J1058+1951		$2.25^{+0.25}_{-0.43}$	$+0.70_{-0.59}$	$+0.99_{-0.79}$	$-7.03^{+1.18}_{-0.66}$	$+1.43_{-2.14}$	$+1.89_{-2.99}$
J1058+5628	<i>m</i>	$1.90^{+1.08}_{-0.65}$	$+2.73_{-0.74}$	$+3.01_{-1.15}$	$-7.36^{+1.61}_{-3.73}$	$+2.11_{-9.46}$	$+2.70_{-10.31}$
J1058+8114		$2.76^{+0.23}_{-0.25}$	$+0.51_{-0.49}$	$+0.68_{-0.65}$	$-7.09^{+0.44}_{-0.69}$	$+0.98_{-1.27}$	$+1.31_{-1.73}$
J1059+2057		$2.10^{+0.12}_{-0.30}$	$+0.45_{-0.40}$	$+0.46_{-0.58}$	$-6.09^{+0.62}_{-0.37}$	$+0.95_{-0.95}$	$+1.26_{-1.28}$
J1102+2757		$3.63^{+0.41}_{-0.66}$	$+1.04_{-1.08}$	$+1.25_{-1.35}$	$-10.96^{+2.04}_{-1.01}$	$+3.11_{-2.84}$	$+3.93_{-3.72}$
J1103+3014		$2.72^{+0.36}_{-0.22}$	$+0.66_{-0.46}$	$+0.79_{-0.71}$	$-7.46^{+0.56}_{-0.84}$	$+1.02_{-1.72}$	$+1.66_{-2.05}$
J1104+0730		$2.37^{+0.29}_{-0.24}$	$+0.52_{-0.53}$	$+0.74_{-0.63}$	$-6.92^{+0.47}_{-0.84}$	$+1.14_{-1.24}$	$+1.41_{-1.85}$
J1104+3812		$2.09^{+0.18}_{-0.21}$	$+0.28_{-0.41}$	$+0.39_{-0.46}$	$-5.58^{+0.56}_{-0.22}$	$+0.75_{-0.66}$	$+0.90_{-0.84}$
J1106+2812		$2.61^{+0.24}_{-0.48}$	$+0.64_{-0.70}$	$+1.12_{-0.84}$	$-7.37^{+0.98}_{-0.79}$	$+1.34_{-2.13}$	$+1.68_{-2.62}$
J1108+0811	<i>m</i>	$2.77^{+0.90}_{-0.75}$	$+2.15_{-1.02}$	$+2.57_{-1.50}$	$-9.12^{+1.47}_{-3.72}$	$+2.85_{-7.81}$	$+3.87_{-8.75}$
J1108+4330		$2.44^{+0.38}_{-0.55}$	$+0.90_{-0.91}$	$+1.29_{-1.07}$	$-8.12^{+1.30}_{-1.19}$	$+2.02_{-3.12}$	$+2.72_{-4.14}$
J1110+4403		$2.62^{+0.30}_{-0.55}$	$+0.77_{-0.88}$	$+1.08_{-0.96}$	$-7.63^{+0.66}_{-1.67}$	$+1.45_{-2.89}$	$+1.71_{-3.95}$
J1112+3503	<i>m</i>	$4.40^{+0.59}_{-1.30}$	$+0.90_{-2.25}$	$+1.10_{-2.65}$	$-14.65^{+4.53}_{-1.80}$	$+6.68_{-3.36}$	$+8.11_{-3.35}$

Table C.1: Results of fitting the simple power-law model over the 1290 selected observations from OVRO dataset. Flag refers to sources well-defined by the model, being (*m*) objects with a $\sigma(\beta)_{68.3\%} \in [1.5, 3]$ (medium quality) and (*ℓ*) to $\sigma(\beta)_{68.3\%} > 3$ (low quality). The absence of a flag means having $\sigma(\beta)_{68.3\%} < 1.5$.

Name	Flag	β	$\beta^{95.5\%}$	$\beta^{99.7\%}$	$\log A$	$\log A^{95.5\%}$	$\log A^{99.7\%}$
J1113+1442		$2.45^{+0.25}_{-0.36}$	$+0.82_{-0.61}$	$+0.99_{-0.81}$	$-7.38^{+0.82}_{-0.81}$	$+1.59_{-2.10}$	$+1.84_{-2.61}$
J1114-0816		$2.46^{+0.47}_{-0.23}$	$+0.67_{-0.62}$	$+1.02_{-0.73}$	$-7.32^{+0.52}_{-1.32}$	$+1.28_{-2.10}$	$+1.73_{-2.93}$
J1116+0829		$2.53^{+0.37}_{-0.30}$	$+0.89_{-0.58}$	$+1.11_{-0.74}$	$-7.91^{+1.06}_{-0.55}$	$+1.88_{-1.81}$	$+2.02_{-2.29}$
J1118+1234		$2.21^{+0.74}_{-0.26}$	$+1.31_{-0.64}$	$+1.73_{-0.86}$	$-6.33^{+0.72}_{-2.13}$	$+1.66_{-3.81}$	$+1.91_{-5.49}$
J1119+0410	<i>m</i>	$3.08^{+2.04}_{-0.18}$	$+2.20_{-1.19}$	$+2.34_{-1.64}$	$-10.41^{+0.50}_{-7.07}$	$+3.87_{-7.07}$	$+4.87_{-7.56}$
J1119+1656		$2.40^{+0.52}_{-0.55}$	$+1.15_{-0.97}$	$+2.02_{-0.97}$	$-8.19^{+1.55}_{-1.47}$	$+2.40_{-3.88}$	$+2.60_{-7.22}$
J1120+0704	<i>m</i>	$4.73^{+0.47}_{-1.10}$	$+0.52_{-2.51}$	$+0.63_{-3.06}$	$-16.62^{+3.70}_{-1.31}$	$+8.48_{-1.37}$	$+10.14_{-1.37}$
J1120-1420		$2.93^{+0.64}_{-0.33}$	$+1.06_{-0.74}$	$+1.24_{-0.99}$	$-9.07^{+1.51}_{-1.18}$	$+1.95_{-3.38}$	$+2.63_{-3.52}$
J1121-0553		$2.29^{+0.22}_{-0.33}$	$+0.51_{-0.59}$	$+0.71_{-0.72}$	$-6.39^{+0.89}_{-0.47}$	$+1.04_{-1.71}$	$+1.56_{-1.71}$
J1121-0711	<i>m</i>	$2.59^{+1.88}_{-0.52}$	$+2.58_{-1.07}$	$+2.82_{-1.33}$	$-8.73^{+2.78}_{-5.10}$	$+2.81_{-9.21}$	$+3.51_{-10.13}$
J1122+1805	<i>m</i>	$2.02^{+2.32}_{-0.39}$	$+3.05_{-0.84}$	$+3.37_{-0.99}$	$-7.09^{+2.11}_{-6.66}$	$+1.93_{-10.62}$	$+2.66_{-10.90}$
J1124+2336		$2.48^{+0.26}_{-0.32}$	$+0.70_{-0.46}$	$+0.78_{-0.59}$	$-6.89^{+0.88}_{-0.50}$	$+1.22_{-1.52}$	$+1.45_{-1.73}$
J1125+0001	<i>m</i>	$2.30^{+1.91}_{-0.46}$	$+2.91_{-0.57}$	$+3.15_{-1.14}$	$-8.61^{+1.20}_{-6.43}$	$+1.59_{-10.32}$	$+2.93_{-10.40}$
J1125+2610		$2.36^{+0.49}_{-0.32}$	$+0.83_{-0.72}$	$+1.08_{-0.75}$	$-6.81^{+1.03}_{-1.13}$	$+1.75_{-2.26}$	$+1.94_{-2.87}$
J1127+0555		$2.41^{+0.37}_{-0.11}$	$+0.57_{-0.39}$	$+0.75_{-0.55}$	$-6.23^{+0.51}_{-0.59}$	$+0.75_{-1.35}$	$+1.16_{-1.72}$
J1127+3620		$1.97^{+0.22}_{-0.29}$	$+0.53_{-0.41}$	$+0.57_{-0.68}$	$-6.16^{+0.52}_{-0.63}$	$+0.78_{-1.62}$	$+1.44_{-1.75}$
J1127+5650		$2.76^{+0.41}_{-0.44}$	$+0.96_{-0.61}$	$+1.22_{-0.80}$	$-8.71^{+1.24}_{-0.98}$	$+1.74_{-2.68}$	$+2.04_{-3.46}$
J1127-1857		$2.67^{+0.29}_{-0.18}$	$+0.55_{-0.42}$	$+0.89_{-0.57}$	$-5.94^{+0.62}_{-0.53}$	$+1.02_{-1.17}$	$+1.38_{-1.96}$
J1128+5925		$2.71^{+0.46}_{-0.30}$	$+0.94_{-0.43}$	$+1.01_{-0.69}$	$-7.94^{+0.87}_{-1.11}$	$+1.33_{-2.22}$	$+1.94_{-2.46}$
J1129-0240	<i>ℓ</i>	$4.08^{+1.12}_{-3.08}$	$+1.05_{-5.31}$	$+1.26_{-5.57}$	$-16.85^{+6.45}_{-2.13}$	$+11.35_{-1.96}$	$+14.06_{-2.12}$
J1130+3815		$2.40^{+0.38}_{-0.27}$	$+0.74_{-0.51}$	$+0.86_{-0.67}$	$-6.41^{+0.72}_{-0.84}$	$+1.37_{-1.64}$	$+1.60_{-2.26}$
J1131-0500		$2.36^{+0.39}_{-0.23}$	$+0.70_{-0.52}$	$+0.92_{-0.74}$	$-7.01^{+1.03}_{-0.58}$	$+1.51_{-1.60}$	$+1.79_{-2.30}$
J1133+0040		$2.42^{+0.33}_{-0.32}$	$+0.74_{-0.53}$	$+0.87_{-0.70}$	$-7.26^{+1.10}_{-0.59}$	$+1.42_{-1.63}$	$+1.83_{-2.10}$
J1135-0428		$1.83^{+0.23}_{-0.37}$	$+0.68_{-0.47}$	$+0.68_{-0.63}$	$-4.57^{+0.81}_{-0.38}$	$+0.85_{-1.40}$	$+1.33_{-1.40}$
J1136+3407		$2.31^{+0.39}_{-0.15}$	$+0.67_{-0.41}$	$+0.77_{-0.65}$	$-7.32^{+0.45}_{-0.87}$	$+1.29_{-1.31}$	$+1.45_{-1.72}$
J1136+7009		$1.90^{+0.34}_{-0.38}$	$+0.88_{-0.56}$	$+1.11_{-0.63}$	$-6.73^{+0.83}_{-0.94}$	$+1.14_{-2.54}$	$+1.63_{-2.99}$
J1136-0330	<i>m</i>	$2.01^{+0.99}_{-0.64}$	$+2.62_{-0.59}$	$+3.08_{-0.86}$	$-6.94^{+1.88}_{-3.16}$	$+1.72_{-9.33}$	$+2.31_{-11.00}$
J1141+6410		$2.65^{+1.04}_{-0.36}$	$+2.12_{-0.69}$	$+2.60_{-0.84}$	$-9.19^{+1.60}_{-2.61}$	$+2.36_{-6.38}$	$+2.65_{-9.50}$
J1145+0455	<i>m</i>	$2.33^{+0.91}_{-0.68}$	$+2.78_{-0.66}$	$+2.77_{-0.97}$	$-8.12^{+1.98}_{-3.28}$	$+2.56_{-9.15}$	$+2.57_{-10.42}$
J1146+3958		$2.78^{+0.27}_{-0.25}$	$+0.60_{-0.49}$	$+0.85_{-0.66}$	$-6.43^{+0.62}_{-0.66}$	$+1.05_{-1.54}$	$+1.53_{-1.95}$

Table C.1: Results of fitting the simple power-law model over the 1290 selected observations from OVRO dataset. Flag refers to sources well-defined by the model, being (*m*) objects with a $\sigma(\beta)_{68.3\%} \in [1.5, 3]$ (medium quality) and (*ℓ*) to $\sigma(\beta)_{68.3\%} > 3$ (low quality). The absence of a flag means having $\sigma(\beta)_{68.3\%} < 1.5$.

Name	Flag	β	$\beta^{95.5\%}$	$\beta^{99.7\%}$	$\log A$	$\log A^{95.5\%}$	$\log A^{99.7\%}$
J1146+5356		$2.92^{+0.35}_{-0.36}$	$+0.82_{-0.58}$	$+1.12_{-0.79}$	$-8.64^{+0.95}_{-0.89}$	$+1.69_{-2.08}$	$+1.88_{-2.81}$
J1146+5848		$3.10^{+0.78}_{-0.55}$	$+1.46_{-0.96}$	$+2.22_{-1.33}$	$-10.21^{+1.83}_{-2.13}$	$+2.62_{-4.88}$	$+3.64_{-7.37}$
J1147+2635		$2.54^{+0.41}_{-0.54}$	$+1.05_{-0.71}$	$+1.72_{-0.99}$	$-7.86^{+1.24}_{-1.36}$	$+1.98_{-2.88}$	$+2.33_{-5.16}$
J1147+3501		$2.25^{+0.57}_{-0.23}$	$+0.95_{-0.65}$	$+1.41_{-0.74}$	$-7.67^{+1.09}_{-1.03}$	$+1.74_{-2.51}$	$+2.05_{-3.87}$
J1147-0724		$2.38^{+0.31}_{-0.26}$	$+0.83_{-0.45}$	$+0.95_{-0.62}$	$-6.19^{+0.73}_{-0.68}$	$+0.93_{-2.29}$	$+1.33_{-2.46}$
J1148+5254	<i>m</i>	$2.54^{+1.18}_{-0.69}$	$+2.50_{-0.94}$	$+2.75_{-1.11}$	$-8.71^{+1.77}_{-4.15}$	$+2.97_{-7.42}$	$+3.28_{-9.24}$
J1148+5924		$2.02^{+0.53}_{-0.19}$	$+0.96_{-0.40}$	$+1.17_{-0.65}$	$-6.87^{+0.65}_{-1.29}$	$+0.94_{-2.84}$	$+1.49_{-3.14}$
J1148-0404		$2.54^{+0.89}_{-0.23}$	$+1.49_{-0.63}$	$+1.58_{-1.12}$	$-8.42^{+1.20}_{-2.00}$	$+2.13_{-3.82}$	$+3.09_{-4.60}$
J1150+2417	<i>m</i>	$2.70^{+1.20}_{-0.48}$	$+2.45_{-0.97}$	$+2.79_{-1.39}$	$-8.64^{+1.70}_{-3.45}$	$+2.77_{-7.69}$	$+3.79_{-9.17}$
J1150+4332	<i>m</i>	$3.52^{+0.82}_{-0.73}$	$+1.82_{-1.25}$	$+1.92_{-1.87}$	$-11.47^{+2.40}_{-2.30}$	$+3.99_{-5.53}$	$+4.89_{-6.27}$
J1150-0640		$2.29^{+0.37}_{-0.45}$	$+1.00_{-0.62}$	$+1.31_{-0.86}$	$-6.62^{+0.90}_{-1.30}$	$+1.63_{-2.91}$	$+1.82_{-4.37}$
J1152+4939		$3.77^{+0.66}_{-0.75}$	$+1.44_{-0.96}$	$+1.53_{-1.48}$	$-12.27^{+2.04}_{-2.42}$	$+2.77_{-4.71}$	$+4.54_{-4.71}$
J1152-0519	<i>m</i>	$2.21^{+1.26}_{-0.57}$	$+2.85_{-0.91}$	$+3.26_{-1.22}$	$-7.71^{+1.82}_{-4.07}$	$+2.09_{-10.02}$	$+2.98_{-11.27}$
J1152-0841		$2.58^{+0.40}_{-0.29}$	$+0.84_{-0.44}$	$+1.09_{-0.65}$	$-7.24^{+0.78}_{-0.92}$	$+1.20_{-2.11}$	$+1.60_{-2.61}$
J1153+8058		$2.77^{+0.52}_{-0.42}$	$+1.05_{-0.81}$	$+1.43_{-0.88}$	$-8.29^{+1.25}_{-1.39}$	$+1.56_{-3.47}$	$+2.42_{-3.89}$
J1154+5934	<i>m</i>	$3.68^{+1.42}_{-1.55}$	$+1.81_{-4.16}$	$+1.75_{-5.16}$	$-13.72^{+2.66}_{-5.69}$	$+7.43_{-5.88}$	$+8.73_{-6.28}$
J1154+6022		$3.00^{+0.49}_{-0.40}$	$+1.10_{-0.72}$	$+1.54_{-0.99}$	$-8.59^{+1.08}_{-1.28}$	$+2.00_{-2.98}$	$+2.29_{-4.42}$
J1157+5527		$2.56^{+0.19}_{-0.37}$	$+0.47_{-0.63}$	$+0.61_{-0.81}$	$-7.44^{+0.65}_{-0.72}$	$+0.94_{-1.62}$	$+1.55_{-1.92}$
J1158+2450	<i>m</i>	$4.76^{+0.41}_{-1.79}$	$+0.50_{-2.96}$	$+0.65_{-3.40}$	$-16.22^{+5.83}_{-1.70}$	$+9.55_{-1.77}$	$+10.81_{-1.76}$
J1158+4825		$2.53^{+0.49}_{-0.41}$	$+1.05_{-0.71}$	$+1.34_{-0.86}$	$-8.24^{+0.90}_{-1.61}$	$+1.87_{-2.86}$	$+2.10_{-4.16}$
J1159+2914		$2.63^{+0.25}_{-0.18}$	$+0.55_{-0.28}$	$+0.66_{-0.43}$	$-5.66^{+0.30}_{-0.60}$	$+0.53_{-1.37}$	$+0.82_{-1.46}$
J1201+1431		$2.47^{+0.61}_{-0.53}$	$+1.53_{-0.73}$	$+1.88_{-0.87}$	$-7.87^{+0.98}_{-2.22}$	$+2.18_{-4.17}$	$+2.46_{-5.65}$
J1202-0528		$2.09^{+0.32}_{-0.29}$	$+0.82_{-0.41}$	$+1.07_{-0.57}$	$-5.76^{+0.46}_{-1.00}$	$+0.91_{-1.98}$	$+1.21_{-3.00}$
J1203+4803		$2.27^{+0.36}_{-0.33}$	$+0.60_{-0.61}$	$+0.80_{-0.79}$	$-6.93^{+1.00}_{-0.70}$	$+1.45_{-1.69}$	$+1.86_{-2.26}$
J1203+6031	<i>m</i>	$3.49^{+1.36}_{-0.81}$	$+1.93_{-1.56}$	$+2.00_{-2.18}$	$-11.07^{+2.16}_{-5.18}$	$+3.76_{-7.78}$	$+5.59_{-7.88}$
J1207+1211		$2.74^{+0.48}_{-0.42}$	$+1.04_{-0.63}$	$+1.68_{-0.96}$	$-7.93^{+1.22}_{-1.24}$	$+1.69_{-2.90}$	$+2.41_{-4.65}$
J1207+2754		$2.87^{+0.49}_{-0.46}$	$+1.13_{-0.75}$	$+1.83_{-1.10}$	$-8.57^{+1.18}_{-1.47}$	$+2.15_{-3.07}$	$+2.74_{-5.38}$
J1209+1810		$3.01^{+0.35}_{-0.39}$	$+0.82_{-0.71}$	$+1.12_{-0.82}$	$-8.57^{+0.88}_{-1.02}$	$+1.92_{-1.80}$	$+1.92_{-2.69}$
J1209+2547	<i>m</i>	$3.22^{+1.20}_{-0.58}$	$+2.12_{-1.02}$	$+2.23_{-1.45}$	$-11.07^{+1.65}_{-4.23}$	$+2.96_{-6.91}$	$+4.40_{-6.91}$
J1209+4119	<i>m</i>	$2.81^{+0.97}_{-0.55}$	$+2.26_{-0.86}$	$+2.48_{-1.25}$	$-9.72^{+1.39}_{-3.42}$	$+3.00_{-6.65}$	$+3.60_{-7.92}$

Table C.1: Results of fitting the simple power-law model over the 1290 selected observations from OVRO dataset. Flag refers to sources well-defined by the model, being (*m*) objects with a $\sigma(\beta)_{68.3\%} \in [1.5, 3]$ (medium quality) and (*ℓ*) to $\sigma(\beta)_{68.3\%} > 3$ (low quality). The absence of a flag means having $\sigma(\beta)_{68.3\%} < 1.5$.

Name	Flag	β	$\beta^{95.5\%}$	$\beta^{99.7\%}$	$\log A$	$\log A^{95.5\%}$	$\log A^{99.7\%}$
J1214+0829	<i>m</i>	$2.82^{+1.06}_{-0.68}$	$+2.30$ -0.73	$+2.64$ -1.14	$-9.31^{+1.84}_{-3.61}$	$+2.64$ -7.05	$+3.33$ -8.65
J1215+1654		$2.17^{+0.32}_{-0.08}$	$+0.56$ -0.30	$+0.68$ -0.39	$-6.04^{+0.31}_{-0.64}$	$+0.72$ -1.26	$+0.91$ -1.52
J1215-1731		$2.07^{+0.55}_{-0.25}$	$+0.99$ -0.61	$+1.37$ -0.61	$-5.64^{+0.91}_{-1.23}$	$+1.38$ -2.62	$+1.68$ -3.85
J1217+3007		$1.67^{+0.40}_{-0.39}$	$+1.44$ -0.52	$+1.77$ -0.54	$-5.46^{+0.83}_{-1.27}$	$+1.11$ -4.39	$+1.35$ -5.55
J1217+5835		$2.39^{+0.88}_{-0.34}$	$+1.51$ -0.83	$+2.40$ -0.90	$-8.18^{+1.59}_{-2.04}$	$+2.44$ -4.42	$+2.75$ -7.03
J1219+4829		$2.45^{+0.27}_{-0.23}$	$+0.47$ -0.46	$+0.66$ -0.61	$-6.86^{+0.55}_{-0.66}$	$+1.10$ -1.19	$+1.47$ -1.53
J1219+6600		$2.00^{+0.30}_{-0.23}$	$+0.49$ -0.46	$+0.63$ -0.83	$-6.57^{+0.75}_{-0.53}$	$+1.17$ -1.14	$+1.69$ -1.55
J1220+3808		$2.68^{+0.27}_{-0.46}$	$+0.67$ -0.69	$+0.97$ -0.88	$-8.13^{+1.21}_{-0.76}$	$+1.95$ -1.55	$+2.18$ -2.62
J1221+2813		$2.22^{+0.27}_{-0.17}$	$+0.42$ -0.40	$+0.60$ -0.59	$-5.98^{+0.49}_{-0.47}$	$+0.80$ -1.10	$+1.26$ -1.36
J1221+4411		$3.30^{+0.41}_{-0.80}$	$+1.14$ -1.10	$+1.60$ -1.78	$-10.71^{+2.32}_{-1.24}$	$+3.30$ -3.55	$+4.79$ -4.86
J1222+0413		$3.03^{+0.21}_{-0.29}$	$+0.40$ -0.49	$+0.67$ -0.61	$-7.04^{+0.37}_{-0.69}$	$+0.95$ -1.00	$+1.24$ -1.55
J1223+8040		$2.25^{+0.32}_{-0.21}$	$+0.50$ -0.51	$+0.71$ -0.61	$-6.39^{+0.74}_{-0.57}$	$+1.21$ -1.24	$+1.43$ -1.72
J1224+4335	<i>m</i>	$2.26^{+1.28}_{-0.86}$	$+2.97$ -0.97	$+3.18$ -1.43	$-7.77^{+2.51}_{-4.16}$	$+2.34$ -10.77	$+3.43$ -11.22
J1226+4340		$3.04^{+0.58}_{-0.81}$	$+1.90$ -1.24	$+2.15$ -1.46	$-9.76^{+1.85}_{-2.11}$	$+3.79$ -5.52	$+3.67$ -7.36
J1226-1328		$2.18^{+0.16}_{-0.38}$	$+0.46$ -0.52	$+0.60$ -0.62	$-6.09^{+0.56}_{-0.61}$	$+0.81$ -1.39	$+1.26$ -1.39
J1227+4932		$2.00^{+0.46}_{-0.44}$	$+1.02$ -0.73	$+1.30$ -0.73	$-6.91^{+1.00}_{-1.41}$	$+1.58$ -3.09	$+1.58$ -4.08
J1228+3706		$2.66^{+0.47}_{-0.29}$	$+0.70$ -0.67	$+0.94$ -0.70	$-7.83^{+0.90}_{-1.09}$	$+1.41$ -2.21	$+1.75$ -2.63
J1229+0203		$2.97^{+0.20}_{-0.37}$	$+0.63$ -0.52	$+0.63$ -0.77	$-5.52^{+0.79}_{-0.59}$	$+1.18$ -1.65	$+1.71$ -1.65
J1230+2518		$2.37^{+0.34}_{-0.21}$	$+0.62$ -0.44	$+0.83$ -0.46	$-6.17^{+0.27}_{-0.97}$	$+0.90$ -1.68	$+0.95$ -2.11
J1231+0418		$2.60^{+0.15}_{-0.36}$	$+0.36$ -0.68	$+0.78$ -0.80	$-7.16^{+0.33}_{-0.92}$	$+1.06$ -1.58	$+1.28$ -2.74
J1232+4821	<i>m</i>	$3.34^{+0.62}_{-0.92}$	$+1.39$ -1.53	$+2.09$ -1.68	$-10.05^{+1.75}_{-2.96}$	$+3.61$ -5.27	$+4.33$ -7.52
J1235+3621	<i>m</i>	$2.77^{+1.28}_{-0.81}$	$+2.47$ -1.14	$+2.63$ -1.34	$-9.43^{+2.56}_{-4.23}$	$+3.23$ -8.57	$+3.82$ -9.14
J1238+0723		$3.23^{+0.40}_{-0.50}$	$+1.01$ -0.81	$+1.36$ -1.11	$-9.67^{+1.44}_{-1.08}$	$+2.54$ -2.71	$+2.89$ -3.90
J1239+0730		$2.18^{+0.36}_{-0.23}$	$+0.74$ -0.40	$+0.80$ -0.52	$-6.12^{+0.45}_{-0.97}$	$+0.79$ -2.01	$+1.19$ -2.01
J1239-1023	<i>m</i>	$2.25^{+0.87}_{-0.68}$	$+2.14$ -0.80	$+2.70$ -0.93	$-7.13^{+1.75}_{-2.89}$	$+2.21$ -6.85	$+2.59$ -9.67
J1242+3750		$2.79^{+0.86}_{-0.58}$	$+1.78$ -0.98	$+2.28$ -1.18	$-9.06^{+1.07}_{-3.21}$	$+2.61$ -5.87	$+3.25$ -7.59
J1243+7442		$2.53^{+0.67}_{-0.46}$	$+1.34$ -0.92	$+1.95$ -1.03	$-8.17^{+1.20}_{-2.08}$	$+2.23$ -3.96	$+2.59$ -6.02
J1245-1617		$2.20^{+0.27}_{-0.20}$	$+0.55$ -0.35	$+0.86$ -0.52	$-5.27^{+0.32}_{-0.75}$	$+0.80$ -1.28	$+1.11$ -2.14
J1248+5820		$2.85^{+0.57}_{-0.52}$	$+1.30$ -0.77	$+2.01$ -1.05	$-9.51^{+0.83}_{-2.32}$	$+2.12$ -4.13	$+3.02$ -5.95
J1248-0632		$2.73^{+0.32}_{-0.44}$	$+0.77$ -0.62	$+1.10$ -0.76	$-8.18^{+1.22}_{-0.81}$	$+1.66$ -2.16	$+1.92$ -3.34

Table C.1: Results of fitting the simple power-law model over the 1290 selected observations from OVRO dataset. Flag refers to sources well-defined by the model, being (*m*) objects with a $\sigma(\beta)_{68.3\%} \in [1.5, 3]$ (medium quality) and (*ℓ*) to $\sigma(\beta)_{68.3\%} > 3$ (low quality). The absence of a flag means having $\sigma(\beta)_{68.3\%} < 1.5$.

Name	Flag	β	$\beta^{95.5\%}$	$\beta^{99.7\%}$	$\log A$	$\log A^{95.5\%}$	$\log A^{99.7\%}$
J1251-1717		$2.39^{+0.70}_{-0.53}$	$+1.61$ -0.69	$+1.91$ -1.02	$-7.66^{+1.28}_{-2.19}$	$+1.51$ -5.30	$+2.62$ -5.30
J1254+1141		$2.63^{+0.47}_{-0.17}$	$+0.57$ -0.61	$+0.81$ -0.75	$-7.61^{+0.73}_{-0.93}$	$+1.26$ -1.67	$+1.92$ -1.67
J1254-1317		$2.74^{+0.55}_{-0.39}$	$+1.10$ -0.66	$+1.46$ -0.92	$-8.93^{+1.21}_{-1.44}$	$+2.22$ -2.91	$+2.63$ -4.02
J1255+1817		$2.13^{+0.34}_{-0.39}$	$+0.70$ -0.72	$+1.01$ -0.92	$-7.18^{+1.08}_{-0.88}$	$+1.91$ -1.98	$+2.15$ -2.93
J1256-0547		$2.43^{+0.34}_{-0.25}$	$+0.70$ -0.48	$+0.99$ -0.60	$-3.65^{+0.60}_{-0.83}$	$+1.08$ -1.66	$+1.42$ -2.75
J1257+3229		$2.12^{+0.25}_{-0.23}$	$+0.48$ -0.33	$+0.55$ -0.49	$-5.91^{+0.45}_{-0.63}$	$+0.63$ -1.35	$+0.97$ -1.40
J1300+0828		$2.94^{+0.70}_{-0.63}$	$+1.63$ -0.94	$+2.29$ -1.36	$-9.58^{+1.82}_{-2.21}$	$+2.70$ -5.66	$+3.88$ -6.64
J1300+1206		$3.04^{+0.68}_{-0.28}$	$+1.30$ -0.67	$+2.25$ -0.86	$-9.38^{+1.07}_{-1.81}$	$+1.86$ -3.77	$+2.58$ -6.64
J1300+2830		$2.17^{+0.88}_{-0.60}$	$+2.07$ -0.77	$+2.89$ -1.05	$-7.64^{+1.51}_{-2.83}$	$+2.01$ -7.06	$+2.77$ -9.10
J1300+5029	<i>m</i>	$2.49^{+1.23}_{-0.73}$	$+2.88$ -0.87	$+3.00$ -1.17	$-8.91^{+2.46}_{-3.81}$	$+3.02$ -8.93	$+3.47$ -9.94
J1302+5748		$2.63^{+0.37}_{-0.19}$	$+0.63$ -0.47	$+0.72$ -0.60	$-7.44^{+0.67}_{-0.69}$	$+1.45$ -1.20	$+1.48$ -1.75
J1305-1033		$3.19^{+0.26}_{-0.30}$	$+0.62$ -0.48	$+0.83$ -0.72	$-7.82^{+0.78}_{-0.50}$	$+1.10$ -1.47	$+1.67$ -1.80
J1306+5529		$2.47^{+0.84}_{-0.52}$	$+1.81$ -0.68	$+2.70$ -0.81	$-8.39^{+1.45}_{-2.66}$	$+1.77$ -6.36	$+2.01$ -9.08
J1306-1718	<i>m</i>	$2.57^{+1.03}_{-0.73}$	$+2.32$ -1.02	$+2.91$ -1.25	$-9.03^{+2.69}_{-2.95}$	$+2.80$ -8.20	$+3.41$ -9.97
J1308+3546		$2.48^{+0.24}_{-0.26}$	$+0.46$ -0.53	$+0.71$ -0.53	$-6.98^{+0.77}_{-0.37}$	$+1.37$ -0.92	$+1.37$ -1.44
J1309+1154		$2.61^{+0.38}_{-0.41}$	$+0.97$ -0.64	$+1.06$ -1.05	$-8.04^{+1.29}_{-0.83}$	$+2.20$ -2.15	$+2.83$ -2.73
J1309+5557		$2.75^{+0.58}_{-0.44}$	$+1.38$ -0.73	$+1.81$ -0.93	$-9.18^{+1.06}_{-1.94}$	$+1.87$ -4.43	$+2.72$ -5.52
J1310+0044	<i>m</i>	$2.48^{+1.41}_{-0.36}$	$+2.61$ -0.81	$+2.81$ -1.16	$-8.66^{+1.55}_{-4.13}$	$+2.89$ -7.82	$+3.32$ -9.23
J1310+3220		$2.69^{+0.31}_{-0.22}$	$+0.59$ -0.40	$+0.81$ -0.58	$-6.61^{+0.71}_{-0.50}$	$+1.31$ -1.02	$+1.53$ -1.56
J1310+3233		$1.48^{+0.28}_{-0.15}$	$+0.52$ -0.32	$+0.63$ -0.48	$-3.55^{+0.33}_{-0.51}$	$+0.79$ -1.08	$+0.93$ -1.56
J1310+4653		$3.63^{+0.46}_{-0.89}$	$+1.22$ -1.35	$+1.85$ -1.47	$-11.06^{+2.45}_{-1.67}$	$+3.36$ -4.40	$+4.04$ -5.90
J1311+5513		$2.50^{+0.39}_{-0.30}$	$+0.81$ -0.55	$+0.90$ -0.88	$-7.83^{+1.06}_{-0.71}$	$+1.54$ -1.98	$+1.89$ -2.23
J1312+4828		$2.20^{+0.27}_{-0.24}$	$+0.50$ -0.40	$+0.66$ -0.56	$-6.57^{+0.51}_{-0.69}$	$+0.85$ -1.27	$+1.17$ -1.66
J1312-0424		$2.24^{+0.25}_{-0.22}$	$+0.54$ -0.34	$+0.61$ -0.50	$-5.96^{+0.52}_{-0.51}$	$+0.86$ -1.07	$+1.07$ -1.38
J1313+1027	<i>m</i>	$4.91^{+0.51}_{-1.05}$	$+0.57$ -2.29	$+0.57$ -3.68	$-17.69^{+3.91}_{-1.16}$	$+8.14$ -1.27	$+12.19$ -1.29
J1314+2348	<i>ℓ</i>	$1.80^{+2.69}_{-1.59}$	$+3.27$ -3.11	$+3.71$ -3.23	$-17.74^{+7.46}_{-3.17}$	$+12.27$ -3.24	$+14.71$ -3.24
J1317+3425		$2.26^{+0.52}_{-0.18}$	$+0.88$ -0.54	$+1.29$ -0.64	$-7.02^{+0.60}_{-1.15}$	$+1.28$ -2.32	$+1.98$ -3.17
J1317-1345		$2.34^{+0.93}_{-0.52}$	$+2.68$ -0.81	$+3.08$ -0.99	$-7.82^{+1.72}_{-2.68}$	$+2.08$ -9.05	$+2.62$ -10.56
J1319-1217		$2.05^{+0.35}_{-0.36}$	$+1.05$ -0.56	$+1.20$ -0.76	$-6.78^{+1.01}_{-0.92}$	$+1.14$ -2.95	$+1.71$ -2.95
J1319-1239	<i>m</i>	$3.21^{+1.05}_{-0.89}$	$+2.02$ -1.03	$+2.03$ -1.90	$-10.32^{+2.66}_{-3.53}$	$+3.04$ -6.66	$+5.36$ -6.65

Table C.1: Results of fitting the simple power-law model over the 1290 selected observations from OVRO dataset. Flag refers to sources well-defined by the model, being (*m*) objects with a $\sigma(\beta)_{68.3\%} \in [1.5, 3]$ (medium quality) and (*ℓ*) to $\sigma(\beta)_{68.3\%} > 3$ (low quality). The absence of a flag means having $\sigma(\beta)_{68.3\%} < 1.5$.

Name	Flag	β	$\beta^{95.5\%}$	$\beta^{99.7\%}$	$\log A$	$\log A^{95.5\%}$	$\log A^{99.7\%}$
J1321+2216		$2.19^{+0.17}_{-0.32}$	$+0.32$ -0.53	$+0.43$ -0.61	$-6.21^{+0.70}_{-0.35}$	$+1.11$ -0.73	$+1.24$ -1.02
J1322-0937		$3.14^{+0.35}_{-0.23}$	$+0.58$ -0.61	$+0.81$ -0.70	$-8.03^{+0.71}_{-0.70}$	$+1.63$ -1.23	$+1.63$ -2.08
J1323+7942		$2.13^{+0.28}_{-0.33}$	$+0.75$ -0.41	$+0.75$ -0.78	$-6.71^{+0.71}_{-0.82}$	$+1.14$ -1.93	$+1.71$ -2.21
J1324+4743		$2.29^{+0.48}_{-0.24}$	$+0.77$ -0.51	$+1.10$ -0.60	$-7.67^{+0.67}_{-1.15}$	$+1.34$ -2.02	$+1.61$ -2.92
J1324-1049		$2.65^{+0.35}_{-0.48}$	$+0.80$ -0.76	$+1.06$ -0.82	$-7.48^{+0.86}_{-1.23}$	$+1.57$ -2.48	$+1.91$ -3.30
J1325-0804	<i>m</i>	$4.19^{+0.90}_{-2.00}$	$+1.15$ -5.05	$+1.20$ -5.64	$-16.91^{+4.84}_{-2.09}$	$+10.87$ -2.09	$+14.55$ -2.09
J1326-0500	<i>ℓ</i>	$2.24^{+2.87}_{-0.84}$	$+2.87$ -3.36	$+3.11$ -3.71	$-15.84^{+5.99}_{-3.07}$	$+9.66$ -3.15	$+12.12$ -3.15
J1327+1223		$2.96^{+0.38}_{-0.34}$	$+0.86$ -0.60	$+0.88$ -1.10	$-8.42^{+0.87}_{-1.07}$	$+1.32$ -2.33	$+2.28$ -2.52
J1327+2210		$2.93^{+0.33}_{-0.24}$	$+0.60$ -0.49	$+0.74$ -0.77	$-7.72^{+0.86}_{-0.56}$	$+1.32$ -1.38	$+1.83$ -1.71
J1327+5008		$2.20^{+0.35}_{-0.36}$	$+0.72$ -0.63	$+1.17$ -0.75	$-7.16^{+0.74}_{-1.20}$	$+1.31$ -2.29	$+1.62$ -3.25
J1329+3154		$2.17^{+0.30}_{-0.24}$	$+0.55$ -0.48	$+0.80$ -0.55	$-6.66^{+0.61}_{-0.69}$	$+1.11$ -1.25	$+1.21$ -1.94
J1332+4722		$2.11^{+0.24}_{-0.23}$	$+0.48$ -0.42	$+0.72$ -0.50	$-6.38^{+0.56}_{-0.53}$	$+0.99$ -1.10	$+1.11$ -1.62
J1332-0509		$3.21^{+0.34}_{-0.32}$	$+0.69$ -0.55	$+0.88$ -0.74	$-8.32^{+0.77}_{-0.90}$	$+1.50$ -1.74	$+1.92$ -2.25
J1332-1256		$2.38^{+0.42}_{-0.53}$	$+1.12$ -0.64	$+1.75$ -0.76	$-6.52^{+1.16}_{-1.20}$	$+1.51$ -3.16	$+1.84$ -4.78
J1333+1649		$4.57^{+0.45}_{-1.02}$	$+0.59$ -2.13	$+0.75$ -2.66	$-16.61^{+3.19}_{-1.39}$	$+6.97$ -1.39	$+9.39$ -1.37
J1333+2725		$2.67^{+0.28}_{-0.29}$	$+0.73$ -0.51	$+0.95$ -0.76	$-7.56^{+0.79}_{-0.64}$	$+1.29$ -1.56	$+1.91$ -2.34
J1333-1950		$2.32^{+0.93}_{-0.54}$	$+2.20$ -0.82	$+2.76$ -1.24	$-7.03^{+1.47}_{-2.64}$	$+2.48$ -6.38	$+2.98$ -9.07
J1334-1150	<i>m</i>	$2.90^{+1.04}_{-0.52}$	$+1.86$ -1.18	$+2.39$ -1.30	$-9.68^{+1.54}_{-3.14}$	$+3.22$ -6.48	$+3.83$ -8.25
J1335+4542	<i>m</i>	$3.15^{+1.28}_{-0.81}$	$+2.18$ -1.27	$+2.32$ -1.67	$-9.64^{+1.79}_{-4.95}$	$+2.74$ -8.34	$+4.40$ -8.34
J1335+5844	<i>m</i>	$2.12^{+1.62}_{-0.83}$	$+3.04$ -0.82	$+3.34$ -1.13	$-7.43^{+2.18}_{-5.47}$	$+2.18$ -10.57	$+2.72$ -11.54
J1336-0829		$2.44^{+0.32}_{-0.32}$	$+0.57$ -0.56	$+0.74$ -0.72	$-7.18^{+0.83}_{-0.80}$	$+1.27$ -1.60	$+1.66$ -2.03
J1337+5501		$2.48^{+0.32}_{-0.26}$	$+0.74$ -0.40	$+0.91$ -0.61	$-7.46^{+0.78}_{-0.64}$	$+1.34$ -1.47	$+1.73$ -2.04
J1337+6532		$2.64^{+0.30}_{-0.42}$	$+0.59$ -0.84	$+0.90$ -0.88	$-7.99^{+0.72}_{-1.20}$	$+1.76$ -1.84	$+1.94$ -2.72
J1337-1257		$3.20^{+0.27}_{-0.49}$	$+0.74$ -0.71	$+0.93$ -0.86	$-7.14^{+1.44}_{-0.46}$	$+1.96$ -1.88	$+2.24$ -2.44
J1341+2816	<i>m</i>	$4.51^{+0.52}_{-1.21}$	$+0.82$ -2.07	$+0.82$ -2.61	$-15.65^{+3.72}_{-2.22}$	$+6.65$ -2.24	$+8.11$ -2.35
J1342+2709		$3.35^{+0.64}_{-0.79}$	$+1.81$ -0.99	$+1.81$ -1.55	$-10.77^{+2.34}_{-1.97}$	$+3.06$ -5.07	$+4.46$ -5.50
J1343+6602		$2.64^{+0.30}_{-0.40}$	$+0.69$ -0.64	$+0.76$ -1.10	$-7.86^{+0.89}_{-1.00}$	$+1.34$ -2.01	$+2.55$ -2.11
J1344+6606		$2.53^{+0.25}_{-0.39}$	$+0.69$ -0.56	$+0.81$ -0.91	$-7.41^{+1.01}_{-0.63}$	$+1.42$ -1.72	$+2.29$ -1.94
J1344-1723		$2.19^{+0.32}_{-0.28}$	$+0.70$ -0.40	$+0.70$ -0.58	$-6.52^{+0.70}_{-0.72}$	$+1.07$ -1.66	$+1.39$ -1.78
J1345+0706		$2.35^{+0.46}_{-0.31}$	$+1.10$ -0.62	$+1.41$ -0.70	$-7.36^{+1.05}_{-0.95}$	$+1.75$ -2.66	$+2.00$ -3.38

Table C.1: Results of fitting the simple power-law model over the 1290 selected observations from OVRO dataset. Flag refers to sources well-defined by the model, being (*m*) objects with a $\sigma(\beta)_{68.3\%} \in [1.5, 3]$ (medium quality) and (*ℓ*) to $\sigma(\beta)_{68.3\%} > 3$ (low quality). The absence of a flag means having $\sigma(\beta)_{68.3\%} < 1.5$.

Name	Flag	β	$\beta^{95.5\%}$	$\beta^{99.7\%}$	$\log A$	$\log A^{95.5\%}$	$\log A^{99.7\%}$
J1347+1835	<i>m</i>	$3.09^{+0.73}_{-0.78}$	$+1.95$ -1.03	$+2.18$ -1.47	$-9.81^{+2.52}_{-2.01}$	$+2.44$ -6.48	$+3.52$ -6.48
J1349+5341		$1.90^{+0.20}_{-0.22}$	$+0.43$ -0.38	$+0.55$ -0.47	$-4.90^{+0.31}_{-0.58}$	$+0.70$ -1.10	$+0.79$ -1.48
J1349-1110		$2.74^{+0.45}_{-0.52}$	$+1.01$ -0.67	$+1.28$ -0.94	$-8.67^{+1.50}_{-1.06}$	$+1.97$ -2.55	$+2.64$ -3.69
J1349-1132		$2.54^{+0.46}_{-0.17}$	$+0.67$ -0.36	$+0.89$ -0.52	$-6.72^{+0.66}_{-0.79}$	$+0.90$ -1.64	$+1.23$ -2.17
J1350+3034		$2.21^{+0.39}_{-0.24}$	$+0.79$ -0.43	$+0.98$ -0.56	$-6.58^{+0.64}_{-0.89}$	$+0.98$ -2.07	$+1.28$ -2.30
J1350-1634		$2.07^{+0.94}_{-0.52}$	$+2.48$ -0.69	$+2.75$ -0.99	$-7.23^{+1.63}_{-2.75}$	$+2.03$ -7.68	$+2.43$ -9.41
J1351+0830		$3.09^{+0.73}_{-0.54}$	$+1.41$ -1.09	$+1.98$ -1.38	$-9.69^{+1.85}_{-2.02}$	$+3.13$ -4.29	$+3.64$ -6.14
J1353+1435	<i>ℓ</i>	$2.40^{+2.23}_{-1.04}$	$+2.75$ -3.54	$+3.04$ -3.83	$-17.09^{+7.64}_{-1.91}$	$+11.52$ -1.91	$+14.86$ -1.91
J1353+7532		$2.10^{+0.31}_{-0.24}$	$+0.55$ -0.49	$+0.57$ -0.72	$-6.73^{+0.64}_{-0.65}$	$+1.01$ -1.30	$+1.42$ -1.41
J1357+7643		$2.90^{+0.33}_{-0.39}$	$+0.77$ -0.66	$+1.01$ -0.92	$-8.31^{+1.22}_{-0.71}$	$+1.67$ -2.10	$+2.39$ -2.67
J1357-1527		$3.64^{+0.53}_{-0.59}$	$+1.07$ -1.03	$+1.65$ -1.10	$-10.27^{+1.57}_{-1.58}$	$+2.76$ -3.28	$+3.23$ -5.23
J1359+4011		$1.99^{+0.25}_{-0.29}$	$+0.54$ -0.55	$+0.72$ -0.72	$-6.26^{+0.75}_{-0.57}$	$+1.42$ -1.04	$+1.60$ -1.77
J1359+5544		$2.89^{+0.33}_{-0.24}$	$+0.71$ -0.47	$+0.87$ -0.68	$-7.71^{+0.52}_{-0.77}$	$+0.90$ -1.80	$+1.27$ -2.28
J1400-1858		$2.60^{+0.48}_{-0.29}$	$+1.07$ -0.57	$+1.29$ -0.76	$-7.58^{+0.85}_{-1.25}$	$+1.52$ -3.00	$+1.94$ -3.56
J1405+0415		$1.62^{+0.20}_{-0.21}$	$+0.35$ -0.44	$+0.57$ -0.49	$-4.57^{+0.26}_{-0.60}$	$+0.70$ -0.88	$+0.88$ -1.19
J1407+2827		$1.88^{+0.57}_{-0.57}$	$+1.57$ -0.68	$+2.26$ -0.72	$-6.51^{+1.30}_{-2.06}$	$+1.66$ -4.91	$+1.93$ -7.69
J1410+0731		$3.10^{+0.67}_{-0.50}$	$+1.09$ -0.91	$+1.81$ -0.91	$-9.36^{+0.98}_{-2.19}$	$+2.08$ -3.72	$+2.42$ -5.22
J1415+0832		$2.30^{+0.29}_{-0.21}$	$+0.60$ -0.42	$+0.77$ -0.55	$-6.49^{+0.46}_{-0.76}$	$+1.28$ -1.35	$+1.26$ -1.94
J1415+1320		$2.92^{+0.29}_{-0.31}$	$+0.69$ -0.46	$+0.87$ -0.68	$-7.06^{+0.55}_{-0.92}$	$+0.97$ -1.81	$+1.41$ -2.42
J1415-0955	<i>m</i>	$3.51^{+1.18}_{-1.59}$	$+1.52$ -4.84	$+1.92$ -5.00	$-14.31^{+4.70}_{-3.04}$	$+8.58$ -3.68	$+10.06$ -3.67
J1416-1705		$2.84^{+0.47}_{-0.63}$	$+1.27$ -0.89	$+1.58$ -1.23	$-9.18^{+1.60}_{-1.54}$	$+2.08$ -4.32	$+3.34$ -4.81
J1419+2706		$2.71^{+0.42}_{-0.32}$	$+0.89$ -0.53	$+0.92$ -0.82	$-7.76^{+0.58}_{-1.38}$	$+1.40$ -2.05	$+1.91$ -2.22
J1419+3821		$2.73^{+0.33}_{-0.24}$	$+0.58$ -0.48	$+0.92$ -0.51	$-7.27^{+0.73}_{-0.61}$	$+1.01$ -1.46	$+1.33$ -2.29
J1419+5423		$2.91^{+0.18}_{-0.24}$	$+0.46$ -0.40	$+0.55$ -0.61	$-6.23^{+0.46}_{-0.45}$	$+0.83$ -1.03	$+1.17$ -1.33
J1420+1703		$2.47^{+0.39}_{-0.32}$	$+0.69$ -0.67	$+1.18$ -0.92	$-7.62^{+0.61}_{-1.24}$	$+1.53$ -1.90	$+2.10$ -2.73
J1421+4645	<i>m</i>	$4.79^{+0.66}_{-1.04}$	$+0.67$ -2.30	$+0.70$ -2.78	$-16.50^{+3.52}_{-2.40}$	$+7.62$ -2.43	$+8.87$ -2.49
J1421-1931		$2.65^{+0.36}_{-0.31}$	$+0.72$ -0.56	$+0.93$ -0.70	$-6.98^{+0.95}_{-0.68}$	$+1.33$ -1.79	$+1.58$ -2.34
J1422+3223		$2.20^{+0.48}_{-0.17}$	$+0.79$ -0.41	$+0.95$ -0.55	$-6.76^{+0.57}_{-1.03}$	$+1.01$ -1.77	$+1.43$ -2.43
J1423+4802		$2.74^{+0.80}_{-0.62}$	$+1.72$ -1.05	$+2.20$ -1.39	$-8.74^{+1.73}_{-2.63}$	$+3.16$ -5.06	$+3.72$ -6.90
J1423+5055		$2.53^{+0.47}_{-0.54}$	$+1.16$ -0.85	$+1.42$ -1.14	$-8.56^{+1.19}_{-1.77}$	$+2.56$ -2.95	$+2.56$ -4.37

Table C.1: Results of fitting the simple power-law model over the 1290 selected observations from OVRO dataset. Flag refers to sources well-defined by the model, being (*m*) objects with a $\sigma(\beta)_{68.3\%} \in [1.5, 3]$ (medium quality) and (*ℓ*) to $\sigma(\beta)_{68.3\%} > 3$ (low quality). The absence of a flag means having $\sigma(\beta)_{68.3\%} < 1.5$.

Name	Flag	β	$\beta^{95.5\%}$	$\beta^{99.7\%}$	$\log A$	$\log A^{95.5\%}$	$\log A^{99.7\%}$
J1424+2256	<i>m</i>	$2.94^{+1.58}_{-0.64}$	$+2.52$ -1.32	$+2.51$ -4.13	$-10.71^{+2.31}_{-5.51}$	$+4.09$ -8.25	$+5.82$ -8.28
J1425+1424		$2.96^{+0.41}_{-0.47}$	$+0.97$ -0.79	$+1.13$ -1.19	$-8.74^{+1.06}_{-1.45}$	$+2.14$ -2.79	$+2.76$ -3.80
J1426+3625		$3.40^{+0.44}_{-0.55}$	$+1.03$ -0.85	$+1.31$ -1.04	$-9.88^{+1.25}_{-1.57}$	$+2.20$ -3.20	$+2.66$ -3.88
J1428+2724		$2.87^{+0.48}_{-0.52}$	$+1.31$ -0.71	$+1.40$ -1.07	$-9.14^{+1.22}_{-1.59}$	$+2.35$ -3.51	$+2.77$ -4.19
J1430+1043		$3.29^{+0.85}_{-0.55}$	$+1.65$ -1.03	$+2.07$ -1.50	$-10.48^{+1.53}_{-2.72}$	$+2.82$ -6.01	$+3.95$ -6.51
J1430+3649		$2.31^{+0.32}_{-0.22}$	$+0.58$ -0.43	$+0.71$ -0.56	$-6.57^{+0.66}_{-0.53}$	$+0.96$ -1.25	$+1.43$ -1.53
J1431+3952	<i>m</i>	$3.82^{+1.08}_{-0.66}$	$+1.34$ -1.51	$+1.42$ -2.04	$-12.52^{+1.34}_{-4.28}$	$+4.55$ -4.35	$+6.19$ -4.47
J1434+1952		$2.40^{+0.22}_{-0.37}$	$+0.55$ -0.68	$+0.80$ -0.84	$-7.03^{+0.65}_{-0.80}$	$+1.59$ -1.48	$+1.88$ -2.18
J1434+4203		$2.31^{+0.41}_{-0.13}$	$+0.49$ -0.45	$+0.75$ -0.54	$-6.92^{+0.41}_{-0.84}$	$+1.04$ -1.16	$+1.34$ -1.59
J1435+3012	<i>m</i>	$4.68^{+0.62}_{-1.18}$	$+0.79$ -2.38	$+0.80$ -3.00	$-17.10^{+4.59}_{-1.81}$	$+8.73$ -1.81	$+10.53$ -1.86
J1436+2321		$2.60^{+0.40}_{-0.26}$	$+0.79$ -0.55	$+0.97$ -0.75	$-7.02^{+0.39}_{-1.21}$	$+1.09$ -2.13	$+1.65$ -2.57
J1436+6336	<i>m</i>	$4.18^{+0.84}_{-1.00}$	$+1.01$ -1.91	$+1.13$ -2.24	$-13.83^{+4.51}_{-1.69}$	$+6.78$ -2.83	$+7.43$ -3.16
J1437+3119		$4.83^{+0.60}_{-0.67}$	$+0.64$ -1.78	$+0.67$ -2.72	$-17.35^{+2.52}_{-1.62}$	$+6.22$ -1.65	$+9.31$ -1.65
J1438+3710		$2.58^{+0.29}_{-0.48}$	$+1.12$ -0.61	$+1.12$ -0.90	$-7.73^{+1.39}_{-0.70}$	$+1.57$ -3.27	$+2.27$ -3.27
J1439+2114		$2.39^{+0.98}_{-0.34}$	$+1.85$ -0.89	$+2.29$ -1.01	$-8.48^{+1.31}_{-2.78}$	$+2.47$ -5.88	$+3.08$ -7.84
J1439+4958		$2.48^{+0.25}_{-0.17}$	$+0.40$ -0.42	$+0.51$ -0.54	$-6.56^{+0.38}_{-0.58}$	$+0.85$ -0.98	$+1.10$ -1.13
J1439-1531		$2.53^{+0.66}_{-0.54}$	$+1.47$ -0.91	$+2.11$ -0.91	$-8.03^{+1.45}_{-1.99}$	$+2.46$ -4.64	$+2.47$ -6.27
J1443+2501		$2.46^{+0.30}_{-0.21}$	$+0.61$ -0.40	$+0.82$ -0.51	$-6.12^{+0.34}_{-0.77}$	$+0.73$ -1.55	$+1.08$ -1.75
J1445-1614	<i>m</i>	$4.12^{+1.01}_{-0.80}$	$+1.15$ -1.85	$+1.29$ -2.43	$-13.86^{+4.76}_{-1.41}$	$+5.78$ -4.05	$+7.56$ -4.11
J1445-1629		$2.39^{+0.42}_{-0.22}$	$+0.63$ -0.56	$+0.77$ -0.67	$-6.83^{+0.67}_{-0.90}$	$+1.08$ -1.81	$+1.50$ -2.20
J1446+1721		$3.16^{+0.25}_{-0.52}$	$+0.88$ -0.61	$+1.00$ -0.84	$-8.93^{+1.23}_{-0.82}$	$+1.62$ -2.27	$+2.24$ -2.53
J1448+7601		$2.31^{+0.50}_{-0.30}$	$+0.81$ -0.75	$+1.29$ -0.86	$-6.99^{+0.66}_{-1.47}$	$+1.68$ -2.31	$+2.06$ -3.86
J1450+0910		$2.75^{+0.30}_{-0.28}$	$+0.67$ -0.42	$+0.77$ -0.64	$-7.99^{+0.71}_{-0.76}$	$+0.92$ -1.85	$+1.33$ -2.03
J1453+2648		$2.51^{+0.31}_{-0.25}$	$+0.59$ -0.54	$+0.79$ -0.74	$-6.96^{+0.49}_{-0.81}$	$+1.21$ -1.47	$+1.51$ -1.97
J1453+3505		$2.01^{+0.48}_{-0.34}$	$+1.07$ -0.54	$+1.29$ -0.68	$-6.67^{+0.69}_{-1.51}$	$+1.11$ -3.55	$+1.55$ -3.77
J1456+5048	<i>m</i>	$2.43^{+1.73}_{-0.53}$	$+2.58$ -0.79	$+2.88$ -1.20	$-9.34^{+1.87}_{-5.67}$	$+2.63$ -8.59	$+3.83$ -8.60
J1458+3720	<i>m</i>	$2.56^{+1.01}_{-0.55}$	$+2.44$ -0.87	$+2.90$ -0.99	$-8.64^{+1.64}_{-3.16}$	$+2.30$ -8.03	$+2.74$ -9.36
J1459+4442		$2.41^{+0.69}_{-0.35}$	$+1.49$ -0.63	$+1.67$ -0.91	$-7.91^{+0.90}_{-1.87}$	$+2.19$ -3.71	$+2.36$ -4.75
J1500+4751	<i>m</i>	$3.56^{+0.98}_{-0.79}$	$+1.68$ -1.32	$+1.80$ -1.70	$-10.76^{+2.23}_{-3.14}$	$+3.63$ -5.62	$+4.65$ -6.08
J1502-1508		$2.71^{+0.49}_{-0.47}$	$+1.18$ -0.81	$+1.34$ -1.01	$-8.36^{+1.44}_{-1.23}$	$+2.20$ -3.43	$+2.97$ -3.77

Table C.1: Results of fitting the simple power-law model over the 1290 selected observations from OVRO dataset. Flag refers to sources well-defined by the model, being (*m*) objects with a $\sigma(\beta)_{68.3\%} \in [1.5, 3]$ (medium quality) and (*ℓ*) to $\sigma(\beta)_{68.3\%} > 3$ (low quality). The absence of a flag means having $\sigma(\beta)_{68.3\%} < 1.5$.

Name	Flag	β	$\beta^{95.5\%}$	$\beta^{99.7\%}$	$\log A$	$\log A^{95.5\%}$	$\log A^{99.7\%}$
J1504+0813	<i>m</i>	$4.74^{+0.50}_{-1.09}$	$+0.75_{-2.07}$	$+0.75_{-2.74}$	$-15.87^{+2.18}_{-3.12}$	$+5.94_{-3.13}$	$+7.98_{-3.12}$
J1504+1029		$2.69^{+0.23}_{-0.28}$	$+0.47_{-0.60}$	$+0.82_{-0.70}$	$-6.13^{+0.60}_{-0.60}$	$+1.27_{-1.20}$	$+1.49_{-1.97}$
J1505+0326		$2.00^{+0.23}_{-0.21}$	$+0.49_{-0.47}$	$+0.69_{-0.52}$	$-5.24^{+0.45}_{-0.50}$	$+0.89_{-1.13}$	$+1.04_{-1.52}$
J1506+3730		$2.77^{+0.45}_{-0.10}$	$+0.59_{-0.36}$	$+0.86_{-0.54}$	$-7.28^{+0.44}_{-0.82}$	$+0.84_{-1.43}$	$+1.21_{-1.83}$
J1506+4239	<i>m</i>	$4.57^{+0.72}_{-1.28}$	$+0.86_{-2.36}$	$+0.91_{-2.98}$	$-14.13^{+4.40}_{-2.18}$	$+7.41_{-2.83}$	$+8.82_{-2.81}$
J1506+4933		$2.86^{+0.40}_{-0.46}$	$+0.87_{-0.80}$	$+1.25_{-0.97}$	$-8.07^{+0.97}_{-1.43}$	$+1.94_{-2.68}$	$+2.47_{-3.68}$
J1506+8319		$3.60^{+0.92}_{-0.55}$	$+1.71_{-0.92}$	$+1.80_{-1.24}$	$-11.85^{+1.87}_{-2.70}$	$+3.20_{-5.14}$	$+3.80_{-5.84}$
J1507-1652		$2.33^{+0.34}_{-0.19}$	$+0.63_{-0.41}$	$+0.91_{-0.55}$	$-6.68^{+0.61}_{-0.74}$	$+0.93_{-1.65}$	$+1.43_{-2.11}$
J1510-1121	<i>m</i>	$4.55^{+0.47}_{-1.46}$	$+0.72_{-2.64}$	$+0.84_{-3.31}$	$-17.02^{+4.81}_{-1.72}$	$+9.20_{-1.97}$	$+11.07_{-1.97}$
J1511+0518	<i>m</i>	$4.52^{+0.79}_{-1.52}$	$+0.85_{-3.03}$	$+0.97_{-3.45}$	$-15.54^{+4.47}_{-3.43}$	$+9.33_{-3.43}$	$+10.67_{-3.45}$
J1513-1012		$2.61^{+0.34}_{-0.35}$	$+0.88_{-0.60}$	$+1.19_{-0.91}$	$-7.04^{+1.10}_{-0.82}$	$+1.55_{-2.36}$	$+2.06_{-2.94}$
J1516+0015		$2.20^{+0.44}_{-0.29}$	$+0.83_{-0.62}$	$+1.17_{-0.62}$	$-6.39^{+0.89}_{-1.01}$	$+1.38_{-2.25}$	$+1.62_{-2.89}$
J1516+1932		$2.66^{+0.39}_{-0.23}$	$+0.62_{-0.52}$	$+0.77_{-0.78}$	$-7.28^{+0.75}_{-0.72}$	$+1.42_{-1.28}$	$+2.00_{-1.72}$
J1521+4336		$2.73^{+0.30}_{-0.50}$	$+0.89_{-0.73}$	$+1.38_{-0.97}$	$-7.94^{+1.34}_{-0.79}$	$+2.12_{-2.13}$	$+2.33_{-3.76}$
J1522+3144		$2.08^{+0.22}_{-0.22}$	$+0.45_{-0.40}$	$+0.69_{-0.49}$	$-6.11^{+0.57}_{-0.46}$	$+0.91_{-1.02}$	$+1.27_{-1.38}$
J1526+6650	<i>ℓ</i>	$2.05^{+2.31}_{-0.95}$	$+2.77_{-3.40}$	$+3.17_{-3.40}$	$-7.87^{+0.89}_{-8.95}$	$+2.23_{-11.11}$	$+4.10_{-11.11}$
J1526-0425		$1.84^{+0.45}_{-0.28}$	$+0.91_{-0.54}$	$+1.17_{-0.61}$	$-6.23^{+0.48}_{-1.46}$	$+1.10_{-2.71}$	$+1.29_{-3.47}$
J1532-1319		$2.12^{+0.48}_{-0.23}$	$+0.97_{-0.51}$	$+1.31_{-0.59}$	$-5.99^{+0.78}_{-0.90}$	$+1.32_{-2.28}$	$+1.43_{-3.14}$
J1533-0421		$2.18^{+0.53}_{-0.48}$	$+1.42_{-0.67}$	$+1.61_{-0.83}$	$-7.48^{+1.41}_{-1.62}$	$+2.13_{-4.26}$	$+2.36_{-5.26}$
J1534+0131		$2.64^{+0.37}_{-0.37}$	$+0.86_{-0.59}$	$+1.00_{-0.76}$	$-7.49^{+1.11}_{-0.76}$	$+1.73_{-1.89}$	$+1.95_{-2.49}$
J1535+4957		$2.95^{+0.33}_{-0.73}$	$+1.08_{-0.98}$	$+1.37_{-1.42}$	$-8.82^{+1.19}_{-1.72}$	$+2.26_{-3.46}$	$+3.11_{-4.73}$
J1539+2744		$2.30^{+0.24}_{-0.22}$	$+0.48_{-0.40}$	$+0.61_{-0.56}$	$-6.16^{+0.47}_{-0.60}$	$+0.83_{-1.18}$	$+1.17_{-1.52}$
J1539+3104	<i>ℓ</i>	$2.37^{+2.81}_{-0.81}$	$+2.90_{-3.46}$	$+3.09_{-3.87}$	$-17.82^{+8.23}_{-1.82}$	$+12.02_{-2.07}$	$+13.67_{-2.17}$
J1540+1447		$2.12^{+0.28}_{-0.23}$	$+0.51_{-0.47}$	$+0.68_{-0.56}$	$-5.89^{+0.69}_{-0.54}$	$+1.00_{-1.34}$	$+1.29_{-1.78}$
J1544+3240		$3.22^{+0.47}_{-0.49}$	$+1.05_{-1.16}$	$+1.59_{-1.31}$	$-10.10^{+1.28}_{-1.35}$	$+2.90_{-3.11}$	$+3.38_{-4.11}$
J1545+5135		$2.53^{+0.84}_{-0.44}$	$+2.27_{-0.73}$	$+2.97_{-1.01}$	$-8.59^{+1.33}_{-2.57}$	$+2.70_{-6.45}$	$+2.69_{-9.84}$
J1548+1727	<i>m</i>	$3.32^{+0.98}_{-0.56}$	$+1.73_{-1.14}$	$+2.15_{-1.40}$	$-11.20^{+2.11}_{-2.57}$	$+3.14_{-5.81}$	$+3.99_{-7.47}$
J1548+3511	<i>ℓ</i>	$2.02^{+1.31}_{-3.04}$	$+2.82_{-3.52}$	$+3.30_{-3.52}$	$-16.52^{+5.98}_{-2.42}$	$+11.02_{-2.35}$	$+13.36_{-2.42}$
J1549+0237		$2.99^{+0.37}_{-0.22}$	$+0.74_{-0.46}$	$+0.86_{-0.76}$	$-6.94^{+0.66}_{-0.77}$	$+1.05_{-1.77}$	$+1.75_{-1.92}$
J1549+5038		$2.24^{+0.30}_{-0.36}$	$+0.67_{-0.74}$	$+0.96_{-0.76}$	$-6.74^{+1.05}_{-0.66}$	$+1.72_{-1.77}$	$+1.99_{-2.38}$

Table C.1: Results of fitting the simple power-law model over the 1290 selected observations from OVRO dataset. Flag refers to sources well-defined by the model, being (*m*) objects with a $\sigma(\beta)_{68.3\%} \in [1.5, 3]$ (medium quality) and (*ℓ*) to $\sigma(\beta)_{68.3\%} > 3$ (low quality). The absence of a flag means having $\sigma(\beta)_{68.3\%} < 1.5$.

Name	Flag	β	$\beta^{95.5\%}$	$\beta^{99.7\%}$	$\log A$	$\log A^{95.5\%}$	$\log A^{99.7\%}$
J1550+0527		$2.24^{+0.39}_{-0.35}$	$+0.84$ -0.56	$+0.98$ -0.71	$-6.32^{+1.16}_{-0.89}$	$+1.58$ -2.37	$+2.00$ -2.92
J1551+5806	<i>m</i>	$2.04^{+0.79}_{-0.85}$	$+2.56$ -0.94	$+3.04$ -0.92	$-7.44^{+2.05}_{-2.57}$	$+2.29$ -8.88	$+2.43$ -11.28
J1552+0850		$1.94^{+0.29}_{-0.38}$	$+0.72$ -0.56	$+0.95$ -0.69	$-6.86^{+1.02}_{-0.66}$	$+1.59$ -1.58	$+1.78$ -2.14
J1555+1111		$2.01^{+0.27}_{-0.28}$	$+0.59$ -0.43	$+0.73$ -0.57	$-6.81^{+0.69}_{-0.69}$	$+1.05$ -1.52	$+1.44$ -1.77
J1557-0001		$2.80^{+0.30}_{-0.37}$	$+0.62$ -0.67	$+1.00$ -0.89	$-7.82^{+0.83}_{-0.88}$	$+1.52$ -1.79	$+2.04$ -2.79
J1558+5625	<i>ℓ</i>	$2.24^{+2.36}_{-0.96}$	$+2.81$ -3.36	$+3.05$ -3.68	$-8.21^{+2.39}_{-6.64}$	$+2.44$ -10.74	$+5.47$ -10.73
J1559+0304		$2.69^{+0.45}_{-0.58}$	$+1.24$ -0.79	$+1.74$ -1.07	$-9.03^{+1.54}_{-1.40}$	$+2.31$ -3.74	$+3.02$ -5.25
J1602+2646	<i>ℓ</i>	$3.69^{+1.20}_{-2.47}$	$+1.29$ -5.04	$+1.58$ -5.11	$-16.76^{+6.34}_{-2.24}$	$+11.54$ -2.24	$+13.25$ -2.23
J1602+3326	<i>m</i>	$3.44^{+0.82}_{-0.88}$	$+1.48$ -1.61	$+2.04$ -1.73	$-10.80^{+2.89}_{-2.52}$	$+4.44$ -4.96	$+5.06$ -5.87
J1603+1105		$2.12^{+0.32}_{-0.29}$	$+0.61$ -0.50	$+0.84$ -0.62	$-6.34^{+0.62}_{-0.87}$	$+1.01$ -1.80	$+1.38$ -2.18
J1603+1554		$4.50^{+0.45}_{-1.01}$	$+0.69$ -2.09	$+0.85$ -2.73	$-16.30^{+3.19}_{-1.59}$	$+7.17$ -1.67	$+9.21$ -1.68
J1603+5730		$2.25^{+0.43}_{-0.49}$	$+1.08$ -0.65	$+1.82$ -0.85	$-7.89^{+1.32}_{-1.22}$	$+1.93$ -3.18	$+2.35$ -5.71
J1603-1007		$2.19^{+0.23}_{-0.26}$	$+0.52$ -0.45	$+0.62$ -0.74	$-6.48^{+0.63}_{-0.51}$	$+1.10$ -0.98	$+1.64$ -1.34
J1604+5714		$2.70^{+0.33}_{-0.26}$	$+0.63$ -0.56	$+0.83$ -0.84	$-7.18^{+0.77}_{-0.64}$	$+1.29$ -1.51	$+2.01$ -1.81
J1605+3001		$2.70^{+0.63}_{-0.51}$	$+2.07$ -0.73	$+2.33$ -0.96	$-8.84^{+1.66}_{-1.51}$	$+1.76$ -6.88	$+2.47$ -6.88
J1605-1139		$1.85^{+0.38}_{-0.22}$	$+0.78$ -0.50	$+1.13$ -0.54	$-5.28^{+0.68}_{-0.86}$	$+0.93$ -2.43	$+1.24$ -3.24
J1606+2717		$2.56^{+0.38}_{-0.31}$	$+0.90$ -0.54	$+1.02$ -0.78	$-7.88^{+0.94}_{-0.88}$	$+1.60$ -2.31	$+1.91$ -2.85
J1606+3124	<i>m</i>	$4.51^{+0.54}_{-1.93}$	$+0.59$ -3.02	$+0.82$ -3.33	$-7.99^{+1.22}_{-7.19}$	$+1.73$ -10.00	$+2.91$ -10.00
J1608+1029		$2.81^{+0.26}_{-0.26}$	$+0.54$ -0.47	$+0.66$ -0.65	$-7.33^{+0.80}_{-0.46}$	$+1.29$ -1.30	$+1.53$ -1.55
J1610+2414		$2.33^{+0.41}_{-0.47}$	$+1.05$ -0.64	$+1.44$ -0.84	$-7.49^{+1.16}_{-1.17}$	$+1.69$ -2.92	$+2.19$ -3.79
J1611+1856		$2.86^{+0.89}_{-0.35}$	$+1.36$ -0.88	$+1.78$ -1.08	$-9.63^{+1.25}_{-2.24}$	$+2.70$ -3.74	$+3.05$ -5.12
J1613+3412		$2.48^{+0.50}_{-0.21}$	$+0.85$ -0.60	$+1.12$ -0.69	$-5.94^{+0.39}_{-1.41}$	$+1.38$ -2.18	$+1.46$ -3.25
J1616+0459		$3.30^{+0.49}_{-0.63}$	$+1.11$ -1.09	$+1.74$ -1.44	$-10.13^{+1.88}_{-1.44}$	$+2.99$ -3.50	$+3.87$ -4.86
J1616+4632		$2.52^{+0.25}_{-0.30}$	$+0.52$ -0.46	$+0.61$ -0.61	$-7.57^{+0.60}_{-0.66}$	$+1.20$ -1.08	$+1.45$ -1.28
J1617+0246		$2.31^{+0.33}_{-0.53}$	$+1.07$ -0.66	$+1.35$ -0.90	$-7.41^{+0.88}_{-1.60}$	$+1.88$ -3.12	$+2.13$ -4.11
J1617-1122	<i>m</i>	$2.64^{+1.20}_{-1.10}$	$+2.62$ -1.11	$+2.84$ -1.38	$-7.58^{+2.55}_{-4.53}$	$+2.49$ -9.91	$+3.21$ -10.20
J1617-1941		$4.94^{+0.35}_{-0.98}$	$+0.38$ -2.27	$+0.55$ -2.60	$-16.42^{+2.76}_{-1.58}$	$+7.04$ -1.57	$+8.27$ -1.58
J1618+0819	<i>m</i>	$2.53^{+0.98}_{-0.70}$	$+2.52$ -1.05	$+2.75$ -1.26	$-8.67^{+1.93}_{-3.21}$	$+2.58$ -8.90	$+2.94$ -10.18
J1619+2247		$2.53^{+0.63}_{-0.77}$	$+1.34$ -1.11	$+1.97$ -1.15	$-8.19^{+1.90}_{-2.28}$	$+2.99$ -4.66	$+2.99$ -6.89
J1620+4901	<i>m</i>	$4.39^{+0.46}_{-1.16}$	$+1.03$ -1.76	$+1.03$ -2.43	$-12.63^{+1.59}_{-3.63}$	$+3.60$ -5.20	$+5.50$ -5.18

Table C.1: Results of fitting the simple power-law model over the 1290 selected observations from OVRO dataset. Flag refers to sources well-defined by the model, being (*m*) objects with a $\sigma(\beta)_{68.3\%} \in [1.5, 3]$ (medium quality) and (*ℓ*) to $\sigma(\beta)_{68.3\%} > 3$ (low quality). The absence of a flag means having $\sigma(\beta)_{68.3\%} < 1.5$.

Name	Flag	β	$\beta^{95.5\%}$	$\beta^{99.7\%}$	$\log A$	$\log A^{95.5\%}$	$\log A^{99.7\%}$
J1624+5652		$2.17^{+0.54}_{-0.44}$	$+1.11$ -0.83	$+1.49$ -1.17	$-7.51^{+1.37}_{-1.44}$	$+2.12$ -3.32	$+2.99$ -4.16
J1624+5741		$2.45^{+0.60}_{-0.33}$	$+1.04$ -0.74	$+1.34$ -0.91	$-7.43^{+0.99}_{-1.59}$	$+1.89$ -2.82	$+2.16$ -4.08
J1625+4134		$2.66^{+0.48}_{-0.33}$	$+1.02$ -0.60	$+1.22$ -0.88	$-8.11^{+0.90}_{-1.33}$	$+1.62$ -2.66	$+2.19$ -3.44
J1628-1415		$2.48^{+0.55}_{-0.57}$	$+1.28$ -0.83	$+1.80$ -1.18	$-7.96^{+1.06}_{-2.11}$	$+2.13$ -3.86	$+2.92$ -5.35
J1630+0701		$3.02^{+0.72}_{-0.35}$	$+1.29$ -0.97	$+1.81$ -1.13	$-9.66^{+1.25}_{-1.80}$	$+2.53$ -3.88	$+2.86$ -5.18
J1631+4927		$2.14^{+0.35}_{-0.39}$	$+0.60$ -0.70	$+0.75$ -0.76	$-7.09^{+1.23}_{-0.71}$	$+1.75$ -1.46	$+1.95$ -1.80
J1632+8232		$2.52^{+0.35}_{-0.36}$	$+0.61$ -0.81	$+1.16$ -0.81	$-7.21^{+0.52}_{-1.43}$	$+1.82$ -1.97	$+1.88$ -3.30
J1635+3808		$3.07^{+0.23}_{-0.38}$	$+0.53$ -0.66	$+0.91$ -0.74	$-6.73^{+0.82}_{-0.65}$	$+1.41$ -1.44	$+1.72$ -2.05
J1636+2112		$2.57^{+0.55}_{-0.49}$	$+1.22$ -0.77	$+1.77$ -1.03	$-8.28^{+1.18}_{-1.82}$	$+1.76$ -3.71	$+2.26$ -5.60
J1637+4717		$2.69^{+0.41}_{-0.26}$	$+0.81$ -0.48	$+1.07$ -0.69	$-7.29^{+0.53}_{-1.25}$	$+1.41$ -1.94	$+1.81$ -2.75
J1638+5720		$2.98^{+0.34}_{-0.31}$	$+0.82$ -0.48	$+1.02$ -0.77	$-7.66^{+0.74}_{-1.01}$	$+1.30$ -2.00	$+1.88$ -2.74
J1639+5357	<i>m</i>	$4.47^{+0.79}_{-1.23}$	$+0.98$ -2.28	$+1.01$ -2.79	$-15.07^{+3.36}_{-3.48}$	$+6.71$ -3.92	$+8.67$ -3.92
J1640+3946		$2.40^{+0.27}_{-0.31}$	$+0.50$ -0.57	$+0.89$ -0.66	$-6.08^{+0.80}_{-0.59}$	$+1.25$ -1.32	$+1.40$ -2.19
J1640-0011		$2.13^{+0.29}_{-0.38}$	$+0.66$ -0.65	$+1.00$ -0.77	$-6.32^{+0.56}_{-1.16}$	$+1.19$ -2.00	$+1.39$ -3.08
J1641+2257		$2.19^{+0.54}_{-0.46}$	$+1.14$ -0.94	$+1.85$ -0.98	$-7.52^{+1.33}_{-1.52}$	$+2.52$ -3.25	$+2.53$ -5.32
J1642+3948		$2.79^{+0.34}_{-0.45}$	$+0.76$ -0.78	$+1.22$ -1.00	$-5.76^{+1.01}_{-1.04}$	$+1.66$ -2.36	$+2.04$ -3.83
J1642+6856		$3.01^{+0.31}_{-0.33}$	$+0.64$ -0.55	$+0.84$ -0.70	$-7.27^{+0.80}_{-0.73}$	$+1.33$ -1.58	$+1.77$ -1.97
J1642-0621		$2.52^{+0.42}_{-0.30}$	$+0.77$ -0.64	$+1.13$ -0.66	$-6.36^{+0.87}_{-0.96}$	$+1.59$ -1.96	$+1.59$ -2.82
J1644+2619	<i>m</i>	$2.01^{+1.61}_{-0.92}$	$+2.68$ -3.44	$+3.42$ -3.44	$-6.96^{+2.28}_{-4.89}$	$+2.48$ -10.36	$+2.63$ -12.02
J1644-0743		$2.89^{+0.32}_{-0.60}$	$+0.88$ -0.85	$+1.49$ -1.00	$-7.56^{+0.83}_{-1.55}$	$+1.82$ -2.63	$+2.09$ -4.55
J1644-1804		$1.95^{+0.47}_{-0.27}$	$+0.91$ -0.50	$+1.10$ -0.67	$-6.63^{+0.75}_{-1.30}$	$+1.26$ -2.64	$+1.70$ -3.20
J1646+4059		$2.38^{+0.44}_{-0.43}$	$+1.00$ -0.71	$+1.17$ -0.90	$-7.17^{+0.92}_{-1.41}$	$+1.81$ -2.76	$+1.81$ -3.77
J1647+4950		$2.19^{+0.25}_{-0.28}$	$+0.52$ -0.51	$+0.80$ -0.69	$-6.87^{+0.70}_{-0.54}$	$+1.01$ -1.31	$+1.31$ -1.75
J1648+2224	<i>m</i>	$2.58^{+1.23}_{-0.66}$	$+2.46$ -1.00	$+2.81$ -1.33	$-9.19^{+1.99}_{-4.01}$	$+2.86$ -8.63	$+4.06$ -8.94
J1649+0412		$2.27^{+0.27}_{-0.25}$	$+0.54$ -0.43	$+0.62$ -0.66	$-6.88^{+0.63}_{-0.68}$	$+0.99$ -1.37	$+1.58$ -1.56
J1650+0824		$2.50^{+0.25}_{-0.40}$	$+0.56$ -0.72	$+1.03$ -0.94	$-7.64^{+1.19}_{-0.52}$	$+1.81$ -1.50	$+2.13$ -2.75
J1651+0129		$2.15^{+0.31}_{-0.28}$	$+0.65$ -0.61	$+0.97$ -0.73	$-6.83^{+0.92}_{-0.62}$	$+1.41$ -1.74	$+1.85$ -2.49
J1652+0618		$2.74^{+0.71}_{-0.42}$	$+1.51$ -0.76	$+2.05$ -1.11	$-8.47^{+1.59}_{-1.61}$	$+2.22$ -4.59	$+2.67$ -6.28
J1652+3902		$2.19^{+0.52}_{-0.24}$	$+0.92$ -0.59	$+1.35$ -0.81	$-6.61^{+0.80}_{-1.10}$	$+1.50$ -2.58	$+1.78$ -3.95
J1653+3107		$5.04^{+0.37}_{-0.86}$	$+0.46$ -1.70	$+0.46$ -2.39	$-15.80^{+3.13}_{-0.91}$	$+5.50$ -1.20	$+7.76$ -1.19

Table C.1: Results of fitting the simple power-law model over the 1290 selected observations from OVRO dataset. Flag refers to sources well-defined by the model, being (*m*) objects with a $\sigma(\beta)_{68.3\%} \in [1.5, 3]$ (medium quality) and (*ℓ*) to $\sigma(\beta)_{68.3\%} > 3$ (low quality). The absence of a flag means having $\sigma(\beta)_{68.3\%} < 1.5$.

Name	Flag	β	$\beta^{95.5\%}$	$\beta^{99.7\%}$	$\log A$	$\log A^{95.5\%}$	$\log A^{99.7\%}$
J1653+3945		$1.79^{+0.70}_{-0.41}$	$+1.51$ -0.69	$+2.26$ -0.84	$-5.72^{+1.28}_{-1.93}$	$+1.33$ -5.37	$+1.81$ -6.84
J1653-1551		$1.76^{+0.52}_{-0.42}$	$+1.20$ -0.58	$+1.48$ -0.74	$-6.44^{+1.07}_{-1.46}$	$+1.38$ -3.61	$+1.65$ -4.50
J1655+4233	<i>m</i>	$2.62^{+1.19}_{-0.78}$	$+2.54$ -0.89	$+2.82$ -1.21	$-9.39^{+2.37}_{-3.77}$	$+2.59$ -8.61	$+3.50$ -9.54
J1656+1826	<i>m</i>	$2.46^{+0.79}_{-0.77}$	$+1.91$ -1.10	$+2.40$ -1.41	$-8.78^{+2.38}_{-2.47}$	$+3.42$ -6.19	$+3.68$ -7.60
J1656+6012		$2.48^{+0.24}_{-0.28}$	$+0.44$ -0.50	$+0.72$ -0.67	$-6.49^{+0.38}_{-0.69}$	$+0.76$ -1.27	$+1.14$ -1.77
J1657+4808		$2.43^{+0.19}_{-0.30}$	$+0.54$ -0.40	$+0.54$ -0.54	$-6.48^{+0.60}_{-0.59}$	$+0.95$ -1.15	$+1.17$ -1.53
J1658+0515		$3.44^{+0.65}_{-0.66}$	$+1.64$ -1.00	$+1.82$ -1.21	$-10.35^{+1.81}_{-2.02}$	$+2.53$ -5.30	$+3.18$ -5.53
J1658+3443	<i>m</i>	$2.11^{+1.97}_{-0.52}$	$+3.12$ -0.79	$+3.25$ -1.73	$-7.84^{+2.07}_{-6.79}$	$+2.15$ -11.12	$+3.19$ -11.12
J1658+4737		$3.33^{+0.80}_{-0.63}$	$+1.48$ -1.21	$+1.94$ -1.60	$-9.93^{+2.06}_{-2.03}$	$+3.41$ -4.28	$+4.08$ -5.96
J1658-0739	<i>m</i>	$4.86^{+0.55}_{-1.43}$	$+0.64$ -2.86	$+0.63$ -3.60	$-15.04^{+3.49}_{-3.37}$	$+8.19$ -3.73	$+9.89$ -3.93
J1700+6830		$2.31^{+0.33}_{-0.11}$	$+0.62$ -0.24	$+0.68$ -0.45	$-5.63^{+0.22}_{-0.68}$	$+0.49$ -1.28	$+0.90$ -1.52
J1701+3954		$2.70^{+0.65}_{-0.34}$	$+1.25$ -0.73	$+1.57$ -0.88	$-8.51^{+1.05}_{-1.84}$	$+2.02$ -3.60	$+2.25$ -4.32
J1706+0953		$2.16^{+0.43}_{-0.30}$	$+0.79$ -0.48	$+1.20$ -0.70	$-7.26^{+1.23}_{-0.60}$	$+1.70$ -1.61	$+1.97$ -2.59
J1707+0148		$2.52^{+0.53}_{-0.40}$	$+1.06$ -0.68	$+1.47$ -0.94	$-7.64^{+1.08}_{-1.38}$	$+2.05$ -2.93	$+2.49$ -3.86
J1707+1331		$2.24^{+0.60}_{-0.53}$	$+1.88$ -0.70	$+2.08$ -0.85	$-6.81^{+1.15}_{-1.96}$	$+1.69$ -5.05	$+2.08$ -6.48
J1707-1415		$2.36^{+0.71}_{-0.57}$	$+1.71$ -0.94	$+2.74$ -0.97	$-7.06^{+1.58}_{-2.16}$	$+2.39$ -5.36	$+2.39$ -8.89
J1709+4318		$2.67^{+0.22}_{-0.41}$	$+0.58$ -0.53	$+0.79$ -0.70	$-6.86^{+0.63}_{-0.85}$	$+1.05$ -1.61	$+1.43$ -2.11
J1709-1728		$2.70^{+0.70}_{-0.30}$	$+1.05$ -0.77	$+1.27$ -0.95	$-8.01^{+0.77}_{-2.06}$	$+2.36$ -2.87	$+2.41$ -4.08
J1712-1820		$2.67^{+0.54}_{-0.49}$	$+1.08$ -0.86	$+1.58$ -0.93	$-7.97^{+1.33}_{-1.33}$	$+2.09$ -3.22	$+2.34$ -4.79
J1713+4916		$2.38^{+0.90}_{-0.49}$	$+1.81$ -0.82	$+2.39$ -0.97	$-8.58^{+1.89}_{-2.31}$	$+2.49$ -5.34	$+2.94$ -7.09
J1716+6836		$1.96^{+0.25}_{-0.38}$	$+0.66$ -0.54	$+1.00$ -0.74	$-6.31^{+0.67}_{-0.89}$	$+1.18$ -1.88	$+1.55$ -2.96
J1716-0452		$2.61^{+0.30}_{-0.36}$	$+0.84$ -0.56	$+1.06$ -0.84	$-7.88^{+0.70}_{-1.11}$	$+1.45$ -2.22	$+2.15$ -3.11
J1719+1745		$1.95^{+0.46}_{-0.20}$	$+0.84$ -0.53	$+1.39$ -0.61	$-5.93^{+0.82}_{-0.86}$	$+1.32$ -2.24	$+1.58$ -3.92
J1719+4858		$2.68^{+0.67}_{-0.50}$	$+1.45$ -0.83	$+2.02$ -0.91	$-9.14^{+1.49}_{-1.92}$	$+2.58$ -4.10	$+2.75$ -5.38
J1719-1420		$2.46^{+0.75}_{-0.25}$	$+1.19$ -0.66	$+1.61$ -0.95	$-7.82^{+0.78}_{-2.03}$	$+1.75$ -3.41	$+2.32$ -4.63
J1721+3542		$2.40^{+0.58}_{-0.63}$	$+1.39$ -0.90	$+1.90$ -1.14	$-8.23^{+1.74}_{-1.71}$	$+2.60$ -4.23	$+3.10$ -5.44
J1722+1013		$1.78^{+0.30}_{-0.19}$	$+0.58$ -0.39	$+0.78$ -0.53	$-5.19^{+0.48}_{-0.62}$	$+0.90$ -1.28	$+1.15$ -1.74
J1722+2815		$2.96^{+0.39}_{-0.47}$	$+0.97$ -0.72	$+1.52$ -0.92	$-9.31^{+1.40}_{-1.00}$	$+2.07$ -2.60	$+2.58$ -4.06
J1722+5856	<i>m</i>	$2.89^{+1.03}_{-0.55}$	$+1.92$ -1.05	$+2.51$ -1.42	$-9.97^{+1.66}_{-3.26}$	$+2.58$ -6.87	$+3.98$ -7.62
J1722+6105		$2.33^{+0.17}_{-0.30}$	$+0.45$ -0.52	$+0.65$ -0.58	$-6.51^{+0.41}_{-0.72}$	$+0.81$ -1.46	$+1.03$ -1.60

Table C.1: Results of fitting the simple power-law model over the 1290 selected observations from OVRO dataset. Flag refers to sources well-defined by the model, being (*m*) objects with a $\sigma(\beta)_{68.3\%} \in [1.5, 3]$ (medium quality) and (*ℓ*) to $\sigma(\beta)_{68.3\%} > 3$ (low quality). The absence of a flag means having $\sigma(\beta)_{68.3\%} < 1.5$.

Name	Flag	β	$\beta^{95.5\%}$	$\beta^{99.7\%}$	$\log A$	$\log A^{95.5\%}$	$\log A^{99.7\%}$
J1724+1648		$2.32^{+0.28}_{-0.60}$	$+0.98_{-0.84}$	$+1.36_{-1.01}$	$-7.32^{+1.11}_{-1.34}$	$+1.96_{-2.94}$	$+1.96_{-4.45}$
J1724+3303		$2.85^{+0.56}_{-0.51}$	$+1.13_{-1.10}$	$+1.79_{-1.15}$	$-8.61^{+1.19}_{-1.98}$	$+3.06_{-3.37}$	$+3.06_{-5.49}$
J1724-1443		$2.87^{+0.58}_{-0.41}$	$+1.16_{-0.80}$	$+1.80_{-0.96}$	$-8.77^{+0.74}_{-1.96}$	$+1.80_{-3.58}$	$+2.30_{-5.54}$
J1725+1152		$2.86^{+0.58}_{-0.52}$	$+1.10_{-0.98}$	$+1.52_{-1.11}$	$-9.36^{+1.52}_{-1.50}$	$+2.84_{-2.86}$	$+2.94_{-4.23}$
J1726+2717		$3.00^{+0.56}_{-0.55}$	$+1.31_{-0.88}$	$+1.74_{-1.13}$	$-9.72^{+1.56}_{-1.73}$	$+2.54_{-4.30}$	$+3.19_{-5.23}$
J1726+3213		$2.60^{+0.66}_{-0.56}$	$+1.73_{-1.06}$	$+2.50_{-1.26}$	$-8.53^{+1.74}_{-1.91}$	$+3.38_{-4.81}$	$+3.32_{-8.30}$
J1727+4530		$2.66^{+0.19}_{-0.24}$	$+0.45_{-0.39}$	$+0.45_{-0.62}$	$-6.21^{+0.52}_{-0.38}$	$+0.79_{-0.94}$	$+1.18_{-1.00}$
J1727+5510	<i>m</i>	$3.91^{+1.14}_{-0.84}$	$+1.52_{-1.77}$	$+1.58_{-2.48}$	$-12.72^{+1.95}_{-4.88}$	$+4.69_{-6.27}$	$+6.53_{-6.26}$
J1728+0427		$2.34^{+0.16}_{-0.25}$	$+0.39_{-0.43}$	$+0.56_{-0.51}$	$-6.03^{+0.62}_{-0.26}$	$+0.86_{-0.92}$	$+1.09_{-1.25}$
J1728+1215		$2.07^{+0.35}_{-0.14}$	$+0.58_{-0.32}$	$+0.66_{-0.47}$	$-5.43^{+0.38}_{-0.73}$	$+0.63_{-1.54}$	$+1.05_{-1.54}$
J1733-0456		$1.89^{+0.34}_{-0.30}$	$+0.73_{-0.52}$	$+1.21_{-0.71}$	$-5.81^{+0.44}_{-1.14}$	$+0.84_{-2.36}$	$+1.25_{-3.53}$
J1733-1304		$1.98^{+0.28}_{-0.25}$	$+0.56_{-0.48}$	$+0.75_{-0.58}$	$-4.38^{+0.61}_{-0.71}$	$+1.05_{-1.55}$	$+1.35_{-1.98}$
J1734+3857		$2.44^{+0.12}_{-0.34}$	$+0.35_{-0.51}$	$+0.50_{-0.57}$	$-5.61^{+0.38}_{-0.63}$	$+0.74_{-1.17}$	$+0.81_{-1.58}$
J1735+3616		$2.30^{+0.42}_{-0.25}$	$+0.62_{-0.65}$	$+1.05_{-0.73}$	$-6.92^{+0.91}_{-0.75}$	$+1.42_{-1.67}$	$+1.65_{-2.41}$
J1735+5049	<i>m</i>	$4.38^{+0.91}_{-1.11}$	$+1.11_{-2.34}$	$+1.12_{-2.98}$	$-14.15^{+3.23}_{-3.58}$	$+7.43_{-4.08}$	$+8.92_{-4.81}$
J1736+0631		$2.93^{+0.44}_{-0.56}$	$+1.02_{-0.99}$	$+1.58_{-0.98}$	$-8.86^{+0.92}_{-1.85}$	$+2.29_{-3.19}$	$+2.34_{-4.89}$
J1738+3224		$2.32^{+0.34}_{-0.15}$	$+0.57_{-0.34}$	$+0.63_{-0.56}$	$-6.46^{+0.39}_{-0.67}$	$+0.73_{-1.11}$	$+1.22_{-1.32}$
J1738+4008		$2.03^{+0.38}_{-0.33}$	$+0.73_{-0.60}$	$+1.09_{-0.71}$	$-7.07^{+1.06}_{-0.82}$	$+1.48_{-2.21}$	$+1.68_{-3.00}$
J1739+4737		$2.10^{+0.25}_{-0.17}$	$+0.48_{-0.39}$	$+0.60_{-0.42}$	$-5.73^{+0.45}_{-0.46}$	$+0.84_{-1.08}$	$+1.00_{-1.30}$
J1739+4955		$2.76^{+0.28}_{-0.31}$	$+0.68_{-0.48}$	$+0.77_{-0.68}$	$-7.64^{+1.05}_{-0.42}$	$+1.39_{-1.44}$	$+1.82_{-1.94}$
J1740+2211		$2.71^{+0.40}_{-0.53}$	$+0.92_{-0.80}$	$+1.12_{-0.99}$	$-8.51^{+1.55}_{-0.99}$	$+2.10_{-2.77}$	$+2.58_{-3.20}$
J1740+4348		$3.12^{+0.57}_{-0.36}$	$+0.81_{-0.89}$	$+1.26_{-1.16}$	$-9.74^{+1.33}_{-1.16}$	$+2.22_{-2.42}$	$+2.98_{-3.61}$
J1740+5211		$2.68^{+0.26}_{-0.29}$	$+0.64_{-0.45}$	$+0.78_{-0.60}$	$-6.67^{+0.45}_{-0.90}$	$+1.04_{-1.74}$	$+1.31_{-2.29}$
J1740-0811		$2.46^{+0.76}_{-0.57}$	$+1.89_{-0.76}$	$+2.59_{-0.97}$	$-6.78^{+1.15}_{-2.67}$	$+1.58_{-6.37}$	$+2.00_{-7.98}$
J1742+5945	<i>ℓ</i>	$1.77^{+2.63}_{-0.90}$	$+3.16_{-3.25}$	$+3.63_{-3.25}$	$-7.52^{+2.28}_{-8.38}$	$+2.11_{-12.38}$	$+3.92_{-12.47}$
J1743+3747		$2.93^{+0.65}_{-0.21}$	$+1.12_{-0.58}$	$+1.40_{-0.84}$	$-8.52^{+0.71}_{-1.60}$	$+1.65_{-2.88}$	$+1.92_{-3.95}$
J1743-0350		$2.86^{+0.46}_{-0.27}$	$+0.87_{-0.61}$	$+1.14_{-0.84}$	$-6.62^{+0.99}_{-0.90}$	$+1.63_{-2.23}$	$+2.23_{-2.99}$
J1745+1720		$3.41^{+0.42}_{-0.46}$	$+0.92_{-0.76}$	$+1.16_{-0.98}$	$-9.66^{+1.14}_{-1.31}$	$+1.97_{-2.81}$	$+2.47_{-3.38}$
J1745+2252		$2.90^{+0.54}_{-0.47}$	$+1.22_{-0.77}$	$+1.45_{-1.07}$	$-9.46^{+1.42}_{-1.42}$	$+2.36_{-3.25}$	$+2.99_{-4.12}$
J1745-0753		$1.90^{+0.24}_{-0.18}$	$+0.49_{-0.30}$	$+0.63_{-0.43}$	$-4.73^{+0.30}_{-0.58}$	$+0.76_{-0.99}$	$+0.89_{-1.44}$

Table C.1: Results of fitting the simple power-law model over the 1290 selected observations from OVRO dataset. Flag refers to sources well-defined by the model, being (*m*) objects with a $\sigma(\beta)_{68.3\%} \in [1.5, 3]$ (medium quality) and (*ℓ*) to $\sigma(\beta)_{68.3\%} > 3$ (low quality). The absence of a flag means having $\sigma(\beta)_{68.3\%} < 1.5$.

Name	Flag	β	$\beta^{95.5\%}$	$\beta^{99.7\%}$	$\log A$	$\log A^{95.5\%}$	$\log A^{99.7\%}$
J1747+4658		$3.54^{+0.68}_{-0.45}$	$+1.46$ -0.96	$+1.90$ -1.15	$-10.41^{+1.58}_{-1.66}$	$+2.98$ -4.17	$+3.22$ -5.59
J1748+3404		$1.91^{+0.39}_{-0.14}$	$+0.66$ -0.31	$+0.81$ -0.52	$-5.61^{+0.46}_{-0.67}$	$+0.86$ -1.28	$+1.24$ -1.67
J1748+7005		$2.06^{+0.29}_{-0.17}$	$+0.62$ -0.26	$+0.79$ -0.37	$-5.59^{+0.59}_{-0.41}$	$+0.63$ -1.49	$+0.91$ -1.56
J1749+4321		$2.56^{+0.30}_{-0.51}$	$+0.86$ -0.83	$+1.27$ -1.00	$-8.07^{+1.28}_{-0.99}$	$+2.29$ -2.35	$+2.51$ -3.75
J1751+0939		$2.38^{+0.16}_{-0.27}$	$+0.48$ -0.38	$+0.68$ -0.42	$-4.34^{+0.44}_{-0.44}$	$+0.63$ -1.17	$+0.83$ -1.65
J1752+1734		$2.65^{+0.73}_{-0.39}$	$+1.14$ -0.99	$+1.55$ -1.09	$-8.01^{+1.34}_{-1.76}$	$+2.53$ -3.38	$+3.10$ -4.89
J1753+2848		$2.60^{+0.16}_{-0.34}$	$+0.39$ -0.54	$+0.67$ -0.66	$-6.41^{+0.70}_{-0.50}$	$+1.02$ -1.03	$+1.47$ -1.47
J1753+4409		$2.45^{+0.95}_{-0.55}$	$+2.46$ -0.93	$+2.98$ -0.94	$-8.17^{+2.21}_{-2.28}$	$+2.14$ -7.76	$+2.72$ -9.43
J1754+6452		$1.86^{+0.43}_{-0.46}$	$+1.14$ -0.56	$+1.14$ -0.98	$-6.57^{+0.75}_{-1.67}$	$+1.84$ -2.86	$+1.83$ -3.83
J1756+1535		$2.40^{+0.21}_{-0.37}$	$+0.71$ -0.51	$+1.06$ -0.69	$-6.57^{+0.46}_{-0.94}$	$+0.91$ -2.06	$+1.40$ -2.75
J1756+1553		$2.24^{+0.29}_{-0.54}$	$+0.75$ -0.83	$+1.15$ -0.89	$-7.26^{+1.15}_{-1.12}$	$+1.73$ -2.33	$+2.05$ -3.34
J1759+2343		$5.18^{+0.28}_{-0.84}$	$+0.32$ -1.85	$+0.31$ -2.40	$-17.86^{+2.64}_{-1.13}$	$+6.05$ -1.13	$+8.01$ -1.13
J1800+3848		$2.32^{+0.88}_{-0.33}$	$+1.49$ -0.77	$+1.98$ -0.83	$-7.38^{+1.02}_{-2.51}$	$+2.12$ -4.33	$+2.36$ -6.18
J1800+7828		$1.60^{+0.14}_{-0.22}$	$+0.40$ -0.37	$+0.53$ -0.41	$-3.50^{+0.40}_{-0.33}$	$+0.66$ -0.82	$+0.87$ -1.33
J1801+4404		$2.67^{+0.35}_{-0.16}$	$+0.59$ -0.40	$+0.73$ -0.49	$-6.68^{+0.40}_{-0.76}$	$+0.95$ -1.28	$+1.02$ -1.76
J1804+0101	<i>m</i>	$3.89^{+1.16}_{-0.55}$	$+1.60$ -1.33	$+1.60$ -1.95	$-12.43^{+2.59}_{-2.75}$	$+4.83$ -4.44	$+6.27$ -4.45
J1805+1714		$2.70^{+0.63}_{-0.35}$	$+1.14$ -0.66	$+1.55$ -0.85	$-8.93^{+0.90}_{-1.80}$	$+1.79$ -3.26	$+2.39$ -4.53
J1806+6949		$2.53^{+0.45}_{-0.26}$	$+0.82$ -0.54	$+1.12$ -0.71	$-6.86^{+0.53}_{-1.41}$	$+1.28$ -2.44	$+1.70$ -2.86
J1808+4542		$2.40^{+0.20}_{-0.44}$	$+0.62$ -0.67	$+0.95$ -0.87	$-6.94^{+1.12}_{-0.44}$	$+1.60$ -1.50	$+2.13$ -2.47
J1809+1849		$2.17^{+0.41}_{-0.51}$	$+1.07$ -0.96	$+1.54$ -1.17	$-7.48^{+1.35}_{-1.18}$	$+2.12$ -3.33	$+2.72$ -4.57
J1811+1704		$2.55^{+0.43}_{-0.45}$	$+0.87$ -0.82	$+1.69$ -0.81	$-7.48^{+1.24}_{-1.11}$	$+1.83$ -2.65	$+2.19$ -4.91
J1813+0615		$2.57^{+0.26}_{-0.37}$	$+0.72$ -0.58	$+1.18$ -0.73	$-7.02^{+0.56}_{-0.94}$	$+1.41$ -1.67	$+1.60$ -3.24
J1813+2952		$2.79^{+0.58}_{-0.30}$	$+1.09$ -0.75	$+1.57$ -0.92	$-8.98^{+1.17}_{-1.27}$	$+2.45$ -2.62	$+2.57$ -4.41
J1815+1623		$2.79^{+0.36}_{-0.56}$	$+0.95$ -0.94	$+1.35$ -1.30	$-8.94^{+1.52}_{-1.06}$	$+2.33$ -2.70	$+3.24$ -4.14
J1818+0903		$1.74^{+0.24}_{-0.19}$	$+0.53$ -0.31	$+0.61$ -0.49	$-5.28^{+0.48}_{-0.44}$	$+0.82$ -0.88	$+1.07$ -1.14
J1818+5017		$2.33^{+0.55}_{-0.16}$	$+0.84$ -0.52	$+1.16$ -0.65	$-7.66^{+0.43}_{-1.48}$	$+1.56$ -2.06	$+1.59$ -2.89
J1824+1044		$2.71^{+0.62}_{-0.33}$	$+1.08$ -0.77	$+1.35$ -0.95	$-8.82^{+1.33}_{-1.38}$	$+2.37$ -2.65	$+2.77$ -3.75
J1824+5651		$2.38^{+0.35}_{-0.24}$	$+0.83$ -0.38	$+0.93$ -0.60	$-6.53^{+0.81}_{-0.64}$	$+1.19$ -1.77	$+1.54$ -2.19
J1827+2658		$2.01^{+0.73}_{-0.40}$	$+1.76$ -0.47	$+1.85$ -0.82	$-7.49^{+1.45}_{-1.78}$	$+1.74$ -4.65	$+2.42$ -5.43
J1832+1357		$3.21^{+0.47}_{-0.57}$	$+1.26$ -0.85	$+1.48$ -1.17	$-9.87^{+1.57}_{-1.24}$	$+2.83$ -3.11	$+3.25$ -3.91

Table C.1: Results of fitting the simple power-law model over the 1290 selected observations from OVRO dataset. Flag refers to sources well-defined by the model, being (*m*) objects with a $\sigma(\beta)_{68.3\%} \in [1.5, 3]$ (medium quality) and (*ℓ*) to $\sigma(\beta)_{68.3\%} > 3$ (low quality). The absence of a flag means having $\sigma(\beta)_{68.3\%} < 1.5$.

Name	Flag	β	$\beta^{95.5\%}$	$\beta^{99.7\%}$	$\log A$	$\log A^{95.5\%}$	$\log A^{99.7\%}$
J1835+3241		$1.70^{+0.60}_{-0.36}$	$+1.22_{-0.65}$	$+1.86_{-0.79}$	$-5.93^{+1.31}_{-1.42}$	$+1.59_{-3.90}$	$+1.88_{-5.45}$
J1835+6119		$2.79^{+0.57}_{-0.34}$	$+0.99_{-0.79}$	$+1.23_{-0.83}$	$-9.03^{+1.24}_{-1.29}$	$+2.33_{-2.69}$	$+2.37_{-3.62}$
J1840+2457		$2.63^{+0.22}_{-0.58}$	$+0.75_{-0.73}$	$+1.09_{-1.07}$	$-8.64^{+1.49}_{-0.64}$	$+2.05_{-1.95}$	$+2.81_{-3.41}$
J1840+3900		$2.48^{+0.36}_{-0.36}$	$+0.87_{-0.72}$	$+1.20_{-0.72}$	$-7.62^{+0.83}_{-1.07}$	$+1.69_{-2.40}$	$+1.86_{-3.04}$
J1842+6809		$2.62^{+0.38}_{-0.29}$	$+0.82_{-0.55}$	$+1.16_{-0.71}$	$-7.11^{+0.54}_{-1.08}$	$+1.27_{-2.31}$	$+1.70_{-2.85}$
J1848+3219		$2.75^{+0.25}_{-0.25}$	$+0.47_{-0.55}$	$+0.84_{-0.55}$	$-6.66^{+0.58}_{-0.55}$	$+1.13_{-1.14}$	$+1.13_{-1.95}$
J1849+3024		$2.23^{+0.41}_{-0.50}$	$+1.10_{-0.86}$	$+1.51_{-0.90}$	$-6.92^{+1.15}_{-1.25}$	$+1.62_{-3.94}$	$+1.96_{-5.06}$
J1849+6705		$2.37^{+0.31}_{-0.18}$	$+0.66_{-0.48}$	$+0.89_{-0.52}$	$-5.29^{+0.41}_{-0.67}$	$+1.10_{-1.28}$	$+1.07_{-1.93}$
J1850+2825	<i>m</i>	$4.06^{+1.08}_{-1.21}$	$+1.41_{-2.29}$	$+1.42_{-2.86}$	$-12.13^{+2.18}_{-5.63}$	$+6.11_{-5.85}$	$+7.53_{-5.85}$
J1852+4019	<i>m</i>	$1.87^{+1.28}_{-0.78}$	$+2.92_{-0.75}$	$+3.44_{-1.05}$	$-6.63^{+1.83}_{-4.56}$	$+1.69_{-10.51}$	$+2.42_{-11.32}$
J1852+4855		$2.38^{+0.28}_{-0.32}$	$+0.68_{-0.53}$	$+0.97_{-0.73}$	$-6.53^{+0.71}_{-0.68}$	$+1.40_{-1.44}$	$+1.60_{-2.56}$
J1854+7351		$2.91^{+0.38}_{-0.38}$	$+0.77_{-0.63}$	$+1.05_{-0.89}$	$-8.96^{+1.18}_{-0.80}$	$+1.84_{-1.84}$	$+2.46_{-2.70}$
J1900+2701		$2.11^{+0.40}_{-0.35}$	$+0.95_{-0.65}$	$+1.40_{-0.72}$	$-6.74^{+0.69}_{-1.31}$	$+1.37_{-2.88}$	$+1.67_{-4.11}$
J1900+2722	<i>m</i>	$4.73^{+0.37}_{-1.65}$	$+0.66_{-2.79}$	$+0.76_{-3.11}$	$-12.68^{+1.39}_{-5.65}$	$+4.80_{-6.13}$	$+6.28_{-6.29}$
J1909+4833		$2.32^{+0.65}_{-0.34}$	$+1.19_{-0.66}$	$+1.83_{-0.89}$	$-7.72^{+0.86}_{-1.59}$	$+1.60_{-3.21}$	$+2.05_{-4.83}$
J1912+3740		$3.15^{+0.63}_{-0.77}$	$+1.39_{-1.29}$	$+2.10_{-1.36}$	$-9.43^{+1.99}_{-2.10}$	$+3.85_{-4.11}$	$+4.11_{-6.78}$
J1916-1519		$1.96^{+0.34}_{-0.19}$	$+0.61_{-0.48}$	$+0.73_{-0.63}$	$-5.77^{+0.45}_{-0.81}$	$+0.86_{-1.50}$	$+1.28_{-1.72}$
J1917-1921	<i>m</i>	$1.98^{+1.57}_{-0.92}$	$+3.51_{-2.44}$	$+3.51_{-3.42}$	$-6.77^{+2.62}_{-6.16}$	$+1.92_{-12.16}$	$+2.92_{-12.19}$
J1918+5520		$2.33^{+0.36}_{-0.41}$	$+0.94_{-0.69}$	$+1.36_{-1.06}$	$-7.53^{+1.05}_{-1.04}$	$+2.11_{-2.25}$	$+2.43_{-3.63}$
J1923+3941	<i>m</i>	$4.64^{+0.50}_{-1.38}$	$+0.62_{-2.74}$	$+0.81_{-3.48}$	$-17.25^{+4.44}_{-1.74}$	$+8.97_{-1.74}$	$+11.19_{-1.74}$
J1923+4754	<i>m</i>	$2.78^{+1.06}_{-0.56}$	$+1.68_{-1.40}$	$+2.65_{-1.39}$	$-8.84^{+2.01}_{-2.58}$	$+3.03_{-5.59}$	$+3.52_{-7.76}$
J1927+6117		$2.39^{+0.32}_{-0.31}$	$+0.72_{-0.47}$	$+0.76_{-0.61}$	$-6.42^{+0.80}_{-0.77}$	$+1.24_{-1.78}$	$+1.38_{-2.14}$
J1927+7358		$3.35^{+0.51}_{-0.40}$	$+1.02_{-0.72}$	$+1.29_{-0.86}$	$-7.98^{+0.95}_{-1.55}$	$+1.64_{-3.25}$	$+2.06_{-4.03}$
J1933+6540		$2.30^{+0.30}_{-0.20}$	$+0.52_{-0.46}$	$+0.68_{-0.60}$	$-6.78^{+0.68}_{-0.46}$	$+1.29_{-0.88}$	$+1.55_{-1.41}$
J1934+6138		$2.23^{+0.56}_{-0.40}$	$+1.18_{-0.76}$	$+1.67_{-0.84}$	$-7.49^{+0.85}_{-1.84}$	$+1.57_{-4.00}$	$+2.06_{-5.34}$
J1936+7131	<i>m</i>	$4.96^{+0.49}_{-1.58}$	$+0.54_{-2.90}$	$+0.53_{-3.64}$	$-16.90^{+5.16}_{-2.01}$	$+9.45_{-2.02}$	$+11.39_{-2.02}$
J1936-0402		$2.66^{+0.49}_{-0.30}$	$+0.73_{-0.75}$	$+1.19_{-1.07}$	$-8.19^{+0.76}_{-1.36}$	$+1.84_{-2.26}$	$+2.53_{-3.39}$
J1938-1749	<i>m</i>	$3.57^{+0.65}_{-0.92}$	$+1.43_{-1.35}$	$+1.65_{-1.63}$	$-10.85^{+2.23}_{-2.60}$	$+3.59_{-5.09}$	$+4.07_{-5.97}$
J1939-1525		$2.59^{+0.43}_{-0.31}$	$+1.05_{-0.50}$	$+1.05_{-0.72}$	$-7.01^{+0.70}_{-1.16}$	$+1.37_{-2.50}$	$+1.63_{-3.08}$
J1947-0103	<i>m</i>	$2.39^{+0.95}_{-0.57}$	$+1.89_{-0.85}$	$+2.62_{-1.05}$	$-7.81^{+1.70}_{-2.65}$	$+2.41_{-5.79}$	$+2.54_{-8.01}$

Table C.1: Results of fitting the simple power-law model over the 1290 selected observations from OVRO dataset. Flag refers to sources well-defined by the model, being (*m*) objects with a $\sigma(\beta)_{68.3\%} \in [1.5, 3]$ (medium quality) and (*ℓ*) to $\sigma(\beta)_{68.3\%} > 3$ (low quality). The absence of a flag means having $\sigma(\beta)_{68.3\%} < 1.5$.

Name	Flag	β	$\beta^{95.5\%}$	$\beta^{99.7\%}$	$\log A$	$\log A^{95.5\%}$	$\log A^{99.7\%}$
J1949-1957		$2.66^{+0.58}_{-0.32}$	$+1.06_{-0.70}$	$+1.26_{-0.86}$	$-8.09^{+1.03}_{-1.39}$	$+2.32_{-2.53}$	$+2.32_{-3.62}$
J1951+0134		$2.02^{+0.56}_{-0.33}$	$+1.09_{-0.63}$	$+1.29_{-0.73}$	$-7.36^{+1.43}_{-0.88}$	$+1.92_{-2.68}$	$+2.08_{-3.53}$
J1951-0509		$2.28^{+0.38}_{-0.37}$	$+0.81_{-0.53}$	$+1.05_{-0.85}$	$-6.97^{+0.68}_{-1.27}$	$+1.20_{-2.39}$	$+2.16_{-2.79}$
J1954-1123		$2.43^{+0.24}_{-0.17}$	$+0.41_{-0.43}$	$+0.62_{-0.50}$	$-5.99^{+0.42}_{-0.44}$	$+0.84_{-0.85}$	$+1.07_{-1.31}$
J1955+0618		$2.38^{+0.54}_{-0.75}$	$+1.28_{-1.18}$	$+2.17_{-1.20}$	$-8.68^{+2.38}_{-1.35}$	$+3.23_{-4.46}$	$+3.39_{-7.32}$
J1955+5131		$2.42^{+0.44}_{-0.28}$	$+0.83_{-0.61}$	$+1.03_{-0.76}$	$-6.58^{+0.55}_{-1.25}$	$+1.20_{-2.32}$	$+1.67_{-2.72}$
J1959+6508		$1.81^{+0.25}_{-0.24}$	$+0.54_{-0.40}$	$+0.63_{-0.58}$	$-6.03^{+0.62}_{-0.57}$	$+0.75_{-1.41}$	$+1.11_{-1.59}$
J2000-1325		$2.39^{+0.24}_{-0.32}$	$+0.54_{-0.56}$	$+0.78_{-0.72}$	$-6.37^{+0.73}_{-0.61}$	$+1.23_{-1.45}$	$+1.66_{-1.86}$
J2000-1748		$2.24^{+0.25}_{-0.16}$	$+0.43_{-0.34}$	$+0.71_{-0.36}$	$-4.58^{+0.38}_{-0.52}$	$+0.65_{-0.91}$	$+0.73_{-1.55}$
J2001+4352		$1.59^{+0.31}_{-0.39}$	$+1.04_{-0.48}$	$+1.40_{-0.63}$	$-5.82^{+0.56}_{-1.20}$	$+1.08_{-2.88}$	$+1.23_{-5.38}$
J2004+7355		$2.45^{+0.58}_{-0.47}$	$+1.19_{-0.74}$	$+1.64_{-1.11}$	$-7.82^{+1.15}_{-1.74}$	$+1.89_{-3.64}$	$+2.75_{-4.89}$
J2005+7752		$2.32^{+0.33}_{-0.13}$	$+0.43_{-0.33}$	$+0.52_{-0.54}$	$-6.13^{+0.35}_{-0.71}$	$+0.69_{-1.08}$	$+1.08_{-1.29}$
J2006+6424		$2.59^{+0.38}_{-0.31}$	$+0.74_{-0.59}$	$+1.05_{-0.77}$	$-7.23^{+0.71}_{-1.11}$	$+1.43_{-2.17}$	$+1.80_{-2.92}$
J2007+0636		$2.32^{+0.38}_{-0.46}$	$+1.00_{-0.69}$	$+1.18_{-0.85}$	$-7.58^{+1.30}_{-0.97}$	$+1.81_{-2.85}$	$+2.22_{-3.21}$
J2007+6607		$2.81^{+0.22}_{-0.47}$	$+0.62_{-0.68}$	$+0.84_{-0.89}$	$-7.98^{+1.15}_{-0.68}$	$+1.83_{-1.59}$	$+2.18_{-2.29}$
J2009+0727		$2.13^{+0.31}_{-0.21}$	$+0.48_{-0.40}$	$+0.58_{-0.64}$	$-6.47^{+0.28}_{-0.90}$	$+0.65_{-1.40}$	$+1.08_{-1.40}$
J2009+7229		$2.24^{+0.44}_{-0.37}$	$+0.91_{-0.66}$	$+1.10_{-0.83}$	$-6.38^{+0.92}_{-1.15}$	$+1.76_{-2.43}$	$+2.07_{-3.15}$
J2011-1546		$2.53^{+0.36}_{-0.22}$	$+0.64_{-0.48}$	$+0.78_{-0.63}$	$-6.37^{+0.51}_{-0.87}$	$+0.98_{-1.83}$	$+1.42_{-2.22}$
J2015+6554		$2.67^{+0.55}_{-0.13}$	$+0.79_{-0.47}$	$+0.94_{-0.71}$	$-7.74^{+0.51}_{-1.17}$	$+1.23_{-1.95}$	$+1.82_{-2.40}$
J2015-0137		$2.73^{+0.52}_{-0.80}$	$+1.60_{-1.08}$	$+1.92_{-1.33}$	$-8.62^{+2.04}_{-1.65}$	$+2.96_{-5.03}$	$+3.43_{-6.27}$
J2015-1252		$2.52^{+0.49}_{-0.43}$	$+1.26_{-0.70}$	$+1.63_{-0.96}$	$-7.93^{+1.05}_{-1.45}$	$+1.59_{-3.87}$	$+2.43_{-4.96}$
J2016+1632		$2.61^{+0.44}_{-0.44}$	$+0.95_{-0.76}$	$+1.91_{-0.94}$	$-7.21^{+0.96}_{-1.31}$	$+1.57_{-3.13}$	$+2.15_{-5.59}$
J2018-0509		$2.43^{+0.42}_{-0.13}$	$+0.67_{-0.40}$	$+0.77_{-0.51}$	$-7.08^{+0.49}_{-0.78}$	$+0.86_{-1.69}$	$+1.23_{-1.75}$
J2020+6747		$2.57^{+0.54}_{-0.67}$	$+1.33_{-1.05}$	$+1.97_{-1.18}$	$-8.26^{+0.99}_{-2.52}$	$+2.17_{-4.80}$	$+2.62_{-7.20}$
J2021+0515	<i>m</i>	$1.77^{+2.04}_{-0.74}$	$+3.50_{-0.59}$	$+3.62_{-1.07}$	$-6.77^{+1.67}_{-7.12}$	$+1.90_{-11.37}$	$+2.54_{-12.19}$
J2022+6136		$1.61^{+0.45}_{-0.34}$	$+1.21_{-0.73}$	$+2.15_{-0.69}$	$-4.77^{+0.82}_{-1.28}$	$+1.64_{-3.70}$	$+1.46_{-6.98}$
J2022+7611		$2.81^{+0.41}_{-0.49}$	$+1.00_{-0.63}$	$+1.29_{-0.85}$	$-7.82^{+1.62}_{-0.83}$	$+1.84_{-2.89}$	$+2.56_{-3.41}$
J2023-0123		$1.82^{+0.17}_{-0.23}$	$+0.59_{-0.34}$	$+0.59_{-0.57}$	$-5.37^{+0.30}_{-0.60}$	$+0.65_{-1.22}$	$+0.92_{-1.22}$
J2024+1718		$3.58^{+0.61}_{-0.62}$	$+1.60_{-0.96}$	$+1.82_{-1.30}$	$-10.78^{+1.79}_{-1.95}$	$+2.39_{-5.57}$	$+3.38_{-5.99}$
J2025+0316		$2.33^{+0.25}_{-0.39}$	$+0.52_{-0.71}$	$+0.69_{-0.88}$	$-6.73^{+0.74}_{-0.87}$	$+1.28_{-1.74}$	$+1.78_{-2.00}$

Table C.1: Results of fitting the simple power-law model over the 1290 selected observations from OVRO dataset. Flag refers to sources well-defined by the model, being (*m*) objects with a $\sigma(\beta)_{68.3\%} \in [1.5, 3]$ (medium quality) and (*ℓ*) to $\sigma(\beta)_{68.3\%} > 3$ (low quality). The absence of a flag means having $\sigma(\beta)_{68.3\%} < 1.5$.

Name	Flag	β	$\beta^{95.5\%}$	$\beta^{99.7\%}$	$\log A$	$\log A^{95.5\%}$	$\log A^{99.7\%}$
J2030-0503		$1.68^{+0.39}_{-0.46}$	$+1.60$ -0.62	$+1.80$ -0.78	$-6.07^{+0.96}_{-1.41}$	$+1.48$ -5.76	$+1.77$ -6.24
J2030-0622		$1.73^{+0.43}_{-0.24}$	$+0.80$ -0.51	$+1.03$ -0.59	$-5.86^{+0.90}_{-0.86}$	$+1.32$ -2.03	$+1.49$ -2.82
J2031+0239		$2.54^{+0.31}_{-0.38}$	$+0.73$ -0.63	$+0.92$ -0.87	$-7.22^{+0.60}_{-1.15}$	$+1.33$ -2.05	$+1.85$ -2.37
J2031+1219		$2.52^{+0.24}_{-0.20}$	$+0.39$ -0.52	$+0.77$ -0.54	$-6.22^{+0.43}_{-0.59}$	$+1.09$ -1.03	$+1.22$ -1.72
J2033+2146		$1.95^{+0.51}_{-0.20}$	$+0.89$ -0.50	$+1.48$ -0.61	$-6.78^{+0.80}_{-1.10}$	$+1.34$ -2.51	$+1.68$ -3.88
J2035+1056		$2.59^{+0.11}_{-0.28}$	$+0.28$ -0.40	$+0.40$ -0.50	$-5.76^{+0.30}_{-0.44}$	$+0.68$ -0.74	$+0.79$ -0.95
J2036-0629		$2.25^{+0.48}_{-0.25}$	$+0.91$ -0.61	$+1.29$ -0.70	$-6.82^{+0.61}_{-1.26}$	$+1.41$ -2.48	$+1.68$ -3.84
J2037-1522		$2.11^{+0.51}_{-0.47}$	$+1.60$ -0.54	$+1.60$ -0.84	$-7.23^{+1.30}_{-1.44}$	$+1.76$ -4.18	$+2.05$ -4.78
J2039-1046		$2.30^{+0.37}_{-0.35}$	$+0.81$ -0.53	$+1.27$ -0.78	$-6.87^{+0.71}_{-1.09}$	$+1.36$ -2.15	$+1.94$ -3.51
J2042+7508		$1.70^{+0.47}_{-0.25}$	$+0.80$ -0.46	$+1.10$ -0.59	$-6.11^{+0.68}_{-1.24}$	$+1.28$ -2.02	$+1.40$ -3.33
J2043+1255		$3.26^{+0.91}_{-0.56}$	$+1.57$ -1.31	$+2.05$ -1.47	$-11.28^{+1.40}_{-3.23}$	$+3.84$ -5.24	$+3.94$ -6.55
J2045-1858		$1.85^{+0.46}_{-0.33}$	$+1.17$ -0.49	$+1.56$ -0.64	$-6.82^{+1.29}_{-0.84}$	$+1.86$ -2.70	$+1.94$ -4.20
J2049+1003		$2.50^{+0.30}_{-0.33}$	$+0.79$ -0.47	$+0.88$ -0.63	$-7.37^{+0.83}_{-0.69}$	$+1.51$ -1.68	$+1.60$ -2.17
J2050+0407		$2.44^{+0.66}_{-0.50}$	$+1.44$ -0.97	$+2.41$ -1.02	$-7.62^{+1.36}_{-1.88}$	$+2.26$ -4.58	$+2.32$ -8.04
J2051+1743		$2.31^{+0.31}_{-0.29}$	$+0.76$ -0.48	$+0.91$ -0.65	$-6.82^{+0.71}_{-0.72}$	$+1.56$ -1.50	$+1.59$ -2.02
J2101+0341		$2.77^{+0.53}_{-0.22}$	$+0.90$ -0.58	$+1.34$ -0.77	$-7.53^{+0.82}_{-1.19}$	$+1.55$ -2.31	$+2.08$ -3.70
J2102+6758		$2.68^{+0.56}_{-0.34}$	$+1.15$ -0.63	$+1.28$ -1.19	$-8.29^{+0.75}_{-1.70}$	$+1.33$ -3.59	$+2.55$ -3.73
J2106+2135		$2.48^{+0.48}_{-0.50}$	$+1.12$ -0.74	$+1.41$ -0.99	$-8.07^{+1.16}_{-1.54}$	$+1.66$ -3.76	$+2.28$ -4.03
J2108+1430		$2.51^{+0.45}_{-0.26}$	$+0.93$ -0.63	$+1.26$ -0.85	$-7.23^{+0.84}_{-1.00}$	$+1.89$ -1.93	$+2.21$ -3.11
J2110+0809		$2.51^{+0.27}_{-0.46}$	$+1.03$ -0.63	$+1.32$ -0.89	$-7.73^{+0.85}_{-1.17}$	$+1.82$ -2.60	$+2.18$ -3.43
J2110-1020	<i>m</i>	$5.03^{+0.47}_{-1.15}$	$+0.47$ -2.69	$+0.47$ -3.65	$-17.64^{+4.46}_{-1.47}$	$+8.87$ -2.32	$+11.92$ -2.33
J2114+2832		$2.25^{+0.33}_{-0.38}$	$+0.70$ -0.66	$+0.99$ -0.75	$-6.29^{+0.71}_{-1.13}$	$+1.46$ -1.96	$+1.65$ -2.80
J2115+2933		$2.18^{+0.27}_{-0.25}$	$+0.45$ -0.54	$+0.65$ -0.70	$-6.13^{+0.53}_{-0.59}$	$+0.98$ -1.18	$+1.30$ -1.71
J2115-1416	<i>m</i>	$2.01^{+1.87}_{-0.65}$	$+3.11$ -0.78	$+3.35$ -0.98	$-7.44^{+2.20}_{-5.83}$	$+1.92$ -11.07	$+2.59$ -11.50
J2117+0503		$2.28^{+0.36}_{-0.32}$	$+0.71$ -0.66	$+1.04$ -0.68	$-7.02^{+0.70}_{-1.05}$	$+1.37$ -1.92	$+1.64$ -2.72
J2118+0013		$2.15^{+0.17}_{-0.32}$	$+0.34$ -0.50	$+0.50$ -0.62	$-6.12^{+0.63}_{-0.44}$	$+0.90$ -0.91	$+1.34$ -0.97
J2118-0636		$2.17^{+0.31}_{-0.42}$	$+1.08$ -0.57	$+1.33$ -0.83	$-7.42^{+0.78}_{-1.25}$	$+1.52$ -2.90	$+2.12$ -3.66
J2120+0533		$2.71^{+0.36}_{-0.37}$	$+0.72$ -0.67	$+1.09$ -0.96	$-8.58^{+1.00}_{-0.93}$	$+1.92$ -1.73	$+2.44$ -2.90
J2123+0535		$2.73^{+0.36}_{-0.20}$	$+0.72$ -0.43	$+0.93$ -0.62	$-6.44^{+0.65}_{-0.64}$	$+1.16$ -1.61	$+1.29$ -2.09
J2125+0441		$2.17^{+0.33}_{-0.31}$	$+0.73$ -0.51	$+0.86$ -0.71	$-7.24^{+0.90}_{-0.78}$	$+1.50$ -1.59	$+1.87$ -2.09

Table C.1: Results of fitting the simple power-law model over the 1290 selected observations from OVRO dataset. Flag refers to sources well-defined by the model, being (*m*) objects with a $\sigma(\beta)_{68.3\%} \in [1.5, 3]$ (medium quality) and (*ℓ*) to $\sigma(\beta)_{68.3\%} > 3$ (low quality). The absence of a flag means having $\sigma(\beta)_{68.3\%} < 1.5$.

Name	Flag	β	$\beta^{95.5\%}$	$\beta^{99.7\%}$	$\log A$	$\log A^{95.5\%}$	$\log A^{99.7\%}$
J2128-0244		$2.66^{+0.56}_{-0.53}$	$+1.71$ -0.62	$+2.18$ -1.00	$-8.72^{+1.27}_{-1.70}$	$+1.83$ -4.61	$+2.50$ -6.23
J2129-1538		$2.62^{+0.55}_{-0.33}$	$+1.00$ -0.65	$+1.27$ -0.87	$-7.69^{+1.14}_{-1.18}$	$+2.02$ -2.49	$+2.42$ -3.66
J2130-0927		$2.09^{+0.45}_{-0.32}$	$+1.06$ -0.54	$+1.25$ -0.78	$-6.23^{+0.95}_{-1.09}$	$+1.75$ -2.85	$+1.99$ -3.52
J2131-1207		$2.10^{+0.34}_{-0.47}$	$+0.91$ -0.70	$+1.60$ -0.82	$-5.97^{+1.15}_{-1.02}$	$+1.78$ -2.50	$+1.95$ -4.62
J2133+1443		$2.77^{+0.41}_{-0.41}$	$+0.89$ -0.60	$+1.08$ -0.87	$-8.58^{+1.14}_{-0.95}$	$+1.68$ -2.21	$+2.33$ -2.50
J2134-0153		$2.31^{+0.24}_{-0.31}$	$+0.51$ -0.48	$+0.69$ -0.66	$-5.82^{+0.58}_{-0.66}$	$+1.01$ -1.34	$+1.47$ -1.49
J2136+0041		$1.67^{+0.21}_{-0.25}$	$+0.52$ -0.44	$+0.64$ -0.52	$-3.83^{+0.60}_{-0.45}$	$+0.84$ -1.18	$+1.12$ -1.52
J2139+0122	<i>m</i>	$4.54^{+0.43}_{-1.25}$	$+0.71$ -2.50	$+0.81$ -2.99	$-16.35^{+4.82}_{-0.90}$	$+8.62$ -1.60	$+10.11$ -1.60
J2139+1423		$2.49^{+0.44}_{-0.40}$	$+0.91$ -0.74	$+1.16$ -0.83	$-6.64^{+0.89}_{-1.39}$	$+1.74$ -2.56	$+2.04$ -3.67
J2142-0437		$2.19^{+0.39}_{-0.21}$	$+0.80$ -0.42	$+1.08$ -0.57	$-6.51^{+0.55}_{-0.92}$	$+1.11$ -1.91	$+1.30$ -2.64
J2143+1743		$1.98^{+0.15}_{-0.20}$	$+0.33$ -0.32	$+0.43$ -0.40	$-4.50^{+0.35}_{-0.29}$	$+0.56$ -0.68	$+0.64$ -0.93
J2145+1115		$1.97^{+0.29}_{-0.38}$	$+0.71$ -0.57	$+1.07$ -0.72	$-6.66^{+0.80}_{-0.97}$	$+1.44$ -1.98	$+1.69$ -3.09
J2146-1525		$2.51^{+0.24}_{-0.32}$	$+0.57$ -0.49	$+0.71$ -0.69	$-6.94^{+0.67}_{-0.69}$	$+1.30$ -1.35	$+1.58$ -1.73
J2147+0929		$2.80^{+0.16}_{-0.30}$	$+0.51$ -0.43	$+0.63$ -0.54	$-6.57^{+0.59}_{-0.47}$	$+1.03$ -1.04	$+1.13$ -1.64
J2148+0657		$2.48^{+0.19}_{-0.48}$	$+0.70$ -0.65	$+0.98$ -0.84	$-5.68^{+0.57}_{-1.16}$	$+1.22$ -2.08	$+1.48$ -3.04
J2148-1723		$3.12^{+0.36}_{-0.43}$	$+0.78$ -0.76	$+1.05$ -1.11	$-9.06^{+1.17}_{-0.98}$	$+1.68$ -2.57	$+2.26$ -2.84
J2149+0322	<i>m</i>	$2.45^{+1.37}_{-0.84}$	$+2.67$ -1.02	$+3.03$ -1.34	$-8.74^{+2.54}_{-4.55}$	$+3.11$ -8.91	$+3.57$ -10.25
J2151+0552	<i>m</i>	$4.75^{+0.71}_{-2.02}$	$+0.72$ -3.40	$+0.71$ -3.87	$-17.12^{+7.06}_{-2.69}$	$+11.49$ -2.72	$+12.39$ -2.87
J2151+0709		$2.57^{+0.37}_{-0.34}$	$+0.68$ -0.58	$+0.76$ -0.87	$-7.66^{+0.85}_{-1.07}$	$+1.50$ -1.99	$+2.20$ -2.24
J2152+1734		$2.46^{+0.29}_{-0.36}$	$+0.62$ -0.69	$+0.89$ -0.91	$-7.37^{+1.03}_{-0.69}$	$+1.59$ -1.75	$+2.03$ -2.58
J2153-1136		$2.26^{+0.19}_{-0.27}$	$+0.45$ -0.39	$+0.61$ -0.51	$-6.13^{+0.60}_{-0.39}$	$+0.83$ -0.93	$+1.01$ -1.28
J2156-0037		$2.30^{+0.15}_{-0.29}$	$+0.31$ -0.51	$+0.58$ -0.54	$-5.91^{+0.64}_{-0.32}$	$+0.90$ -0.91	$+1.13$ -1.19
J2157+3127		$2.39^{+0.33}_{-0.26}$	$+0.59$ -0.47	$+0.83$ -0.55	$-6.06^{+0.68}_{-0.70}$	$+1.01$ -1.53	$+1.27$ -2.03
J2158-1501		$2.46^{+0.11}_{-0.32}$	$+0.36$ -0.52	$+0.50$ -0.74	$-4.89^{+0.38}_{-0.54}$	$+0.73$ -1.20	$+1.21$ -1.29
J2200+0234		$2.55^{+0.51}_{-0.18}$	$+0.74$ -0.56	$+1.00$ -0.90	$-8.13^{+0.75}_{-1.03}$	$+1.28$ -2.12	$+2.31$ -2.48
J2203+1725		$2.40^{+0.26}_{-0.16}$	$+0.51$ -0.38	$+0.64$ -0.56	$-6.11^{+0.57}_{-0.38}$	$+0.77$ -1.25	$+1.16$ -1.33
J2203+3145		$2.59^{+0.39}_{-0.34}$	$+0.82$ -0.59	$+1.22$ -0.71	$-6.24^{+0.81}_{-1.07}$	$+1.27$ -2.22	$+1.71$ -3.29
J2204+0440		$1.65^{+0.48}_{-0.27}$	$+0.97$ -0.50	$+1.53$ -0.65	$-5.93^{+0.63}_{-1.41}$	$+1.20$ -2.76	$+1.52$ -4.24
J2204+3632	<i>m</i>	$4.49^{+0.58}_{-1.86}$	$+0.78$ -2.94	$+0.93$ -3.59	$-16.65^{+6.86}_{-1.41}$	$+9.90$ -2.30	$+11.66$ -2.30
J2206-0031		$2.56^{+0.37}_{-0.29}$	$+0.67$ -0.66	$+0.94$ -0.70	$-7.29^{+0.86}_{-0.75}$	$+1.44$ -1.68	$+1.48$ -2.67

Table C.1: Results of fitting the simple power-law model over the 1290 selected observations from OVRO dataset. Flag refers to sources well-defined by the model, being (*m*) objects with a $\sigma(\beta)_{68.3\%} \in [1.5, 3]$ (medium quality) and (*ℓ*) to $\sigma(\beta)_{68.3\%} > 3$ (low quality). The absence of a flag means having $\sigma(\beta)_{68.3\%} < 1.5$.

Name	Flag	β	$\beta^{95.5\%}$	$\beta^{99.7\%}$	$\log A$	$\log A^{95.5\%}$	$\log A^{99.7\%}$
J2207+1652		$2.58^{+0.53}_{-0.41}$	$+1.14$ -0.82	$+2.09$ -0.90	$-8.17^{+1.02}_{-1.54}$	$+2.05$ -3.62	$+2.46$ -6.55
J2210+2013		$1.99^{+0.31}_{-0.27}$	$+0.64$ -0.50	$+0.99$ -0.61	$-6.38^{+0.64}_{-0.80}$	$+1.16$ -1.83	$+1.46$ -2.60
J2211+1841		$2.34^{+0.10}_{-0.26}$	$+0.26$ -0.39	$+0.33$ -0.53	$-6.28^{+0.52}_{-0.22}$	$+0.85$ -0.54	$+1.04$ -0.66
J2212+2355		$2.34^{+0.24}_{-0.28}$	$+0.65$ -0.42	$+0.79$ -0.53	$-6.04^{+0.64}_{-0.58}$	$+0.93$ -1.59	$+1.18$ -1.77
J2214+0711		$2.59^{+0.44}_{-0.46}$	$+0.82$ -0.84	$+1.31$ -0.84	$-7.47^{+0.81}_{-1.46}$	$+1.60$ -2.62	$+1.77$ -4.44
J2214+3739	<i>m</i>	$4.72^{+0.53}_{-2.24}$	$+0.68$ -3.29	$+0.72$ -3.84	$-16.51^{+8.82}_{-0.86}$	$+10.62$ -3.01	$+11.60$ -3.46
J2216+3102		$2.86^{+0.80}_{-0.58}$	$+1.78$ -0.97	$+2.35$ -1.33	$-9.29^{+1.47}_{-2.57}$	$+2.35$ -6.06	$+3.72$ -6.84
J2216+3518		$2.62^{+0.29}_{-0.27}$	$+0.50$ -0.56	$+0.66$ -0.62	$-7.07^{+0.71}_{-0.61}$	$+1.12$ -1.33	$+1.44$ -1.65
J2217+2421		$1.75^{+0.18}_{-0.17}$	$+0.38$ -0.31	$+0.57$ -0.35	$-4.05^{+0.27}_{-0.47}$	$+0.54$ -0.91	$+0.68$ -1.40
J2218+1520		$2.95^{+0.26}_{-0.50}$	$+0.81$ -0.65	$+0.95$ -0.84	$-8.17^{+1.31}_{-0.67}$	$+1.76$ -2.13	$+2.08$ -2.54
J2218-0335		$2.89^{+0.24}_{-0.50}$	$+0.69$ -0.78	$+1.39$ -0.91	$-7.56^{+0.89}_{-1.04}$	$+1.65$ -2.31	$+1.89$ -4.19
J2219+1806		$2.35^{+0.30}_{-0.22}$	$+0.57$ -0.37	$+0.77$ -0.51	$-6.29^{+0.36}_{-0.78}$	$+0.74$ -1.36	$+0.98$ -1.84
J2225+2118		$3.16^{+0.22}_{-0.41}$	$+0.66$ -0.56	$+0.77$ -0.79	$-8.32^{+0.88}_{-0.71}$	$+1.48$ -1.53	$+1.84$ -2.04
J2226+0052		$2.44^{+0.55}_{-0.19}$	$+0.96$ -0.46	$+1.04$ -0.78	$-7.58^{+0.77}_{-1.16}$	$+1.49$ -2.30	$+2.06$ -2.94
J2228+2503	<i>m</i>	$4.53^{+0.65}_{-1.95}$	$+0.65$ -3.33	$+0.84$ -4.02	$-17.10^{+7.00}_{-1.76}$	$+11.17$ -1.85	$+12.75$ -1.85
J2229-0832		$2.81^{+0.33}_{-0.21}$	$+0.60$ -0.45	$+0.94$ -0.56	$-6.24^{+0.44}_{-0.87}$	$+0.88$ -1.55	$+1.16$ -2.09
J2230+6946		$2.28^{+0.30}_{-0.35}$	$+0.78$ -0.52	$+0.89$ -0.68	$-6.59^{+0.84}_{-0.72}$	$+1.45$ -1.63	$+1.57$ -2.47
J2230-1325		$1.92^{+0.36}_{-0.19}$	$+0.60$ -0.42	$+0.73$ -0.61	$-5.69^{+0.42}_{-0.90}$	$+0.81$ -1.69	$+1.27$ -2.04
J2236+2828		$2.50^{+0.22}_{-0.29}$	$+0.61$ -0.46	$+0.82$ -0.62	$-6.02^{+0.57}_{-0.61}$	$+1.16$ -1.33	$+1.33$ -2.00
J2236-1433		$2.28^{+0.16}_{-0.27}$	$+0.42$ -0.40	$+0.54$ -0.46	$-5.38^{+0.44}_{-0.46}$	$+0.64$ -1.12	$+0.89$ -1.31
J2238+2749		$2.49^{+0.20}_{-0.53}$	$+0.81$ -0.65	$+0.89$ -0.84	$-7.33^{+0.68}_{-1.21}$	$+1.01$ -2.84	$+1.76$ -2.84
J2241+0953		$2.88^{+0.30}_{-0.26}$	$+0.55$ -0.49	$+0.97$ -0.68	$-7.93^{+0.64}_{-0.75}$	$+1.12$ -1.40	$+1.50$ -2.47
J2241+4120		$2.48^{+0.37}_{-0.44}$	$+0.83$ -0.75	$+1.18$ -0.90	$-7.79^{+1.12}_{-1.00}$	$+1.89$ -2.50	$+2.18$ -3.23
J2244+4057		$1.74^{+0.39}_{-0.30}$	$+0.93$ -0.34	$+1.15$ -0.45	$-3.83^{+0.60}_{-1.00}$	$+0.74$ -2.33	$+0.89$ -2.99
J2245+0324		$2.05^{+0.50}_{-0.27}$	$+0.95$ -0.65	$+1.96$ -0.69	$-7.12^{+0.94}_{-1.22}$	$+1.85$ -2.46	$+1.86$ -5.50
J2245+0500		$3.15^{+0.79}_{-0.34}$	$+1.44$ -0.74	$+1.64$ -1.11	$-10.28^{+1.09}_{-2.16}$	$+2.42$ -3.61	$+3.42$ -4.74
J2246-1206		$2.51^{+0.44}_{-0.32}$	$+0.95$ -0.54	$+1.19$ -0.69	$-6.49^{+0.87}_{-1.13}$	$+1.41$ -2.61	$+1.84$ -3.00
J2247+0310		$2.59^{+0.15}_{-0.39}$	$+0.59$ -0.55	$+0.74$ -0.79	$-7.27^{+0.65}_{-0.77}$	$+1.26$ -1.45	$+1.68$ -2.02
J2247-1237		$2.32^{+0.48}_{-0.39}$	$+1.14$ -0.63	$+1.39$ -0.95	$-7.34^{+1.08}_{-1.32}$	$+1.75$ -3.36	$+2.40$ -3.97
J2249+2107		$2.37^{+0.33}_{-0.46}$	$+0.81$ -0.75	$+1.32$ -0.78	$-7.41^{+1.35}_{-0.74}$	$+1.82$ -2.38	$+2.10$ -3.46

Table C.1: Results of fitting the simple power-law model over the 1290 selected observations from OVRO dataset. Flag refers to sources well-defined by the model, being (*m*) objects with a $\sigma(\beta)_{68.3\%} \in [1.5, 3]$ (medium quality) and (*ℓ*) to $\sigma(\beta)_{68.3\%} > 3$ (low quality). The absence of a flag means having $\sigma(\beta)_{68.3\%} < 1.5$.

Name	Flag	β	$\beta^{95.5\%}$	$\beta^{99.7\%}$	$\log A$	$\log A^{95.5\%}$	$\log A^{99.7\%}$
J2253+1608		$2.90^{+0.36}_{-0.21}$	$+0.64_{-0.53}$	$+0.91_{-0.66}$	$-5.04^{+0.58}_{-0.82}$	$+1.21_{-1.63}$	$+1.52_{-2.10}$
J2253+1942		$3.75^{+0.57}_{-0.72}$	$+1.25_{-0.95}$	$+1.37_{-1.29}$	$-11.33^{+2.25}_{-1.61}$	$+3.09_{-3.59}$	$+3.50_{-4.31}$
J2257+0243		$4.97^{+0.44}_{-0.92}$	$+0.52_{-2.24}$	$+0.52_{-3.41}$	$-17.26^{+2.83}_{-1.72}$	$+7.28_{-1.74}$	$+10.94_{-1.72}$
J2259-0811	<i>ℓ</i>	$1.99^{+0.54}_{-3.49}$	$+2.59_{-3.48}$	$+3.30_{-3.49}$	$-16.60^{+7.32}_{-1.84}$	$+11.33_{-2.40}$	$+13.83_{-2.40}$
J2300+1655		$2.69^{+0.41}_{-0.35}$	$+0.78_{-0.68}$	$+1.03_{-1.00}$	$-8.39^{+1.00}_{-1.00}$	$+1.81_{-2.18}$	$+2.46_{-2.85}$
J2301-0158		$2.88^{+0.42}_{-0.24}$	$+0.80_{-0.55}$	$+1.03_{-0.59}$	$-7.44^{+0.50}_{-1.10}$	$+1.08_{-2.24}$	$+1.39_{-2.81}$
J2305+8242		$2.81^{+0.54}_{-0.60}$	$+1.10_{-1.22}$	$+1.77_{-1.22}$	$-9.34^{+1.81}_{-1.51}$	$+3.58_{-3.29}$	$+3.58_{-5.43}$
J2307+1450		$2.75^{+0.26}_{-0.55}$	$+0.70_{-0.94}$	$+1.28_{-0.94}$	$-8.93^{+1.53}_{-0.72}$	$+2.47_{-1.87}$	$+2.65_{-3.83}$
J2308+2008		$3.09^{+0.85}_{-0.53}$	$+1.63_{-1.13}$	$+2.33_{-1.30}$	$-9.72^{+1.37}_{-2.79}$	$+3.28_{-5.07}$	$+3.32_{-7.85}$
J2310+1055		$2.61^{+0.33}_{-0.43}$	$+0.84_{-0.74}$	$+0.97_{-1.01}$	$-8.44^{+1.58}_{-0.53}$	$+2.20_{-2.12}$	$+2.71_{-2.56}$
J2311+4543		$3.06^{+0.44}_{-0.36}$	$+0.93_{-0.70}$	$+1.20_{-0.88}$	$-8.49^{+0.96}_{-1.09}$	$+1.68_{-2.54}$	$+2.03_{-3.09}$
J2321+2732		$2.08^{+0.35}_{-0.25}$	$+0.80_{-0.42}$	$+1.11_{-0.65}$	$-5.87^{+0.56}_{-0.89}$	$+1.17_{-1.79}$	$+1.53_{-2.66}$
J2321+3204		$2.72^{+0.26}_{-0.23}$	$+0.49_{-0.48}$	$+0.81_{-0.58}$	$-6.42^{+0.51}_{-0.52}$	$+0.98_{-1.11}$	$+1.15_{-1.74}$
J2322+1843		$1.98^{+0.45}_{-0.41}$	$+1.10_{-0.62}$	$+1.37_{-0.94}$	$-7.12^{+1.08}_{-1.23}$	$+1.42_{-3.60}$	$+2.17_{-3.90}$
J2322+4445		$2.72^{+0.75}_{-0.39}$	$+1.55_{-0.61}$	$+1.68_{-0.88}$	$-8.54^{+1.52}_{-1.87}$	$+1.53_{-4.75}$	$+2.30_{-5.33}$
J2323-0317		$2.64^{+0.29}_{-0.27}$	$+0.65_{-0.48}$	$+0.92_{-0.72}$	$-6.44^{+0.50}_{-0.81}$	$+0.88_{-1.64}$	$+1.14_{-2.54}$
J2327+0940		$3.02^{+0.27}_{-0.22}$	$+0.56_{-0.43}$	$+0.82_{-0.55}$	$-6.89^{+0.37}_{-0.70}$	$+0.87_{-1.28}$	$+1.16_{-1.77}$
J2327+1524		$2.23^{+0.44}_{-0.21}$	$+0.75_{-0.44}$	$+1.05_{-0.62}$	$-6.92^{+0.49}_{-1.04}$	$+1.00_{-1.85}$	$+1.31_{-2.48}$
J2327+1533	<i>m</i>	$4.12^{+0.71}_{-1.06}$	$+1.20_{-1.75}$	$+1.31_{-2.50}$	$-13.05^{+2.65}_{-3.21}$	$+4.07_{-4.93}$	$+6.77_{-4.92}$
J2329+0834		$2.72^{+0.30}_{-0.42}$	$+0.67_{-0.62}$	$+0.79_{-0.87}$	$-7.69^{+0.89}_{-0.94}$	$+1.32_{-2.02}$	$+1.93_{-2.14}$
J2330+1100		$3.27^{+0.60}_{-0.47}$	$+1.11_{-0.96}$	$+1.63_{-1.09}$	$-9.19^{+1.09}_{-1.95}$	$+2.21_{-3.80}$	$+3.06_{-4.35}$
J2330+3348		$2.34^{+0.41}_{-0.40}$	$+0.85_{-0.72}$	$+1.21_{-0.81}$	$-7.08^{+0.68}_{-1.62}$	$+1.45_{-2.99}$	$+1.83_{-3.74}$
J2331-1556		$2.52^{+0.37}_{-0.49}$	$+0.94_{-0.71}$	$+1.15_{-0.88}$	$-7.46^{+0.89}_{-1.38}$	$+2.13_{-2.39}$	$+2.39_{-3.17}$
J2334+0736		$2.47^{+0.25}_{-0.21}$	$+0.55_{-0.40}$	$+0.78_{-0.57}$	$-6.56^{+0.41}_{-0.65}$	$+0.92_{-1.34}$	$+1.14_{-1.73}$
J2335-0131		$2.89^{+0.41}_{-0.19}$	$+0.75_{-0.43}$	$+1.08_{-0.63}$	$-7.89^{+0.79}_{-0.65}$	$+1.21_{-1.65}$	$+1.53_{-2.45}$
J2337+2617	<i>m</i>	$2.79^{+1.28}_{-0.65}$	$+2.35_{-0.87}$	$+2.59_{-1.19}$	$-9.59^{+2.12}_{-3.95}$	$+2.67_{-8.01}$	$+3.29_{-8.84}$
J2337-0230		$2.45^{+0.34}_{-0.32}$	$+0.73_{-0.67}$	$+0.93_{-0.85}$	$-6.67^{+0.75}_{-0.86}$	$+1.61_{-1.80}$	$+1.84_{-2.32}$
J2339-1206		$4.53^{+0.50}_{-0.83}$	$+0.94_{-1.37}$	$+0.97_{-2.00}$	$-13.48^{+1.99}_{-2.06}$	$+3.26_{-3.57}$	$+5.13_{-3.67}$
J2343+1543		$2.42^{+0.44}_{-0.23}$	$+0.71_{-0.58}$	$+0.95_{-0.65}$	$-7.49^{+0.67}_{-1.08}$	$+1.19_{-1.96}$	$+1.54_{-2.59}$
J2343+2339		$3.05^{+0.55}_{-0.38}$	$+1.41_{-0.72}$	$+1.76_{-1.24}$	$-9.28^{+1.04}_{-1.43}$	$+1.87_{-4.01}$	$+3.39_{-4.61}$

Table C.1: Results of fitting the simple power-law model over the 1290 selected observations from OVRO dataset. Flag refers to sources well-defined by the model, being (*m*) objects with a $\sigma(\beta)_{68.3\%} \in [1.5, 3]$ (medium quality) and (*ℓ*) to $\sigma(\beta)_{68.3\%} > 3$ (low quality). The absence of a flag means having $\sigma(\beta)_{68.3\%} < 1.5$.

Name	Flag	β	$\beta^{95.5\%}$	$\beta^{99.7\%}$	$\log A$	$\log A^{95.5\%}$	$\log A^{99.7\%}$
J2345-1555		$2.38^{+0.17}_{-0.25}$	$+0.45_{-0.35}$	$+0.53_{-0.53}$	$-5.52^{+0.42}_{-0.43}$	$+0.66_{-1.01}$	$+1.06_{-1.05}$
J2346+0930		$3.26^{+0.60}_{-0.55}$	$+1.45_{-0.85}$	$+1.84_{-1.09}$	$-9.24^{+1.11}_{-2.14}$	$+1.96_{-4.44}$	$+2.73_{-5.66}$
J2346+8007		$2.41^{+0.31}_{-0.29}$	$+0.59_{-0.56}$	$+0.74_{-0.62}$	$-7.12^{+0.76}_{-0.70}$	$+1.35_{-1.43}$	$+1.42_{-1.70}$
J2348-0425		$3.08^{+0.62}_{-0.28}$	$+0.89_{-0.67}$	$+1.27_{-0.87}$	$-8.92^{+0.90}_{-1.40}$	$+1.52_{-2.65}$	$+2.02_{-3.33}$
J2348-1631		$2.57^{+0.29}_{-0.19}$	$+0.56_{-0.36}$	$+0.69_{-0.46}$	$-5.93^{+0.36}_{-0.78}$	$+0.83_{-1.21}$	$+1.05_{-1.51}$
J2350+1106		$2.16^{+0.79}_{-0.40}$	$+2.37_{-0.80}$	$+3.05_{-0.92}$	$-7.66^{+1.26}_{-2.27}$	$+2.53_{-7.54}$	$+2.53_{-10.22}$
J2352+3947		$2.75^{+0.54}_{-0.61}$	$+1.30_{-0.90}$	$+1.69_{-1.36}$	$-8.76^{+1.52}_{-1.82}$	$+2.46_{-3.84}$	$+3.40_{-5.43}$
J2354-1513		$2.33^{+0.31}_{-0.29}$	$+0.70_{-0.40}$	$+0.70_{-0.67}$	$-6.48^{+0.49}_{-0.91}$	$+0.80_{-1.64}$	$+1.41_{-1.69}$
J2357-0152		$2.41^{+0.22}_{-0.45}$	$+0.65_{-0.71}$	$+0.93_{-0.79}$	$-7.46^{+0.83}_{-0.87}$	$+1.57_{-1.84}$	$+1.59_{-2.63}$
J2357-1125		$2.26^{+0.21}_{-0.39}$	$+0.46_{-0.64}$	$+0.83_{-0.94}$	$-6.48^{+0.85}_{-0.63}$	$+1.30_{-1.53}$	$+1.90_{-2.27}$
J2358+0430	<i>m</i>	$2.87^{+1.45}_{-0.56}$	$+2.58_{-0.76}$	$+2.62_{-1.26}$	$-10.01^{+1.60}_{-5.00}$	$+2.51_{-8.72}$	$+3.42_{-9.63}$
J2358+1955		$2.51^{+0.57}_{-0.31}$	$+0.84_{-0.82}$	$+1.21_{-0.88}$	$-7.81^{+0.70}_{-1.65}$	$+1.95_{-2.35}$	$+2.23_{-3.24}$
J2358-1020		$3.29^{+0.28}_{-0.32}$	$+0.61_{-0.48}$	$+0.85_{-0.69}$	$-7.92^{+0.53}_{-0.79}$	$+1.10_{-1.45}$	$+1.35_{-2.04}$
M81		$1.98^{+0.19}_{-0.30}$	$+0.62_{-0.36}$	$+0.62_{-0.58}$	$-5.31^{+0.60}_{-0.46}$	$+0.70_{-1.44}$	$+1.03_{-1.44}$
MG1J183001+1323		$2.54^{+0.58}_{-0.49}$	$+1.24_{-0.90}$	$+1.68_{-1.10}$	$-8.19^{+0.92}_{-1.95}$	$+2.36_{-3.66}$	$+2.44_{-5.21}$
MG1J235704+0447	<i>m</i>	$3.06^{+0.83}_{-0.78}$	$+1.95_{-1.32}$	$+2.43_{-1.43}$	$-9.96^{+1.81}_{-3.03}$	$+3.86_{-6.01}$	$+3.86_{-7.82}$
MG2J043338+3236	<i>m</i>	$2.79^{+1.84}_{-0.66}$	$+2.71_{-0.99}$	$+2.70_{-1.69}$	$-10.12^{+2.91}_{-5.52}$	$+3.21_{-8.80}$	$+5.01_{-8.82}$
MG2J045613+2702		$1.94^{+0.35}_{-0.22}$	$+0.68_{-0.45}$	$+0.79_{-0.69}$	$-6.19^{+0.44}_{-0.84}$	$+1.08_{-1.41}$	$+1.28_{-1.83}$
MG2J174753+2323	<i>m</i>	$1.66^{+2.16}_{-0.77}$	$+3.51_{-0.76}$	$+3.79_{-0.95}$	$-6.07^{+2.00}_{-7.23}$	$+1.95_{-12.01}$	$+1.95_{-12.91}$
MG2J184929+2748	<i>m</i>	$4.16^{+0.90}_{-1.57}$	$+0.92_{-2.59}$	$+1.27_{-2.98}$	$-6.76^{+1.00}_{-6.80}$	$+1.28_{-9.84}$	$+2.10_{-10.22}$
MG2J195919+3847		$1.69^{+0.31}_{-0.33}$	$+0.75_{-0.55}$	$+1.10_{-0.68}$	$-4.87^{+0.64}_{-0.85}$	$+1.00_{-1.96}$	$+1.20_{-3.00}$
MG3J021846+3641		$2.18^{+0.26}_{-0.28}$	$+0.60_{-0.54}$	$+0.76_{-0.65}$	$-6.43^{+0.68}_{-0.61}$	$+1.02_{-1.60}$	$+1.35_{-1.91}$
MG3J025334+3217		$2.60^{+0.31}_{-0.47}$	$+0.89_{-0.79}$	$+1.12_{-0.93}$	$-7.74^{+1.09}_{-0.87}$	$+1.88_{-2.15}$	$+2.08_{-3.09}$
MG4J015630+3913		$2.64^{+0.30}_{-0.31}$	$+0.54_{-0.60}$	$+0.91_{-0.66}$	$-6.82^{+0.60}_{-0.78}$	$+0.99_{-1.65}$	$+1.35_{-2.36}$
MG4J195957+4213		$1.91^{+0.76}_{-0.30}$	$+1.40_{-0.65}$	$+1.91_{-0.84}$	$-5.66^{+0.88}_{-1.80}$	$+1.49_{-3.92}$	$+2.00_{-5.05}$
MG4J202932+4925		$1.91^{+0.29}_{-0.21}$	$+0.57_{-0.40}$	$+0.81_{-0.48}$	$-5.67^{+0.54}_{-0.46}$	$+0.78_{-1.13}$	$+0.94_{-1.35}$
MS14588+2249		$2.66^{+0.92}_{-0.55}$	$+1.46_{-1.12}$	$+1.97_{-1.23}$	$-8.91^{+1.84}_{-2.34}$	$+2.71_{-4.96}$	$+3.10_{-6.00}$
NGC1068	<i>m</i>	$-0.68^{+1.98}_{-0.79}$	$+4.44_{-0.79}$	$+5.41_{-0.79}$	$-16.77^{+6.60}_{-1.94}$	$+12.53_{-2.13}$	$+14.05_{-2.17}$
NGC1218		$1.98^{+0.29}_{-0.22}$	$+0.66_{-0.45}$	$+0.74_{-0.65}$	$-5.73^{+0.46}_{-0.68}$	$+1.15_{-1.41}$	$+1.33_{-1.77}$
NRAO676	<i>m</i>	$3.13^{+0.85}_{-0.83}$	$+2.00_{-1.17}$	$+2.35_{-1.43}$	$-9.06^{+2.59}_{-2.24}$	$+3.65_{-5.94}$	$+4.06_{-7.44}$

Table C.1: Results of fitting the simple power-law model over the 1290 selected observations from OVRO dataset. Flag refers to sources well-defined by the model, being (*m*) objects with a $\sigma(\beta)_{68.3\%} \in [1.5, 3]$ (medium quality) and (*ℓ*) to $\sigma(\beta)_{68.3\%} > 3$ (low quality). The absence of a flag means having $\sigma(\beta)_{68.3\%} < 1.5$.

Name	Flag	β	$\beta^{95.5\%}$	$\beta^{99.7\%}$	$\log A$	$\log A^{95.5\%}$	$\log A^{99.7\%}$
NVSSJ020344+304238		$2.18^{+0.21}_{-0.28}$	$+0.46$ -0.57	$+0.93$ -0.65	$-5.84^{+0.47}_{-0.51}$	$+0.85$ -1.33	$+1.06$ -2.38
NVSSJ025357+510256		$2.07^{+0.37}_{-0.30}$	$+0.95$ -0.50	$+1.20$ -0.57	$-5.98^{+0.75}_{-0.88}$	$+1.12$ -2.40	$+1.27$ -3.17
NVSSJ030943-074427	<i>ℓ</i>	$0.20^{+3.77}_{-0.61}$	$+4.57$ -1.69	$+5.03$ -1.69	$-16.76^{+5.11}_{-2.19}$	$+11.29$ -2.19	$+13.37$ -2.24
NVSSJ033223-111951	<i>ℓ</i>	$-0.62^{+2.45}_{-0.85}$	$+4.79$ -0.88	$+5.75$ -0.87	$-17.90^{+6.50}_{-2.08}$	$+12.81$ -2.10	$+15.40$ -2.10
NVSSJ070651+774137	<i>m</i>	$2.74^{+1.69}_{-0.62}$	$+2.44$ -1.06	$+2.63$ -1.56	$-10.05^{+2.34}_{-5.16}$	$+2.66$ -8.80	$+4.19$ -8.87
NVSSJ090226+205045		$2.75^{+0.40}_{-0.51}$	$+0.94$ -0.89	$+1.41$ -1.13	$-8.29^{+1.32}_{-1.20}$	$+2.11$ -2.62	$+2.74$ -4.22
NVSSJ210833-160724	<i>m</i>	$2.72^{+1.39}_{-0.83}$	$+2.61$ -1.02	$+2.61$ -1.46	$-9.91^{+3.08}_{-4.07}$	$+3.53$ -8.30	$+4.23$ -9.02
NVSSJ231101+020504		$2.62^{+0.59}_{-0.61}$	$+1.78$ -0.94	$+2.07$ -1.08	$-8.44^{+1.45}_{-1.97}$	$+2.20$ -5.82	$+2.59$ -7.07
OM484		$3.43^{+0.47}_{-0.46}$	$+1.09$ -0.77	$+1.26$ -1.04	$-8.83^{+1.05}_{-1.37}$	$+1.81$ -3.05	$+2.75$ -3.05
PB00198	<i>m</i>	$4.46^{+0.64}_{-1.07}$	$+0.77$ -2.40	$+0.79$ -3.12	$-15.50^{+3.09}_{-2.48}$	$+7.57$ -2.50	$+9.58$ -2.50
PKS 0214-085		$2.28^{+0.64}_{-0.47}$	$+1.31$ -0.75	$+1.46$ -0.94	$-7.41^{+1.40}_{-1.86}$	$+1.98$ -3.67	$+2.36$ -4.44
PKS 0459+060		$2.52^{+0.46}_{-0.39}$	$+1.06$ -0.64	$+1.59$ -0.74	$-6.42^{+0.55}_{-1.47}$	$+1.10$ -3.11	$+1.62$ -4.14
PKS 0519+01	<i>m</i>	$4.69^{+0.34}_{-1.87}$	$+0.45$ -3.05	$+0.65$ -3.74	$-15.95^{+5.60}_{-1.97}$	$+9.10$ -2.02	$+11.30$ -2.02
PKS 0648-16		$2.55^{+0.36}_{-0.45}$	$+0.85$ -0.66	$+1.06$ -0.86	$-6.92^{+0.90}_{-1.10}$	$+1.52$ -2.38	$+2.07$ -2.80
PKS 0723-008		$3.37^{+0.36}_{-0.46}$	$+0.70$ -0.95	$+1.20$ -0.99	$-7.16^{+0.69}_{-1.46}$	$+1.66$ -2.58	$+2.15$ -3.75
PKS 0727-115		$2.35^{+0.34}_{-0.16}$	$+0.62$ -0.28	$+0.83$ -0.45	$-4.79^{+0.37}_{-0.66}$	$+0.70$ -1.24	$+1.04$ -1.97
PKS 0855-19		$2.38^{+0.52}_{-0.38}$	$+1.15$ -0.96	$+1.91$ -0.96	$-6.21^{+1.10}_{-1.24}$	$+2.12$ -3.18	$+2.15$ -5.07
PKS 1217+02		$2.91^{+0.78}_{-0.46}$	$+1.43$ -0.92	$+1.96$ -1.05	$-8.69^{+1.18}_{-2.39}$	$+2.46$ -4.23	$+2.81$ -5.69
PKS 1348+007		$1.88^{+0.32}_{-0.21}$	$+0.51$ -0.49	$+0.88$ -0.57	$-5.96^{+0.29}_{-0.98}$	$+0.91$ -1.45	$+1.19$ -2.38
PKS 1508-05	<i>ℓ</i>	$1.77^{+2.50}_{-1.59}$	$+3.14$ -3.13	$+3.62$ -3.27	$-16.71^{+7.90}_{-3.28}$	$+12.28$ -3.29	$+14.81$ -3.28
PKS 1509+022		$2.19^{+0.34}_{-0.26}$	$+0.75$ -0.42	$+0.89$ -0.60	$-6.64^{+0.64}_{-0.90}$	$+1.08$ -1.82	$+1.36$ -2.37
PKS 1510-089		$2.53^{+0.25}_{-0.16}$	$+0.42$ -0.39	$+0.63$ -0.45	$-4.87^{+0.56}_{-0.31}$	$+0.88$ -0.85	$+1.00$ -1.34
PKS 1728+004		$2.74^{+0.32}_{-0.36}$	$+0.67$ -0.71	$+0.93$ -0.80	$-7.58^{+0.80}_{-0.94}$	$+1.47$ -2.12	$+1.77$ -2.63
PKS 1734+063		$2.40^{+0.29}_{-0.42}$	$+0.80$ -0.61	$+1.23$ -0.69	$-6.84^{+0.89}_{-0.87}$	$+1.50$ -2.01	$+1.76$ -3.13
PKS 1830-211		$3.41^{+0.39}_{-0.39}$	$+0.83$ -0.68	$+1.17$ -0.82	$-7.43^{+1.26}_{-0.75}$	$+2.02$ -1.94	$+2.40$ -2.86
PKS 2320-021		$2.16^{+0.41}_{-0.67}$	$+1.38$ -0.93	$+1.87$ -1.11	$-7.01^{+1.17}_{-1.82}$	$+2.14$ -4.37	$+2.27$ -5.90
PMN J0124-0624	<i>m</i>	$4.73^{+0.59}_{-2.13}$	$+0.76$ -3.98	$+0.74$ -5.95	$-17.20^{+6.79}_{-1.70}$	$+10.71$ -1.69	$+13.49$ -1.75
PMN J0643+0857		$2.36^{+0.31}_{-0.17}$	$+0.62$ -0.30	$+0.84$ -0.41	$-6.26^{+0.36}_{-0.66}$	$+0.73$ -1.18	$+0.93$ -1.55
PMN J0656-032		$2.61^{+0.19}_{-0.35}$	$+0.51$ -0.48	$+0.57$ -0.65	$-6.01^{+0.52}_{-0.63}$	$+0.83$ -1.46	$+1.26$ -1.55
PMN J0709-0255		$2.36^{+0.45}_{-0.47}$	$+1.22$ -0.68	$+1.49$ -0.82	$-6.62^{+1.29}_{-1.08}$	$+1.98$ -3.29	$+2.04$ -3.99

Table C.1: Results of fitting the simple power-law model over the 1290 selected observations from OVRO dataset. Flag refers to sources well-defined by the model, being (*m*) objects with a $\sigma(\beta)_{68.3\%} \in [1.5, 3]$ (medium quality) and (*ℓ*) to $\sigma(\beta)_{68.3\%} > 3$ (low quality). The absence of a flag means having $\sigma(\beta)_{68.3\%} < 1.5$.

Name	Flag	β	$\beta^{95.5\%}$	$\beta^{99.7\%}$	$\log A$	$\log A^{95.5\%}$	$\log A^{99.7\%}$
PMN J0721+0406		$2.59^{+0.28}_{-0.35}$	$+0.77_{-0.45}$	$+0.95_{-0.58}$	$-6.34^{+0.86}_{-0.70}$	$+1.09_{-1.89}$	$+1.31_{-2.36}$
PMN J0746-0709	<i>m</i>	$2.30^{+1.70}_{-0.55}$	$+2.79_{-0.78}$	$+3.11_{-1.17}$	$-8.28^{+2.14}_{-5.17}$	$+1.97_{-9.47}$	$+3.17_{-9.71}$
PMN J0906-0905	<i>m</i>	$3.54^{+0.65}_{-0.86}$	$+1.48_{-1.23}$	$+1.96_{-1.80}$	$-10.97^{+2.65}_{-1.91}$	$+3.79_{-4.77}$	$+4.91_{-6.39}$
PMN J0941-0754	<i>m</i>	$2.60^{+1.68}_{-1.15}$	$+2.43_{-3.45}$	$+2.59_{-4.01}$	$-9.72^{+1.42}_{-6.75}$	$+3.78_{-8.28}$	$+6.38_{-8.22}$
PMN J1238-1959		$2.32^{+0.31}_{-0.43}$	$+0.73_{-0.71}$	$+0.90_{-1.10}$	$-6.78^{+0.93}_{-0.92}$	$+1.44_{-2.01}$	$+2.32_{-2.40}$
PMN J1318-1235	<i>ℓ</i>	$-0.68^{+3.27}_{-0.81}$	$+5.45_{-0.79}$	$+6.12_{-0.80}$	$-17.55^{+6.54}_{-2.39}$	$+12.16_{-2.37}$	$+14.60_{-2.38}$
PMN J1420-1118	<i>ℓ</i>	$1.80^{+1.83}_{-1.81}$	$+2.62_{-3.24}$	$+3.52_{-3.30}$	$-6.66^{+1.30}_{-8.15}$	$+2.19_{-11.45}$	$+4.29_{-12.24}$
PMN J2016-0903	<i>m</i>	$2.42^{+1.78}_{-0.79}$	$+2.97_{-0.88}$	$+3.07_{-1.42}$	$-8.62^{+2.05}_{-6.07}$	$+2.09_{-10.27}$	$+3.51_{-10.38}$
PMN J2324+0801	<i>m</i>	$-0.24^{+1.66}_{-1.23}$	$+4.11_{-1.25}$	$+4.90_{-1.25}$	$-16.74^{+6.64}_{-2.18}$	$+11.85_{-2.27}$	$+13.21_{-2.26}$
RGBJ2056+496	<i>ℓ</i>	$1.76^{+2.31}_{-0.85}$	$+3.37_{-2.64}$	$+3.50_{-3.24}$	$-7.02^{+1.74}_{-7.92}$	$+1.86_{-11.58}$	$+3.09_{-11.91}$
RXJ0132.6-0804	<i>ℓ</i>	$1.30^{+3.83}_{-0.75}$	$+3.97_{-2.51}$	$+4.14_{-2.80}$	$-16.70^{+6.11}_{-2.25}$	$+12.33_{-2.24}$	$+14.85_{-2.24}$
RXJ1931.1+0937	<i>m</i>	$2.44^{+1.88}_{-0.63}$	$+2.99_{-0.93}$	$+3.04_{-1.31}$	$-8.34^{+2.25}_{-5.73}$	$+2.27_{-10.78}$	$+3.08_{-11.64}$
S40859+47		$2.29^{+0.44}_{-0.31}$	$+0.86_{-0.45}$	$+0.86_{-0.70}$	$-6.47^{+0.89}_{-1.05}$	$+1.07_{-2.24}$	$+1.69_{-2.41}$
S40900+42		$2.09^{+0.86}_{-0.46}$	$+1.73_{-0.86}$	$+2.48_{-0.98}$	$-6.46^{+1.05}_{-2.55}$	$+2.02_{-4.84}$	$+2.15_{-7.20}$
S40913+39		$2.63^{+0.28}_{-0.34}$	$+0.57_{-0.54}$	$+0.96_{-0.71}$	$-6.73^{+0.61}_{-0.81}$	$+1.11_{-1.50}$	$+1.45_{-2.47}$
S51027+74		$2.25^{+0.24}_{-0.28}$	$+0.59_{-0.50}$	$+0.71_{-0.70}$	$-5.58^{+0.47}_{-0.72}$	$+0.95_{-1.33}$	$+1.33_{-1.71}$
TB0110+6805		$2.10^{+0.35}_{-0.32}$	$+0.85_{-0.58}$	$+0.94_{-0.74}$	$-6.92^{+0.71}_{-1.04}$	$+1.35_{-2.39}$	$+1.69_{-2.86}$
TB0423+4150		$2.96^{+0.54}_{-0.32}$	$+0.96_{-0.68}$	$+1.36_{-0.96}$	$-7.88^{+0.79}_{-1.50}$	$+1.56_{-2.80}$	$+2.28_{-3.96}$
TB0754-1147		$3.23^{+0.73}_{-0.51}$	$+1.58_{-0.99}$	$+2.20_{-1.22}$	$-9.14^{+1.39}_{-2.31}$	$+2.31_{-5.21}$	$+2.89_{-6.73}$
TXS 0106+612		$1.92^{+0.29}_{-0.19}$	$+0.61_{-0.31}$	$+0.80_{-0.40}$	$-4.88^{+0.37}_{-0.58}$	$+0.62_{-1.24}$	$+0.77_{-1.82}$
TXS 0259+681		$2.87^{+0.42}_{-0.37}$	$+0.97_{-0.60}$	$+1.15_{-0.88}$	$-8.07^{+1.06}_{-0.95}$	$+1.80_{-2.22}$	$+2.52_{-2.67}$
TXS 0329+654	<i>m</i>	$4.46^{+0.76}_{-1.46}$	$+0.91_{-2.62}$	$+1.02_{-2.99}$	$-11.76^{+1.77}_{-5.83}$	$+4.04_{-7.24}$	$+5.44_{-7.24}$
TXS 0330+291	<i>m</i>	$2.46^{+1.25}_{-0.77}$	$+2.70_{-1.05}$	$+3.00_{-1.33}$	$-8.74^{+2.65}_{-3.57}$	$+2.64_{-9.32}$	$+3.29_{-10.09}$
TXS 0354+599		$2.28^{+0.35}_{-0.28}$	$+0.67_{-0.66}$	$+0.89_{-0.72}$	$-6.57^{+0.70}_{-0.94}$	$+1.60_{-1.59}$	$+1.83_{-2.45}$
TXS 0529+483		$2.87^{+0.35}_{-0.38}$	$+0.75_{-0.60}$	$+1.01_{-0.78}$	$-7.07^{+1.03}_{-0.68}$	$+1.45_{-1.70}$	$+1.92_{-2.41}$
TXS 0646-176		$3.45^{+0.63}_{-0.56}$	$+1.29_{-0.98}$	$+1.87_{-1.06}$	$-9.43^{+1.30}_{-2.03}$	$+2.40_{-3.98}$	$+2.87_{-5.29}$
TXS 0657+172		$2.68^{+0.45}_{-0.26}$	$+0.84_{-0.57}$	$+1.02_{-0.71}$	$-7.03^{+0.53}_{-1.19}$	$+1.23_{-2.23}$	$+1.64_{-2.37}$
TXS 0700-197		$2.16^{+0.39}_{-0.24}$	$+0.75_{-0.55}$	$+1.00_{-0.67}$	$-5.59^{+0.83}_{-0.69}$	$+1.35_{-1.81}$	$+1.45_{-2.40}$
TXS 0745-165		$2.12^{+0.91}_{-0.56}$	$+2.60_{-0.87}$	$+3.21_{-0.89}$	$-6.39^{+1.71}_{-2.32}$	$+2.35_{-8.53}$	$+2.35_{-11.61}$
TXS 0936-173		$2.48^{+0.48}_{-0.29}$	$+1.00_{-0.50}$	$+1.16_{-0.77}$	$-7.47^{+0.91}_{-0.95}$	$+1.39_{-2.28}$	$+1.74_{-2.85}$

Table C.1: Results of fitting the simple power-law model over the 1290 selected observations from OVRO dataset. Flag refers to sources well-defined by the model, being (*m*) objects with a $\sigma(\beta)_{68.3\%} \in [1.5, 3]$ (medium quality) and (*ℓ*) to $\sigma(\beta)_{68.3\%} > 3$ (low quality). The absence of a flag means having $\sigma(\beta)_{68.3\%} < 1.5$.

Name	Flag	β	$\beta^{95.5\%}$	$\beta^{99.7\%}$	$\log A$	$\log A^{95.5\%}$	$\log A^{99.7\%}$
TXS 1801+253		$2.32^{+0.35}_{-0.35}$	$+0.84$ -0.56	$+1.20$ -0.76	$-7.01^{+0.79}_{-0.94}$	$+1.25$ -2.19	$+1.59$ -2.97
TXS 1827+062		$2.78^{+0.47}_{-0.44}$	$+0.79$ -1.02	$+1.31$ -1.00	$-7.43^{+0.91}_{-1.43}$	$+2.19$ -2.53	$+2.40$ -3.77
TXS 2016+386		$1.31^{+0.16}_{-0.22}$	$+0.39$ -0.42	$+0.61$ -0.50	$-4.22^{+0.37}_{-0.41}$	$+0.80$ -0.93	$+0.84$ -1.43
TXS 2157+102		$2.01^{+0.47}_{-0.32}$	$+0.95$ -0.57	$+1.08$ -0.83	$-6.72^{+0.94}_{-1.07}$	$+1.37$ -2.38	$+1.74$ -2.82
TXS 2206+650		$1.30^{+0.24}_{-0.25}$	$+0.88$ -0.45	$+1.49$ -0.45	$-3.78^{+0.51}_{-0.57}$	$+0.73$ -2.51	$+0.77$ -4.17
VER J0521+211		$2.28^{+0.48}_{-0.36}$	$+0.94$ -0.74	$+1.40$ -0.83	$-7.11^{+0.98}_{-1.20}$	$+1.69$ -2.91	$+2.00$ -3.53
WNB1016.6+8038	<i>m</i>	$3.42^{+1.56}_{-0.27}$	$+1.89$ -1.08	$+2.07$ -1.66	$-11.31^{+2.31}_{-3.57}$	$+2.80$ -6.57	$+4.52$ -6.61
WNB1609.6+8517	<i>ℓ</i>	$4.37^{+0.90}_{-2.39}$	$+1.01$ -5.29	$+1.10$ -5.80	$-16.96^{+6.51}_{-1.91}$	$+11.53$ -1.98	$+14.07$ -2.02
Z8276	<i>ℓ</i>	$-0.52^{+2.35}_{-0.97}$	$+5.13$ -0.97	$+5.69$ -0.97	$-16.95^{+5.24}_{-2.05}$	$+11.75$ -2.05	$+14.00$ -2.05

Table C.2: Results of fitting the broken power-law model over the 1290 selected observations from OVRO dataset. Break significance refers to the source having a possible break frequency being (1σ) at 68.3%, (2σ) at 95.5% and (3σ) at 99.7%. The absence of break significance means that the source is not well-fitted at any level.

Name	Break significance	β_l	$\beta_l^{95.5\%}$	$\beta_l^{99.7\%}$	β_h	$\beta_h^{95.5\%}$	$\beta_h^{99.7\%}$	$\log f_{br}$	$\log f_{br}^{95.5\%}$	$\log f_{br}^{99.7\%}$	$\log A$	$\log A^{95.5\%}$	$\log A^{99.7\%}$
0010+405		1.92 ^{+0.66} _{-0.97}	+1.20 -3.41	+3.17 -3.41	2.74 ^{+1.09} _{-0.82}	+2.72 -1.52	+2.71 -2.84	-2.04 ^{+0.14} _{-1.11}	+0.68 -1.14	+0.86 -1.14	-6.88 ^{+1.67} _{-1.98}	+2.30 -4.80	+3.88 -5.40
0059+581		2.20 ^{+0.56} _{-1.06}	+0.97 -3.11	+1.03 -3.70	2.29 ^{+1.32} _{-0.62}	+2.97 -2.81	+3.09 -3.69	-3.04 ^{+1.42} _{-0.29}	+1.93 -0.22	+1.96 -0.28	-4.17 ^{+1.03} _{-2.31}	+4.03 -3.78	+4.34 -5.23
0136+176		3.17 ^{+2.04} _{-0.83}	+2.31 -3.31	+2.31 -4.65	3.51 ^{+1.99} _{-1.52}	+1.99 -4.25	+2.00 -4.93	-2.91 ^{+1.07} _{-0.24}	+1.54 -0.26	+1.63 -0.26	-11.85 ^{+5.55} _{-2.77}	+8.03 -4.98	+9.06 -6.76
0224+671		2.42 ^{+1.06} _{-1.99}	+1.52 -3.77	+2.82 -3.89	3.86 ^{+0.90} _{-0.73}	+1.64 -1.01	+1.63 -1.75	-2.79 ^{+0.38} _{-0.31}	+0.95 -0.38	+1.38 -0.38	-9.33 ^{+1.21} _{-2.30}	+2.45 -3.61	+3.64 -4.00
0241+622		2.38 ^{+0.89} _{-1.01}	+1.01 -3.78	+1.79 -3.88	2.95 ^{+1.30} _{-1.00}	+2.53 -2.08	+2.52 -3.86	-2.90 ^{+1.07} _{-0.28}	+1.64 -0.27	+1.74 -0.27	-7.71 ^{+1.96} _{-2.39}	+3.30 -5.40	+5.66 -5.40
0300+471		2.39 ^{+0.67} _{-0.87}	+1.79 -3.41	+3.10 -3.88	2.53 ^{+1.39} _{-0.86}	+2.89 -2.96	+2.92 -3.99	-1.39 ^{+0.07} _{-1.61}	+0.28 -1.89	+0.31 -1.93	-5.89 ^{+1.47} _{-2.57}	+4.07 -4.41	+4.75 -5.61
0333+321		2.67 ^{+0.77} _{-0.55}	+2.19 -1.77	+2.68 -3.76	2.32 ^{+1.85} _{-0.94}	+3.17 -2.57	+3.16 -3.66	-1.50 ^{+0.28} _{-1.25}	+0.21 -1.82	+0.30 -1.82	-6.13 ^{+1.84} _{-3.25}	+3.15 -6.61	+4.67 -6.81
0355+508		2.79 ^{+1.13} _{-1.10}	+2.65 -2.34	+2.67 -3.93	1.86 ^{+2.74} _{-0.61}	+3.08 -3.17	+3.63 -3.17	-3.04 ^{+1.23} _{-0.28}	+1.74 -0.28	+1.85 -0.28	-3.60 ^{+1.96} _{-4.99}	+2.91 -8.75	+4.07 -10.37
0415+379	1 σ	1.35 ^{+1.20} _{-1.51}	+1.67 -2.84	+3.33 -2.81	3.29 ^{+1.01} _{-0.31}	+1.78 -0.67	+2.17 -0.87	-2.89 ^{+0.44} _{-0.22}	+0.64 -0.42	+1.08 -0.43	-7.11 ^{+0.51} _{-2.42}	+1.54 -3.87	+1.94 -4.76
0536+145		2.33 ^{+1.13} _{-0.90}	+2.50 -2.68	+2.95 -3.80	2.56 ^{+1.59} _{-0.89}	+2.91 -1.66	+2.94 -3.45	-2.92 ^{+1.03} _{-0.25}	+1.56 -0.25	+1.64 -0.25	-6.68 ^{+1.66} _{-2.98}	+3.10 -5.85	+4.41 -6.57
0836+710		2.65 ^{+0.92} _{-1.62}	+1.06 -3.92	+1.70 -4.08	3.44 ^{+1.97} _{-0.51}	+2.06 -2.72	+2.06 -4.60	-2.96 ^{+0.81} _{-0.36}	+1.57 -0.32	+1.63 -0.36	-8.59 ^{+2.20} _{-3.60}	+4.79 -5.29	+7.24 -5.29
0859-140		-0.41 ^{+3.29} _{-1.09}	+5.48 -1.08	+5.90 -1.09	-0.55 ^{+2.62} _{-0.94}	+5.40 -0.90	+6.01 -0.94	-2.95 ^{+1.04} _{-0.21}	+1.61 -0.19	+1.67 -0.23	-17.11 ^{+6.13} _{-2.83}	+13.53 -2.87	+15.27 -2.86
1243-072		2.25 ^{+1.14} _{-1.05}	+2.46 -2.69	+2.46 -3.58	2.81 ^{+2.25} _{-0.78}	+2.69 -3.17	+2.69 -3.93	-2.84 ^{+0.91} _{-0.30}	+1.42 -0.28	+1.44 -0.34	-8.43 ^{+2.84} _{-3.76}	+6.16 -5.49	+6.62 -7.03
1406-076		2.99 ^{+1.00} _{-1.42}	+1.19 -3.92	+1.59 -4.37	3.94 ^{+1.39} _{-0.84}	+1.56 -3.73	+1.54 -5.35	-2.99 ^{+0.97} _{-0.33}	+1.68 -0.26	+1.68 -0.33	-10.10 ^{+2.54} _{-2.91}	+6.65 -4.19	+9.14 -4.82
1458+718		5.04 ^{+0.46} _{-1.15}	+0.46 -2.57	+0.45 -3.59	4.11 ^{+1.39} _{-2.56}	+1.39 -5.14	+1.39 -5.59	-1.60 ^{+0.33} _{-0.80}	+0.29 -1.49	+0.33 -1.56	-12.53 ^{+6.61} _{-1.77}	+8.97 -4.09	+10.84 -5.09
1655+077		3.34 ^{+0.88} _{-0.82}	+2.10 -2.10	+2.10 -4.69	3.40 ^{+1.95} _{-1.02}	+2.05 -4.00	+2.05 -4.87	-1.57 ^{+0.40} _{-1.00}	+0.37 -1.57	+0.40 -1.61	-8.92 ^{+2.57} _{-3.56}	+6.72 -4.43	+7.37 -6.20
1845+797		2.89 ^{+1.29} _{-1.15}	+2.16 -3.68	+2.34 -4.39	3.21 ^{+2.13} _{-0.76}	+2.26 -3.50	+2.26 -4.65	-2.91 ^{+0.99} _{-0.26}	+1.67 -0.23	+1.74 -0.26	-9.22 ^{+2.81} _{-4.09}	+6.42 -5.62	+7.51 -6.59
1923+210		2.71 ^{+1.75} _{-1.19}	+2.80 -3.19	+2.80 -4.14	4.35 ^{+1.11} _{-2.36}	+1.11 -4.98	+1.14 -5.84	-2.88 ^{+0.99} _{-0.30}	+1.57 -0.24	+1.60 -0.30	-10.66 ^{+5.32} _{-2.72}	+8.25 -5.17	+9.09 -6.33
1924+507		4.87 ^{+0.63} _{-1.97}	+0.62 -3.84	+0.62 -5.24	4.03 ^{+1.47} _{-2.45}	+1.45 -4.80	+1.46 -5.48	-2.25 ^{+0.89} _{-0.31}	+0.99 -0.78	+0.99 -0.91	-10.22 ^{+3.77} _{-4.90}	+7.00 -7.61	+8.15 -9.61
1926+42		1.50 ^{+1.05} _{-1.04}	+1.61 -2.70	+2.12 -2.84	1.99 ^{+2.25} _{-0.55}	+3.50 -0.94	+3.50 -2.83	-2.72 ^{+0.96} _{-0.27}	+1.43 -0.35	+1.44 -0.45	-6.18 ^{+1.18} _{-4.28}	+2.01 -7.66	+3.67 -8.85
1RXS002209.2-185333		4.61 ^{+0.75} _{-2.37}	+0.89 -4.12	+0.87 -5.31	3.64 ^{+1.51} _{-2.10}	+1.76 -4.47	+1.82 -5.09	-1.49 ^{+0.27} _{-1.11}	+0.25 -1.67	+0.29 -1.73	-9.42 ^{+2.46} _{-5.33}	+5.72 -8.27	+6.61 -9.91
1RXSJ154604.6+08191		2.17 ^{+2.90} _{-1.48}	+3.01 -3.38	+3.33 -3.62	1.24 ^{+2.89} _{-1.42}	+3.64 -2.74	+4.23 -2.74	-1.73 ^{+0.39} _{-0.88}	+0.34 -1.48	+0.41 -1.49	-17.62 ^{+6.32} _{-2.28}	+12.36 -2.22	+14.93 -2.32
2005+403		2.15 ^{+1.06} _{-0.88}	+2.15 -3.13	+3.32 -3.59	2.09 ^{+1.94} _{-0.76}	+3.28 -1.85	+3.33 -3.21	-1.43 ^{+0.24} _{-1.18}	+0.25 -1.68	+0.27 -1.75	-5.41 ^{+1.61} _{-3.34}	+2.58 -6.10	+4.25 -7.32
2021+317		2.64 ^{+1.35} _{-0.90}	+2.81 -2.17	+2.80 -4.11	2.93 ^{+2.55} _{-0.90}	+2.56 -3.58	+2.55 -4.41	-1.59 ^{+0.30} _{-0.99}	+0.28 -1.55	+0.31 -1.59	-5.92 ^{+1.83} _{-5.27}	+3.78 -8.17	+4.91 -10.27

Table C.2: Results of fitting the broken power-law model over the 1290 selected observations from OVRO dataset. Break significance refers to the source having a possible break frequency being (1σ) at 68.3%, (2σ) at 95.5% and (3σ) at 99.7%. The absence of break significance means that the source is not well-fitted at any level.

Name	Break significance	β_l	$\beta_l^{95.5\%}$	$\beta_l^{99.7\%}$	β_h	$\beta_h^{95.5\%}$	$\beta_h^{99.7\%}$	$\log f_{br}$	$\log f_{br}^{95.5\%}$	$\log f_{br}^{99.7\%}$	$\log A$	$\log A^{95.5\%}$	$\log A^{99.7\%}$
CR1928-0456		4.82 ^{+0.68} _{-1.30}	+0.68 -3.22	+0.68 -5.50	4.03 ^{+1.12} _{-2.70}	+1.43 -4.63	+1.47 -5.49	-1.69 ^{+0.34} _{-0.95}	+0.41 -1.47	+0.41 -1.60	-12.91 ^{+4.42} _{-3.82}	+8.56 -4.80	+10.71 -6.25
CR2228-0753		2.42 ^{+0.73} _{-0.89}	+1.64 -3.25	+2.25 -3.76	2.90 ^{+1.59} _{-1.02}	+2.57 -1.78	+2.58 -3.63	-2.41 ^{+0.48} _{-0.90}	+1.16 -0.87	+1.20 -0.92	-9.06 ^{+2.73} _{-2.47}	+4.07 -5.22	+5.88 -5.67
CRJ0305-0607		5.01 ^{+0.44} _{-1.17}	+0.49 -2.76	+0.49 -5.08	4.61 ^{+0.89} _{-2.74}	+0.89 -5.58	+0.89 -6.07	-1.79 ^{+0.52} _{-0.76}	+0.51 -1.36	+0.53 -1.48	-13.00 ^{+2.85} _{-5.42}	+8.07 -5.52	+9.82 -5.92
CRJ0505-0419		1.70 ^{+0.81} _{-0.98}	+1.56 -3.03	+3.52 -3.14	1.91 ^{+2.01} _{-0.81}	+3.56 -1.37	+3.54 -3.06	-1.56 ^{+0.26} _{-1.07}	+0.19 -1.72	+0.29 -1.72	-5.41 ^{+1.40} _{-4.13}	+2.72 -7.85	+4.01 -9.29
CRJ1012+0630		2.40 ^{+0.85} _{-1.00}	+1.99 -2.87	+2.46 -3.54	3.26 ^{+2.17} _{-0.80}	+2.17 -3.73	+2.23 -4.44	-1.52 ^{+0.25} _{-1.09}	+0.24 -1.67	+0.24 -1.77	-10.05 ^{+4.66} _{-1.56}	+6.03 -5.42	+7.40 -6.84
CRJ1142+1547		4.23 ^{+1.27} _{-2.46}	+1.27 -5.33	+1.27 -5.72	4.37 ^{+1.06} _{-3.39}	+0.98 -5.59	+1.12 -5.86	-1.63 ^{+0.28} _{-1.07}	+0.33 -1.57	+0.34 -1.66	-12.93 ^{+2.79} _{-6.77}	+8.42 -6.83	+10.66 -7.07
CRJ1220+7105	2σ	0.26 ^{+1.18} _{-0.72}	+1.44 -1.77	+2.00 -1.77	3.23 ^{+1.13} _{-0.74}	+2.26 -0.73	+2.26 -1.10	-2.32 ^{+0.15} _{-0.37}	+0.39 -0.58	+0.50 -0.78	-7.89 ^{+1.37} _{-2.39}	+1.57 -4.42	+2.15 -4.65
CRJ1305+7854		3.58 ^{+1.88} _{-0.78}	+1.92 -2.65	+1.92 -5.02	3.34 ^{+2.16} _{-1.19}	+2.15 -3.59	+2.16 -4.59	-3.03 ^{+1.13} _{-0.25}	+1.75 -0.19	+1.75 -0.25	-11.13 ^{+3.23} _{-4.83}	+5.98 -6.92	+8.19 -7.36
CRJ1321+8316	2σ	-0.68 ^{+1.45} _{-0.76}	+2.85 -0.77	+3.84 -0.79	3.75 ^{+0.96} _{-0.90}	+1.66 -1.44	+1.73 -2.06	-2.78 ^{+0.22} _{-0.25}	+0.57 -0.48	+0.96 -0.48	-10.45 ^{+2.25} _{-2.15}	+3.20 -4.13	+4.40 -4.79
CRJ1803+0341	1σ	2.08 ^{+0.48} _{-2.13}	+0.63 -3.50	+1.40 -3.58	3.21 ^{+1.58} _{-0.58}	+2.25 -1.35	+2.25 -2.70	-2.77 ^{+0.33} _{-0.48}	+1.25 -0.51	+1.59 -0.52	-9.44 ^{+2.21} _{-2.81}	+3.77 -4.88	+5.50 -5.21
CRJ1925-1018		2.21 ^{+3.07} _{-1.04}	+3.23 -3.36	+3.27 -3.69	0.84 ^{+2.32} _{-2.24}	+4.29 -2.34	+4.63 -2.34	-2.53 ^{+0.61} _{-0.76}	+1.27 -0.76	+1.37 -0.76	-14.42 ^{+3.85} _{-4.93}	+9.57 -5.57	+11.15 -5.55
CT_1419-0838		1.56 ^{+0.99} _{-1.05}	+1.12 -2.87	+1.60 -3.05	2.48 ^{+1.21} _{-0.58}	+2.69 -0.65	+2.98 -0.96	-2.25 ^{+0.14} _{-0.86}	+0.73 -1.00	+0.84 -1.02	-6.19 ^{+0.84} _{-2.72}	+1.56 -5.22	+1.46 -6.32
CT_1625+4118		2.24 ^{+0.70} _{-1.02}	+0.92 -3.22	+1.67 -3.72	2.95 ^{+2.31} _{-0.13}	+2.55 -1.16	+2.54 -2.69	-2.30 ^{+0.27} _{-0.78}	+0.89 -0.86	+0.96 -0.93	-8.59 ^{+0.49} _{-4.43}	+2.61 -5.02	+4.38 -5.89
CT_2255+2410		2.83 ^{+1.30} _{-1.32}	+2.66 -3.02	+2.62 -4.32	3.54 ^{+1.90} _{-1.31}	+1.91 -4.16	+1.91 -5.02	-2.98 ^{+1.23} _{-0.22}	+1.78 -0.23	+1.83 -0.29	-11.66 ^{+5.15} _{-2.46}	+7.51 -5.56	+8.16 -7.21
GAJ1054+8629		4.60 ^{+0.84} _{-1.06}	+0.90 -3.22	+0.90 -5.79	4.73 ^{+0.73} _{-2.94}	+0.73 -5.71	+0.73 -6.22	-1.61 ^{+0.31} _{-0.99}	+0.30 -1.63	+0.32 -1.69	-14.43 ^{+5.58} _{-2.80}	+9.02 -5.01	+11.06 -5.42
GB10751+485		1.87 ^{+1.40} _{-0.98}	+3.37 -2.12	+3.51 -2.96	2.74 ^{+2.21} _{-0.96}	+2.75 -3.38	+2.75 -4.15	-2.36 ^{+1.14} _{-0.19}	+1.14 -0.77	+1.16 -0.84	-8.53 ^{+3.52} _{-3.06}	+6.34 -6.62	+6.34 -8.96
GB6J0009+0625		1.37 ^{+0.62} _{-0.93}	+0.92 -2.73	+1.84 -2.73	1.87 ^{+1.73} _{-0.71}	+3.60 -0.70	+3.59 -1.45	-1.67 ^{+0.29} _{-1.07}	+0.37 -1.50	+0.47 -1.54	-5.94 ^{+1.22} _{-2.75}	+1.97 -5.20	+1.97 -7.01
GB6J0047+5657		1.93 ^{+0.84} _{-1.46}	+1.79 -2.99	+2.78 -3.32	2.79 ^{+2.44} _{-0.47}	+2.70 -2.20	+2.70 -3.35	-2.75 ^{+0.80} _{-0.46}	+1.66 -0.35	+1.66 -0.65	-8.56 ^{+2.60} _{-3.65}	+4.38 -5.80	+5.68 -6.87
GB6J0515+1527		4.64 ^{+0.85} _{-2.18}	+0.85 -5.22	+0.85 -5.98	3.08 ^{+2.39} _{-1.63}	+2.42 -4.17	+2.40 -4.57	-1.62 ^{+0.30} _{-0.86}	+0.22 -1.60	+0.30 -1.60	-13.15 ^{+3.41} _{-5.46}	+8.16 -6.45	+9.97 -6.75
GB6J0526+6317		4.47 ^{+0.98} _{-3.11}	+1.00 -5.41	+1.00 -5.94	0.32 ^{+2.76} _{-1.62}	+4.85 -1.74	+5.14 -1.81	-2.93 ^{+1.05} _{-0.28}	+1.66 -0.27	+1.73 -0.28	-13.90 ^{+3.84} _{-5.28}	+9.18 -6.10	+10.65 -6.11
GB6J0636+7138	1σ	1.14 ^{+0.96} _{-1.46}	+1.24 -2.54	+1.60 -2.63	2.91 ^{+1.81} _{-0.38}	+2.42 -1.03	+2.55 -1.46	-2.60 ^{+0.29} _{-0.41}	+0.82 -0.58	+1.35 -0.60	-8.76 ^{+1.94} _{-2.62}	+2.59 -4.97	+3.27 -5.61
GB6J0856+7146	2σ	0.58 ^{+1.04} _{-0.47}	+1.32 -1.50	+1.57 -2.00	3.52 ^{+1.59} _{-0.48}	+1.98 -1.24	+1.97 -1.89	-2.24 ^{+0.19} _{-0.20}	+0.53 -0.36	+0.53 -0.74	-8.97 ^{+1.10} _{-3.06}	+2.75 -4.02	+3.41 -4.70
GB6J0922+0433	1σ	0.98 ^{+1.17} _{-1.15}	+1.37 -2.42	+2.56 -2.42	4.15 ^{+0.63} _{-1.77}	+1.24 -2.29	+1.33 -2.66	-2.53 ^{+0.27} _{-0.37}	+0.77 -0.68	+1.17 -0.64	-11.23 ^{+3.76} _{-1.39}	+5.33 -2.40	+6.41 -2.75
GB6J0941+2721		4.30 ^{+0.50} _{-2.48}	+1.20 -3.98	+1.20 -5.59	4.26 ^{+1.21} _{-2.42}	+1.23 -4.72	+1.23 -5.64	-1.71 ^{+0.40} _{-0.87}	+0.38 -1.43	+0.40 -1.50	-8.59 ^{+2.51} _{-5.72}	+4.23 -8.93	+5.73 -9.94

Table C.2: Results of fitting the broken power-law model over the 1290 selected observations from OVRO dataset. Break significance refers to the source having a possible break frequency being (1σ) at 68.3%, (2σ) at 95.5% and (3σ) at 99.7%. The absence of break significance means that the source is not well-fitted at any level.

Name	Break significance	β_l	$\beta_l^{95.5\%}$	$\beta_l^{99.7\%}$	β_h	$\beta_h^{95.5\%}$	$\beta_h^{99.7\%}$	$\log f_{br}$	$\log f_{br}^{95.5\%}$	$\log f_{br}^{99.7\%}$	$\log A$	$\log A^{95.5\%}$	$\log A^{99.7\%}$
GB6J1439+3711		4.64 ^{+0.84} _{-2.51}	+0.84 -5.65	+0.84 -6.13	1.27 ^{+3.05} _{-1.45}	+3.85 -2.71	+4.22 -2.76	-1.78 ^{+0.47} _{-0.79}	+0.47 -1.34	+0.46 -1.44	-16.15 ^{+6.43} _{-2.87}	+11.31 -3.67	+13.05 -3.84
GB6J2102+4702		2.15 ^{+2.75} _{-0.57}	+3.35 -2.34	+3.34 -3.65	2.72 ^{+2.60} _{-1.41}	+2.76 -3.50	+2.75 -4.22	-2.86 ^{+1.06} _{-0.31}	+1.62 -0.30	+1.66 -0.35	-6.51 ^{+3.07} _{-5.47}	+3.76 -10.77	+4.66 -12.08
J0001+1914		4.14 ^{+0.99} _{-1.07}	+1.34 -2.88	+1.35 -5.23	4.60 ^{+0.79} _{-2.61}	+0.81 -5.44	+0.90 -6.03	-1.43 ^{+0.28} _{-1.21}	+0.26 -1.87	+0.30 -1.94	-13.78 ^{+4.72} _{-2.82}	+9.35 -3.41	+10.40 -4.95
J0001-1551		4.99 ^{+0.48} _{-1.27}	+0.51 -2.53	+0.51 -3.37	4.31 ^{+1.16} _{-2.52}	+1.18 -5.06	+1.20 -5.67	-1.56 ^{+0.31} _{-0.87}	+0.32 -1.65	+0.31 -1.81	-12.47 ^{+4.35} _{-3.68}	+8.34 -5.44	+9.74 -6.62
J0004+2019		2.69 ^{+1.46} _{-0.54}	+2.62 -1.27	+2.80 -3.15	2.33 ^{+2.17} _{-1.19}	+3.16 -2.77	+3.14 -3.79	-1.53 ^{+0.40} _{-1.11}	+0.40 -1.73	+0.40 -1.84	-7.76 ^{+2.06} _{-4.67}	+4.14 -6.92	+5.11 -9.13
J0004+4615		2.40 ^{+0.87} _{-0.66}	+2.25 -3.13	+3.09 -3.80	2.47 ^{+2.28} _{-0.78}	+2.94 -3.07	+2.94 -3.97	-1.54 ^{+0.39} _{-1.14}	+0.29 -1.81	+2.94 -1.83	-7.89 ^{+1.69} _{-4.43}	+5.01 -5.95	+5.46 -7.51
J0004-1148		2.26 ^{+0.46} _{-0.70}	+1.22 -3.10	+2.46 -3.67	2.53 ^{+1.69} _{-0.47}	+2.94 -0.71	+2.94 -2.22	-2.04 ^{+0.84} _{-0.60}	+0.75 -1.28	+0.84 -1.29	-6.96 ^{+1.09} _{-2.71}	+1.59 -5.51	+2.89 -6.26
J0005+3820	1 σ	1.33 ^{+0.63} _{-1.04}	+0.95 -2.49	+1.26 -2.79	2.98 ^{+1.61} _{-0.41}	+2.42 -0.72	+2.49 -0.98	-2.33 ^{+0.39} _{-0.32}	+0.45 -0.85	+0.73 -1.03	-7.91 ^{+0.87} _{-3.14}	+2.00 -4.32	+2.16 -4.99
J0006-0623		2.46 ^{+0.56} _{-0.83}	+0.97 -3.32	+1.76 -3.91	2.88 ^{+1.31} _{-0.75}	+2.57 -1.37	+2.58 -3.05	-2.10 ^{+0.15} _{-1.22}	+0.89 -1.15	+0.90 -1.22	-6.43 ^{+1.45} _{-2.42}	+2.50 -5.21	+4.90 -5.53
J0009+0628		1.85 ^{+1.57} _{-1.12}	+3.01 -2.83	+3.52 -3.29	3.13 ^{+1.84} _{-1.52}	+2.38 -3.76	+2.36 -4.51	-2.25 ^{+0.39} _{-1.02}	+0.95 -1.01	+1.03 -1.07	-10.56 ^{+4.35} _{-2.77}	+6.70 -5.83	+7.32 -8.62
J0010+1058	3 σ	-0.58 ^{+0.76} _{-0.92}	+2.02 -0.92	+2.76 -0.91	4.22 ^{+0.64} _{-0.77}	+1.12 -1.09	+1.27 -1.23	-2.79 ^{+0.11} _{-0.15}	+0.24 -0.33	+0.35 -0.42	-10.06 ^{+1.53} _{-1.67}	+2.08 -3.23	+2.72 -3.23
J0010+1724		2.53 ^{+0.79} _{-0.76}	+1.24 -3.35	+2.49 -3.35	3.12 ^{+1.80} _{-1.04}	+2.38 -3.36	+2.38 -4.46	-1.50 ^{+0.38} _{-1.16}	+0.30 -1.86	+0.37 -1.86	-9.69 ^{+2.81} _{-2.62}	+6.19 -4.36	+7.17 -5.74
J0010+2047		1.79 ^{+0.75} _{-1.80}	+0.93 -3.28	+1.85 -3.28	2.54 ^{+1.56} _{-0.59}	+2.91 -0.54	+2.90 -1.23	-2.92 ^{+0.65} _{-0.37}	+1.52 -0.38	+1.68 -0.44	-10.23 ^{+3.44} _{-1.07}	+3.84 -3.67	+4.94 -4.98
J0011+0057	1 σ	1.19 ^{+0.85} _{-1.19}	+1.47 -2.36	+1.67 -2.61	2.81 ^{+1.11} _{-0.75}	+2.23 -0.92	+2.53 -1.15	-2.57 ^{+0.32} _{-0.34}	+0.62 -0.71	+1.11 -0.72	-8.59 ^{+1.95} _{-2.09}	+2.14 -4.81	+2.69 -5.70
J0012+3353	1 σ	1.30 ^{+0.50} _{-2.11}	+1.34 -2.74	+1.84 -2.79	2.76 ^{+1.67} _{-0.64}	+2.51 -1.03	+2.71 -1.72	-2.91 ^{+0.39} _{-0.34}	+1.19 -0.43	+1.63 -0.43	-8.93 ^{+1.69} _{-3.51}	+2.56 -6.18	+4.20 -6.80
J0013+1910		2.09 ^{+0.79} _{-1.51}	+0.70 -3.55	+1.20 -3.55	3.28 ^{+1.68} _{-0.98}	+2.22 -2.66	+2.21 -4.77	-2.87 ^{+0.77} _{-0.45}	+1.74 -0.37	+1.74 -0.49	-9.41 ^{+2.34} _{-3.72}	+4.37 -6.37	+6.58 -6.65
J0013-0423		1.94 ^{+0.62} _{-0.70}	+2.24 -3.20	+3.42 -3.20	2.04 ^{+1.27} _{-0.78}	+3.37 -1.59	+3.37 -2.48	-1.57 ^{+0.34} _{-1.21}	+0.27 -1.75	+0.37 -1.76	-5.49 ^{+1.16} _{-2.09}	+2.53 -5.14	+3.10 -5.88
J0013-1513	1 σ	2.02 ^{+0.47} _{-2.21}	+0.84 -3.42	+1.45 -3.49	3.05 ^{+1.95} _{-0.54}	+2.41 -1.39	+2.45 -1.64	-2.83 ^{+0.39} _{-0.45}	+1.53 -0.49	+1.70 -0.52	-11.31 ^{+4.35} _{-1.27}	+4.58 -3.98	+5.69 -5.34
J0015-1812		2.94 ^{+0.83} _{-0.95}	+2.13 -3.42	+2.40 -4.32	3.23 ^{+1.63} _{-1.19}	+2.26 -2.88	+2.25 -4.31	-3.07 ^{+1.16} _{-0.26}	+1.77 -0.26	+1.87 -0.26	-9.02 ^{+2.60} _{-3.07}	+4.48 -6.13	+6.33 -6.31
J0016-0015	2 σ	0.53 ^{+0.78} _{-0.88}	+1.29 -1.83	+1.81 -1.93	4.02 ^{+0.76} _{-1.07}	+1.46 -1.45	+1.48 -1.78	-2.44 ^{+0.17} _{-0.21}	+0.25 -0.58	+0.36 -0.71	-10.57 ^{+2.96} _{-1.06}	+3.77 -2.77	+4.30 -3.32
J0017+8135		2.22 ^{+0.82} _{-1.31}	+1.10 -3.62	+2.04 -3.68	3.35 ^{+1.20} _{-1.70}	+1.79 -4.12	+2.14 -4.31	-2.84 ^{+0.97} _{-0.47}	+1.53 -0.47	+1.64 -0.49	-7.11 ^{+1.86} _{-4.36}	+3.78 -6.84	+5.07 -8.63
J0017-0512	1 σ	1.33 ^{+0.66} _{-0.96}	+1.15 -2.36	+1.42 -2.64	3.04 ^{+1.26} _{-0.69}	+2.38 -0.71	+2.45 -0.94	-2.06 ^{+0.10} _{-0.57}	+0.35 -0.92	+0.40 -1.28	-7.54 ^{+0.61} _{-3.12}	+1.40 -4.47	+1.86 -4.61
J0019+2021		2.41 ^{+0.50} _{-0.57}	+1.17 -3.00	+2.66 -3.85	2.50 ^{+1.74} _{-0.69}	+2.98 -2.49	+2.98 -3.88	-1.58 ^{+0.44} _{-0.89}	+0.43 -1.70	+0.44 -1.79	-6.56 ^{+1.28} _{-2.61}	+3.55 -4.90	+4.26 -5.85
J0019+2602		2.80 ^{+1.01} _{-0.74}	+1.52 -3.62	+1.94 -4.25	3.33 ^{+1.88} _{-0.51}	+2.09 -2.90	+2.08 -4.72	-3.01 ^{+1.20} _{-0.33}	+1.80 -0.26	+1.80 -0.32	-9.58 ^{+2.74} _{-1.73}	+5.16 -4.01	+7.29 -4.31

Table C.2: Results of fitting the broken power-law model over the 1290 selected observations from OVRO dataset. Break significance refers to the source having a possible break frequency being (1σ) at 68.3%, (2σ) at 95.5% and (3σ) at 99.7%. The absence of break significance means that the source is not well-fitted at any level.

Name	Break significance	β_l	$\beta_l^{95.5\%}$	$\beta_l^{99.7\%}$	β_h	$\beta_h^{95.5\%}$	$\beta_h^{99.7\%}$	$\log f_{br}$	$\log f_{br}^{95.5\%}$	$\log f_{br}^{99.7\%}$	$\log A$	$\log A^{95.5\%}$	$\log A^{99.7\%}$
J0019+7327		3.20 ^{+0.78} _{-1.48}	+1.15 -4.50	+1.93 -4.66	3.79 ^{+1.59} _{-0.50}	+1.71 -1.93	+1.69 -3.52	-3.03 ^{+0.79} _{-0.30}	+1.64 -0.29	+1.83 -0.29	-9.22 ^{+2.20} _{-2.55}	+4.07 -4.25	+6.36 -4.25
J0022+0608		2.08 ^{+0.67} _{-0.91}	+0.99 -3.29	+1.80 -3.54	2.57 ^{+1.22} _{-0.59}	+2.68 -0.71	+2.90 -0.92	-3.02 ^{+1.01} _{-0.29}	+1.66 -0.30	+1.78 -0.30	-6.79 ^{+1.12} _{-2.29}	+0.98 -5.44	+1.78 -5.45
J0022+4525		1.89 ^{+0.97} _{-0.80}	+2.13 -2.73	+3.20 -3.33	2.30 ^{+2.35} _{-0.57}	+2.97 -1.61	+3.19 -2.19	-2.34 ^{+0.35} _{-1.03}	+1.01 -1.03	+1.20 -1.03	-8.31 ^{+3.24} _{-2.77}	+3.45 -6.02	+4.65 -6.94
J0023+4456		2.23 ^{+0.59} _{-0.81}	+2.17 -2.29	+2.65 -3.65	2.41 ^{+2.12} _{-0.83}	+3.07 -2.06	+3.07 -3.36	-1.45 ^{+0.32} _{-1.21}	+0.32 -1.81	+0.33 -1.90	-7.68 ^{+2.18} _{-3.09}	+3.44 -7.25	+5.11 -7.25
J0024+2439		2.26 ^{+0.58} _{-1.27}	+0.98 -3.02	+2.28 -3.75	3.15 ^{+1.83} _{-0.51}	+2.34 -1.81	+2.30 -4.00	-2.56 ^{+0.54} _{-0.62}	+1.21 -0.77	+1.32 -0.79	-9.27 ^{+1.91} _{-3.01}	+3.17 -5.40	+6.02 -5.40
J0027+2241		3.90 ^{+1.38} _{-0.77}	+1.60 -2.13	+1.59 -3.19	4.51 ^{+0.95} _{-2.75}	+0.91 -5.58	+0.95 -5.94	-1.64 ^{+0.49} _{-0.92}	+0.49 -1.65	+0.50 -1.73	-11.90 ^{+3.91} _{-4.71}	+7.88 -5.72	+9.06 -7.11
J0029+0554		1.50 ^{+0.56} _{-0.97}	+1.49 -1.87	+1.49 -2.93	2.57 ^{+1.88} _{-0.79}	+2.91 -0.87	+2.90 -1.70	-2.48 ^{+0.67} _{-0.32}	+1.03 -0.86	+1.16 -0.89	-7.68 ^{+0.81} _{-4.46}	+1.95 -6.75	+2.80 -7.25
J0035-1305		2.49 ^{+1.31} _{-0.82}	+2.39 -2.78	+2.71 -3.94	4.16 ^{+0.61} _{-2.42}	+1.32 -4.26	+1.32 -5.41	-3.10 ^{+1.32} _{-0.26}	+1.82 -0.21	+1.86 -0.26	-11.07 ^{+4.04} _{-2.65}	+6.76 -4.48	+8.01 -6.05
J0037+1109		2.02 ^{+0.55} _{-0.73}	+0.96 -2.45	+1.60 -3.49	2.68 ^{+1.88} _{-0.55}	+2.80 -0.84	+2.80 -1.89	-2.26 ^{+0.30} _{-1.11}	+0.91 -1.10	+1.01 -1.10	-7.86 ^{+1.26} _{-3.04}	+1.98 -5.73	+3.13 -6.23
J0038+1227		2.20 ^{+1.59} _{-0.85}	+3.29 -1.77	+3.29 -2.95	2.75 ^{+2.66} _{-0.63}	+2.73 -2.94	+2.73 -4.23	-1.59 ^{+0.15} _{-1.24}	+0.40 -1.59	+0.40 -1.71	-8.51 ^{+1.47} _{-6.23}	+4.52 -8.04	+6.31 -9.48
J0038+1856		2.31 ^{+0.61} _{-2.08}	+0.87 -3.73	+1.96 -3.81	3.40 ^{+1.50} _{-0.78}	+2.08 -1.82	+2.10 -2.95	-2.91 ^{+0.50} _{-0.41}	+1.46 -0.46	+1.67 -0.45	-10.13 ^{+2.04} _{-3.16}	+4.01 -5.11	+5.06 -5.64
J0038+4137		1.89 ^{+0.81} _{-1.02}	+1.15 -3.26	+2.41 -3.31	2.68 ^{+1.79} _{-0.88}	+2.80 -1.57	+2.79 -3.38	-3.04 ^{+1.05} _{-0.26}	+1.79 -0.28	+1.90 -0.32	-8.41 ^{+2.29} _{-3.37}	+3.30 -6.51	+5.57 -6.72
J0039+1411		2.20 ^{+1.31} _{-0.67}	+3.11 -1.65	+3.11 -3.65	2.34 ^{+2.28} _{-0.68}	+3.16 -2.40	+3.16 -3.28	-1.58 ^{+0.32} _{-1.08}	+0.32 -1.71	+0.34 -1.78	-7.81 ^{+1.23} _{-5.22}	+3.74 -7.20	+4.98 -9.50
J0040-0146		1.55 ^{+0.82} _{-0.76}	+1.57 -2.45	+2.47 -2.90	2.38 ^{+1.91} _{-1.05}	+3.11 -2.07	+3.10 -3.52	-2.41 ^{+1.10} _{-0.19}	+1.10 -0.87	+1.19 -0.91	-6.98 ^{+1.80} _{-3.76}	+2.57 -7.57	+4.45 -7.57
J0042+1009		3.41 ^{+1.45} _{-0.85}	+1.99 -2.78	+2.07 -4.60	3.68 ^{+1.27} _{-1.98}	+1.79 -4.08	+1.81 -4.77	-3.10 ^{+1.27} _{-0.26}	+1.79 -0.25	+1.86 -0.26	-10.41 ^{+3.14} _{-4.13}	+6.00 -6.01	+6.84 -7.72
J0042+2320		2.16 ^{+0.55} _{-0.94}	+1.12 -3.18	+1.51 -3.64	2.47 ^{+1.72} _{-0.62}	+3.02 -1.39	+3.02 -2.71	-3.03 ^{+1.15} _{-0.24}	+1.82 -0.24	+1.90 -0.33	-8.66 ^{+2.57} _{-1.91}	+3.78 -4.96	+5.11 -4.97
J0046+3900		2.26 ^{+0.85} _{-1.00}	+1.40 -3.36	+2.20 -3.76	3.01 ^{+1.96} _{-0.88}	+2.48 -2.50	+2.48 -4.42	-2.54 ^{+0.53} _{-0.82}	+1.28 -0.82	+1.39 -0.83	-10.67 ^{+3.26} _{-2.52}	+5.38 -4.75	+7.45 -4.94
J0047+2435		2.03 ^{+0.66} _{-1.05}	+0.92 -2.89	+2.28 -3.49	2.63 ^{+1.91} _{-0.58}	+2.87 -1.90	+2.87 -3.13	-2.12 ^{+0.32} _{-1.02}	+0.91 -1.08	+0.91 -1.20	-9.17 ^{+2.14} _{-2.72}	+3.76 -5.43	+5.39 -5.43
J0048+3157	2 σ	1.64 ^{+1.01} _{-1.47}	+1.24 -3.00	+1.91 -3.08	3.69 ^{+1.04} _{-0.34}	+1.72 -0.68	+1.81 -0.86	-2.78 ^{+0.23} _{-0.26}	+0.53 -0.54	+0.72 -0.58	-9.42 ^{+0.77} _{-2.40}	+1.67 -3.86	+2.34 -4.40
J0049+0237		2.31 ^{+0.50} _{-1.36}	+0.86 -3.45	+1.26 -3.75	2.84 ^{+1.14} _{-0.64}	+2.59 -0.89	+2.59 -2.72	-2.58 ^{+0.62} _{-0.60}	+1.09 -0.78	+1.28 -0.78	-7.78 ^{+1.31} _{-2.19}	+1.92 -5.06	+4.38 -5.44
J0049+5128		2.50 ^{+0.81} _{-1.95}	+0.99 -3.85	+2.80 -3.96	4.01 ^{+1.41} _{-0.83}	+1.45 -2.08	+1.47 -2.73	-2.87 ^{+0.41} _{-0.44}	+1.40 -0.43	+1.66 -0.45	-11.10 ^{+2.50} _{-2.86}	+4.56 -3.94	+5.72 -4.25
J0050-0452	1 σ	0.98 ^{+1.02} _{-0.95}	+1.39 -2.12	+1.44 -2.46	3.28 ^{+1.23} _{-0.68}	+2.09 -1.00	+2.22 -1.20	-2.33 ^{+0.16} _{-0.41}	+0.40 -0.77	+0.48 -0.95	-8.68 ^{+2.21} _{-1.78}	+2.36 -4.06	+3.06 -4.06
J0050-0929		1.81 ^{+0.69} _{-0.81}	+0.85 -2.46	+0.85 -3.28	2.70 ^{+1.67} _{-0.30}	+2.56 -0.55	+2.80 -0.70	-2.29 ^{+0.32} _{-0.68}	+0.78 -1.00	+0.95 -1.08	-6.44 ^{+0.59} _{-3.00}	+1.12 -4.98	+1.50 -5.70
J0051-0650		2.30 ^{+0.82} _{-0.76}	+2.82 -1.61	+2.95 -3.64	2.22 ^{+2.16} _{-0.82}	+3.24 -2.77	+3.25 -3.59	-1.49 ^{+0.28} _{-1.22}	+0.22 -1.81	+0.28 -1.85	-6.12 ^{+1.36} _{-3.83}	+3.76 -6.54	+4.73 -7.47

Table C.2: Results of fitting the broken power-law model over the 1290 selected observations from OVRO dataset. Break significance refers to the source having a possible break frequency being (1σ) at 68.3%, (2σ) at 95.5% and (3σ) at 99.7%. The absence of break significance means that the source is not well-fitted at any level.

Name	Break significance	β_l	$\beta_l^{95.5\%}$	$\beta_l^{99.7\%}$	β_h	$\beta_h^{95.5\%}$	$\beta_h^{99.7\%}$	$\log f_{br}$	$\log f_{br}^{95.5\%}$	$\log f_{br}^{99.7\%}$	$\log A$	$\log A^{95.5\%}$	$\log A^{99.7\%}$
J0121+0422		2.35 ^{+0.62} _{-1.06}	+0.93 -3.56	+2.61 -3.85	2.87 ^{+1.77} _{-0.71}	+2.62 -1.59	+2.62 -3.83	-2.46 ^{+0.43} _{-0.87}	+1.18 -0.83	+1.25 -0.88	-7.63 ^{+2.26} _{-2.68}	+2.80 -5.74	+5.73 -5.73
J0121+1149		2.23 ^{+0.85} _{-1.32}	+0.87 -3.47	+1.99 -3.69	3.21 ^{+0.65} _{-1.02}	+2.16 -1.12	+2.27 -1.61	-2.98 ^{+0.65} _{-0.38}	+1.63 -0.38	+1.82 -0.38	-7.41 ^{+1.07} _{-2.46}	+2.09 -4.97	+2.74 -5.60
J0122+2502		2.34 ^{+0.79} _{-0.77}	+1.24 -3.34	+1.52 -3.72	3.28 ^{+1.60} _{-1.30}	+2.21 -3.23	+2.22 -4.53	-2.98 ^{+1.19} _{-0.34}	+1.85 -0.27	+1.85 -0.37	-10.43 ^{+3.92} _{-1.83}	+6.11 -4.66	+7.52 -5.19
J0123+2615		3.10 ^{+1.15} _{-1.24}	+2.29 -3.24	+2.29 -4.56	4.31 ^{+1.00} _{-2.37}	+1.14 -5.44	+1.18 -5.81	-3.07 ^{+1.26} _{-0.29}	+1.86 -0.27	+1.95 -0.29	-11.33 ^{+3.57} _{-4.50}	+6.67 -5.92	+9.07 -7.11
J0125-0005		2.33 ^{+0.71} _{-0.92}	+0.95 -3.63	+2.06 -3.63	2.72 ^{+1.69} _{-0.67}	+2.78 -1.33	+2.78 -2.87	-2.38 ^{+0.32} _{-0.94}	+0.99 -0.93	+1.06 -0.94	-7.63 ^{+1.71} _{-3.00}	+2.51 -6.05	+4.85 -6.05
J0126+2559	1 σ	1.74 ^{+0.53} _{-1.88}	+0.66 -3.23	+1.25 -3.24	3.21 ^{+1.69} _{-0.68}	+2.24 -1.24	+2.28 -1.88	-2.77 ^{+0.36} _{-0.46}	+1.34 -0.59	+1.56 -0.59	-10.01 ^{+3.47} _{-1.61}	+4.10 -4.15	+4.56 -5.13
J0127-0821		2.40 ^{+1.25} _{-1.30}	+1.38 -3.58	+2.04 -3.88	3.49 ^{+1.45} _{-1.07}	+1.98 -2.74	+2.00 -4.65	-3.04 ^{+1.06} _{-0.33}	+1.68 -0.31	+1.80 -0.33	-11.27 ^{+3.56} _{-1.72}	+5.37 -4.71	+8.40 -4.75
J0128+4901	2 σ	0.92 ^{+0.39} _{-0.75}	+1.05 -1.59	+1.21 -2.20	2.97 ^{+0.91} _{-0.44}	+2.05 -0.82	+2.50 -1.01	-2.20 ^{+0.14} _{-0.28}	+0.38 -0.60	+0.45 -0.98	-6.27 ^{+1.06} _{-1.46}	+1.56 -3.61	+1.84 -4.57
J0130+0842	2 σ	-0.44 ^{+0.86} _{-0.94}	+2.04 -1.06	+2.62 -1.07	3.70 ^{+0.95} _{-0.77}	+1.78 -1.11	+1.78 -1.56	-2.78 ^{+0.18} _{-0.18}	+0.33 -0.44	+0.52 -0.57	-9.89 ^{+0.98} _{-3.20}	+2.21 -4.73	+3.07 -5.07
J0131+3834		3.05 ^{+1.17} _{-0.97}	+2.30 -2.94	+2.33 -4.40	2.95 ^{+2.54} _{-0.86}	+2.55 -3.51	+2.54 -4.32	-1.55 ^{+0.43} _{-1.14}	+0.35 -1.79	+0.43 -1.81	-9.48 ^{+3.46} _{-3.36}	+5.92 -6.14	+6.70 -7.12
J0132+4325		2.15 ^{+0.72} _{-0.92}	+1.00 -3.27	+1.31 -3.59	2.63 ^{+1.09} _{-0.63}	+2.87 -0.97	+2.87 -2.03	-3.05 ^{+1.16} _{-0.32}	+1.82 -0.30	+1.90 -0.32	-6.64 ^{+1.28} _{-1.78}	+1.54 -4.92	+2.89 -5.82
J0132-1654		2.58 ^{+0.77} _{-1.08}	+0.94 -3.57	+1.60 -3.99	3.04 ^{+1.32} _{-0.70}	+2.43 -1.92	+2.44 -3.63	-3.05 ^{+1.12} _{-0.20}	+1.74 -0.26	+1.80 -0.31	-7.32 ^{+1.84} _{-2.23}	+2.80 -4.51	+5.37 -5.12
J0136+4751		2.38 ^{+0.83} _{-1.63}	+1.05 -3.57	+2.24 -3.83	3.14 ^{+1.05} _{-0.57}	+2.18 -0.90	+2.28 -1.27	-2.92 ^{+0.45} _{-0.40}	+1.30 -0.43	+1.75 -0.44	-6.34 ^{+1.11} _{-2.45}	+1.45 -5.81	+2.49 -5.82
J0140-1532		2.22 ^{+0.97} _{-0.90}	+1.76 -3.68	+3.17 -3.68	2.47 ^{+1.84} _{-1.09}	+3.01 -2.39	+2.99 -3.57	-2.78 ^{+0.92} _{-0.56}	+1.52 -0.51	+1.54 -0.59	-8.04 ^{+2.22} _{-3.64}	+3.76 -6.58	+5.03 -8.21
J0141-0202		2.35 ^{+0.93} _{-1.15}	+1.38 -3.77	+2.81 -3.77	2.93 ^{+1.71} _{-1.05}	+2.56 -2.00	+2.55 -4.27	-3.07 ^{+1.07} _{-0.30}	+1.73 -0.30	+1.82 -0.30	-9.39 ^{+2.44} _{-3.38}	+4.18 -5.90	+7.31 -6.73
J0141-0928	2 σ	1.40 ^{+0.55} _{-1.68}	+0.68 -2.82	+1.42 -2.87	3.19 ^{+0.93} _{-0.42}	+2.07 -0.60	+2.22 -0.82	-2.79 ^{+0.46} _{-0.22}	+0.77 -0.43	+1.42 -0.51	-7.86 ^{+0.77} _{-2.19}	+1.46 -4.00	+1.75 -4.52
J0143+4129		1.67 ^{+0.67} _{-1.30}	+1.02 -2.79	+1.07 -3.15	2.95 ^{+0.93} _{-0.95}	+2.35 -0.94	+2.49 -1.22	-2.62 ^{+0.51} _{-0.34}	+0.98 -0.69	+1.27 -0.72	-8.29 ^{+1.98} _{-2.27}	+2.06 -5.23	+2.63 -5.67
J0148+3854		2.08 ^{+0.74} _{-0.77}	+0.87 -3.38	+1.96 -3.56	2.65 ^{+1.71} _{-0.64}	+2.83 -1.92	+2.83 -3.75	-2.98 ^{+1.08} _{-0.39}	+1.80 -0.34	+1.85 -0.39	-8.06 ^{+1.15} _{-3.42}	+2.99 -6.36	+5.11 -6.36
J0148+4215		2.86 ^{+1.97} _{-0.53}	+2.63 -1.26	+2.63 -2.51	4.55 ^{+0.59} _{-2.89}	+0.92 -5.11	+0.94 -6.00	-1.56 ^{+0.32} _{-0.99}	+0.32 -1.69	+0.32 -1.78	-11.21 ^{+4.69} _{-3.26}	+8.05 -6.09	+8.23 -7.70
J0149+0555	1 σ	0.56 ^{+1.15} _{-0.88}	+1.70 -1.85	+2.19 -2.00	2.77 ^{+1.82} _{-0.57}	+2.72 -0.71	+2.73 -1.40	-2.57 ^{+0.18} _{-0.31}	+0.47 -0.59	+0.53 -0.79	-10.60 ^{+3.36} _{-2.17}	+4.12 -4.29	+5.93 -4.29
J0149+1857		2.94 ^{+0.51} _{-0.76}	+1.55 -3.03	+2.35 -4.22	3.35 ^{+2.14} _{-0.56}	+2.14 -3.72	+2.13 -4.84	-1.45 ^{+0.31} _{-1.16}	+0.31 -1.83	+0.32 -1.92	-9.39 ^{+2.49} _{-2.56}	+5.47 -4.63	+6.89 -4.81
J0151+2744		2.27 ^{+0.99} _{-0.75}	+2.39 -3.00	+3.03 -3.41	2.54 ^{+2.17} _{-0.59}	+2.92 -2.03	+2.93 -2.96	-2.91 ^{+1.41} _{-0.13}	+1.71 -0.44	+1.79 -0.45	-7.88 ^{+2.16} _{-3.04}	+3.50 -5.72	+4.39 -6.98
J0151-1732	1 σ	-0.59 ^{+1.92} _{-0.27}	+2.63 -0.91	+3.28 -0.91	2.61 ^{+1.24} _{-0.43}	+2.34 -0.72	+2.76 -0.90	-2.85 ^{+0.26} _{-0.28}	+0.70 -0.52	+1.18 -0.51	-8.04 ^{+1.00} _{-2.93}	+1.67 -5.74	+2.16 -6.98
J0152+2207		2.53 ^{+0.82} _{-0.97}	+1.01 -3.81	+2.43 -3.95	2.99 ^{+1.57} _{-1.07}	+2.43 -3.26	+2.44 -4.35	-2.99 ^{+1.21} _{-0.37}	+1.86 -0.31	+1.86 -0.38	-7.61 ^{+1.50} _{-3.41}	+5.38 -4.51	+6.34 -5.98

Table C.2: Results of fitting the broken power-law model over the 1290 selected observations from OVRO dataset. Break significance refers to the source having a possible break frequency being (1σ) at 68.3%, (2σ) at 95.5% and (3σ) at 99.7%. The absence of break significance means that the source is not well-fitted at any level.

Name	Break significance	β_l	$\beta_l^{95.5\%}$	$\beta_l^{99.7\%}$	β_h	$\beta_h^{95.5\%}$	$\beta_h^{99.7\%}$	$\log f_{br}$	$\log f_{br}^{95.5\%}$	$\log f_{br}^{99.7\%}$	$\log A$	$\log A^{95.5\%}$	$\log A^{99.7\%}$
J0154+4743		2.59 ^{+0.64} _{-0.91}	+2.64 -2.52	+2.64 -3.97	2.67 ^{+2.13} _{-0.91}	+2.83 -3.14	+2.81 -4.13	-1.39 ^{+0.27} _{-1.28}	+0.20 -1.93	+0.26 -1.98	-7.72 ^{+2.21} _{-3.60}	+4.39 -6.21	+5.50 -6.82
J0202+3943		2.67 ^{+0.85} _{-0.70}	+2.71 -2.46	+2.71 -4.14	2.72 ^{+1.94} _{-0.47}	+2.77 -2.41	+2.75 -4.21	-3.13 ^{+1.35} _{-0.22}	+1.99 -0.16	+1.99 -0.24	-8.14 ^{+1.02} _{-3.67}	+3.48 -6.18	+5.24 -6.35
J0202+4205		3.07 ^{+0.79} _{-0.82}	+2.21 -2.14	+2.32 -4.10	3.11 ^{+2.26} _{-0.75}	+2.36 -3.18	+2.36 -4.48	-1.53 ^{+0.39} _{-1.12}	+0.35 -1.79	+0.39 -1.84	-9.56 ^{+3.44} _{-2.64}	+5.25 -5.67	+6.95 -6.05
J0202-0559		1.25 ^{+1.11} _{-2.62}	+3.82 -2.60	+4.09 -2.73	2.40 ^{+2.87} _{-0.85}	+3.08 -3.03	+3.07 -3.84	-2.64 ^{+0.52} _{-0.73}	+1.17 -0.73	+1.28 -0.73	-9.28 ^{+3.48} _{-5.40}	+4.67 -10.08	+5.94 -10.65
J0203+1134		2.60 ^{+0.64} _{-0.55}	+1.10 -3.36	+1.92 -3.64	2.70 ^{+2.11} _{-0.81}	+2.76 -2.92	+2.76 -4.15	-1.43 ^{+0.31} _{-1.20}	+0.31 -1.87	+0.31 -1.93	-7.28 ^{+1.09} _{-3.94}	+3.58 -5.66	+5.04 -5.76
J0203+7232		2.82 ^{+0.72} _{-0.62}	+2.38 -0.91	+2.60 -1.82	2.87 ^{+1.98} _{-0.95}	+2.62 -2.99	+2.62 -4.20	-1.47 ^{+0.26} _{-1.00}	+0.25 -1.78	+2.88 -1.85	-9.12 ^{+2.88} _{-2.43}	+4.91 -5.63	+6.60 -6.34
J0204+1514		2.51 ^{+0.60} _{-1.52}	+0.77 -3.99	+1.56 -3.97	3.17 ^{+1.23} _{-0.50}	+2.03 -0.98	+2.32 -1.54	-2.72 ^{+0.36} _{-0.62}	+1.24 -0.65	+1.54 -0.65	-8.27 ^{+1.32} _{-2.24}	+2.44 -4.14	+3.41 -5.47
J0204+4005		3.58 ^{+0.94} _{-1.08}	+1.89 -3.81	+1.89 -4.77	4.29 ^{+1.20} _{-1.84}	+1.20 -4.98	+1.20 -5.75	-3.11 ^{+1.34} _{-0.26}	+1.88 -0.24	+1.97 -0.26	-13.07 ^{+5.08} _{-2.25}	+8.66 -3.78	+10.36 -3.92
J0204-1701		2.45 ^{+0.84} _{-0.67}	+2.33 -2.50	+2.83 -3.88	2.56 ^{+1.71} _{-0.71}	+2.92 -1.56	+2.94 -3.06	-2.41 ^{+1.17} _{-0.31}	+1.09 -0.95	+1.45 -0.95	-6.68 ^{+1.45} _{-3.22}	+2.47 -6.36	+4.37 -6.44
J0205+3212	1 σ	1.76 ^{+1.04} _{-1.87}	+1.77 -3.22	+2.53 -3.23	4.16 ^{+1.09} _{-0.48}	+1.29 -1.16	+1.33 -1.70	-2.78 ^{+0.12} _{-0.41}	+0.49 -0.58	+0.83 -0.58	-11.08 ^{+1.71} _{-2.16}	+3.59 -2.60	+4.62 -3.04
J0206-1150	1 σ	-0.11 ^{+1.39} _{-1.20}	+2.74 -1.37	+3.68 -1.36	3.09 ^{+0.56} _{-0.46}	+1.29 -0.66	+1.64 -0.96	-2.86 ^{+0.18} _{-0.35}	+0.60 -0.44	+0.78 -0.51	-8.22 ^{+1.02} _{-1.35}	+1.52 -3.19	+2.15 -3.67
J0209+1352		2.20 ^{+0.57} _{-0.62}	+1.68 -3.00	+3.11 -3.62	2.50 ^{+1.51} _{-0.65}	+3.00 -0.67	+3.00 -3.24	-1.99 ^{+0.56} _{-0.92}	+0.65 -1.38	+0.74 -1.38	-7.31 ^{+0.64} _{-3.29}	+1.42 -5.77	+4.77 -5.77
J0209+7229	2 σ	0.45 ^{+0.93} _{-1.47}	+1.83 -1.92	+2.27 -1.94	3.33 ^{+0.65} _{-0.77}	+1.63 -0.99	+2.15 -1.09	-2.83 ^{+0.29} _{-0.24}	+0.70 -0.48	+1.02 -0.48	-8.74 ^{+1.84} _{-1.27}	+2.13 -3.31	+2.43 -4.33
J0211+1051		2.46 ^{+0.64} _{-0.48}	+3.01 -2.43	+3.01 -3.92	2.57 ^{+1.57} _{-0.88}	+2.91 -2.98	+2.91 -3.87	-1.38 ^{+0.26} _{-1.31}	+0.23 -1.93	+1.36 -1.97	-5.99 ^{+1.36} _{-2.47}	+3.99 -4.13	+4.50 -5.29
J0211-1558		2.39 ^{+0.76} _{-0.82}	+1.39 -2.59	+2.71 -3.64	3.78 ^{+1.14} _{-1.69}	+1.72 -3.77	+1.72 -5.06	-2.46 ^{+1.22} _{-0.10}	+1.21 -0.76	+1.22 -0.91	-10.77 ^{+3.46} _{-2.26}	+7.30 -3.21	+8.35 -4.22
J0215-0222		2.33 ^{+1.00} _{-1.14}	+2.79 -2.63	+3.10 -3.68	2.57 ^{+2.26} _{-0.81}	+2.73 -2.61	+2.89 -4.01	-1.60 ^{+0.34} _{-1.14}	+0.28 -1.75	+0.35 -1.76	-7.31 ^{+1.27} _{-4.40}	+3.07 -7.20	+5.25 -7.34
J0217+0144		2.65 ^{+0.57} _{-0.83}	+1.66 -3.92	+2.68 -4.10	2.77 ^{+1.15} _{-0.53}	+2.65 -1.21	+2.65 -2.14	-1.73 ^{+0.10} _{-1.64}	+0.40 -1.63	+0.48 -1.64	-7.01 ^{+0.81} _{-2.41}	+1.83 -4.95	+2.93 -5.14
J0217+0837		2.35 ^{+0.77} _{-1.46}	+1.01 -3.85	+2.59 -3.85	2.79 ^{+0.90} _{-0.90}	+2.67 -1.09	+2.67 -2.41	-3.06 ^{+0.88} _{-0.31}	+1.81 -0.31	+1.92 -0.31	-7.17 ^{+1.23} _{-2.32}	+2.29 -5.28	+3.57 -6.10
J0217+7349		2.43 ^{+0.60} _{-1.37}	+0.69 -3.64	+1.27 -3.87	2.94 ^{+1.81} _{-0.61}	+2.50 -3.02	+2.50 -4.15	-2.89 ^{+0.99} _{-0.44}	+1.79 -0.31	+1.79 -0.44	-7.19 ^{+1.56} _{-3.04}	+4.48 -5.38	+5.71 -6.68
J0219+0120		1.75 ^{+0.78} _{-0.55}	+1.80 -2.65	+3.64 -2.94	2.08 ^{+2.00} _{-0.73}	+3.37 -0.90	+3.41 -2.18	-1.76 ^{+0.44} _{-0.81}	+0.48 -1.52	+0.52 -1.60	-6.41 ^{+1.36} _{-3.62}	+1.73 -7.42	+2.92 -7.42
J0219+4727		3.45 ^{+1.39} _{-1.47}	+2.05 -4.08	+2.05 -4.80	4.58 ^{+0.91} _{-2.08}	+0.92 -4.84	+0.92 -5.92	-3.08 ^{+1.20} _{-0.29}	+1.82 -0.29	+1.94 -0.29	-14.38 ^{+5.69} _{-1.78}	+9.36 -3.38	+10.84 -4.12
J0219-1842	1 σ	2.15 ^{+0.71} _{-1.17}	+1.17 -3.06	+1.36 -3.61	3.53 ^{+1.69} _{-0.18}	+1.93 -0.97	+1.96 -1.73	-2.48 ^{+0.20} _{-0.64}	+0.74 -0.82	+1.22 -0.88	-9.54 ^{+0.96} _{-3.22}	+2.55 -4.18	+3.68 -4.82
J0220-1305		-0.34 ^{+3.92} _{-0.48}	+5.67 -0.87	+5.81 -1.12	1.05 ^{+1.83} _{-2.52}	+4.00 -2.53	+4.43 -2.53	-2.98 ^{+1.25} _{-0.22}	+1.65 -0.39	+1.74 -0.39	-15.04 ^{+3.93} _{-4.94}	+10.28 -4.89	+12.66 -4.66
J0221+3556		1.89 ^{+0.63} _{-0.57}	+1.15 -3.00	+2.46 -3.38	2.22 ^{+1.88} _{-0.67}	+3.28 -1.41	+3.26 -3.64	-1.83 ^{+0.68} _{-0.73}	+0.68 -1.45	+0.69 -1.54	-6.18 ^{+1.65} _{-2.70}	+2.08 -6.44	+4.43 -6.44

Table C.2: Results of fitting the broken power-law model over the 1290 selected observations from OVRO dataset. Break significance refers to the source having a possible break frequency being (1σ) at 68.3%, (2σ) at 95.5% and (3σ) at 99.7%. The absence of break significance means that the source is not well-fitted at any level.

Name	Break significance	β_l	$\beta_l^{95.5\%}$	$\beta_l^{99.7\%}$	β_h	$\beta_h^{95.5\%}$	$\beta_h^{99.7\%}$	$\log f_{br}$	$\log f_{br}^{95.5\%}$	$\log f_{br}^{99.7\%}$	$\log A$	$\log A^{95.5\%}$	$\log A^{99.7\%}$
J0222-1615	3σ	$-0.12^{+0.29}_{-1.01}$	$+0.83_{-1.38}$	$+1.20_{-1.38}$	$4.40^{+0.76}_{-1.02}$	$+1.01_{-1.87}$	$+1.07_{-2.22}$	$-2.45^{+0.11}_{-0.09}$	$+0.26_{-0.23}$	$+0.30_{-0.38}$	$-9.31^{+0.95}_{-2.97}$	$+2.44_{-3.86}$	$+2.90_{-4.31}$
J0224+0659		$2.64^{+0.60}_{-1.70}$	$+0.88_{-4.14}$	$+2.56_{-4.14}$	$3.10^{+1.31}_{-0.80}$	$+2.33_{-1.80}$	$+2.40_{-3.59}$	$-3.02^{+0.93}_{-0.32}$	$+1.70_{-0.32}$	$+1.81_{-0.32}$	$-7.52^{+1.12}_{-2.95}$	$+2.94_{-5.28}$	$+5.27_{-5.28}$
J0225+1846		$2.52^{+0.58}_{-2.13}$	$+0.98_{-3.67}$	$+1.73_{-4.01}$	$3.14^{+1.02}_{-0.55}$	$+2.01_{-1.32}$	$+2.29_{-2.76}$	$-2.99^{+0.70}_{-0.36}$	$+1.85_{-0.31}$	$+1.85_{-0.38}$	$-8.54^{+1.28}_{-2.00}$	$+2.37_{-4.28}$	$+5.06_{-4.44}$
J0226-1843		$2.57^{+0.90}_{-0.81}$	$+1.54_{-3.09}$	$+2.76_{-3.99}$	$2.93^{+1.86}_{-0.54}$	$+2.55_{-1.83}$	$+2.53_{-3.73}$	$-2.59^{+0.56}_{-0.76}$	$+1.23_{-0.70}$	$+1.24_{-0.76}$	$-9.08^{+2.47}_{-2.40}$	$+3.32_{-5.25}$	$+5.98_{-5.25}$
J0230+4032		$2.26^{+0.92}_{-1.38}$	$+1.14_{-3.40}$	$+1.56_{-3.74}$	$3.29^{+0.90}_{-0.58}$	$+2.17_{-0.54}$	$+2.20_{-0.98}$	$-2.31^{+0.14}_{-0.86}$	$+0.61_{-1.06}$	$+0.93_{-1.06}$	$-8.58^{+0.99}_{-2.15}$	$+1.33_{-4.23}$	$+2.02_{-4.65}$
J0231+1322		$2.30^{+0.63}_{-2.15}$	$+0.77_{-3.77}$	$+1.49_{-3.77}$	$3.23^{+1.19}_{-1.02}$	$+2.18_{-1.33}$	$+2.24_{-1.56}$	$-2.85^{+0.44}_{-0.38}$	$+1.22_{-0.50}$	$+1.43_{-0.51}$	$-8.53^{+1.55}_{-3.44}$	$+3.11_{-5.10}$	$+3.67_{-5.46}$
J0237+0526		$1.92^{+1.48}_{-1.37}$	$+1.99_{-3.32}$	$+3.41_{-3.33}$	$4.09^{+1.18}_{-1.91}$	$+1.40_{-4.37}$	$+1.41_{-5.32}$	$-2.92^{+0.95}_{-0.41}$	$+1.70_{-0.33}$	$+1.70_{-0.41}$	$-8.76^{+1.68}_{-5.81}$	$+3.84_{-9.31}$	$+5.79_{-9.31}$
J0237+2848		$2.45^{+0.71}_{-1.20}$	$+0.89_{-3.57}$	$+1.84_{-3.91}$	$2.89^{+0.92}_{-0.60}$	$+2.56_{-0.82}$	$+2.56_{-1.66}$	$-3.04^{+0.98}_{-0.33}$	$+1.81_{-0.30}$	$+1.91_{-0.33}$	$-6.53^{+1.53}_{-1.43}$	$+1.94_{-4.30}$	$+2.78_{-5.28}$
J0237+3022		$2.79^{+1.27}_{-1.27}$	$+1.45_{-4.03}$	$+2.24_{-4.24}$	$4.28^{+1.19}_{-1.76}$	$+1.20_{-4.57}$	$+1.19_{-5.69}$	$-3.09^{+1.13}_{-0.28}$	$+1.77_{-0.28}$	$+1.85_{-0.27}$	$-12.62^{+5.65}_{-1.45}$	$+8.37_{-3.65}$	$+10.37_{-4.47}$
J0238+1636		$2.36^{+0.60}_{-1.51}$	$+0.87_{-3.35}$	$+1.83_{-3.85}$	$2.99^{+0.89}_{-0.38}$	$+2.18_{-0.69}$	$+2.46_{-1.01}$	$-3.00^{+0.89}_{-0.34}$	$+1.63_{-0.36}$	$+1.87_{-0.37}$	$-6.11^{+0.78}_{-1.45}$	$+1.33_{-3.49}$	$+1.58_{-4.58}$
J0239+0416		$2.10^{+0.81}_{-0.79}$	$+1.12_{-3.58}$	$+2.74_{-3.58}$	$3.05^{+1.78}_{-0.24}$	$+2.45_{-0.41}$	$+2.44_{-0.66}$	$-2.20^{+0.20}_{-0.75}$	$+0.51_{-1.08}$	$+0.82_{-1.11}$	$-11.62^{+4.20}_{-0.15}$	$+4.80_{-1.19}$	$+5.03_{-1.72}$
J0239-0234		$2.44^{+0.72}_{-0.74}$	$+1.40_{-3.56}$	$+2.91_{-3.64}$	$2.66^{+1.24}_{-0.90}$	$+2.80_{-2.07}$	$+2.84_{-3.59}$	$-1.53^{+-0.24}_{-1.76}$	$+0.19_{-1.84}$	$+0.29_{-1.83}$	$-6.92^{+1.09}_{-3.16}$	$+3.18_{-5.41}$	$+4.73_{-5.90}$
J0240+1848		$4.99^{+0.50}_{-1.80}$	$+0.50_{-3.27}$	$+0.50_{-6.32}$	$4.36^{+0.60}_{-2.99}$	$+1.12_{-4.77}$	$+1.13_{-5.84}$	$-1.61^{+0.17}_{-1.32}$	$+0.36_{-1.68}$	$+0.36_{-1.77}$	$-10.31^{+4.29}_{-4.24}$	$+5.96_{-7.62}$	$+7.44_{-8.59}$
J0241-0815		$3.01^{+0.68}_{-1.04}$	$+1.72_{-4.25}$	$+2.48_{-4.42}$	$3.23^{+1.14}_{-1.06}$	$+2.17_{-3.39}$	$+2.17_{-4.42}$	$-3.10^{+1.22}_{-0.25}$	$+1.86_{-0.17}$	$+1.86_{-0.26}$	$-8.19^{+2.62}_{-1.84}$	$+5.48_{-3.93}$	$+6.28_{-4.99}$
J0242+1101		$3.28^{+0.78}_{-0.63}$	$+1.33_{-3.16}$	$+2.21_{-4.69}$	$3.83^{+1.21}_{-1.28}$	$+1.66_{-3.81}$	$+1.67_{-5.01}$	$-1.43^{+0.30}_{-1.29}$	$+0.30_{-1.85}$	$+0.30_{-1.93}$	$-10.05^{+2.37}_{-2.81}$	$+6.92_{-3.66}$	$+7.56_{-4.65}$
J0242+1742		$1.99^{+0.59}_{-1.46}$	$+0.84_{-3.29}$	$+2.13_{-3.41}$	$2.67^{+1.75}_{-0.64}$	$+2.81_{-1.07}$	$+2.81_{-3.25}$	$-2.66^{+0.49}_{-0.65}$	$+1.22_{-0.66}$	$+1.42_{-0.70}$	$-8.18^{+1.44}_{-3.29}$	$+2.48_{-6.67}$	$+4.53_{-6.67}$
J0242+2653		$0.95^{+1.00}_{-1.38}$	$+1.40_{-2.33}$	$+3.26_{-2.42}$	$2.26^{+2.03}_{-0.48}$	$+3.23_{-0.67}$	$+3.22_{-1.36}$	$-2.72^{+0.26}_{-0.41}$	$+0.85_{-0.63}$	$+1.26_{-0.63}$	$-8.49^{+1.78}_{-4.13}$	$+3.39_{-6.19}$	$+3.82_{-7.14}$
J0243+7120		$2.98^{+1.72}_{-0.82}$	$+2.51_{-2.98}$	$+2.51_{-4.33}$	$4.10^{+1.32}_{-2.17}$	$+1.36_{-4.80}$	$+1.35_{-5.59}$	$-1.67^{+0.21}_{-1.30}$	$+0.47_{-1.59}$	$+0.49_{-1.64}$	$-9.11^{+2.43}_{-5.39}$	$+5.24_{-7.90}$	$+6.65_{-9.15}$
J0243-0550		$2.05^{+0.88}_{-1.58}$	$+1.21_{-3.55}$	$+2.69_{-3.55}$	$3.37^{+1.16}_{-0.76}$	$+2.07_{-0.88}$	$+2.11_{-1.39}$	$-2.83^{+0.47}_{-0.39}$	$+1.01_{-0.52}$	$+1.28_{-0.53}$	$-9.04^{+1.27}_{-2.90}$	$+2.22_{-4.50}$	$+3.10_{-5.30}$
J0246-1236		$3.04^{+0.95}_{-1.04}$	$+1.66_{-3.79}$	$+2.28_{-4.47}$	$3.86^{+1.62}_{-1.08}$	$+1.62_{-3.82}$	$+1.62_{-5.14}$	$-3.03^{+1.20}_{-0.33}$	$+1.68_{-0.32}$	$+1.79_{-0.33}$	$-11.55^{+3.43}_{-2.49}$	$+6.78_{-4.16}$	$+9.20_{-4.31}$
J0249+0619		$1.98^{+0.77}_{-1.19}$	$+1.26_{-2.92}$	$+2.74_{-3.42}$	$2.98^{+1.69}_{-0.81}$	$+2.47_{-1.35}$	$+2.47_{-3.57}$	$-2.49^{+0.34}_{-0.76}$	$+1.15_{-0.85}$	$+1.28_{-0.85}$	$-9.79^{+2.77}_{-2.32}$	$+4.41_{-4.32}$	$+6.59_{-5.17}$
J0251+3734		$2.98^{+1.30}_{-1.20}$	$+2.30_{-3.63}$	$+2.51_{-4.45}$	$3.86^{+1.63}_{-1.52}$	$+1.63_{-4.59}$	$+1.63_{-5.22}$	$-3.00^{+1.18}_{-0.37}$	$+1.77_{-0.31}$	$+1.77_{-0.36}$	$-11.31^{+4.53}_{-2.52}$	$+6.72_{-5.23}$	$+7.90_{-6.19}$
J0251+4315		$2.08^{+0.71}_{-0.82}$	$+1.39_{-2.50}$	$+2.44_{-3.12}$	$2.77^{+1.80}_{-0.96}$	$+2.58_{-2.33}$	$+2.72_{-2.78}$	$-2.52^{+0.96}_{-0.46}$	$+1.36_{-0.73}$	$+1.36_{-0.85}$	$-8.18^{+2.17}_{-3.45}$	$+3.28_{-6.37}$	$+4.58_{-6.73}$
J0251+7226		$2.57^{+0.69}_{-1.44}$	$+1.12_{-3.83}$	$+2.59_{-3.94}$	$3.52^{+0.88}_{-1.11}$	$+1.95_{-1.49}$	$+1.98_{-2.58}$	$-3.07^{+0.83}_{-0.26}$	$+1.62_{-0.26}$	$+1.75_{-0.26}$	$-10.33^{+3.00}_{-1.31}$	$+3.57_{-3.99}$	$+4.94_{-4.45}$

Table C.2: Results of fitting the broken power-law model over the 1290 selected observations from OVRO dataset. Break significance refers to the source having a possible break frequency being (1σ) at 68.3%, (2σ) at 95.5% and (3σ) at 99.7%. The absence of break significance means that the source is not well-fitted at any level.

Name	Break significance	β_l	$\beta_l^{95.5\%}$	$\beta_l^{99.7\%}$	β_h	$\beta_h^{95.5\%}$	$\beta_h^{99.7\%}$	$\log f_{br}$	$\log f_{br}^{95.5\%}$	$\log f_{br}^{99.7\%}$	$\log A$	$\log A^{95.5\%}$	$\log A^{99.7\%}$
J0339-0133		$4.14^{+1.35}_{-0.87}$	$+1.35_{-2.04}$	$+1.35_{-2.68}$	$3.45^{+1.59}_{-2.13}$	$+1.98_{-4.55}$	$+2.01_{-4.93}$	$-1.60^{+0.30}_{-0.92}$	$+0.30_{-1.57}$	$+0.30_{-1.70}$	$-11.56^{+5.73}_{-2.10}$	$+7.86_{-5.20}$	$+9.26_{-6.19}$
J0339-0146		$2.00^{+1.11}_{-1.40}$	$+1.12_{-3.28}$	$+1.60_{-3.49}$	$3.10^{+0.72}_{-0.47}$	$+1.72_{-0.75}$	$+2.28_{-0.80}$	$-2.96^{+0.37}_{-0.40}$	$+0.93_{-0.41}$	$+1.46_{-0.40}$	$-6.86^{+0.86}_{-1.71}$	$+1.70_{-3.83}$	$+1.90_{-4.98}$
J0343+3622		$2.57^{+0.71}_{-1.52}$	$+0.74_{-3.67}$	$+1.10_{-4.04}$	$3.30^{+1.27}_{-1.03}$	$+2.19_{-3.05}$	$+2.17_{-4.49}$	$-2.92^{+0.83}_{-0.45}$	$+1.71_{-0.45}$	$+1.79_{-0.45}$	$-9.06^{+2.20}_{-2.85}$	$+5.20_{-4.70}$	$+6.50_{-4.92}$
J0345+1453		$2.89^{+0.67}_{-1.06}$	$+2.06_{-3.12}$	$+2.49_{-4.25}$	$3.54^{+0.81}_{-1.40}$	$+1.95_{-2.51}$	$+1.95_{-3.93}$	$-3.08^{+1.08}_{-0.29}$	$+1.64_{-0.29}$	$+1.84_{-0.29}$	$-9.66^{+2.59}_{-1.97}$	$+4.63_{-4.01}$	$+6.50_{-4.67}$
J0348-1610		$2.52^{+0.78}_{-0.67}$	$+2.85_{-2.20}$	$+2.78_{-3.91}$	$2.70^{+1.75}_{-1.25}$	$+2.78_{-2.53}$	$+2.78_{-3.62}$	$-1.62^{+0.36}_{-1.07}$	$+0.34_{-1.68}$	$+0.38_{-1.73}$	$-7.51^{+1.81}_{-3.84}$	$+3.52_{-7.06}$	$+5.02_{-7.06}$
J0351-1153		$4.15^{+0.99}_{-1.53}$	$+1.35_{-3.16}$	$+1.34_{-5.62}$	$4.32^{+1.00}_{-2.69}$	$+0.99_{-5.43}$	$+1.13_{-5.78}$	$-1.56^{+0.31}_{-1.14}$	$+0.24_{-1.78}$	$+0.33_{-1.79}$	$-8.56^{+3.51}_{-4.67}$	$+4.32_{-8.64}$	$+6.76_{-9.38}$
J0354+8009		$1.57^{+0.73}_{-0.91}$	$+0.92_{-2.82}$	$+1.67_{-2.99}$	$2.44^{+1.62}_{-0.34}$	$+2.99_{-0.49}$	$+3.05_{-0.85}$	$-2.02^{+0.17}_{-0.88}$	$+0.49_{-1.29}$	$+0.78_{-1.29}$	$-7.07^{+1.11}_{-2.72}$	$+1.11_{-5.23}$	$+1.99_{-5.72}$
J0357+2319		$2.15^{+0.69}_{-1.79}$	$+0.63_{-3.65}$	$+1.64_{-3.65}$	$2.77^{+1.06}_{-0.86}$	$+2.71_{-1.25}$	$+2.71_{-2.23}$	$-2.97^{+0.69}_{-0.37}$	$+1.65_{-0.34}$	$+1.71_{-0.39}$	$-7.19^{+2.40}_{-1.66}$	$+3.61_{-4.38}$	$+3.66_{-5.95}$
J0359+3220		$3.10^{+1.09}_{-1.17}$	$+2.38_{-2.40}$	$+2.35_{-4.22}$	$4.57^{+0.56}_{-3.06}$	$+0.93_{-5.00}$	$+0.93_{-5.95}$	$-3.01^{+1.77}_{-0.23}$	$+1.74_{-0.33}$	$+1.76_{-0.36}$	$-8.36^{+3.12}_{-4.99}$	$+4.86_{-7.77}$	$+6.19_{-8.86}$
J0400+0550		$2.24^{+1.05}_{-0.95}$	$+1.05_{-3.71}$	$+1.84_{-3.70}$	$2.78^{+1.85}_{-1.13}$	$+2.70_{-2.62}$	$+2.70_{-3.90}$	$-2.96^{+1.22}_{-0.32}$	$+1.70_{-0.29}$	$+1.72_{-0.39}$	$-8.11^{+1.95}_{-4.23}$	$+4.10_{-6.89}$	$+6.07_{-8.32}$
J0401+0413	2σ	$-0.35^{+1.03}_{-1.13}$	$+2.38_{-1.15}$	$+3.07_{-1.15}$	$4.74^{+0.74}_{-0.97}$	$+0.75_{-2.11}$	$+0.74_{-2.65}$	$-2.79^{+0.15}_{-0.14}$	$+0.26_{-0.43}$	$+0.66_{-0.42}$	$-11.32^{+1.87}_{-2.44}$	$+4.43_{-2.93}$	$+5.65_{-2.94}$
J0401+2110	2σ	$1.43^{+0.72}_{-0.69}$	$+0.74_{-2.55}$	$+1.05_{-2.82}$	$2.80^{+1.31}_{-0.51}$	$+2.60_{-0.63}$	$+2.68_{-0.97}$	$-2.22^{+0.26}_{-0.60}$	$+0.62_{-0.99}$	$+0.96_{-1.12}$	$-7.22^{+1.12}_{-2.36}$	$+1.42_{-4.85}$	$+1.75_{-5.68}$
J0401-1606		$4.87^{+0.62}_{-1.38}$	$+0.63_{-3.12}$	$+0.61_{-4.10}$	$3.50^{+1.85}_{-2.08}$	$+1.97_{-4.48}$	$+1.98_{-4.93}$	$-1.65^{+0.40}_{-0.90}$	$+0.34_{-1.70}$	$+0.41_{-1.72}$	$-11.55^{+5.05}_{-4.14}$	$+8.43_{-6.21}$	$+9.48_{-7.66}$
J0403+2600		$2.53^{+0.70}_{-0.74}$	$+2.35_{-2.29}$	$+2.62_{-3.71}$	$2.93^{+1.62}_{-1.00}$	$+2.56_{-2.73}$	$+2.56_{-4.41}$	$-3.13^{+1.97}_{-0.44}$	$+1.93_{-0.22}$	$+2.00_{-0.24}$	$-8.04^{+1.74}_{-3.25}$	$+4.67_{-4.76}$	$+6.34_{-6.09}$
J0405-1308	1σ	$0.47^{+1.83}_{-0.99}$	$+2.47_{-1.96}$	$+2.89_{-1.96}$	$3.60^{+0.67}_{-0.88}$	$+1.89_{-0.95}$	$+1.89_{-1.32}$	$-2.88^{+0.17}_{-0.36}$	$+0.71_{-0.42}$	$+1.10_{-0.42}$	$-8.64^{+1.74}_{-1.88}$	$+2.70_{-4.20}$	$+2.94_{-4.86}$
J0406+0637		$1.89^{+0.75}_{-1.87}$	$+0.94_{-3.37}$	$+1.70_{-3.37}$	$3.16^{+1.45}_{-0.63}$	$+2.33_{-0.96}$	$+2.33_{-1.73}$	$-2.83^{+0.32}_{-0.39}$	$+1.16_{-0.51}$	$+1.37_{-0.52}$	$-8.99^{+2.40}_{-2.37}$	$+2.40_{-5.57}$	$+4.00_{-5.56}$
J0407+0742		$1.95^{+0.71}_{-0.82}$	$+1.71_{-2.79}$	$+3.33_{-3.34}$	$2.27^{+1.27}_{-0.67}$	$+3.16_{-0.66}$	$+3.16_{-1.57}$	$-2.26^{+0.24}_{-1.09}$	$+0.93_{-1.08}$	$+1.01_{-1.10}$	$-5.84^{+1.42}_{-2.31}$	$+1.71_{-5.50}$	$+2.33_{-6.76}$
J0409+1217		$2.87^{+0.80}_{-0.91}$	$+1.46_{-3.71}$	$+2.49_{-4.00}$	$3.65^{+1.56}_{-1.44}$	$+1.84_{-4.00}$	$+1.83_{-4.87}$	$-1.56^{+0.29}_{-1.25}$	$+0.28_{-1.74}$	$+0.33_{-1.80}$	$-10.51^{+3.69}_{-3.16}$	$+7.43_{-4.22}$	$+8.41_{-5.24}$
J0409-1238		$3.95^{+1.07}_{-0.85}$	$+1.53_{-1.74}$	$+1.51_{-4.31}$	$4.38^{+1.12}_{-2.50}$	$+1.12_{-4.98}$	$+1.12_{-5.75}$	$-1.58^{+0.26}_{-1.18}$	$+0.26_{-1.74}$	$+0.34_{-1.78}$	$-11.71^{+4.12}_{-3.83}$	$+6.99_{-5.05}$	$+9.04_{-5.94}$
J0412+0010		$2.29^{+0.73}_{-1.28}$	$+1.27_{-3.14}$	$+1.60_{-3.76}$	$3.57^{+1.34}_{-1.34}$	$+1.81_{-4.52}$	$+1.93_{-4.97}$	$-3.00^{+1.00}_{-0.35}$	$+1.67_{-0.35}$	$+1.76_{-0.35}$	$-10.87^{+3.22}_{-2.42}$	$+7.92_{-3.98}$	$+8.27_{-5.89}$
J0412+0438		$2.57^{+1.86}_{-0.82}$	$+2.54_{-3.40}$	$+2.90_{-3.86}$	$4.56^{+0.83}_{-2.30}$	$+0.90_{-5.00}$	$+0.91_{-5.97}$	$-3.05^{+1.10}_{-0.31}$	$+1.71_{-0.31}$	$+1.81_{-0.31}$	$-9.64^{+1.72}_{-6.13}$	$+5.45_{-7.64}$	$+6.67_{-9.79}$
J0412+1856		$0.71^{+2.23}_{-2.10}$	$+4.43_{-2.07}$	$+4.78_{-2.13}$	$-0.44^{+2.56}_{-1.05}$	$+5.16_{-1.06}$	$+5.87_{-1.06}$	$-1.81^{+0.44}_{-0.95}$	$+0.47_{-1.54}$	$+0.57_{-1.54}$	$-17.85^{+6.42}_{-2.11}$	$+11.91_{-2.13}$	$+15.24_{-2.14}$
J0414+3418		$1.16^{+0.79}_{-1.79}$	$+3.03_{-2.51}$	$+4.19_{-2.66}$	$1.94^{+2.68}_{-0.63}$	$+3.53_{-2.32}$	$+3.56_{-3.25}$	$-2.39^{+0.57}_{-0.66}$	$+1.12_{-0.84}$	$+1.14_{-0.84}$	$-6.13^{+1.38}_{-5.05}$	$+2.04_{-8.39}$	$+4.29_{-9.41}$
J0416-1851	1σ	$1.57^{+1.06}_{-1.08}$	$+1.36_{-2.84}$	$+1.79_{-3.05}$	$3.75^{+0.78}_{-0.86}$	$+1.64_{-1.18}$	$+1.73_{-1.51}$	$-2.60^{+0.30}_{-0.34}$	$+0.54_{-0.71}$	$+0.81_{-0.71}$	$-9.49^{+1.77}_{-1.97}$	$+2.59_{-3.90}$	$+3.46_{-4.12}$

Table C.2: Results of fitting the broken power-law model over the 1290 selected observations from OVRO dataset. Break significance refers to the source having a possible break frequency being (1σ) at 68.3%, (2σ) at 95.5% and (3σ) at 99.7%. The absence of break significance means that the source is not well-fitted at any level.

Name	Break significance	β_l	$\beta_l^{95.5\%}$	$\beta_l^{99.7\%}$	β_h	$\beta_h^{95.5\%}$	$\beta_h^{99.7\%}$	$\log f_{br}$	$\log f_{br}^{95.5\%}$	$\log f_{br}^{99.7\%}$	$\log A$	$\log A^{95.5\%}$	$\log A^{99.7\%}$
J0422+0219		$2.57_{-0.75}^{+0.63}$	$+1.07_{-3.38}$	$+2.04_{-3.81}$	$2.87_{-0.75}^{+1.50}$	$+2.62_{-2.30}$	$+2.62_{-3.55}$	$-1.58_{-1.37}^{+0.19}$	$+0.23_{-1.79}$	$+0.34_{-1.79}$	$-7.56_{-2.62}^{+1.74}$	$+3.91_{-5.10}$	$+5.82_{-5.97}$
J0422-0643	2σ	$1.16_{-0.49}^{+0.30}$	$+0.59_{-1.13}$	$+0.89_{-1.57}$	$4.75_{-1.81}^{+0.49}$	$+0.74_{-2.98}$	$+0.74_{-3.27}$	$-1.75_{-0.25}^{+0.19}$	$+0.36_{-0.56}$	$+0.54_{-0.98}$	$-9.49_{-0.71}^{+3.01}$	$+5.04_{-1.23}$	$+5.04_{-2.04}$
J0423-0120		$3.10_{-0.82}^{+0.69}$	$+1.05_{-3.42}$	$+1.65_{-4.47}$	$3.37_{-0.85}^{+1.39}$	$+2.12_{-3.36}$	$+2.12_{-4.68}$	$-1.54_{-1.37}^{+0.20}$	$+0.20_{-1.82}$	$+0.30_{-1.82}$	$-7.24_{-2.81}^{+1.72}$	$+4.86_{-4.68}$	$+6.62_{-4.84}$
J0424+0805		$2.27_{-0.80}^{+1.11}$	$+1.38_{-3.62}$	$+3.03_{-3.62}$	$3.56_{-1.38}^{+1.71}$	$+1.88_{-3.70}$	$+1.94_{-4.73}$	$-1.57_{-1.23}^{+0.25}$	$+0.22_{-1.80}$	$+0.32_{-1.79}$	$-10.62_{-1.99}^{+3.98}$	$+6.49_{-4.65}$	$+8.19_{-5.45}$
J0426+0518		$2.27_{-1.02}^{+0.86}$	$+1.13_{-3.19}$	$+1.75_{-3.60}$	$3.15_{-0.44}^{+2.28}$	$+2.34_{-2.73}$	$+2.34_{-4.34}$	$-2.64_{-0.63}^{+0.61}$	$+1.43_{-0.56}$	$+1.45_{-0.64}$	$-8.73_{-4.41}^{+1.48}$	$+4.27_{-6.14}$	$+6.99_{-6.34}$
J0426+2327		$3.40_{-0.63}^{+1.46}$	$+2.08_{-1.86}$	$+2.04_{-4.87}$	$3.65_{-1.54}^{+1.79}$	$+1.82_{-4.17}$	$+1.86_{-4.93}$	$-1.54_{-1.12}^{+0.30}$	$+0.27_{-1.75}$	$+0.30_{-1.83}$	$-10.13_{-4.91}^{+2.53}$	$+5.76_{-6.91}$	$+7.60_{-7.51}$
J0426+2350		$5.01_{-0.96}^{+0.48}$	$+0.48_{-2.28}$	$+0.48_{-3.02}$	$4.21_{-2.90}^{+1.28}$	$+1.28_{-5.23}$	$+1.27_{-5.71}$	$-1.65_{-0.78}^{+0.39}$	$+0.39_{-1.52}$	$+0.40_{-1.71}$	$-13.85_{-2.43}^{+6.72}$	$+10.51_{-3.88}$	$+11.10_{-4.90}$
J0428+1732		$4.41_{-1.24}^{+0.95}$	$+1.08_{-2.75}$	$+1.08_{-4.25}$	$4.31_{-2.49}^{+1.15}$	$+1.18_{-5.04}$	$+1.19_{-5.78}$	$-1.59_{-1.01}^{+0.35}$	$+0.35_{-1.69}$	$+0.35_{-1.77}$	$-14.01_{-2.33}^{+6.45}$	$+10.00_{-4.03}$	$+11.75_{-5.21}$
J0430+1655		$1.28_{-1.57}^{+0.73}$	$+0.98_{-2.79}$	$+1.76_{-2.78}$	$2.23_{-0.25}^{+2.39}$	$+3.11_{-0.69}$	$+3.22_{-1.23}$	$-2.69_{-0.44}^{+0.36}$	$+1.10_{-0.54}$	$+1.26_{-0.62}$	$-7.27_{-4.54}^{+1.25}$	$+1.78_{-7.50}$	$+2.67_{-8.40}$
J0431+1731		$1.92_{-1.44}^{+1.11}$	$+1.36_{-3.15}$	$+1.68_{-3.41}$	$4.08_{-1.41}^{+1.14}$	$+1.42_{-3.12}$	$+1.39_{-5.56}$	$-2.87_{-0.44}^{+0.58}$	$+1.48_{-0.39}$	$+1.57_{-0.44}$	$-11.26_{-1.33}^{+4.86}$	$+6.42_{-3.97}$	$+9.33_{-4.59}$
J0433+0521	3σ	$1.56_{-0.33}^{+0.55}$	$+0.77_{-0.86}$	$+1.14_{-1.26}$	$4.40_{-0.69}^{+0.77}$	$+1.08_{-1.16}$	$+1.08_{-1.55}$	$-2.19_{-0.14}^{+0.17}$	$+0.42_{-0.25}$	$+0.42_{-0.42}$	$-8.61_{-1.38}^{+1.37}$	$+2.12_{-2.21}$	$+2.83_{-2.21}$
J0433+2905		$1.50_{-1.74}^{+0.60}$	$+0.79_{-2.92}$	$+1.14_{-2.99}$	$2.68_{-0.71}^{+0.78}$	$+2.68_{-0.70}$	$+2.78_{-0.99}$	$-2.86_{-0.15}^{+0.74}$	$+1.08_{-0.50}$	$+1.50_{-0.51}$	$-7.02_{-1.68}^{+1.48}$	$+2.03_{-4.92}$	$+1.93_{-6.01}$
J0434-1442		$3.13_{-0.76}^{+1.36}$	$+2.35_{-2.26}$	$+2.36_{-4.19}$	$2.73_{-0.85}^{+2.38}$	$+2.77_{-3.09}$	$+2.77_{-4.00}$	$-1.55_{-1.19}^{+0.30}$	$+0.32_{-1.73}$	$+0.32_{-1.80}$	$-8.26_{-4.97}^{+1.92}$	$+3.96_{-7.96}$	$+5.86_{-8.46}$
J0437-1844		$4.12_{-0.67}^{+1.36}$	$+1.36_{-2.13}$	$+1.37_{-3.97}$	$4.61_{-2.78}^{+0.86}$	$+0.86_{-5.53}$	$+0.87_{-6.02}$	$-1.60_{-0.92}^{+0.40}$	$+0.40_{-1.62}$	$+0.40_{-1.73}$	$-13.22_{-3.04}^{+5.40}$	$+9.42_{-3.88}$	$+11.50_{-5.10}$
J0438+3004		$2.41_{-0.87}^{+0.58}$	$+1.48_{-3.41}$	$+2.82_{-3.56}$	$2.48_{-0.77}^{+2.09}$	$+2.96_{-2.37}$	$+3.01_{-3.21}$	$-1.60_{-1.14}^{+0.34}$	$+0.28_{-1.77}$	$+0.34_{-1.77}$	$-7.69_{-2.97}^{+2.24}$	$+3.35_{-6.75}$	$+5.17_{-6.78}$
J0438-1251		$2.82_{-1.75}^{+0.89}$	$+0.87_{-4.29}$	$+2.65_{-4.31}$	$3.99_{-0.97}^{+1.49}$	$+1.45_{-3.98}$	$+1.50_{-4.71}$	$-3.03_{-0.32}^{+0.84}$	$+1.64_{-0.31}$	$+1.81_{-0.32}$	$-10.35_{-3.68}^{+2.46}$	$+7.00_{-4.45}$	$+8.19_{-4.81}$
J0439+0520		$0.84_{-1.20}^{+2.81}$	$+3.91_{-2.32}$	$+4.54_{-2.32}$	$2.73_{-1.92}^{+2.33}$	$+2.56_{-3.87}$	$+2.77_{-4.16}$	$-2.50_{-0.21}^{+1.24}$	$+1.13_{-0.87}$	$+1.26_{-0.87}$	$-11.81_{-6.94}^{+2.75}$	$+6.89_{-8.20}$	$+9.39_{-8.20}$
J0439+3045		$2.62_{-1.15}^{+1.20}$	$+2.74_{-2.57}$	$+2.74_{-3.92}$	$2.28_{-0.56}^{+2.64}$	$+3.20_{-2.34}$	$+3.21_{-3.53}$	$-3.08_{-0.28}^{+1.15}$	$+1.75_{-0.28}$	$+1.84_{-0.37}$	$-9.48_{-3.07}^{+4.06}$	$+5.83_{-6.14}$	$+6.72_{-7.60}$
J0440+1437		$2.98_{-1.88}^{+0.68}$	$+1.13_{-4.35}$	$+2.47_{-4.39}$	$3.94_{-0.79}^{+1.45}$	$+1.56_{-2.74}$	$+1.56_{-3.30}$	$-3.00_{-0.31}^{+0.77}$	$+1.67_{-0.30}$	$+1.80_{-0.31}$	$-11.33_{-2.50}^{+2.81}$	$+6.32_{-3.57}$	$+7.42_{-3.69}$
J0442-0017		$2.25_{-0.80}^{+0.62}$	$+1.20_{-2.60}$	$+2.89_{-3.07}$	$2.75_{-0.39}^{+1.84}$	$+2.71_{-1.10}$	$+2.75_{-2.27}$	$-2.35_{-0.73}^{+0.54}$	$+0.97_{-1.02}$	$+1.10_{-1.02}$	$-6.81_{-3.31}^{+1.11}$	$+2.28_{-5.46}$	$+3.84_{-5.99}$
J0449+1121		$1.87_{-1.09}^{+0.98}$	$+1.03_{-3.22}$	$+2.47_{-3.36}$	$1.89_{-0.79}^{+1.41}$	$+2.76_{-2.81}$	$+3.51_{-3.13}$	$-3.00_{-0.35}^{+1.20}$	$+1.77_{-0.34}$	$+1.88_{-0.37}$	$-4.35_{-2.62}^{+1.49}$	$+3.60_{-5.76}$	$+3.74_{-8.98}$
J0449+6332	2σ	$-0.99_{-0.51}^{+1.32}$	$+2.96_{-0.50}$	$+4.09_{-0.51}$	$4.46_{-0.46}^{+1.02}$	$+1.02_{-1.41}$	$+1.02_{-1.87}$	$-2.86_{-0.14}^{+0.14}$	$+0.31_{-0.29}$	$+0.38_{-0.44}$	$-11.77_{-1.85}^{+1.81}$	$+3.81_{-2.44}$	$+4.81_{-2.54}$
J0452+1236		$2.27_{-1.27}^{+1.15}$	$+1.59_{-3.39}$	$+2.38_{-3.73}$	$3.87_{-1.38}^{+1.59}$	$+1.63_{-3.54}$	$+1.62_{-5.32}$	$-3.03_{-0.32}^{+1.01}$	$+1.68_{-0.31}$	$+1.79_{-0.33}$	$-10.46_{-2.45}^{+4.46}$	$+6.40_{-5.46}$	$+8.27_{-6.00}$
J0456+0400		$1.57_{-1.11}^{+1.47}$	$+3.08_{-2.46}$	$+3.79_{-3.03}$	$2.00_{-0.78}^{+2.38}$	$+3.44_{-1.75}$	$+3.46_{-3.26}$	$-2.26_{-1.07}^{+0.31}$	$+0.93_{-1.07}$	$+1.02_{-1.09}$	$-7.23_{-4.24}^{+2.49}$	$+3.29_{-8.32}$	$+4.10_{-11.26}$

Table C.2: Results of fitting the broken power-law model over the 1290 selected observations from OVRO dataset. Break significance refers to the source having a possible break frequency being (1σ) at 68.3%, (2σ) at 95.5% and (3σ) at 99.7%. The absence of break significance means that the source is not well-fitted at any level.

Name	Break significance	β_l	$\beta_l^{95.5\%}$	$\beta_l^{99.7\%}$	β_h	$\beta_h^{95.5\%}$	$\beta_h^{99.7\%}$	$\log f_{br}$	$\log f_{br}^{95.5\%}$	$\log f_{br}^{99.7\%}$	$\log A$	$\log A^{95.5\%}$	$\log A^{99.7\%}$
J0457+0645	3σ	$-0.96^{+1.63}_{-0.47}$	$+2.77_{-0.54}$	$+3.10_{-0.54}$	$3.44^{+1.04}_{-0.71}$	$+2.01_{-0.73}$	$+2.06_{-1.13}$	$-2.82^{+0.15}_{-0.20}$	$+0.32_{-0.38}$	$+0.41_{-0.52}$	$-8.37^{+1.63}_{-2.58}$	$+1.80_{-5.02}$	$+2.58_{-5.38}$
J0501+1356		$2.40^{+1.44}_{-0.72}$	$+2.56_{-2.57}$	$+2.74_{-3.82}$	$2.91^{+2.04}_{-0.98}$	$+2.47_{-2.98}$	$+2.56_{-4.32}$	$-3.07^{+1.30}_{-0.13}$	$+1.78_{-0.22}$	$+1.83_{-0.88}$	$-10.53^{+4.91}_{-1.48}$	$+6.61_{-4.79}$	$+7.99_{-5.93}$
J0501-0159		$2.53^{+0.52}_{-1.03}$	$+0.80_{-4.00}$	$+2.53_{-4.00}$	$2.94^{+1.42}_{-0.70}$	$+2.53_{-1.21}$	$+2.53_{-2.16}$	$-2.47^{+0.42}_{-0.90}$	$+1.05_{-0.90}$	$+1.20_{-0.90}$	$-7.02^{+0.92}_{-3.37}$	$+2.46_{-5.14}$	$+3.70_{-6.09}$
J0502+1338		$3.77^{+1.63}_{-0.82}$	$+1.73_{-2.10}$	$+1.72_{-4.02}$	$1.77^{+2.96}_{-0.69}$	$+3.71_{-2.45}$	$+3.71_{-3.21}$	$-3.01^{+1.14}_{-0.32}$	$+1.70_{-0.32}$	$+1.76_{-0.36}$	$-5.59^{+1.37}_{-6.71}$	$+2.73_{-10.24}$	$+4.28_{-11.23}$
J0503+6600		$1.87^{+1.37}_{-1.13}$	$+3.40_{-2.47}$	$+3.62_{-3.18}$	$2.40^{+2.09}_{-0.83}$	$+3.07_{-3.02}$	$+3.07_{-3.76}$	$-1.60^{+0.32}_{-1.06}$	$+0.33_{-1.68}$	$+0.40_{-1.72}$	$-7.27^{+1.40}_{-4.60}$	$+3.60_{-7.00}$	$+4.65_{-7.99}$
J0505+0459	2σ	$1.26^{+0.75}_{-1.46}$	$+0.76_{-2.68}$	$+1.37_{-2.75}$	$3.60^{+0.90}_{-0.80}$	$+1.80_{-0.89}$	$+1.90_{-1.19}$	$-2.72^{+0.42}_{-0.17}$	$+0.65_{-0.32}$	$+0.84_{-0.40}$	$-8.84^{+1.30}_{-2.16}$	$+1.97_{-3.56}$	$+2.69_{-3.91}$
J0508+8432		$2.64^{+1.25}_{-0.86}$	$+1.57_{-3.29}$	$+2.20_{-4.02}$	$3.78^{+1.23}_{-1.47}$	$+1.63_{-3.81}$	$+1.66_{-5.18}$	$-2.99^{+0.95}_{-0.37}$	$+1.66_{-0.37}$	$+1.75_{-0.37}$	$-11.42^{+3.42}_{-3.06}$	$+7.38_{-4.33}$	$+8.57_{-5.54}$
J0509+0541		$2.61^{+0.78}_{-1.46}$	$+1.04_{-4.10}$	$+1.87_{-4.10}$	$3.17^{+2.31}_{-0.46}$	$+2.32_{-3.62}$	$+2.31_{-4.64}$	$-3.03^{+1.04}_{-0.34}$	$+1.71_{-0.33}$	$+1.78_{-0.34}$	$-8.97^{+2.26}_{-3.83}$	$+5.50_{-6.33}$	$+7.70_{-6.32}$
J0510+1800	1σ	$1.91^{+0.66}_{-0.72}$	$+1.11_{-2.42}$	$+1.23_{-3.19}$	$4.94^{+0.53}_{-1.26}$	$+0.47_{-2.39}$	$+0.54_{-2.72}$	$-2.40^{+0.23}_{-0.24}$	$+0.28_{-0.87}$	$+0.49_{-0.97}$	$-11.33^{+2.94}_{-0.95}$	$+5.26_{-1.03}$	$+6.03_{-1.45}$
J0511+1357		$2.82^{+1.63}_{-0.72}$	$+2.67_{-1.14}$	$+2.66_{-2.39}$	$2.92^{+2.45}_{-1.04}$	$+2.58_{-3.55}$	$+2.59_{-4.28}$	$-1.63^{+0.39}_{-0.95}$	$+0.35_{-1.70}$	$+0.39_{-1.74}$	$-9.86^{+3.76}_{-4.16}$	$+5.74_{-8.05}$	$+7.81_{-8.55}$
J0522-0725		$2.51^{+1.04}_{-1.39}$	$+1.65_{-3.87}$	$+2.82_{-3.94}$	$4.78^{+0.42}_{-2.33}$	$+0.72_{-4.04}$	$+0.72_{-6.22}$	$-3.04^{+0.93}_{-0.31}$	$+1.59_{-0.31}$	$+1.70_{-0.31}$	$-8.66^{+1.99}_{-4.59}$	$+3.42_{-7.91}$	$+5.65_{-8.42}$
J0527+0331	3σ	$-0.26^{+0.32}_{-1.17}$	$+1.50_{-1.12}$	$+1.86_{-1.22}$	$4.85^{+0.63}_{-0.65}$	$+0.64_{-1.62}$	$+0.65_{-2.15}$	$-2.51^{+0.08}_{-0.12}$	$+0.23_{-0.17}$	$+0.25_{-0.25}$	$-11.51^{+2.06}_{-0.92}$	$+3.94_{-1.54}$	$+5.23_{-1.55}$
J0529-0519		$2.50^{+1.50}_{-1.10}$	$+1.74_{-3.61}$	$+2.36_{-3.99}$	$4.36^{+0.98}_{-2.10}$	$+1.09_{-4.77}$	$+1.10_{-5.79}$	$-2.99^{+0.96}_{-0.36}$	$+1.64_{-0.37}$	$+1.76_{-0.36}$	$-11.31^{+4.69}_{-3.03}$	$+9.20_{-3.62}$	$+10.28_{-4.53}$
J0530+1331		$3.38^{+1.19}_{-2.05}$	$+1.62_{-4.25}$	$+1.62_{-4.88}$	$4.64^{+0.86}_{-0.90}$	$+0.83_{-5.27}$	$+0.86_{-5.70}$	$-3.03^{+0.79}_{-0.33}$	$+1.60_{-0.33}$	$+1.77_{-0.34}$	$-11.87^{+2.39}_{-2.26}$	$+8.37_{-2.83}$	$+9.43_{-3.08}$
J0532+0732		$2.48^{+0.63}_{-1.23}$	$+0.82_{-3.59}$	$+1.47_{-3.83}$	$3.18^{+1.25}_{-0.75}$	$+2.32_{-1.99}$	$+2.32_{-2.90}$	$-2.54^{+0.40}_{-0.81}$	$+1.30_{-0.73}$	$+1.30_{-0.82}$	$-7.42^{+1.61}_{-2.23}$	$+4.44_{-3.93}$	$+4.44_{-5.38}$
J0541+5312		$2.91^{+1.13}_{-1.41}$	$+2.57_{-2.40}$	$+2.57_{-4.15}$	$2.85^{+2.65}_{-0.67}$	$+2.64_{-3.45}$	$+2.65_{-4.30}$	$-3.07^{+1.20}_{-0.27}$	$+1.76_{-0.24}$	$+1.86_{-0.26}$	$-10.17^{+4.39}_{-2.98}$	$+6.31_{-6.85}$	$+7.82_{-8.43}$
J0541-0541		$1.69^{+0.66}_{-1.26}$	$+1.05_{-2.95}$	$+1.86_{-3.19}$	$2.14^{+1.85}_{-0.84}$	$+3.35_{-0.96}$	$+3.35_{-1.82}$	$-2.49^{+0.30}_{-0.80}$	$+1.13_{-0.84}$	$+1.24_{-0.85}$	$-5.33^{+1.41}_{-4.08}$	$+1.71_{-7.52}$	$+2.87_{-8.54}$
J0542+498		$1.67^{+0.71}_{-1.05}$	$+0.99_{-2.70}$	$+1.47_{-3.05}$	$2.56^{+2.49}_{-0.62}$	$+2.84_{-2.96}$	$+2.93_{-3.86}$	$-2.27^{+1.02}_{-0.26}$	$+1.39_{-0.76}$	$+1.52_{-0.89}$	$-6.23^{+1.22}_{-4.87}$	$+4.35_{-6.14}$	$+4.69_{-6.88}$
J0542-0913	3σ	$0.25^{+0.84}_{-1.09}$	$+1.91_{-1.45}$	$+1.96_{-1.74}$	$3.80^{+1.07}_{-0.68}$	$+1.60_{-1.22}$	$+1.67_{-1.53}$	$-2.64^{+0.16}_{-0.14}$	$+0.35_{-0.39}$	$+0.48_{-0.42}$	$-8.77^{+1.56}_{-2.42}$	$+2.59_{-3.87}$	$+3.46_{-4.35}$
J0552+0313		$2.54^{+1.23}_{-0.73}$	$+2.35_{-2.74}$	$+2.74_{-3.95}$	$2.08^{+2.99}_{-0.85}$	$+3.41_{-3.03}$	$+3.41_{-3.57}$	$-3.10^{+1.24}_{-0.26}$	$+1.78_{-0.26}$	$+1.86_{-0.26}$	$-5.32^{+3.36}_{-4.68}$	$+4.01_{-9.21}$	$+5.09_{-10.31}$
J0554+6857		$3.51^{+1.62}_{-1.01}$	$+1.96_{-4.07}$	$+1.96_{-4.98}$	$4.09^{+1.33}_{-1.99}$	$+1.39_{-4.48}$	$+1.40_{-5.45}$	$-3.06^{+1.20}_{-0.23}$	$+1.75_{-0.26}$	$+1.86_{-0.26}$	$-13.18^{+6.02}_{-2.30}$	$+8.71_{-4.22}$	$+10.69_{-5.46}$
J0558-1317		$2.30^{+0.94}_{-0.64}$	$+1.47_{-3.30}$	$+2.83_{-3.30}$	$2.63^{+1.74}_{-1.44}$	$+2.82_{-2.66}$	$+2.87_{-4.12}$	$-1.53^{+0.27}_{-1.12}$	$+0.27_{-1.73}$	$+0.28_{-1.84}$	$-7.32^{+2.88}_{-2.93}$	$+4.75_{-5.99}$	$+5.40_{-7.45}$
J0559+5804		$2.74^{+1.29}_{-1.37}$	$+2.24_{-3.43}$	$+2.74_{-4.19}$	$3.20^{+1.78}_{-1.28}$	$+2.29_{-3.22}$	$+2.29_{-4.43}$	$-3.01^{+1.09}_{-0.30}$	$+1.74_{-0.30}$	$+1.81_{-0.30}$	$-9.67^{+2.81}_{-4.01}$	$+5.20_{-6.66}$	$+7.22_{-7.24}$
J0559-1817		$4.62^{+0.87}_{-1.04}$	$+0.87_{-2.63}$	$+0.87_{-5.45}$	$4.27^{+1.17}_{-2.89}$	$+1.23_{-5.17}$	$+1.23_{-5.76}$	$-1.79^{+0.02}_{-1.49}$	$+0.55_{-1.49}$	$+0.55_{-1.58}$	$-9.03^{+5.10}_{-3.94}$	$+5.90_{-7.69}$	$+7.19_{-8.71}$

Table C.2: Results of fitting the broken power-law model over the 1290 selected observations from OVRO dataset. Break significance refers to the source having a possible break frequency being (1σ) at 68.3%, (2σ) at 95.5% and (3σ) at 99.7%. The absence of break significance means that the source is not well-fitted at any level.

Name	Break significance	β_l	$\beta_l^{95.5\%}$	$\beta_l^{99.7\%}$	β_h	$\beta_h^{95.5\%}$	$\beta_h^{99.7\%}$	$\log f_{br}$	$\log f_{br}^{95.5\%}$	$\log f_{br}^{99.7\%}$	$\log A$	$\log A^{95.5\%}$	$\log A^{99.7\%}$
J0606-0724	1σ	$1.80^{+0.37}_{-2.30}$	$+0.84_{-3.29}$	$+1.27_{-3.30}$	$3.60^{+1.45}_{-0.55}$	$+1.83_{-1.30}$	$+1.90_{-2.03}$	$-2.90^{+0.28}_{-0.30}$	$+0.99_{-0.47}$	$+1.66_{-0.47}$	$-10.58^{+3.06}_{-1.75}$	$+3.76_{-3.92}$	$+5.49_{-4.48}$
J0607+4739		$2.33^{+1.07}_{-0.92}$	$+1.18_{-3.34}$	$+2.04_{-3.79}$	$3.35^{+1.77}_{-0.93}$	$+2.12_{-3.59}$	$+2.14_{-4.76}$	$-2.90^{+1.01}_{-0.45}$	$+1.70_{-0.46}$	$+1.78_{-0.46}$	$-9.07^{+1.57}_{-4.50}$	$+4.61_{-6.00}$	$+6.98_{-6.00}$
J0607+6720		$2.43^{+0.84}_{-0.57}$	$+1.43_{-3.32}$	$+2.88_{-3.68}$	$2.50^{+1.71}_{-0.90}$	$+2.70_{-2.66}$	$+2.96_{-3.89}$	$-1.54^{+0.28}_{-1.20}$	$+0.26_{-1.76}$	$+0.34_{-1.79}$	$-7.76^{+2.18}_{-2.82}$	$+4.13_{-5.55}$	$+6.06_{-6.99}$
J0607-0834		$2.82^{+0.90}_{-0.58}$	$+2.46_{-2.19}$	$+2.46_{-3.45}$	$2.95^{+2.33}_{-1.22}$	$+2.50_{-3.91}$	$+2.50_{-4.36}$	$-1.64^{+0.37}_{-0.98}$	$+0.36_{-1.65}$	$+0.40_{-1.72}$	$-7.49^{+3.63}_{-3.14}$	$+7.69_{-4.18}$	$+7.69_{-6.40}$
J0609-1542		$1.97^{+0.75}_{-1.80}$	$+0.76_{-3.41}$	$+1.70_{-3.47}$	$2.92^{+1.06}_{-0.82}$	$+2.43_{-0.95}$	$+2.53_{-1.37}$	$-2.82^{+0.58}_{-0.36}$	$+1.35_{-0.50}$	$+1.58_{-0.49}$	$-6.33^{+1.71}_{-2.34}$	$+1.96_{-5.33}$	$+3.01_{-5.36}$
J0610-1847		$2.26^{+0.85}_{-1.23}$	$+1.02_{-3.54}$	$+1.39_{-3.72}$	$2.21^{+2.57}_{-1.00}$	$+3.29_{-3.06}$	$+3.28_{-3.69}$	$-2.90^{+1.05}_{-0.40}$	$+1.62_{-0.40}$	$+1.68_{-0.43}$	$-5.02^{+1.84}_{-5.76}$	$+4.36_{-8.27}$	$+4.36_{-9.82}$
J0612+4122		$2.31^{+0.66}_{-0.89}$	$+0.82_{-3.36}$	$+1.31_{-3.74}$	$2.96^{+1.19}_{-0.81}$	$+2.50_{-1.42}$	$+2.48_{-2.75}$	$-2.29^{+0.30}_{-1.04}$	$+1.06_{-0.96}$	$+1.06_{-1.05}$	$-8.41^{+1.90}_{-2.08}$	$+3.28_{-4.83}$	$+4.54_{-5.20}$
J0616-1041	3σ	$-1.21^{+0.49}_{-0.29}$	$+1.57_{-0.29}$	$+2.15_{-0.29}$	$4.74^{+0.63}_{-1.22}$	$+0.70_{-2.49}$	$+0.75_{-3.03}$	$-2.56^{+0.11}_{-0.12}$	$+0.23_{-0.26}$	$+0.26_{-0.35}$	$-11.50^{+2.86}_{-1.45}$	$+5.59_{-1.92}$	$+6.59_{-2.15}$
J0617+5701		$2.76^{+0.77}_{-0.50}$	$+1.13_{-3.49}$	$+2.70_{-3.78}$	$3.17^{+2.16}_{-0.52}$	$+2.22_{-3.60}$	$+2.33_{-4.34}$	$-1.46^{+0.27}_{-1.21}$	$+0.22_{-1.81}$	$+0.27_{-1.85}$	$-9.83^{+2.46}_{-2.69}$	$+5.94_{-4.83}$	$+7.22_{-5.11}$
J0617+7816		$2.35^{+1.62}_{-0.79}$	$+3.04_{-2.02}$	$+3.08_{-3.42}$	$2.26^{+2.12}_{-1.02}$	$+3.22_{-2.29}$	$+3.22_{-3.71}$	$-3.01^{+1.17}_{-0.26}$	$+1.69_{-0.21}$	$+1.69_{-0.32}$	$-7.93^{+2.17}_{-4.10}$	$+3.98_{-7.64}$	$+6.00_{-9.51}$
J0618+4620		$2.64^{+0.85}_{-0.75}$	$+2.04_{-2.04}$	$+2.74_{-2.91}$	$2.52^{+2.05}_{-0.66}$	$+2.97_{-2.44}$	$+2.97_{-4.01}$	$-1.55^{+0.30}_{-1.10}$	$+0.26_{-1.78}$	$+0.31_{-1.82}$	$-7.97^{+1.46}_{-3.81}$	$+3.36_{-6.09}$	$+5.68_{-6.24}$
J0619-1140		$2.03^{+0.76}_{-0.67}$	$+2.20_{-3.10}$	$+3.44_{-3.45}$	$2.00^{+1.82}_{-0.70}$	$+3.20_{-2.14}$	$+3.48_{-2.47}$	$-1.66^{+0.40}_{-1.11}$	$+0.37_{-1.69}$	$+0.41_{-1.71}$	$-5.59^{+1.88}_{-2.66}$	$+2.01_{-6.24}$	$+3.25_{-7.96}$
J0624+3856		$2.75^{+0.73}_{-0.74}$	$+1.93_{-3.47}$	$+2.49_{-4.17}$	$2.84^{+2.09}_{-0.79}$	$+2.65_{-3.11}$	$+2.66_{-4.12}$	$-1.52^{+0.31}_{-1.27}$	$+0.30_{-1.77}$	$+0.31_{-1.82}$	$-8.29^{+2.23}_{-3.81}$	$+4.02_{-6.37}$	$+5.60_{-6.37}$
J0625+4440	2σ	$1.34^{+0.38}_{-2.11}$	$+1.01_{-2.83}$	$+2.14_{-2.83}$	$3.42^{+0.98}_{-0.51}$	$+1.86_{-0.68}$	$+2.02_{-0.89}$	$-2.88^{+0.20}_{-0.23}$	$+0.44_{-0.47}$	$+0.85_{-0.48}$	$-9.29^{+1.28}_{-2.33}$	$+1.94_{-4.18}$	$+2.23_{-5.00}$
J0626+8202		$2.86^{+0.95}_{-1.31}$	$+1.30_{-4.02}$	$+2.32_{-4.23}$	$3.47^{+1.55}_{-0.93}$	$+1.92_{-3.37}$	$+1.99_{-4.18}$	$-3.03^{+0.99}_{-0.30}$	$+1.72_{-0.23}$	$+1.72_{-0.30}$	$-9.62^{+1.49}_{-4.20}$	$+4.48_{-6.02}$	$+6.06_{-6.02}$
J0629-1959		$2.07^{+0.62}_{-1.00}$	$+1.05_{-3.53}$	$+2.27_{-3.53}$	$2.42^{+1.64}_{-0.60}$	$+3.06_{-0.95}$	$+3.06_{-1.96}$	$-2.40^{+1.16}_{-0.26}$	$+1.09_{-0.88}$	$+1.18_{-0.92}$	$-6.28^{+1.09}_{-3.10}$	$+2.42_{-5.28}$	$+3.15_{-6.12}$
J0630-1323		$2.64^{+0.83}_{-0.81}$	$+2.48_{-2.98}$	$+2.75_{-4.04}$	$2.95^{+1.61}_{-1.24}$	$+2.53_{-2.97}$	$+2.52_{-4.42}$	$-1.64^{+0.21}_{-1.71}$	$+0.33_{-1.72}$	$+0.40_{-1.71}$	$-9.49^{+2.68}_{-3.26}$	$+5.76_{-5.05}$	$+7.10_{-5.68}$
J0631-1410		$2.32^{+0.71}_{-1.05}$	$+1.88_{-3.09}$	$+2.06_{-3.72}$	$2.56^{+1.50}_{-0.78}$	$+2.93_{-1.76}$	$+2.93_{-3.19}$	$-3.14^{+1.16}_{-0.23}$	$+1.81_{-0.23}$	$+1.90_{-0.22}$	$-7.11^{+1.36}_{-3.07}$	$+2.87_{-5.90}$	$+4.65_{-6.38}$
J0637+3322		$2.67^{+0.67}_{-2.60}$	$+1.69_{-4.16}$	$+2.58_{-4.11}$	$4.65^{+0.82}_{-1.49}$	$+0.81_{-3.54}$	$+0.84_{-4.75}$	$-3.00^{+0.58}_{-0.33}$	$+1.67_{-0.27}$	$+1.67_{-0.33}$	$-12.20^{+3.25}_{-3.31}$	$+6.16_{-3.73}$	$+7.74_{-4.09}$
J0638+5933		$1.52^{+0.49}_{-0.65}$	$+1.14_{-2.24}$	$+1.11_{-3.01}$	$2.27^{+1.87}_{-0.61}$	$+3.21_{-0.67}$	$+3.21_{-1.39}$	$-2.10^{+0.81}_{-0.36}$	$+0.81_{-1.11}$	$+0.90_{-1.19}$	$-6.71^{+0.90}_{-3.62}$	$+1.88_{-5.65}$	$+2.76_{-6.58}$
J0639+7324		$2.81^{+0.76}_{-0.73}$	$+1.20_{-3.49}$	$+1.70_{-4.25}$	$3.21^{+1.63}_{-0.94}$	$+2.28_{-3.49}$	$+2.28_{-4.62}$	$-3.10^{+1.89}_{-0.32}$	$+1.88_{-0.18}$	$+1.89_{-0.24}$	$-8.33^{+1.70}_{-3.22}$	$+5.20_{-5.01}$	$+6.28_{-6.35}$
J0642+3509		$1.96^{+0.69}_{-1.13}$	$+1.24_{-2.98}$	$+3.35_{-3.22}$	$2.70^{+1.78}_{-0.96}$	$+2.80_{-1.91}$	$+2.80_{-3.21}$	$-2.52^{+0.58}_{-0.59}$	$+1.07_{-0.80}$	$+1.18_{-0.81}$	$-8.62^{+2.07}_{-3.83}$	$+3.77_{-6.30}$	$+5.60_{-6.59}$
J0642+8811		$2.72^{+0.84}_{-2.12}$	$+0.83_{-4.05}$	$+1.20_{-4.22}$	$4.34^{+0.72}_{-1.18}$	$+1.12_{-2.84}$	$+1.12_{-3.25}$	$-3.02^{+0.53}_{-0.34}$	$+1.58_{-0.28}$	$+1.67_{-0.34}$	$-11.52^{+2.30}_{-2.38}$	$+5.97_{-2.72}$	$+5.97_{-3.80}$
J0644+3914		$2.33^{+0.83}_{-0.81}$	$+1.51_{-2.58}$	$+1.92_{-3.59}$	$2.45^{+2.01}_{-0.79}$	$+2.73_{-3.31}$	$+3.01_{-3.77}$	$-1.49^{+0.26}_{-1.07}$	$+0.22_{-1.84}$	$+0.26_{-1.85}$	$-7.47^{+1.41}_{-3.86}$	$+4.43_{-5.67}$	$+5.00_{-6.45}$

Table C.2: Results of fitting the broken power-law model over the 1290 selected observations from OVRO dataset. Break significance refers to the source having a possible break frequency being (1σ) at 68.3%, (2σ) at 95.5% and (3σ) at 99.7%. The absence of break significance means that the source is not well-fitted at any level.

Name	Break significance	β_l	$\beta_l^{95.5\%}$	$\beta_l^{99.7\%}$	β_h	$\beta_h^{95.5\%}$	$\beta_h^{99.7\%}$	$\log f_{br}$	$\log f_{br}^{95.5\%}$	$\log f_{br}^{99.7\%}$	$\log A$	$\log A^{95.5\%}$	$\log A^{99.7\%}$
J0646+4451		2.27 ^{+0.87} _{-0.64}	+1.68 -3.47	+3.08 -3.59	2.47 ^{+1.66} _{-0.96}	+2.97 -2.01	+3.02 -3.80	-1.56 ^{+0.32} _{-1.07}	+0.26 -1.79	+0.32 -1.80	-6.33 ^{+2.00} _{-3.06}	+2.91 -6.29	+5.26 -6.55
J0650+5616		2.44 ^{+0.83} _{-1.23}	+1.41 -3.18	+1.83 -3.89	3.06 ^{+2.03} _{-0.58}	+2.43 -2.49	+2.44 -4.30	-2.86 ^{+0.82} _{-0.51}	+1.56 -0.47	+1.62 -0.50	-9.13 ^{+1.85} _{-3.81}	+3.98 -6.44	+6.39 -6.70
J0650+6001		2.26 ^{+0.48} _{-0.93}	+1.58 -2.98	+3.21 -3.44	2.77 ^{+1.62} _{-1.12}	+2.64 -2.18	+2.64 -3.79	-2.27 ^{+1.06} _{-0.26}	+0.96 -1.07	+1.05 -1.07	-9.12 ^{+3.08} _{-2.05}	+4.74 -4.14	+6.26 -4.75
J0653+3705		3.13 ^{+1.13} _{-0.98}	+2.02 -3.58	+2.34 -4.29	4.30 ^{+1.05} _{-2.15}	+1.19 -4.55	+1.19 -5.46	-1.63 ^{+0.15} _{-1.68}	+0.36 -1.68	+0.42 -1.70	-11.51 ^{+4.64} _{-2.73}	+7.28 -4.62	+8.67 -5.03
J0654+4514	3 σ	1.45 ^{+0.38} _{-0.58}	+0.77 -1.10	+1.04 -1.48	5.18 ^{+0.28} _{-0.93}	+0.32 -1.75	+0.32 -2.31	-2.23 ^{+0.10} _{-0.09}	+0.19 -0.36	+0.26 -0.52	-11.50 ^{+1.84} _{-0.63}	+3.51 -0.80	+4.63 -0.80
J0654+5042		1.67 ^{+0.56} _{-0.43}	+0.71 -2.87	+1.26 -3.14	2.38 ^{+1.82} _{-0.61}	+3.11 -0.68	+3.11 -1.72	-1.81 ^{+0.57} _{-0.49}	+0.54 -1.40	+0.57 -1.53	-7.07 ^{+1.07} _{-3.00}	+1.73 -4.96	+2.93 -5.58
J0655+4100		3.18 ^{+1.30} _{-0.84}	+2.10 -2.97	+2.19 -4.54	3.75 ^{+1.74} _{-1.50}	+1.74 -4.44	+1.74 -5.24	-3.02 ^{+1.34} _{-0.18}	+1.69 -0.32	+1.80 -0.32	-11.67 ^{+5.38} _{-2.09}	+7.77 -4.14	+9.92 -4.79
J0657+2423		2.24 ^{+1.04} _{-1.50}	+1.07 -3.48	+1.36 -3.74	4.39 ^{+0.33} _{-2.00}	+1.11 -3.20	+1.11 -5.45	-2.90 ^{+0.64} _{-0.36}	+1.52 -0.36	+1.56 -0.42	-11.36 ^{+3.73} _{-1.45}	+5.62 -3.53	+8.94 -4.07
J0702+2644		2.23 ^{+1.34} _{-0.87}	+2.43 -2.73	+3.08 -3.71	3.06 ^{+1.87} _{-1.27}	+2.41 -3.47	+2.44 -4.43	-2.99 ^{+1.03} _{-0.33}	+1.57 -0.33	+1.65 -0.33	-12.07 ^{+4.97} _{-2.09}	+9.21 -2.83	+9.97 -4.44
J0702+8549		2.39 ^{+2.53} _{-0.64}	+3.09 -2.56	+3.10 -3.83	4.33 ^{+0.93} _{-2.39}	+1.12 -4.59	+1.12 -5.81	-3.09 ^{+1.08} _{-0.20}	+1.71 -0.27	+1.85 -0.27	-12.55 ^{+5.62} _{-2.32}	+8.31 -5.83	+9.41 -7.41
J0712+5033	3 σ	-0.75 ^{+0.76} _{-0.53}	+1.63 -0.71	+2.20 -0.71	2.86 ^{+0.83} _{-0.38}	+1.60 -0.67	+2.23 -1.04	-2.51 ^{+0.16} _{-0.11}	+0.35 -0.26	+0.43 -0.47	-7.12 ^{+1.04} _{-1.45}	+1.49 -3.20	+2.06 -4.73
J0717+4538		3.12 ^{+0.81} _{-0.60}	+1.81 -2.92	+2.19 -4.33	3.12 ^{+1.51} _{-1.05}	+2.32 -2.94	+2.32 -4.62	-1.67 ^{+0.17} _{-1.70}	+0.34 -1.70	+0.43 -1.70	-8.76 ^{+2.01} _{-3.17}	+4.74 -5.43	+6.50 -6.10
J0720+4737		2.43 ^{+1.05} _{-1.14}	+2.43 -2.48	+2.94 -3.77	2.41 ^{+2.49} _{-0.91}	+3.08 -3.00	+3.09 -3.48	-1.60 ^{+0.36} _{-1.15}	+0.33 -1.72	+0.35 -1.77	-10.50 ^{+5.96} _{-1.35}	+7.58 -4.93	+8.17 -6.32
J0721+7120	3 σ	0.93 ^{+0.60} _{-0.70}	+0.82 -1.89	+0.88 -2.25	2.88 ^{+1.22} _{-0.42}	+2.44 -0.56	+2.57 -0.74	-1.80 ^{+0.12} _{-0.51}	+0.23 -0.77	+0.26 -1.01	-4.78 ^{+0.65} _{-1.79}	+1.13 -3.40	+1.13 -3.99
J0725+1425		1.73 ^{+0.84} _{-0.63}	+2.96 -2.04	+3.25 -2.98	1.61 ^{+1.88} _{-1.25}	+3.71 -2.34	+3.88 -3.06	-1.53 ^{+0.28} _{-1.19}	+0.28 -1.78	+0.29 -1.84	-4.09 ^{+2.04} _{-3.30}	+3.41 -7.54	+3.63 -9.14
J0726+0636		2.37 ^{+1.00} _{-1.13}	+2.57 -2.97	+3.00 -3.72	2.91 ^{+2.23} _{-0.71}	+2.50 -2.50	+2.59 -3.95	-3.04 ^{+1.11} _{-0.27}	+1.72 -0.18	+1.72 -0.29	-9.97 ^{+2.59} _{-3.67}	+5.80 -5.20	+6.62 -7.06
J0726+2153		3.02 ^{+0.93} _{-0.91}	+2.13 -2.92	+2.13 -4.18	3.31 ^{+1.92} _{-0.74}	+2.11 -3.36	+2.18 -4.54	-3.06 ^{+1.12} _{-0.27}	+1.68 -0.27	+1.74 -0.27	-9.18 ^{+2.67} _{-3.22}	+5.25 -5.58	+7.01 -6.33
J0728+2153		2.44 ^{+0.80} _{-0.86}	+1.40 -2.90	+2.21 -3.42	2.59 ^{+1.97} _{-0.63}	+2.89 -2.24	+2.88 -3.32	-3.08 ^{+1.16} _{-0.20}	+1.69 -0.20	+1.76 -0.24	-7.71 ^{+1.33} _{-4.02}	+3.85 -6.04	+5.17 -6.83
J0728+5701		2.55 ^{+0.69} _{-0.78}	+0.91 -3.42	+1.54 -3.89	2.91 ^{+2.04} _{-0.39}	+2.56 -2.59	+2.56 -4.02	-1.54 ^{+0.29} _{-1.15}	+0.26 -1.76	+0.30 -1.82	-8.61 ^{+1.00} _{-3.75}	+3.88 -5.51	+6.05 -6.04
J0730+4049		4.44 ^{+0.72} _{-2.33}	+1.05 -4.12	+1.05 -5.75	3.35 ^{+2.04} _{-1.42}	+2.12 -3.78	+2.14 -4.78	-2.94 ^{+0.99} _{-0.40}	+1.61 -0.32	+1.62 -0.40	-10.73 ^{+2.39} _{-6.69}	+6.29 -7.73	+7.94 -8.80
J0731+2451		3.10 ^{+1.02} _{-1.09}	+2.36 -1.67	+2.35 -3.21	2.64 ^{+2.78} _{-0.70}	+2.85 -2.98	+2.85 -4.08	-2.24 ^{+0.35} _{-0.93}	+0.91 -0.94	+0.93 -1.08	-8.54 ^{+3.34} _{-4.55}	+5.74 -7.89	+5.73 -10.04
J0732+2548	1 σ	1.57 ^{+0.53} _{-0.79}	+0.91 -2.33	+0.92 -2.93	2.85 ^{+1.57} _{-0.57}	+2.53 -0.81	+2.64 -1.01	-2.09 ^{+0.31} _{-0.51}	+0.47 -1.10	+0.77 -1.18	-7.64 ^{+1.01} _{-2.86}	+1.68 -4.71	+2.23 -5.14
J0733+0456		2.35 ^{+0.68} _{-0.60}	+1.59 -3.78	+3.09 -3.78	2.65 ^{+1.88} _{-0.66}	+2.76 -1.39	+2.82 -3.10	-3.07 ^{+1.12} _{-0.25}	+1.67 -0.24	+1.75 -0.25	-7.56 ^{+1.91} _{-2.83}	+2.66 -5.78	+4.87 -6.17
J0733+5022		2.60 ^{+0.71} _{-0.67}	+1.34 -3.44	+2.47 -3.94	2.82 ^{+1.38} _{-1.06}	+2.65 -3.03	+2.65 -4.31	-1.44 ^{+0.31} _{-1.21}	+0.31 -1.80	+0.31 -1.92	-7.77 ^{+1.26} _{-3.39}	+3.97 -5.24	+5.77 -5.40

Table C.2: Results of fitting the broken power-law model over the 1290 selected observations from OVRO dataset. Break significance refers to the source having a possible break frequency being (1σ) at 68.3%, (2σ) at 95.5% and (3σ) at 99.7%. The absence of break significance means that the source is not well-fitted at any level.

Name	Break significance	β_l	$\beta_l^{95.5\%}$	$\beta_l^{99.7\%}$	β_h	$\beta_h^{95.5\%}$	$\beta_h^{99.7\%}$	$\log f_{br}$	$\log f_{br}^{95.5\%}$	$\log f_{br}^{99.7\%}$	$\log A$	$\log A^{95.5\%}$	$\log A^{99.7\%}$
J0735+4750		$3.44^{+1.17}_{-1.15}$	$+2.02_{-3.08}$	$+2.03_{-4.55}$	$4.00^{+1.05}_{-2.23}$	$+1.19_{-5.36}$	$+1.47_{-5.36}$	$-3.13^{+1.30}_{-0.19}$	$+1.78_{-0.22}$	$+1.87_{-0.25}$	$-10.33^{+4.44}_{-3.21}$	$+6.35_{-5.98}$	$+7.81_{-6.87}$
J0736+2604		$4.12^{+1.14}_{-0.85}$	$+1.38_{-2.74}$	$+1.37_{-5.12}$	$3.35^{+2.12}_{-1.10}$	$+2.13_{-3.67}$	$+2.15_{-4.74}$	$-1.66^{+0.31}_{-1.02}$	$+0.31_{-1.61}$	$+0.31_{-1.71}$	$-11.81^{+4.49}_{-2.92}$	$+6.35_{-6.51}$	$+8.82_{-6.51}$
J0738+1742		$2.34^{+0.73}_{-0.68}$	$+2.43_{-1.96}$	$+2.91_{-3.70}$	$2.13^{+2.34}_{-0.69}$	$+3.34_{-2.23}$	$+3.34_{-3.55}$	$-1.54^{+0.34}_{-1.07}$	$+0.29_{-1.75}$	$+0.34_{-1.78}$	$-5.79^{+1.68}_{-3.87}$	$+2.65_{-7.26}$	$+4.36_{-7.75}$
J0739+0137	1σ	$1.20^{+0.65}_{-1.74}$	$+1.16_{-2.67}$	$+1.49_{-2.68}$	$2.93^{+0.68}_{-0.32}$	$+1.84_{-0.63}$	$+2.50_{-0.70}$	$-2.71^{+0.39}_{-0.33}$	$+0.76_{-0.40}$	$+0.89_{-0.51}$	$-6.38^{+0.77}_{-1.17}$	$+1.34_{-3.57}$	$+1.38_{-4.91}$
J0740+2852		$2.67^{+0.84}_{-1.15}$	$+1.67_{-3.91}$	$+2.58_{-4.07}$	$3.00^{+1.77}_{-0.83}$	$+2.50_{-2.47}$	$+2.50_{-3.95}$	$-3.04^{+1.07}_{-0.33}$	$+1.67_{-0.26}$	$+1.69_{-0.33}$	$-8.81^{+1.39}_{-4.17}$	$+3.74_{-6.50}$	$+6.08_{-7.28}$
J0741+3112		$2.78^{+0.68}_{-0.78}$	$+1.79_{-3.06}$	$+2.69_{-4.00}$	$2.91^{+1.72}_{-0.85}$	$+2.34_{-3.36}$	$+2.56_{-4.32}$	$-1.54^{+0.29}_{-1.15}$	$+0.26_{-1.78}$	$+0.29_{-1.82}$	$-7.39^{+2.02}_{-3.04}$	$+4.76_{-5.47}$	$+6.39_{-6.01}$
J0742+4900	1σ	$2.11^{+0.51}_{-0.56}$	$+0.93_{-1.64}$	$+1.04_{-2.74}$	$2.98^{+2.17}_{-0.13}$	$+2.48_{-0.88}$	$+2.51_{-2.09}$	$-2.18^{+0.52}_{-0.37}$	$+0.76_{-1.08}$	$+0.93_{-1.16}$	$-8.16^{+1.40}_{-3.02}$	$+2.24_{-4.45}$	$+3.66_{-5.04}$
J0742+5444		$1.63^{+0.79}_{-1.38}$	$+0.79_{-2.81}$	$+1.23_{-3.09}$	$2.92^{+0.67}_{-0.64}$	$+2.35_{-0.64}$	$+2.58_{-0.84}$	$-2.65^{+0.59}_{-0.35}$	$+1.08_{-0.57}$	$+1.45_{-0.63}$	$-7.29^{+1.10}_{-1.34}$	$+1.37_{-3.68}$	$+1.75_{-4.51}$
J0743+1714		$2.76^{+0.94}_{-1.08}$	$+1.52_{-3.81}$	$+2.41_{-4.21}$	$3.08^{+1.67}_{-0.64}$	$+2.41_{-1.70}$	$+2.41_{-2.90}$	$-3.02^{+0.90}_{-0.31}$	$+1.50_{-0.31}$	$+1.67_{-0.31}$	$-9.26^{+1.70}_{-3.49}$	$+3.75_{-5.25}$	$+5.29_{-6.14}$
J0745+1011		$2.17^{+0.62}_{-1.41}$	$+0.77_{-3.35}$	$+1.21_{-3.64}$	$2.81^{+2.01}_{-0.42}$	$+2.67_{-1.76}$	$+2.65_{-4.04}$	$-2.89^{+0.85}_{-0.41}$	$+1.66_{-0.36}$	$+1.66_{-0.46}$	$-7.77^{+1.79}_{-3.15}$	$+3.31_{-5.85}$	$+5.34_{-6.87}$
J0745-0044		$2.40^{+1.12}_{-0.67}$	$+1.63_{-3.17}$	$+2.64_{-3.68}$	$2.71^{+1.95}_{-0.93}$	$+2.77_{-2.44}$	$+2.78_{-3.77}$	$-1.55^{+0.29}_{-1.21}$	$+0.22_{-1.80}$	$+0.30_{-1.81}$	$-7.61^{+2.36}_{-3.13}$	$+4.12_{-6.24}$	$+5.73_{-6.86}$
J0746+2549	1σ	$1.52^{+0.61}_{-1.76}$	$+1.05_{-2.87}$	$+1.75_{-3.02}$	$3.06^{+0.74}_{-0.48}$	$+1.80_{-0.65}$	$+2.31_{-0.88}$	$-2.81^{+0.41}_{-0.33}$	$+0.93_{-0.42}$	$+1.18_{-0.50}$	$-7.87^{+1.05}_{-1.45}$	$+1.52_{-3.29}$	$+1.88_{-4.57}$
J0746+2734		$2.53^{+0.88}_{-0.97}$	$+1.75_{-3.35}$	$+2.59_{-3.94}$	$3.12^{+1.53}_{-1.07}$	$+2.38_{-3.17}$	$+2.38_{-4.10}$	$-3.13^{+1.17}_{-0.23}$	$+1.79_{-0.23}$	$+1.89_{-0.23}$	$-8.99^{+2.61}_{-2.90}$	$+5.20_{-4.43}$	$+6.50_{-5.22}$
J0748+2400		$2.32^{+0.86}_{-1.70}$	$+0.91_{-3.81}$	$+1.84_{-3.80}$	$3.16^{+1.52}_{-0.62}$	$+2.30_{-1.52}$	$+2.30_{-2.28}$	$-2.98^{+0.57}_{-0.35}$	$+1.39_{-0.37}$	$+1.61_{-0.37}$	$-8.73^{+2.02}_{-2.83}$	$+3.77_{-4.95}$	$+4.32_{-6.06}$
J0749+7420		$2.35^{+0.80}_{-1.94}$	$+0.91_{-3.72}$	$+1.96_{-3.83}$	$2.99^{+1.53}_{-0.57}$	$+2.50_{-1.41}$	$+2.50_{-3.82}$	$-2.91^{+0.64}_{-0.41}$	$+1.48_{-0.41}$	$+1.60_{-0.41}$	$-8.68^{+2.27}_{-2.50}$	$+3.22_{-5.22}$	$+5.92_{-5.73}$
J0750+1021		$2.15^{+0.67}_{-1.00}$	$+1.13_{-3.17}$	$+3.08_{-3.37}$	$2.75^{+1.56}_{-0.89}$	$+2.74_{-1.45}$	$+2.74_{-3.01}$	$-2.85^{+0.95}_{-0.49}$	$+1.54_{-0.49}$	$+1.60_{-0.51}$	$-8.08^{+1.12}_{-3.36}$	$+2.84_{-6.16}$	$+4.33_{-6.69}$
J0750+1231		$2.79^{+0.71}_{-0.76}$	$+1.29_{-3.96}$	$+2.64_{-4.20}$	$2.96^{+1.81}_{-0.84}$	$+2.50_{-2.75}$	$+2.50_{-4.47}$	$-1.52^{+0.28}_{-1.24}$	$+0.22_{-1.83}$	$+0.28_{-1.85}$	$-7.26^{+1.61}_{-3.54}$	$+4.40_{-5.57}$	$+6.21_{-6.25}$
J0750+1823		$1.69^{+0.60}_{-1.14}$	$+0.84_{-3.05}$	$+1.57_{-3.16}$	$2.91^{+1.49}_{-0.75}$	$+2.52_{-0.83}$	$+2.56_{-1.34}$	$-2.45^{+0.23}_{-0.55}$	$+0.59_{-0.91}$	$+1.02_{-0.92}$	$-8.12^{+0.63}_{-4.46}$	$+1.89_{-5.75}$	$+2.82_{-6.14}$
J0750+4814		$2.43^{+0.80}_{-0.59}$	$+1.21_{-2.90}$	$+2.13_{-3.60}$	$2.73^{+1.86}_{-0.91}$	$+2.76_{-2.70}$	$+2.76_{-4.04}$	$-1.55^{+0.31}_{-1.02}$	$+0.31_{-1.73}$	$+0.32_{-1.80}$	$-7.49^{+1.83}_{-3.30}$	$+3.99_{-5.38}$	$+4.94_{-6.09}$
J0751+3313		$2.63^{+0.85}_{-0.99}$	$+0.95_{-3.79}$	$+2.11_{-4.04}$	$3.09^{+1.41}_{-0.83}$	$+2.37_{-1.77}$	$+2.38_{-4.19}$	$-3.08^{+1.04}_{-0.25}$	$+1.71_{-0.28}$	$+1.84_{-0.28}$	$-9.06^{+2.08}_{-2.55}$	$+4.06_{-4.45}$	$+6.59_{-5.78}$
J0752+3730		$2.03^{+0.80}_{-1.15}$	$+1.17_{-3.02}$	$+1.94_{-3.45}$	$2.83^{+1.69}_{-1.01}$	$+2.67_{-2.05}$	$+2.66_{-3.14}$	$-2.85^{+0.83}_{-0.44}$	$+1.48_{-0.45}$	$+1.60_{-0.51}$	$-10.15^{+3.63}_{-1.96}$	$+5.73_{-4.45}$	$+6.75_{-5.38}$
J0753+5352	1σ	$1.38^{+0.71}_{-1.42}$	$+0.94_{-2.71}$	$+1.37_{-2.87}$	$2.96^{+1.02}_{-0.79}$	$+2.15_{-0.90}$	$+2.53_{-1.01}$	$-2.38^{+0.09}_{-0.65}$	$+0.35_{-0.86}$	$+0.67_{-0.97}$	$-7.64^{+1.36}_{-2.60}$	$+1.71_{-4.90}$	$+2.29_{-5.50}$
J0756+6347		$2.50^{+1.49}_{-1.55}$	$+2.94_{-2.95}$	$+2.96_{-3.91}$	$4.46^{+0.95}_{-2.39}$	$+1.03_{-4.92}$	$+1.02_{-5.96}$	$-3.10^{+1.25}_{-0.26}$	$+1.80_{-0.24}$	$+1.84_{-0.24}$	$-10.93^{+3.90}_{-4.01}$	$+7.02_{-6.19}$	$+8.45_{-8.43}$
J0757+0956	2σ	$0.87^{+0.88}_{-1.24}$	$+1.67_{-2.36}$	$+2.35_{-2.34}$	$4.07^{+0.85}_{-0.88}$	$+1.34_{-1.36}$	$+1.42_{-1.65}$	$-2.63^{+0.21}_{-0.23}$	$+0.35_{-0.67}$	$+0.76_{-0.70}$	$-9.44^{+1.61}_{-2.39}$	$+2.85_{-3.40}$	$+3.58_{-3.49}$

Table C.2: Results of fitting the broken power-law model over the 1290 selected observations from OVRO dataset. Break significance refers to the source having a possible break frequency being (1σ) at 68.3%, (2σ) at 95.5% and (3σ) at 99.7%. The absence of break significance means that the source is not well-fitted at any level.

Name	Break significance	β_l	$\beta_l^{95.5\%}$	$\beta_l^{99.7\%}$	β_h	$\beta_h^{95.5\%}$	$\beta_h^{99.7\%}$	$\log f_{br}$	$\log f_{br}^{95.5\%}$	$\log f_{br}^{99.7\%}$	$\log A$	$\log A^{95.5\%}$	$\log A^{99.7\%}$
J0802+1809		1.69 ^{+0.94} _{-0.99}	+1.59 -2.49	+1.83 -3.05	2.39 ^{+1.95} _{-0.54}	+2.92 -0.91	+3.09 -1.58	-2.57 ^{+0.49} _{-0.54}	+1.06 -0.72	+1.24 -0.75	-9.04 ^{+2.15} _{-3.16}	+3.64 -4.74	+4.44 -6.01
J0805+6144		2.50 ^{+0.62} _{-1.19}	+0.90 -3.49	+2.02 -3.99	3.09 ^{+1.49} _{-0.79}	+2.39 -2.26	+2.39 -4.31	-2.60 ^{+0.60} _{-0.76}	+1.43 -0.68	+1.46 -0.77	-8.53 ^{+2.20} _{-2.43}	+3.81 -5.10	+6.17 -5.69
J0805-0111		2.37 ^{+0.57} _{-0.89}	+1.03 -3.29	+2.94 -3.75	2.82 ^{+1.43} _{-0.60}	+2.65 -1.34	+2.65 -3.78	-2.14 ^{+0.16} _{-1.17}	+0.84 -1.16	+0.90 -1.22	-7.61 ^{+1.01} _{-2.62}	+2.18 -5.62	+4.93 -5.61
J0806+4504		2.16 ^{+0.69} _{-1.77}	+0.89 -3.64	+1.95 -3.64	2.95 ^{+1.43} _{-1.19}	+2.48 -1.70	+2.48 -3.71	-2.98 ^{+0.78} _{-0.36}	+1.65 -0.36	+1.73 -0.38	-10.22 ^{+4.20} _{-1.64}	+5.50 -4.84	+6.79 -5.72
J0807+5117		2.86 ^{+1.17} _{-0.99}	+2.38 -3.14	+2.58 -4.13	4.61 ^{+0.87} _{-2.08}	+0.87 -4.92	+0.87 -6.03	-3.03 ^{+1.00} _{-0.33}	+1.57 -0.34	+1.68 -0.33	-12.96 ^{+5.07} _{-2.21}	+8.53 -4.04	+10.55 -4.37
J0807-0541		1.44 ^{+4.01} _{-0.36}	+3.97 -2.56	+4.01 -2.93	3.64 ^{+1.85} _{-2.50}	+1.85 -4.62	+1.85 -5.09	-2.05 ^{+0.63} _{-0.67}	+0.75 -1.15	+0.75 -1.26	-15.96 ^{+8.82} _{-1.51}	+11.80 -3.75	+13.38 -3.83
J0808+4052		2.37 ^{+0.57} _{-0.60}	+1.09 -3.04	+2.05 -3.81	2.66 ^{+2.15} _{-0.64}	+2.81 -2.34	+2.81 -3.98	-1.50 ^{+0.26} _{-1.05}	+0.24 -1.77	+0.26 -1.85	-7.14 ^{+1.92} _{-3.45}	+3.63 -5.96	+5.72 -6.62
J0808+4950		2.41 ^{+0.43} _{-1.17}	+1.24 -3.25	+2.26 -3.91	2.90 ^{+1.57} _{-0.42}	+2.30 -1.10	+2.52 -1.28	-2.51 ^{+0.41} _{-0.86}	+1.14 -0.84	+1.25 -0.86	-7.69 ^{+1.83} _{-1.98}	+1.83 -4.82	+2.58 -5.60
J0808+7315		3.82 ^{+1.16} _{-0.96}	+1.67 -3.06	+1.64 -5.16	4.49 ^{+0.97} _{-2.49}	+0.90 -5.15	+0.97 -5.82	-1.64 ^{+0.32} _{-1.03}	+0.32 -1.61	+0.32 -1.69	-12.83 ^{+5.23} _{-2.46}	+9.53 -3.65	+10.16 -5.61
J0808-0751		2.73 ^{+0.72} _{-0.78}	+1.37 -3.19	+2.16 -4.17	2.88 ^{+1.42} _{-0.82}	+2.61 -2.01	+2.60 -3.72	-2.27 ^{+1.03} _{-0.42}	+0.96 -1.09	+1.03 -1.09	-7.26 ^{+1.32} _{-3.02}	+3.01 -5.41	+4.84 -5.53
J0809+5341		1.95 ^{+0.69} _{-0.84}	+0.81 -3.36	+2.05 -3.34	2.69 ^{+1.54} _{-0.52}	+2.64 -0.74	+2.78 -0.92	-2.20 ^{+0.31} _{-0.88}	+0.66 -1.16	+0.94 -1.16	-7.62 ^{+1.32} _{-2.81}	+1.72 -5.21	+2.11 -5.79
J0810+4134		2.61 ^{+0.81} _{-1.44}	+0.99 -4.04	+2.66 -4.11	3.73 ^{+1.14} _{-1.06}	+1.77 -2.04	+1.77 -3.51	-3.02 ^{+0.59} _{-0.27}	+1.48 -0.35	+1.73 -0.35	-10.70 ^{+2.58} _{-2.62}	+4.24 -4.40	+6.79 -4.57
J0811+0146		2.33 ^{+0.59} _{-0.82}	+1.39 -3.28	+2.68 -3.65	2.50 ^{+1.00} _{-0.43}	+2.85 -0.62	+2.97 -2.51	-3.12 ^{+1.30} _{-0.24}	+1.79 -0.24	+1.87 -0.24	-5.76 ^{+1.14} _{-1.44}	+1.24 -4.69	+3.40 -5.26
J0811+4533		2.17 ^{+0.70} _{-2.22}	+1.23 -3.62	+2.71 -3.65	3.80 ^{+1.27} _{-1.03}	+1.70 -2.06	+1.69 -2.98	-2.97 ^{+0.44} _{-0.30}	+1.34 -0.39	+1.63 -0.40	-10.42 ^{+1.85} _{-4.00}	+4.20 -5.19	+5.24 -5.65
J0813+2542	1 σ	0.45 ^{+0.87} _{-1.47}	+1.80 -1.90	+2.32 -1.94	3.05 ^{+1.34} _{-0.90}	+2.44 -1.03	+2.45 -1.43	-2.73 ^{+0.23} _{-0.39}	+0.83 -0.61	+1.18 -0.62	-9.04 ^{+2.78} _{-2.42}	+2.81 -5.35	+3.60 -6.15
J0814+5609		2.58 ^{+1.58} _{-1.36}	+2.53 -3.51	+2.89 -4.01	4.58 ^{+0.87} _{-2.26}	+0.91 -5.03	+0.91 -5.93	-2.84 ^{+0.97} _{-0.15}	+1.46 -0.22	+1.48 -0.29	-12.18 ^{+5.39} _{-1.95}	+7.24 -4.82	+9.16 -4.96
J0814+6431		2.43 ^{+0.90} _{-0.76}	+1.53 -2.88	+2.61 -3.35	2.81 ^{+2.01} _{-0.70}	+2.65 -2.27	+2.67 -4.14	-1.47 ^{+0.30} _{-1.22}	+0.28 -1.83	+0.34 -1.89	-7.96 ^{+1.57} _{-3.39}	+3.30 -6.15	+5.60 -6.15
J0815+3635		2.21 ^{+0.76} _{-0.98}	+2.82 -2.39	+2.82 -3.54	2.55 ^{+1.92} _{-1.18}	+2.94 -2.87	+2.93 -3.74	-3.05 ^{+1.07} _{-0.29}	+1.79 -0.23	+1.83 -0.23	-8.08 ^{+2.95} _{-3.55}	+5.29 -6.11	+6.18 -8.42
J0818+4222		2.64 ^{+0.65} _{-0.57}	+2.23 -2.47	+2.83 -3.80	2.75 ^{+1.64} _{-0.57}	+2.74 -1.46	+2.74 -3.57	-2.07 ^{+0.83} _{-0.60}	+0.77 -1.29	+0.83 -1.29	-7.19 ^{+1.12} _{-2.79}	+2.81 -5.14	+4.81 -5.80
J0819+3226		2.22 ^{+0.81} _{-0.96}	+1.62 -2.79	+2.48 -3.66	2.76 ^{+1.86} _{-0.45}	+2.74 -0.93	+2.74 -1.63	-2.29 ^{+0.18} _{-1.05}	+0.78 -1.05	+0.96 -1.05	-7.81 ^{+1.32} _{-3.30}	+2.05 -5.43	+2.56 -6.28
J0823+2928		2.05 ^{+0.94} _{-1.29}	+1.73 -3.20	+2.35 -3.47	2.48 ^{+2.37} _{-0.63}	+2.73 -2.80	+2.97 -3.66	-2.97 ^{+1.06} _{-0.32}	+1.55 -0.35	+1.65 -0.35	-7.18 ^{+1.82} _{-4.60}	+3.30 -7.37	+4.62 -8.40
J0824+3916	2 σ	-0.80 ^{+1.18} _{-0.70}	+2.49 -0.69	+3.52 -0.69	4.80 ^{+0.66} _{-0.68}	+0.70 -1.61	+0.70 -2.45	-2.82 ^{+0.11} _{-0.15}	+0.25 -0.30	+0.41 -0.36	-12.41 ^{+1.73} _{-1.67}	+4.08 -1.99	+5.97 -1.99
J0824+5552	2 σ	2.14 ^{+1.04} _{-1.51}	+1.04 -3.38	+1.33 -3.62	5.10 ^{+0.38} _{-1.00}	+0.39 -1.76	+0.39 -2.34	-2.66 ^{+0.23} _{-0.38}	+0.38 -0.65	+0.53 -0.65	-11.80 ^{+1.36} _{-1.96}	+3.24 -2.32	+4.02 -2.74
J0824-1527		3.24 ^{+1.62} _{-0.81}	+2.23 -2.99	+2.22 -4.59	3.81 ^{+1.27} _{-2.24}	+1.53 -4.37	+1.68 -5.25	-1.61 ^{+0.30} _{-1.12}	+0.30 -1.63	+0.30 -1.71	-11.15 ^{+5.35} _{-2.52}	+7.81 -4.68	+9.65 -5.69

Table C.2: Results of fitting the broken power-law model over the 1290 selected observations from OVRO dataset. Break significance refers to the source having a possible break frequency being (1σ) at 68.3%, (2σ) at 95.5% and (3σ) at 99.7%. The absence of break significance means that the source is not well-fitted at any level.

Name	Break significance	β_l	$\beta_l^{95.5\%}$	$\beta_l^{99.7\%}$	β_h	$\beta_h^{95.5\%}$	$\beta_h^{99.7\%}$	$\log f_{br}$	$\log f_{br}^{95.5\%}$	$\log f_{br}^{99.7\%}$	$\log A$	$\log A^{95.5\%}$	$\log A^{99.7\%}$
J0825+0309		$2.85^{+0.74}_{-0.81}$	$+0.99_{-3.85}$	$+2.16_{-4.33}$	$3.17^{+1.12}_{-0.68}$	$+2.19_{-1.74}$	$+2.19_{-3.90}$	$-3.08^{+1.10}_{-0.29}$	$+1.81_{-0.23}$	$+1.83_{-0.29}$	$-7.42^{+1.36}_{-1.96}$	$+2.38_{-4.21}$	$+5.61_{-4.67}$
J0825+1332		$2.00^{+0.73}_{-0.73}$	$+0.91_{-3.49}$	$+2.44_{-3.49}$	$2.41^{+1.83}_{-0.77}$	$+3.04_{-1.62}$	$+3.03_{-3.23}$	$-1.65^{+0.31}_{-1.07}$	$+0.26_{-1.63}$	$+0.34_{-1.66}$	$-7.76^{+1.61}_{-3.49}$	$+2.96_{-6.55}$	$+4.97_{-7.31}$
J0825+6157		$3.00^{+0.97}_{-1.14}$	$+2.23_{-3.54}$	$+2.23_{-4.47}$	$4.31^{+1.10}_{-1.48}$	$+1.15_{-4.21}$	$+1.15_{-5.71}$	$-3.04^{+1.12}_{-0.24}$	$+1.79_{-0.24}$	$+1.80_{-0.33}$	$-10.23^{+2.12}_{-3.91}$	$+5.60_{-5.53}$	$+7.16_{-5.98}$
J0827+3525		$2.26^{+0.78}_{-1.53}$	$+2.04_{-3.01}$	$+2.04_{-3.73}$	$3.32^{+1.16}_{-1.49}$	$+2.12_{-2.79}$	$+2.15_{-4.32}$	$-2.99^{+1.12}_{-0.25}$	$+1.73_{-0.24}$	$+1.79_{-0.34}$	$-10.56^{+3.74}_{-1.70}$	$+5.43_{-4.62}$	$+7.69_{-6.59}$
J0830+2410	1 σ	$1.95^{+0.68}_{-1.06}$	$+1.25_{-2.87}$	$+1.42_{-3.39}$	$3.57^{+1.11}_{-0.44}$	$+1.92_{-0.58}$	$+1.92_{-1.03}$	$-2.29^{+0.15}_{-0.53}$	$+0.31_{-0.96}$	$+0.60_{-1.01}$	$-8.62^{+0.83}_{-2.35}$	$+1.34_{-3.76}$	$+2.29_{-3.85}$
J0831+0429		$2.37^{+0.76}_{-1.19}$	$+1.00_{-3.86}$	$+2.70_{-3.85}$	$2.96^{+0.88}_{-0.68}$	$+2.52_{-0.80}$	$+2.52_{-1.83}$	$-3.04^{+0.87}_{-0.33}$	$+1.78_{-0.26}$	$+1.78_{-0.33}$	$-7.22^{+1.17}_{-2.06}$	$+1.98_{-4.09}$	$+3.33_{-5.05}$
J0833+0350		$2.16^{+1.04}_{-1.07}$	$+1.28_{-3.29}$	$+2.68_{-3.62}$	$2.56^{+1.67}_{-0.82}$	$+2.95_{-1.68}$	$+2.94_{-3.06}$	$-2.96^{+0.88}_{-0.41}$	$+1.58_{-0.41}$	$+1.71_{-0.41}$	$-7.79^{+1.93}_{-3.44}$	$+3.01_{-6.65}$	$+4.65_{-6.96}$
J0833+4224		$2.37^{+0.87}_{-1.21}$	$+1.09_{-3.65}$	$+2.02_{-3.75}$	$2.71^{+1.59}_{-0.65}$	$+2.77_{-2.00}$	$+2.73_{-3.54}$	$-3.08^{+1.15}_{-0.26}$	$+1.77_{-0.26}$	$+1.86_{-0.26}$	$-7.72^{+1.72}_{-2.59}$	$+3.13_{-5.66}$	$+5.26_{-5.80}$
J0834+6019		$2.69^{+0.67}_{-1.19}$	$+1.26_{-3.14}$	$+1.84_{-4.16}$	$3.49^{+1.52}_{-0.56}$	$+2.00_{-1.72}$	$+1.99_{-3.31}$	$-2.59^{+0.28}_{-0.77}$	$+1.05_{-0.77}$	$+1.19_{-0.77}$	$-9.96^{+2.09}_{-2.63}$	$+3.92_{-4.25}$	$+6.37_{-4.64}$
J0835+6835	3 σ	$-1.12^{+0.94}_{-0.38}$	$+2.24_{-0.37}$	$+3.13_{-0.38}$	$3.99^{+1.09}_{-0.79}$	$+1.49_{-1.46}$	$+1.50_{-1.82}$	$-2.78^{+0.12}_{-0.11}$	$+0.22_{-0.27}$	$+0.59_{-0.27}$	$-11.40^{+2.46}_{-2.08}$	$+3.63_{-3.70}$	$+4.67_{-3.74}$
J0836+2728	1 σ	$2.78^{+0.80}_{-2.22}$	$+0.86_{-4.23}$	$+1.27_{-4.28}$	$4.97^{+0.52}_{-1.04}$	$+0.52_{-2.26}$	$+0.53_{-3.82}$	$-2.96^{+0.35}_{-0.28}$	$+1.19_{-0.36}$	$+1.47_{-0.39}$	$-12.68^{+1.78}_{-2.12}$	$+4.38_{-2.70}$	$+7.15_{-2.69}$
J0837+2454		$2.39^{+0.81}_{-0.79}$	$+1.55_{-3.87}$	$+3.04_{-3.87}$	$2.73^{+1.18}_{-0.94}$	$+2.68_{-1.17}$	$+2.72_{-2.76}$	$-3.07^{+1.00}_{-0.26}$	$+1.67_{-0.26}$	$+1.74_{-0.26}$	$-8.18^{+2.47}_{-1.81}$	$+3.17_{-4.63}$	$+4.62_{-5.32}$
J0837+5825		$3.45^{+0.81}_{-1.12}$	$+2.04_{-3.65}$	$+2.04_{-4.93}$	$4.02^{+1.11}_{-1.97}$	$+1.47_{-4.33}$	$+1.47_{-5.35}$	$-1.78^{+ -0.04}_{-1.56}$	$+0.46_{-1.56}$	$+0.54_{-1.57}$	$-11.37^{+4.21}_{-2.47}$	$+7.73_{-3.55}$	$+8.75_{-4.65}$
J0839+0104		$2.13^{+0.62}_{-0.99}$	$+0.82_{-3.09}$	$+1.01_{-3.51}$	$2.82^{+1.19}_{-0.78}$	$+2.63_{-1.08}$	$+2.63_{-2.20}$	$-2.58^{+0.45}_{-0.77}$	$+1.22_{-0.77}$	$+1.34_{-0.78}$	$-8.06^{+2.20}_{-1.86}$	$+2.77_{-4.76}$	$+3.86_{-5.51}$
J0842+1835		$1.42^{+0.78}_{-1.35}$	$+0.99_{-2.86}$	$+1.58_{-2.88}$	$2.49^{+1.97}_{-0.59}$	$+2.94_{-0.99}$	$+2.99_{-1.25}$	$-2.62^{+0.30}_{-0.65}$	$+0.92_{-0.71}$	$+1.19_{-0.71}$	$-8.18^{+1.70}_{-3.80}$	$+2.71_{-6.25}$	$+3.36_{-7.59}$
J0847-0703		$2.20^{+0.73}_{-1.05}$	$+1.01_{-3.21}$	$+1.18_{-3.62}$	$3.30^{+0.99}_{-0.48}$	$+1.86_{-0.79}$	$+2.18_{-0.86}$	$-2.58^{+0.38}_{-0.52}$	$+0.72_{-0.79}$	$+1.13_{-0.79}$	$-8.52^{+1.25}_{-1.79}$	$+1.87_{-3.68}$	$+2.21_{-4.30}$
J0849+5108	3 σ	$1.04^{+0.39}_{-0.50}$	$+0.66_{-1.23}$	$+0.75_{-1.73}$	$4.82^{+0.53}_{-1.40}$	$+0.65_{-2.28}$	$+0.68_{-2.63}$	$-2.00^{+0.19}_{-0.19}$	$+0.34_{-0.50}$	$+0.37_{-0.64}$	$-10.16^{+2.34}_{-0.93}$	$+4.03_{-1.21}$	$+4.62_{-1.38}$
J0850-1213	2 σ	$-0.81^{+1.45}_{-0.69}$	$+2.94_{-0.62}$	$+3.47_{-0.69}$	$2.87^{+0.52}_{-0.35}$	$+1.26_{-0.64}$	$+1.75_{-0.63}$	$-2.82^{+0.18}_{-0.26}$	$+0.84_{-0.28}$	$+0.84_{-0.47}$	$-6.49^{+0.42}_{-1.39}$	$+1.17_{-2.83}$	$+1.18_{-3.95}$
J0854+2006	2 σ	$1.34^{+0.57}_{-1.08}$	$+0.88_{-2.46}$	$+1.23_{-2.79}$	$3.15^{+1.32}_{-0.55}$	$+2.24_{-0.63}$	$+2.34_{-0.88}$	$-2.17^{+0.18}_{-0.43}$	$+0.26_{-0.98}$	$+0.38_{-1.09}$	$-5.41^{+1.06}_{-2.52}$	$+1.07_{-4.41}$	$+1.77_{-4.41}$
J0854+5757		$4.83^{+0.67}_{-1.29}$	$+0.67_{-3.77}$	$+0.67_{-6.14}$	$4.65^{+0.83}_{-2.76}$	$+0.83_{-5.35}$	$+0.83_{-6.12}$	$-2.17^{+0.90}_{-0.51}$	$+0.87_{-1.16}$	$+0.95_{-1.16}$	$-14.65^{+5.32}_{-3.05}$	$+10.22_{-3.66}$	$+12.99_{-4.26}$
J0856+2111		$1.54^{+1.60}_{-1.70}$	$+3.88_{-2.42}$	$+3.88_{-2.96}$	$4.21^{+1.22}_{-1.98}$	$+1.28_{-4.75}$	$+1.29_{-5.59}$	$-2.57^{+0.53}_{-0.75}$	$+1.19_{-0.77}$	$+1.33_{-0.77}$	$-8.48^{+2.89}_{-5.13}$	$+6.28_{-8.25}$	$+6.28_{-10.66}$
J0856-1105		$2.55^{+0.45}_{-0.87}$	$+1.11_{-3.62}$	$+2.57_{-3.62}$	$2.79^{+1.86}_{-0.44}$	$+2.69_{-2.00}$	$+2.69_{-4.25}$	$-3.09^{+1.22}_{-0.26}$	$+1.82_{-0.22}$	$+1.84_{-0.28}$	$-7.57^{+1.74}_{-2.76}$	$+3.51_{-5.46}$	$+5.90_{-6.45}$
J0900+4108		$2.85^{+1.28}_{-1.13}$	$+2.19_{-3.55}$	$+2.29_{-4.22}$	$4.39^{+0.86}_{-2.05}$	$+1.10_{-4.67}$	$+1.10_{-5.34}$	$-1.65^{+0.34}_{-1.10}$	$+0.34_{-1.59}$	$+0.34_{-1.68}$	$-10.08^{+3.50}_{-3.77}$	$+5.10_{-6.57}$	$+6.66_{-7.30}$
J0901+0448		$3.28^{+0.99}_{-0.93}$	$+1.59_{-3.51}$	$+1.89_{-4.66}$	$3.87^{+1.41}_{-1.26}$	$+1.61_{-3.87}$	$+1.62_{-5.30}$	$-3.07^{+1.19}_{-0.27}$	$+1.63_{-0.28}$	$+1.71_{-0.28}$	$-11.26^{+2.97}_{-3.41}$	$+5.95_{-5.42}$	$+8.24_{-5.42}$

Table C.2: Results of fitting the broken power-law model over the 1290 selected observations from OVRO dataset. Break significance refers to the source having a possible break frequency being (1σ) at 68.3%, (2σ) at 95.5% and (3σ) at 99.7%. The absence of break significance means that the source is not well-fitted at any level.

Name	Break significance	β_l	$\beta_l^{95.5\%}$	$\beta_l^{99.7\%}$	β_h	$\beta_h^{95.5\%}$	$\beta_h^{99.7\%}$	$\log f_{br}$	$\log f_{br}^{95.5\%}$	$\log f_{br}^{99.7\%}$	$\log A$	$\log A^{95.5\%}$	$\log A^{99.7\%}$
J0902+0443		2.12 ^{+2.13} _{-1.41}	+3.38 -2.77	+3.38 -3.51	4.25 ^{+1.15} _{-2.17}	+1.24 -4.69	+1.24 -5.67	-2.75 ^{+1.02} _{-0.17}	+1.40 -0.28	+1.40 -0.38	-8.61 ^{+1.95} _{-5.95}	+3.55 -8.78	+5.62 -10.66
J0902+4310		2.70 ^{+0.90} _{-0.89}	+1.64 -3.90	+2.66 -4.18	2.86 ^{+1.97} _{-0.69}	+2.64 -2.10	+2.63 -4.32	-3.07 ^{+1.04} _{-0.25}	+1.67 -0.25	+1.76 -0.25	-8.48 ^{+1.70} _{-3.96}	+3.85 -6.28	+5.70 -7.20
J0902+5402		4.48 ^{+0.95} _{-1.75}	+1.01 -3.80	+1.01 -5.92	4.57 ^{+0.90} _{-2.88}	+0.93 -5.44	+0.91 -6.07	-1.73 ^{+0.34} _{-1.02}	+0.34 -1.56	+0.42 -1.59	-8.13 ^{+2.28} _{-6.41}	+3.45 -10.21	+5.06 -10.66
J0903+6757		2.40 ^{+0.91} _{-1.06}	+1.72 -3.36	+2.49 -3.89	3.17 ^{+1.16} _{-1.13}	+2.33 -1.29	+2.33 -2.17	-2.97 ^{+0.85} _{-0.35}	+1.56 -0.34	+1.66 -0.35	-8.86 ^{+2.12} _{-2.74}	+3.21 -4.88	+4.11 -6.33
J0903-1721	2 σ	0.43 ^{+0.61} _{-0.77}	+1.53 -1.17	+1.62 -1.88	5.08 ^{+0.42} _{-1.02}	+0.42 -2.14	+0.42 -3.17	-2.37 ^{+0.10} _{-0.12}	+0.20 -0.28	+0.34 -0.34	-12.78 ^{+2.36} _{-0.99}	+4.63 -1.22	+6.42 -1.35
J0905+2849		3.24 ^{+1.89} _{-0.70}	+2.14 -3.37	+2.22 -4.46	3.98 ^{+1.41} _{-2.05}	+1.39 -5.14	+1.51 -5.43	-1.73 ^{+0.15} _{-1.60}	+0.32 -1.60	+0.41 -1.60	-11.83 ^{+4.71} _{-3.38}	+7.76 -5.24	+9.80 -6.56
J0906+6930		4.74 ^{+0.76} _{-1.46}	+0.76 -3.28	+0.76 -5.39	4.40 ^{+1.10} _{-2.57}	+1.10 -5.27	+1.10 -5.81	-1.65 ^{+0.29} _{-0.98}	+0.29 -1.62	+0.34 -1.67	-10.62 ^{+3.93} _{-4.58}	+6.08 -8.21	+7.51 -8.91
J0908+1609		3.31 ^{+1.49} _{-0.92}	+2.14 -2.68	+2.18 -4.34	3.35 ^{+2.14} _{-1.10}	+2.14 -4.46	+2.14 -4.84	-1.58 ^{+0.32} _{-1.15}	+0.25 -1.78	+0.34 -1.78	-11.23 ^{+3.99} _{-3.86}	+6.98 -6.01	+8.47 -7.36
J0909+0121	2 σ	0.94 ^{+0.47} _{-1.97}	+1.23 -2.44	+1.82 -2.44	3.75 ^{+0.57} _{-0.83}	+1.47 -0.93	+1.75 -1.14	-2.80 ^{+0.18} _{-0.21}	+0.34 -0.48	+0.67 -0.48	-9.02 ^{+1.56} _{-1.70}	+2.09 -3.45	+2.63 -4.16
J0909+0200		1.86 ^{+0.60} _{-1.52}	+0.83 -3.24	+1.23 -3.34	2.71 ^{+1.74} _{-0.50}	+2.77 -1.02	+2.77 -2.84	-2.60 ^{+0.24} _{-0.69}	+1.20 -0.75	+1.38 -0.74	-8.17 ^{+1.40} _{-3.46}	+2.36 -5.94	+4.56 -6.20
J0910+2248		2.79 ^{+1.01} _{-0.54}	+2.20 -1.49	+2.70 -2.89	3.18 ^{+1.49} _{-1.43}	+2.31 -3.70	+2.31 -4.53	-1.57 ^{+0.33} _{-1.06}	+0.33 -1.71	+0.33 -1.80	-9.63 ^{+3.00} _{-2.76}	+5.81 -4.67	+7.33 -5.39
J0910+3329		2.24 ^{+1.86} _{-0.96}	+3.22 -2.12	+3.21 -3.23	2.53 ^{+1.61} _{-1.43}	+2.85 -2.98	+2.94 -3.99	-3.04 ^{+1.22} _{-0.23}	+1.81 -0.20	+1.83 -0.27	-10.35 ^{+3.83} _{-3.00}	+6.59 -4.54	+8.31 -7.39
J0914+0245		2.63 ^{+0.82} _{-1.81}	+1.07 -4.09	+2.03 -4.09	4.12 ^{+0.57} _{-1.63}	+1.38 -2.93	+1.36 -5.58	-3.01 ^{+0.84} _{-0.34}	+1.66 -0.32	+1.78 -0.34	-8.87 ^{+1.38} _{-3.49}	+3.71 -5.28	+6.90 -5.97
J0917-1345		3.28 ^{+2.10} _{-1.57}	+2.20 -3.91	+2.19 -4.74	2.70 ^{+2.71} _{-1.52}	+2.79 -3.79	+2.80 -4.10	-2.49 ^{+1.03} _{-0.27}	+1.06 -0.80	+1.18 -0.82	-14.88 ^{+6.61} _{-2.44}	+10.49 -4.45	+11.99 -4.74
J0919+3324		2.68 ^{+1.01} _{-0.83}	+2.39 -2.58	+2.39 -4.06	3.08 ^{+1.34} _{-1.46}	+2.40 -3.38	+2.40 -4.42	-3.05 ^{+1.21} _{-0.20}	+1.70 -0.22	+1.74 -0.27	-9.83 ^{+3.34} _{-2.77}	+5.92 -5.58	+7.00 -6.59
J0920+4441		2.85 ^{+0.85} _{-0.78}	+2.64 -2.76	+2.64 -4.34	3.06 ^{+1.39} _{-0.93}	+2.44 -2.16	+2.43 -3.86	-3.07 ^{+1.09} _{-0.24}	+1.71 -0.20	+1.76 -0.25	-7.49 ^{+1.71} _{-3.09}	+3.30 -6.03	+5.48 -6.03
J0921+6215		2.10 ^{+0.64} _{-0.92}	+2.00 -2.77	+2.36 -3.57	2.61 ^{+1.95} _{-0.66}	+2.87 -2.25	+2.87 -3.94	-2.54 ^{+1.28} _{-0.14}	+1.22 -0.81	+1.28 -0.83	-7.22 ^{+1.74} _{-3.45}	+4.38 -5.85	+5.31 -6.97
J0922-0529		2.16 ^{+0.58} _{-0.51}	+1.95 -1.85	+2.32 -3.32	2.39 ^{+1.96} _{-0.59}	+3.11 -1.80	+3.11 -3.01	-1.64 ^{+0.38} _{-0.94}	+0.38 -1.60	+0.39 -1.73	-6.88 ^{+1.14} _{-3.55}	+3.82 -5.19	+4.37 -6.71
J0923+2815	3 σ	1.07 ^{+0.89} _{-1.29}	+1.14 -2.56	+1.57 -2.56	4.61 ^{+0.17} _{-1.39}	+0.88 -1.48	+0.88 -1.93	-2.59 ^{+0.15} _{-0.24}	+0.24 -0.55	+0.39 -0.62	-10.87 ^{+2.02} _{-1.42}	+3.26 -2.07	+3.93 -2.27
J0923+3849	1 σ	1.65 ^{+0.61} _{-1.46}	+0.99 -3.02	+1.42 -3.12	4.17 ^{+0.36} _{-1.48}	+1.31 -1.66	+1.31 -1.90	-2.47 ^{+0.30} _{-0.36}	+0.42 -0.85	+0.77 -0.84	-10.55 ^{+3.00} _{-1.02}	+3.80 -2.73	+4.18 -3.36
J0923+4125		0.99 ^{+1.52} _{-0.60}	+1.72 -2.26	+3.56 -2.41	3.00 ^{+1.10} _{-0.84}	+2.30 -0.96	+2.42 -1.25	-2.66 ^{+0.38} _{-0.42}	+1.06 -0.60	+1.33 -0.66	-8.12 ^{+1.57} _{-2.55}	+2.33 -4.71	+2.74 -5.93
J0925+1658		4.62 ^{+0.42} _{-1.73}	+0.87 -2.51	+0.87 -3.30	4.16 ^{+1.12} _{-2.71}	+1.30 -4.98	+1.33 -5.53	-1.64 ^{+0.39} _{-0.88}	+0.39 -1.61	+0.39 -1.70	-13.43 ^{+6.40} _{-2.17}	+9.07 -4.34	+10.48 -5.42
J0926+4029		4.17 ^{+1.09} _{-0.83}	+1.34 -2.02	+1.34 -3.16	4.32 ^{+1.13} _{-2.44}	+1.16 -4.75	+1.17 -5.51	-1.68 ^{+0.32} _{-0.96}	+0.25 -1.63	+0.36 -1.64	-14.42 ^{+7.57} _{-0.92}	+9.52 -3.24	+11.74 -3.82
J0927+3902		4.65 ^{+0.83} _{-2.36}	+0.85 -4.49	+0.85 -5.86	4.42 ^{+1.02} _{-2.54}	+1.07 -4.81	+1.07 -5.69	-2.13 ^{+0.81} _{-0.47}	+0.81 -1.10	+0.82 -1.19	-7.76 ^{+3.17} _{-5.88}	+6.65 -7.40	+8.02 -8.89

Table C.2: Results of fitting the broken power-law model over the 1290 selected observations from OVRO dataset. Break significance refers to the source having a possible break frequency being (1σ) at 68.3%, (2σ) at 95.5% and (3σ) at 99.7%. The absence of break significance means that the source is not well-fitted at any level.

Name	Break significance	β_l	$\beta_l^{95.5\%}$	$\beta_l^{99.7\%}$	β_h	$\beta_h^{95.5\%}$	$\beta_h^{99.7\%}$	$\log f_{br}$	$\log f_{br}^{95.5\%}$	$\log f_{br}^{99.7\%}$	$\log A$	$\log A^{95.5\%}$	$\log A^{99.7\%}$
J0956+2515		2.55 ^{+0.67} _{-1.17}	+1.15 -3.90	+2.29 -4.04	3.08 ^{+1.48} _{-0.52}	+2.30 -1.14	+2.41 -2.79	-2.42 ^{+0.23} _{-0.89}	+1.10 -0.93	+1.24 -0.95	-7.83 ^{+1.33} _{-2.83}	+2.33 -4.74	+4.56 -5.06
J0957-1350	3 σ	0.49 ^{+0.78} _{-1.38}	+1.47 -1.97	+2.35 -1.97	5.04 ^{+0.31} _{-0.96}	+0.46 -1.69	+0.46 -2.11	-2.80 ^{+0.15} _{-0.14}	+0.33 -0.28	+0.36 -0.46	-13.22 ^{+2.28} _{-0.80}	+3.99 -1.37	+5.10 -1.37
J0958+4725	1 σ	0.92 ^{+1.84} _{-1.27}	+2.33 -2.41	+3.21 -2.41	4.32 ^{+1.11} _{-0.55}	+1.16 -1.34	+1.17 -2.13	-2.92 ^{+0.25} _{-0.26}	+0.58 -0.42	+0.93 -0.42	-11.48 ^{+1.99} _{-2.16}	+3.52 -2.85	+5.08 -3.11
J0958+5039		2.87 ^{+0.74} _{-2.29}	+1.46 -4.09	+1.95 -4.34	4.59 ^{+0.90} _{-1.27}	+0.89 -3.30	+0.90 -4.44	-3.03 ^{+0.73} _{-0.31}	+1.55 -0.31	+1.68 -0.31	-11.88 ^{+2.62} _{-2.91}	+6.10 -3.65	+7.02 -4.68
J0958+6533	2 σ	0.76 ^{+0.65} _{-1.15}	+1.14 -2.13	+1.65 -2.23	2.84 ^{+0.80} _{-0.22}	+1.40 -0.62	+1.92 -0.71	-2.52 ^{+0.30} _{-0.21}	+0.40 -0.60	+0.61 -0.75	-6.23 ^{+0.79} _{-1.24}	+1.39 -2.77	+1.39 -3.98
J1001+2911	2 σ	0.74 ^{+0.40} _{-1.73}	+0.95 -2.23	+1.46 -2.23	2.55 ^{+0.52} _{-0.30}	+1.55 -0.53	+2.65 -0.57	-2.72 ^{+0.30} _{-0.26}	+0.78 -0.39	+0.86 -0.53	-6.16 ^{+0.50} _{-1.15}	+1.18 -3.12	+1.18 -5.03
J1001+3424		2.50 ^{+0.83} _{-1.71}	+1.27 -3.69	+1.51 -3.99	3.44 ^{+1.77} _{-0.74}	+2.05 -3.04	+2.05 -4.88	-3.01 ^{+1.04} _{-0.29}	+1.65 -0.25	+1.67 -0.33	-10.32 ^{+2.61} _{-3.22}	+5.19 -5.45	+7.56 -5.67
J1002+1216		3.06 ^{+1.53} _{-1.21}	+2.44 -2.42	+2.43 -3.69	4.21 ^{+1.20} _{-1.99}	+1.27 -4.60	+1.28 -5.57	-1.71 ^{+0.26} _{-1.65}	+0.30 -1.64	+0.36 -1.65	-13.22 ^{+6.32} _{-1.26}	+8.43 -4.38	+10.07 -5.73
J1007+1356		2.10 ^{+1.07} _{-1.02}	+2.55 -2.69	+3.15 -3.57	2.29 ^{+2.20} _{-0.74}	+3.21 -1.47	+3.21 -2.95	-3.09 ^{+1.13} _{-0.26}	+1.67 -0.26	+1.73 -0.27	-9.14 ^{+3.64} _{-2.53}	+6.30 -5.70	+6.49 -7.52
J1007-0207		2.43 ^{+1.52} _{-1.34}	+2.52 -3.28	+2.52 -3.89	3.17 ^{+2.17} _{-0.78}	+2.33 -3.50	+2.31 -4.64	-3.07 ^{+1.13} _{-0.29}	+1.76 -0.29	+1.83 -0.29	-9.99 ^{+2.58} _{-5.14}	+6.61 -7.51	+7.75 -8.04
J1008+0621	3 σ	0.58 ^{+0.78} _{-0.66}	+1.62 -1.44	+1.88 -2.06	4.06 ^{+1.29} _{-0.18}	+1.44 -0.83	+1.44 -1.42	-2.39 ^{+0.15} _{-0.14}	+0.26 -0.36	+0.47 -0.55	-10.37 ^{+1.16} _{-1.89}	+2.69 -2.14	+3.58 -2.47
J1010+3330		2.02 ^{+0.77} _{-0.88}	+1.04 -3.27	+1.49 -3.43	2.71 ^{+1.41} _{-0.76}	+2.72 -1.07	+2.72 -1.76	-3.04 ^{+0.95} _{-0.25}	+1.58 -0.28	+1.69 -0.31	-8.27 ^{+1.44} _{-3.32}	+2.32 -6.16	+3.61 -6.15
J1010+8250	1 σ	1.70 ^{+1.17} _{-1.54}	+1.21 -3.19	+1.83 -3.19	3.65 ^{+1.25} _{-0.37}	+1.83 -0.81	+1.83 -1.17	-2.94 ^{+0.33} _{-0.25}	+0.53 -0.42	+0.76 -0.43	-9.64 ^{+1.43} _{-2.48}	+2.16 -4.08	+2.91 -4.51
J1010-0200		2.73 ^{+0.72} _{-0.89}	+1.42 -3.53	+2.55 -3.93	3.22 ^{+1.70} _{-0.76}	+2.27 -3.00	+2.27 -4.27	-3.05 ^{+1.72} _{-0.32}	+1.71 -0.20	+1.73 -0.28	-10.35 ^{+3.45} _{-1.84}	+5.86 -4.32	+7.52 -4.33
J1012+2312	2 σ	0.47 ^{+0.39} _{-1.76}	+1.40 -1.95	+2.06 -1.96	3.12 ^{+1.07} _{-0.78}	+2.27 -0.89	+2.37 -1.36	-2.78 ^{+0.27} _{-0.24}	+0.48 -0.55	+0.80 -0.54	-8.66 ^{+1.53} _{-2.74}	+1.95 -5.37	+3.19 -5.58
J1013+2449		2.31 ^{+2.34} _{-0.60}	+3.18 -1.47	+3.19 -3.47	2.13 ^{+2.61} _{-0.89}	+3.36 -2.62	+3.35 -3.61	-1.89 ^{+0.61} _{-0.80}	+0.61 -1.38	+0.65 -1.48	-7.02 ^{+2.57} _{-4.71}	+3.08 -10.39	+5.04 -10.39
J1013+3445		3.09 ^{+1.49} _{-1.10}	+2.24 -4.08	+2.40 -4.57	3.97 ^{+1.46} _{-1.80}	+1.48 -4.86	+1.51 -5.42	-1.56 ^{+0.21} _{-1.76}	+0.27 -1.75	+0.34 -1.79	-8.49 ^{+1.22} _{-6.47}	+4.90 -7.98	+5.99 -9.30
J1014+2301		3.34 ^{+0.81} _{-2.13}	+1.02 -4.54	+1.79 -4.80	4.49 ^{+0.82} _{-1.12}	+1.00 -3.99	+1.00 -5.56	-3.03 ^{+0.78} _{-0.34}	+1.75 -0.26	+1.76 -0.34	-11.67 ^{+2.80} _{-1.83}	+7.69 -2.79	+9.63 -3.07
J1015+1227		2.64 ^{+0.97} _{-1.20}	+1.15 -4.11	+2.58 -4.11	3.33 ^{+1.57} _{-0.33}	+2.09 -0.81	+2.13 -1.75	-3.06 ^{+0.75} _{-0.20}	+1.53 -0.26	+1.70 -0.28	-9.57 ^{+1.31} _{-2.67}	+2.19 -4.44	+3.88 -4.61
J1015+6728		4.53 ^{+0.96} _{-2.56}	+0.96 -5.47	+0.96 -5.96	0.73 ^{+2.56} _{-1.86}	+4.42 -2.23	+4.76 -2.22	-2.89 ^{+1.25} _{-0.11}	+1.58 -0.32	+1.58 -0.44	-17.75 ^{+6.50} _{-2.21}	+11.92 -2.22	+14.87 -2.21
J1016+2037		1.89 ^{+1.10} _{-0.91}	+2.54 -1.82	+3.35 -2.97	1.91 ^{+2.37} _{-0.69}	+3.58 -2.39	+3.54 -3.33	-1.66 ^{+0.42} _{-0.96}	+0.41 -1.63	+0.42 -1.71	-6.16 ^{+1.36} _{-4.66}	+2.55 -8.14	+4.50 -8.38
J1017+6116		4.66 ^{+0.68} _{-1.96}	+0.82 -4.71	+0.83 -5.90	4.61 ^{+0.89} _{-2.59}	+0.89 -5.44	+0.89 -6.07	-3.05 ^{+1.15} _{-0.27}	+1.70 -0.24	+1.74 -0.27	-12.38 ^{+6.30} _{-2.21}	+7.96 -5.73	+10.46 -5.81
J1018+0530		2.69 ^{+0.69} _{-1.38}	+1.09 -3.72	+2.13 -4.10	3.32 ^{+1.37} _{-0.91}	+2.09 -2.99	+2.16 -4.77	-3.07 ^{+1.14} _{-0.30}	+1.73 -0.29	+1.81 -0.29	-9.27 ^{+2.22} _{-2.65}	+4.48 -5.24	+6.72 -5.83
J1018+3542		2.78 ^{+1.12} _{-1.18}	+1.25 -4.26	+2.20 -4.26	4.41 ^{+0.98} _{-1.60}	+1.04 -3.80	+1.07 -5.30	-3.06 ^{+1.05} _{-0.29}	+1.73 -0.29	+1.83 -0.29	-9.48 ^{+2.33} _{-3.72}	+4.14 -6.21	+6.14 -6.58

Table C.2: Results of fitting the broken power-law model over the 1290 selected observations from OVRO dataset. Break significance refers to the source having a possible break frequency being (1σ) at 68.3%, (2σ) at 95.5% and (3σ) at 99.7%. The absence of break significance means that the source is not well-fitted at any level.

Name	Break significance	β_l	$\beta_l^{95.5\%}$	$\beta_l^{99.7\%}$	β_h	$\beta_h^{95.5\%}$	$\beta_h^{99.7\%}$	$\log f_{br}$	$\log f_{br}^{95.5\%}$	$\log f_{br}^{99.7\%}$	$\log A$	$\log A^{95.5\%}$	$\log A^{99.7\%}$
J1019+6320		2.03 ^{+0.72} _{-1.72}	+0.73 -3.38	+1.49 -3.47	3.18 ^{+0.64} _{-0.52}	+2.04 -0.69	+2.23 -0.95	-2.75 ^{+0.34} _{-0.44}	+0.95 -0.58	+1.43 -0.56	-8.16 ^{+1.06} _{-1.40}	+1.97 -3.92	+1.97 -4.71
J1021+3437		2.60 ^{+1.74} _{-0.91}	+2.90 -2.67	+2.87 -3.90	4.49 ^{+0.77} _{-2.23}	+0.96 -4.68	+1.00 -5.75	-3.05 ^{+1.11} _{-0.29}	+1.70 -0.23	+1.72 -0.29	-8.92 ^{+1.83} _{-5.99}	+4.53 -7.92	+6.21 -8.50
J1022+4239		3.21 ^{+1.49} _{-1.05}	+2.20 -3.78	+2.24 -4.70	4.06 ^{+1.39} _{-1.44}	+1.42 -4.13	+1.43 -5.12	-3.11 ^{+1.04} _{-0.23}	+1.66 -0.23	+1.78 -0.23	-13.13 ^{+5.30} _{-1.71}	+8.91 -4.11	+9.50 -5.40
J1023+3948		2.71 ^{+0.91} _{-0.86}	+1.06 -4.02	+2.29 -4.20	2.92 ^{+1.71} _{-0.77}	+2.46 -2.45	+2.56 -4.29	-2.99 ^{+1.21} _{-0.33}	+1.70 -0.33	+1.78 -0.35	-7.42 ^{+1.94} _{-2.70}	+3.19 -6.77	+5.64 -6.77
J1024+1912		2.50 ^{+1.58} _{-0.69}	+2.88 -2.81	+2.88 -3.77	2.84 ^{+2.11} _{-1.24}	+2.64 -3.12	+2.66 -3.97	-1.70 ^{+0.16} _{-1.67}	+0.31 -1.67	+0.44 -1.67	-8.18 ^{+3.11} _{-3.92}	+4.56 -7.48	+5.65 -8.77
J1025+1253		2.60 ^{+1.11} _{-1.11}	+1.20 -4.08	+2.42 -4.07	3.07 ^{+1.92} _{-0.94}	+2.42 -3.41	+2.42 -4.35	-3.04 ^{+1.14} _{-0.28}	+1.62 -0.29	+1.71 -0.30	-9.34 ^{+3.09} _{-3.25}	+7.24 -4.65	+7.36 -5.91
J1025-0509		3.61 ^{+1.16} _{-0.93}	+1.88 -2.89	+1.88 -4.31	4.49 ^{+0.97} _{-2.15}	+0.97 -5.01	+1.01 -5.94	-1.72 ^{+0.36} _{-1.10}	+0.28 -1.65	+0.36 -1.65	-12.78 ^{+5.17} _{-2.59}	+8.04 -4.24	+10.19 -4.77
J1028+0255		3.19 ^{+1.30} _{-1.10}	+2.29 -3.34	+2.28 -4.56	4.27 ^{+1.20} _{-1.54}	+1.22 -4.50	+1.23 -5.56	-3.13 ^{+1.28} _{-0.23}	+1.71 -0.22	+1.76 -0.24	-11.95 ^{+3.43} _{-3.53}	+7.53 -4.64	+9.17 -5.48
J1029-1852		3.36 ^{+1.65} _{-0.84}	+2.11 -3.35	+2.11 -4.69	4.26 ^{+1.05} _{-2.30}	+1.21 -4.94	+1.23 -5.47	-1.77 ^{+0.11} _{-1.27}	+0.38 -1.53	+0.46 -1.54	-11.82 ^{+5.39} _{-2.61}	+8.83 -4.43	+9.90 -5.06
J1033+0711		2.48 ^{+1.14} _{-0.96}	+2.48 -3.04	+2.85 -3.86	2.58 ^{+2.05} _{-0.92}	+2.89 -2.00	+2.86 -3.57	-3.06 ^{+1.02} _{-0.30}	+1.69 -0.24	+1.70 -0.30	-7.52 ^{+1.46} _{-4.86}	+3.41 -7.37	+4.97 -8.50
J1033+4116		2.60 ^{+0.99} _{-0.78}	+1.23 -3.97	+2.56 -4.05	2.95 ^{+1.77} _{-1.14}	+2.50 -3.37	+2.51 -4.45	-3.03 ^{+1.24} _{-0.31}	+1.81 -0.24	+1.81 -0.32	-7.57 ^{+2.30} _{-3.56}	+5.72 -5.66	+5.72 -6.98
J1033+6051		1.94 ^{+0.64} _{-2.20}	+0.99 -3.42	+2.46 -3.42	3.19 ^{+0.40} _{-0.64}	+1.96 -0.85	+2.28 -1.06	-2.95 ^{+0.40} _{-0.32}	+1.12 -0.32	+1.26 -0.38	-7.14 ^{+1.02} _{-1.12}	+1.59 -3.74	+1.96 -4.42
J1036+1440		2.00 ^{+3.06} _{-0.77}	+3.48 -2.77	+3.50 -3.40	3.46 ^{+1.97} _{-1.74}	+2.01 -4.22	+2.03 -4.93	-2.47 ^{+1.10} _{-0.24}	+1.01 -0.88	+1.13 -0.88	-12.91 ^{+4.15} _{-5.37}	+8.19 -6.51	+9.57 -7.05
J1036+2203		1.44 ^{+0.90} _{-1.22}	+0.90 -2.80	+1.30 -2.92	2.41 ^{+1.80} _{-0.54}	+3.06 -0.71	+3.06 -1.17	-2.89 ^{+0.92} _{-0.33}	+1.53 -0.42	+1.65 -0.45	-7.54 ^{+1.63} _{-2.97}	+2.27 -5.61	+2.68 -7.28
J1038+0512	2σ	1.47 ^{+0.84} _{-1.31}	+1.15 -2.67	+1.60 -2.96	3.70 ^{+0.89} _{-0.68}	+1.72 -0.75	+1.78 -1.36	-2.56 ^{+0.21} _{-0.34}	+0.35 -0.72	+0.57 -0.80	-8.66 ^{+1.42} _{-2.04}	+1.87 -3.83	+3.23 -4.10
J1039-1541		1.77 ^{+0.72} _{-0.90}	+0.72 -3.23	+1.15 -3.27	2.25 ^{+1.45} _{-0.59}	+3.22 -0.85	+3.20 -1.94	-2.96 ^{+1.30} _{-0.14}	+1.63 -0.27	+1.64 -0.36	-5.87 ^{+1.06} _{-2.78}	+1.47 -5.81	+2.47 -6.75
J1041+0610		2.67 ^{+1.30} _{-0.89}	+2.07 -3.29	+2.78 -3.75	2.72 ^{+1.81} _{-0.80}	+2.77 -1.97	+2.77 -3.24	-3.12 ^{+1.14} _{-0.25}	+1.75 -0.25	+1.88 -0.25	-7.59 ^{+3.04} _{-2.65}	+3.47 -6.11	+4.83 -6.89
J1041+5233		2.63 ^{+1.09} _{-0.96}	+1.09 -4.01	+1.94 -4.01	3.35 ^{+1.55} _{-0.80}	+2.15 -2.56	+2.15 -3.99	-3.07 ^{+1.10} _{-0.28}	+1.65 -0.28	+1.73 -0.28	-9.33 ^{+2.17} _{-3.08}	+4.52 -5.50	+6.57 -5.50
J1043+2408	2σ	0.82 ^{+1.22} _{-0.66}	+1.22 -2.14	+1.61 -2.26	3.28 ^{+1.31} _{-0.33}	+2.15 -0.63	+2.19 -1.00	-2.54 ^{+0.20} _{-0.29}	+0.35 -0.66	+0.53 -0.72	-7.81 ^{+1.38} _{-2.14}	+1.43 -4.61	+2.23 -4.69
J1044+5322		1.69 ^{+0.94} _{-1.02}	+1.25 -2.86	+2.35 -3.18	2.53 ^{+1.53} _{-0.76}	+2.91 -1.14	+2.97 -1.97	-2.98 ^{+0.91} _{-0.36}	+1.62 -0.30	+1.62 -0.36	-7.57 ^{+0.85} _{-3.81}	+2.52 -5.45	+3.07 -6.25
J1044+8054		2.63 ^{+0.73} _{-1.72}	+0.73 -4.09	+1.17 -4.13	3.53 ^{+1.01} _{-0.74}	+1.97 -1.69	+1.97 -3.61	-2.99 ^{+0.72} _{-0.38}	+1.74 -0.28	+1.74 -0.38	-8.81 ^{+1.18} _{-2.62}	+3.10 -4.52	+5.25 -4.76
J1045+0624		4.49 ^{+0.99} _{-1.51}	+0.99 -3.65	+0.99 -5.40	2.61 ^{+2.75} _{-0.71}	+2.90 -3.33	+2.85 -4.10	-1.63 ^{+0.25} _{-1.06}	+0.28 -1.66	+0.28 -1.74	-8.66 ^{+0.93} _{-7.34}	+4.82 -8.68	+5.61 -10.18
J1046+5354		2.16 ^{+0.84} _{-2.06}	+1.35 -3.60	+2.45 -3.59	3.69 ^{+0.85} _{-1.16}	+1.80 -1.53	+1.80 -2.60	-2.91 ^{+0.29} _{-0.42}	+1.26 -0.44	+1.53 -0.44	-10.70 ^{+1.94} _{-2.96}	+4.54 -3.86	+5.75 -4.81
J1047-1308		4.95 ^{+0.54} _{-1.51}	+0.54 -3.53	+0.54 -4.44	4.61 ^{+0.73} _{-3.02}	+0.87 -5.42	+0.89 -5.93	-1.79 ^{+0.38} _{-0.94}	+0.42 -1.49	+0.44 -1.57	-11.40 ^{+5.65} _{-3.37}	+7.68 -6.54	+9.75 -7.67

Table C.2: Results of fitting the broken power-law model over the 1290 selected observations from OVRO dataset. Break significance refers to the source having a possible break frequency being (1σ) at 68.3%, (2σ) at 95.5% and (3σ) at 99.7%. The absence of break significance means that the source is not well-fitted at any level.

Name	Break significance	β_l	$\beta_l^{95.5\%}$	$\beta_l^{99.7\%}$	β_h	$\beta_h^{95.5\%}$	$\beta_h^{99.7\%}$	$\log f_{br}$	$\log f_{br}^{95.5\%}$	$\log f_{br}^{99.7\%}$	$\log A$	$\log A^{95.5\%}$	$\log A^{99.7\%}$
J1048+7143		$2.41^{+0.73}_{-1.78}$	$+0.71_{-3.87}$	$+1.42_{-3.87}$	$2.73^{+0.80}_{-0.48}$	$+2.13_{-0.80}$	$+2.58_{-1.48}$	$-3.06^{+0.66}_{-0.31}$	$+1.59_{-0.31}$	$+1.79_{-0.31}$	$-5.83^{+0.80}_{-1.95}$	$+1.56_{-3.83}$	$+2.62_{-4.55}$
J1048-1909		$2.45^{+1.01}_{-1.98}$	$+0.99_{-3.85}$	$+1.82_{-3.94}$	$3.88^{+0.91}_{-1.59}$	$+1.48_{-3.45}$	$+1.58_{-3.51}$	$-2.91^{+0.51}_{-0.41}$	$+1.58_{-0.32}$	$+1.58_{-0.41}$	$-7.63^{+1.70}_{-3.99}$	$+4.49_{-5.79}$	$+4.49_{-6.83}$
J1051+2027		$2.48^{+0.94}_{-0.77}$	$+1.54_{-3.02}$	$+1.81_{-3.86}$	$2.87^{+1.32}_{-0.81}$	$+2.63_{-1.09}$	$+2.63_{-1.90}$	$-2.96^{+1.05}_{-0.36}$	$+1.66_{-0.33}$	$+1.72_{-0.39}$	$-8.34^{+1.26}_{-3.01}$	$+2.49_{-5.08}$	$+3.46_{-5.78}$
J1051+2119		$3.07^{+1.24}_{-0.86}$	$+2.34_{-1.37}$	$+2.43_{-2.74}$	$4.11^{+1.05}_{-2.46}$	$+1.23_{-4.96}$	$+1.36_{-5.17}$	$-1.75^{+0.03}_{-1.46}$	$+0.43_{-1.59}$	$+0.53_{-1.59}$	$-6.56^{+1.99}_{-5.74}$	$+2.43_{-9.76}$	$+3.97_{-10.07}$
J1054-0713		$3.11^{+1.29}_{-1.29}$	$+2.32_{-3.37}$	$+2.36_{-4.40}$	$4.38^{+1.05}_{-1.72}$	$+1.11_{-4.61}$	$+1.12_{-5.65}$	$-3.12^{+1.23}_{-0.25}$	$+1.77_{-0.21}$	$+1.77_{-0.25}$	$-10.90^{+2.20}_{-4.98}$	$+5.72_{-6.72}$	$+8.14_{-7.25}$
J1056+7011		$3.25^{+0.78}_{-2.70}$	$+0.78_{-4.73}$	$+1.82_{-4.73}$	$4.20^{+1.04}_{-0.31}$	$+1.29_{-0.93}$	$+1.29_{-2.40}$	$-3.02^{+0.32}_{-0.30}$	$+1.29_{-0.30}$	$+1.66_{-0.30}$	$-10.71^{+0.70}_{-2.56}$	$+2.26_{-3.25}$	$+4.94_{-3.36}$
J1058+0133		$3.06^{+0.86}_{-1.41}$	$+1.03_{-4.37}$	$+1.74_{-4.42}$	$4.24^{+0.96}_{-1.05}$	$+1.24_{-2.82}$	$+1.25_{-5.22}$	$-3.05^{+0.78}_{-0.31}$	$+1.57_{-0.31}$	$+1.69_{-1.61}$	$-9.44^{+3.01}_{-1.61}$	$+5.37_{-3.42}$	$+8.79_{-3.38}$
J1058+1951		$2.33^{+0.74}_{-0.79}$	$+2.48_{-2.60}$	$+3.15_{-3.82}$	$2.58^{+1.87}_{-0.89}$	$+2.77_{-3.02}$	$+2.87_{-3.88}$	$-1.59^{+0.34}_{-1.03}$	$+0.25_{-1.77}$	$+0.34_{-1.76}$	$-7.67^{+1.56}_{-3.83}$	$+4.97_{-5.42}$	$+5.52_{-7.57}$
J1058+5628		$1.92^{+2.02}_{-1.42}$	$+2.90_{-3.41}$	$+3.56_{-3.38}$	$4.50^{+0.73}_{-2.45}$	$+1.00_{-4.84}$	$+0.99_{-5.93}$	$-2.93^{+0.88}_{-0.40}$	$+1.59_{-0.40}$	$+1.71_{-0.40}$	$-11.10^{+5.41}_{-2.28}$	$+6.55_{-6.83}$	$+8.27_{-7.78}$
J1058+8114		$2.32^{+0.66}_{-1.62}$	$+0.94_{-3.34}$	$+2.24_{-3.77}$	$3.16^{+0.75}_{-0.62}$	$+2.19_{-0.62}$	$+2.28_{-1.33}$	$-2.87^{+0.51}_{-0.44}$	$+1.24_{-0.50}$	$+1.60_{-0.49}$	$-8.03^{+1.30}_{-1.73}$	$+1.59_{-4.12}$	$+2.59_{-5.19}$
J1059+2057	1σ	$0.87^{+0.26}_{-2.03}$	$+1.22_{-2.28}$	$+1.70_{-2.36}$	$2.55^{+0.52}_{-0.58}$	$+1.63_{-0.72}$	$+2.29_{-0.88}$	$-2.86^{+0.36}_{-0.26}$	$+0.87_{-0.40}$	$+1.22_{-0.50}$	$-7.13^{+1.32}_{-1.06}$	$+1.75_{-3.34}$	$+1.98_{-4.99}$
J1102+2757		$3.73^{+1.05}_{-0.88}$	$+1.67_{-3.27}$	$+1.68_{-5.05}$	$4.17^{+1.31}_{-1.63}$	$+1.32_{-4.65}$	$+1.32_{-5.59}$	$-1.58^{+-0.19}_{-1.78}$	$+0.34_{-1.69}$	$+0.34_{-1.78}$	$-11.45^{+2.84}_{-3.97}$	$+6.69_{-4.08}$	$+8.50_{-4.55}$
J1103+3014		$2.69^{+0.69}_{-1.30}$	$+0.72_{-3.65}$	$+1.01_{-4.16}$	$3.41^{+0.89}_{-1.03}$	$+2.08_{-1.71}$	$+2.07_{-3.55}$	$-2.97^{+0.80}_{-0.32}$	$+1.70_{-0.29}$	$+1.71_{-0.39}$	$-8.89^{+1.68}_{-2.31}$	$+3.42_{-4.75}$	$+5.79_{-4.83}$
J1104+0730		$1.75^{+0.73}_{-1.16}$	$+0.90_{-2.85}$	$+1.04_{-3.17}$	$3.05^{+1.30}_{-0.69}$	$+2.44_{-0.75}$	$+2.44_{-1.10}$	$-2.42^{+0.34}_{-0.64}$	$+0.84_{-0.83}$	$+0.99_{-0.87}$	$-8.38^{+1.30}_{-2.50}$	$+2.11_{-4.77}$	$+2.55_{-5.59}$
J1104+3812	1σ	$1.60^{+0.43}_{-0.51}$	$+0.55_{-2.21}$	$+0.67_{-2.75}$	$2.37^{+2.01}_{-0.30}$	$+2.92_{-0.42}$	$+3.11_{-0.55}$	$-1.81^{+0.31}_{-0.40}$	$+0.33_{-1.50}$	$+0.64_{-1.51}$	$-6.04^{+0.51}_{-3.21}$	$+0.83_{-4.55}$	$+1.08_{-5.11}$
J1106+2812	3σ	$-0.12^{+1.05}_{-0.70}$	$+1.47_{-1.36}$	$+1.95_{-1.37}$	$4.94^{+0.55}_{-0.70}$	$+0.56_{-1.58}$	$+0.56_{-2.31}$	$-2.61^{+0.07}_{-0.13}$	$+0.18_{-0.20}$	$+0.23_{-0.27}$	$-12.73^{+2.07}_{-0.96}$	$+3.66_{-1.65}$	$+5.55_{-1.65}$
J1108+0811		$2.98^{+1.54}_{-1.21}$	$+2.33_{-3.35}$	$+2.49_{-4.41}$	$4.42^{+1.05}_{-1.69}$	$+1.07_{-4.28}$	$+1.08_{-5.38}$	$-3.09^{+1.12}_{-0.27}$	$+1.63_{-0.27}$	$+1.73_{-0.27}$	$-10.81^{+2.03}_{-5.17}$	$+5.80_{-6.92}$	$+7.70_{-7.61}$
J1108+4330		$2.49^{+0.97}_{-1.46}$	$+1.55_{-3.96}$	$+2.88_{-3.97}$	$2.98^{+1.70}_{-1.12}$	$+2.52_{-2.90}$	$+2.52_{-4.22}$	$-3.10^{+1.23}_{-0.26}$	$+1.78_{-0.25}$	$+1.85_{-0.26}$	$-9.81^{+2.62}_{-3.67}$	$+5.07_{-6.22}$	$+7.05_{-7.88}$
J1110+4403	2σ	$-0.93^{+1.50}_{-0.47}$	$+2.98_{-0.54}$	$+3.41_{-0.57}$	$5.02^{+0.42}_{-1.00}$	$+0.48_{-2.11}$	$+0.47_{-2.76}$	$-2.85^{+0.12}_{-0.17}$	$+0.29_{-0.36}$	$+0.57_{-0.45}$	$-14.32^{+2.49}_{-1.35}$	$+5.36_{-1.59}$	$+7.37_{-1.59}$
J1112+3503		$4.69^{+0.77}_{-1.21}$	$+0.81_{-2.51}$	$+0.80_{-3.57}$	$4.68^{+0.81}_{-2.85}$	$+0.82_{-5.15}$	$+0.82_{-6.15}$	$-1.58^{+0.28}_{-0.95}$	$+0.28_{-1.62}$	$+0.28_{-1.72}$	$-11.88^{+4.42}_{-4.18}$	$+7.39_{-5.75}$	$+9.52_{-6.57}$
J1113+1442		$2.32^{+0.61}_{-0.82}$	$+1.23_{-3.77}$	$+2.66_{-3.77}$	$2.76^{+2.01}_{-0.74}$	$+2.71_{-2.54}$	$+2.70_{-4.18}$	$-2.38^{+1.15}_{-0.25}$	$+1.15_{-0.91}$	$+1.14_{-0.98}$	$-8.03^{+1.18}_{-4.21}$	$+3.77_{-6.17}$	$+5.41_{-6.31}$
J1114-0816		$2.01^{+0.60}_{-1.52}$	$+0.81_{-3.18}$	$+1.75_{-3.49}$	$3.37^{+1.26}_{-0.80}$	$+2.02_{-1.23}$	$+2.13_{-1.63}$	$-2.72^{+0.36}_{-0.44}$	$+1.04_{-0.65}$	$+1.29_{-0.65}$	$-9.97^{+3.05}_{-1.71}$	$+3.09_{-4.45}$	$+4.09_{-4.92}$
J1116+0829	2σ	$-0.66^{+1.14}_{-0.73}$	$+2.35_{-0.84}$	$+3.16_{-0.83}$	$4.31^{+0.34}_{-1.39}$	$+1.09_{-1.61}$	$+1.16_{-2.23}$	$-2.79^{+0.13}_{-0.22}$	$+0.43_{-0.33}$	$+0.43_{-0.58}$	$-11.86^{+2.77}_{-1.46}$	$+3.89_{-2.85}$	$+5.33_{-2.98}$
J1118+1234		$2.58^{+0.81}_{-0.97}$	$+2.32_{-2.51}$	$+2.78_{-4.02}$	$2.29^{+2.51}_{-0.67}$	$+3.19_{-2.31}$	$+3.19_{-3.51}$	$-1.62^{+0.38}_{-1.15}$	$+0.31_{-1.73}$	$+0.38_{-1.75}$	$-7.03^{+2.49}_{-4.13}$	$+4.05_{-7.36}$	$+5.52_{-9.13}$

Table C.2: Results of fitting the broken power-law model over the 1290 selected observations from OVRO dataset. Break significance refers to the source having a possible break frequency being (1σ) at 68.3%, (2σ) at 95.5% and (3σ) at 99.7%. The absence of break significance means that the source is not well-fitted at any level.

Name	Break significance	β_l	$\beta_l^{95.5\%}$	$\beta_l^{99.7\%}$	β_h	$\beta_h^{95.5\%}$	$\beta_h^{99.7\%}$	$\log f_{br}$	$\log f_{br}^{95.5\%}$	$\log f_{br}^{99.7\%}$	$\log A$	$\log A^{95.5\%}$	$\log A^{99.7\%}$
J1119+0410		4.61 ^{+0.83} _{-1.53}	+0.89 -3.12	+0.88 -5.64	3.86 ^{+1.52} _{-2.29}	+1.53 -5.08	+1.60 -5.34	-2.20 ^{+0.85} _{-0.29}	+0.85 -0.98	+0.85 -1.15	-9.67 ^{+3.46} _{-5.31}	+6.10 -7.71	+6.74 -8.73
J1119+1656		2.41 ^{+1.94} _{-0.77}	+3.00 -3.25	+2.99 -3.89	2.89 ^{+1.58} _{-1.24}	+2.54 -2.65	+2.58 -3.64	-3.09 ^{+1.08} _{-0.28}	+1.74 -0.28	+1.84 -0.28	-13.02 ^{+6.47} _{-0.48}	+8.91 -3.06	+9.65 -4.39
J1120+0704		4.93 ^{+0.56} _{-1.12}	+0.57 -3.01	+0.57 -3.86	4.54 ^{+0.95} _{-2.77}	+0.95 -5.42	+0.95 -6.00	-1.77 ^{+0.24} _{-0.84}	+0.36 -1.42	+0.35 -1.55	-13.22 ^{+5.01} _{-4.24}	+8.64 -5.68	+9.54 -6.67
J1120-1420		3.17 ^{+1.03} _{-1.03}	+2.17 -3.72	+2.17 -4.67	3.60 ^{+1.86} _{-0.85}	+1.89 -3.44	+1.89 -5.07	-3.10 ^{+1.13} _{-0.26}	+1.71 -0.23	+1.74 -0.26	-10.20 ^{+2.67} _{-3.92}	+5.11 -6.05	+7.45 -6.04
J1121-0553	1 σ	1.57 ^{+0.61} _{-1.00}	+1.17 -2.12	+1.17 -2.70	4.74 ^{+0.58} _{-1.54}	+0.71 -2.54	+0.75 -3.00	-2.39 ^{+0.22} _{-0.33}	+0.88 -0.58	+0.88 -0.92	-11.75 ^{+3.49} _{-1.11}	+5.90 -1.58	+6.74 -2.39
J1121-0711		4.39 ^{+1.05} _{-1.91}	+1.05 -4.25	+1.09 -5.88	3.08 ^{+2.20} _{-1.18}	+2.36 -3.54	+2.40 -4.58	-1.88 ^{+0.13} _{-1.43}	+0.37 -1.43	+0.41 -1.48	-10.42 ^{+4.56} _{-3.87}	+6.29 -7.47	+7.93 -8.40
J1122+1805		3.49 ^{+1.84} _{-1.03}	+2.00 -3.21	+2.00 -4.92	4.49 ^{+0.89} _{-3.00}	+0.99 -5.30	+0.99 -5.97	-1.61 ^{+0.36} _{-1.03}	+0.36 -1.67	+0.36 -1.76	-8.31 ^{+3.42} _{+5.37}	+4.29 -9.67	+6.56 -11.12
J1124+2336		2.36 ^{+0.67} _{-0.90}	+1.10 -3.66	+2.90 -3.79	2.79 ^{+1.18} _{-0.87}	+2.58 -1.66	+2.69 -2.39	-3.07 ^{+1.14} _{-0.28}	+1.78 -0.25	+1.82 -0.29	-7.54 ^{+1.88} _{-1.97}	+2.41 -5.48	+4.01 -5.67
J1125+0001		4.68 ^{+0.69} _{-1.95}	+0.82 -4.34	+0.82 -6.13	4.50 ^{+0.99} _{-2.59}	+0.99 -5.32	+0.99 -5.96	-1.76 ^{+0.41} _{-0.95}	+0.39 -1.53	+0.41 -1.60	-13.06 ^{+4.63} _{-4.46}	+8.99 -5.49	+10.02 -6.89
J1125+2610		2.45 ^{+0.86} _{-0.85}	+2.91 -2.36	+2.96 -3.87	2.23 ^{+1.77} _{-0.93}	+3.26 -2.18	+3.26 -3.45	-1.59 ^{+0.22} _{-1.78}	+0.29 -1.76	+0.35 -1.77	-6.54 ^{+1.60} _{-3.65}	+3.13 -6.33	+4.48 -6.81
J1127+0555		2.01 ^{+0.73} _{-0.74}	+0.82 -3.08	+1.04 -3.50	2.81 ^{+1.53} _{-0.41}	+2.49 -0.68	+2.69 -0.70	-2.16 ^{+0.45} _{-0.67}	+0.55 -1.13	+0.78 -1.21	-7.04 ^{+0.69} _{-3.09}	+1.33 -4.82	+1.71 -5.37
J1127+3620	1 σ	1.36 ^{+0.61} _{-0.60}	+0.80 -2.10	+1.17 -2.82	4.87 ^{+0.24} _{-2.23}	+0.48 -3.15	+0.62 -3.26	-2.29 ^{+0.36} _{-0.32}	+0.71 -1.06	+1.03 -1.06	-7.87 ^{+0.29} _{-4.62}	+1.89 -5.33	+2.36 -5.99
J1127+5650		2.88 ^{+0.80} _{-0.97}	+1.59 -3.57	+1.67 -4.25	3.65 ^{+1.66} _{-1.04}	+1.81 -3.37	+1.83 -4.77	-1.49 ^{+0.23} _{-1.30}	+0.23 -1.83	+0.25 -1.88	-10.93 ^{+3.82} _{-2.09}	+5.89 -4.44	+7.74 -4.96
J1127-1857		2.67 ^{+0.74} _{-0.89}	+0.94 -3.77	+2.02 -4.11	2.93 ^{+1.22} _{-0.76}	+2.54 -2.51	+2.54 -4.12	-3.14 ^{+1.36} _{-0.20}	+1.87 -0.20	+1.89 -0.23	-6.37 ^{+0.97} _{-2.51}	+4.16 -4.35	+5.68 -5.26
J1128+5925		2.68 ^{+1.24} _{-1.41}	+1.31 -3.90	+1.75 -4.12	3.60 ^{+1.42} _{-1.01}	+1.90 -2.88	+1.87 -4.02	-3.02 ^{+1.07} _{-0.35}	+1.70 -0.32	+1.76 -0.35	-9.68 ^{+2.00} _{-2.89}	+5.20 -5.10	+6.54 -5.10
J1129-0240		4.39 ^{+0.99} _{-3.00}	+0.90 -5.68	+1.09 -5.87	1.32 ^{+3.00} _{-1.37}	+4.06 -2.43	+4.15 -2.80	-3.07 ^{+1.09} _{-0.26}	+1.66 -0.26	+1.71 -0.30	-13.56 ^{+5.29} _{-4.43}	+8.51 -6.37	+11.23 -6.42
J1130+3815		2.45 ^{+0.80} _{-0.61}	+0.96 -3.12	+1.65 -3.78	2.76 ^{+1.72} _{-0.83}	+2.72 -2.52	+2.68 -3.06	-1.52 ^{+0.28} _{-1.14}	+0.18 -1.84	+0.28 -1.85	-7.23 ^{+2.43} _{-2.44}	+4.28 -4.50	+4.28 -5.66
J1131-0500		2.34 ^{+0.71} _{-0.80}	+2.20 -2.09	+2.99 -2.96	2.48 ^{+1.55} _{-0.82}	+3.00 -1.21	+3.00 -2.88	-2.09 ^{+0.68} _{-0.71}	+0.64 -1.28	+0.73 -1.28	-7.01 ^{+1.56} _{-3.31}	+2.36 -5.92	+4.64 -6.35
J1133+0040	1 σ	1.72 ^{+0.50} _{-1.46}	+0.80 -2.98	+1.35 -3.19	3.22 ^{+1.69} _{-0.39}	+2.17 -0.87	+2.28 -1.18	-2.60 ^{+0.45} _{-0.26}	+0.62 -0.65	+0.98 -0.76	-9.03 ^{+0.70} _{-3.83}	+2.33 -4.73	+2.82 -5.42
J1135-0428	3 σ	-0.36 ^{+0.48} _{-0.91}	+1.14 -1.13	+1.52 -1.12	3.45 ^{+1.10} _{-0.64}	+2.04 -0.81	+2.04 -1.07	-2.27 ^{+0.10} _{-0.23}	+0.27 -0.36	+0.37 -0.43	-7.56 ^{+1.31} _{-1.95}	+1.95 -3.41	+2.21 -3.99
J1136+3407	1 σ	1.50 ^{+0.79} _{-0.77}	+1.02 -2.84	+2.00 -2.94	3.03 ^{+1.73} _{-0.42}	+2.45 -0.71	+2.45 -1.29	-2.29 ^{+0.24} _{-0.47}	+0.30 -0.96	+0.38 -1.08	-8.74 ^{+0.45} _{-3.93}	+1.70 -5.04	+2.81 -5.26
J1136+7009		1.73 ^{+1.21} _{-1.20}	+1.19 -3.23	+3.34 -3.23	2.46 ^{+1.80} _{-0.67}	+3.02 -1.06	+3.02 -2.22	-2.97 ^{+0.86} _{-0.35}	+1.64 -0.35	+1.72 -0.40	-8.11 ^{+1.71} _{-3.87}	+2.49 -6.77	+4.09 -7.61
J1136-0330		2.09 ^{+2.18} _{-1.07}	+3.40 -2.57	+3.40 -3.19	4.45 ^{+1.02} _{-2.46}	+0.99 -5.67	+1.03 -5.89	-1.65 ^{+0.28} _{-1.04}	+0.22 -1.68	+0.30 -1.70	-8.66 ^{+2.36} _{-5.95}	+5.17 -9.10	+6.32 -11.12
J1141+6410		3.08 ^{+1.07} _{-1.07}	+2.41 -2.69	+2.41 -4.51	3.07 ^{+1.90} _{-1.10}	+2.41 -3.34	+2.38 -4.56	-3.10 ^{+1.22} _{-0.26}	+1.75 -0.26	+1.85 -0.26	-9.93 ^{+2.57} _{-4.27}	+5.74 -6.21	+7.02 -7.29

Table C.2: Results of fitting the broken power-law model over the 1290 selected observations from OVRO dataset. Break significance refers to the source having a possible break frequency being (1σ) at 68.3 %, (2σ) at 95.5 % and (3σ) at 99.7 %. The absence of break significance means that the source is not well-fitted at any level.

Name	Break significance	β_l	$\beta_l^{95.5\%}$	$\beta_l^{99.7\%}$	β_h	$\beta_h^{95.5\%}$	$\beta_h^{99.7\%}$	$\log f_{br}$	$\log f_{br}^{95.5\%}$	$\log f_{br}^{99.7\%}$	$\log A$	$\log A^{95.5\%}$	$\log A^{99.7\%}$
J1145+0455		$2.66^{+1.48}_{-1.63}$	$+2.82_{-2.77}$	$+2.82_{-4.00}$	$4.27^{+0.78}_{-2.34}$	$+1.23_{-4.34}$	$+1.22_{-5.54}$	$-3.07^{+1.07}_{-0.30}$	$+1.62_{-0.28}$	$+1.71_{-0.30}$	$-13.96^{+6.00}_{-1.61}$	$+10.19_{-3.00}$	$+10.33_{-5.43}$
J1146+3958		$2.85^{+0.69}_{-0.79}$	$+1.68_{-3.59}$	$+2.09_{-4.28}$	$3.01^{+1.38}_{-0.62}$	$+2.46_{-2.28}$	$+2.46_{-4.39}$	$-1.55^{+0.29}_{-1.31}$	$+0.27_{-1.78}$	$+0.30_{-1.82}$	$-7.03^{+1.24}_{-2.49}$	$+3.73_{-4.15}$	$+5.69_{-4.89}$
J1146+5356	1σ	$1.83^{+0.90}_{-1.67}$	$+1.47_{-2.93}$	$+1.59_{-3.32}$	$3.91^{+0.88}_{-0.73}$	$+1.50_{-1.16}$	$+1.58_{-1.56}$	$-2.74^{+0.27}_{-0.36}$	$+0.50_{-0.61}$	$+1.14_{-0.62}$	$-11.12^{+1.91}_{-1.90}$	$+2.91_{-3.55}$	$+4.03_{-3.89}$
J1146+5848		$3.04^{+0.98}_{-1.78}$	$+1.68_{-3.88}$	$+1.89_{-4.53}$	$4.82^{+0.67}_{-1.57}$	$+0.67_{-4.94}$	$+0.66_{-5.69}$	$-3.07^{+1.00}_{-0.30}$	$+1.72_{-0.29}$	$+1.82_{-0.30}$	$-13.27^{+3.68}_{-2.79}$	$+8.41_{-3.58}$	$+10.19_{-4.38}$
J1147+2635		$2.61^{+0.81}_{-1.89}$	$+2.05_{-3.46}$	$+2.05_{-4.08}$	$3.42^{+1.84}_{-0.62}$	$+2.06_{-3.01}$	$+2.06_{-4.21}$	$-2.99^{+0.83}_{-0.37}$	$+1.72_{-0.35}$	$+1.87_{-0.37}$	$-11.32^{+3.77}_{-2.28}$	$+5.94_{-4.27}$	$+7.95_{-4.49}$
J1147+3501		$2.01^{+0.75}_{-1.77}$	$+0.99_{-3.40}$	$+1.93_{-3.41}$	$3.02^{+2.21}_{-0.27}$	$+2.48_{-1.52}$	$+2.47_{-2.42}$	$-2.94^{+0.65}_{-0.37}$	$+1.62_{-0.33}$	$+1.70_{-0.42}$	$-9.92^{+1.76}_{-4.11}$	$+3.26_{-6.97}$	$+5.30_{-6.97}$
J1147-0724		$2.36^{+0.56}_{-0.74}$	$+2.74_{-2.26}$	$+2.87_{-3.77}$	$2.45^{+1.61}_{-0.70}$	$+2.94_{-1.44}$	$+3.04_{-2.33}$	$-1.73^{+0.37}_{-1.01}$	$+0.34_{-1.59}$	$+0.37_{-1.64}$	$-6.52^{+1.64}_{-2.81}$	$+2.95_{-4.87}$	$+3.69_{-6.25}$
J1148+5254		$3.69^{+0.86}_{-1.92}$	$+1.79_{-3.74}$	$+1.79_{-4.84}$	$4.67^{+0.82}_{-2.40}$	$+0.83_{-4.72}$	$+0.83_{-6.06}$	$-1.69^{+0.10}_{-1.64}$	$+0.41_{-1.64}$	$+0.45_{-1.67}$	$-9.86^{+2.98}_{-5.12}$	$+5.14_{-7.75}$	$+6.79_{-8.96}$
J1148+5924		$2.10^{+0.70}_{-0.78}$	$+1.81_{-1.84}$	$+3.01_{-2.17}$	$2.37^{+2.01}_{-0.56}$	$+3.13_{-1.30}$	$+3.13_{-3.09}$	$-2.00^{+0.76}_{-0.59}$	$+0.71_{-1.31}$	$+0.76_{-1.37}$	$-8.06^{+2.08}_{-3.03}$	$+3.09_{-5.40}$	$+4.97_{-6.57}$
J1148-0404		$2.37^{+0.90}_{-1.64}$	$+1.46_{-3.44}$	$+1.54_{-3.86}$	$4.70^{+0.79}_{-1.57}$	$+0.80_{-3.58}$	$+0.80_{-5.87}$	$-3.00^{+0.72}_{-0.35}$	$+1.59_{-0.32}$	$+1.64_{-0.36}$	$-10.77^{+2.39}_{-3.73}$	$+5.42_{-5.64}$	$+8.13_{-6.13}$
J1150+2417		$3.10^{+1.83}_{-0.72}$	$+2.14_{-4.17}$	$+2.36_{-4.56}$	$3.09^{+1.82}_{-1.46}$	$+2.34_{-3.51}$	$+2.36_{-4.40}$	$-3.11^{+1.28}_{-0.24}$	$+1.92_{-0.23}$	$+1.98_{-0.24}$	$-9.74^{+4.51}_{-3.24}$	$+5.46_{-6.70}$	$+7.37_{-7.86}$
J1150+4332		$3.55^{+1.45}_{-1.08}$	$+1.80_{-3.72}$	$+1.90_{-4.79}$	$4.79^{+0.71}_{-2.33}$	$+0.71_{-5.26}$	$+0.71_{-6.25}$	$-3.12^{+1.37}_{-0.25}$	$+1.88_{-0.18}$	$+1.88_{-0.24}$	$-12.53^{+2.83}_{-4.50}$	$+7.10_{-4.71}$	$+9.32_{-4.99}$
J1150-0640		$2.32^{+0.84}_{-0.91}$	$+2.11_{-3.23}$	$+3.01_{-3.69}$	$2.58^{+1.64}_{-1.12}$	$+2.89_{-2.38}$	$+2.89_{-3.86}$	$-1.67^{+0.29}_{-1.11}$	$+0.32_{-1.63}$	$+0.32_{-1.70}$	$-7.43^{+1.98}_{-3.45}$	$+4.02_{-6.19}$	$+5.40_{-7.26}$
J1152+4939		$3.89^{+1.30}_{-0.51}$	$+1.59_{-2.45}$	$+1.59_{-4.00}$	$4.62^{+0.87}_{-2.14}$	$+0.86_{-5.45}$	$+0.86_{-5.91}$	$-1.57^{+0.30}_{-1.08}$	$+0.27_{-1.75}$	$+0.31_{-1.80}$	$-14.21^{+5.06}_{-2.13}$	$+10.88_{-2.28}$	$+11.16_{-3.12}$
J1152-0519		$3.00^{+1.62}_{-1.26}$	$+2.44_{-2.57}$	$+2.49_{-4.08}$	$4.63^{+0.78}_{-2.58}$	$+0.81_{-4.86}$	$+0.87_{-5.60}$	$-3.10^{+1.73}_{-0.34}$	$+1.69_{-0.20}$	$+1.74_{-0.27}$	$-10.67^{+4.44}_{-3.49}$	$+5.89_{-6.99}$	$+7.72_{-8.21}$
J1152-0841		$2.73^{+0.76}_{-0.92}$	$+1.99_{-2.89}$	$+2.69_{-4.05}$	$2.85^{+1.39}_{-0.87}$	$+2.65_{-1.44}$	$+2.64_{-2.50}$	$-3.09^{+1.14}_{-0.24}$	$+1.66_{-0.25}$	$+1.72_{-0.28}$	$-7.61^{+0.74}_{-3.89}$	$+2.62_{-5.61}$	$+3.86_{-6.70}$
J1153+8058		$2.99^{+0.97}_{-0.94}$	$+2.12_{-3.24}$	$+2.26_{-4.19}$	$3.63^{+1.79}_{-0.93}$	$+1.86_{-4.21}$	$+1.86_{-5.07}$	$-3.04^{+1.13}_{-0.32}$	$+1.74_{-0.32}$	$+1.80_{-0.32}$	$-10.32^{+2.98}_{-3.37}$	$+7.61_{-4.15}$	$+8.39_{-5.65}$
J1154+5934		$4.46^{+0.97}_{-2.46}$	$+1.01_{-5.23}$	$+1.03_{-5.91}$	$3.22^{+1.29}_{-2.99}$	$+2.01_{-4.67}$	$+2.26_{-4.71}$	$-1.81^{+0.47}_{-0.96}$	$+0.46_{-1.55}$	$+0.57_{-1.55}$	$-14.45^{+5.08}_{-4.05}$	$+10.08_{-4.81}$	$+11.50_{-5.52}$
J1154+6022		$2.85^{+1.19}_{-1.51}$	$+1.30_{-3.75}$	$+1.45_{-4.33}$	$4.73^{+0.75}_{-1.44}$	$+0.77_{-3.99}$	$+0.75_{-6.05}$	$-2.96^{+0.81}_{-0.35}$	$+1.62_{-0.28}$	$+1.64_{-0.35}$	$-10.87^{+2.42}_{-3.06}$	$+5.71_{-4.32}$	$+8.86_{-4.75}$
J1157+5527	2σ	$1.24^{+1.03}_{-0.90}$	$+1.09_{-2.45}$	$+1.54_{-2.70}$	$5.03^{+0.20}_{-1.68}$	$+0.43_{-2.44}$	$+0.47_{-2.88}$	$-2.51^{+0.19}_{-0.31}$	$+0.51_{-0.61}$	$+0.65_{-0.80}$	$-12.00^{+2.80}_{-1.33}$	$+4.39_{-2.16}$	$+5.25_{-2.36}$
J1158+2450		$4.92^{+0.58}_{-1.48}$	$+0.59_{-3.17}$	$+0.57_{-4.95}$	$4.41^{+1.05}_{-2.86}$	$+1.05_{-5.33}$	$+1.07_{-5.85}$	$-1.72^{+0.59}_{-0.90}$	$+0.59_{-1.54}$	$+0.59_{-1.65}$	$-9.11^{+1.92}_{-6.57}$	$+4.61_{-9.02}$	$+6.32_{-9.41}$
J1158+4825		$2.67^{+0.96}_{-0.76}$	$+2.17_{-2.26}$	$+2.76_{-3.95}$	$2.71^{+2.11}_{-0.66}$	$+2.52_{-3.63}$	$+2.75_{-4.05}$	$-1.58^{+0.34}_{-1.16}$	$+0.25_{-1.76}$	$+0.34_{-1.76}$	$-9.07^{+1.84}_{-4.03}$	$+5.29_{-5.35}$	$+6.16_{-6.08}$
J1159+2914		$2.08^{+0.65}_{-0.94}$	$+0.74_{-3.13}$	$+1.01_{-3.58}$	$3.01^{+0.91}_{-0.32}$	$+2.08_{-0.63}$	$+2.47_{-0.71}$	$-2.48^{+0.67}_{-0.31}$	$+0.74_{-0.89}$	$+1.32_{-0.89}$	$-6.43^{+0.64}_{-1.77}$	$+1.20_{-3.78}$	$+1.41_{-4.65}$
J1201+1431		$2.72^{+1.30}_{-1.01}$	$+1.73_{-3.38}$	$+2.07_{-4.20}$	$3.21^{+2.22}_{-0.53}$	$+2.23_{-3.25}$	$+2.27_{-4.63}$	$-3.03^{+1.10}_{-0.34}$	$+1.70_{-0.34}$	$+1.79_{-0.34}$	$-9.58^{+2.73}_{-3.65}$	$+4.50_{-6.61}$	$+6.53_{-6.66}$

Table C.2: Results of fitting the broken power-law model over the 1290 selected observations from OVRO dataset. Break significance refers to the source having a possible break frequency being (1σ) at 68.3%, (2σ) at 95.5% and (3σ) at 99.7%. The absence of break significance means that the source is not well-fitted at any level.

Name	Break significance	β_l	$\beta_l^{95.5\%}$	$\beta_l^{99.7\%}$	β_h	$\beta_h^{95.5\%}$	$\beta_h^{99.7\%}$	$\log f_{br}$	$\log f_{br}^{95.5\%}$	$\log f_{br}^{99.7\%}$	$\log A$	$\log A^{95.5\%}$	$\log A^{99.7\%}$
J1202-0528		$1.68^{+0.56}_{-1.88}$	$+0.86_{-2.99}$	$+1.09_{-3.18}$	$2.57^{+1.38}_{-0.48}$	$+2.76_{-0.59}$	$+2.88_{-1.02}$	$-2.85^{+0.42}_{-0.37}$	$+1.15_{-0.49}$	$+1.47_{-0.49}$	$-6.77^{+0.81}_{-3.09}$	$+1.95_{-5.82}$	$+2.25_{-6.72}$
J1203+4803		$2.19^{+0.72}_{-0.61}$	$+1.52_{-2.09}$	$+1.92_{-2.94}$	$2.46^{+2.32}_{-0.40}$	$+3.04_{-2.19}$	$+3.04_{-3.50}$	$-1.57^{+0.32}_{-1.03}$	$+0.25_{-1.79}$	$+0.32_{-1.80}$	$-7.36^{+0.81}_{-4.45}$	$+3.53_{-6.07}$	$+4.67_{-7.19}$
J1203+6031		$4.82^{+0.67}_{-1.96}$	$+0.68_{-4.97}$	$+0.68_{-6.25}$	$4.44^{+0.90}_{-2.45}$	$+1.06_{-5.17}$	$+1.05_{-5.80}$	$-3.02^{+1.04}_{-0.29}$	$+1.65_{-0.26}$	$+1.71_{-0.29}$	$-14.13^{+5.67}_{-2.71}$	$+10.45_{-3.96}$	$+11.64_{-5.74}$
J1207+1211		$2.95^{+0.71}_{-0.77}$	$+1.83_{-2.56}$	$+2.42_{-3.47}$	$3.32^{+1.62}_{-1.13}$	$+2.18_{-3.59}$	$+2.17_{-4.68}$	$-1.53^{+0.28}_{-1.10}$	$+0.26_{-1.78}$	$+0.29_{-1.83}$	$-9.76^{+3.01}_{-2.64}$	$+5.75_{-4.87}$	$+7.47_{-5.30}$
J1207+2754		$2.99^{+0.97}_{-0.53}$	$+2.37_{-1.12}$	$+2.51_{-2.99}$	$2.71^{+2.54}_{-0.88}$	$+2.76_{-3.45}$	$+2.76_{-4.10}$	$-1.50^{+0.37}_{-1.00}$	$+0.37_{-1.75}$	$+0.37_{-1.86}$	$-6.77^{+0.99}_{-5.01}$	$+3.85_{-7.11}$	$+4.52_{-8.50}$
J1209+1810	1σ	$2.16^{+0.64}_{-1.98}$	$+0.99_{-3.62}$	$+1.95_{-3.63}$	$3.92^{+0.89}_{-0.80}$	$+1.58_{-1.07}$	$+1.58_{-1.77}$	$-2.85^{+0.36}_{-0.31}$	$+0.64_{-0.45}$	$+1.14_{-0.46}$	$-10.75^{+1.82}_{-2.04}$	$+2.80_{-3.77}$	$+4.54_{-3.98}$
J1209+2547		$3.81^{+1.08}_{-1.19}$	$+1.61_{-2.74}$	$+1.68_{-4.10}$	$4.66^{+0.82}_{-2.74}$	$+0.83_{-5.31}$	$+0.82_{-6.09}$	$-3.11^{+1.25}_{-0.23}$	$+1.77_{-0.26}$	$+1.86_{-0.26}$	$-11.37^{+3.02}_{-5.39}$	$+7.09_{-6.21}$	$+8.23_{-7.35}$
J1209+4119		$3.27^{+1.33}_{-1.15}$	$+2.15_{-3.50}$	$+2.22_{-4.70}$	$4.36^{+1.10}_{-2.05}$	$+1.11_{-5.13}$	$+1.10_{-5.67}$	$-3.12^{+1.27}_{-0.25}$	$+1.75_{-0.25}$	$+1.87_{-0.25}$	$-11.15^{+3.02}_{-4.68}$	$+6.49_{-6.01}$	$+8.14_{-6.74}$
J1214+0829		$3.84^{+1.34}_{-1.00}$	$+1.66_{-2.12}$	$+1.66_{-4.86}$	$3.45^{+1.59}_{-1.54}$	$+1.94_{-3.83}$	$+2.03_{-4.92}$	$-1.71^{+0.32}_{-1.04}$	$+0.31_{-1.59}$	$+0.35_{-1.65}$	$-8.61^{+1.63}_{-5.44}$	$+3.44_{-8.86}$	$+5.76_{-9.46}$
J1215+1654		$2.01^{+0.66}_{-1.15}$	$+0.74_{-3.08}$	$+1.30_{-3.49}$	$2.63^{+1.07}_{-0.48}$	$+2.85_{-0.87}$	$+2.85_{-1.68}$	$-2.83^{+0.76}_{-0.53}$	$+1.47_{-0.54}$	$+1.69_{-0.53}$	$-6.83^{+0.99}_{-1.91}$	$+2.27_{-4.05}$	$+2.27_{-5.08}$
J1215-1731		$2.19^{+1.15}_{-0.64}$	$+1.45_{-3.67}$	$+3.09_{-3.69}$	$2.35^{+1.99}_{-0.80}$	$+3.13_{-2.91}$	$+3.12_{-3.68}$	$-1.65^{+0.34}_{-1.15}$	$+0.24_{-1.68}$	$+0.34_{-1.68}$	$-5.78^{+1.28}_{-4.39}$	$+4.81_{-5.93}$	$+4.81_{-7.22}$
J1217+3007		$1.79^{+1.47}_{-0.73}$	$+2.02_{-3.13}$	$+3.44_{-3.13}$	$1.83^{+2.30}_{-0.74}$	$+3.61_{-1.83}$	$+3.64_{-2.96}$	$-1.58^{+0.35}_{-1.19}$	$+0.26_{-1.77}$	$+0.35_{-1.78}$	$-5.67^{+1.45}_{-4.17}$	$+2.12_{-8.19}$	$+3.18_{-9.49}$
J1217+5835		$2.60^{+1.49}_{-0.96}$	$+1.49_{-4.07}$	$+2.32_{-4.07}$	$4.34^{+0.60}_{-2.25}$	$+1.16_{-3.69}$	$+1.13_{-5.83}$	$-3.10^{+1.09}_{-0.27}$	$+1.78_{-0.24}$	$+1.85_{-0.27}$	$-10.47^{+3.54}_{-3.40}$	$+5.88_{-5.35}$	$+8.23_{-6.12}$
J1219+4829		$2.37^{+0.51}_{-0.76}$	$+1.34_{-2.91}$	$+3.11_{-3.51}$	$2.72^{+1.37}_{-0.86}$	$+2.74_{-1.23}$	$+2.74_{-2.73}$	$-1.50^{+0.23}_{-1.12}$	$+0.22_{-1.81}$	$+0.25_{-1.87}$	$-7.44^{+1.75}_{-2.22}$	$+1.99_{-5.21}$	$+4.17_{-5.63}$
J1219+6600	1σ	$1.55^{+0.64}_{-0.60}$	$+0.87_{-1.65}$	$+1.16_{-2.30}$	$2.86^{+2.53}_{-0.09}$	$+2.59_{-1.30}$	$+2.60_{-1.99}$	$-2.31^{+0.58}_{-0.33}$	$+1.00_{-0.80}$	$+1.06_{-1.05}$	$-8.64^{+0.91}_{-4.21}$	$+2.96_{-5.00}$	$+3.88_{-5.72}$
J1220+3808		$2.66^{+0.78}_{-0.84}$	$+1.39_{-4.13}$	$+2.58_{-4.13}$	$3.08^{+1.31}_{-1.10}$	$+2.41_{-2.27}$	$+2.39_{-4.54}$	$-3.12^{+1.17}_{-0.25}$	$+1.77_{-0.25}$	$+1.86_{-0.25}$	$-8.98^{+2.38}_{-2.71}$	$+3.88_{-5.78}$	$+6.15_{-5.77}$
J1221+2813		$1.83^{+0.68}_{-0.48}$	$+1.14_{-1.97}$	$+2.26_{-2.88}$	$2.70^{+1.57}_{-0.56}$	$+2.79_{-0.66}$	$+2.80_{-1.82}$	$-2.09^{+0.55}_{-0.43}$	$+0.81_{-1.13}$	$+0.83_{-1.27}$	$-7.19^{+1.59}_{-2.36}$	$+1.87_{-4.69}$	$+2.92_{-5.50}$
J1221+4411		$3.26^{+1.43}_{-1.37}$	$+1.81_{-4.56}$	$+2.18_{-4.66}$	$4.38^{+1.06}_{-1.83}$	$+1.12_{-4.53}$	$+1.12_{-5.82}$	$-3.16^{+1.19}_{-0.21}$	$+1.84_{-0.21}$	$+1.91_{-0.21}$	$-12.43^{+4.55}_{-2.61}$	$+7.49_{-4.24}$	$+9.25_{-4.65}$
J1222+0413	2σ	$-0.00^{+0.95}_{-1.08}$	$+1.82_{-1.45}$	$+2.59_{-1.49}$	$3.92^{+0.47}_{-0.49}$	$+1.37_{-0.83}$	$+1.45_{-1.35}$	$-2.81^{+0.25}_{-0.13}$	$+0.52_{-0.27}$	$+0.54_{-0.45}$	$-8.91^{+0.99}_{-1.02}$	$+1.75_{-3.01}$	$+2.80_{-3.00}$
J1223+8040		$2.08^{+0.66}_{-0.98}$	$+1.80_{-3.35}$	$+3.10_{-3.56}$	$2.46^{+1.43}_{-0.67}$	$+3.02_{-0.87}$	$+2.99_{-2.77}$	$-3.08^{+1.09}_{-0.23}$	$+1.70_{-0.23}$	$+1.78_{-0.23}$	$-6.89^{+1.54}_{-2.49}$	$+1.74_{-5.40}$	$+3.82_{-5.81}$
J1224+4335		$2.04^{+2.43}_{-0.86}$	$+3.44_{-2.47}$	$+3.46_{-3.40}$	$3.59^{+1.85}_{-1.57}$	$+1.90_{-4.16}$	$+1.90_{-4.97}$	$-1.76^{+0.07}_{-1.35}$	$+0.44_{-1.55}$	$+0.57_{-1.55}$	$-12.81^{+6.21}_{-2.36}$	$+9.54_{-4.35}$	$+10.23_{-6.58}$
J1226+4340		$2.94^{+1.59}_{-1.44}$	$+1.60_{-4.07}$	$+2.50_{-4.39}$	$4.66^{+0.80}_{-1.75}$	$+0.80_{-4.81}$	$+0.80_{-6.05}$	$-3.01^{+0.90}_{-0.30}$	$+1.60_{-0.29}$	$+1.70_{-0.30}$	$-13.71^{+3.84}_{-2.63}$	$+8.98_{-2.95}$	$+11.24_{-3.52}$
J1226-1328	2σ	$0.42^{+0.31}_{-1.68}$	$+1.42_{-1.90}$	$+2.27_{-1.90}$	$3.03^{+1.25}_{-0.56}$	$+2.32_{-0.81}$	$+2.40_{-1.17}$	$-2.59^{+0.15}_{-0.28}$	$+0.37_{-0.52}$	$+0.67_{-0.73}$	$-7.96^{+1.66}_{-2.55}$	$+1.61_{-5.68}$	$+2.46_{-5.69}$
J1227+4932		$1.91^{+0.98}_{-1.35}$	$+1.31_{-3.26}$	$+1.95_{-3.38}$	$2.80^{+2.05}_{-0.67}$	$+2.70_{-1.97}$	$+2.70_{-4.19}$	$-2.95^{+0.98}_{-0.32}$	$+1.58_{-0.42}$	$+1.71_{-0.42}$	$-9.44^{+2.51}_{-3.33}$	$+5.13_{-5.90}$	$+7.23_{-7.06}$

Table C.2: Results of fitting the broken power-law model over the 1290 selected observations from OVRO dataset. Break significance refers to the source having a possible break frequency being (1σ) at 68.3%, (2σ) at 95.5% and (3σ) at 99.7%. The absence of break significance means that the source is not well-fitted at any level.

Name	Break significance	β_l	$\beta_l^{95.5\%}$	$\beta_l^{99.7\%}$	β_h	$\beta_h^{95.5\%}$	$\beta_h^{99.7\%}$	$\log f_{br}$	$\log f_{br}^{95.5\%}$	$\log f_{br}^{99.7\%}$	$\log A$	$\log A^{95.5\%}$	$\log A^{99.7\%}$
J1228+3706		2.82 ^{+0.87} _{-0.90}	+2.58 -1.71	+2.55 -3.61	2.56 ^{+1.52} _{-0.72}	+2.93 -2.26	+2.93 -3.87	-3.13 ^{+1.31} _{-0.24}	+1.82 -0.23	+1.89 -0.23	-7.79 ^{+1.48} _{-3.21}	+3.49 -5.46	+5.23 -6.13
J1229+0203		2.77 ^{+0.63} _{-0.90}	+1.12 -3.63	+2.25 -4.16	3.36 ^{+1.75} _{-0.49}	+2.12 -2.79	+2.12 -3.73	-2.62 ^{+0.64} _{-0.75}	+1.47 -0.69	+1.49 -0.75	-6.41 ^{+1.79} _{-2.49}	+4.51 -4.25	+4.99 -5.06
J1230+2518		2.37 ^{+0.72} _{-0.88}	+1.24 -3.51	+2.06 -3.77	2.66 ^{+1.15} _{-0.77}	+2.77 -1.56	+2.84 -2.78	-3.12 ^{+1.32} _{-0.25}	+1.94 -0.22	+2.00 -0.24	-6.74 ^{+1.49} _{-1.85}	+1.75 -5.32	+3.38 -5.32
J1231+0418	1 σ	1.82 ^{+0.63} _{-1.46}	+0.99 -3.02	+1.58 -3.25	3.03 ^{+1.15} _{-0.46}	+2.45 -0.64	+2.47 -1.04	-2.85 ^{+0.54} _{-0.40}	+1.27 -0.52	+1.45 -0.52	-8.63 ^{+1.08} _{-2.57}	+1.76 -5.32	+2.46 -6.17
J1232+4821		3.41 ^{+1.46} _{-0.64}	+1.99 -1.89	+1.99 -3.35	4.36 ^{+1.07} _{-2.58}	+1.02 -5.35	+1.13 -5.85	-1.55 ^{+0.31} _{-1.04}	+0.31 -1.70	+0.31 -1.82	-9.47 ^{+3.60} _{-4.24}	+5.72 -6.73	+6.27 -8.06
J1235+3621		2.89 ^{+1.90} _{-0.80}	+2.56 -2.46	+2.56 -4.07	2.85 ^{+2.55} _{-0.96}	+2.65 -3.50	+2.65 -4.25	-1.70 ^{+0.26} _{-1.09}	+0.33 -1.65	+0.45 -1.66	-9.92 ^{+4.22} _{-4.07}	+6.11 -7.83	+7.36 -8.61
J1238+0723		3.15 ^{+1.35} _{-0.75}	+1.35 -3.81	+1.87 -4.63	4.19 ^{+1.22} _{-1.27}	+1.24 -3.87	+1.29 -5.69	-3.06 ^{+1.17} _{-0.23}	+1.59 -0.30	+1.70 -0.30	-12.11 ^{+3.85} _{-1.96}	+7.20 -3.44	+9.73 -4.40
J1239+0730		2.13 ^{+0.73} _{-0.69}	+1.99 -3.05	+3.28 -3.48	2.41 ^{+1.43} _{-0.93}	+3.09 -1.15	+3.07 -3.27	-2.04 ^{+0.80} _{-0.59}	+0.68 -1.32	+0.80 -1.33	-6.64 ^{+1.56} _{-2.59}	+2.04 -6.16	+4.61 -6.64
J1239-1023		2.79 ^{+1.55} _{-1.20}	+2.65 -2.79	+2.63 -4.21	4.32 ^{+1.18} _{-2.15}	+1.18 -4.40	+1.18 -5.72	-3.11 ^{+1.20} _{-0.25}	+1.71 -0.23	+1.75 -0.26	-9.01 ^{+3.50} _{-4.41}	+5.60 -7.34	+7.22 -8.29
J1242+3750		3.10 ^{+1.57} _{-0.90}	+2.35 -2.53	+2.37 -3.46	2.84 ^{+2.24} _{-1.06}	+2.66 -3.10	+2.63 -4.31	-1.62 ^{+0.36} _{-1.14}	+0.36 -1.68	+0.38 -1.75	-10.65 ^{+5.07} _{-2.30}	+6.61 -5.67	+7.59 -6.97
J1243+7442		2.56 ^{+1.06} _{-1.32}	+1.43 -3.96	+2.50 -3.96	4.73 ^{+0.75} _{-1.98}	+0.77 -4.65	+0.77 -6.08	-3.02 ^{+0.99} _{-0.31}	+1.60 -0.30	+1.71 -0.31	-12.53 ^{+4.23} _{-2.60}	+7.97 -3.60	+10.37 -3.61
J1245-1617		2.20 ^{+0.73} _{-0.77}	+3.26 -2.05	+3.26 -3.69	2.36 ^{+1.44} _{-0.82}	+3.05 -0.84	+3.11 -2.02	-1.74 ^{+0.06} _{-1.53}	+0.30 -1.58	+0.41 -1.58	-5.64 ^{+1.59} _{-2.49}	+1.87 -5.18	+3.17 -5.82
J1248+5820		2.87 ^{+1.20} _{-0.85}	+2.62 -3.03	+2.61 -4.18	3.47 ^{+1.82} _{-0.81}	+2.02 -3.37	+2.02 -4.78	-3.10 ^{+1.16} _{-0.27}	+1.78 -0.25	+1.86 -0.27	-11.03 ^{+2.79} _{-3.36}	+6.05 -5.12	+7.50 -5.64
J1248-0632		2.82 ^{+0.81} _{-0.76}	+2.09 -2.80	+2.35 -4.24	3.01 ^{+1.66} _{-0.82}	+2.49 -2.80	+2.48 -4.26	-1.65 ^{+0.30} _{-1.02}	+0.26 -1.63	+0.30 -1.71	-8.93 ^{+2.07} _{-3.21}	+4.42 -5.56	+6.22 -5.56
J1251-1717		2.58 ^{+1.07} _{-1.18}	+1.75 -3.57	+2.31 -4.08	3.72 ^{+1.13} _{-1.83}	+1.77 -4.14	+1.76 -5.02	-3.07 ^{+1.11} _{-0.26}	+1.70 -0.21	+1.75 -0.26	-10.23 ^{+3.66} _{-3.40}	+7.15 -5.33	+7.44 -6.79
J1254+1141		2.65 ^{+0.72} _{-0.78}	+2.30 -2.61	+2.75 -4.15	2.88 ^{+1.80} _{-1.06}	+2.60 -3.00	+2.60 -4.36	-1.47 ^{+0.31} _{-1.23}	+0.32 -1.85	+0.33 -1.91	-7.99 ^{+2.00} _{-3.39}	+4.59 -5.46	+5.86 -6.18
J1254-1317		3.08 ^{+0.97} _{-1.06}	+1.71 -3.93	+2.31 -4.40	3.45 ^{+1.60} _{-1.01}	+2.04 -3.11	+2.05 -4.50	-3.09 ^{+0.94} _{-0.27}	+1.67 -0.27	+1.73 -0.27	-11.80 ^{+4.32} _{-1.52}	+7.60 -3.62	+8.46 -4.64
J1255+1817		2.02 ^{+0.81} _{-0.82}	+1.55 -2.83	+1.77 -3.45	2.39 ^{+2.03} _{-0.68}	+3.05 -2.02	+3.06 -3.00	-3.00 ^{+1.21} _{-0.30}	+1.73 -0.30	+1.88 -0.35	-7.93 ^{+1.71} _{-3.63}	+4.54 -6.10	+4.54 -8.06
J1256-0547		2.48 ^{+0.77} _{-1.09}	+1.46 -3.90	+2.74 -3.94	2.71 ^{+1.05} _{-0.86}	+2.70 -1.61	+2.77 -3.40	-3.13 ^{+1.19} _{-0.24}	+1.78 -0.24	+1.87 -0.24	-4.52 ^{+1.77} _{-1.93}	+2.87 -4.79	+4.71 -5.64
J1257+3229		2.11 ^{+0.74} _{-1.35}	+0.75 -3.46	+1.72 -3.58	2.50 ^{+1.04} _{-0.68}	+2.97 -0.83	+2.97 -2.26	-2.96 ^{+1.23} _{-0.30}	+1.71 -0.40	+1.83 -0.41	-6.47 ^{+1.19} _{-2.21}	+1.67 -4.84	+2.89 -5.88
J1300+0828		2.94 ^{+1.57} _{-0.84}	+1.57 -3.95	+2.02 -4.35	4.62 ^{+0.83} _{-1.97}	+0.88 -4.82	+0.88 -6.02	-3.04 ^{+1.00} _{-0.27}	+1.65 -0.26	+1.73 -0.27	-12.78 ^{+4.10} _{-3.13}	+7.46 -4.27	+9.20 -4.27
J1300+1206		3.12 ^{+1.15} _{-0.79}	+1.77 -3.53	+2.16 -4.44	4.27 ^{+1.22} _{-1.20}	+1.22 -4.17	+1.22 -5.52	-3.10 ^{+1.20} _{-0.27}	+1.77 -0.27	+1.86 -0.27	-11.36 ^{+2.63} _{-3.11}	+6.96 -4.43	+8.23 -5.31
J1300+2830		2.49 ^{+1.71} _{-1.15}	+2.99 -2.30	+2.99 -3.92	4.59 ^{+0.59} _{-2.64}	+0.85 -5.17	+0.87 -6.00	-1.75 ^{+0.04} _{-1.51}	+0.50 -1.62	+0.62 -1.62	-8.81 ^{+2.83} _{-4.87}	+5.27 -7.82	+6.22 -9.35
J1300+5029		2.82 ^{+1.92} _{-1.05}	+2.67 -2.80	+2.67 -4.31	2.72 ^{+2.77} _{-0.59}	+2.77 -3.35	+2.77 -4.16	-3.04 ^{+1.18} _{-0.31}	+1.77 -0.27	+1.79 -0.33	-9.91 ^{+3.37} _{-4.67}	+5.91 -7.99	+6.95 -9.96

Table C.2: Results of fitting the broken power-law model over the 1290 selected observations from OVRO dataset. Break significance refers to the source having a possible break frequency being (1σ) at 68.3%, (2σ) at 95.5% and (3σ) at 99.7%. The absence of break significance means that the source is not well-fitted at any level.

Name	Break significance	β_l	$\beta_l^{95.5\%}$	$\beta_l^{99.7\%}$	β_h	$\beta_h^{95.5\%}$	$\beta_h^{99.7\%}$	$\log f_{br}$	$\log f_{br}^{95.5\%}$	$\log f_{br}^{99.7\%}$	$\log A$	$\log A^{95.5\%}$	$\log A^{99.7\%}$
J1302+5748		2.50 ^{+1.05} _{-1.17}	+1.13 -3.86	+2.26 -3.92	3.01 ^{+1.35} _{-0.74}	+2.49 -1.37	+2.49 -2.93	-3.12 ^{+1.02} _{-0.24}	+1.76 -0.23	+1.89 -0.24	-8.31 ^{+0.96} _{-3.40}	+2.54 -5.11	+4.68 -5.11
J1305-1033	3 σ	0.64 ^{+1.48} _{-0.51}	+1.71 -1.95	+2.29 -2.13	5.00 ^{+0.48} _{-0.55}	+0.47 -1.46	+0.50 -1.94	-2.54 ^{+0.12} _{-0.22}	+0.19 -0.51	+0.28 -0.58	-11.66 ^{+1.25} _{-1.06}	+3.13 -1.53	+4.20 -1.52
J1306+5529		2.81 ^{+1.60} _{-1.01}	+2.69 -2.04	+2.68 -3.19	4.42 ^{+0.99} _{-2.47}	+1.03 -4.66	+1.06 -5.85	-1.61 ^{+0.37} _{-1.15}	+0.31 -1.70	+0.37 -1.75	-9.03 ^{+2.89} _{-4.70}	+4.77 -7.64	+6.15 -9.56
J1306-1718		2.79 ^{+2.27} _{-0.88}	+2.70 -3.32	+2.70 -4.16	4.53 ^{+0.91} _{-2.21}	+0.91 -5.06	+0.95 -5.98	-2.92 ^{+1.49} _{-0.10}	+1.49 -0.40	+1.60 -0.41	-12.21 ^{+3.99} _{-4.01}	+7.92 -5.53	+9.74 -7.14
J1308+3546		2.20 ^{+0.68} _{-0.98}	+0.93 -3.26	+1.37 -3.65	2.90 ^{+1.46} _{-0.46}	+2.57 -0.81	+2.59 -1.39	-2.27 ^{+0.20} _{-1.05}	+1.00 -1.07	+1.13 -1.09	-7.91 ^{+1.32} _{-2.33}	+2.10 -4.86	+2.79 -5.64
J1309+1154		2.55 ^{+0.72} _{-0.76}	+1.36 -3.22	+2.14 -4.00	3.48 ^{+1.51} _{-1.26}	+2.01 -3.60	+2.01 -4.84	-1.43 ^{+0.29} _{-1.27}	+0.27 -1.83	+0.30 -1.94	-10.45 ^{+3.22} _{-2.38}	+6.63 -3.68	+8.16 -4.61
J1309+5557		2.84 ^{+1.25} _{-0.71}	+1.87 -2.66	+2.57 -4.12	4.06 ^{+1.25} _{-1.59}	+1.37 -4.43	+1.41 -5.34	-3.02 ^{+1.75} _{-0.26}	+1.75 -0.26	+1.77 -0.35	-12.38 ^{+5.15} _{-1.29}	+8.07 -3.29	+8.76 -4.35
J1310+0044		3.17 ^{+1.65} _{-1.40}	+2.31 -3.52	+2.33 -4.58	4.54 ^{+0.91} _{-2.18}	+0.95 -4.50	+0.95 -5.79	-3.06 ^{+1.02} _{-0.24}	+1.56 -0.26	+1.63 -0.26	-13.42 ^{+6.30} _{-1.73}	+9.27 -4.57	+10.57 -5.92
J1310+3220		2.60 ^{+0.46} _{-0.93}	+1.23 -3.23	+2.22 -3.91	3.01 ^{+1.27} _{-0.65}	+2.49 -1.99	+2.47 -4.48	-3.07 ^{+1.30} _{-0.25}	+1.91 -0.20	+1.94 -0.29	-6.98 ^{+1.98} _{-2.52}	+3.19 -4.97	+6.29 -4.97
J1310+3233		1.46 ^{+0.66} _{-0.63}	+2.65 -1.97	+3.86 -1.97	1.55 ^{+1.57} _{-0.66}	+3.85 -1.93	+3.89 -2.96	-1.36 ^{+0.31} _{-1.14}	+0.27 -1.79	+0.31 -1.81	-3.60 ^{+0.79} _{-2.37}	+2.64 -4.89	+3.26 -6.02
J1310+4653		3.72 ^{+0.75} _{-1.29}	+1.77 -2.95	+1.76 -4.85	4.59 ^{+0.89} _{-2.06}	+0.91 -4.83	+0.89 -6.06	-1.57 ^{+0.33} _{-1.20}	+0.26 -1.79	+0.33 -1.79	-10.61 ^{+3.23} _{-3.84}	+6.20 -5.15	+7.46 -6.29
J1311+5513	2 σ	0.03 ^{+1.41} _{-0.73}	+2.10 -1.52	+2.95 -1.52	4.94 ^{+0.51} _{-1.14}	+0.51 -2.31	+0.56 -2.66	-2.74 ^{+0.21} _{-0.15}	+0.40 -0.38	+0.52 -0.55	-13.33 ^{+2.93} _{-1.01}	+5.36 -1.63	+6.34 -1.92
J1312+4828		1.61 ^{+0.74} _{-1.45}	+0.95 -3.11	+1.97 -3.10	2.74 ^{+1.30} _{-0.70}	+2.69 -0.69	+2.74 -1.07	-2.60 ^{+0.53} _{-0.38}	+1.04 -0.69	+1.33 -0.77	-7.71 ^{+1.20} _{-3.01}	+1.83 -5.48	+2.17 -6.14
J1312-0424	1 σ	1.78 ^{+0.51} _{-1.30}	+0.80 -2.74	+1.05 -3.25	2.89 ^{+1.48} _{-0.57}	+2.59 -0.68	+2.59 -0.98	-2.35 ^{+0.25} _{-0.75}	+0.78 -0.96	+0.97 -0.97	-7.28 ^{+1.03} _{-2.77}	+1.96 -4.85	+2.06 -5.80
J1313+1027		4.79 ^{+0.65} _{-0.96}	+0.70 -2.37	+0.71 -3.88	4.42 ^{+0.89} _{-3.05}	+1.05 -5.43	+1.07 -5.85	-1.53 ^{+0.29} _{-0.99}	+0.29 -1.70	+0.29 -1.83	-11.50 ^{+3.67} _{-4.70}	+7.12 -7.19	+8.43 -7.33
J1314+2348		3.14 ^{+2.35} _{-1.86}	+2.22 -4.47	+2.34 -4.63	1.65 ^{+1.24} _{-3.15}	+3.39 -3.15	+3.84 -3.15	-3.00 ^{+1.24} _{-0.30}	+1.94 -0.21	+1.94 -0.30	-13.71 ^{+4.66} _{-5.31}	+8.82 -6.27	+10.93 -6.27
J1317+3425		2.38 ^{+0.85} _{-1.61}	+1.01 -3.57	+1.87 -3.84	3.36 ^{+1.35} _{-1.13}	+2.14 -2.83	+2.14 -4.72	-2.88 ^{+0.79} _{-0.49}	+1.76 -0.40	+1.76 -0.48	-9.68 ^{+3.40} _{-1.88}	+5.34 -4.62	+7.43 -5.58
J1317-1345		2.30 ^{+1.70} _{-0.74}	+3.06 -1.53	+3.19 -3.49	2.50 ^{+2.38} _{-0.75}	+2.82 -3.09	+2.97 -3.65	-1.63 ^{+0.32} _{-1.04}	+0.32 -1.62	+0.32 -1.70	-9.18 ^{+2.20} _{-4.37}	+6.08 -5.85	+6.36 -7.82
J1319-1217	1 σ	1.66 ^{+0.60} _{-1.21}	+1.35 -2.52	+1.74 -3.13	2.86 ^{+2.25} _{-0.44}	+2.63 -1.49	+2.63 -2.00	-2.43 ^{+0.35} _{-0.50}	+0.98 -0.76	+1.04 -0.89	-8.71 ^{+2.39} _{-3.50}	+3.08 -6.05	+4.10 -6.23
J1319-1239		3.43 ^{+1.25} _{-1.20}	+2.06 -3.06	+2.05 -4.83	3.88 ^{+1.48} _{-1.77}	+1.62 -3.93	+1.61 -5.29	-3.08 ^{+1.16} _{-0.23}	+1.71 -0.22	+1.73 -0.25	-11.47 ^{+3.68} _{-4.04}	+7.44 -5.44	+9.17 -6.19
J1321+2216	2 σ	0.95 ^{+0.70} _{-0.71}	+1.15 -1.75	+1.44 -2.33	3.26 ^{+1.15} _{-0.59}	+2.17 -0.86	+2.23 -1.26	-2.35 ^{+0.32} _{-0.19}	+0.53 -0.55	+0.72 -0.86	-8.28 ^{+1.13} _{-2.33}	+1.79 -4.01	+2.48 -4.33
J1322-0937		2.88 ^{+0.64} _{-1.24}	+1.15 -3.41	+2.10 -4.20	3.53 ^{+1.05} _{-0.65}	+1.97 -1.73	+1.95 -2.79	-3.09 ^{+0.84} _{-0.28}	+1.66 -0.28	+1.84 -0.28	-8.79 ^{+1.23} _{-2.47}	+2.76 -4.58	+4.86 -4.57
J1323+7942		1.94 ^{+0.71} _{-0.96}	+1.07 -2.83	+1.85 -3.36	2.61 ^{+1.55} _{-0.60}	+2.87 -0.68	+2.86 -1.55	-2.32 ^{+0.29} _{-0.82}	+0.84 -0.95	+0.99 -0.98	-9.17 ^{+2.94} _{-1.55}	+2.94 -4.61	+4.67 -5.31
J1324+4743	2 σ	1.27 ^{+0.45} _{-2.06}	+0.97 -2.75	+1.70 -2.76	4.11 ^{+1.14} _{-0.81}	+1.39 -1.69	+1.39 -2.16	-2.77 ^{+0.23} _{-0.24}	+0.39 -0.58	+0.71 -0.58	-12.00 ^{+1.91} _{-2.93}	+4.40 -3.32	+5.32 -3.82

Table C.2: Results of fitting the broken power-law model over the 1290 selected observations from OVRO dataset. Break significance refers to the source having a possible break frequency being (1σ) at 68.3%, (2σ) at 95.5% and (3σ) at 99.7%. The absence of break significance means that the source is not well-fitted at any level.

Name	Break significance	β_l	$\beta_l^{95.5\%}$	$\beta_l^{99.7\%}$	β_h	$\beta_h^{95.5\%}$	$\beta_h^{99.7\%}$	$\log f_{br}$	$\log f_{br}^{95.5\%}$	$\log f_{br}^{99.7\%}$	$\log A$	$\log A^{95.5\%}$	$\log A^{99.7\%}$
J1324-1049		$2.64^{+0.60}_{-1.00}$	$+0.89$ -3.36	$+2.00$ -3.87	$3.41^{+1.13}_{-1.14}$	$+2.09$ -2.41	$+2.09$ -4.85	$-2.58^{+1.15}_{-0.24}$	$+1.22$ -0.79	$+1.34$ -0.79	$-10.26^{+3.10}_{-1.44}$	$+5.46$ -4.34	$+7.87$ -4.34
J1325-0804		$4.64^{+0.86}_{-2.13}$	$+0.84$ -5.11	$+0.86$ -5.80	$2.23^{+3.07}_{-1.18}$	$+3.15$ -3.38	$+3.27$ -3.72	$-1.84^{+0.48}_{-0.85}$	$+0.48$ -1.44	$+0.48$ -1.52	$-13.50^{+3.02}_{-6.10}$	$+7.76$ -6.39	$+10.48$ -6.47
J1326-0500		$4.43^{+0.68}_{-3.52}$	$+0.88$ -5.67	$+1.03$ -5.91	$1.92^{+2.87}_{-1.65}$	$+3.16$ -3.41	$+3.56$ -3.41	$-2.83^{+1.48}_{-0.08}$	$+1.48$ -0.47	$+1.48$ -0.54	$-12.31^{+4.24}_{-4.86}$	$+6.76$ -7.62	$+9.25$ -7.62
J1327+1223		$2.95^{+0.77}_{-1.54}$	$+0.78$ -4.14	$+1.16$ -4.44	$4.10^{+0.94}_{-1.27}$	$+1.33$ -3.87	$+1.33$ -5.41	$-3.05^{+0.89}_{-0.32}$	$+1.69$ -0.31	$+1.79$ -0.32	$-10.86^{+2.42}_{-2.65}$	$+6.47$ -3.80	$+8.07$ -4.28
J1327+2210		$2.90^{+0.73}_{-1.28}$	$+0.76$ -4.12	$+1.50$ -4.39	$3.56^{+1.03}_{-1.05}$	$+1.87$ -3.51	$+1.87$ -5.04	$-3.06^{+1.17}_{-0.31}$	$+1.88$ -0.24	$+1.90$ -0.31	$-9.11^{+2.20}_{-1.92}$	$+6.05$ -3.38	$+7.01$ -4.58
J1327+5008		$2.24^{+0.92}_{-0.86}$	$+1.40$ -3.31	$+3.15$ -3.73	$2.53^{+2.69}_{-0.28}$	$+2.95$ -2.28	$+2.95$ -3.43	$-3.01^{+1.11}_{-0.34}$	$+1.78$ -0.27	$+1.78$ -0.34	$-10.07^{+3.98}_{-1.94}$	$+5.70$ -4.76	$+6.88$ -5.75
J1329+3154		$2.15^{+0.61}_{-0.87}$	$+1.22$ -3.16	$+2.34$ -3.62	$2.53^{+2.33}_{-0.35}$	$+2.97$ -1.88	$+2.96$ -4.01	$-1.46^{+0.34}_{-1.20}$	$+0.34$ -1.81	$+0.34$ -1.91	$-7.46^{+1.57}_{-2.84}$	$+2.78$ -5.35	$+4.94$ -5.70
J1332+4722		$1.67^{+0.78}_{-0.69}$	$+1.19$ -2.39	$+1.46$ -3.13	$2.50^{+1.74}_{-0.63}$	$+2.93$ -0.63	$+2.97$ -1.48	$-2.08^{+0.64}_{-0.48}$	$+0.64$ -1.23	$+0.75$ -1.27	$-7.33^{+1.28}_{-3.06}$	$+1.73$ -5.19	$+2.77$ -5.96
J1332-0509		$3.06^{+0.80}_{-0.68}$	$+2.20$ -2.62	$+2.38$ -4.37	$3.71^{+1.72}_{-0.57}$	$+1.79$ -2.80	$+1.78$ -4.50	$-2.36^{+1.01}_{-0.34}$	$+0.95$ -0.97	$+1.01$ -0.99	$-10.23^{+3.08}_{-1.80}$	$+5.62$ -3.10	$+7.83$ -3.09
J1332-1256		$2.33^{+0.81}_{-2.10}$	$+1.39$ -3.80	$+3.14$ -3.80	$2.71^{+2.11}_{-0.62}$	$+2.79$ -1.76	$+2.77$ -3.05	$-2.95^{+0.67}_{-0.35}$	$+1.48$ -0.35	$+1.63$ -0.36	$-7.23^{+2.20}_{-3.88}$	$+3.16$ -7.25	$+4.46$ -7.60
J1333+1649		$4.99^{+0.50}_{-1.08}$	$+0.51$ -2.84	$+0.51$ -4.23	$4.64^{+0.85}_{-2.94}$	$+0.86$ -5.56	$+0.86$ -6.11	$-1.65^{+0.41}_{-0.87}$	$+0.33$ -1.72	$+0.41$ -1.72	$-15.40^{+6.36}_{-2.55}$	$+10.65$ -3.37	$+12.85$ -4.04
J1333+2725		$2.60^{+0.85}_{-1.14}$	$+1.23$ -3.83	$+2.62$ -4.05	$2.94^{+1.57}_{-0.70}$	$+2.55$ -1.74	$+2.55$ -2.44	$-3.02^{+1.04}_{-0.35}$	$+1.94$ -0.30	$+2.00$ -0.35	$-8.03^{+1.36}_{-3.07}$	$+2.67$ -5.14	$+3.75$ -5.85
J1333-1950		$2.62^{+1.22}_{-1.03}$	$+2.03$ -3.42	$+2.56$ -4.04	$4.64^{+0.86}_{-2.40}$	$+0.84$ -5.03	$+0.85$ -5.99	$-3.03^{+1.06}_{-0.30}$	$+1.64$ -0.30	$+1.72$ -0.29	$-9.17^{+4.75}_{-3.25}$	$+6.01$ -6.90	$+7.55$ -7.93
J1334-1150		$3.25^{+1.06}_{-1.73}$	$+2.16$ -3.93	$+2.15$ -4.74	$4.45^{+1.04}_{-1.81}$	$+1.05$ -4.49	$+1.05$ -5.74	$-3.04^{+1.07}_{-0.29}$	$+1.61$ -0.28	$+1.73$ -0.29	$-12.67^{+4.46}_{-2.59}$	$+8.57$ -3.86	$+10.12$ -4.54
J1335+4542		$4.29^{+1.19}_{-1.25}$	$+1.18$ -2.54	$+1.21$ -3.13	$3.27^{+2.23}_{-1.28}$	$+2.23$ -4.02	$+2.23$ -4.75	$-1.64^{+0.18}_{-1.11}$	$+0.37$ -1.57	$+0.39$ -1.72	$-10.53^{+2.94}_{-5.63}$	$+7.26$ -6.30	$+8.29$ -8.35
J1335+5844		$3.28^{+2.09}_{-0.74}$	$+2.21$ -2.64	$+2.21$ -4.64	$2.53^{+2.67}_{-0.76}$	$+2.92$ -2.63	$+2.95$ -4.02	$-2.31^{+0.88}_{-0.54}$	$+1.01$ -1.00	$+1.06$ -1.06	$-11.32^{+5.92}_{-2.33}$	$+6.91$ -6.46	$+8.51$ -7.92
J1336-0829		$2.58^{+1.09}_{-0.76}$	$+2.86$ -2.66	$+2.88$ -3.82	$2.29^{+1.62}_{-0.76}$	$+3.20$ -1.52	$+3.20$ -2.98	$-3.12^{+1.15}_{-0.22}$	$+1.69$ -0.22	$+1.75$ -0.25	$-6.97^{+1.85}_{-2.61}$	$+2.14$ -6.01	$+4.43$ -6.90
J1337+5501	1σ	$1.04^{+0.91}_{-1.64}$	$+1.50$ -2.46	$+2.28$ -2.53	$3.58^{+1.11}_{-0.66}$	$+1.78$ -1.23	$+1.91$ -1.68	$-2.85^{+0.35}_{-0.15}$	$+0.56$ -0.40	$+1.09$ -0.46	$-9.57^{+1.76}_{-2.33}$	$+2.70$ -4.59	$+3.65$ -5.18
J1337+6532		$2.36^{+0.93}_{-1.06}$	$+1.27$ -3.57	$+2.39$ -3.85	$3.00^{+1.15}_{-0.90}$	$+2.48$ -1.16	$+2.49$ -2.54	$-3.07^{+0.99}_{-0.25}$	$+1.60$ -0.25	$+1.74$ -0.25	$-9.18^{+1.90}_{-2.47}$	$+3.15$ -4.56	$+4.39$ -5.75
J1337-1257		$2.98^{+0.80}_{-1.24}$	$+1.73$ -3.49	$+2.35$ -4.45	$3.41^{+1.62}_{-0.62}$	$+2.09$ -2.84	$+2.09$ -4.71	$-3.05^{+0.94}_{-0.27}$	$+1.65$ -0.26	$+1.73$ -0.27	$-7.57^{+1.63}_{-3.20}$	$+4.60$ -4.83	$+7.34$ -4.83
J1341+2816		$4.98^{+0.52}_{-1.37}$	$+0.52$ -2.55	$+0.52$ -3.55	$4.54^{+0.95}_{-2.91}$	$+0.92$ -5.61	$+0.94$ -5.95	$-1.44^{+0.30}_{-0.97}$	$+0.31$ -1.77	$+0.31$ -1.92	$-13.85^{+6.12}_{-2.60}$	$+9.51$ -4.24	$+11.39$ -4.98
J1342+2709		$3.60^{+1.27}_{-1.07}$	$+1.88$ -3.87	$+1.88$ -5.07	$4.61^{+0.88}_{-1.96}$	$+0.88$ -5.02	$+0.88$ -5.97	$-3.09^{+1.17}_{-0.26}$	$+1.85$ -0.28	$+1.97$ -0.28	$-13.50^{+4.56}_{-2.88}$	$+9.15$ -3.24	$+10.73$ -4.22
J1343+6602		$2.56^{+0.94}_{-1.58}$	$+1.20$ -4.04	$+2.51$ -4.05	$2.99^{+1.63}_{-0.56}$	$+2.49$ -1.65	$+2.49$ -2.56	$-2.99^{+0.84}_{-0.33}$	$+1.56$ -0.31	$+1.67$ -0.33	$-8.72^{+1.03}_{-3.83}$	$+3.84$ -5.26	$+3.84$ -7.00
J1344+6606		$2.41^{+0.74}_{-0.92}$	$+1.20$ -3.40	$+2.55$ -3.83	$2.90^{+1.60}_{-0.84}$	$+2.54$ -2.60	$+2.54$ -3.55	$-2.99^{+1.20}_{-0.18}$	$+1.71$ -0.27	$+1.77$ -0.34	$-8.21^{+1.73}_{-3.35}$	$+4.42$ -5.16	$+5.50$ -5.64

Table C.2: Results of fitting the broken power-law model over the 1290 selected observations from OVRO dataset. Break significance refers to the source having a possible break frequency being (1σ) at 68.3%, (2σ) at 95.5% and (3σ) at 99.7%. The absence of break significance means that the source is not well-fitted at any level.

Name	Break significance	β_l	$\beta_l^{95.5\%}$	$\beta_l^{99.7\%}$	β_h	$\beta_h^{95.5\%}$	$\beta_h^{99.7\%}$	$\log f_{br}$	$\log f_{br}^{95.5\%}$	$\log f_{br}^{99.7\%}$	$\log A$	$\log A^{95.5\%}$	$\log A^{99.7\%}$
J1344-1723		$2.13^{+0.85}_{-0.66}$	$+2.44$ -2.02	$+2.44$ -3.46	$2.45^{+1.36}_{-0.82}$	$+3.03$ -1.35	$+3.04$ -2.58	$-1.86^{+0.48}_{-0.79}$	$+0.50$ -1.40	$+0.54$ -1.46	$-6.93^{+0.69}_{-3.52}$	$+2.12$ -5.81	$+3.99$ -5.94
J1345+0706		$2.29^{+0.62}_{-2.67}$	$+0.75$ -3.73	$+1.45$ -3.78	$3.52^{+1.26}_{-1.17}$	$+1.96$ -2.28	$+1.96$ -3.22	$-2.89^{+0.27}_{-0.37}$	$+1.39$ -0.41	$+1.54$ -0.41	$-9.89^{+3.13}_{-2.70}$	$+4.57$ -5.19	$+5.45$ -5.19
J1347+1835		$3.29^{+1.04}_{-1.02}$	$+2.10$ -3.44	$+2.09$ -4.39	$4.14^{+1.24}_{-1.81}$	$+1.32$ -4.69	$+1.32$ -5.58	$-3.08^{+1.27}_{-0.26}$	$+1.79$ -0.26	$+1.84$ -0.29	$-12.46^{+4.80}_{-2.15}$	$+8.37$ -4.18	$+9.88$ -4.91
J1349+5341	2σ	$1.43^{+0.33}_{-0.39}$	$+0.46$ -0.70	$+0.70$ -0.87	$4.97^{+0.53}_{-1.30}$	$+0.53$ -2.72	$+0.53$ -3.33	$-1.91^{+0.17}_{-0.13}$	$+0.39$ -0.48	$+0.60$ -0.80	$-9.89^{+1.96}_{-1.47}$	$+4.29$ -1.74	$+5.51$ -1.73
J1349-1110		$2.38^{+1.13}_{-1.77}$	$+1.13$ -3.70	$+2.11$ -3.88	$4.28^{+1.09}_{-0.92}$	$+1.21$ -2.87	$+1.20$ -4.79	$-2.92^{+0.36}_{-0.41}$	$+1.46$ -0.35	$+1.49$ -0.40	$-13.05^{+3.16}_{-1.86}$	$+7.04$ -2.81	$+9.03$ -2.81
J1349-1132	2σ	$1.60^{+0.61}_{-1.42}$	$+1.03$ -2.75	$+1.29$ -3.08	$3.35^{+1.30}_{-0.57}$	$+2.11$ -0.72	$+2.15$ -1.00	$-2.42^{+0.18}_{-0.53}$	$+0.44$ -0.79	$+0.64$ -0.90	$-8.11^{+1.38}_{-2.69}$	$+1.38$ -4.74	$+1.96$ -5.06
J1350+3034		$2.16^{+0.68}_{-1.73}$	$+0.76$ -3.35	$+1.10$ -3.62	$2.86^{+1.03}_{-0.77}$	$+2.49$ -0.98	$+2.64$ -1.29	$-2.85^{+0.65}_{-0.40}$	$+1.51$ -0.47	$+1.76$ -0.47	$-8.83^{+2.35}_{-1.18}$	$+3.16$ -3.39	$+4.10$ -5.31
J1350-1634		$2.17^{+2.58}_{-0.85}$	$+3.21$ -2.85	$+3.21$ -3.64	$4.08^{+1.08}_{-2.02}$	$+1.16$ -4.54	$+1.42$ -5.12	$-2.95^{+1.00}_{-0.37}$	$+1.58$ -0.37	$+1.64$ -0.37	$-7.77^{+1.14}_{-6.62}$	$+4.66$ -8.36	$+5.17$ -10.02
J1351+0830		$3.22^{+0.81}_{-1.08}$	$+2.09$ -1.81	$+2.06$ -3.75	$3.43^{+1.84}_{-1.16}$	$+2.06$ -3.74	$+2.07$ -4.76	$-1.63^{+0.11}_{-1.58}$	$+0.28$ -1.73	$+0.38$ -1.73	$-10.66^{+3.11}_{-3.89}$	$+6.85$ -4.76	$+7.91$ -5.54
J1353+1435		$2.08^{+2.94}_{-0.96}$	$+3.38$ -3.09	$+3.42$ -3.56	$3.94^{+1.08}_{-3.21}$	$+1.54$ -4.97	$+1.54$ -5.44	$-2.92^{+1.17}_{-0.17}$	$+1.61$ -0.28	$+1.63$ -0.39	$-13.51^{+7.11}_{-2.07}$	$+8.76$ -6.42	$+11.23$ -6.43
J1353+7532		$1.87^{+0.96}_{-0.73}$	$+1.02$ -3.09	$+2.61$ -3.34	$2.63^{+1.66}_{-0.59}$	$+2.84$ -0.82	$+2.83$ -1.48	$-2.12^{+0.19}_{-1.04}$	$+0.68$ -1.21	$+0.81$ -1.20	$-7.99^{+1.40}_{-2.83}$	$+2.16$ -5.64	$+2.67$ -6.01
J1357+7643		$2.85^{+1.18}_{-1.27}$	$+1.42$ -4.02	$+2.37$ -4.29	$3.21^{+1.54}_{-0.69}$	$+2.29$ -2.12	$+2.27$ -3.90	$-3.06^{+0.91}_{-0.31}$	$+1.66$ -0.30	$+1.81$ -0.30	$-9.11^{+1.55}_{-3.36}$	$+4.22$ -5.16	$+6.46$ -5.74
J1357-1527		$3.54^{+1.08}_{-0.95}$	$+1.92$ -3.43	$+1.92$ -4.92	$4.48^{+0.92}_{-1.64}$	$+1.02$ -4.52	$+1.02$ -5.87	$-3.10^{+1.18}_{-0.22}$	$+1.73$ -0.20	$+1.79$ -0.22	$-12.38^{+4.58}_{-1.38}$	$+8.55$ -2.54	$+10.35$ -3.05
J1359+4011		$1.57^{+0.66}_{-0.85}$	$+1.56$ -2.26	$+3.12$ -2.76	$2.13^{+2.53}_{-0.18}$	$+3.28$ -0.58	$+3.35$ -1.02	$-2.14^{+0.56}_{-0.42}$	$+0.67$ -1.19	$+0.90$ -1.19	$-6.64^{+0.98}_{-4.02}$	$+1.78$ -5.89	$+1.99$ -7.06
J1359+5544		$2.03^{+0.91}_{-1.41}$	$+1.16$ -2.96	$+1.38$ -3.47	$3.54^{+0.81}_{-0.73}$	$+1.91$ -0.74	$+1.95$ -1.08	$-2.70^{+0.33}_{-0.47}$	$+0.94$ -0.60	$+1.23$ -0.59	$-9.17^{+1.60}_{-1.61}$	$+1.48$ -3.95	$+2.28$ -4.26
J1400-1858		$2.64^{+0.92}_{-1.13}$	$+1.16$ -3.62	$+1.33$ -4.13	$3.19^{+1.80}_{-0.55}$	$+2.27$ -1.90	$+2.31$ -3.12	$-3.05^{+1.08}_{-0.28}$	$+1.61$ -0.28	$+1.72$ -0.28	$-10.01^{+3.71}_{-1.38}$	$+5.08$ -4.11	$+6.63$ -5.14
J1405+0415	3σ	$1.16^{+0.26}_{-0.28}$	$+0.63$ -0.53	$+0.63$ -0.69	$3.98^{+1.51}_{-0.57}$	$+1.50$ -1.86	$+1.51$ -1.94	$-1.68^{+0.12}_{-0.24}$	$+0.44$ -0.39	$+0.44$ -0.63	$-8.67^{+1.43}_{-2.01}$	$+3.45$ -1.93	$+3.46$ -2.29
J1407+2827		$2.02^{+1.80}_{-1.07}$	$+3.35$ -2.51	$+3.34$ -3.43	$2.35^{+2.83}_{-0.47}$	$+3.14$ -2.20	$+3.15$ -3.72	$-3.05^{+1.15}_{-0.28}$	$+1.82$ -0.23	$+1.85$ -0.23	$-7.58^{+1.85}_{-5.37}$	$+3.98$ -8.48	$+5.24$ -9.98
J1410+0731		$3.14^{+0.97}_{-0.77}$	$+2.16$ -3.25	$+2.04$ -4.59	$3.55^{+1.95}_{-0.60}$	$+1.95$ -2.79	$+1.95$ -3.98	$-3.08^{+1.31}_{-0.24}$	$+1.80$ -0.22	$+1.84$ -0.27	$-11.51^{+3.62}_{-2.38}$	$+6.76$ -3.75	$+7.97$ -4.63
J1415+0832		$2.10^{+0.49}_{-1.36}$	$+0.91$ -3.16	$+1.56$ -3.51	$2.75^{+0.90}_{-0.68}$	$+2.51$ -0.68	$+2.51$ -1.62	$-2.51^{+0.44}_{-0.65}$	$+1.07$ -0.86	$+1.26$ -0.86	$-7.57^{+1.32}_{-1.91}$	$+1.86$ -4.86	$+3.05$ -6.02
J1415+1320		$1.33^{+1.97}_{-1.27}$	$+2.21$ -2.70	$+3.72$ -2.80	$3.31^{+0.86}_{-0.41}$	$+1.63$ -0.79	$+2.07$ -1.20	$-2.98^{+0.24}_{-0.37}$	$+1.12$ -0.39	$+1.63$ -0.38	$-8.17^{+0.97}_{-2.01}$	$+1.63$ -3.77	$+2.47$ -4.85
J1415-0955		$4.37^{+1.08}_{-1.94}$	$+1.01$ -5.23	$+1.11$ -5.73	$3.37^{+0.92}_{-3.28}$	$+1.82$ -4.64	$+2.09$ -4.70	$-1.67^{+0.23}_{-1.06}$	$+0.24$ -1.54	$+0.26$ -1.64	$-14.33^{+5.71}_{-3.26}$	$+9.91$ -5.64	$+11.76$ -5.63
J1416-1705		$2.82^{+1.56}_{-1.37}$	$+2.03$ -4.11	$+2.42$ -4.31	$4.43^{+0.87}_{-1.69}$	$+1.04$ -4.21	$+1.07$ -5.46	$-3.02^{+0.86}_{-0.30}$	$+1.59$ -0.31	$+1.71$ -0.30	$-12.95^{+4.64}_{-1.58}$	$+7.86$ -3.51	$+10.24$ -3.64
J1419+2706		$2.82^{+0.73}_{-0.86}$	$+1.48$ -3.44	$+2.29$ -4.19	$3.00^{+1.41}_{-0.91}$	$+2.49$ -2.24	$+2.49$ -4.27	$-3.07^{+1.14}_{-0.26}$	$+1.66$ -0.26	$+1.75$ -0.26	$-8.21^{+1.17}_{-3.69}$	$+3.18$ -5.97	$+5.86$ -5.97

Table C.2: Results of fitting the broken power-law model over the 1290 selected observations from OVRO dataset. Break significance refers to the source having a possible break frequency being (1σ) at 68.3%, (2σ) at 95.5% and (3σ) at 99.7%. The absence of break significance means that the source is not well-fitted at any level.

Name	Break significance	β_l	$\beta_l^{95.5\%}$	$\beta_l^{99.7\%}$	β_h	$\beta_h^{95.5\%}$	$\beta_h^{99.7\%}$	$\log f_{br}$	$\log f_{br}^{95.5\%}$	$\log f_{br}^{99.7\%}$	$\log A$	$\log A^{95.5\%}$	$\log A^{99.7\%}$
J1419+3821		$2.08^{+0.85}_{-1.69}$	$+1.06$ -3.47	$+1.87$ -3.51	$3.33^{+0.69}_{-0.79}$	$+1.98$ -0.81	$+2.13$ -1.11	$-2.91^{+0.50}_{-0.31}$	$+1.45$ -0.42	$+1.64$ -0.43	$-8.57^{+1.63}_{-1.56}$	$+1.99$ -3.98	$+2.53$ -4.71
J1419+5423		$2.65^{+0.67}_{-1.82}$	$+0.79$ -3.93	$+2.03$ -4.13	$3.17^{+0.59}_{-0.42}$	$+2.21$ -0.68	$+2.33$ -1.13	$-3.08^{+0.87}_{-0.29}$	$+1.62$ -0.27	$+1.78$ -0.29	$-6.72^{+0.65}_{-1.29}$	$+1.80$ -2.83	$+2.01$ -4.34
J1420+1703		$1.97^{+0.79}_{-1.53}$	$+1.60$ -3.17	$+3.12$ -3.42	$2.94^{+1.71}_{-0.56}$	$+2.56$ -0.87	$+2.55$ -1.34	$-2.51^{+0.22}_{-0.72}$	$+0.88$ -0.86	$+1.11$ -0.86	$-8.71^{+1.56}_{-3.42}$	$+2.38$ -5.45	$+2.91$ -6.09
J1421+4645		$4.57^{+0.92}_{-0.92}$	$+0.93$ -3.18	$+0.93$ -5.85	$4.61^{+0.89}_{-2.69}$	$+0.89$ -5.33	$+0.89$ -5.99	$-1.56^{+0.32}_{-1.07}$	$+0.30$ -1.73	$+0.31$ -1.81	$-14.30^{+5.56}_{-3.14}$	$+9.54$ -4.33	$+11.27$ -4.33
J1421-1931		$1.78^{+1.07}_{-1.17}$	$+1.32$ -2.94	$+1.58$ -3.28	$3.37^{+1.21}_{-0.79}$	$+2.13$ -0.77	$+2.13$ -1.31	$-2.48^{+0.17}_{-0.56}$	$+0.43$ -0.84	$+0.92$ -0.84	$-9.06^{+2.49}_{-2.08}$	$+2.54$ -4.33	$+3.38$ -4.59
J1422+3223	1σ	$1.46^{+0.68}_{-1.56}$	$+0.81$ -2.93	$+1.54$ -2.93	$2.96^{+1.55}_{-0.34}$	$+2.47$ -0.71	$+2.51$ -1.30	$-2.70^{+0.32}_{-0.38}$	$+0.87$ -0.55	$+1.09$ -0.62	$-8.59^{+1.91}_{-2.36}$	$+2.28$ -5.14	$+3.11$ -5.90
J1423+4802		$3.04^{+1.02}_{-1.15}$	$+1.95$ -3.73	$+2.04$ -4.45	$4.27^{+1.17}_{-2.11}$	$+1.22$ -4.70	$+1.19$ -5.75	$-3.13^{+1.21}_{-0.23}$	$+1.80$ -0.23	$+1.89$ -4.70	$-10.65^{+4.95}_{-2.91}$	$+7.29$ -5.50	$+8.64$ -6.14
J1423+5055		$2.33^{+1.00}_{-1.31}$	$+2.15$ -2.67	$+2.41$ -3.80	$3.61^{+1.64}_{-1.26}$	$+1.85$ -3.71	$+1.87$ -4.92	$-1.54^{+0.30}_{-1.20}$	$+0.22$ -1.81	$+0.30$ -1.82	$-11.40^{+4.46}_{-1.83}$	$+6.37$ -5.22	$+8.43$ -5.22
J1424+2256		$4.54^{+0.94}_{-2.29}$	$+0.94$ -5.21	$+0.96$ -5.91	$4.40^{+0.89}_{-2.54}$	$+1.03$ -4.95	$+1.06$ -5.89	$-3.03^{+0.99}_{-0.32}$	$+1.66$ -0.28	$+1.70$ -0.32	$-13.02^{+4.58}_{-3.97}$	$+8.05$ -6.37	$+9.75$ -6.93
J1425+1424		$2.99^{+0.96}_{-1.06}$	$+1.77$ -3.18	$+2.44$ -4.48	$3.42^{+1.39}_{-1.47}$	$+2.08$ -3.48	$+2.08$ -4.78	$-1.77^{+0.10}_{-1.57}$	$+0.32$ -1.60	$+0.41$ -1.60	$-9.93^{+3.15}_{-2.85}$	$+5.87$ -4.84	$+7.83$ -5.78
J1426+3625		$3.45^{+1.05}_{-1.02}$	$+1.38$ -4.27	$+2.02$ -4.80	$4.44^{+0.90}_{-1.56}$	$+1.06$ -4.35	$+1.05$ -5.93	$-3.10^{+1.17}_{-0.25}$	$+1.75$ -0.25	$+1.86$ -0.25	$-11.93^{+3.48}_{-2.38}$	$+7.90$ -3.46	$+9.78$ -4.48
J1428+2724		$2.99^{+1.02}_{-0.93}$	$+1.84$ -3.57	$+2.29$ -4.07	$4.20^{+1.01}_{-1.86}$	$+1.29$ -3.90	$+1.29$ -5.66	$-3.03^{+1.14}_{-0.27}$	$+1.72$ -0.21	$+1.72$ -0.27	$-11.17^{+3.39}_{-2.89}$	$+6.72$ -4.37	$+8.03$ -5.34
J1430+1043		$3.56^{+1.04}_{-1.06}$	$+1.92$ -3.34	$+1.92$ -4.81	$4.13^{+1.36}_{-1.74}$	$+1.35$ -4.55	$+1.35$ -5.63	$-3.08^{+1.23}_{-0.26}$	$+1.76$ -0.26	$+1.82$ -0.29	$-10.75^{+2.87}_{-4.63}$	$+6.35$ -6.03	$+7.89$ -6.43
J1430+3649	2σ	$0.95^{+0.82}_{-0.86}$	$+1.20$ -2.44	$+1.65$ -2.44	$3.27^{+1.30}_{-0.62}$	$+2.23$ -0.77	$+2.22$ -1.28	$-2.33^{+0.10}_{-0.35}$	$+0.24$ -0.71	$+0.37$ -0.83	$-7.99^{+0.69}_{-3.18}$	$+1.37$ -4.97	$+2.11$ -5.31
J1431+3952		$4.69^{+0.53}_{-1.42}$	$+0.80$ -2.67	$+0.79$ -3.77	$2.74^{+2.39}_{-1.18}$	$+2.76$ -3.34	$+2.76$ -4.22	$-1.76^{+0.55}_{-0.87}$	$+0.47$ -1.57	$+0.54$ -1.58	$-12.21^{+4.70}_{-3.81}$	$+8.38$ -4.77	$+9.60$ -5.70
J1434+1952	1σ	$0.92^{+1.34}_{-0.85}$	$+1.55$ -2.29	$+2.39$ -2.42	$3.40^{+1.03}_{-0.97}$	$+2.01$ -1.00	$+2.08$ -1.38	$-2.62^{+0.35}_{-0.27}$	$+0.43$ -0.70	$+0.73$ -0.73	$-9.34^{+1.25}_{-3.19}$	$+2.33$ -4.68	$+3.31$ -4.89
J1434+4203		$2.14^{+0.82}_{-0.78}$	$+1.14$ -3.15	$+1.68$ -3.63	$2.90^{+1.44}_{-0.81}$	$+2.60$ -1.14	$+2.60$ -2.33	$-2.94^{+1.14}_{-0.21}$	$+1.56$ -0.38	$+1.71$ -0.40	$-8.57^{+1.77}_{-2.32}$	$+3.02$ -4.33	$+4.59$ -5.23
J1435+3012		$4.90^{+0.60}_{-1.36}$	$+0.59$ -2.90	$+0.60$ -4.38	$4.41^{+1.01}_{-2.77}$	$+1.08$ -5.13	$+1.08$ -5.80	$-1.71^{+0.39}_{-0.83}$	$+0.40$ -1.52	$+0.40$ -1.60	$-13.77^{+7.25}_{-1.52}$	$+8.91$ -4.95	$+10.65$ -5.24
J1436+2321	1σ	$1.30^{+1.13}_{-1.52}$	$+1.74$ -2.56	$+2.07$ -2.78	$3.33^{+1.39}_{-0.59}$	$+2.01$ -1.06	$+2.12$ -1.19	$-2.66^{+0.19}_{-0.40}$	$+0.58$ -0.65	$+0.93$ -0.66	$-8.62^{+1.26}_{-3.33}$	$+2.33$ -4.80	$+2.48$ -5.27
J1436+6336		$4.65^{+0.85}_{-1.04}$	$+0.85$ -2.30	$+0.85$ -3.15	$4.06^{+1.42}_{-2.44}$	$+1.43$ -5.02	$+1.41$ -5.56	$-1.67^{+0.39}_{-0.87}$	$+0.39$ -1.61	$+0.42$ -1.67	$-12.78^{+6.12}_{-2.71}$	$+10.08$ -3.32	$+10.66$ -5.19
J1437+3119		$5.04^{+0.43}_{-0.82}$	$+0.44$ -2.11	$+0.44$ -3.80	$3.55^{+1.79}_{-2.29}$	$+1.91$ -4.37	$+1.94$ -4.96	$-2.09^{+0.72}_{-0.43}$	$+0.77$ -1.04	$+0.78$ -1.23	$-12.27^{+5.78}_{-3.31}$	$+7.67$ -6.35	$+9.23$ -7.10
J1438+3710		$2.57^{+0.90}_{-0.93}$	$+2.92$ -2.87	$+2.84$ -3.98	$2.64^{+1.90}_{-0.74}$	$+2.86$ -2.17	$+2.85$ -3.50	$-3.10^{+1.21}_{-0.23}$	$+1.81$ -0.23	$+1.90$ -0.23	$-7.82^{+1.69}_{-3.54}$	$+3.13$ -6.60	$+4.97$ -7.12
J1439+2114		$2.40^{+1.49}_{-1.67}$	$+2.29$ -3.61	$+3.03$ -3.90	$4.75^{+0.28}_{-2.67}$	$+0.73$ -3.95	$+0.74$ -5.02	$-3.03^{+0.87}_{-0.27}$	$+1.61$ -0.26	$+1.70$ -0.31	$-8.73^{+0.99}_{-6.03}$	$+2.97$ -8.78	$+4.82$ -9.38
J1439+4958	1σ	$1.48^{+0.72}_{-1.33}$	$+0.91$ -2.89	$+1.36$ -2.93	$2.95^{+1.20}_{-0.43}$	$+2.35$ -0.64	$+2.52$ -0.88	$-2.25^{+0.10}_{-0.68}$	$+0.34$ -0.94	$+0.52$ -1.09	$-7.52^{+1.14}_{-2.26}$	$+1.23$ -4.78	$+1.83$ -5.24

Table C.2: Results of fitting the broken power-law model over the 1290 selected observations from OVRO dataset. Break significance refers to the source having a possible break frequency being (1σ) at 68.3%, (2σ) at 95.5% and (3σ) at 99.7%. The absence of break significance means that the source is not well-fitted at any level.

Name	Break significance	β_l	$\beta_l^{95.5\%}$	$\beta_l^{99.7\%}$	β_h	$\beta_h^{95.5\%}$	$\beta_h^{99.7\%}$	$\log f_{br}$	$\log f_{br}^{95.5\%}$	$\log f_{br}^{99.7\%}$	$\log A$	$\log A^{95.5\%}$	$\log A^{99.7\%}$
J1439-1531		$2.88^{+0.75}_{-1.55}$	$+2.10$ -3.49	$+2.59$ -4.38	$4.19^{+1.22}_{-1.75}$	$+1.28$ -4.08	$+1.28$ -5.52	$-3.10^{+1.10}_{-0.22}$	$+1.68$ -0.22	$+1.80$ -0.22	$-8.58^{+1.77}_{-5.29}$	$+3.81$ -7.48	$+6.04$ -7.90
J1443+2501		$2.37^{+0.66}_{-0.80}$	$+0.90$ -3.70	$+3.09$ -3.82	$2.80^{+1.10}_{-0.63}$	$+2.40$ -0.84	$+2.68$ -0.99	$-2.12^{+0.09}_{-1.17}$	$+0.66$ -1.19	$+0.83$ -1.19	$-6.83^{+1.39}_{-2.03}$	$+1.61$ -4.81	$+1.88$ -5.62
J1445-1614		$3.34^{+1.55}_{-0.80}$	$+2.16$ -2.49	$+2.16$ -4.67	$4.58^{+0.92}_{-2.12}$	$+0.88$ -5.40	$+0.92$ -6.01	$-1.78^{+0.36}_{-0.89}$	$+0.30$ -1.52	$+0.36$ -1.54	$-12.97^{+3.84}_{-4.29}$	$+9.07$ -4.22	$+10.02$ -5.15
J1445-1629		$2.23^{+0.72}_{-0.79}$	$+1.00$ -2.59	$+1.90$ -3.64	$2.91^{+1.50}_{-0.94}$	$+2.45$ -1.61	$+2.58$ -2.18	$-2.44^{+0.34}_{-0.85}$	$+1.05$ -0.84	$+1.13$ -0.87	$-8.01^{+1.39}_{-3.55}$	$+2.63$ -5.25	$+3.79$ -5.89
J1446+1721		$2.97^{+0.65}_{-1.96}$	$+0.81$ -4.36	$+1.49$ -4.45	$4.22^{+0.86}_{-1.03}$	$+1.28$ -3.08	$+1.28$ -4.89	$-3.03^{+0.75}_{-0.33}$	$+1.66$ -0.33	$+1.77$ -0.33	$-10.86^{+2.07}_{-2.27}$	$+5.66$ -3.49	$+7.64$ -4.26
J1448+7601		$1.92^{+0.65}_{-1.87}$	$+0.93$ -3.40	$+1.51$ -3.40	$2.95^{+1.52}_{-0.49}$	$+2.54$ -0.84	$+2.52$ -2.30	$-2.92^{+0.37}_{-0.38}$	$+1.03$ -0.38	$+1.55$ -0.41	$-8.72^{+1.66}_{-3.24}$	$+2.49$ -5.67	$+5.04$ -6.14
J1450+0910		$2.49^{+0.74}_{-1.56}$	$+0.93$ -3.64	$+1.23$ -3.93	$3.30^{+1.17}_{-0.58}$	$+2.16$ -0.87	$+2.15$ -1.41	$-2.87^{+0.49}_{-0.45}$	$+1.48$ -0.45	$+1.63$ -0.45	$-9.87^{+2.04}_{-1.89}$	$+2.73$ -3.95	$+3.42$ -4.21
J1453+2648	1σ	$1.77^{+0.65}_{-1.23}$	$+0.92$ -3.08	$+1.75$ -3.27	$3.28^{+1.25}_{-0.72}$	$+2.21$ -0.69	$+2.21$ -1.08	$-2.44^{+0.29}_{-0.40}$	$+0.45$ -0.87	$+0.81$ -0.87	$-8.83^{+1.57}_{-2.72}$	$+1.78$ -4.61	$+2.65$ -4.82
J1453+3505		$1.80^{+0.86}_{-0.97}$	$+1.64$ -2.77	$+2.14$ -3.30	$2.74^{+1.46}_{-1.33}$	$+2.76$ -1.81	$+2.76$ -3.57	$-2.28^{+0.24}_{-0.91}$	$+0.91$ -0.97	$+0.96$ -1.05	$-8.31^{+2.01}_{-3.90}$	$+3.41$ -6.53	$+5.79$ -7.05
J1456+5048		$4.46^{+1.00}_{-1.68}$	$+1.03$ -4.16	$+1.03$ -5.85	$2.22^{+3.29}_{-0.60}$	$+3.29$ -3.06	$+3.29$ -3.71	$-1.67^{+0.40}_{-1.10}$	$+0.43$ -1.61	$+0.43$ -1.70	$-12.12^{+5.43}_{-2.97}$	$+7.89$ -6.00	$+9.77$ -6.59
J1458+3720		$2.68^{+1.52}_{-0.79}$	$+2.71$ -1.26	$+2.80$ -2.91	$2.71^{+2.57}_{-0.59}$	$+2.79$ -2.91	$+2.79$ -4.03	$-1.70^{+0.09}_{-1.49}$	$+0.39$ -1.50	$+0.39$ -1.62	$-8.68^{+2.64}_{-4.62}$	$+4.01$ -7.96	$+5.73$ -9.67
J1459+4442		$2.38^{+0.67}_{-2.01}$	$+0.98$ -3.81	$+1.54$ -3.87	$4.73^{+0.66}_{-1.72}$	$+0.77$ -3.62	$+0.77$ -5.44	$-2.95^{+0.69}_{-0.37}$	$+1.62$ -0.29	$+1.62$ -0.38	$-12.52^{+4.49}_{-1.85}$	$+7.14$ -3.51	$+9.39$ -3.86
J1500+4751		$3.74^{+1.44}_{-0.77}$	$+1.70$ -2.73	$+1.70$ -4.28	$4.54^{+0.95}_{-2.26}$	$+0.96$ -4.83	$+0.96$ -5.82	$-1.65^{+0.31}_{-1.12}$	$+0.32$ -1.62	$+0.33$ -1.68	$-9.64^{+2.84}_{-5.20}$	$+5.25$ -6.89	$+6.91$ -7.80
J1502-1508		$2.56^{+1.47}_{-0.76}$	$+1.45$ -3.58	$+2.89$ -4.03	$3.95^{+1.54}_{-0.96}$	$+1.54$ -2.88	$+1.54$ -4.61	$-3.02^{+0.94}_{-0.23}$	$+1.50$ -0.30	$+1.60$ -0.30	$-10.88^{+3.49}_{-2.26}$	$+5.91$ -4.76	$+8.67$ -4.76
J1504+0813		$4.97^{+0.53}_{-1.14}$	$+0.53$ -2.47	$+0.53$ -3.05	$4.54^{+0.92}_{-3.15}$	$+0.93$ -5.45	$+0.94$ -6.01	$-1.59^{+0.35}_{-0.93}$	$+0.31$ -1.74	$+0.35$ -1.77	$-14.98^{+5.99}_{-3.29}$	$+10.23$ -4.06	$+12.25$ -4.50
J1504+1029		$2.64^{+0.45}_{-0.65}$	$+2.77$ -1.40	$+2.77$ -3.66	$2.72^{+1.38}_{-0.80}$	$+2.70$ -1.31	$+2.78$ -1.54	$-1.54^{+0.41}_{-1.18}$	$+0.39$ -1.77	$+0.41$ -1.83	$-6.32^{+1.81}_{-1.87}$	$+2.20$ -4.15	$+2.39$ -5.57
J1505+0326	3σ	$-1.03^{+0.90}_{-0.43}$	$+2.09$ -0.47	$+2.46$ -0.47	$2.88^{+0.40}_{-0.57}$	$+1.08$ -0.86	$+1.76$ -0.97	$-2.65^{+0.20}_{-0.12}$	$+0.46$ -0.33	$+0.61$ -0.38	$-6.89^{+1.09}_{-0.91}$	$+1.52$ -2.26	$+1.88$ -3.59
J1506+3730	1σ	$1.64^{+1.10}_{-1.44}$	$+1.14$ -3.12	$+1.78$ -3.12	$3.22^{+0.87}_{-0.43}$	$+1.83$ -0.54	$+2.23$ -0.76	$-2.80^{+0.39}_{-0.28}$	$+0.68$ -0.52	$+1.00$ -0.52	$-8.08^{+0.57}_{-2.29}$	$+1.10$ -4.07	$+1.51$ -4.89
J1506+4239		$5.04^{+0.42}_{-1.37}$	$+0.43$ -2.76	$+0.44$ -3.45	$4.51^{+0.92}_{-2.84}$	$+0.99$ -5.42	$+0.97$ -6.00	$-1.63^{+0.27}_{-0.95}$	$+0.32$ -1.51	$+0.32$ -1.67	$-11.21^{+5.57}_{-2.87}$	$+7.67$ -5.16	$+9.60$ -5.65
J1506+4933		$2.97^{+0.70}_{-0.90}$	$+1.61$ -3.92	$+2.33$ -4.41	$2.90^{+2.32}_{-0.66}$	$+2.48$ -3.41	$+2.60$ -4.03	$-1.56^{+0.24}_{-1.25}$	$+0.24$ -1.69	$+0.24$ -1.76	$-7.77^{+1.84}_{-4.79}$	$+4.83$ -6.54	$+5.63$ -7.23
J1506+8319		$3.79^{+1.05}_{-0.94}$	$+1.71$ -2.29	$+1.70$ -5.29	$4.67^{+0.80}_{-2.04}$	$+0.83$ -5.09	$+0.83$ -6.07	$-1.82^{+0.46}_{-0.97}$	$+0.46$ -1.47	$+0.46$ -1.54	$-13.25^{+3.50}_{-3.57}$	$+8.71$ -3.77	$+10.74$ -4.14
J1507-1652		$2.36^{+0.83}_{-0.56}$	$+1.02$ -3.85	$+2.84$ -3.84	$2.72^{+1.21}_{-0.72}$	$+2.78$ -1.16	$+2.78$ -2.59	$-1.98^{+0.03}_{-1.38}$	$+0.63$ -1.33	$+0.63$ -1.38	$-7.94^{+1.93}_{-1.89}$	$+2.97$ -4.32	$+4.84$ -5.76
J1510-1121		$3.87^{+1.63}_{-0.69}$	$+1.63$ -3.33	$+1.63$ -5.18	$3.60^{+1.78}_{-1.89}$	$+1.88$ -4.25	$+1.89$ -5.06	$-2.10^{+0.48}_{-0.83}$	$+0.69$ -1.19	$+0.73$ -1.26	$-14.65^{+8.19}_{-1.07}$	$+10.25$ -4.15	$+11.41$ -4.97
J1511+0518		$4.90^{+0.59}_{-1.97}$	$+0.56$ -3.86	$+0.59$ -4.49	$3.43^{+2.05}_{-1.96}$	$+2.03$ -4.42	$+2.05$ -4.90	$-1.61^{+0.36}_{-0.89}$	$+0.35$ -1.67	$+0.36$ -1.76	$-11.32^{+6.02}_{-2.83}$	$+6.53$ -7.93	$+8.33$ -8.27

Table C.2: Results of fitting the broken power-law model over the 1290 selected observations from OVRO dataset. Break significance refers to the source having a possible break frequency being (1σ) at 68.3%, (2σ) at 95.5% and (3σ) at 99.7%. The absence of break significance means that the source is not well-fitted at any level.

Name	Break significance	β_l	$\beta_l^{95.5\%}$	$\beta_l^{99.7\%}$	β_h	$\beta_h^{95.5\%}$	$\beta_h^{99.7\%}$	$\log f_{br}$	$\log f_{br}^{95.5\%}$	$\log f_{br}^{99.7\%}$	$\log A$	$\log A^{95.5\%}$	$\log A^{99.7\%}$
J1513-1012		$2.38^{+0.76}_{-1.03}$	$+1.02$ -3.50	$+1.57$ -3.72	$2.89^{+1.71}_{-0.71}$	$+2.61$ -1.31	$+2.60$ -2.86	$-2.46^{+0.27}_{-0.91}$	$+1.13$ -0.91	$+1.22$ -0.91	$-7.73^{+1.63}_{-3.32}$	$+2.30$ -6.07	$+4.73$ -6.07
J1516+0015		$2.27^{+0.78}_{-1.58}$	$+1.29$ -3.47	$+3.20$ -3.77	$2.78^{+1.70}_{-0.83}$	$+2.70$ -1.84	$+2.70$ -3.64	$-2.98^{+0.97}_{-0.39}$	$+1.63$ -0.37	$+1.73$ -0.38	$-7.59^{+1.06}_{-4.17}$	$+4.07$ -5.78	$+5.89$ -7.56
J1516+1932		$2.37^{+0.75}_{-1.57}$	$+0.73$ -3.77	$+2.33$ -3.85	$3.09^{+1.09}_{-0.77}$	$+2.17$ -0.77	$+2.36$ -1.28	$-3.01^{+0.60}_{-0.34}$	$+1.65$ -0.36	$+1.88$ -0.36	$-8.08^{+0.97}_{-2.89}$	$+1.63$ -5.00	$+2.59$ -5.95
J1521+4336		$2.75^{+0.74}_{-0.93}$	$+1.98$ -3.26	$+2.67$ -4.23	$2.95^{+2.04}_{-0.68}$	$+2.55$ -2.55	$+2.55$ -4.00	$-3.03^{+1.22}_{-0.29}$	$+1.74$ -0.30	$+1.83$ -0.29	$-8.58^{+2.38}_{-3.32}$	$+4.64$ -5.48	$+5.62$ -6.64
J1522+3144		$1.77^{+0.57}_{-0.77}$	$+0.76$ -2.74	$+0.86$ -3.26	$2.58^{+1.51}_{-0.64}$	$+2.73$ -0.59	$+2.85$ -0.94	$-1.97^{+0.20}_{-0.86}$	$+0.55$ -1.22	$+0.71$ -1.40	$-7.09^{+1.28}_{-2.54}$	$+1.24$ -5.47	$+1.82$ -5.62
J1526+6650		$4.27^{+1.02}_{-2.73}$	$+1.22$ -5.37	$+1.20$ -5.77	$-0.16^{+3.45}_{-1.33}$	$+5.63$ -1.08	$+5.63$ -1.33	$-1.69^{+0.44}_{-1.01}$	$+0.38$ -1.64	$+0.45$ -1.67	$-16.85^{+6.94}_{-1.93}$	$+11.37$ -3.08	$+13.55$ -3.10
J1526-0425		$1.82^{+0.97}_{-1.35}$	$+1.49$ -3.19	$+3.30$ -3.29	$2.94^{+1.53}_{-1.16}$	$+2.52$ -1.61	$+2.56$ -2.39	$-2.91^{+0.83}_{-0.46}$	$+1.52$ -0.45	$+1.66$ -0.65	$-8.07^{+1.80}_{-4.01}$	$+2.77$ -6.99	$+3.75$ -8.07
J1532-1319	1σ	$-0.41^{+1.84}_{-0.71}$	$+2.78$ -1.08	$+3.92$ -1.06	$3.21^{+1.19}_{-0.83}$	$+2.24$ -1.13	$+2.28$ -1.44	$-2.78^{+0.29}_{-0.29}$	$+0.81$ -0.51	$+1.03$ -0.52	$-9.43^{+3.62}_{-1.03}$	$+3.74$ -3.96	$+4.42$ -4.61
J1533-0421		$2.25^{+1.11}_{-0.85}$	$+2.00$ -3.38	$+2.98$ -3.75	$3.56^{+1.18}_{-1.91}$	$+1.92$ -3.59	$+1.92$ -4.92	$-1.58^{+0.33}_{-1.10}$	$+0.28$ -1.75	$+0.34$ -1.78	$-9.82^{+3.51}_{-2.96}$	$+7.09$ -5.26	$+7.11$ -7.42
J1534+0131	1σ	$1.80^{+0.78}_{-1.73}$	$+0.84$ -3.15	$+1.65$ -3.26	$3.16^{+1.59}_{-0.35}$	$+2.33$ -0.67	$+2.33$ -1.09	$-2.85^{+0.29}_{-0.27}$	$+0.63$ -0.51	$+0.93$ -0.51	$-8.77^{+0.62}_{-4.24}$	$+1.95$ -5.40	$+2.60$ -5.85
J1535+4957	1σ	$2.08^{+0.41}_{-2.64}$	$+1.28$ -3.36	$+2.01$ -3.58	$4.83^{+0.40}_{-1.44}$	$+0.65$ -2.72	$+0.65$ -3.70	$-2.91^{+0.22}_{-0.41}$	$+1.10$ -0.41	$+1.54$ -0.41	$-11.87^{+1.64}_{-3.20}$	$+5.17$ -3.79	$+6.68$ -4.71
J1539+2744		$2.06^{+0.82}_{-1.03}$	$+0.82$ -3.38	$+1.70$ -3.47	$2.59^{+1.01}_{-0.61}$	$+2.58$ -1.09	$+2.79$ -1.38	$-2.97^{+0.94}_{-0.34}$	$+1.69$ -0.34	$+1.83$ -0.40	$-6.81^{+1.19}_{-1.83}$	$+1.92$ -4.63	$+1.92$ -5.41
J1539+3104		$2.38^{+3.10}_{-1.15}$	$+3.10$ -3.55	$+3.10$ -3.85	$3.07^{+2.16}_{-2.06}$	$+2.17$ -4.41	$+2.39$ -4.49	$-2.44^{+0.32}_{-0.91}$	$+0.96$ -0.92	$+1.08$ -0.93	$-12.98^{+3.67}_{-5.87}$	$+7.96$ -7.00	$+10.42$ -6.98
J1540+1447		$1.82^{+0.70}_{-1.07}$	$+0.95$ -2.82	$+0.95$ -3.28	$2.75^{+1.17}_{-0.75}$	$+2.74$ -0.93	$+2.74$ -1.81	$-2.46^{+0.35}_{-0.73}$	$+0.94$ -0.88	$+1.23$ -0.88	$-7.44^{+1.75}_{-2.23}$	$+2.81$ -5.03	$+3.24$ -5.78
J1544+3240	1σ	$0.53^{+1.81}_{-1.56}$	$+2.89$ -2.01	$+3.67$ -2.02	$5.13^{+0.34}_{-1.06}$	$+0.37$ -1.93	$+0.37$ -2.63	$-3.01^{+0.14}_{-0.28}$	$+0.48$ -0.36	$+1.30$ -0.36	$-14.60^{+2.58}_{-1.44}$	$+4.71$ -1.73	$+6.20$ -1.73
J1545+5135		$2.72^{+1.82}_{-0.72}$	$+2.74$ -2.63	$+2.74$ -4.12	$2.45^{+2.50}_{-0.82}$	$+3.05$ -2.59	$+3.04$ -3.92	$-3.07^{+1.16}_{-0.30}$	$+1.81$ -0.24	$+1.82$ -0.30	$-8.22^{+1.02}_{-5.98}$	$+3.18$ -9.02	$+4.64$ -9.31
J1548+1727		$3.39^{+1.27}_{-1.12}$	$+2.10$ -3.42	$+2.10$ -4.74	$4.43^{+1.03}_{-1.84}$	$+1.03$ -4.72	$+1.07$ -5.65	$-3.07^{+1.12}_{-0.25}$	$+1.84$ -0.21	$+1.86$ -0.27	$-11.97^{+2.99}_{-3.94}$	$+6.97$ -5.58	$+9.04$ -6.22
J1548+3511		$4.16^{+1.24}_{-3.29}$	$+1.28$ -5.31	$+1.33$ -5.65	$-0.58^{+3.44}_{-0.89}$	$+5.69$ -0.89	$+6.03$ -0.89	$-2.31^{+0.97}_{-0.20}$	$+0.96$ -0.74	$+0.97$ -0.81	$-15.29^{+5.18}_{-4.60}$	$+10.24$ -4.60	$+12.25$ -4.68
J1549+0237		$3.08^{+0.65}_{-0.85}$	$+1.58$ -3.81	$+2.16$ -4.46	$3.21^{+1.44}_{-0.63}$	$+2.29$ -2.80	$+2.29$ -4.31	$-3.08^{+1.40}_{-0.28}$	$+1.93$ -0.25	$+1.96$ -0.28	$-7.49^{+1.07}_{-2.90}$	$+4.22$ -4.18	$+6.11$ -4.60
J1549+5038		$2.19^{+0.91}_{-0.97}$	$+1.27$ -3.25	$+3.12$ -3.58	$2.59^{+1.67}_{-0.68}$	$+2.86$ -1.34	$+2.86$ -3.04	$-2.99^{+0.96}_{-0.38}$	$+1.69$ -0.34	$+1.74$ -0.38	$-7.43^{+1.95}_{-3.00}$	$+2.87$ -5.95	$+4.78$ -7.18
J1550+0527		$2.38^{+1.02}_{-0.69}$	$+1.82$ -3.54	$+3.08$ -3.54	$2.36^{+2.03}_{-0.96}$	$+3.07$ -2.63	$+3.13$ -3.65	$-3.07^{+1.24}_{-0.27}$	$+1.76$ -0.26	$+1.86$ -0.27	$-5.96^{+1.70}_{-4.07}$	$+4.46$ -6.80	$+4.46$ -8.66
J1551+5806		$2.24^{+2.08}_{-0.99}$	$+3.05$ -2.77	$+3.17$ -3.55	$4.06^{+0.53}_{-2.72}$	$+1.44$ -4.06	$+1.43$ -5.48	$-3.03^{+1.11}_{-0.32}$	$+1.69$ -0.32	$+1.79$ -0.32	$-10.60^{+3.83}_{-4.01}$	$+6.34$ -6.59	$+7.99$ -7.95
J1552+0850		$1.67^{+0.96}_{-1.09}$	$+1.01$ -3.00	$+1.53$ -3.16	$2.63^{+1.44}_{-1.07}$	$+2.83$ -1.21	$+2.86$ -1.66	$-2.82^{+0.76}_{-0.36}$	$+1.43$ -0.46	$+1.63$ -0.47	$-8.62^{+2.79}_{-2.29}$	$+3.15$ -5.80	$+3.70$ -6.53
J1555+1111		$1.93^{+0.64}_{-1.23}$	$+0.98$ -3.10	$+1.80$ -3.31	$2.50^{+1.82}_{-0.78}$	$+3.00$ -1.39	$+2.97$ -3.40	$-2.47^{+0.52}_{-0.80}$	$+1.31$ -0.75	$+1.32$ -0.88	$-7.68^{+1.20}_{-3.61}$	$+2.34$ -6.30	$+5.05$ -6.30

Table C.2: Results of fitting the broken power-law model over the 1290 selected observations from OVRO dataset. Break significance refers to the source having a possible break frequency being (1σ) at 68.3%, (2σ) at 95.5% and (3σ) at 99.7%. The absence of break significance means that the source is not well-fitted at any level.

Name	Break significance	β_l	$\beta_l^{95.5\%}$	$\beta_l^{99.7\%}$	β_h	$\beta_h^{95.5\%}$	$\beta_h^{99.7\%}$	$\log f_{br}$	$\log f_{br}^{95.5\%}$	$\log f_{br}^{99.7\%}$	$\log A$	$\log A^{95.5\%}$	$\log A^{99.7\%}$
J1557-0001		$2.85^{+0.81}_{-1.15}$	$+1.38$ -4.28	$+2.58$ -4.28	$3.08^{+1.27}_{-1.15}$	$+2.26$ -2.89	$+2.41$ -3.74	$-3.09^{+1.21}_{-0.27}$	$+1.80$ -0.24	$+1.85$ -0.27	$-8.14^{+1.44}_{-3.36}$	$+4.41$ -4.89	$+5.28$ -6.65
J1558+5625		$1.95^{+1.55}_{-2.33}$	$+3.11$ -3.24	$+3.53$ -3.41	$4.40^{+1.01}_{-2.80}$	$+1.10$ -5.21	$+1.10$ -5.83	$-2.89^{+1.02}_{-0.29}$	$+1.60$ -0.30	$+1.60$ -0.42	$-12.32^{+4.73}_{-3.98}$	$+7.84$ -6.69	$+10.00$ -7.53
J1559+0304		$2.74^{+0.97}_{-0.95}$	$+2.42$ -3.00	$+2.68$ -3.87	$2.91^{+2.04}_{-0.80}$	$+2.59$ -2.88	$+2.58$ -4.36	$-3.12^{+1.23}_{-0.21}$	$+1.79$ -0.24	$+1.88$ -0.24	$-9.28^{+2.34}_{-4.28}$	$+5.35$ -6.26	$+6.81$ -7.64
J1602+2646		$4.48^{+1.01}_{-2.49}$	$+1.02$ -5.21	$+1.01$ -5.94	$4.12^{+1.02}_{-3.35}$	$+1.32$ -5.24	$+1.35$ -5.61	$-1.65^{+0.41}_{-1.04}$	$+0.39$ -1.63	$+0.40$ -1.72	$-14.53^{+8.40}_{-1.57}$	$+9.95$ -5.39	$+11.81$ -5.38
J1602+3326		$3.70^{+1.20}_{-1.15}$	$+1.79$ -3.48	$+1.78$ -5.17	$3.81^{+1.56}_{-1.49}$	$+1.69$ -4.15	$+1.69$ -5.09	$-3.12^{+1.28}_{-0.22}$	$+1.80$ -0.23	$+1.88$ -0.24	$-11.32^{+4.23}_{-3.33}$	$+7.02$ -5.10	$+8.96$ -5.96
J1603+1105		$2.03^{+0.86}_{-0.86}$	$+0.99$ -3.27	$+2.61$ -3.53	$2.38^{+1.35}_{-0.74}$	$+3.03$ -0.76	$+3.09$ -1.90	$-3.01^{+1.01}_{-0.34}$	$+1.70$ -0.33	$+1.79$ -0.34	$-7.14^{+1.46}_{-2.90}$	$+2.28$ -5.83	$+3.31$ -6.46
J1603+1554		$4.80^{+0.70}_{-1.00}$	$+0.68$ -2.56	$+0.70$ -3.13	$4.37^{+1.07}_{-3.14}$	$+1.09$ -5.31	$+1.09$ -5.83	$-1.59^{+0.37}_{-0.86}$	$+0.37$ -1.59	$+0.37$ -1.74	$-14.25^{+6.00}_{-2.75}$	$+10.19$ -3.95	$+11.13$ -5.07
J1603+5730		$2.32^{+1.08}_{-1.16}$	$+2.51$ -2.71	$+2.73$ -3.79	$3.04^{+1.46}_{-1.66}$	$+2.46$ -3.40	$+2.45$ -4.29	$-3.05^{+1.17}_{-0.28}$	$+1.76$ -0.27	$+1.81$ -0.31	$-10.36^{+3.43}_{-3.03}$	$+6.04$ -5.33	$+7.36$ -7.10
J1603-1007		$1.61^{+0.68}_{-1.02}$	$+0.82$ -2.76	$+1.06$ -3.09	$2.86^{+1.09}_{-0.69}$	$+2.37$ -0.90	$+2.64$ -1.13	$-2.52^{+0.36}_{-0.56}$	$+0.86$ -0.79	$+1.17$ -0.80	$-7.64^{+1.46}_{-2.43}$	$+1.91$ -4.89	$+2.15$ -5.85
J1604+5714	2σ	$0.84^{+0.83}_{-1.12}$	$+1.39$ -2.04	$+1.82$ -2.33	$4.36^{+0.48}_{-1.04}$	$+1.14$ -1.22	$+1.14$ -1.75	$-2.61^{+0.19}_{-0.22}$	$+0.38$ -0.45	$+0.60$ -0.48	$-10.55^{+1.98}_{-1.39}$	$+2.88$ -2.35	$+3.89$ -2.56
J1605+3001		$2.72^{+1.05}_{-0.75}$	$+2.76$ -2.01	$+2.76$ -4.17	$3.53^{+1.78}_{-1.14}$	$+1.96$ -3.41	$+1.96$ -5.01	$-1.58^{+0.32}_{-1.15}$	$+0.32$ -1.76	$+0.33$ -1.79	$-10.82^{+4.16}_{-2.27}$	$+5.77$ -6.03	$+7.91$ -6.53
J1605-1139		$1.94^{+0.77}_{-0.71}$	$+1.80$ -2.75	$+3.08$ -3.06	$2.05^{+1.81}_{-0.81}$	$+3.39$ -2.04	$+3.41$ -3.42	$-1.61^{+0.30}_{-1.06}$	$+0.30$ -1.66	$+0.30$ -1.71	$-5.69^{+1.84}_{-3.08}$	$+3.04$ -6.47	$+4.58$ -7.83
J1606+2717		$2.48^{+0.82}_{-1.14}$	$+1.77$ -3.50	$+2.87$ -3.69	$3.20^{+1.88}_{-0.86}$	$+2.30$ -3.01	$+2.29$ -4.40	$-3.05^{+1.07}_{-0.32}$	$+1.73$ -0.31	$+1.79$ -0.32	$-9.28^{+2.37}_{-3.41}$	$+5.98$ -4.69	$+6.43$ -5.75
J1606+3124		$4.20^{+1.30}_{-1.51}$	$+1.25$ -4.61	$+1.30$ -5.35	$2.68^{+2.71}_{-0.87}$	$+2.82$ -3.06	$+2.82$ -4.14	$-1.52^{+0.28}_{-1.15}$	$+0.23$ -1.80	$+0.28$ -1.84	$-8.61^{+2.96}_{-5.50}$	$+4.13$ -9.38	$+5.69$ -10.37
J1608+1029		$2.61^{+0.63}_{-1.96}$	$+0.91$ -4.11	$+2.12$ -4.08	$3.08^{+0.73}_{-0.72}$	$+2.39$ -0.87	$+2.39$ -1.67	$-3.01^{+0.66}_{-0.34}$	$+1.57$ -0.33	$+1.72$ -0.34	$-7.77^{+1.26}_{-1.63}$	$+1.89$ -4.25	$+2.67$ -5.21
J1610+2414		$2.37^{+1.44}_{-0.96}$	$+1.44$ -3.78	$+2.61$ -3.78	$2.84^{+2.22}_{-0.60}$	$+2.66$ -2.57	$+2.65$ -4.23	$-2.99^{+0.87}_{-0.36}$	$+1.63$ -0.35	$+1.76$ -0.36	$-8.63^{+1.39}_{-5.15}$	$+4.27$ -6.69	$+6.34$ -7.49
J1611+1856		$2.88^{+1.17}_{-1.34}$	$+1.25$ -4.09	$+2.34$ -4.35	$4.50^{+1.00}_{-1.51}$	$+0.99$ -4.52	$+1.00$ -5.37	$-2.99^{+1.03}_{-0.36}$	$+1.71$ -0.29	$+1.76$ -0.35	$-10.76^{+1.65}_{-4.90}$	$+5.20$ -6.09	$+7.46$ -6.09
J1613+3412		$2.36^{+0.64}_{-0.78}$	$+1.22$ -2.04	$+1.66$ -3.40	$2.96^{+2.03}_{-0.39}$	$+2.53$ -2.09	$+2.53$ -3.49	$-2.46^{+0.81}_{-0.45}$	$+1.22$ -0.80	$+1.22$ -0.91	$-7.06^{+1.46}_{-3.52}$	$+3.42$ -5.27	$+5.43$ -6.33
J1616+0459		$3.26^{+0.87}_{-0.85}$	$+2.08$ -1.39	$+2.23$ -3.34	$3.49^{+1.77}_{-1.39}$	$+1.95$ -3.78	$+1.98$ -4.58	$-1.44^{+0.32}_{-1.13}$	$+0.28$ -1.86	$+0.32$ -1.92	$-11.00^{+4.91}_{-1.36}$	$+6.80$ -4.33	$+8.58$ -5.32
J1616+4632		$1.91^{+0.67}_{-2.00}$	$+0.91$ -3.24	$+1.33$ -3.38	$3.08^{+0.81}_{-0.52}$	$+1.84$ -0.86	$+2.42$ -0.99	$-2.90^{+0.50}_{-0.37}$	$+1.33$ -0.36	$+1.68$ -0.40	$-8.73^{+1.23}_{-1.42}$	$+1.80$ -3.46	$+2.30$ -4.71
J1617+0246		$2.31^{+1.01}_{-1.18}$	$+1.17$ -3.81	$+3.18$ -3.81	$3.06^{+1.66}_{-1.13}$	$+2.43$ -3.11	$+2.44$ -4.33	$-3.00^{+1.00}_{-0.37}$	$+1.67$ -0.36	$+1.76$ -0.36	$-9.73^{+2.84}_{-3.42}$	$+6.24$ -5.75	$+7.48$ -6.44
J1617-1122		$2.91^{+1.60}_{-1.21}$	$+2.58$ -2.06	$+2.58$ -3.86	$3.52^{+1.35}_{-2.22}$	$+1.96$ -4.22	$+1.96$ -4.81	$-1.62^{+0.29}_{-1.15}$	$+0.23$ -1.70	$+0.31$ -1.70	$-7.79^{+2.25}_{-5.70}$	$+5.00$ -8.12	$+6.55$ -9.15
J1617-1941		$5.08^{+0.38}_{-0.98}$	$+0.41$ -2.15	$+0.41$ -2.73	$4.45^{+1.04}_{-2.56}$	$+1.05$ -5.28	$+1.05$ -5.92	$-1.62^{+0.27}_{-0.86}$	$+0.27$ -1.54	$+0.27$ -1.73	$-11.61^{+2.89}_{-5.04}$	$+7.52$ -6.25	$+8.70$ -7.29
J1618+0819		$2.70^{+1.91}_{-0.93}$	$+2.79$ -2.48	$+2.79$ -4.15	$3.90^{+1.39}_{-2.13}$	$+1.60$ -4.36	$+1.60$ -5.25	$-3.02^{+1.18}_{-0.25}$	$+1.78$ -0.24	$+1.78$ -0.34	$-12.46^{+6.68}_{-1.50}$	$+8.52$ -4.33	$+9.43$ -6.37

Table C.2: Results of fitting the broken power-law model over the 1290 selected observations from OVRO dataset. Break significance refers to the source having a possible break frequency being (1σ) at 68.3%, (2σ) at 95.5% and (3σ) at 99.7%. The absence of break significance means that the source is not well-fitted at any level.

Name	Break significance	β_l	$\beta_l^{95.5\%}$	$\beta_l^{99.7\%}$	β_h	$\beta_h^{95.5\%}$	$\beta_h^{99.7\%}$	$\log f_{br}$	$\log f_{br}^{95.5\%}$	$\log f_{br}^{99.7\%}$	$\log A$	$\log A^{95.5\%}$	$\log A^{99.7\%}$
J1619+2247		$2.51^{+1.48}_{-1.26}$	$+2.80_{-3.38}$	$+2.98_{-3.94}$	$4.52^{+0.78}_{-2.25}$	$+0.98_{-4.74}$	$+0.96_{-5.88}$	$-3.02^{+1.09}_{-0.33}$	$+1.73_{-0.31}$	$+1.80_{-0.33}$	$-10.35^{+2.91}_{-4.88}$	$+7.13_{-6.12}$	$+8.41_{-7.68}$
J1620+4901		$4.34^{+0.71}_{-1.48}$	$+1.16_{-4.25}$	$+1.16_{-5.70}$	$4.60^{+0.88}_{-2.22}$	$+0.90_{-5.29}$	$+0.90_{-6.05}$	$-3.14^{+1.28}_{-0.23}$	$+1.82_{-0.23}$	$+1.90_{-0.23}$	$-14.25^{+4.29}_{-2.99}$	$+10.10_{-3.08}$	$+11.74_{-3.91}$
J1624+5652		$2.24^{+0.63}_{-1.99}$	$+0.84_{-3.70}$	$+2.12_{-3.69}$	$3.72^{+1.06}_{-1.55}$	$+1.76_{-3.60}$	$+1.76_{-5.06}$	$-2.93^{+0.55}_{-0.44}$	$+1.58_{-0.37}$	$+1.69_{-0.43}$	$-9.99^{+2.53}_{-4.07}$	$+5.48_{-5.88}$	$+7.63_{-6.36}$
J1624+5741		$2.51^{+0.98}_{-1.65}$	$+1.09_{-3.83}$	$+2.01_{-3.99}$	$3.19^{+1.73}_{-0.84}$	$+2.31_{-2.92}$	$+2.28_{-4.62}$	$-3.00^{+0.84}_{-0.37}$	$+1.69_{-0.29}$	$+1.77_{-0.36}$	$-9.54^{+1.56}_{-4.39}$	$+4.76_{-6.17}$	$+7.41_{-6.07}$
J1625+4134		$2.79^{+0.81}_{-0.89}$	$+2.03_{-3.05}$	$+2.63_{-4.02}$	$3.09^{+1.25}_{-1.18}$	$+2.39_{-3.11}$	$+2.35_{-4.46}$	$-3.08^{+1.18}_{-0.29}$	$+1.71_{-0.29}$	$+1.83_{-0.29}$	$-9.16^{+1.96}_{-3.15}$	$+4.94_{-4.45}$	$+6.68_{-5.17}$
J1628-1415		$2.55^{+1.14}_{-1.61}$	$+1.39_{-3.71}$	$+2.56_{-3.87}$	$4.28^{+0.99}_{-1.63}$	$+1.21_{-4.24}$	$+1.21_{-5.17}$	$-3.04^{+0.85}_{-0.31}$	$+1.62_{-0.27}$	$+1.68_{-0.32}$	$-11.43^{+3.37}_{-3.36}$	$+7.20_{-4.32}$	$+8.17_{-4.80}$
J1630+0701		$2.95^{+1.10}_{-1.12}$	$+1.22_{-4.35}$	$+2.19_{-4.33}$	$4.48^{+0.99}_{-1.24}$	$+1.02_{-3.98}$	$+1.01_{-5.51}$	$-3.06^{+0.96}_{-0.28}$	$+1.71_{-0.27}$	$+1.81_{-0.30}$	$-12.76^{+3.10}_{-2.85}$	$+8.10_{-3.21}$	$+9.62_{-3.85}$
J1631+4927		$1.69^{+0.82}_{-1.49}$	$+1.01_{-3.10}$	$+1.84_{-3.15}$	$2.97^{+1.67}_{-0.76}$	$+2.44_{-1.58}$	$+2.51_{-3.38}$	$-2.80^{+0.56}_{-0.38}$	$+1.43_{-0.51}$	$+1.56_{-0.54}$	$-9.31^{+2.94}_{-2.63}$	$+3.45_{-6.12}$	$+6.32_{-6.12}$
J1632+8232		$2.36^{+0.79}_{-1.19}$	$+1.85_{-3.20}$	$+2.75_{-3.77}$	$2.72^{+1.75}_{-0.70}$	$+2.72_{-1.34}$	$+2.77_{-2.11}$	$-3.07^{+0.88}_{-0.30}$	$+1.71_{-0.30}$	$+1.83_{-0.30}$	$-7.87^{+0.98}_{-4.10}$	$+3.36_{-5.88}$	$+3.85_{-7.12}$
J1635+3808		$2.53^{+0.71}_{-1.89}$	$+0.91_{-3.75}$	$+1.29_{-4.03}$	$3.49^{+0.84}_{-0.62}$	$+1.82_{-0.75}$	$+1.95_{-1.29}$	$-2.80^{+0.29}_{-0.50}$	$+0.97_{-0.50}$	$+1.44_{-0.53}$	$-7.72^{+1.29}_{-1.94}$	$+1.81_{-3.78}$	$+2.70_{-4.15}$
J1636+2112		$2.74^{+0.68}_{-1.19}$	$+1.78_{-3.12}$	$+2.30_{-4.20}$	$2.86^{+2.18}_{-0.71}$	$+2.57_{-3.39}$	$+2.63_{-4.24}$	$-1.52^{+0.19}_{-1.29}$	$+0.28_{-1.76}$	$+0.29_{-1.82}$	$-9.01^{+2.24}_{-3.81}$	$+5.48_{-5.78}$	$+5.74_{-7.20}$
J1637+4717		$2.84^{+0.72}_{-0.75}$	$+1.27_{-3.57}$	$+2.29_{-4.25}$	$3.08^{+1.53}_{-1.15}$	$+2.41_{-3.27}$	$+2.41_{-4.44}$	$-1.52^{+0.26}_{-1.22}$	$+0.23_{-1.80}$	$+0.27_{-1.85}$	$-8.29^{+3.02}_{-1.99}$	$+5.77_{-4.27}$	$+6.42_{-5.82}$
J1638+5720		$3.05^{+0.67}_{-0.70}$	$+1.80_{-2.57}$	$+2.44_{-4.06}$	$3.43^{+1.26}_{-0.99}$	$+2.04_{-2.81}$	$+2.05_{-4.68}$	$-3.10^{+1.32}_{-0.20}$	$+1.84_{-0.17}$	$+1.86_{-0.26}$	$-8.72^{+2.02}_{-2.29}$	$+4.84_{-3.89}$	$+6.30_{-4.57}$
J1639+5357		$4.60^{+0.89}_{-1.28}$	$+0.89_{-3.38}$	$+0.88_{-4.97}$	$4.71^{+0.73}_{-2.97}$	$+0.78_{-5.36}$	$+0.78_{-6.09}$	$-1.71^{+0.46}_{-0.85}$	$+0.46_{-1.54}$	$+0.46_{-1.65}$	$-15.66^{+7.05}_{-1.38}$	$+11.58_{-2.29}$	$+12.89_{-3.40}$
J1640+3946	1σ	$1.61^{+0.72}_{-0.89}$	$+1.10_{-2.58}$	$+1.80_{-2.97}$	$3.30^{+1.32}_{-0.69}$	$+2.19_{-0.88}$	$+2.19_{-1.33}$	$-2.40^{+0.28}_{-0.39}$	$+0.67_{-0.82}$	$+0.99_{-0.89}$	$-7.47^{+0.88}_{-3.39}$	$+1.50_{-5.27}$	$+2.07_{-5.63}$
J1640-0011	2σ	$-0.26^{+0.99}_{-0.90}$	$+1.75_{-1.24}$	$+2.35_{-1.23}$	$4.74^{+-0.01}_{-2.03}$	$+0.76_{-2.37}$	$+0.76_{-2.93}$	$-2.70^{+0.14}_{-0.15}$	$+0.27_{-0.40}$	$+0.41_{-0.65}$	$-9.26^{+1.26}_{-3.70}$	$+2.11_{-5.66}$	$+3.42_{-5.66}$
J1641+2257		$2.17^{+1.30}_{-1.05}$	$+1.86_{-3.25}$	$+3.15_{-3.56}$	$3.59^{+1.53}_{-1.39}$	$+1.91_{-3.55}$	$+1.91_{-5.06}$	$-3.01^{+1.02}_{-0.31}$	$+1.74_{-0.28}$	$+1.80_{-0.33}$	$-10.11^{+2.35}_{-4.45}$	$+5.48_{-5.93}$	$+7.86_{-6.33}$
J1642+3948		$2.46^{+0.57}_{-2.37}$	$+1.01_{-3.92}$	$+2.38_{-3.89}$	$3.33^{+1.55}_{-0.61}$	$+2.14_{-1.60}$	$+2.14_{-3.05}$	$-2.91^{+0.39}_{-0.42}$	$+1.55_{-0.38}$	$+1.70_{-0.42}$	$-7.51^{+2.40}_{-2.62}$	$+3.11_{-5.68}$	$+5.50_{-5.62}$
J1642+6856		$2.93^{+0.64}_{-0.86}$	$+1.32_{-3.65}$	$+1.85_{-4.34}$	$3.33^{+1.61}_{-0.52}$	$+2.14_{-2.79}$	$+2.14_{-4.53}$	$-3.07^{+1.27}_{-0.24}$	$+1.87_{-0.18}$	$+1.87_{-0.25}$	$-7.98^{+1.51}_{-2.81}$	$+5.18_{-3.75}$	$+6.71_{-4.79}$
J1642-0621		$2.62^{+0.89}_{-0.84}$	$+1.39_{-3.96}$	$+2.82_{-3.96}$	$2.78^{+1.68}_{-1.02}$	$+2.72_{-2.73}$	$+2.72_{-4.11}$	$-3.08^{+1.29}_{-0.24}$	$+1.82_{-0.23}$	$+1.88_{-0.24}$	$-6.92^{+1.82}_{-3.41}$	$+4.65_{-5.32}$	$+5.61_{-6.75}$
J1644+2619		$1.80^{+0.94}_{-2.86}$	$+3.52_{-2.92}$	$+3.65_{-3.28}$	$3.39^{+1.44}_{-1.96}$	$+2.06_{-3.54}$	$+2.07_{-4.58}$	$-2.58^{+0.54}_{-0.54}$	$+1.17_{-0.52}$	$+1.24_{-0.54}$	$-10.98^{+5.23}_{-2.41}$	$+6.77_{-6.42}$	$+7.25_{-8.88}$
J1644-0743		$2.59^{+0.66}_{-2.41}$	$+0.91_{-4.05}$	$+1.37_{-4.08}$	$4.04^{+1.18}_{-1.08}$	$+1.46_{-2.43}$	$+1.46_{-4.15}$	$-2.94^{+0.41}_{-0.38}$	$+1.51_{-0.38}$	$+1.63_{-0.38}$	$-10.08^{+2.32}_{-3.25}$	$+4.57_{-4.55}$	$+6.67_{-4.85}$
J1644-1804		$1.98^{+1.11}_{-0.80}$	$+2.31_{-2.28}$	$+3.00_{-3.34}$	$2.24^{+2.75}_{-0.45}$	$+3.26_{-2.33}$	$+3.25_{-3.50}$	$-1.55^{+0.31}_{-1.13}$	$+0.31_{-1.76}$	$+0.31_{-1.80}$	$-7.19^{+1.48}_{-4.98}$	$+3.34_{-8.45}$	$+4.34_{-8.76}$
J1646+4059		$2.44^{+0.78}_{-0.80}$	$+2.45_{-2.68}$	$+2.76_{-3.91}$	$2.90^{+1.97}_{-1.07}$	$+2.60_{-3.34}$	$+2.60_{-4.29}$	$-1.42^{+0.23}_{-1.22}$	$+0.23_{-1.79}$	$+0.22_{-1.90}$	$-9.19^{+2.76}_{-3.36}$	$+5.76_{-5.52}$	$+7.01_{-6.17}$

Table C.2: Results of fitting the broken power-law model over the 1290 selected observations from OVRO dataset. Break significance refers to the source having a possible break frequency being (1σ) at 68.3%, (2σ) at 95.5% and (3σ) at 99.7%. The absence of break significance means that the source is not well-fitted at any level.

Name	Break significance	β_l	$\beta_l^{95.5\%}$	$\beta_l^{99.7\%}$	β_h	$\beta_h^{95.5\%}$	$\beta_h^{99.7\%}$	$\log f_{br}$	$\log f_{br}^{95.5\%}$	$\log f_{br}^{99.7\%}$	$\log A$	$\log A^{95.5\%}$	$\log A^{99.7\%}$
J1647+4950		1.71 ^{+0.48} _{-0.88}	+1.01 -2.62	+1.83 -3.17	2.64 ^{+1.47} _{-0.67}	+2.81 -0.62	+2.81 -0.99	-2.27 ^{+0.67} _{-0.38}	+0.77 -1.04	+0.77 -1.09	-7.57 ^{+1.10} _{-2.93}	+1.31 -5.70	+1.82 -6.54
J1648+2224		3.08 ^{+2.17} _{-0.85}	+2.34 -3.35	+2.34 -4.58	4.44 ^{+1.05} _{-2.44}	+1.05 -5.27	+1.05 -5.90	-1.65 ^{+0.23} _{-1.70}	+0.37 -1.65	+0.43 -1.70	-13.48 ^{+6.24} _{-2.38}	+9.26 -4.90	+10.58 -5.64
J1649+0412		2.16 ^{+0.89} _{-1.06}	+0.89 -3.44	+2.05 -3.62	2.67 ^{+0.99} _{-0.85}	+2.59 -0.90	+2.81 -1.60	-3.05 ^{+0.92} _{-0.31}	+1.69 -0.31	+1.80 -0.32	-7.83 ^{+1.58} _{-2.10}	+2.06 -4.86	+2.85 -5.40
J1650+0824		2.51 ^{+0.65} _{-0.67}	+1.89 -2.85	+2.82 -3.65	2.68 ^{+1.93} _{-0.72}	+2.77 -2.56	+2.80 -3.90	-1.47 ^{+0.33} _{-1.26}	+0.25 -1.88	+0.33 -1.89	-8.53 ^{+2.91} _{-1.86}	+4.30 -5.01	+5.91 -5.70
J1651+0129		2.11 ^{+0.70} _{-0.73}	+2.25 -2.41	+3.36 -3.31	2.31 ^{+1.72} _{-0.80}	+3.18 -1.57	+3.17 -2.62	-2.16 ^{+0.92} _{-0.46}	+0.86 -1.18	+0.92 -1.20	-7.07 ^{+1.53} _{-3.04}	+2.58 -6.58	+3.44 -7.37
J1652+0618		2.98 ^{+1.12} _{-0.94}	+1.44 -4.38	+2.37 -4.38	3.98 ^{+1.14} _{-1.79}	+1.51 -3.87	+1.51 -5.19	-3.11 ^{+1.21} _{-0.25}	+1.77 -0.24	+1.87 -0.25	-10.05 ^{+3.62} _{-2.79}	+5.29 -6.02	+7.42 -6.28
J1652+3902		2.33 ^{+0.84} _{-1.28}	+1.92 -3.53	+2.58 -3.73	2.85 ^{+1.63} _{-1.23}	+2.63 -3.09	+2.63 -4.24	-3.04 ^{+1.22} _{-0.29}	+1.76 -0.29	+1.84 -1.89	-8.68 ^{+3.14} _{-2.54}	+5.22 -5.87	+6.65 -6.25
J1653+3107		5.14 ^{+0.34} _{-0.88}	+0.35 -1.80	+0.35 -2.61	4.32 ^{+1.15} _{-2.73}	+1.17 -5.39	+1.17 -5.80	-1.57 ^{+0.26} _{-0.89}	+0.25 -1.58	+0.26 -1.72	-13.07 ^{+6.40} _{-1.89}	+9.50 -3.40	+11.49 -3.72
J1653+3945		1.87 ^{+1.59} _{-1.12}	+2.99 -2.84	+3.47 -3.28	4.08 ^{+0.68} _{-2.65}	+1.41 -4.47	+1.41 -5.41	-3.00 ^{+1.09} _{-0.31}	+1.70 -0.32	+1.80 -0.32	-6.37 ^{+2.47} _{-5.18}	+3.07 -9.32	+4.43 -10.98
J1653-1551		1.68 ^{+1.44} _{-1.12}	+2.09 -3.09	+3.11 -3.11	2.37 ^{+2.67} _{-0.36}	+3.13 -2.05	+3.11 -3.54	-2.93 ^{+0.90} _{-0.42}	+1.62 -0.38	+1.70 -0.42	-11.07 ^{+4.96} _{-2.07}	+6.21 -6.09	+8.40 -6.09
J1655+4233		3.14 ^{+1.58} _{-1.20}	+2.34 -3.05	+2.34 -4.58	4.49 ^{+0.90} _{-2.46}	+0.86 -5.42	+1.00 -5.96	-3.06 ^{+1.27} _{-0.18}	+1.73 -0.20	+1.76 -0.26	-13.06 ^{+6.57} _{-1.90}	+8.87 -4.33	+10.01 -6.16
J1656+1826		2.36 ^{+1.76} _{-0.97}	+2.55 -3.67	+2.91 -3.83	3.06 ^{+2.09} _{-0.99}	+2.44 -3.15	+2.44 -4.49	-3.05 ^{+1.13} _{-0.29}	+1.75 -0.29	+1.80 -0.31	-11.72 ^{+4.94} _{-2.83}	+7.28 -5.22	+8.81 -6.02
J1656+6012	3 σ	0.99 ^{+0.63} _{-1.43}	+0.79 -2.46	+1.27 -2.46	3.35 ^{+0.87} _{-0.54}	+1.63 -0.89	+2.06 -1.01	-2.62 ^{+0.34} _{-0.22}	+0.57 -0.36	+0.74 -0.44	-8.58 ^{+1.10} _{-1.74}	+2.02 -3.02	+2.31 -3.93
J1657+4808		2.11 ^{+0.61} _{-1.88}	+0.86 -3.58	+3.32 -3.57	2.70 ^{+0.78} _{-0.59}	+2.25 -0.83	+2.75 -1.87	-2.99 ^{+0.70} _{-0.37}	+1.64 -0.38	+1.75 -0.37	-7.18 ^{+1.31} _{-1.45}	+2.00 -3.71	+3.08 -4.60
J1658+0515		3.69 ^{+0.84} _{-1.06}	+1.73 -3.26	+1.68 -5.01	4.41 ^{+0.94} _{-1.96}	+1.05 -4.90	+1.05 -5.74	-3.05 ^{+1.33} _{-0.26}	+1.80 -0.30	+1.92 -0.32	-10.48 ^{+2.45} _{-4.47}	+5.75 -5.42	+7.71 -5.96
J1658+3443		2.60 ^{+2.88} _{-0.48}	+2.88 -2.95	+2.89 -3.92	2.52 ^{+2.89} _{-1.08}	+2.84 -3.74	+2.94 -3.99	-2.91 ^{+1.27} _{-0.06}	+1.58 -0.30	+1.59 -0.41	-12.28 ^{+5.12} _{-3.55}	+8.62 -5.91	+8.68 -7.46
J1658+4737		3.28 ^{+0.89} _{-1.03}	+2.19 -3.15	+2.19 -4.71	4.34 ^{+1.05} _{-2.07}	+1.09 -5.01	+1.15 -5.68	-3.07 ^{+1.22} _{-0.30}	+1.78 -0.29	+1.83 -0.30	-12.26 ^{+4.34} _{-2.58}	+9.16 -2.79	+9.64 -4.56
J1658-0739		4.70 ^{+0.80} _{-1.39}	+0.80 -4.96	+0.79 -5.86	4.24 ^{+1.25} _{-2.17}	+1.25 -4.99	+1.25 -5.74	-1.67 ^{+0.26} _{-1.66}	+0.28 -1.66	+0.36 -1.66	-13.32 ^{+4.75} _{-3.63}	+8.87 -4.47	+10.95 -5.65
J1700+6830	2 σ	-0.85 ^{+1.34} _{-0.62}	+2.58 -0.62	+3.15 -0.64	3.09 ^{+0.26} _{-0.49}	+1.01 -0.60	+1.32 -0.80	-2.65 ^{+0.30} _{-0.17}	+0.58 -0.38	+0.77 -0.52	-7.13 ^{+0.91} _{-0.59}	+1.51 -1.64	+1.64 -2.55
J1701+3954		2.92 ^{+0.93} _{-0.85}	+1.91 -3.28	+2.39 -4.31	3.75 ^{+1.20} _{-1.64}	+1.75 -3.35	+1.75 -4.89	-1.66 ^{+0.27} _{-1.66}	+0.24 -1.65	+0.35 -1.66	-11.17 ^{+4.16} _{-1.91}	+6.58 -4.45	+8.55 -5.33
J1706+0953	2 σ	0.24 ^{+1.11} _{-0.74}	+1.46 -1.73	+2.14 -1.73	5.01 ^{+0.49} _{-1.11}	+0.49 -2.31	+0.49 -2.98	-2.59 ^{+0.20} _{-0.12}	+0.34 -0.40	+0.44 -0.59	-13.48 ^{+2.95} _{-0.84}	+5.50 -1.17	+6.95 -1.65
J1707+0148		2.57 ^{+0.93} _{-1.15}	+1.55 -3.68	+2.61 -4.05	3.26 ^{+1.42} _{-1.17}	+2.23 -2.90	+2.21 -4.59	-3.03 ^{+1.05} _{-0.33}	+1.81 -0.32	+1.90 -0.33	-9.83 ^{+3.20} _{-2.57}	+5.91 -5.02	+7.86 -5.21
J1707+1331		2.21 ^{+1.08} _{-1.26}	+1.33 -3.54	+2.31 -3.66	4.20 ^{+0.40} _{-2.61}	+1.26 -4.78	+1.30 -5.67	-3.00 ^{+1.06} _{-0.37}	+1.65 -0.37	+1.76 -0.37	-9.82 ^{+4.62} _{-2.16}	+6.74 -5.55	+8.26 -5.76
J1707-1415		2.51 ^{+1.53} _{-0.78}	+2.95 -2.77	+2.95 -3.89	3.41 ^{+1.07} _{-2.37}	+2.04 -4.18	+2.07 -4.85	-1.51 ^{+0.25} _{-1.27}	+0.20 -1.83	+0.27 -1.85	-6.03 ^{+1.59} _{-5.86}	+4.19 -8.37	+4.53 -9.93

Table C.2: Results of fitting the broken power-law model over the 1290 selected observations from OVRO dataset. Break significance refers to the source having a possible break frequency being (1σ) at 68.3 %, (2σ) at 95.5 % and (3σ) at 99.7 %. The absence of break significance means that the source is not well-fitted at any level.

Name	Break significance	β_l	$\beta_l^{95.5\%}$	$\beta_l^{99.7\%}$	β_h	$\beta_h^{95.5\%}$	$\beta_h^{99.7\%}$	$\log f_{br}$	$\log f_{br}^{95.5\%}$	$\log f_{br}^{99.7\%}$	$\log A$	$\log A^{95.5\%}$	$\log A^{99.7\%}$
J1709+4318		2.25 ^{+0.72} _{-1.89}	+0.79 -3.58	+1.47 -3.70	3.22 ^{+0.93} _{-0.60}	+1.95 -0.89	+2.27 -0.99	-2.81 ^{+0.31} _{-0.47}	+1.19 -0.52	+1.60 -0.52	-8.07 ^{+1.35} _{-1.90}	+1.72 -4.04	+2.18 -4.83
J1709-1728		2.84 ^{+0.96} _{-1.03}	+1.89 -3.53	+2.57 -4.27	3.38 ^{+1.63} _{-1.22}	+2.10 -3.20	+2.09 -4.56	-3.05 ^{+1.13} _{-0.26}	+1.76 -0.25	+1.85 -0.26	-9.33 ^{+2.02} _{-4.21}	+5.86 -5.39	+7.68 -5.91
J1712-1820		2.59 ^{+0.79} _{-1.46}	+1.68 -3.98	+2.81 -4.03	3.21 ^{+1.81} _{-0.80}	+2.29 -2.29	+2.29 -2.85	-3.08 ^{+0.98} _{-0.28}	+1.63 -0.27	+1.73 -0.28	-9.04 ^{+1.59} _{-4.35}	+4.97 -4.93	+4.97 -6.42
J1713+4916		2.70 ^{+1.48} _{-0.89}	+2.68 -2.96	+2.68 -3.93	2.84 ^{+2.50} _{-0.61}	+2.66 -2.94	+2.64 -3.99	-3.09 ^{+1.23} _{-0.28}	+1.78 -0.28	+1.85 -0.28	-9.48 ^{+2.93} _{-4.08}	+5.21 -6.63	+6.21 -8.01
J1716+6836		1.77 ^{+0.86} _{-0.80}	+1.07 -2.86	+2.89 -3.02	2.35 ^{+1.80} _{-0.90}	+3.12 -1.27	+3.12 -3.26	-2.23 ^{+0.37} _{-1.03}	+1.03 -0.99	+1.03 -1.08	-7.16 ^{+1.60} _{-3.57}	+2.04 -6.65	+4.22 -7.06
J1716-0452		2.63 ^{+0.88} _{-0.76}	+1.10 -3.86	+2.05 -4.07	3.08 ^{+1.47} _{-0.93}	+2.42 -2.80	+2.42 -4.48	-3.11 ^{+1.29} _{-0.23}	+1.84 -0.19	+1.87 -0.26	-9.06 ^{+1.80} _{-3.28}	+5.67 -4.51	+6.68 -5.79
J1719+1745		2.12 ^{+0.60} _{-0.71}	+3.35 -1.01	+3.35 -2.39	1.86 ^{+1.55} _{-0.80}	+3.31 -2.06	+3.61 -3.27	-1.48 ^{+0.23} _{-1.89}	+0.25 -1.88	+0.34 -1.89	-5.53 ^{+1.77} _{-2.48}	+2.23 -6.77	+4.04 -7.77
J1719+4858		2.93 ^{+1.33} _{-1.18}	+1.63 -4.19	+2.39 -4.42	4.25 ^{+1.15} _{-1.52}	+1.23 -3.97	+1.24 -5.53	-3.08 ^{+1.16} _{-0.28}	+1.73 -0.29	+1.83 -0.29	-12.46 ^{+4.01} _{-2.06}	+7.21 -3.56	+9.48 -4.30
J1719-1420		2.67 ^{+0.97} _{-1.06}	+1.86 -3.60	+2.60 -4.16	3.16 ^{+1.77} _{-1.01}	+2.33 -2.97	+2.33 -4.44	-3.07 ^{+1.22} _{-0.28}	+1.83 -0.23	+1.84 -0.28	-9.23 ^{+2.09} _{-3.77}	+5.51 -5.48	+6.20 -6.83
J1721+3542		2.39 ^{+1.36} _{-0.86}	+2.28 -3.39	+3.11 -3.80	3.02 ^{+2.46} _{-0.65}	+2.47 -2.95	+2.46 -4.47	-3.07 ^{+1.20} _{-0.26}	+1.80 -0.24	+1.86 -0.26	-10.60 ^{+3.98} _{-3.07}	+7.49 -4.94	+8.31 -6.72
J1722+1013		1.66 ^{+0.46} _{-1.06}	+0.77 -2.57	+1.35 -3.15	2.19 ^{+2.00} _{-0.58}	+3.18 -0.58	+3.30 -0.84	-2.21 ^{+0.27} _{-0.82}	+0.86 -1.03	+0.97 -1.11	-6.01 ^{+1.20} _{-3.75}	+1.16 -6.61	+1.65 -7.08
J1722+2815		2.92 ^{+0.78} _{-0.78}	+1.74 -3.60	+2.34 -4.39	3.76 ^{+1.70} _{-1.08}	+1.73 -3.70	+1.73 -4.91	-1.54 ^{+0.29} _{-1.21}	+0.30 -1.77	+0.30 -1.83	-10.72 ^{+3.39} _{-2.19}	+7.04 -4.01	+7.93 -5.29
J1722+5856		3.20 ^{+0.91} _{-1.27}	+2.28 -3.06	+2.27 -4.60	3.59 ^{+1.78} _{-1.65}	+1.91 -4.24	+1.91 -4.85	-3.13 ^{+1.20} _{-0.22}	+1.76 -0.23	+1.89 -0.23	-10.67 ^{+3.95} _{-4.18}	+6.29 -6.24	+7.61 -6.90
J1722+6105	2 σ	0.99 ^{+0.88} _{-1.22}	+1.15 -2.42	+1.55 -2.47	2.86 ^{+1.14} _{-0.62}	+2.34 -0.64	+2.60 -0.92	-2.71 ^{+0.52} _{-0.17}	+0.69 -0.57	+1.21 -0.64	-7.83 ^{+1.47} _{-2.21}	+1.21 -5.05	+1.99 -5.14
J1724+1648		2.17 ^{+1.25} _{-1.85}	+2.03 -3.53	+3.19 -3.66	3.76 ^{+1.63} _{-1.36}	+1.73 -3.42	+1.73 -4.98	-2.98 ^{+0.95} _{-0.33}	+1.79 -0.31	+1.82 -0.39	-7.71 ^{+1.82} _{-4.98}	+2.31 -8.72	+4.78 -9.26
J1724+3303		2.94 ^{+1.13} _{-0.77}	+2.55 -2.78	+2.55 -3.81	2.53 ^{+2.60} _{-0.86}	+2.97 -3.09	+2.97 -3.98	-1.63 ^{+0.39} _{-1.10}	+0.34 -1.70	+0.39 -1.73	-8.02 ^{+1.96} _{-5.36}	+4.76 -7.06	+6.56 -8.06
J1724-1443		2.83 ^{+1.13} _{-1.51}	+1.28 -4.06	+1.98 -4.26	4.33 ^{+1.03} _{-1.25}	+1.15 -3.83	+1.15 -5.18	-3.05 ^{+0.89} _{-0.31}	+1.69 -0.30	+1.82 -0.30	-12.28 ^{+3.43} _{-2.26}	+7.57 -3.59	+9.22 -4.22
J1725+1152		2.80 ^{+0.58} _{-2.21}	+1.18 -3.90	+1.48 -4.25	4.41 ^{+1.07} _{-1.27}	+1.07 -3.82	+1.07 -5.91	-2.97 ^{+0.72} _{-0.40}	+1.68 -0.39	+1.82 -0.39	-12.06 ^{+2.44} _{-3.66}	+6.86 -4.08	+9.29 -4.58
J1726+2717		3.11 ^{+0.96} _{-0.84}	+2.34 -2.90	+2.34 -4.59	3.90 ^{+1.60} _{-1.75}	+1.60 -4.97	+1.60 -5.38	-1.62 ^{+0.38} _{-1.08}	+0.38 -1.68	+0.38 -1.75	-9.88 ^{+2.79} _{-4.16}	+5.89 -5.87	+7.01 -6.94
J1726+3213		2.70 ^{+1.01} _{-1.18}	+2.61 -2.86	+2.61 -4.19	3.83 ^{+1.55} _{-1.39}	+1.58 -4.02	+1.67 -5.05	-3.07 ^{+1.07} _{-0.29}	+1.72 -0.29	+1.83 -0.29	-11.86 ^{+4.57} _{-2.07}	+8.35 -3.28	+8.69 -4.89
J1727+4530		2.10 ^{+0.45} _{-1.18}	+0.83 -2.90	+1.07 -3.51	3.08 ^{+0.89} _{-0.55}	+2.32 -0.58	+2.41 -0.84	-2.08 ^{+0.34} _{-0.72}	+0.43 -1.25	+0.63 -1.25	-6.98 ^{+1.04} _{-1.70}	+1.13 -4.20	+1.67 -4.42
J1727+5510		4.69 ^{+0.47} _{-1.58}	+0.81 -2.57	+0.80 -4.72	3.86 ^{+1.62} _{-2.13}	+1.59 -4.87	+1.62 -5.34	-1.73 ^{+0.47} _{-0.83}	+0.45 -1.55	+0.48 -1.63	-13.75 ^{+6.65} _{-1.75}	+9.15 -4.22	+10.77 -4.97
J1728+0427	2 σ	1.43 ^{+0.51} _{-0.48}	+1.03 -1.39	+1.11 -2.34	4.66 ^{+0.32} _{-1.72}	+0.84 -2.11	+0.84 -2.46	-2.13 ^{+0.19} _{-0.22}	+0.30 -0.76	+0.40 -1.20	-10.52 ^{+2.56} _{-1.41}	+4.46 -1.41	+4.88 -1.76
J1728+1215		2.12 ^{+0.71} _{-0.53}	+1.90 -2.78	+2.96 -3.58	2.23 ^{+1.27} _{-0.69}	+3.27 -1.61	+3.26 -3.13	-1.57 ^{+0.33} _{-1.09}	+0.25 -1.78	+0.33 -1.80	-5.73 ^{+1.19} _{-2.34}	+2.85 -5.53	+4.23 -6.24

Table C.2: Results of fitting the broken power-law model over the 1290 selected observations from OVRO dataset. Break significance refers to the source having a possible break frequency being (1σ) at 68.3%, (2σ) at 95.5% and (3σ) at 99.7%. The absence of break significance means that the source is not well-fitted at any level.

Name	Break significance	β_l	$\beta_l^{95.5\%}$	$\beta_l^{99.7\%}$	β_h	$\beta_h^{95.5\%}$	$\beta_h^{99.7\%}$	$\log f_{br}$	$\log f_{br}^{95.5\%}$	$\log f_{br}^{99.7\%}$	$\log A$	$\log A^{95.5\%}$	$\log A^{99.7\%}$
J1827+2658		2.29 ^{+1.17} _{-1.11}	+1.61 -3.61	+2.56 -3.79	4.10 ^{+1.11} _{-1.92}	+1.36 -4.15	+1.40 -5.02	-2.99 ^{+1.20} _{-0.20}	+1.66 -0.37	+1.75 -0.38	-10.92 ^{+4.66} _{-2.16}	+6.21 -5.61	+7.92 -7.35
J1832+1357		3.05 ^{+1.15} _{-1.11}	+1.50 -4.26	+2.17 -4.46	4.41 ^{+1.09} _{-1.67}	+1.08 -4.28	+1.09 -5.67	-3.05 ^{+1.29} _{-0.31}	+1.87 -0.30	+1.93 -0.31	-11.95 ^{+4.28} _{-1.93}	+6.99 -3.79	+8.35 -3.93
J1835+3241		1.83 ^{+1.73} _{-0.99}	+2.48 -3.08	+3.36 -3.24	2.44 ^{+2.82} _{-0.42}	+3.06 -2.31	+3.06 -3.62	-3.04 ^{+1.09} _{-0.27}	+1.66 -0.31	+1.79 -0.33	-8.48 ^{+3.54} _{-3.86}	+4.57 -8.52	+6.77 -8.52
J1835+6119		3.02 ^{+0.72} _{-0.76}	+2.48 -1.29	+2.43 -3.33	2.57 ^{+1.94} _{-0.75}	+2.93 -2.35	+2.93 -3.94	-1.55 ^{+0.28} _{-1.13}	+0.28 -1.74	+0.30 -1.83	-8.58 ^{+1.45} _{-4.06}	+4.41 -5.96	+6.16 -6.90
J1840+2457		2.48 ^{+1.08} _{-0.75}	+1.61 -3.07	+2.27 -3.86	2.91 ^{+1.94} _{-0.82}	+2.51 -3.11	+2.55 -4.15	-1.52 ^{+0.24} _{-1.25}	+0.23 -1.80	+0.27 -1.85	-9.04 ^{+1.93} _{-3.75}	+4.70 -5.73	+5.99 -6.53
J1840+3900		2.44 ^{+0.75} _{-0.69}	+3.01 -1.15	+3.04 -2.39	2.42 ^{+1.56} _{-0.91}	+3.03 -2.05	+3.02 -3.33	-1.53 ^{+0.29} _{-1.21}	+0.26 -1.81	+0.29 -1.83	-7.71 ^{+1.64} _{-3.08}	+3.77 -5.27	+4.88 -6.47
J1842+6809		1.91 ^{+0.95} _{-1.29}	+1.46 -3.01	+3.17 -3.37	3.29 ^{+1.19} _{-0.68}	+2.11 -0.96	+2.20 -1.58	-2.60 ^{+0.22} _{-0.51}	+0.76 -0.73	+1.20 -0.76	-8.54 ^{+1.01} _{-3.17}	+1.94 -5.39	+3.38 -5.38
J1848+3219		2.59 ^{+0.59} _{-0.88}	+0.96 -3.30	+1.79 -4.07	3.06 ^{+1.23} _{-0.71}	+2.32 -1.86	+2.44 -3.40	-2.33 ^{+0.33} _{-1.03}	+1.04 -1.03	+1.19 -1.03	-7.33 ^{+1.40} _{-2.20}	+3.09 -4.32	+4.78 -5.21
J1849+3024		2.27 ^{+1.03} _{-0.87}	+2.80 -2.75	+3.01 -3.77	2.39 ^{+2.43} _{-0.75}	+3.09 -2.72	+3.07 -3.88	-3.14 ^{+1.25} _{-0.23}	+1.79 -0.23	+1.88 -0.23	-7.12 ^{+1.41} _{-4.99}	+3.96 -7.20	+5.08 -9.29
J1849+6705		2.15 ^{+0.55} _{-1.56}	+0.59 -3.42	+0.97 -3.61	2.79 ^{+0.61} _{-0.68}	+2.47 -0.74	+2.50 -1.35	-2.83 ^{+0.47} _{-0.54}	+1.45 -0.53	+1.58 -0.54	-6.09 ^{+1.13} _{-1.51}	+1.72 -3.73	+2.29 -5.20
J1850+2825		4.38 ^{+1.12} _{-1.24}	+1.12 -2.89	+1.11 -4.80	4.60 ^{+0.86} _{-2.87}	+0.88 -5.23	+0.86 -6.07	-1.64 ^{+0.51} _{-0.99}	+0.50 -1.64	+0.51 -1.72	-11.57 ^{+5.01} _{-4.28}	+7.90 -5.89	+9.78 -6.45
J1852+4019		2.53 ^{+2.43} _{-0.85}	+2.94 -3.11	+2.94 -3.96	2.12 ^{+3.17} _{-0.48}	+3.31 -3.03	+3.38 -3.55	-1.59 ^{+0.37} _{-1.20}	+0.28 -1.76	+0.36 -1.76	-6.89 ^{+2.44} _{-5.39}	+3.72 -9.67	+4.53 -12.25
J1852+4855	2 σ	-0.65 ^{+1.10} _{-0.85}	+2.50 -0.82	+3.63 -0.85	3.56 ^{+0.70} _{-0.89}	+1.86 -1.03	+1.93 -1.36	-2.75 ^{+0.21} _{-0.19}	+0.45 -0.46	+0.66 -0.51	-8.82 ^{+1.71} _{-1.82}	+2.13 -4.34	+2.62 -5.05
J1854+7351		2.66 ^{+1.02} _{-1.31}	+1.25 -3.70	+1.99 -4.13	3.44 ^{+1.36} _{-0.59}	+1.95 -2.29	+2.03 -3.56	-3.06 ^{+0.88} _{-0.31}	+1.68 -0.28	+1.77 -0.31	-10.92 ^{+2.64} _{-1.72}	+5.21 -3.73	+7.23 -4.38
J1900+2701		2.22 ^{+0.94} _{-0.53}	+1.97 -2.49	+2.69 -3.35	2.30 ^{+1.89} _{-0.87}	+3.08 -2.20	+3.18 -3.75	-1.57 ^{+0.31} _{-1.13}	+0.31 -1.73	+0.32 -1.80	-7.14 ^{+1.35} _{-3.89}	+3.24 -6.62	+4.42 -7.89
J1900+2722		3.93 ^{+1.44} _{-0.82}	+1.56 -2.79	+1.55 -5.06	4.42 ^{+1.08} _{-2.38}	+1.05 -5.13	+1.08 -5.70	-1.70 ^{+0.37} _{-1.10}	+0.34 -1.66	+0.46 -1.66	-13.66 ^{+6.12} _{-1.93}	+10.15 -3.73	+11.65 -5.06
J1909+4833		2.52 ^{+1.15} _{-1.51}	+1.39 -4.02	+2.76 -4.02	3.55 ^{+1.73} _{-0.90}	+1.92 -3.06	+1.92 -4.31	-2.82 ^{+0.77} _{-0.31}	+1.49 -0.30	+1.55 -0.33	-9.93 ^{+2.27} _{-3.24}	+4.24 -5.51	+6.59 -5.51
J1912+3740		3.27 ^{+0.99} _{-1.34}	+2.17 -3.66	+2.17 -4.72	4.50 ^{+0.94} _{-2.34}	+0.97 -5.09	+0.97 -5.96	-3.11 ^{+1.16} _{-0.24}	+1.76 -0.24	+1.87 -0.25	-11.12 ^{+4.58} _{-3.34}	+8.15 -4.78	+9.36 -5.12
J1916-1519	1 σ	0.57 ^{+1.16} _{-0.81}	+1.47 -1.86	+1.86 -2.01	2.69 ^{+1.67} _{-0.67}	+2.67 -0.75	+2.77 -1.09	-2.40 ^{+0.17} _{-0.45}	+0.49 -0.85	+0.85 -0.88	-7.38 ^{+1.65} _{-3.14}	+1.88 -5.48	+2.25 -6.07
J1917-1921		1.68 ^{+1.98} _{-1.55}	+3.57 -2.54	+3.76 -3.12	2.68 ^{+2.15} _{-1.13}	+2.77 -2.96	+2.79 -4.12	-2.93 ^{+1.09} _{-0.17}	+1.56 -0.32	+1.63 -0.38	-8.53 ^{+2.30} _{-6.09}	+6.02 -8.44	+6.92 -11.41
J1918+5520		2.27 ^{+0.85} _{-0.88}	+1.53 -3.27	+3.08 -3.70	2.58 ^{+1.78} _{-1.07}	+2.92 -2.78	+2.91 -4.04	-1.54 ^{+0.29} _{-1.22}	+0.24 -1.81	+0.29 -1.82	-7.99 ^{+0.92} _{-4.85}	+4.21 -6.36	+5.41 -7.43
J1923+3941		4.75 ^{+0.74} _{-1.27}	+0.75 -3.35	+0.75 -5.28	4.44 ^{+0.98} _{-2.69}	+0.96 -5.45	+1.03 -5.92	-2.09 ^{+0.87} _{-0.52}	+0.87 -1.15	+0.87 -1.26	-15.29 ^{+7.46} _{-1.36}	+10.56 -3.52	+11.84 -4.12
J1923+4754		2.93 ^{+1.47} _{-1.26}	+2.55 -3.01	+2.55 -4.25	4.61 ^{+0.81} _{-2.49}	+0.87 -5.08	+0.86 -6.04	-2.90 ^{+1.11} _{-0.21}	+1.60 -0.21	+1.65 -0.21	-12.01 ^{+5.94} _{-1.37}	+8.26 -3.67	+9.37 -5.24
J1927+6117		2.42 ^{+0.85} _{-0.57}	+1.85 -3.27	+2.73 -3.90	2.64 ^{+1.46} _{-1.03}	+2.76 -3.18	+2.83 -4.12	-1.43 ^{+0.28} _{-1.31}	+0.22 -1.93	+0.30 -1.94	-7.02 ^{+2.11} _{-2.28}	+4.83 -4.22	+5.46 -5.41

Table C.2: Results of fitting the broken power-law model over the 1290 selected observations from OVRO dataset. Break significance refers to the source having a possible break frequency being (1σ) at 68.3%, (2σ) at 95.5% and (3σ) at 99.7%. The absence of break significance means that the source is not well-fitted at any level.

Name	Break significance	β_l	$\beta_l^{95.5\%}$	$\beta_l^{99.7\%}$	β_h	$\beta_h^{95.5\%}$	$\beta_h^{99.7\%}$	$\log f_{br}$	$\log f_{br}^{95.5\%}$	$\log f_{br}^{99.7\%}$	$\log A$	$\log A^{95.5\%}$	$\log A^{99.7\%}$
J1927+7358		$3.40^{+0.72}_{-0.79}$	$+1.60_{-3.52}$	$+1.60_{-4.85}$	$4.29^{+1.09}_{-1.43}$	$+1.19_{-4.75}$	$+1.19_{-5.74}$	$-3.09^{+1.27}_{-0.27}$	$+1.75_{-0.27}$	$+1.85_{-0.28}$	$-10.22^{+3.66}_{-1.89}$	$+8.07_{-2.87}$	$+9.02_{-3.73}$
J1933+6540		$2.31^{+0.87}_{-0.82}$	$+1.20_{-3.24}$	$+2.28_{-3.72}$	$2.66^{+1.42}_{-0.76}$	$+2.82_{-1.81}$	$+2.82_{-3.33}$	$-1.60^{+0.35}_{-1.11}$	$+0.30_{-1.72}$	$+0.36_{-1.76}$	$-7.19^{+1.13}_{-2.90}$	$+2.57_{-5.77}$	$+3.97_{-5.77}$
J1934+6138		$2.43^{+0.85}_{-0.89}$	$+2.26_{-2.62}$	$+2.82_{-3.54}$	$2.30^{+2.27}_{-0.88}$	$+3.18_{-2.62}$	$+3.19_{-3.33}$	$-1.67^{+0.43}_{-1.08}$	$+0.43_{-1.62}$	$+0.43_{-1.70}$	$-7.77^{+2.37}_{-3.61}$	$+3.26_{-7.89}$	$+4.92_{-8.21}$
J1936+7131		$4.92^{+0.57}_{-1.38}$	$+0.57_{-3.23}$	$+0.57_{-4.40}$	$4.39^{+0.88}_{-2.66}$	$+1.11_{-5.20}$	$+1.10_{-5.85}$	$-1.53^{+0.33}_{-1.00}$	$+0.33_{-1.67}$	$+0.33_{-1.80}$	$-13.96^{+5.10}_{-3.39}$	$+9.47_{-4.49}$	$+11.86_{-5.36}$
J1936-0402		$2.61^{+0.82}_{-0.82}$	$+1.16_{-3.37}$	$+1.67_{-4.01}$	$3.03^{+2.10}_{-0.60}$	$+2.47_{-2.63}$	$+2.47_{-4.00}$	$-1.58^{+0.33}_{-1.20}$	$+0.33_{-1.70}$	$+0.33_{-1.78}$	$-9.16^{+2.24}_{-3.16}$	$+4.29_{-5.71}$	$+6.12_{-6.79}$
J1938-1749		$3.79^{+0.90}_{-1.27}$	$+1.70_{-2.19}$	$+1.70_{-4.08}$	$4.34^{+1.05}_{-2.38}$	$+1.16_{-5.17}$	$+1.12_{-5.80}$	$-1.60^{+0.39}_{-0.98}$	$+0.36_{-1.65}$	$+0.40_{-1.71}$	$-11.98^{+3.76}_{-3.74}$	$+7.77_{-5.26}$	$+10.11_{-5.04}$
J1939-1525		$2.61^{+0.68}_{-0.63}$	$+1.45_{-2.05}$	$+2.39_{-2.72}$	$2.83^{+2.04}_{-0.90}$	$+2.65_{-3.06}$	$+2.65_{-4.21}$	$-1.60^{+0.39}_{-0.88}$	$+0.39_{-1.61}$	$+0.39_{-1.74}$	$-7.97^{+2.22}_{-3.20}$	$+4.56_{-5.32}$	$+6.27_{-5.37}$
J1947-0103		$2.64^{+1.26}_{-0.95}$	$+2.38_{-2.59}$	$+2.56_{-4.03}$	$2.35^{+2.43}_{-0.95}$	$+3.15_{-2.72}$	$+3.15_{-3.83}$	$-1.54^{+0.30}_{-1.21}$	$+0.27_{-1.78}$	$+0.30_{-1.83}$	$-7.89^{+2.95}_{-4.20}$	$+4.13_{-7.48}$	$+5.63_{-9.33}$
J1949-1957		$3.00^{+0.72}_{-0.64}$	$+1.75_{-2.47}$	$+2.48_{-4.23}$	$2.75^{+1.94}_{-1.10}$	$+2.56_{-3.85}$	$+2.71_{-4.12}$	$-1.50^{+0.29}_{-1.14}$	$+0.28_{-1.76}$	$+0.29_{-1.84}$	$-8.19^{+2.97}_{-3.12}$	$+3.98_{-6.74}$	$+5.94_{-6.74}$
J1951+0134		$2.13^{+1.01}_{-1.11}$	$+1.80_{-2.99}$	$+3.20_{-3.58}$	$2.65^{+2.16}_{-1.00}$	$+2.82_{-2.74}$	$+2.82_{-4.06}$	$-2.95^{+1.03}_{-0.35}$	$+1.61_{-0.36}$	$+1.74_{-0.37}$	$-8.54^{+3.47}_{-3.52}$	$+4.65_{-6.98}$	$+5.92_{-8.05}$
J1951-0509		$2.31^{+0.68}_{-0.81}$	$+2.17_{-2.95}$	$+2.88_{-3.80}$	$2.46^{+1.91}_{-0.67}$	$+3.04_{-1.65}$	$+3.04_{-2.73}$	$-2.14^{+0.21}_{-1.14}$	$+0.78_{-1.21}$	$+0.89_{-1.22}$	$-7.42^{+1.47}_{-3.45}$	$+3.27_{-5.77}$	$+4.11_{-6.29}$
J1954-1123		$2.18^{+0.51}_{-1.08}$	$+0.77_{-3.63}$	$+2.40_{-3.63}$	$2.64^{+0.92}_{-0.50}$	$+2.44_{-0.59}$	$+2.85_{-0.67}$	$-3.03^{+1.10}_{-0.24}$	$+1.78_{-0.23}$	$+1.81_{-0.30}$	$-6.42^{+0.91}_{-1.66}$	$+1.12_{-3.88}$	$+1.29_{-5.02}$
J1955+0618		$2.28^{+1.45}_{-1.37}$	$+2.88_{-3.34}$	$+3.19_{-3.76}$	$3.49^{+2.01}_{-1.25}$	$+2.01_{-4.03}$	$+2.01_{-4.77}$	$-3.00^{+0.98}_{-0.31}$	$+1.55_{-0.31}$	$+1.70_{-0.31}$	$-12.38^{+5.64}_{-1.87}$	$+8.14_{-4.99}$	$+9.54_{-5.68}$
J1955+5131	1σ	$0.56^{+1.04}_{-1.67}$	$+2.11_{-2.03}$	$+3.02_{-2.05}$	$3.28^{+1.47}_{-0.48}$	$+2.21_{-0.84}$	$+2.21_{-1.22}$	$-2.88^{+0.23}_{-0.26}$	$+0.79_{-0.49}$	$+1.56_{-0.49}$	$-9.14^{+1.55}_{-3.11}$	$+2.90_{-4.64}$	$+3.58_{-5.73}$
J1959+6508		$1.57^{+0.65}_{-0.73}$	$+1.33_{-2.65}$	$+3.87_{-2.71}$	$2.10^{+2.29}_{-0.56}$	$+3.40_{-1.28}$	$+3.40_{-2.43}$	$-2.33^{+1.01}_{-0.28}$	$+1.13_{-0.95}$	$+1.20_{-1.04}$	$-6.81^{+1.76}_{-3.47}$	$+1.95_{-6.93}$	$+3.03_{-6.93}$
J2000-1325		$2.25^{+0.62}_{-0.84}$	$+1.32_{-3.14}$	$+2.81_{-3.60}$	$2.56^{+1.79}_{-0.71}$	$+2.95_{-2.18}$	$+2.94_{-3.64}$	$-1.49^{+0.28}_{-1.79}$	$+0.27_{-1.75}$	$+0.29_{-1.83}$	$-6.63^{+1.62}_{-2.77}$	$+3.40_{-5.59}$	$+4.98_{-5.99}$
J2000-1748		$2.29^{+0.68}_{-1.23}$	$+1.54_{-3.77}$	$+2.72_{-3.77}$	$2.44^{+0.87}_{-0.55}$	$+2.86_{-1.84}$	$+3.02_{-2.83}$	$-3.04^{+1.34}_{-0.29}$	$+1.88_{-0.29}$	$+1.94_{-0.29}$	$-4.84^{+1.19}_{-1.29}$	$+2.97_{-3.45}$	$+3.49_{-4.41}$
J2001+4352		$1.36^{+0.78}_{-0.96}$	$+1.35_{-2.78}$	$+2.57_{-2.77}$	$1.99^{+2.25}_{-0.63}$	$+3.51_{-1.46}$	$+3.51_{-3.27}$	$-2.33^{+0.94}_{-0.45}$	$+1.28_{-0.80}$	$+1.31_{-0.94}$	$-6.77^{+1.54}_{-3.83}$	$+2.83_{-6.64}$	$+4.02_{-8.00}$
J2004+7355		$2.63^{+1.09}_{-0.97}$	$+1.61_{-3.97}$	$+2.76_{-3.97}$	$2.86^{+2.09}_{-0.78}$	$+2.63_{-2.65}$	$+2.63_{-3.23}$	$-3.06^{+1.17}_{-0.25}$	$+1.76_{-0.25}$	$+1.85_{-0.26}$	$-9.48^{+2.52}_{-4.08}$	$+5.26_{-5.44}$	$+6.13_{-6.52}$
J2005+7752		$2.38^{+0.41}_{-0.59}$	$+1.00_{-3.12}$	$+2.52_{-3.77}$	$2.52^{+1.51}_{-0.62}$	$+2.96_{-1.42}$	$+2.95_{-3.20}$	$-1.51^{+0.38}_{-1.19}$	$+0.37_{-1.78}$	$+0.38_{-1.86}$	$-6.52^{+1.09}_{-2.30}$	$+2.33_{-4.41}$	$+4.22_{-5.23}$
J2006+6424		$2.56^{+0.81}_{-0.60}$	$+1.78_{-2.43}$	$+1.79_{-3.97}$	$2.94^{+1.67}_{-0.92}$	$+2.25_{-3.75}$	$+2.53_{-4.27}$	$-1.55^{+0.23}_{-1.27}$	$+0.22_{-1.81}$	$+0.31_{-1.82}$	$-8.32^{+2.09}_{-3.09}$	$+5.84_{-4.49}$	$+6.67_{-5.70}$
J2007+0636		$2.45^{+0.74}_{-1.34}$	$+1.48_{-3.47}$	$+2.96_{-3.89}$	$3.51^{+1.23}_{-1.54}$	$+1.97_{-3.07}$	$+1.98_{-4.52}$	$-2.97^{+1.02}_{-0.36}$	$+1.66_{-0.36}$	$+1.77_{-0.36}$	$-8.08^{+1.49}_{-4.45}$	$+3.58_{-7.05}$	$+5.20_{-8.20}$
J2007+6607		$2.71^{+0.96}_{-0.72}$	$+1.48_{-3.73}$	$+2.72_{-4.17}$	$3.13^{+1.42}_{-1.13}$	$+2.19_{-2.97}$	$+2.36_{-4.26}$	$-3.12^{+1.35}_{-0.19}$	$+1.84_{-0.20}$	$+1.88_{-0.20}$	$-8.83^{+2.92}_{-2.32}$	$+4.61_{-5.12}$	$+7.03_{-5.12}$
J2009+0727		$1.96^{+0.66}_{-0.95}$	$+1.13_{-3.09}$	$+2.32_{-3.45}$	$2.47^{+1.04}_{-0.71}$	$+2.77_{-0.71}$	$+2.98_{-1.68}$	$-3.04^{+1.32}_{-0.17}$	$+1.68_{-0.28}$	$+1.82_{-0.28}$	$-7.38^{+1.26}_{-2.09}$	$+1.72_{-4.73}$	$+2.79_{-5.29}$

Table C.2: Results of fitting the broken power-law model over the 1290 selected observations from OVRO dataset. Break significance refers to the source having a possible break frequency being (1σ) at 68.3%, (2σ) at 95.5% and (3σ) at 99.7%. The absence of break significance means that the source is not well-fitted at any level.

Name	Break significance	β_l	$\beta_l^{95.5\%}$	$\beta_l^{99.7\%}$	β_h	$\beta_h^{95.5\%}$	$\beta_h^{99.7\%}$	$\log f_{br}$	$\log f_{br}^{95.5\%}$	$\log f_{br}^{99.7\%}$	$\log A$	$\log A^{95.5\%}$	$\log A^{99.7\%}$
J2009+7229		2.25 ^{+0.79} _{-0.79}	+1.46 -3.41	+3.07 -3.40	2.36 ^{+1.74} _{-0.82}	+3.07 -2.43	+3.15 -3.63	-1.46 ^{+0.26} _{-1.26}	+0.20 -1.86	+0.26 -1.86	-6.77 ^{+1.96} _{-2.84}	+3.78 -5.68	+5.47 -6.29
J2011-1546		2.25 ^{+0.79} _{-1.30}	+1.20 -3.49	+2.77 -3.75	3.11 ^{+0.92} _{-0.74}	+2.15 -1.03	+2.29 -1.96	-3.07 ^{+0.81} _{-0.25}	+1.75 -0.30	+1.94 -0.29	-7.93 ^{+2.21} _{-1.38}	+2.66 -3.92	+3.97 -4.77
J2015+6554		2.62 ^{+1.05} _{-1.00}	+1.14 -4.10	+2.33 -4.08	3.03 ^{+1.66} _{-0.47}	+2.47 -2.29	+2.46 -4.29	-3.09 ^{+1.06} _{-0.28}	+1.71 -0.28	+1.84 -0.28	-8.34 ^{+1.09} _{-3.64}	+3.62 -5.12	+5.66 -6.01
J2015-0137		2.67 ^{+1.16} _{-0.69}	+2.44 -3.05	+2.40 -4.02	3.06 ^{+2.16} _{-1.26}	+2.34 -3.80	+2.42 -4.40	-1.55 ^{+0.31} _{-1.17}	+0.35 -1.66	+0.35 -1.76	-8.58 ^{+3.07} _{-4.17}	+5.72 -5.81	+6.42 -7.05
J2015-1252		2.61 ^{+0.93} _{-0.84}	+1.51 -4.05	+2.84 -4.05	2.40 ^{+2.46} _{-0.59}	+2.98 -2.57	+3.09 -3.57	-1.58 ^{+0.36} _{-1.07}	+0.37 -1.68	+0.36 -1.76	-7.74 ^{+1.90} _{-3.87}	+3.18 -7.41	+5.10 -7.67
J2016+1632		2.72 ^{+0.84} _{-0.68}	+1.66 -2.44	+2.72 -2.92	2.41 ^{+2.11} _{-0.56}	+3.07 -1.39	+3.06 -3.76	-1.54 ^{+0.34} _{-1.24}	+0.32 -1.83	+0.41 -1.83	-6.92 ^{+1.42} _{-4.03}	+2.32 -6.15	+5.16 -6.49
J2018-0509	2σ	1.31 ^{+0.82} _{-1.46}	+0.84 -2.78	+1.88 -2.78	3.09 ^{+1.16} _{-0.40}	+2.29 -0.53	+2.37 -0.96	-2.85 ^{+0.55} _{-0.08}	+0.79 -0.34	+0.99 -0.48	-8.49 ^{+0.92} _{-2.43}	+1.27 -4.69	+2.17 -4.94
J2020+6747		2.64 ^{+1.79} _{-0.98}	+2.27 -3.57	+2.77 -4.03	2.90 ^{+2.56} _{-0.54}	+2.56 -3.18	+2.58 -4.37	-3.09 ^{+1.10} _{-0.27}	+1.78 -0.26	+1.84 -0.28	-8.72 ^{+1.14} _{-6.61}	+3.81 -8.61	+5.96 -8.72
J2021+0515		2.77 ^{+2.71} _{-0.49}	+2.72 -2.34	+2.72 -3.81	2.06 ^{+3.42} _{-0.43}	+3.43 -2.71	+3.43 -3.47	-1.48 ^{+0.29} _{-1.18}	+0.28 -1.78	+0.29 -1.84	-8.99 ^{+3.31} _{-4.86}	+5.69 -8.38	+6.41 -10.03
J2022+6136		1.66 ^{+0.90} _{-1.07}	+3.34 -2.11	+3.73 -3.02	1.99 ^{+1.80} _{-1.19}	+3.50 -1.96	+3.48 -3.41	-1.53 ^{+0.40} _{-1.16}	+0.40 -1.75	+0.41 -1.84	-5.88 ^{+1.90} _{-3.95}	+3.66 -6.90	+4.73 -8.03
J2022+7611		2.81 ^{+1.05} _{-0.62}	+1.55 -4.27	+2.56 -4.27	2.78 ^{+2.24} _{-0.70}	+2.72 -2.92	+2.72 -4.13	-1.59 ^{+0.18} _{-1.34}	+0.38 -1.64	+0.39 -1.73	-9.72 ^{+4.39} _{-1.47}	+7.16 -3.37	+8.28 -4.54
J2023-0123		1.22 ^{+0.71} _{-0.86}	+0.76 -2.44	+1.07 -2.70	2.27 ^{+1.63} _{-0.50}	+3.00 -0.55	+3.20 -0.69	-1.93 ^{+0.35} _{-0.66}	+0.61 -1.11	+0.66 -1.37	-6.26 ^{+0.88} _{-2.86}	+0.88 -5.34	+1.25 -6.16
J2024+1718		3.79 ^{+0.83} _{-0.94}	+1.67 -1.96	+1.66 -3.53	4.37 ^{+0.93} _{-2.41}	+1.10 -5.20	+1.10 -5.86	-1.54 ^{+0.41} _{-1.06}	+0.40 -1.77	+0.40 -1.83	-12.30 ^{+6.11} _{-1.10}	+8.34 -3.40	+9.99 -4.13
J2025+0316	1σ	0.92 ^{+0.65} _{-1.47}	+1.27 -2.40	+1.78 -2.41	3.16 ^{+1.59} _{-0.45}	+2.21 -1.08	+2.33 -1.32	-2.73 ^{+0.37} _{-0.24}	+0.62 -0.54	+1.03 -0.58	-8.69 ^{+1.38} _{-3.21}	+2.40 -4.93	+2.78 -5.69
J2030-0503		1.81 ^{+2.34} _{-1.16}	+3.69 -2.25	+3.69 -3.25	1.95 ^{+2.62} _{-0.91}	+3.52 -2.58	+3.52 -3.40	-2.25 ^{+0.32} _{-1.12}	+0.93 -1.09	+1.01 -1.12	-7.56 ^{+2.03} _{-5.66}	+3.17 -10.30	+4.98 -11.14
J2030-0622		1.79 ^{+0.74} _{-0.71}	+1.78 -2.91	+3.70 -2.88	1.85 ^{+2.02} _{-0.75}	+3.65 -1.45	+3.63 -2.24	-1.74 ^{+0.56} _{-0.85}	+0.53 -1.50	+0.56 -1.57	-6.14 ^{+1.55} _{-3.52}	+2.11 -7.02	+3.03 -7.76
J2031+0239	1σ	1.22 ^{+1.26} _{-0.92}	+1.47 -2.53	+2.52 -2.72	3.13 ^{+1.34} _{-0.50}	+2.37 -0.67	+2.37 -1.19	-2.53 ^{+0.22} _{-0.51}	+0.50 -0.70	+0.68 -0.79	-9.09 ^{+1.33} _{-2.81}	+2.03 -4.71	+3.02 -5.28
J2031+1219		2.53 ^{+0.71} _{-0.55}	+1.13 -3.13	+2.07 -3.98	2.63 ^{+1.57} _{-0.79}	+2.87 -1.89	+2.84 -3.54	-1.45 ^{+0.32} _{-1.28}	+0.32 -1.86	+0.32 -1.92	-6.34 ^{+1.43} _{-2.21}	+2.67 -4.97	+4.49 -5.48
J2033+2146		2.08 ^{+1.00} _{-0.79}	+1.34 -3.43	+3.25 -3.43	2.32 ^{+2.23} _{-0.60}	+3.13 -2.00	+3.13 -3.77	-3.08 ^{+1.31} _{-0.25}	+1.89 -0.26	+1.97 -0.26	-7.42 ^{+1.67} _{-3.75}	+3.14 -6.17	+4.97 -6.92
J2035+1056	3σ	1.56 ^{+0.41} _{-0.27}	+0.63 -0.66	+0.79 -0.94	5.11 ^{+0.39} _{-0.96}	+0.38 -1.99	+0.39 -2.41	-1.92 ^{+0.09} _{-0.14}	+0.14 -0.38	+0.21 -0.51	-10.17 ^{+1.81} _{-0.61}	+3.27 -0.77	+4.08 -0.88
J2036-0629		2.23 ^{+0.92} _{-0.99}	+1.01 -3.38	+2.45 -3.71	2.81 ^{+1.91} _{-0.69}	+2.69 -1.82	+2.66 -3.87	-2.62 ^{+0.70} _{-0.72}	+1.44 -0.72	+1.50 -0.74	-7.96 ^{+2.12} _{-3.09}	+3.20 -6.02	+5.99 -7.06
J2037-1522		2.23 ^{+0.90} _{-1.26}	+1.53 -3.68	+2.97 -3.61	2.63 ^{+2.26} _{-0.79}	+2.87 -2.55	+2.87 -3.84	-3.07 ^{+1.22} _{-0.29}	+1.77 -0.29	+1.84 -0.29	-8.29 ^{+1.57} _{-5.03}	+4.08 -7.06	+5.48 -9.35
J2039-1046		2.29 ^{+0.89} _{-1.15}	+1.44 -3.32	+3.10 -3.73	2.72 ^{+1.93} _{-0.68}	+2.66 -2.24	+2.66 -4.15	-2.94 ^{+1.03} _{-0.37}	+1.63 -0.36	+1.75 -0.37	-7.69 ^{+1.90} _{-3.68}	+3.78 -5.86	+5.27 -6.49
J2042+7508		1.80 ^{+1.33} _{-0.87}	+2.88 -2.63	+3.58 -3.08	2.24 ^{+2.17} _{-1.12}	+3.13 -2.47	+3.23 -3.63	-1.85 ^{+0.03} _{-1.42}	+0.61 -1.41	+0.65 -1.47	-6.83 ^{+2.17} _{-4.35}	+3.04 -8.96	+4.44 -9.55

Table C.2: Results of fitting the broken power-law model over the 1290 selected observations from OVRO dataset. Break significance refers to the source having a possible break frequency being (1σ) at 68.3%, (2σ) at 95.5% and (3σ) at 99.7%. The absence of break significance means that the source is not well-fitted at any level.

Name	Break significance	β_l	$\beta_l^{95.5\%}$	$\beta_l^{99.7\%}$	β_h	$\beta_h^{95.5\%}$	$\beta_h^{99.7\%}$	$\log f_{br}$	$\log f_{br}^{95.5\%}$	$\log f_{br}^{99.7\%}$	$\log A$	$\log A^{95.5\%}$	$\log A^{99.7\%}$
J2043+1255		$3.40^{+1.11}_{-1.55}$	$+2.09$ -4.17	$+2.09$ -4.89	$4.49^{+1.00}_{-2.12}$	$+1.00$ -4.83	$+0.99$ -5.95	$-3.07^{+1.27}_{-0.30}$	$+1.93$ -0.22	$+1.93$ -0.30	$-13.85^{+4.25}_{-3.35}$	$+9.41$ -3.68	$+11.03$ -5.31
J2045-1858		$1.95^{+0.98}_{-0.68}$	$+2.15$ -2.45	$+3.50$ -3.23	$2.22^{+2.40}_{-0.73}$	$+3.24$ -2.86	$+3.24$ -3.52	$-1.71^{+0.46}_{-0.92}$	$+0.36$ -1.64	$+0.45$ -1.66	$-7.37^{+2.06}_{-4.25}$	$+3.79$ -7.64	$+4.98$ -8.52
J2049+1003		$2.44^{+0.70}_{-0.81}$	$+1.12$ -3.53	$+1.75$ -3.93	$2.87^{+1.89}_{-0.59}$	$+2.62$ -2.28	$+2.62$ -3.60	$-3.08^{+1.32}_{-0.21}$	$+1.98$ -0.16	$+1.99$ -0.24	$-8.06^{+1.75}_{-2.90}$	$+4.17$ -5.09	$+5.33$ -6.52
J2050+0407		$2.49^{+0.97}_{-0.83}$	$+2.99$ -1.72	$+2.97$ -3.84	$2.54^{+2.15}_{-1.18}$	$+2.94$ -3.00	$+2.94$ -4.03	$-1.51^{+0.42}_{-1.07}$	$+0.39$ -1.74	$+0.43$ -1.81	$-7.61^{+2.61}_{-4.10}$	$+4.33$ -7.14	$+5.27$ -8.66
J2051+1743		$2.08^{+0.63}_{-1.60}$	$+0.74$ -3.38	$+1.10$ -3.55	$2.85^{+1.40}_{-0.66}$	$+2.44$ -1.08	$+2.64$ -2.14	$-2.83^{+0.55}_{-0.49}$	$+1.55$ -0.52	$+1.70$ -0.53	$-8.21^{+1.84}_{-2.32}$	$+2.73$ -4.46	$+3.93$ -5.61
J2101+0341		$2.94^{+0.66}_{-0.93}$	$+1.19$ -3.73	$+1.89$ -4.40	$3.22^{+1.79}_{-0.79}$	$+2.28$ -3.15	$+2.27$ -4.64	$-3.05^{+1.25}_{-0.32}$	$+1.83$ -0.32	$+1.83$ -0.32	$-8.38^{+1.88}_{-3.15}$	$+5.07$ -4.73	$+6.51$ -5.54
J2102+6758		$2.67^{+0.92}_{-1.82}$	$+1.28$ -3.77	$+1.63$ -4.15	$3.65^{+1.64}_{-0.73}$	$+1.80$ -2.78	$+1.80$ -3.91	$-3.00^{+0.63}_{-0.36}$	$+1.64$ -0.34	$+1.75$ -0.37	$-10.31^{+1.70}_{-4.07}$	$+5.00$ -5.49	$+6.66$ -5.49
J2106+2135		$2.53^{+1.27}_{-0.81}$	$+1.90$ -3.42	$+2.96$ -3.84	$3.01^{+2.02}_{-1.12}$	$+2.49$ -3.64	$+2.49$ -4.45	$-3.10^{+1.31}_{-0.27}$	$+1.87$ -0.27	$+1.96$ -0.27	$-10.47^{+4.47}_{-2.21}$	$+6.72$ -5.15	$+8.19$ -5.85
J2108+1430		$2.30^{+0.86}_{-1.92}$	$+1.06$ -3.75	$+1.70$ -3.74	$3.12^{+1.49}_{-0.74}$	$+2.38$ -1.64	$+2.38$ -3.76	$-2.89^{+0.59}_{-0.46}$	$+1.59$ -0.44	$+1.76$ -0.47	$-8.59^{+1.74}_{-3.05}$	$+2.77$ -5.89	$+6.01$ -5.89
J2110+0809		$2.46^{+0.86}_{-0.68}$	$+1.51$ -3.20	$+2.50$ -3.92	$3.09^{+1.61}_{-1.09}$	$+2.41$ -3.07	$+2.38$ -4.27	$-1.40^{+0.33}_{-1.23}$	$+0.33$ -1.80	$+0.33$ -1.90	$-9.41^{+2.53}_{-2.55}$	$+5.22$ -4.45	$+7.05$ -6.68
J2110-1020		$4.94^{+0.55}_{-1.12}$	$+0.56$ -3.10	$+0.55$ -3.74	$3.00^{+2.29}_{-1.64}$	$+2.30$ -4.01	$+2.50$ -4.42	$-1.56^{+0.34}_{-0.97}$	$+0.42$ -1.60	$+0.43$ -1.76	$-12.35^{+4.41}_{-4.54}$	$+8.81$ -5.66	$+9.63$ -7.22
J2114+2832		$2.24^{+0.92}_{-0.81}$	$+1.82$ -3.57	$+3.20$ -3.57	$2.45^{+2.39}_{-0.77}$	$+3.02$ -2.78	$+3.02$ -3.87	$-1.41^{+0.26}_{-1.31}$	$+0.18$ -1.94	$+0.31$ -1.94	$-7.06^{+2.45}_{-3.18}$	$+4.45$ -6.27	$+5.29$ -6.76
J2115+2933		$1.96^{+0.51}_{-1.84}$	$+0.68$ -3.33	$+0.97$ -3.44	$2.63^{+1.06}_{-0.66}$	$+2.49$ -1.07	$+2.83$ -1.22	$-2.89^{+0.70}_{-0.45}$	$+1.69$ -0.37	$+1.75$ -0.45	$-7.54^{+1.74}_{-1.56}$	$+2.77$ -3.85	$+2.77$ -5.79
J2115-1416		$4.45^{+0.39}_{-2.80}$	$+1.05$ -4.22	$+1.05$ -5.27	$4.51^{+0.93}_{-2.91}$	$+0.99$ -5.41	$+0.99$ -5.95	$-1.55^{+0.35}_{-1.03}$	$+0.35$ -1.67	$+0.35$ -1.77	$-7.51^{+1.87}_{-7.33}$	$+3.58$ -10.72	$+4.62$ -11.67
J2117+0503		$2.27^{+0.56}_{-0.94}$	$+1.64$ -2.72	$+3.08$ -3.57	$2.99^{+2.32}_{-0.70}$	$+2.51$ -3.37	$+2.50$ -4.35	$-2.47^{+1.29}_{-0.13}$	$+1.29$ -0.85	$+1.34$ -0.89	$-10.06^{+4.76}_{-1.00}$	$+6.31$ -4.43	$+8.29$ -4.53
J2118+0013	2σ	$1.12^{+0.43}_{-0.61}$	$+0.72$ -1.39	$+1.40$ -1.76	$4.53^{+0.79}_{-1.01}$	$+0.87$ -2.13	$+0.97$ -2.51	$-2.17^{+0.17}_{-0.15}$	$+0.31$ -0.44	$+0.54$ -0.60	$-10.70^{+1.99}_{-1.49}$	$+4.25$ -1.74	$+4.92$ -2.00
J2118-0636		$2.05^{+1.10}_{-0.68}$	$+1.38$ -2.91	$+1.78$ -3.28	$3.28^{+1.47}_{-1.38}$	$+2.21$ -2.29	$+2.20$ -4.26	$-2.38^{+0.33}_{-0.99}$	$+0.98$ -0.99	$+1.14$ -0.99	$-10.27^{+3.81}_{-1.99}$	$+5.30$ -5.13	$+7.43$ -6.07
J2120+0533		$2.79^{+0.70}_{-0.91}$	$+1.16$ -3.40	$+1.21$ -4.05	$3.20^{+1.75}_{-0.77}$	$+2.30$ -2.99	$+2.28$ -4.68	$-3.11^{+1.33}_{-0.25}$	$+1.92$ -0.24	$+1.98$ -0.25	$-9.58^{+2.66}_{-2.56}$	$+5.26$ -5.20	$+7.30$ -5.65
J2123+0535		$2.48^{+0.75}_{-1.40}$	$+0.81$ -3.66	$+1.10$ -3.89	$3.10^{+0.83}_{-0.66}$	$+2.15$ -0.81	$+2.40$ -1.15	$-2.99^{+0.75}_{-0.34}$	$+1.49$ -0.37	$+1.83$ -0.38	$-7.21^{+1.05}_{-1.92}$	$+1.86$ -4.09	$+2.16$ -4.90
J2125+0441		$2.12^{+0.60}_{-0.72}$	$+1.46$ -3.57	$+3.09$ -3.58	$2.47^{+2.17}_{-0.65}$	$+2.97$ -2.71	$+3.02$ -3.65	$-2.21^{+1.08}_{-0.42}$	$+1.04$ -1.11	$+1.08$ -1.16	$-7.81^{+1.73}_{-3.67}$	$+4.43$ -5.71	$+5.10$ -6.78
J2128-0244		$2.68^{+0.88}_{-2.15}$	$+0.87$ -4.05	$+1.80$ -4.18	$4.49^{+0.80}_{-1.50}$	$+0.99$ -4.07	$+0.99$ -5.84	$-3.02^{+0.53}_{-0.35}$	$+1.64$ -0.35	$+1.77$ -0.35	$-10.98^{+1.66}_{-4.22}$	$+5.84$ -5.19	$+7.59$ -5.38
J2129-1538		$2.61^{+0.83}_{-0.77}$	$+1.75$ -3.93	$+2.88$ -3.95	$2.93^{+1.84}_{-1.01}$	$+2.55$ -2.81	$+2.57$ -4.41	$-3.10^{+1.29}_{-0.22}$	$+1.81$ -0.22	$+1.88$ -0.24	$-8.34^{+2.25}_{-3.54}$	$+4.10$ -6.57	$+6.14$ -6.57
J2130-0927		$2.24^{+0.74}_{-0.95}$	$+3.26$ -1.92	$+3.26$ -3.61	$2.17^{+1.93}_{-1.06}$	$+3.25$ -2.42	$+3.28$ -3.55	$-1.48^{+0.35}_{-1.16}$	$+0.35$ -1.80	$+0.35$ -1.89	$-6.12^{+1.66}_{-3.22}$	$+2.97$ -6.51	$+4.12$ -7.21
J2131-1207		$2.22^{+1.10}_{-0.71}$	$+2.09$ -2.85	$+3.20$ -3.46	$2.23^{+2.23}_{-0.74}$	$+3.26$ -2.38	$+3.25$ -3.71	$-1.52^{+0.31}_{-1.14}$	$+0.31$ -1.73	$+0.32$ -1.80	$-6.43^{+1.98}_{-3.91}$	$+4.07$ -6.03	$+4.82$ -7.19

Table C.2: Results of fitting the broken power-law model over the 1290 selected observations from OVRO dataset. Break significance refers to the source having a possible break frequency being (1σ) at 68.3%, (2σ) at 95.5% and (3σ) at 99.7%. The absence of break significance means that the source is not well-fitted at any level.

Name	Break significance	β_l	$\beta_l^{95.5\%}$	$\beta_l^{99.7\%}$	β_h	$\beta_h^{95.5\%}$	$\beta_h^{99.7\%}$	$\log f_{br}$	$\log f_{br}^{95.5\%}$	$\log f_{br}^{99.7\%}$	$\log A$	$\log A^{95.5\%}$	$\log A^{99.7\%}$
J2133+1443		2.59 ^{+0.59} _{-2.29}	+0.97 -3.81	+1.44 -4.08	3.89 ^{+1.18} _{-0.96}	+1.60 -2.75	+1.59 -4.06	-2.90 ^{+0.45} _{-0.44}	+1.67 -0.39	+1.77 -0.46	-11.11 ^{+2.53} _{-2.41}	+5.40 -4.57	+6.73 -4.46
J2134-0153		2.19 ^{+0.72} _{-0.94}	+3.22 -2.57	+3.25 -3.67	2.41 ^{+1.83} _{-0.57}	+3.08 -1.86	+3.08 -3.36	-3.17 ^{+1.31} _{-0.18}	+1.98 -0.18	+2.05 -0.18	-6.01 ^{+1.23} _{-3.04}	+2.87 -5.78	+4.48 -6.29
J2136+0041		1.00 ^{+0.59} _{-1.32}	+0.94 -2.31	+1.77 -2.49	2.21 ^{+1.67} _{-0.66}	+2.93 -0.86	+3.29 -0.86	-2.44 ^{+0.51} _{-0.36}	+0.98 -0.79	+1.28 -0.90	-4.92 ^{+1.09} _{-3.41}	+1.45 -5.99	+1.85 -6.70
J2139+0122		4.76 ^{+0.74} _{-1.37}	+0.73 -3.32	+0.73 -4.84	4.52 ^{+0.89} _{-2.99}	+0.94 -5.40	+0.98 -5.96	-1.53 ^{+0.29} _{-1.18}	+0.30 -1.83	+0.40 -1.83	-12.53 ^{+6.13} _{-3.07}	+8.06 -6.08	+9.91 -6.43
J2139+1423		2.61 ^{+0.85} _{-0.70}	+2.88 -1.20	+2.87 -3.11	2.48 ^{+2.21} _{-0.81}	+3.01 -2.53	+3.01 -3.48	-1.48 ^{+0.35} _{-1.10}	+0.26 -1.88	+0.35 -1.88	-6.83 ^{+1.69} _{-4.16}	+4.21 -6.15	+5.29 -7.71
J2142-0437		2.11 ^{+0.72} _{-1.06}	+0.90 -3.28	+2.11 -3.55	2.74 ^{+1.81} _{-0.52}	+2.73 -1.69	+2.73 -2.46	-2.65 ^{+0.62} _{-0.69}	+1.35 -0.66	+1.39 -0.72	-7.71 ^{+1.61} _{-3.02}	+2.79 -5.53	+4.06 -6.18
J2143+1743	2σ	0.93 ^{+0.59} _{-0.75}	+0.89 -1.89	+0.91 -2.39	2.60 ^{+0.93} _{-0.47}	+2.62 -0.56	+2.80 -0.83	-1.90 ^{+0.14} _{-0.56}	+0.22 -0.90	+0.26 -1.07	-5.53 ^{+0.90} _{-1.45}	+0.97 -4.14	+1.35 -4.44
J2145+1115		1.95 ^{+0.86} _{-0.65}	+2.47 -2.11	+2.73 -3.39	2.22 ^{+2.23} _{-0.81}	+3.28 -1.99	+3.26 -3.59	-1.45 ^{+0.32} _{-1.16}	+0.32 -1.82	+0.32 -1.92	-8.72 ^{+2.97} _{-2.64}	+5.22 -5.53	+6.33 -7.02
J2146-1525		1.99 ^{+0.76} _{-1.68}	+0.95 -3.38	+2.47 -3.49	2.93 ^{+0.86} _{-0.67}	+2.19 -0.85	+2.46 -1.12	-2.87 ^{+0.35} _{-0.45}	+1.05 -0.47	+1.39 -0.47	-7.91 ^{+1.59} _{-1.81}	+1.65 -4.87	+2.61 -5.44
J2147+0929	1σ	1.67 ^{+0.56} _{-1.53}	+1.38 -2.75	+1.61 -3.17	3.29 ^{+0.86} _{-0.42}	+2.18 -0.44	+2.20 -0.75	-2.58 ^{+0.29} _{-0.43}	+0.62 -0.64	+0.83 -0.77	-7.64 ^{+0.92} _{-1.68}	+1.14 -4.04	+1.87 -4.33
J2148+0657		2.46 ^{+0.74} _{-0.58}	+2.30 -1.49	+2.96 -1.49	2.24 ^{+1.79} _{-1.12}	+3.25 -2.23	+3.25 -3.34	-1.46 ^{+0.34} _{-1.25}	+0.25 -1.91	+0.34 -1.91	-5.68 ^{+1.96} _{-3.02}	+4.05 -5.98	+4.16 -7.67
J2148-1723		3.12 ^{+0.93} _{-0.64}	+2.31 -2.16	+2.31 -3.72	3.28 ^{+1.70} _{-1.02}	+2.22 -3.74	+2.20 -4.59	-1.54 ^{+0.30} _{-1.15}	+0.26 -1.79	+0.33 -1.79	-9.26 ^{+2.70} _{-3.00}	+5.79 -4.61	+6.95 -5.48
J2149+0322		2.73 ^{+1.68} _{-1.15}	+2.76 -2.65	+2.74 -4.14	4.28 ^{+1.00} _{-2.58}	+1.22 -4.79	+1.22 -5.75	-1.53 ^{+0.34} _{-1.08}	+0.26 -1.75	+0.33 -1.79	-10.15 ^{+4.22} _{-4.29}	+6.23 -7.62	+7.33 -9.38
J2151+0552		4.57 ^{+0.93} _{-1.80}	+0.93 -4.36	+0.93 -5.63	2.05 ^{+3.20} _{-0.77}	+3.36 -2.95	+3.45 -3.41	-1.52 ^{+0.38} _{-1.02}	+0.30 -1.84	+0.39 -1.84	-8.94 ^{+3.12} _{-5.72}	+5.68 -8.82	+6.24 -10.76
J2151+0709		2.73 ^{+0.47} _{-0.70}	+2.09 -1.10	+2.75 -1.28	2.40 ^{+2.00} _{-0.94}	+3.08 -2.98	+3.10 -3.64	-1.41 ^{+0.29} _{-1.08}	+0.29 -1.83	+0.29 -1.95	-7.47 ^{+1.92} _{-3.24}	+4.65 -5.17	+5.27 -6.33
J2152+1734		2.35 ^{+0.83} _{-0.78}	+1.30 -2.94	+1.73 -3.68	2.90 ^{+1.39} _{-1.16}	+2.58 -2.95	+2.58 -4.12	-3.00 ^{+1.14} _{-0.36}	+1.86 -0.28	+1.86 -0.36	-8.08 ^{+1.26} _{-3.84}	+5.08 -5.34	+5.68 -6.64
J2153-1136	1σ	1.36 ^{+0.49} _{-0.92}	+0.92 -1.98	+1.26 -2.40	3.00 ^{+1.43} _{-0.39}	+2.24 -0.76	+2.50 -1.08	-2.30 ^{+0.27} _{-0.24}	+0.55 -0.66	+0.86 -0.74	-7.61 ^{+0.91} _{-2.51}	+1.46 -4.34	+2.42 -4.77
J2156-0037	2σ	-0.03 ^{+0.54} _{-1.35}	+1.57 -1.43	+2.34 -1.45	2.79 ^{+0.66} _{-0.37}	+1.43 -0.69	+2.00 -0.86	-2.72 ^{+0.20} _{-0.21}	+0.46 -0.41	+0.68 -0.63	-6.93 ^{+0.84} _{-1.34}	+1.46 -3.23	+1.78 -3.98
J2157+3127		2.33 ^{+0.75} _{-1.42}	+0.86 -3.61	+1.20 -3.81	2.85 ^{+1.11} _{-0.78}	+2.42 -2.99	+2.64 -4.21	-2.96 ^{+0.98} _{-0.37}	+1.76 -0.37	+1.84 -0.39	-6.92 ^{+1.44} _{-2.21}	+4.36 -4.83	+5.74 -5.79
J2158-1501		2.34 ^{+0.51} _{-0.68}	+1.38 -3.77	+2.98 -3.77	2.48 ^{+1.42} _{-0.51}	+2.88 -0.51	+3.01 -1.47	-1.74 ^{+0.01} _{-1.60}	+0.55 -1.59	+0.61 -1.60	-5.14 ^{+0.96} _{-2.33}	+1.02 -4.91	+2.39 -5.53
J2200+0234	2σ	0.73 ^{+0.87} _{-1.30}	+1.51 -2.20	+2.08 -2.22	4.71 ^{+0.78} _{-0.63}	+0.78 -1.85	+0.78 -2.26	-2.67 ^{+0.16} _{-0.17}	+0.27 -0.47	+0.46 -0.64	-13.12 ^{+1.97} _{-1.75}	+4.50 -2.15	+5.19 -2.46
J2203+1725		2.38 ^{+0.59} _{-0.63}	+1.33 -3.66	+2.51 -3.76	2.58 ^{+0.93} _{-0.85}	+2.88 -2.17	+2.91 -3.44	-1.47 ^{+0.31} _{-1.32}	+0.32 -1.83	+0.34 -1.89	-6.42 ^{+1.20} _{-1.68}	+3.67 -3.91	+4.29 -5.22
J2203+3145		2.56 ^{+0.79} _{-1.27}	+1.56 -3.32	+1.88 -3.98	3.21 ^{+1.90} _{-0.65}	+2.29 -3.43	+2.29 -4.44	-2.98 ^{+1.04} _{-0.37}	+1.84 -0.29	+1.87 -0.36	-8.09 ^{+2.35} _{-3.00}	+5.68 -5.03	+6.62 -5.28
J2204+0440		1.84 ^{+1.29} _{-0.65}	+2.31 -3.15	+3.54 -3.33	1.91 ^{+2.08} _{-0.90}	+3.56 -1.61	+3.55 -2.97	-3.07 ^{+1.23} _{-0.22}	+1.78 -0.24	+1.88 -0.24	-6.68 ^{+1.96} _{-3.46}	+2.81 -7.35	+4.22 -9.21

Table C.2: Results of fitting the broken power-law model over the 1290 selected observations from OVRO dataset. Break significance refers to the source having a possible break frequency being (1σ) at 68.3%, (2σ) at 95.5% and (3σ) at 99.7%. The absence of break significance means that the source is not well-fitted at any level.

Name	Break significance	β_l	$\beta_l^{95.5\%}$	$\beta_l^{99.7\%}$	β_h	$\beta_h^{95.5\%}$	$\beta_h^{99.7\%}$	$\log f_{br}$	$\log f_{br}^{95.5\%}$	$\log f_{br}^{99.7\%}$	$\log A$	$\log A^{95.5\%}$	$\log A^{99.7\%}$
J2204+3632		$4.89_{-1.64}^{+0.61}$	$+0.61_{-3.57}$	$+0.61_{-5.48}$	$4.24_{-2.65}^{+1.20}$	$+1.23_{-5.15}$	$+1.27_{-5.64}$	$-1.67_{-1.00}^{+0.33}$	$+0.46_{-1.55}$	$+0.48_{-1.64}$	$-12.13_{-3.38}^{+5.54}$	$+8.53_{-6.24}$	$+9.37_{-7.65}$
J2206-0031	1σ	$0.22_{-1.72}^{+1.00}$	$+2.57_{-1.71}$	$+3.79_{-1.71}$	$3.15_{-0.49}^{+0.94}$	$+1.74_{-0.91}$	$+2.35_{-1.03}$	$-2.92_{-0.31}^{+0.24}$	$+0.67_{-0.43}$	$+0.96_{-0.44}$	$-8.37_{-1.85}^{+1.46}$	$+1.71_{-4.29}$	$+2.11_{-5.69}$
J2207+1652		$2.76_{-0.82}^{+1.01}$	$+2.66_{-2.35}$	$+2.71_{-4.10}$	$3.00_{-1.55}^{+1.39}$	$+2.44_{-3.13}$	$+2.44_{-4.27}$	$-3.09_{-0.28}^{+1.27}$	$+1.85_{-0.27}$	$+1.95_{-0.27}$	$-9.51_{-3.21}^{+2.91}$	$+5.27_{-5.45}$	$+7.15_{-7.55}$
J2210+2013		$2.01_{-0.72}^{+0.63}$	$+2.34_{-2.96}$	$+3.38_{-3.23}$	$2.05_{-0.73}^{+2.09}$	$+3.27_{-2.16}$	$+3.42_{-2.79}$	$-1.53_{-1.13}^{+0.36}$	$+0.36_{-1.79}$	$+0.40_{-1.83}$	$-6.64_{-3.44}^{+1.62}$	$+2.99_{-6.49}$	$+3.98_{-6.91}$
J2211+1841		$1.96_{-1.72}^{+0.38}$	$+0.71_{-3.06}$	$+1.09_{-3.38}$	$2.59_{-0.45}^{+0.48}$	$+1.79_{-0.43}$	$+1.79_{-0.72}$	$-2.85_{-0.41}^{+0.57}$	$+1.52_{-0.50}$	$+1.72_{-0.50}$	$-6.84_{-0.75}^{+1.01}$	$+1.17_{-2.43}$	$+1.46_{-2.78}$
J2212+2355		$2.25_{-1.35}^{+0.61}$	$+0.91_{-3.65}$	$+2.58_{-3.72}$	$2.59_{-0.63}^{+1.16}$	$+2.88_{-1.12}$	$+2.90_{-3.17}$	$-3.04_{-0.33}^{+1.11}$	$+1.85_{-0.30}$	$+1.92_{-0.32}$	$-6.53_{-2.43}^{+0.99}$	$+2.43_{-5.08}$	$+4.50_{-5.93}$
J2214+0711		$2.45_{-0.90}^{+1.15}$	$+1.65_{-3.43}$	$+2.72_{-3.94}$	$3.03_{-0.96}^{+1.98}$	$+2.45_{-3.47}$	$+2.45_{-4.11}$	$-3.06_{-0.25}^{+1.25}$	$+1.80_{-0.24}$	$+1.88_{-0.25}$	$-9.04_{-3.07}^{+3.02}$	$+4.83_{-6.04}$	$+6.26_{-6.67}$
J2214+3739		$4.85_{-2.24}^{+0.64}$	$+0.63_{-4.33}$	$+0.64_{-5.11}$	$4.06_{-2.46}^{+1.44}$	$+1.34_{-5.06}$	$+1.44_{-5.50}$	$-1.71_{-0.94}^{+0.51}$	$+0.50_{-1.51}$	$+0.51_{-1.61}$	$-14.72_{-1.40}^{+7.70}$	$+10.95_{-3.74}$	$+11.96_{-5.09}$
J2216+3102		$2.98_{-1.21}^{+1.08}$	$+2.00_{-3.97}$	$+2.48_{-4.46}$	$3.95_{-1.43}^{+1.55}$	$+1.55_{-4.39}$	$+1.55_{-5.19}$	$-3.05_{-0.27}^{+1.16}$	$+1.76_{-0.27}$	$+1.86_{-0.27}$	$-12.32_{-3.29}^{+4.04}$	$+8.33_{-3.72}$	$+9.86_{-4.72}$
J2216+3518		$2.35_{-1.04}^{+0.59}$	$+1.26_{-3.08}$	$+3.04_{-3.85}$	$2.95_{-0.55}^{+1.58}$	$+2.48_{-0.87}$	$+2.54_{-2.36}$	$-2.27_{-0.96}^{+0.18}$	$+0.94_{-1.04}$	$+1.06_{-1.04}$	$-7.97_{-2.84}^{+1.29}$	$+2.10_{-5.06}$	$+4.01_{-5.31}$
J2217+2421		$1.74_{-0.74}^{+0.53}$	$+1.72_{-3.15}$	$+3.51_{-3.20}$	$1.84_{-0.57}^{+1.26}$	$+3.63_{-1.37}$	$+3.63_{-2.61}$	$-1.40_{-1.42}^{+0.28}$	$+0.28_{-1.89}$	$+0.28_{-1.96}$	$-4.24_{-1.69}^{+0.95}$	$+1.93_{-5.40}$	$+2.89_{-5.76}$
J2218+1520		$3.00_{-0.75}^{+0.64}$	$+2.26_{-3.06}$	$+2.26_{-4.34}$	$3.33_{-1.40}^{+1.31}$	$+2.17_{-3.50}$	$+2.16_{-4.61}$	$-1.45_{-1.29}^{+0.31}$	$+0.25_{-1.88}$	$+0.31_{-1.91}$	$-9.31_{-1.76}^{+3.46}$	$+5.70_{-4.66}$	$+7.19_{-5.64}$
J2218-0335		$2.80_{-0.65}^{+0.79}$	$+2.37_{-3.23}$	$+2.68_{-4.29}$	$2.85_{-0.87}^{+1.32}$	$+2.62_{-2.67}$	$+2.61_{-3.97}$	$-1.55_{-1.26}^{+0.26}$	$+0.26_{-1.76}$	$+0.30_{-1.82}$	$-7.74_{-2.75}^{+1.85}$	$+3.91_{-5.13}$	$+5.78_{-5.54}$
J2219+1806	1σ	$1.57_{-1.12}^{+0.53}$	$+0.87_{-2.82}$	$+1.25_{-3.02}$	$3.07_{-0.43}^{+1.51}$	$+2.43_{-0.67}$	$+2.43_{-1.03}$	$-2.27_{-0.54}^{+0.20}$	$+0.45_{-0.89}$	$+0.58_{-1.02}$	$-7.91_{-2.71}^{+1.23}$	$+1.88_{-4.43}$	$+2.15_{-4.92}$
J2225+2118		$3.10_{-0.99}^{+0.57}$	$+1.13_{-3.89}$	$+2.18_{-4.59}$	$3.45_{-0.58}^{+1.71}$	$+2.01_{-3.44}$	$+2.05_{-4.66}$	$-3.09_{-0.20}^{+1.37}$	$+1.95_{-0.18}$	$+1.95_{-0.28}$	$-9.03_{-2.64}^{+1.73}$	$+5.23_{-4.34}$	$+7.26_{-4.35}$
J2226+0052	1σ	$2.45_{-1.21}^{+0.45}$	$+0.94_{-2.87}$	$+1.16_{-3.88}$	$3.33_{-0.39}^{+2.15}$	$+2.15_{-2.71}$	$+2.17_{-4.11}$	$-2.49_{-0.87}^{+0.38}$	$+1.23_{-0.74}$	$+1.25_{-0.87}$	$-9.64_{-3.58}^{+1.99}$	$+4.48_{-5.29}$	$+7.26_{-5.29}$
J2228+2503		$4.69_{-1.67}^{+0.81}$	$+0.80_{-3.47}$	$+0.81_{-4.40}$	$2.33_{-0.91}^{+3.16}$	$+2.89_{-3.73}$	$+3.14_{-3.81}$	$-1.59_{-1.03}^{+0.29}$	$+0.40_{-1.70}$	$+0.46_{-1.76}$	$-9.54_{-5.45}^{+3.42}$	$+5.38_{-8.97}$	$+6.59_{-10.35}$
J2229-0832	1σ	$2.02_{-0.83}^{+0.80}$	$+0.99_{-2.54}$	$+1.28_{-3.47}$	$4.17_{-1.03}^{+0.76}$	$+1.33_{-1.28}$	$+1.33_{-1.67}$	$-2.41_{-0.40}^{+0.27}$	$+0.60_{-0.81}$	$+0.86_{-0.88}$	$-8.99_{-2.71}^{+1.11}$	$+2.83_{-2.81}$	$+3.43_{-3.11}$
J2230+6946		$2.06_{-0.95}^{+0.76}$	$+0.97_{-3.46}$	$+2.11_{-3.46}$	$2.72_{-0.81}^{+1.50}$	$+2.78_{-1.30}$	$+2.77_{-2.53}$	$-2.49_{-0.81}^{+0.44}$	$+1.19_{-0.80}$	$+1.28_{-0.83}$	$-7.66_{-2.77}^{+1.77}$	$+2.67_{-5.39}$	$+4.31_{-6.21}$
J2230-1325		$1.80_{-0.71}^{+0.86}$	$+1.19_{-2.66}$	$+2.24_{-3.23}$	$2.32_{-0.79}^{+1.82}$	$+3.17_{-1.12}$	$+3.17_{-3.18}$	$-2.46_{-0.25}^{+1.05}$	$+1.23_{-0.76}$	$+1.24_{-0.88}$	$-6.67_{-3.43}^{+1.58}$	$+2.29_{-6.59}$	$+4.32_{-7.21}$
J2236+2828	2σ	$1.06_{-1.02}^{+0.59}$	$+1.21_{-1.90}$	$+1.39_{-2.55}$	$3.72_{-0.59}^{+1.04}$	$+1.58_{-1.10}$	$+1.76_{-1.32}$	$-2.48_{-0.21}^{+0.15}$	$+0.36_{-0.52}$	$+0.54_{-0.73}$	$-8.74_{-1.92}^{+1.60}$	$+2.50_{-3.14}$	$+2.97_{-3.84}$
J2236-1433	1σ	$0.32_{-1.64}^{+0.47}$	$+1.92_{-1.74}$	$+2.49_{-1.81}$	$2.79_{-0.58}^{+0.44}$	$+1.25_{-0.77}$	$+1.61_{-0.83}$	$-2.66_{-0.30}^{+0.14}$	$+0.42_{-0.67}$	$+0.68_{-0.67}$	$-6.42_{-1.01}^{+1.08}$	$+1.59_{-2.89}$	$+1.59_{-3.79}$
J2238+2749		$2.42_{-0.83}^{+0.67}$	$+1.28_{-3.10}$	$+1.32_{-3.82}$	$3.03_{-0.99}^{+1.76}$	$+2.45_{-3.58}$	$+2.44_{-4.33}$	$-1.43_{-1.18}^{+0.30}$	$+0.29_{-1.84}$	$+0.30_{-1.93}$	$-9.46_{-2.16}^{+3.27}$	$+6.72_{-3.60}$	$+6.71_{-5.42}$
J2241+0953		$2.65_{-1.46}^{+0.66}$	$+1.29_{-3.63}$	$+2.55_{-4.12}$	$3.16_{-0.51}^{+1.30}$	$+2.34_{-1.03}$	$+2.34_{-1.97}$	$-2.59_{-0.76}^{+0.27}$	$+1.20_{-0.78}$	$+1.43_{-0.77}$	$-8.82_{-2.98}^{+1.02}$	$+2.25_{-4.81}$	$+3.72_{-4.81}$

Table C.2: Results of fitting the broken power-law model over the 1290 selected observations from OVRO dataset. Break significance refers to the source having a possible break frequency being (1σ) at 68.3%, (2σ) at 95.5% and (3σ) at 99.7%. The absence of break significance means that the source is not well-fitted at any level.

Name	Break significance	β_l	$\beta_l^{95.5\%}$	$\beta_l^{99.7\%}$	β_h	$\beta_h^{95.5\%}$	$\beta_h^{99.7\%}$	$\log f_{br}$	$\log f_{br}^{95.5\%}$	$\log f_{br}^{99.7\%}$	$\log A$	$\log A^{95.5\%}$	$\log A^{99.7\%}$
J2241+4120		$2.33^{+0.75}_{-2.05}$	$+1.36$ -3.77	$+2.94$ -3.77	$3.18^{+1.58}_{-0.82}$	$+2.30$ -2.27	$+2.30$ -3.81	$-2.93^{+0.65}_{-0.43}$	$+1.66$ -0.44	$+1.80$ -0.44	$-8.57^{+1.15}_{-4.48}$	$+3.28$ -6.73	$+5.47$ -6.81
J2244+4057		$2.17^{+0.79}_{-0.58}$	$+2.17$ -2.54	$+3.22$ -3.30	$1.49^{+0.61}_{-2.08}$	$+2.90$ -2.98	$+3.86$ -2.98	$-1.52^{+0.33}_{-0.92}$	$+0.30$ -1.75	$+0.33$ -1.79	$-3.25^{+2.50}_{-1.13}$	$+3.20$ -5.80	$+3.33$ -8.65
J2245+0324		$2.36^{+0.71}_{-1.05}$	$+2.31$ -2.93	$+2.86$ -3.80	$2.42^{+2.55}_{-0.58}$	$+3.08$ -2.02	$+3.07$ -3.46	$-1.61^{+0.49}_{-1.11}$	$+0.46$ -1.69	$+0.49$ -1.76	$-6.94^{+1.61}_{-4.04}$	$+2.35$ -7.62	$+3.98$ -8.92
J2245+0500		$3.28^{+1.11}_{-0.99}$	$+1.38$ -3.99	$+1.68$ -4.75	$4.67^{+0.81}_{-1.77}$	$+0.81$ -5.08	$+0.81$ -5.84	$-3.09^{+1.13}_{-0.28}$	$+1.77$ -0.26	$+1.85$ -0.27	$-13.51^{+4.57}_{-2.14}$	$+8.75$ -2.99	$+10.27$ -2.99
J2246-1206		$2.73^{+0.71}_{-0.75}$	$+1.50$ -3.55	$+2.61$ -4.10	$2.71^{+1.88}_{-0.86}$	$+2.73$ -2.43	$+2.73$ -4.00	$-1.48^{+0.26}_{-1.30}$	$+0.26$ -1.78	$+0.26$ -1.86	$-6.78^{+1.88}_{-3.48}$	$+3.64$ -5.84	$+5.62$ -6.58
J2247+0310		$2.52^{+0.77}_{-0.68}$	$+1.37$ -2.84	$+2.43$ -3.63	$2.81^{+1.66}_{-0.76}$	$+2.69$ -2.35	$+2.68$ -4.19	$-2.24^{+0.32}_{-1.13}$	$+1.00$ -1.04	$+1.00$ -1.13	$-8.08^{+1.58}_{-3.34}$	$+3.87$ -5.36	$+5.81$ -5.70
J2247-1237		$2.31^{+0.76}_{-0.75}$	$+3.00$ -2.07	$+3.04$ -3.31	$2.38^{+2.12}_{-0.93}$	$+3.02$ -2.59	$+3.07$ -3.40	$-1.62^{+0.38}_{-1.08}$	$+0.33$ -1.70	$+0.41$ -1.72	$-7.93^{+2.53}_{-3.48}$	$+4.21$ -6.28	$+5.66$ -7.21
J2249+2107		$2.20^{+0.84}_{-1.64}$	$+0.93$ -3.66	$+2.15$ -3.67	$3.04^{+1.68}_{-0.95}$	$+2.36$ -3.17	$+2.44$ -4.06	$-2.92^{+0.73}_{-0.45}$	$+1.71$ -0.45	$+1.80$ -0.45	$-8.97^{+2.72}_{-3.19}$	$+4.89$ -6.13	$+6.73$ -6.39
J2253+1608		$2.94^{+0.55}_{-0.64}$	$+2.46$ -2.52	$+2.46$ -4.00	$3.09^{+1.73}_{-0.82}$	$+2.40$ -3.10	$+2.40$ -4.53	$-1.39^{+0.27}_{-1.17}$	$+0.27$ -1.87	$+0.27$ -1.98	$-5.58^{+2.03}_{-2.60}$	$+4.47$ -4.84	$+6.47$ -4.91
J2253+1942		$3.79^{+0.70}_{-1.06}$	$+1.62$ -2.66	$+1.68$ -4.45	$4.30^{+1.20}_{-1.79}$	$+1.20$ -4.87	$+1.20$ -5.74	$-1.46^{+0.29}_{-1.18}$	$+0.29$ -1.83	$+0.32$ -1.91	$-11.68^{+3.84}_{-3.02}$	$+7.30$ -4.71	$+9.18$ -5.04
J2257+0243		$4.99^{+0.51}_{-0.95}$	$+0.50$ -2.34	$+0.50$ -3.20	$4.28^{+1.19}_{-2.96}$	$+1.10$ -5.40	$+1.19$ -5.76	$-1.67^{+0.47}_{-0.77}$	$+0.47$ -1.54	$+0.47$ -1.65	$-15.39^{+6.81}_{-1.84}$	$+10.62$ -3.46	$+12.61$ -3.80
J2259-0811		$2.81^{+1.49}_{-3.03}$	$+2.28$ -4.24	$+2.68$ -4.30	$-0.28^{+2.95}_{-1.22}$	$+5.19$ -1.22	$+5.68$ -1.22	$-1.92^{+0.23}_{-1.19}$	$+0.67$ -1.32	$+0.70$ -1.41	$-15.85^{+5.00}_{-3.91}$	$+10.65$ -3.88	$+13.07$ -3.98
J2300+1655		$2.68^{+0.77}_{-1.14}$	$+1.50$ -3.08	$+1.50$ -3.98	$3.25^{+1.93}_{-0.69}$	$+2.25$ -3.06	$+2.25$ -4.46	$-2.64^{+0.64}_{-0.73}$	$+1.40$ -0.73	$+1.51$ -0.73	$-10.01^{+2.25}_{-3.43}$	$+5.45$ -5.29	$+7.44$ -5.29
J2301-0158		$2.61^{+0.59}_{-2.45}$	$+0.73$ -4.11	$+1.46$ -4.11	$3.50^{+0.88}_{-0.56}$	$+1.62$ -0.93	$+1.98$ -1.55	$-2.96^{+0.30}_{-0.31}$	$+1.37$ -0.36	$+1.69$ -0.37	$-9.02^{+1.46}_{-1.76}$	$+2.29$ -3.98	$+3.52$ -4.70
J2305+8242		$2.82^{+1.04}_{-1.44}$	$+1.91$ -3.96	$+2.61$ -4.30	$3.10^{+2.26}_{-0.49}$	$+2.39$ -3.13	$+2.36$ -4.27	$-3.05^{+1.07}_{-0.27}$	$+1.69$ -0.26	$+1.74$ -0.27	$-10.17^{+2.38}_{-4.21}$	$+6.26$ -5.21	$+6.83$ -7.25
J2307+1450		$2.58^{+1.06}_{-1.11}$	$+1.06$ -3.63	$+1.47$ -4.07	$4.09^{+0.99}_{-1.46}$	$+1.35$ -4.00	$+1.38$ -5.36	$-2.96^{+0.99}_{-0.37}$	$+1.73$ -0.38	$+1.84$ -0.39	$-10.11^{+2.20}_{-3.48}$	$+4.68$ -5.95	$+7.40$ -5.95
J2308+2008		$3.14^{+1.35}_{-0.67}$	$+2.13$ -2.55	$+2.26$ -4.44	$3.31^{+2.14}_{-1.11}$	$+2.17$ -4.15	$+2.17$ -4.71	$-1.46^{+0.33}_{-1.22}$	$+0.28$ -1.83	$+0.33$ -1.90	$-11.23^{+3.54}_{-3.68}$	$+6.98$ -5.08	$+8.46$ -5.96
J2310+1055		$2.59^{+0.67}_{-0.86}$	$+2.24$ -2.56	$+2.84$ -3.42	$2.55^{+2.16}_{-0.74}$	$+2.92$ -2.56	$+2.93$ -3.70	$-1.44^{+0.32}_{-1.17}$	$+0.23$ -1.92	$+0.32$ -1.92	$-7.91^{+1.15}_{-4.54}$	$+4.23$ -5.88	$+5.39$ -7.46
J2311+4543		$3.05^{+0.93}_{-0.75}$	$+1.21$ -4.32	$+2.34$ -4.52	$3.99^{+1.27}_{-1.26}$	$+1.48$ -4.19	$+1.50$ -5.31	$-3.08^{+1.26}_{-0.29}$	$+1.87$ -0.28	$+1.95$ -0.29	$-10.53^{+3.02}_{-2.44}$	$+7.09$ -3.23	$+8.23$ -4.00
J2321+2732		$1.92^{+0.74}_{-1.65}$	$+0.86$ -3.12	$+1.09$ -3.40	$2.72^{+1.23}_{-0.72}$	$+2.57$ -1.06	$+2.78$ -1.30	$-2.79^{+0.60}_{-0.40}$	$+1.34$ -0.51	$+1.57$ -0.52	$-7.08^{+1.16}_{-3.01}$	$+2.29$ -4.98	$+2.49$ -6.81
J2321+3204	2σ	$1.26^{+0.76}_{-0.95}$	$+1.48$ -2.11	$+1.48$ -2.71	$3.81^{+0.62}_{-0.72}$	$+1.66$ -0.96	$+1.67$ -1.37	$-2.46^{+0.21}_{-0.18}$	$+0.53$ -0.51	$+0.53$ -0.86	$-8.61^{+1.67}_{-1.15}$	$+2.50$ -2.79	$+2.77$ -3.51
J2322+1843		$2.02^{+1.10}_{-0.89}$	$+1.96$ -3.47	$+3.33$ -3.47	$2.20^{+2.22}_{-0.91}$	$+3.20$ -2.42	$+3.30$ -3.58	$-3.00^{+1.14}_{-0.35}$	$+1.80$ -0.35	$+2.23$ -0.36	$-7.82^{+2.23}_{-3.95}$	$+3.39$ -8.26	$+4.75$ -9.39
J2322+4445		$2.91^{+1.13}_{-0.80}$	$+2.50$ -1.61	$+2.50$ -3.99	$3.37^{+1.75}_{-1.27}$	$+2.12$ -3.65	$+2.12$ -4.58	$-3.03^{+1.28}_{-0.34}$	$+1.91$ -0.27	$+1.90$ -0.34	$-9.88^{+3.05}_{-3.61}$	$+6.11$ -5.89	$+7.17$ -6.87
J2323-0317		$1.99^{+0.70}_{-1.37}$	$+1.00$ -3.44	$+2.12$ -3.42	$3.12^{+1.39}_{-0.43}$	$+2.36$ -0.68	$+2.36$ -1.06	$-2.38^{+0.23}_{-0.67}$	$+0.67$ -0.95	$+0.92$ -0.95	$-7.73^{+1.02}_{-2.76}$	$+2.12$ -4.44	$+2.23$ -5.21

Table C.2: Results of fitting the broken power-law model over the 1290 selected observations from OVRO dataset. Break significance refers to the source having a possible break frequency being (1σ) at 68.3%, (2σ) at 95.5% and (3σ) at 99.7%. The absence of break significance means that the source is not well-fitted at any level.

Name	Break significance	β_l	$\beta_l^{95.5\%}$	$\beta_l^{99.7\%}$	β_h	$\beta_h^{95.5\%}$	$\beta_h^{99.7\%}$	$\log f_{br}$	$\log f_{br}^{95.5\%}$	$\log f_{br}^{99.7\%}$	$\log A$	$\log A^{95.5\%}$	$\log A^{99.7\%}$
J2327+0940	2σ	$-0.60^{+1.41}_{-0.90}$	$+2.78_{-0.90}$	$+3.49_{-0.90}$	$3.57^{+0.42}_{-0.32}$	$+0.84_{-0.59}$	$+1.27_{-0.70}$	$-2.91^{+0.17}_{-0.18}$	$+0.53_{-0.34}$	$+0.64_{-0.46}$	$-7.82^{+0.58}_{-0.97}$	$+1.23_{-1.88}$	$+1.26_{-2.75}$
J2327+1524	1σ	$0.44^{+0.97}_{-1.28}$	$+1.96_{-1.90}$	$+2.38_{-1.94}$	$2.93^{+1.51}_{-0.40}$	$+2.57_{-0.55}$	$+2.57_{-1.03}$	$-2.74^{+0.23}_{-0.30}$	$+0.52_{-0.61}$	$+1.01_{-0.63}$	$-8.73^{+1.30}_{-3.21}$	$+1.77_{-5.52}$	$+2.62_{-6.27}$
J2327+1533		$3.95^{+1.53}_{-0.44}$	$+1.54_{-2.29}$	$+1.53_{-3.13}$	$4.52^{+0.97}_{-2.78}$	$+0.98_{-5.27}$	$+0.97_{-5.97}$	$-1.54^{+0.34}_{-1.13}$	$+0.34_{-1.79}$	$+0.41_{-1.81}$	$-10.61^{+2.92}_{-5.42}$	$+5.99_{-7.53}$	$+7.84_{-8.05}$
J2329+0834	2σ	$-0.84^{+1.70}_{-0.53}$	$+3.20_{-0.64}$	$+3.87_{-0.63}$	$4.23^{+0.54}_{-1.37}$	$+1.24_{-1.56}$	$+1.27_{-1.99}$	$-2.86^{+0.15}_{-0.20}$	$+0.31_{-0.39}$	$+0.45_{-0.49}$	$-11.16^{+2.91}_{-1.88}$	$+3.56_{-3.64}$	$+4.34_{-3.80}$
J2330+1100		$3.38^{+1.07}_{-0.72}$	$+1.86_{-3.65}$	$+2.06_{-4.78}$	$4.01^{+1.34}_{-1.72}$	$+1.49_{-4.32}$	$+1.49_{-5.28}$	$-1.46^{+0.24}_{-1.90}$	$+0.27_{-1.90}$	$+0.33_{-1.91}$	$-10.05^{+3.55}_{-3.01}$	$+6.43_{-4.78}$	$+7.78_{-5.34}$
J2330+3348		$2.38^{+0.83}_{-0.70}$	$+1.46_{-3.83}$	$+2.85_{-3.83}$	$2.77^{+1.54}_{-1.27}$	$+2.72_{-2.50}$	$+2.72_{-3.57}$	$-3.12^{+1.31}_{-0.24}$	$+1.88_{-0.20}$	$+1.88_{-0.25}$	$-8.57^{+2.99}_{-2.61}$	$+4.76_{-5.43}$	$+6.08_{-6.35}$
J2331-1556		$2.56^{+0.92}_{-0.65}$	$+1.92_{-2.54}$	$+2.93_{-3.07}$	$2.96^{+1.77}_{-1.40}$	$+2.53_{-3.47}$	$+2.52_{-4.40}$	$-1.47^{+0.33}_{-1.17}$	$+0.27_{-1.90}$	$+0.33_{-1.90}$	$-8.86^{+3.95}_{-2.24}$	$+5.34_{-5.84}$	$+7.10_{-5.84}$
J2334+0736		$2.38^{+0.54}_{-0.80}$	$+0.93_{-3.28}$	$+2.33_{-3.86}$	$2.85^{+1.36}_{-0.75}$	$+2.34_{-2.84}$	$+2.59_{-3.11}$	$-2.16^{+0.94}_{-0.47}$	$+0.88_{-1.21}$	$+0.99_{-1.21}$	$-7.22^{+1.10}_{-2.65}$	$+3.99_{-4.47}$	$+4.59_{-5.31}$
J2335-0131	2σ	$1.27^{+1.04}_{-0.82}$	$+1.60_{-2.31}$	$+1.61_{-2.68}$	$5.08^{+0.41}_{-0.99}$	$+0.41_{-1.85}$	$+0.41_{-2.23}$	$-2.49^{+0.16}_{-0.25}$	$+0.25_{-0.73}$	$+0.36_{-0.80}$	$-12.56^{+2.39}_{-0.77}$	$+4.28_{-0.94}$	$+5.01_{-1.28}$
J2337+2617		$3.09^{+2.34}_{-0.32}$	$+2.33_{-2.70}$	$+2.40_{-4.28}$	$3.71^{+1.78}_{-1.61}$	$+1.78_{-4.47}$	$+1.77_{-5.18}$	$-1.49^{+0.23}_{-1.27}$	$+0.23_{-1.87}$	$+0.36_{-1.88}$	$-11.07^{+3.99}_{-3.70}$	$+7.80_{-6.70}$	$+7.79_{-8.82}$
J2337-0230	2σ	$-0.27^{+0.93}_{-1.21}$	$+2.07_{-1.23}$	$+2.86_{-1.22}$	$3.11^{+1.06}_{-0.59}$	$+2.24_{-0.78}$	$+2.39_{-0.96}$	$-2.84^{+0.11}_{-0.24}$	$+0.39_{-0.37}$	$+0.48_{-0.48}$	$-8.17^{+1.40}_{-2.60}$	$+2.15_{-5.01}$	$+2.36_{-5.81}$
J2339-1206		$4.48^{+0.67}_{-0.99}$	$+0.99_{-3.37}$	$+0.99_{-5.78}$	$4.74^{+0.74}_{-2.21}$	$+0.75_{-5.42}$	$+0.75_{-6.22}$	$-1.68^{+0.05}_{-1.63}$	$+0.45_{-1.68}$	$+0.55_{-1.68}$	$-14.33^{+4.44}_{-2.21}$	$+9.65_{-2.60}$	$+11.50_{-3.00}$
J2343+1543	1σ	$1.35^{+0.90}_{-1.08}$	$+1.46_{-2.36}$	$+1.92_{-2.79}$	$4.76^{+0.57}_{-1.44}$	$+0.72_{-2.31}$	$+0.73_{-2.69}$	$-2.53^{+0.23}_{-0.29}$	$+0.43_{-0.77}$	$+0.68_{-0.83}$	$-12.95^{+3.74}_{-0.69}$	$+5.41_{-1.62}$	$+6.39_{-1.73}$
J2343+2339		$3.11^{+1.17}_{-0.81}$	$+1.37_{-4.15}$	$+2.30_{-4.48}$	$4.35^{+0.99}_{-1.53}$	$+1.06_{-5.15}$	$+1.11_{-5.67}$	$-3.04^{+1.25}_{-0.31}$	$+1.85_{-0.31}$	$+1.91_{-0.32}$	$-11.11^{+2.85}_{-3.03}$	$+7.24_{-3.94}$	$+8.63_{-4.33}$
J2345-1555	3σ	$0.42^{+0.47}_{-0.94}$	$+0.96_{-1.72}$	$+1.31_{-1.88}$	$3.45^{+0.78}_{-0.74}$	$+2.03_{-0.74}$	$+2.03_{-1.13}$	$-2.35^{+0.12}_{-0.23}$	$+0.24_{-0.49}$	$+0.26_{-0.66}$	$-7.49^{+1.08}_{-1.93}$	$+1.53_{-3.91}$	$+2.18_{-4.14}$
J2346+0930		$3.48^{+0.83}_{-1.02}$	$+1.77_{-3.61}$	$+2.02_{-4.57}$	$4.45^{+1.05}_{-1.86}$	$+1.04_{-4.80}$	$+1.05_{-5.82}$	$-3.10^{+1.36}_{-0.23}$	$+1.88_{-0.25}$	$+1.96_{-0.27}$	$-11.07^{+4.16}_{-2.60}$	$+7.63_{-4.16}$	$+8.57_{-5.10}$
J2346+8007	1σ	$1.19^{+0.86}_{-1.28}$	$+1.33_{-2.51}$	$+1.85_{-2.65}$	$3.14^{+1.49}_{-0.49}$	$+2.32_{-0.72}$	$+2.35_{-1.14}$	$-2.50^{+0.22}_{-0.44}$	$+0.47_{-0.82}$	$+0.82_{-0.82}$	$-8.76^{+1.40}_{-2.97}$	$+1.77_{-5.00}$	$+2.67_{-5.49}$
J2348-0425	1σ	$-0.40^{+2.39}_{-0.62}$	$+3.45_{-1.04}$	$+4.31_{-1.07}$	$4.13^{+1.12}_{-0.42}$	$+1.36_{-1.10}$	$+1.37_{-1.42}$	$-2.95^{+0.13}_{-0.29}$	$+0.51_{-0.33}$	$+0.63_{-0.36}$	$-11.38^{+0.85}_{-3.05}$	$+2.65_{-3.59}$	$+3.54_{-4.09}$
J2348-1631		$2.54^{+0.53}_{-0.97}$	$+0.68_{-3.93}$	$+1.57_{-3.95}$	$2.93^{+1.67}_{-0.56}$	$+2.53_{-2.29}$	$+2.55_{-4.19}$	$-2.00^{+0.88}_{-0.66}$	$+0.88_{-1.27}$	$+0.88_{-1.36}$	$-6.66^{+1.33}_{-2.55}$	$+3.53_{-4.98}$	$+5.22_{-4.98}$
J2350+1106		$2.48^{+1.26}_{-1.14}$	$+2.32_{-3.38}$	$+2.93_{-3.85}$	$4.10^{+1.41}_{-1.76}$	$+1.41_{-4.76}$	$+1.40_{-5.54}$	$-3.10^{+1.35}_{-0.27}$	$+1.90_{-0.27}$	$+1.97_{-0.27}$	$-9.48^{+3.35}_{-4.20}$	$+5.08_{-7.48}$	$+6.97_{-7.47}$
J2352+3947		$2.78^{+0.80}_{-1.18}$	$+2.20_{-3.33}$	$+2.20_{-4.16}$	$3.97^{+1.39}_{-1.74}$	$+1.52_{-4.11}$	$+1.52_{-5.42}$	$-3.08^{+1.21}_{-0.28}$	$+1.78_{-0.25}$	$+1.84_{-0.28}$	$-11.01^{+4.40}_{-2.69}$	$+7.24_{-4.67}$	$+8.84_{-5.53}$
J2354-1513		$1.82^{+0.77}_{-0.89}$	$+1.29_{-3.03}$	$+2.84_{-3.23}$	$2.95^{+1.52}_{-0.62}$	$+2.49_{-0.69}$	$+2.53_{-1.10}$	$-2.38^{+0.46}_{-0.42}$	$+0.80_{-0.99}$	$+1.13_{-0.98}$	$-7.99^{+1.46}_{-3.02}$	$+1.75_{-5.11}$	$+2.16_{-5.67}$
J2357-0152		$1.90^{+0.94}_{-1.19}$	$+1.06_{-3.04}$	$+1.30_{-3.40}$	$3.08^{+1.61}_{-0.75}$	$+2.37_{-1.32}$	$+2.40_{-3.05}$	$-2.67^{+0.38}_{-0.56}$	$+1.37_{-0.56}$	$+1.45_{-0.64}$	$-9.06^{+2.30}_{-2.74}$	$+2.86_{-5.32}$	$+5.33_{-6.43}$
J2357-1125		$2.01^{+0.64}_{-0.88}$	$+1.86_{-3.11}$	$+3.18_{-3.47}$	$2.56^{+1.61}_{-0.98}$	$+2.93_{-1.21}$	$+2.93_{-2.62}$	$-2.30^{+0.35}_{-1.02}$	$+1.05_{-1.02}$	$+1.16_{-1.07}$	$-7.23^{+1.61}_{-3.36}$	$+2.43_{-6.28}$	$+4.10_{-6.58}$

Table C.2: Results of fitting the broken power-law model over the 1290 selected observations from OVRO dataset. Break significance refers to the source having a possible break frequency being (1σ) at 68.3%, (2σ) at 95.5% and (3σ) at 99.7%. The absence of break significance means that the source is not well-fitted at any level.

Name	Break significance	β_l	$\beta_l^{95.5\%}$	$\beta_l^{99.7\%}$	β_h	$\beta_h^{95.5\%}$	$\beta_h^{99.7\%}$	$\log f_{br}$	$\log f_{br}^{95.5\%}$	$\log f_{br}^{99.7\%}$	$\log A$	$\log A^{95.5\%}$	$\log A^{99.7\%}$
J2358+0430		$3.60^{+1.90}_{-0.71}$	$+1.90$ -3.24	$+1.90$ -5.05	$4.00^{+1.10}_{-2.34}$	$+1.47$ -4.75	$+1.49$ -5.45	$-1.50^{+0.30}_{-1.10}$	$+0.25$ -1.76	$+0.30$ -1.80	$-12.02^{+4.03}_{-4.31}$	$+7.81$ -6.15	$+9.50$ -7.19
J2358+1955		$2.73^{+0.69}_{-1.01}$	$+2.50$ -2.96	$+2.50$ -4.16	$2.83^{+1.65}_{-1.11}$	$+2.66$ -2.55	$+2.66$ -4.25	$-1.48^{+0.35}_{-1.20}$	$+0.26$ -1.89	$+0.35$ -1.89	$-7.62^{+0.97}_{-4.30}$	$+4.28$ -6.16	$+4.65$ -7.45
J2358-1020	3σ	$-0.32^{+1.21}_{-1.14}$	$+2.75$ -1.18	$+3.47$ -1.18	$4.32^{+0.63}_{-0.50}$	$+1.18$ -0.73	$+1.18$ -1.12	$-2.83^{+0.16}_{-0.22}$	$+0.52$ -0.34	$+0.64$ -0.42	$-10.31^{+1.15}_{-1.29}$	$+1.87$ -2.49	$+2.50$ -2.79
M81		$1.71^{+0.53}_{-1.10}$	$+0.88$ -2.82	$+1.62$ -3.21	$2.33^{+1.52}_{-0.66}$	$+3.16$ -0.70	$+3.16$ -1.61	$-2.55^{+1.07}_{-0.20}$	$+1.14$ -0.74	$+1.24$ -0.77	$-6.06^{+1.22}_{-2.67}$	$+1.62$ -5.48	$+2.53$ -6.69
MG1J183001+1323		$2.52^{+0.64}_{-1.86}$	$+1.20$ -3.69	$+2.20$ -3.95	$4.06^{+0.90}_{-1.66}$	$+1.43$ -3.94	$+1.43$ -4.50	$-2.87^{+0.77}_{-0.34}$	$+1.52$ -0.34	$+1.63$ -0.34	$-10.77^{+3.17}_{-2.78}$	$+6.24$ -4.61	$+7.26$ -5.48
MG1J235704+0447		$3.40^{+1.54}_{-0.91}$	$+2.02$ -3.68	$+2.02$ -4.89	$4.69^{+0.81}_{-2.15}$	$+0.81$ -4.57	$+0.81$ -5.75	$-2.98^{+1.11}_{-0.21}$	$+1.66$ -0.21	$+1.78$ -0.22	$-12.27^{+3.18}_{-4.09}$	$+7.88$ -4.22	$+9.46$ -5.33
MG2J043338+3236		$4.28^{+1.21}_{-1.52}$	$+1.20$ -4.39	$+1.20$ -5.63	$4.35^{+1.01}_{-2.55}$	$+1.14$ -4.77	$+1.14$ -5.77	$-2.90^{+1.11}_{-0.20}$	$+1.62$ -0.30	$+1.70$ -0.30	$-11.91^{+3.94}_{-4.40}$	$+7.74$ -5.88	$+8.77$ -7.58
MG2J045613+2702	3σ	$0.14^{+0.56}_{-1.31}$	$+1.24$ -1.61	$+1.74$ -1.61	$4.72^{+0.64}_{-1.39}$	$+0.67$ -2.72	$+0.78$ -2.81	$-2.41^{+0.19}_{-0.19}$	$+0.32$ -0.66	$+0.55$ -0.66	$-11.76^{+2.66}_{-1.78}$	$+5.45$ -1.78	$+5.67$ -2.09
MG2J174753+2323		$1.81^{+3.44}_{-0.31}$	$+3.68$ -2.31	$+3.68$ -3.12	$4.46^{+0.70}_{-3.44}$	$+1.04$ -5.39	$+1.02$ -5.96	$-2.21^{+0.35}_{-0.94}$	$+0.87$ -0.94	$+0.90$ -1.00	$-8.23^{+4.21}_{-5.39}$	$+4.91$ -10.53	$+6.30$ -11.71
MG2J184929+2748		$3.96^{+1.41}_{-1.02}$	$+1.52$ -2.30	$+1.52$ -3.17	$3.93^{+1.23}_{-2.56}$	$+1.55$ -4.54	$+1.55$ -5.30	$-1.54^{+0.34}_{-0.93}$	$+0.31$ -1.58	$+0.34$ -1.67	$-9.49^{+4.92}_{-3.18}$	$+6.43$ -7.14	$+7.30$ -8.17
MG2J195919+3847	1σ	$0.18^{+0.42}_{-1.67}$	$+1.77$ -1.68	$+2.40$ -1.67	$2.47^{+1.65}_{-0.62}$	$+2.98$ -0.72	$+3.03$ -1.09	$-2.57^{+0.25}_{-0.26}$	$+0.61$ -0.64	$+1.26$ -0.64	$-6.67^{+1.58}_{-3.39}$	$+1.96$ -6.37	$+2.45$ -7.42
MG3J021846+3641		$2.01^{+0.70}_{-0.85}$	$+1.04$ -2.93	$+1.30$ -3.50	$2.62^{+1.63}_{-0.86}$	$+2.76$ -1.46	$+2.88$ -2.26	$-2.66^{+0.91}_{-0.44}$	$+1.46$ -0.45	$+1.46$ -0.55	$-7.51^{+1.43}_{-2.87}$	$+2.66$ -5.22	$+3.89$ -5.98
MG3J025334+3217		$2.37^{+0.87}_{-1.55}$	$+0.87$ -3.85	$+1.43$ -3.83	$3.60^{+1.11}_{-1.17}$	$+1.89$ -2.79	$+1.88$ -4.30	$-2.81^{+0.64}_{-0.39}$	$+1.48$ -0.39	$+1.62$ -0.39	$-9.86^{+2.56}_{-2.53}$	$+5.26$ -4.34	$+6.84$ -5.26
MG4J015630+3913		$2.29^{+0.74}_{-1.19}$	$+0.85$ -3.58	$+1.34$ -3.79	$3.03^{+1.70}_{-0.39}$	$+2.45$ -0.89	$+2.46$ -1.53	$-2.33^{+0.20}_{-0.85}$	$+0.99$ -0.85	$+1.11$ -0.88	$-7.83^{+1.10}_{-3.02}$	$+2.29$ -4.69	$+2.75$ -5.82
MG4J195957+4213		$2.17^{+1.22}_{-0.88}$	$+1.44$ -3.49	$+2.51$ -3.66	$2.28^{+2.17}_{-1.02}$	$+3.12$ -2.69	$+3.19$ -3.76	$-2.85^{+1.15}_{-0.34}$	$+1.77$ -0.26	$+1.77$ -0.35	$-6.59^{+2.54}_{-3.73}$	$+3.68$ -7.37	$+4.90$ -7.97
MG4J202932+4925	3σ	$-1.09^{+0.95}_{-0.36}$	$+2.01$ -0.41	$+2.30$ -0.41	$3.20^{+0.93}_{-0.66}$	$+2.02$ -0.86	$+2.23$ -1.28	$-2.32^{+0.13}_{-0.11}$	$+0.16$ -0.34	$+0.23$ -0.48	$-7.92^{+0.94}_{-2.16}$	$+1.58$ -4.22	$+2.50$ -4.62
MS14588+2249		$2.53^{+1.43}_{-1.43}$	$+2.14$ -3.88	$+2.92$ -4.02	$4.63^{+0.84}_{-2.03}$	$+0.85$ -4.22	$+0.84$ -5.86	$-2.97^{+0.95}_{-0.32}$	$+1.67$ -0.25	$+1.70$ -0.31	$-10.72^{+3.47}_{-3.66}$	$+5.68$ -5.88	$+7.87$ -6.45
NGC1068		$-0.28^{+2.94}_{-1.22}$	$+5.29$ -1.22	$+5.77$ -1.22	$-0.09^{+2.34}_{-1.30}$	$+4.83$ -1.40	$+5.52$ -1.41	$-2.79^{+0.89}_{-0.39}$	$+1.47$ -0.39	$+1.58$ -0.39	$-17.24^{+5.74}_{-2.72}$	$+11.90$ -2.73	$+14.79$ -2.73
NGC1218		$1.55^{+0.62}_{-1.14}$	$+0.91$ -2.83	$+1.62$ -2.87	$2.63^{+1.96}_{-0.58}$	$+2.86$ -0.96	$+2.86$ -2.48	$-2.43^{+0.41}_{-0.54}$	$+1.02$ -0.88	$+1.23$ -0.88	$-7.04^{+2.21}_{-2.96}$	$+2.30$ -6.36	$+3.74$ -6.70
NRAO676		$3.33^{+1.21}_{-0.97}$	$+2.17$ -2.78	$+2.14$ -4.78	$3.89^{+1.57}_{-1.88}$	$+1.61$ -4.84	$+1.60$ -5.29	$-1.45^{+0.29}_{-1.02}$	$+0.20$ -1.72	$+0.29$ -1.73	$-10.97^{+5.66}_{-1.92}$	$+9.02$ -3.85	$+9.55$ -6.07
NVSSJ020344+304238	1σ	$1.29^{+0.46}_{-1.51}$	$+0.70$ -2.77	$+1.23$ -2.77	$2.74^{+0.97}_{-0.70}$	$+2.41$ -1.04	$+2.71$ -1.04	$-2.40^{+0.24}_{-0.46}$	$+0.56$ -0.78	$+0.98$ -0.79	$-7.04^{+1.61}_{-1.80}$	$+1.91$ -4.73	$+1.91$ -6.04
NVSSJ025357+510256		$2.23^{+0.56}_{-0.93}$	$+3.05$ -2.30	$+3.08$ -3.71	$2.04^{+1.94}_{-0.51}$	$+3.29$ -1.84	$+3.33$ -3.38	$-1.65^{+0.08}_{-1.55}$	$+0.37$ -1.57	$+0.44$ -1.56	$-5.93^{+1.19}_{-3.41}$	$+3.09$ -5.30	$+4.13$ -6.67
NVSSJ030943-074427		$4.62^{+0.87}_{-3.39}$	$+0.87$ -5.69	$+0.87$ -6.06	$-0.39^{+2.99}_{-1.11}$	$+5.23$ -1.11	$+5.83$ -1.10	$-1.71^{+0.33}_{-0.86}$	$+0.33$ -1.47	$+0.39$ -1.51	$-15.45^{+4.58}_{-4.01}$	$+9.79$ -4.50	$+12.46$ -4.51
NVSSJ033223-111951		$0.66^{+2.93}_{-1.45}$	$+4.45$ -2.11	$+4.83$ -2.11	$-0.50^{+2.54}_{-0.96}$	$+5.36$ -0.97	$+5.96$ -0.99	$-2.67^{+0.89}_{-0.38}$	$+1.29$ -0.54	$+1.36$ -0.54	$-15.60^{+3.60}_{-4.31}$	$+9.89$ -4.34	$+12.72$ -4.33

Table C.2: Results of fitting the broken power-law model over the 1290 selected observations from OVRO dataset. Break significance refers to the source having a possible break frequency being (1σ) at 68.3%, (2σ) at 95.5% and (3σ) at 99.7%. The absence of break significance means that the source is not well-fitted at any level.

Name	Break significance	β_l	$\beta_l^{95.5\%}$	$\beta_l^{99.7\%}$	β_h	$\beta_h^{95.5\%}$	$\beta_h^{99.7\%}$	$\log f_{br}$	$\log f_{br}^{95.5\%}$	$\log f_{br}^{99.7\%}$	$\log A$	$\log A^{95.5\%}$	$\log A^{99.7\%}$
NVSSJ070651+774137		$3.44^{+1.86}_{-0.96}$	$+2.05$ -3.26	$+2.05$ -4.23	$3.90^{+1.50}_{-1.78}$	$+1.60$ -4.16	$+1.58$ -5.21	$-2.93^{+1.07}_{-0.19}$	$+1.57$ -0.25	$+1.61$ -0.28	$-12.02^{+3.06}_{-4.81}$	$+7.79$ -5.81	$+8.34$ -7.71
NVSSJ090226+205045		$2.71^{+0.99}_{-1.05}$	$+2.55$ -3.10	$+2.55$ -4.09	$3.77^{+1.04}_{-1.74}$	$+1.73$ -3.44	$+1.72$ -4.62	$-2.94^{+1.01}_{-0.26}$	$+1.62$ -0.21	$+1.63$ -0.27	$-9.94^{+3.82}_{-2.30}$	$+5.83$ -4.63	$+7.66$ -5.67
NVSSJ210833-160724		$2.69^{+2.31}_{-0.61}$	$+2.79$ -2.74	$+2.79$ -4.11	$4.49^{+0.99}_{-2.33}$	$+1.00$ -5.06	$+0.99$ -5.78	$-1.79^{+0.17}_{-1.08}$	$+0.28$ -1.41	$+0.37$ -1.41	$-8.09^{+1.01}_{-7.10}$	$+3.51$ -10.24	$+5.04$ -11.18
NVSSJ231101+020504		$2.75^{+1.22}_{-1.20}$	$+2.17$ -3.69	$+2.55$ -4.16	$4.43^{+0.82}_{-2.12}$	$+1.02$ -4.70	$+1.02$ -5.90	$-2.93^{+1.11}_{-0.28}$	$+1.66$ -0.28	$+1.73$ -0.28	$-11.42^{+4.25}_{-3.02}$	$+6.45$ -5.62	$+8.82$ -5.62
OM484		$3.30^{+0.95}_{-1.60}$	$+1.06$ -4.41	$+2.01$ -4.53	$4.62^{+0.79}_{-1.15}$	$+0.88$ -3.81	$+0.87$ -5.05	$-2.95^{+0.70}_{-0.26}$	$+1.51$ -0.27	$+1.63$ -0.26	$-11.12^{+2.24}_{-2.57}$	$+6.93$ -2.70	$+8.67$ -3.09
PB00198		$4.89^{+0.58}_{-1.34}$	$+0.61$ -3.41	$+0.61$ -5.06	$4.45^{+0.29}_{-3.64}$	$+1.03$ -5.46	$+1.04$ -5.79	$-1.72^{+0.39}_{-0.91}$	$+0.34$ -1.47	$+0.41$ -1.47	$-9.56^{+1.11}_{-7.47}$	$+5.09$ -8.92	$+6.52$ -9.83
PKS 0214-085		$2.44^{+1.19}_{-1.07}$	$+1.76$ -3.68	$+2.47$ -3.93	$3.23^{+1.76}_{-1.25}$	$+2.27$ -3.09	$+2.27$ -4.49	$-2.95^{+1.08}_{-0.34}$	$+1.61$ -0.30	$+1.68$ -0.33	$-9.06^{+1.97}_{-5.09}$	$+5.25$ -6.46	$+6.80$ -7.30
PKS 0459+060	1σ	$0.18^{+0.97}_{-1.53}$	$+2.67$ -1.52	$+2.88$ -1.68	$4.30^{+0.83}_{-1.16}$	$+1.20$ -1.97	$+1.20$ -2.28	$-2.75^{+0.20}_{-0.22}$	$+0.44$ -0.43	$+0.81$ -0.44	$-8.52^{+0.76}_{-3.92}$	$+2.28$ -4.95	$+2.82$ -5.38
PKS 0519+01		$4.74^{+0.72}_{-1.84}$	$+0.74$ -5.04	$+0.74$ -5.98	$3.68^{+1.82}_{-1.91}$	$+1.78$ -4.69	$+1.82$ -5.10	$-1.51^{+0.29}_{-1.06}$	$+0.22$ -1.70	$+0.30$ -1.70	$-11.21^{+4.57}_{-3.46}$	$+7.13$ -6.27	$+8.03$ -7.64
PKS 0648-16		$2.64^{+1.01}_{-0.82}$	$+2.01$ -3.33	$+2.80$ -3.80	$2.61^{+2.12}_{-0.82}$	$+2.86$ -2.27	$+2.88$ -3.47	$-1.50^{+0.29}_{-1.15}$	$+0.29$ -1.63	$+0.29$ -1.71	$-6.73^{+1.42}_{-4.14}$	$+3.22$ -6.07	$+4.82$ -6.77
PKS 0723-008		$3.27^{+1.11}_{-1.28}$	$+1.11$ -4.31	$+1.38$ -4.70	$4.23^{+1.22}_{-0.79}$	$+1.27$ -4.03	$+1.26$ -5.64	$-2.93^{+0.87}_{-0.28}$	$+1.48$ -0.28	$+1.61$ -0.28	$-9.39^{+2.88}_{-1.99}$	$+6.87$ -3.69	$+9.52$ -3.69
PKS 0727-115		$2.29^{+0.55}_{-1.15}$	$+0.76$ -3.27	$+1.19$ -3.66	$2.75^{+1.15}_{-0.66}$	$+2.73$ -0.84	$+2.73$ -1.84	$-2.95^{+1.02}_{-0.37}$	$+1.66$ -0.37	$+1.74$ -0.38	$-5.56^{+1.15}_{-2.05}$	$+1.88$ -4.82	$+2.80$ -5.82
PKS 0855-19		$2.27^{+1.19}_{-1.22}$	$+1.19$ -3.70	$+1.93$ -3.77	$3.18^{+2.08}_{-0.76}$	$+2.23$ -3.52	$+2.31$ -4.51	$-2.84^{+0.83}_{-0.37}$	$+1.47$ -0.34	$+1.51$ -0.37	$-8.64^{+2.81}_{-3.60}$	$+7.05$ -4.77	$+7.74$ -5.86
PKS 1217+02		$3.11^{+1.35}_{-0.84}$	$+2.35$ -2.94	$+2.35$ -4.51	$4.30^{+0.98}_{-2.13}$	$+1.14$ -5.02	$+1.19$ -5.73	$-1.62^{+0.19}_{-1.58}$	$+0.22$ -1.58	$+0.31$ -1.59	$-11.91^{+5.33}_{-1.85}$	$+9.28$ -2.90	$+9.48$ -5.01
PKS 1348+007		$1.76^{+0.77}_{-0.80}$	$+1.12$ -2.95	$+2.54$ -3.16	$2.21^{+2.02}_{-0.60}$	$+3.17$ -1.14	$+3.27$ -1.96	$-1.86^{+0.38}_{-0.83}$	$+0.46$ -1.35	$+0.55$ -1.35	$-6.64^{+1.18}_{-3.35}$	$+1.59$ -6.49	$+2.87$ -7.40
PKS 1508-05		$1.47^{+3.16}_{-1.17}$	$+3.64$ -2.89	$+4.03$ -2.89	$3.61^{+1.71}_{-2.73}$	$+1.82$ -4.71	$+1.89$ -5.04	$-2.34^{+0.37}_{-0.94}$	$+1.04$ -0.87	$+1.04$ -0.97	$-11.37^{+4.18}_{-6.41}$	$+7.71$ -8.31	$+10.02$ -8.57
PKS 1509+022	1σ	$0.74^{+0.86}_{-1.60}$	$+1.68$ -2.19	$+2.88$ -2.19	$2.96^{+1.43}_{-0.50}$	$+2.46$ -0.71	$+2.52$ -1.07	$-2.69^{+0.22}_{-0.33}$	$+0.70$ -0.55	$+1.25$ -0.57	$-8.36^{+1.13}_{-3.36}$	$+1.92$ -5.71	$+2.46$ -6.25
PKS 1510-089		$2.26^{+0.56}_{-0.66}$	$+1.37$ -2.79	$+2.00$ -3.72	$2.86^{+1.51}_{-0.47}$	$+2.64$ -0.44	$+2.64$ -0.83	$-1.92^{+0.44}_{-0.66}$	$+0.36$ -1.41	$+0.55$ -1.41	$-5.48^{+1.23}_{-2.34}$	$+1.18$ -4.44	$+1.59$ -5.25
PKS 1728+004		$2.81^{+0.79}_{-0.84}$	$+1.40$ -3.98	$+2.65$ -4.19	$3.14^{+1.11}_{-1.08}$	$+2.33$ -1.64	$+2.33$ -2.38	$-3.02^{+1.12}_{-0.26}$	$+1.81$ -0.22	$+1.84$ -0.26	$-8.87^{+2.42}_{-1.89}$	$+3.66$ -3.68	$+4.03$ -5.37
PKS 1734+063		$2.37^{+0.96}_{-0.87}$	$+1.44$ -3.84	$+2.51$ -3.84	$2.70^{+1.87}_{-0.85}$	$+2.78$ -2.24	$+2.78$ -4.14	$-1.99^{+0.15}_{-1.22}$	$+0.77$ -1.16	$+0.79$ -1.22	$-7.54^{+2.11}_{-3.31}$	$+3.58$ -5.81	$+5.42$ -5.81
PKS 1830-211		$3.40^{+0.91}_{-1.18}$	$+1.19$ -4.13	$+2.10$ -4.64	$3.98^{+1.42}_{-0.74}$	$+1.50$ -3.33	$+1.50$ -4.87	$-3.01^{+1.06}_{-0.25}$	$+1.64$ -0.25	$+1.75$ -0.25	$-8.36^{+1.79}_{-3.14}$	$+6.31$ -3.66	$+7.49$ -3.99
PKS 2320-021		$1.96^{+1.01}_{-1.76}$	$+1.40$ -3.41	$+2.18$ -3.46	$3.81^{+1.41}_{-1.41}$	$+1.68$ -3.65	$+1.68$ -5.11	$-2.73^{+0.58}_{-0.55}$	$+1.40$ -0.55	$+1.57$ -0.55	$-11.42^{+4.45}_{-2.18}$	$+7.28$ -4.20	$+8.50$ -5.45
PMN J0124-0624		$4.70^{+0.80}_{-2.35}$	$+0.80$ -5.22	$+0.80$ -6.10	$4.15^{+1.31}_{-2.81}$	$+1.31$ -5.21	$+1.31$ -5.59	$-1.80^{+0.09}_{-1.23}$	$+0.41$ -1.40	$+0.49$ -1.40	$-12.08^{+5.01}_{-4.53}$	$+10.02$ -5.80	$+10.02$ -7.91
PMN J0643+0857		$2.13^{+0.74}_{-0.65}$	$+1.16$ -2.63	$+1.16$ -3.51	$2.83^{+1.56}_{-0.52}$	$+2.63$ -0.65	$+2.64$ -1.73	$-1.96^{+0.63}_{-0.50}$	$+0.48$ -1.25	$+0.63$ -1.25	$-7.06^{+0.92}_{-2.95}$	$+1.21$ -5.03	$+2.21$ -5.16

Table C.2: Results of fitting the broken power-law model over the 1290 selected observations from OVRO dataset. Break significance refers to the source having a possible break frequency being (1σ) at 68.3%, (2σ) at 95.5% and (3σ) at 99.7%. The absence of break significance means that the source is not well-fitted at any level.

Name	Break significance	β_l	$\beta_l^{95.5\%}$	$\beta_l^{99.7\%}$	β_h	$\beta_h^{95.5\%}$	$\beta_h^{99.7\%}$	$\log f_{br}$	$\log f_{br}^{95.5\%}$	$\log f_{br}^{99.7\%}$	$\log A$	$\log A^{95.5\%}$	$\log A^{99.7\%}$
PMN J0656-032	3σ	$0.92^{+0.69}_{-0.91}$	$+1.25$ -1.90	$+1.53$ -2.42	$5.08^{+0.42}_{-0.96}$	$+0.42$ -1.80	$+0.42$ -2.52	$-2.42^{+0.16}_{-0.16}$	$+0.21$ -0.40	$+0.24$ -0.55	$-10.63^{+1.69}_{-1.44}$	$+3.08$ -1.95	$+4.87$ -2.04
PMN J0709-0255		$2.28^{+0.90}_{-1.15}$	$+1.26$ -3.64	$+2.60$ -3.77	$2.81^{+1.93}_{-0.81}$	$+2.55$ -2.58	$+2.67$ -3.28	$-2.86^{+0.82}_{-0.33}$	$+1.42$ -0.35	$+1.55$ -0.35	$-7.83^{+2.71}_{-3.16}$	$+4.93$ -5.84	$+5.48$ -6.71
PMN J0721+0406		$2.61^{+0.60}_{-0.84}$	$+1.58$ -3.79	$+2.77$ -3.90	$2.72^{+1.35}_{-0.98}$	$+2.73$ -2.03	$+2.76$ -3.45	$-1.61^{+0.28}_{-1.10}$	$+0.25$ -1.55	$+0.27$ -1.61	$-6.67^{+1.80}_{-2.76}$	$+3.57$ -4.77	$+5.06$ -5.79
PMN J0746-0709		$4.73^{+0.65}_{-2.45}$	$+0.74$ -4.80	$+0.74$ -6.18	$2.84^{+2.65}_{-0.91}$	$+2.66$ -3.48	$+2.65$ -4.02	$-2.95^{+1.01}_{-0.27}$	$+1.54$ -0.26	$+1.64$ -0.26	$-11.56^{+6.22}_{-2.15}$	$+7.20$ -6.80	$+8.44$ -7.74
PMN J0906-0905		$3.47^{+1.10}_{-0.93}$	$+2.03$ -2.97	$+2.03$ -4.68	$4.21^{+0.98}_{-2.22}$	$+1.26$ -4.74	$+1.26$ -5.58	$-2.97^{+1.10}_{-0.24}$	$+1.59$ -0.22	$+1.66$ -0.24	$-12.05^{+4.74}_{-2.33}$	$+8.34$ -3.45	$+9.69$ -5.16
PMN J0941-0754		$3.81^{+1.01}_{-2.77}$	$+1.68$ -4.63	$+1.68$ -5.31	$3.72^{+1.64}_{-2.36}$	$+1.77$ -4.69	$+1.77$ -5.22	$-2.88^{+0.87}_{-0.33}$	$+1.47$ -0.33	$+1.56$ -0.33	$-14.37^{+6.30}_{-2.66}$	$+9.31$ -5.57	$+11.37$ -5.56
PMN J1238-1959		$1.99^{+0.97}_{-1.49}$	$+1.60$ -3.22	$+1.93$ -3.48	$2.92^{+1.38}_{-0.96}$	$+2.55$ -1.17	$+2.55$ -1.79	$-2.77^{+0.52}_{-0.41}$	$+1.26$ -0.40	$+1.33$ -0.44	$-8.36^{+2.08}_{-2.78}$	$+3.02$ -5.50	$+3.63$ -6.04
PMN J1318-1235		$0.15^{+3.64}_{-0.72}$	$+5.26$ -1.35	$+5.31$ -1.64	$-0.48^{+3.37}_{-0.90}$	$+5.50$ -0.99	$+5.97$ -0.99	$-2.70^{+1.23}_{-0.01}$	$+1.20$ -0.50	$+1.28$ -0.51	$-14.98^{+5.02}_{-4.14}$	$+9.39$ -5.00	$+12.68$ -4.98
PMN J1420-1118		$0.92^{+1.24}_{-2.04}$	$+4.04$ -2.42	$+4.40$ -2.41	$3.23^{+2.27}_{-1.57}$	$+2.00$ -4.68	$+2.27$ -4.68	$-2.65^{+0.69}_{-0.48}$	$+1.27$ -0.50	$+1.34$ -0.55	$-12.42^{+5.40}_{-3.24}$	$+6.80$ -7.47	$+9.44$ -7.46
PMN J2016-0903		$4.17^{+0.51}_{-2.43}$	$+1.33$ -4.50	$+1.33$ -5.51	$2.74^{+2.71}_{-1.06}$	$+2.77$ -3.55	$+2.76$ -4.21	$-1.46^{+0.26}_{-1.17}$	$+0.22$ -1.70	$+0.26$ -1.75	$-9.63^{+3.34}_{-4.44}$	$+5.38$ -7.77	$+6.12$ -9.76
PMN J2324+0801		$0.30^{+2.85}_{-1.35}$	$+4.68$ -1.67	$+5.16$ -1.79	$-0.59^{+2.81}_{-0.87}$	$+5.50$ -0.87	$+6.08$ -0.90	$-2.83^{+1.04}_{-0.30}$	$+1.59$ -0.33	$+1.64$ -0.37	$-16.71^{+4.59}_{-3.28}$	$+11.32$ -3.28	$+13.71$ -3.29
RGBJ2056+496		$1.84^{+2.82}_{-1.18}$	$+3.59$ -2.85	$+3.65$ -3.32	$3.23^{+2.15}_{-1.64}$	$+2.21$ -3.99	$+2.25$ -4.61	$-2.78^{+1.00}_{-0.34}$	$+1.56$ -0.34	$+1.57$ -0.43	$-9.12^{+2.19}_{-7.19}$	$+4.74$ -9.96	$+5.46$ -10.53
RXJ0132.6-0804		$3.57^{+1.57}_{-2.56}$	$+1.91$ -4.55	$+1.90$ -5.07	$1.04^{+2.11}_{-2.29}$	$+3.94$ -2.55	$+4.45$ -2.51	$-2.16^{+0.29}_{-0.99}$	$+0.89$ -0.94	$+0.91$ -1.00	$-15.02^{+4.62}_{-4.80}$	$+10.65$ -4.81	$+12.81$ -4.81
RXJ1931.1+0937		$2.44^{+2.49}_{-0.78}$	$+3.06$ -2.60	$+3.06$ -3.86	$2.97^{+2.13}_{-1.26}$	$+2.52$ -3.57	$+2.52$ -4.35	$-1.54^{+0.32}_{-1.09}$	$+0.31$ -1.64	$+0.35$ -1.67	$-9.68^{+2.91}_{-5.21}$	$+5.83$ -7.28	$+6.30$ -9.30
S40859+47		$2.24^{+0.89}_{-0.98}$	$+1.20$ -3.27	$+2.74$ -3.67	$2.82^{+1.71}_{-0.91}$	$+2.65$ -2.45	$+2.65$ -3.64	$-2.88^{+0.92}_{-0.32}$	$+1.51$ -0.28	$+1.56$ -0.33	$-7.72^{+1.55}_{-3.83}$	$+3.82$ -6.77	$+5.26$ -6.77
S40900+42		$2.13^{+0.94}_{-1.85}$	$+1.86$ -3.38	$+2.27$ -3.58	$4.05^{+0.91}_{-2.02}$	$+1.45$ -4.22	$+1.44$ -5.55	$-2.86^{+0.65}_{-0.35}$	$+1.44$ -0.34	$+1.55$ -0.35	$-10.63^{+4.09}_{-3.33}$	$+6.96$ -4.95	$+8.73$ -5.83
S40913+39		$2.41^{+0.83}_{-0.94}$	$+1.16$ -3.59	$+2.73$ -3.88	$2.95^{+1.67}_{-0.45}$	$+2.38$ -1.57	$+2.52$ -2.35	$-2.08^{+0.13}_{-1.06}$	$+0.65$ -1.13	$+0.76$ -1.13	$-7.53^{+1.63}_{-2.31}$	$+2.39$ -4.63	$+3.81$ -5.19
S51027+74	3σ	$0.13^{+0.63}_{-0.92}$	$+1.04$ -1.49	$+1.45$ -1.52	$4.49^{+0.97}_{-0.52}$	$+1.01$ -1.50	$+1.01$ -2.20	$-2.26^{+0.11}_{-0.11}$	$+0.25$ -0.21	$+0.29$ -0.37	$-9.83^{+1.42}_{-1.54}$	$+3.14$ -2.10	$+4.16$ -2.55
TB0110+6805		$2.04^{+0.70}_{-1.12}$	$+1.28$ -3.33	$+3.13$ -3.38	$2.32^{+2.63}_{-0.34}$	$+3.16$ -1.98	$+3.15$ -3.72	$-2.48^{+0.56}_{-0.82}$	$+1.28$ -0.83	$+1.39$ -0.84	$-7.43^{+1.51}_{-4.49}$	$+2.99$ -8.04	$+5.10$ -8.03
TB0423+4150		$3.14^{+1.07}_{-0.70}$	$+2.28$ -2.68	$+2.27$ -4.55	$3.71^{+1.55}_{-1.47}$	$+1.75$ -4.13	$+1.75$ -5.03	$-1.40^{+0.32}_{-1.26}$	$+0.28$ -1.85	$+0.32$ -1.92	$-10.30^{+3.85}_{-1.72}$	$+7.85$ -2.69	$+8.77$ -4.30
TB0754-1147		$3.26^{+1.24}_{-0.81}$	$+2.23$ -3.59	$+2.23$ -4.71	$4.24^{+1.23}_{-1.77}$	$+1.26$ -4.77	$+1.23$ -5.74	$-3.08^{+1.23}_{-0.24}$	$+1.77$ -0.24	$+1.88$ -0.24	$-11.35^{+3.91}_{-3.34}$	$+8.54$ -4.22	$+9.82$ -5.46
TXS 0106+612		$1.12^{+0.90}_{-1.03}$	$+1.10$ -2.49	$+1.61$ -2.61	$2.43^{+1.37}_{-0.47}$	$+2.86$ -0.51	$+2.96$ -0.77	$-2.12^{+0.25}_{-0.54}$	$+0.29$ -1.01	$+0.83$ -1.05	$-5.84^{+1.13}_{-2.37}$	$+1.13$ -5.20	$+1.52$ -5.73
TXS 0259+681	1σ	$2.30^{+0.75}_{-2.05}$	$+0.77$ -3.70	$+1.16$ -3.80	$4.14^{+0.65}_{-1.01}$	$+1.35$ -1.28	$+1.35$ -1.68	$-2.85^{+0.28}_{-0.34}$	$+1.07$ -0.35	$+1.50$ -0.36	$-9.84^{+0.94}_{-2.70}$	$+2.02$ -4.37	$+2.86$ -4.70
TXS 0329+654		$3.55^{+1.93}_{-0.92}$	$+1.93$ -4.27	$+1.92$ -5.06	$4.15^{+1.33}_{-2.62}$	$+1.35$ -5.08	$+1.33$ -5.60	$-1.55^{+0.31}_{-1.09}$	$+0.29$ -1.64	$+0.35$ -1.66	$-14.93^{+6.60}_{-1.93}$	$+10.93$ -3.74	$+12.74$ -4.81

Table C.2: Results of fitting the broken power-law model over the 1290 selected observations from OVRO dataset. Break significance refers to the source having a possible break frequency being (1σ) at 68.3%, (2σ) at 95.5% and (3σ) at 99.7%. The absence of break significance means that the source is not well-fitted at any level.

Name	Break significance	β_l	$\beta_l^{95.5\%}$	$\beta_l^{99.7\%}$	β_h	$\beta_h^{95.5\%}$	$\beta_h^{99.7\%}$	$\log f_{br}$	$\log f_{br}^{95.5\%}$	$\log f_{br}^{99.7\%}$	$\log A$	$\log A^{95.5\%}$	$\log A^{99.7\%}$
TXS 0330+291		$2.60^{+1.72}_{-0.88}$	$+2.78$ -2.57	$+2.85$ -3.73	$4.19^{+1.31}_{-2.21}$	$+1.31$ -4.76	$+1.31$ -5.52	$-1.57^{+0.36}_{-1.02}$	$+0.27$ -1.62	$+0.36$ -1.63	$-9.72^{+2.37}_{-5.48}$	$+5.60$ -7.49	$+7.05$ -9.74
TXS 0354+599		$2.37^{+0.54}_{-0.82}$	$+1.20$ -2.08	$+2.10$ -2.81	$2.75^{+1.80}_{-0.77}$	$+2.75$ -2.15	$+2.75$ -4.03	$-2.19^{+0.87}_{-0.21}$	$+0.86$ -0.91	$+0.87$ -1.02	$-7.41^{+1.79}_{-3.53}$	$+3.29$ -6.03	$+5.64$ -6.03
TXS 0529+483		$2.90^{+0.82}_{-0.92}$	$+1.68$ -4.21	$+2.60$ -4.21	$3.00^{+1.55}_{-0.92}$	$+2.40$ -3.20	$+2.48$ -3.88	$-3.00^{+1.24}_{-0.20}$	$+1.75$ -0.18	$+1.80$ -0.22	$-7.02^{+1.04}_{-3.59}$	$+4.12$ -4.83	$+5.22$ -5.50
TXS 0646-176		$3.61^{+0.88}_{-0.72}$	$+1.76$ -1.53	$+1.88$ -2.23	$3.39^{+1.81}_{-1.31}$	$+2.11$ -3.99	$+2.11$ -4.88	$-1.49^{+0.30}_{-1.04}$	$+0.30$ -1.59	$+0.30$ -1.72	$-8.09^{+1.55}_{-4.60}$	$+4.62$ -5.84	$+6.62$ -6.16
TXS 0657+172		$2.69^{+0.73}_{-0.84}$	$+1.07$ -3.17	$+1.36$ -4.14	$3.30^{+1.33}_{-0.81}$	$+2.19$ -2.46	$+2.19$ -4.23	$-2.89^{+0.91}_{-0.33}$	$+1.55$ -0.27	$+1.58$ -0.32	$-8.22^{+1.36}_{-2.75}$	$+4.20$ -4.74	$+5.78$ -5.15
TXS 0700-197		$2.17^{+1.09}_{-0.87}$	$+1.85$ -2.96	$+1.85$ -3.64	$2.48^{+1.80}_{-0.65}$	$+2.99$ -1.72	$+2.99$ -3.94	$-2.92^{+1.05}_{-0.30}$	$+1.64$ -0.30	$+1.71$ -0.30	$-6.16^{+1.47}_{-3.26}$	$+3.09$ -6.01	$+5.17$ -6.62
TXS 0745-165		$2.35^{+1.35}_{-1.18}$	$+3.05$ -2.28	$+3.15$ -3.64	$2.76^{+1.89}_{-1.77}$	$+2.72$ -3.25	$+2.73$ -4.15	$-2.96^{+1.11}_{-0.25}$	$+1.60$ -0.25	$+1.65$ -0.25	$-7.91^{+4.24}_{-3.28}$	$+5.64$ -7.43	$+6.50$ -9.02
TXS 0936-173	2σ	$-0.21^{+0.84}_{-1.20}$	$+2.15$ -1.28	$+2.96$ -1.28	$5.08^{+0.41}_{-0.94}$	$+0.41$ -2.06	$+0.41$ -2.65	$-2.64^{+0.13}_{-0.17}$	$+0.28$ -0.37	$+0.49$ -0.42	$-13.28^{+2.41}_{-0.84}$	$+4.75$ -1.12	$+6.01$ -1.42
TXS 1801+253	1σ	$1.77^{+0.67}_{-1.84}$	$+0.77$ -3.25	$+1.61$ -3.25	$3.97^{+0.71}_{-1.45}$	$+1.53$ -1.79	$+1.53$ -2.25	$-2.70^{+0.43}_{-0.29}$	$+0.89$ -0.41	$+1.22$ -0.49	$-9.74^{+2.49}_{-2.20}$	$+3.51$ -4.42	$+4.10$ -4.98
TXS 1827+062		$2.74^{+0.83}_{-1.22}$	$+1.25$ -3.97	$+2.41$ -4.23	$3.53^{+1.78}_{-0.85}$	$+1.97$ -2.96	$+1.96$ -3.77	$-2.93^{+0.91}_{-0.28}$	$+1.65$ -0.26	$+1.73$ -0.28	$-9.82^{+3.54}_{-2.25}$	$+5.81$ -4.04	$+7.18$ -4.81
TXS 2016+386		$1.11^{+0.52}_{-0.67}$	$+2.37$ -2.08	$+3.78$ -2.55	$1.42^{+2.06}_{-0.58}$	$+3.95$ -0.66	$+3.95$ -1.47	$-1.55^{+0.45}_{-0.79}$	$+0.43$ -1.57	$+0.45$ -1.64	$-4.45^{+0.88}_{-2.89}$	$+1.15$ -5.74	$+1.81$ -6.71
TXS 2157+102	1σ	$-0.14^{+2.14}_{-0.48}$	$+2.70$ -1.22	$+3.03$ -1.35	$3.99^{+0.87}_{-1.37}$	$+1.46$ -1.83	$+1.51$ -2.28	$-2.72^{+0.23}_{-0.27}$	$+0.77$ -0.49	$+1.39$ -0.49	$-10.71^{+2.55}_{-2.75}$	$+3.98$ -4.16	$+5.04$ -4.44
TXS 2206+650		$1.67^{+0.93}_{-0.71}$	$+2.29$ -2.96	$+3.70$ -2.98	$1.14^{+1.32}_{-0.94}$	$+2.72$ -2.58	$+4.08$ -2.59	$-1.57^{+0.32}_{-1.07}$	$+0.32$ -1.58	$+0.37$ -1.64	$-3.54^{+1.15}_{-2.07}$	$+2.81$ -6.24	$+2.81$ -8.90
VER J0521+211		$2.27^{+0.75}_{-1.50}$	$+1.26$ -3.53	$+2.09$ -3.75	$2.96^{+2.10}_{-0.56}$	$+2.54$ -1.95	$+2.53$ -3.62	$-2.78^{+0.65}_{-0.43}$	$+1.44$ -0.38	$+1.46$ -0.43	$-8.53^{+1.88}_{-3.81}$	$+3.92$ -6.38	$+5.93$ -7.16
WNB1016.6+8038		$3.72^{+1.45}_{-0.65}$	$+1.78$ -2.41	$+1.77$ -5.19	$4.36^{+0.98}_{-2.40}$	$+1.10$ -5.34	$+1.11$ -5.80	$-1.58^{+0.27}_{-0.98}$	$+0.27$ -1.59	$+0.27$ -1.63	$-12.83^{+5.36}_{-1.79}$	$+8.53$ -3.93	$+10.00$ -4.83
WNB1609.6+8517		$4.56^{+0.93}_{-2.48}$	$+0.92$ -5.51	$+0.94$ -6.02	$1.77^{+3.22}_{-1.12}$	$+3.70$ -2.74	$+3.70$ -3.22	$-1.77^{+0.43}_{-0.83}$	$+0.42$ -1.35	$+0.44$ -1.44	$-12.38^{+5.38}_{-4.18}$	$+8.43$ -6.91	$+9.70$ -7.58
Z8276		$0.63^{+3.10}_{-1.36}$	$+4.67$ -1.94	$+4.87$ -2.11	$-0.21^{+2.34}_{-1.29}$	$+4.95$ -1.28	$+5.71$ -1.28	$-2.38^{+0.90}_{-0.38}$	$+1.12$ -0.68	$+1.12$ -0.76	$-17.29^{+5.24}_{-2.71}$	$+11.32$ -2.71	$+14.53$ -2.72